![UCOR logo — an Amentum-led partnership with Jacobs]

Performance Assessment for the Environmental Management Disposal Facility at the Y-12 National Security Complex, Oak Ridge, Tennessee

This document is approved for public release per review by:

Peter Kortman (signature on file)   04-23-2020

UCOR Classification &   Date
Information Control Office

Performance Assessment for the Environmental Management Disposal Facility at the Y-12 National Security Complex, Oak Ridge, Tennessee

Date Issued—April 2020

Prepared for the
U.S. Department of Energy
Office of Environmental Management

This page intentionally left blank.

APPROVALS

Performance Assessment for the Environmental Management Disposal Facility at the Y-12 National Security Complex, Oak Ridge, Tennessee	UCOR-5094/R2
	April 2020

USQD Review Determination	☐ USQD ☐ UCD ☐ CAT X ☐ Exempt (Select Criteria 1–3 below.) USQD/UCD/CAT X No.: _____
Exemption Criteria	☐ (1) Non-Intent Change ☐ (2) DOE-Approved Safety Basis Document ☐ (3) Chief Accounting Officer, Internal Audit, Labor Relations, General Counsel, Outreach & Public Affairs, or Project Controls Services OR ☒ (4) Document identified in USQD-MS-CX-REPORTS-1074
USQD Preparer:	KAREN BALO (Affiliate) Digitally signed by KAREN BALO (Affiliate) Date: 2020.04.27 12:28:18 -04'00' Name Date
Exhibit L Mandatory Contractor Document	☒ No (No PCCB Reviewer Signature Required.) ☐ Yes (Requires review by the Proforma Change Control Board.)
PCCB Reviewer:	Name Date

Prepared by:

Stephen Kenworthy   Digitally signed by Stephen Kenworthy
Date: 2020.04.27 14:30:13 -04'00'

Steve Kenworthy, Senior Hydrogeologist   Date
UCOR

Concurred by:

JULIE PFEFFER (Affiliate)   Digitally signed by JULIE PFEFFER (Affiliate)
Date: 2020.04.27 18:54:20 -04'00'

Julie Pfeffer, EMDF Project Manager   Date
UCOR

Approved by:

John Wrapp (signature on file)   04-28-2020

John Wrapp, Waste Program and Disposition Manager   Date
UCOR

This page intentionally left blank.

REVISION LOG

Revision Number	Description of Changes	Pages Affected
0	Initial issue of document.	All
1	Addressed OREM comments.	All
2	Addressed LFRG comments	All

This page intentionally left blank.

CONTENTS

This page intentionally left blank.

FIGURES

This page intentionally left blank.

TABLES

ACRONYMS

ALARA	as low as reasonably achievable
ANA	aquatic natural area
ARAR	applicable or relevant and appropriate requirement
ASTM	American Society for Testing and Materials
BCBG	Bear Creek Burial Ground
BCK	Bear Creek kilometer
BCV	Bear Creek Valley
BG	burial ground
bgs	below ground surface
BJC	Bechtel Jacobs Company LLC
C2DF	Class L-II Disposal Facility
CA	Composite Analysis
CBCV	Central Bear Creek Valley
CERCLA	Comprehensive Environmental Response, Compensation, and Liability Act of 1980
CFR	*Code of Federal Regulations*
D	dimensional
DAS	Disposal Authorization Statement
DCS	Derived Concentration Standard
D&D	deactivation and decommissioning
DMC	Document Management Center
DOE	U.S. Department of Energy
DOE O	DOE Order
DOE M	DOE Manual
EBCV	East Bear Creek Valley
Eh	oxidation-reduction potential
EMDF	Environmental Management Disposal Facility
EMWMF	Environmental Management Waste Management Facility
EOW	edge of waste
EPA	U.S. Environmental Protection Agency
EPM	equivalent porous medium
ETSZ	East Tennessee Seismic Zone
ETTP	East Tennessee Technology Park
FLUTe^{TM}	Flexible Liner Underground Technologies, LLC
FFA	Federal Facility Agreement
Golder	Golder Associates, Inc.
HA	habitat area
HDPE	high-density polyethylene
HELP	Hydrologic Evaluation of Landfill Performance
IAEA	International Atomic Energy Agency
IHI	inadvertent human intrusion
K_d	partition coefficient
LDR	Land Disposal Restriction
LLW	low-level (radioactive) waste
MCL	maximum contaminant level
MEI	maximally exposed individual
MSL	mean sea level
NA	natural area
NQA	Nuclear Quality Assurance

NRC	U.S. Nuclear Regulatory Commission
NT	North Tributary
NWS	National Weather Service
Ogden	Ogden Environmental and Energy Services Co., Inc.
OM	organic matter
OREM	Oak Ridge Office of Environmental Management
ORERP	Oak Ridge Environmental Research Park
ORNL	Oak Ridge National Laboratory
ORR	Oak Ridge Reservation
PA	Performance Assessment
PNNL	Pacific Northwest National Laboratory
POA	point of assessment
QA	quality assurance
RCRA	Resource Conservation and Recovery Act of 1976
RER	Remediation Effectiveness Report
RESRAD	RESidual RADioactivity
RI/FS	Remedial Investigation/Feasibility Study
ROD	Record of Decision
SR	State Route
SRS	Savannah River Site
SRSG	Single Radionuclide Soil Guideline
STOMP	Subsurface Transport Over Multiple Phases
SWSA	Solid Waste Storage Area
TDEC	Tennessee Department of Environment and Conservation
TVA	Tennessee Valley Authority
UCL	upper confidence limit
USDA	U.S. Department of Agriculture
USGS	U.S. Geological Survey
VMC	volumetric moisture content
WAC	waste acceptance criteria
WAG	Waste Area Grouping
WBCV	West Bear Creek Valley
WMFS	Waste Management Federal Services, Inc.
Y-12	Y-12 National Security Complex

EXECUTIVE SUMMARY

This report documents the Performance Assessment (PA) for the Environmental Management Disposal Facility (EMDF). The EMDF is a proposed, new low-level (radioactive) waste (LLW) disposal facility on the U.S. Department of Energy (DOE) Oak Ridge Reservation (ORR). This executive summary includes an overview of the following:

- Need for EMDF and basis for the PA

- Features and safety functions of the EMDF disposal system, including a summary of the estimated radionuclide inventory

- Key assumptions

- Conceptual models and model codes implemented for analysis of performance and quality assurance (QA) processes

- Summary of results, including sensitivity and uncertainty analysis

- Evaluation of EMDF performance relative to the requirements of DOE Manual (M) 435.1-1 (DOE 2011a).

NEED FOR THE EMDF AND BASIS FOR THE PA

A detailed description of the basis for the PA is provided in Sect. 1.1.

Mission Need and PA Development

DOE is responsible for sitewide waste management and environmental restoration activities on the ORR under its Office of Environmental Management Program at the national level and locally under the Oak Ridge Office of Environmental Management (OREM). OREM is responsible for minimizing potential hazards to human health and the environment associated with contamination from past DOE practices and addressing the waste management and disposal needs of the ORR. Under the requirements of the Federal Facility Agreement (FFA) for the ORR (DOE 1992a) established by DOE, the U.S. Environmental Protection Agency, and the Tennessee Department of Environment and Conservation, environmental restoration activities on the ORR are performed in accordance with the Comprehensive Environmental Response, Compensation, and Liability Act of 1980 (CERCLA).

Timely and effective ORR cleanup is essential to facilitate reindustrialization of the East Tennessee Technology Park, and to ensure worker safety and the success of DOE missions at the Y-12 National Security Complex (Y-12) and Oak Ridge National Laboratory (ORNL). The Environmental Management Waste Management Facility (EMWMF), constructed in Bear Creek Valley (BCV) near Y-12 (Fig. ES.1), is accepting CERCLA cleanup wastes. The authorized disposal capacity of EMWMF is 2.3 million cy (DOE 1999a, DOE 2010a). The scope of the OREM cleanup effort has expanded since EMWMF began operations in 2002. Approximately 1.6 million cy of additional CERCLA waste is expected to be generated and require disposal after EMWMF has reached maximum capacity in the late-2020s.
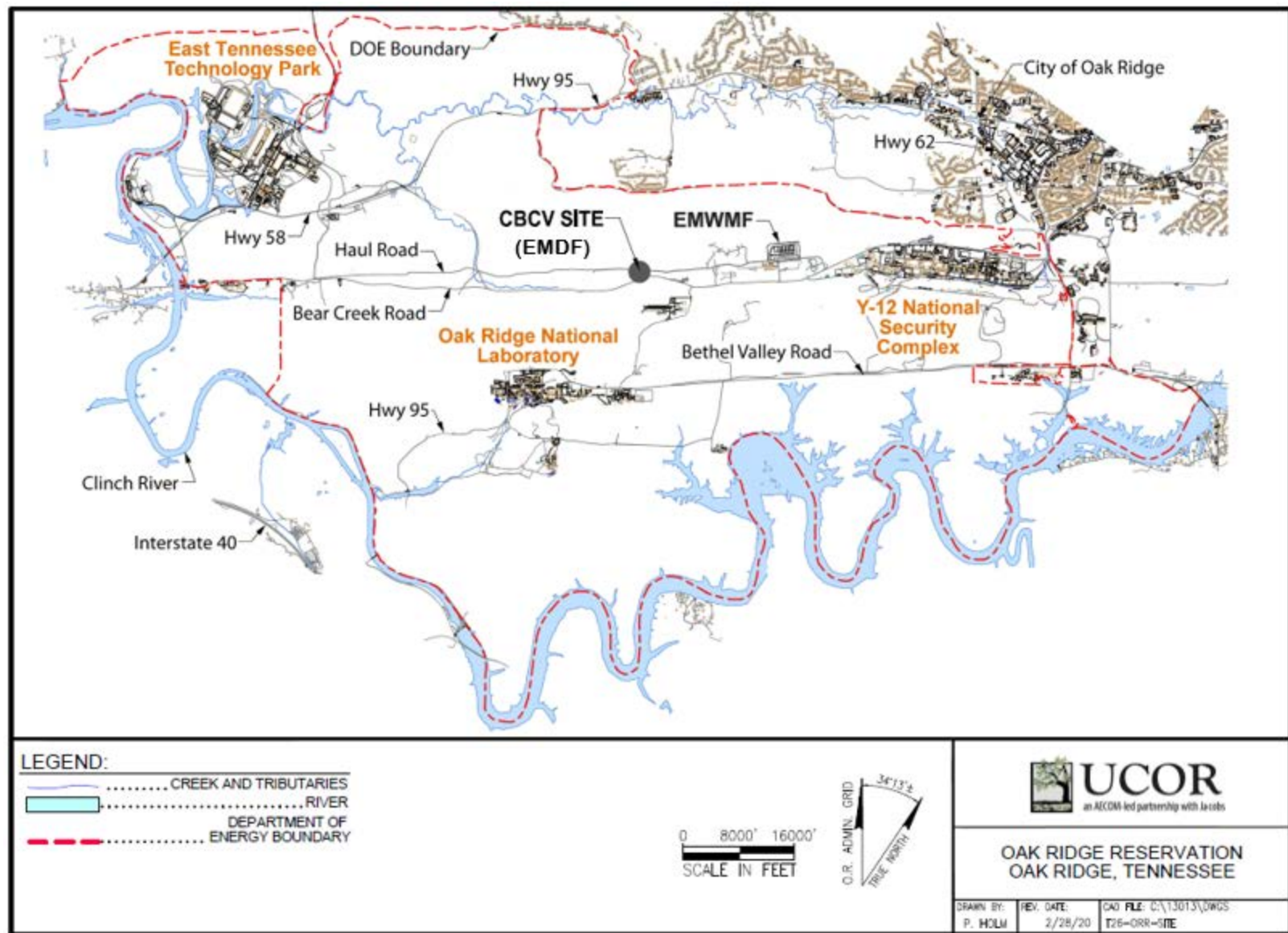
Fig. ES.1. ORR map with locations of DOE facilities, including EMWMF and EMDF sites

A new facility is required to ensure sufficient future LLW disposal capacity for CERCLA environmental cleanup activities on the ORR. The FFA parties issued a Proposed Plan (DOE 2018a) for the disposal of future ORR CERCLA waste for public comment in 2018. Since the Proposed Plan was issued, the design of the EMDF has been advanced to a preliminary design (60 percent) stage and is the basis for technical analyses in this PA. The total airspace capacity of the EMDF preliminary design is 2.2 million cy.

This EMDF PA has been developed to support DOE approval of a Disposal Authorization Statement (DAS) for construction of EMDF. Development of the EMDF PA and facility design activities are being conducted in parallel with activities required for approval of EMDF for onsite LLW disposal under the FFA. Documentation to support a final Disposal Authorization Statement for operations of the landfill will occur in parallel with the final design of the facility. A Composite Analysis (CA) (UCOR, an Amentum-led partnership with Jacobs, 2020a) has been prepared to evaluate the cumulative impacts of potential releases from historical waste disposal sites, the existing EMWMF, and the future EMDF in BCV.

The EMDF PA includes site-specific model simulations for release of radionuclides from the facility and dose analyses for post-closure exposure to releases, as well as analysis of inadvertent human intrusion (IHI) scenarios. The primary purpose of the EMDF PA is to provide a reasonable expectation that DOE M 435.1-1 performance objectives will be met.

Performance Objectives

EMDF performance objectives for the PA analysis are summarized in Table ES.1. Additional detail is provided in Sect. 1.5.1. The performance objectives are taken directly from DOE M 435.1-1 and do not reflect any site-specific regulatory requirements other than the application of drinking water maximum contaminant levels for water resources protection objectives.

Table ES.1. Exposure scenarios, performance objectives and measures, and points of assessment for the EMDF PA

Exposure scenario	Performance objective or measure	Point of assessment
All pathways	25 mrem/year	Groundwater: 100 m from waste margin at the point of maximum concentration (plume centerline)
		Surface water: Bear Creek downstream of NT-11
Air pathway[a]	10 mrem/year[b]	100 m from waste margin
Radon flux	20 pCi/m^2/sec	EMDF cover surface
Water resources (groundwater) • Ra-226 + Ra-228 • Gross alpha activity[c] • Beta/photon activity • H-3 • Sr-90 • Uranium (total)	5 pCi/L 15 pCi/L 4 mrem/year 20,000 pCi/L 8 pCi/L 30 µg/L	Groundwater at 100 m
Water resources (surface water)	DOE *Derived Concentration Technical Standard*[d]	Bear Creek at NT-11 tributary junction

**Table ES.1. Exposure scenarios, performance objectives and measures,
and points of assessment for the EMDF PA (cont.)**

Exposure scenario	Performance objective or measure	Point of assessment
Inadvertent human intrusion		
• Chronic exposure	100 mrem/year	At EMDF
• Acute exposure	500 mrem	At EMDF

[a]Air pathway is screened from the EMDF PA.
[b]Excluding radon in air.
[c]Including Ra-226, but excluding radon and uranium.
[d]DOE 2011b.

DOE = U.S. Department of Energy	NT = North Tributary
EMDF = Environmental Management Disposal Facility	PA = Performance Assessment

Point of Assessment, Institutional Control, and Timing Assumptions

A point of assessment (POA) is provided for each exposure scenario listed in Table ES.1. For the EMDF PA, the POAs are identical to DOE M 435.1-1 requirements and consistent with the Disposal Authorization Statement and Tank Closure Documentation standard (DOE 2017a). The assumed POAs do not vary with the post-closure time period, even though expected future land use and institutional controls would preclude public exposure at the 100-m buffer zone boundary for as long as waste remains above unrestricted use criteria in the area (as required under CERCLA). Institutional controls limiting site access are assumed to be effective for 100 years following closure. For analysis of IHI, intrusion is assumed to occur no earlier than 100 years post-closure as a result of a temporary loss of institutional control of the Central Bear Creek Valley (CBCV) site. These assumptions are pessimistic given that DOE is required to maintain control over land containing radionuclide sources until the land can be safely released pursuant to DOE Order (O) 458.1, *Radiation Protection of the Public and the Environment* (DOE 2013a), and CERCLA. Additional consideration of land use and institutional controls is provided in Sect. 1.6.

EMDF performance with respect to the performance objectives or performance measures is based on deterministic model results for specific pathways and environmental media. Compliance with performance objectives and measures is based on PA results for the compliance period from EMDF closure to 1000 years post-closure, with the exception of the IHI analysis for which compliance is assessed beginning at the assumed end of institutional control (100 years). Quantitative dose estimates are presented for a period of 10,000 years post-closure to provide perspective on the potential impacts beyond the compliance period. For long-lived, relatively immobile radionuclides that are significant components of the estimated EMDF inventory (e.g., radionuclides of uranium), PA model saturated zone concentration results beyond 10,000 years also are provided. These model predictions for the period beyond 10,000 years are highly uncertain and are presented only to indicate very long-term trends, rather than for comparison to regulatory standards.

AS LOW AS REASONABLY ACHIEVALBE ANALYSIS

The As Low As Reasonably Achievable (ALARA) process (DOE 2013a) is used to optimize EMDF performance and maintain doses to members of the public (both individual and collective) and releases to the environment ALARA. DOE M 435.1-1 includes a requirement for an ALARA analysis as part of the PA. The ALARA handbook (DOE 2014) describes a graded approach to implementing the ALARA process, including the use of reference doses for determining the level of analysis required for a given project. The reference dose for a maximally exposed individual and the reference collective dose below which only qualitative ALARA analysis is sufficient are 1 mrem/year and 10 person-rem/year, respectively.

For a LLW disposal project, the timeframe of consideration for an ALARA analysis of any level should be no greater than 1000 years (DOE 2014, pages 5–8), so the peak total dose within the compliance period and the estimated EMDF dose at 1000 years are compared to the reference values.

The EMDF PA modeling predicts a base case all-pathways maximum individual dose within the 1000-year compliance period of 1.03 mrem/year (Sect. 4.5.1). The results of the probabilistic uncertainty analysis (Sect. 5.4 and Appendix G, Sect. G.6.3.3) suggest a median peak individual dose of 1.0 mrem/year and a mean all pathways dose of 1.0 mrem/year at 1000 years. These results for individual exposure indicate that a semi-quantitative ALARA analysis could be considered; however, the ALARA guidance also states that "it is the collective dose that is utilized in the ALARA analysis to select a radiation protection alternative". Given the likelihood that BCV and the CBCV site will remain under DOE control indefinitely, there are a limited range of collective exposure scenarios that are credible, and the collective dose from EMDF release is expected to remain far below the reference collective dose of 10 person-rem/year (refer to Sect. 1.5.4 for additional detail). Based on the 10 person-rem/year reference value for collective dose, these model-based quantitative estimates indicate that a qualitative ALARA analysis for EMDF design and operations is sufficient.

The EMDF Remedial Investigation/Feasibility Study (RI/FS) (DOE 2017b) includes an analysis of alternatives for disposition of LLW from CERCLA actions on the ORR. The RI/FS includes identification and screening of disposal technologies and process options (DOE 2017b, Sect. 5) and considers broader social, economic, and public policy aspects in the analysis of remedial alternatives (DOE 2017b, Sect. 7). The disposal technology screening and conceptual facility design for the CBCV site (DOE 2017b, Sect. 6) served as the foundation for preliminary engineering design of the Resource Conservation and Recovery Act of 1976-type disposal facility at the CBCV site.

The EMDF Proposed Plan (DOE 2018a) describes the remedial action objectives for CERCLA waste disposal and presents onsite disposal at the CBCV site as the preferred (optimal) alternative based on the range of considerations required under CERCLA and the FFA. CERCLA alternative evaluation threshold criteria for remedial actions include overall protection of human health and the environment and compliance with applicable or relevant and appropriate requirements (ARARs). Balancing criteria include long-term effectiveness and permanence; reduction of toxicity, mobility, or volume through treatment; short-term effectiveness; implementability; and cost. Considerations of state and community acceptance are incorporated following public review of the Proposed Plan. Thus, the FFA remedy selection process has addressed key considerations for an ALARA analysis and the disposal options considered and conclusions presented in the EMDF RI/FS and Proposed Plan are considered to meet the intent of the DOE ALARA requirements for the EMDF PA.

EMDF DISPOSAL SYSTEM

The proposed site for EMDF in BCV is southwest of the city of Oak Ridge, Tennessee, and Y-12 (Fig. ES.1). The LLW disposal concept and preliminary design are similar to EMWMF (i.e., an engineered multicell, near-surface disposal unit for solid LLW derived from CERCLA response actions on ORR). The EMDF disposal system encompasses the natural features of the CBCV site, design features of the engineered disposal unit, waste characteristics, and the operating limits (e.g., waste acceptance criteria [WAC]) and other waste and safety management practices that ensure worker protection and post-closure facility performance.

Site Characteristics

The ORR lies in the western portion of the Valley and Ridge physiographic province, which is characterized by long, parallel ridges and valleys that follow a northeast-to-southwest trend. EMDF will be located on DOE property approximately 3 miles southwest of Y-12 (Fig. ES.1). BCV lies between Pine Ridge to the northwest and Chestnut Ridge to the southeast. The upper portion of the Bear Creek watershed between Y-12 and the EMDF site contains several closed disposal facilities, contaminant source areas, and groundwater contaminant plumes, in addition to the currently operating EMWMF.

The EMDF PA analysis incorporates an extensive body of environmental information drawn from over two decades of RIs and monitoring in BCV. CBCV site characterization efforts have been completed to support FFA approval of the proposed site and to support engineering design (DOE 2018b, DOE 2019). Proposed activities, new regulatory requirements, or other new information that could challenge key assumptions for the EMDF performance analysis (Sect. 1.7) will be evaluated in accordance with the EMDF change control process to assess the potential for such changes to require a Special Analysis or revisions to the PA.

An extensive review of the ORR, BCV, and CBCV site characteristics, including demographics, climate, geology, ecology and natural resources, hydrology and hydrogeology, and subsurface geochemistry is provided in Sect. 2.1. The geologic and hydrogeologic setting are briefly summarized in the following paragraphs.

The Valley and Ridge physiographic province developed on thick, folded and thrust-faulted beds of sedimentary rock (Figs. ES.2 and ES.3). The interbedded clastic and carbonate sedimentary rocks are variably fractured and weathered, resulting in significant vertical and horizontal subsurface heterogeneity. The sequence of geologic formations underlying BCV from Pine Ridge southward to Bear Creek includes the Rome Formation of lower Cambrian age and formations of the Middle Cambrian Conasauga Group (Fig. ES.3). The EMDF footprint is underlain by the moderately to steeply dipping beds of the Maryville Formation on the northern end and by the Nolichucky Formation on the southern end of the site (Sect. 2.1.3).

The hydrogeologic system in BCV reflects the geologic complexity of the location and the abundant precipitation associated with a humid subtropical climate. The depth to the water table (unsaturated zone thickness) varies from greater than 30 ft below the crest of Pine Ridge and other upland areas to near zero in seasonal wetland belts along the margins of some Bear Creek tributaries. Shallow groundwater also occurs at springs in narrow headwater ravines of Pine Ridge and across broader seepage areas along tributary valleys. In most of the lower elevation areas, the water table is at depths of less than 20 ft below the surface. Groundwater flow in the saturated zone is strongly influenced by the orientation of bedding surfaces and the distribution of fracture systems in the rock units. Shallow groundwater within the saturated zone converges and discharges into stream channels along the tributary valley floors, supporting dry-weather base flow, primarily during the wetter portions of the year. Deeper groundwater that does not discharge to the tributaries moves southward from Pine Ridge toward Bear Creek along pathways that reflect the bedding geometry and fracture characteristics of the sedimentary strata. Additional detail on BCV hydrogeology is provided in Sect. 2.1.5.

Selection of the CBCV site for construction of EMDF is based on the objective of hydrologically isolating the waste from natural drainage systems. Natural topographic and hydrologic boundaries and the properties of geologic materials that influence groundwater flow and subsurface geochemistry are fundamentally important to the isolation of EMDF waste from potential receptors. Natural surface and subsurface boundaries limit the potential for short and long-term contaminant migration via surface water and groundwater pathways to the nearest populations in the city of Oak Ridge located north of the EMDF site.
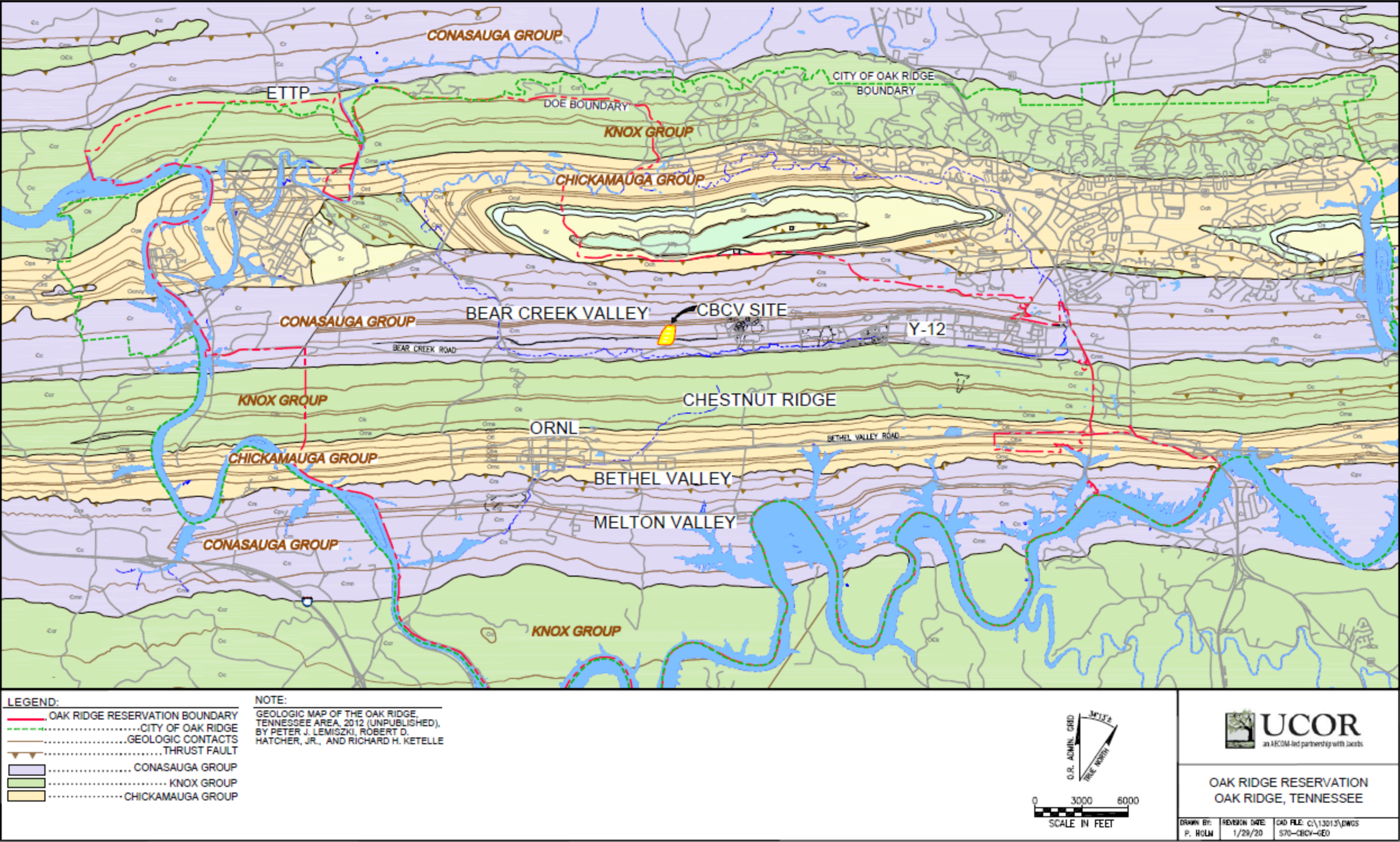
Fig. ES.2. Geologic map of the ORR

This page intentionally left blank.

NW

SE

ENVIRONMENTAL MANAGEMENT
DISPOSAL FACILITY (EMDF)

WHITEOAK MOUNTAIN FAULT

COPPER CREEK FAULT

EAST FORK RIDGE

PINE RIDGE

BEAR CREEK VALLEY

CHESTNUT RIDGE

BETHEL VALLEY

MDc   MDc
Or Os   Mfp
Sr   Och
Ocncy
Omc
Ord   Omc   OЄk
Orb

Єrs   Єrs   Єrs
Єra
Єcu   Єmn   Єcr   Oc   Ok

Olv
Oma Ofo
Obw Owi
Ofl Ork   Obe
Єpv
Єrs   Єrs
Omc

CROSS-SECTION
(No Vertical Exaggeration)

Єra/Єrs - Lower Cambrian Rome Formation; Apison Shale Member and Sandstone Member.
Єcu - Middle Cambrian Conasauga Shale Undivided (including the Nolichucky Shale).
Єmn - Upper Cambrian Maynardville Limestone.
Єcr - Upper Cambrian Copper Ridge Dolomite.

UCOR
an AECOM-led partnership with Jacobs

Source:

Lemiszki 2000. *Geologic Map of the Bethel Valley Quadrangle, Tennessee*, Geologic Quadrangle Map 130-NE, Lemiszki, P.J., Tennessee Division of Geology, Nashville.

CENTRAL BEAR CREEK VALLEY
OAK RIDGE, TENNESSEE

DRAWN BY:	REV. NO./DATE:	CAD FILE: C:\13013\DWGS
P. HOLM	0— 9/26/19	T04—CBCV—GEO—XSEC

Fig. ES.3. Northwest-southeast geologic cross-section across the ORR

Under a long-term performance scenario, contaminant retardation in the vadose zone beneath EMDF and within the saturated matrix of the fractured rock at the CBCV site serve disposal system safety functions by delaying and attenuating impacts of radionuclide release at potential groundwater and surface water exposure points.

EMDF Design Features and Safety Functions

In accordance with CERCLA, the EMDF preliminary design will satisfy ARARs for hazardous and toxic waste disposal units (Sect. 1.5.5). The engineered disposal unit consists of a multilayer liner, leachate collection and treatment systems, lined embankments for lateral containment and stability, and a multilayer final cover (cap) to completely encapsulate the waste in the post-closure period. A CBCV site map showing key EMDF disposal system features and safety functions is provided as Fig. ES.4. A typical EMDF cross-section, based on the preliminary design (UCOR 2020b), is shown on Fig. ES.5 and a schematic profile of EMDF disposal system components and associated safety functions is shown on Fig. ES.6.

The engineered barriers of the cover and liner systems are designed to impede the percolation of water into the waste and to retard the (post-closure) release of radionuclides through the bottom liner and into the surrounding environmental media. Perimeter berms and the cover system also serve to deter biointrusion and/or IHI that could lead to direct exposure to the waste. Engineered surface and subsurface drainage systems outside of the liner footprint serve to maintain groundwater drainage and to limit increases in water table elevation below the liner in the event of cover and/or liner system failure. The facility is designed to maintain vertical separation of the waste from groundwater in the saturated zone beneath the disposal facility and includes a 10-ft-thick layer of geologic buffer material between the waste and the water table (Fig. ES.6). Detailed descriptions of the EMDF design features and safety functions are provided in Sects. 1.3, 2.2, and Appendix C. The natural characteristics of the EMDF site, as well as the fact that DOE is required to maintain control of the site as long as there is a potential risk from the waste, also represent important safety functions that are factored into site selection.

The EMDF will begin accepting waste after the first phase of construction is completed, projected for the late-2020s. The current scope of ORR cleanup work is projected to be completed in the 2050s timeframe; therefore, the approximate duration of EMDF operations is 25 years. EMDF operations will include waste receipt and placement, water management, and environmental monitoring of facility performance. EMDF waste certification practices are expected to be carried over from current EMWMF WAC attainment and tracking systems (DOE 2001a). EMDF waste receipt operations will include unloading and placing waste into the landfill and spreading and compacting bulk waste using heavy equipment while placing fill materials, as required, to fill voids. As portions of the landfill are filled to design capacity, an interim cover will be put in place to limit infiltration and leachate generation from that portion of the disposal facility. The EMDF interim cover design is assumed to be similar to that implemented for the EMWMF, which consists of a geotextile separator layer and an approximately 1-ft-thick contouring soil layer on top of the waste, overlain by a temporary flexible geomembrane to minimize infiltration into the waste zone.

EMDF closure activities will involve construction of the final cover system and removal of any unneeded infrastructure. Post-closure activities will involve cap maintenance, continued leachate collection and management, and site environmental monitoring. Final closure plans will be detailed in approved documents required under DOE orders and manuals and by the FFA. Post-closure performance monitoring will include CERCLA 5-year reviews of remedial effectiveness.
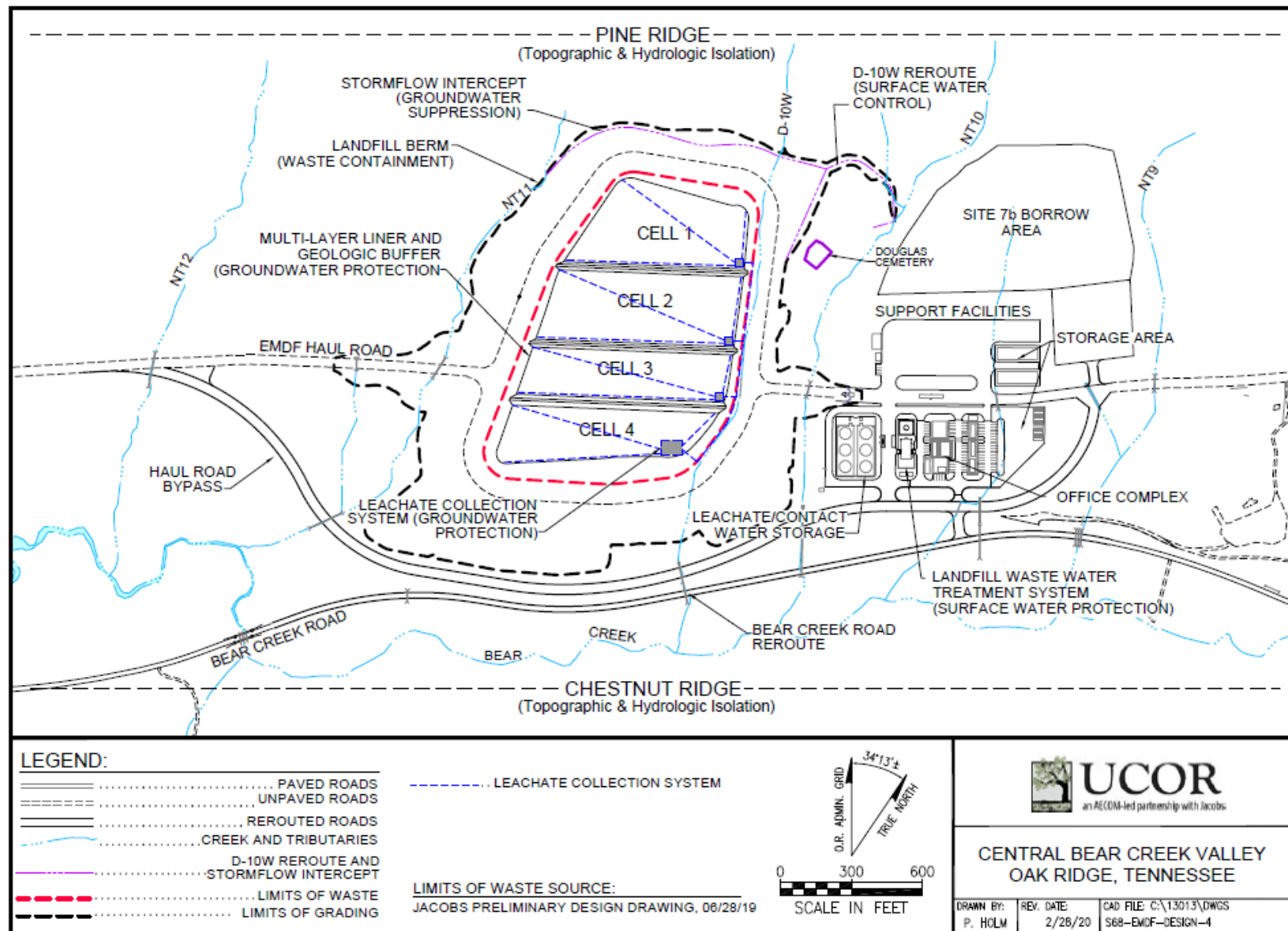
Fig. ES.4. EMDF site and design features and safety functions

Typical Width, 1,000 ft

Final Cover System

Perimeter Berms

Liner System

Existing Grade

Typical Waste
Height 75 ft

NT-11

NT-10

Waste

Geologic Buffer

Predicted Future Groundwater

NOT TO SCALE

UCOR
an AECOM-led partnership with Jacobs

CENTRAL BEAR CREEK VALLEY
OAK RIDGE, TENNESSEE

| DRAWN BY: | REV. DATE: | CAD FILE: C:\13013\DWGS |
| P. HOLM | 2/24/20 | T26-CBCV-COVER-SECT |
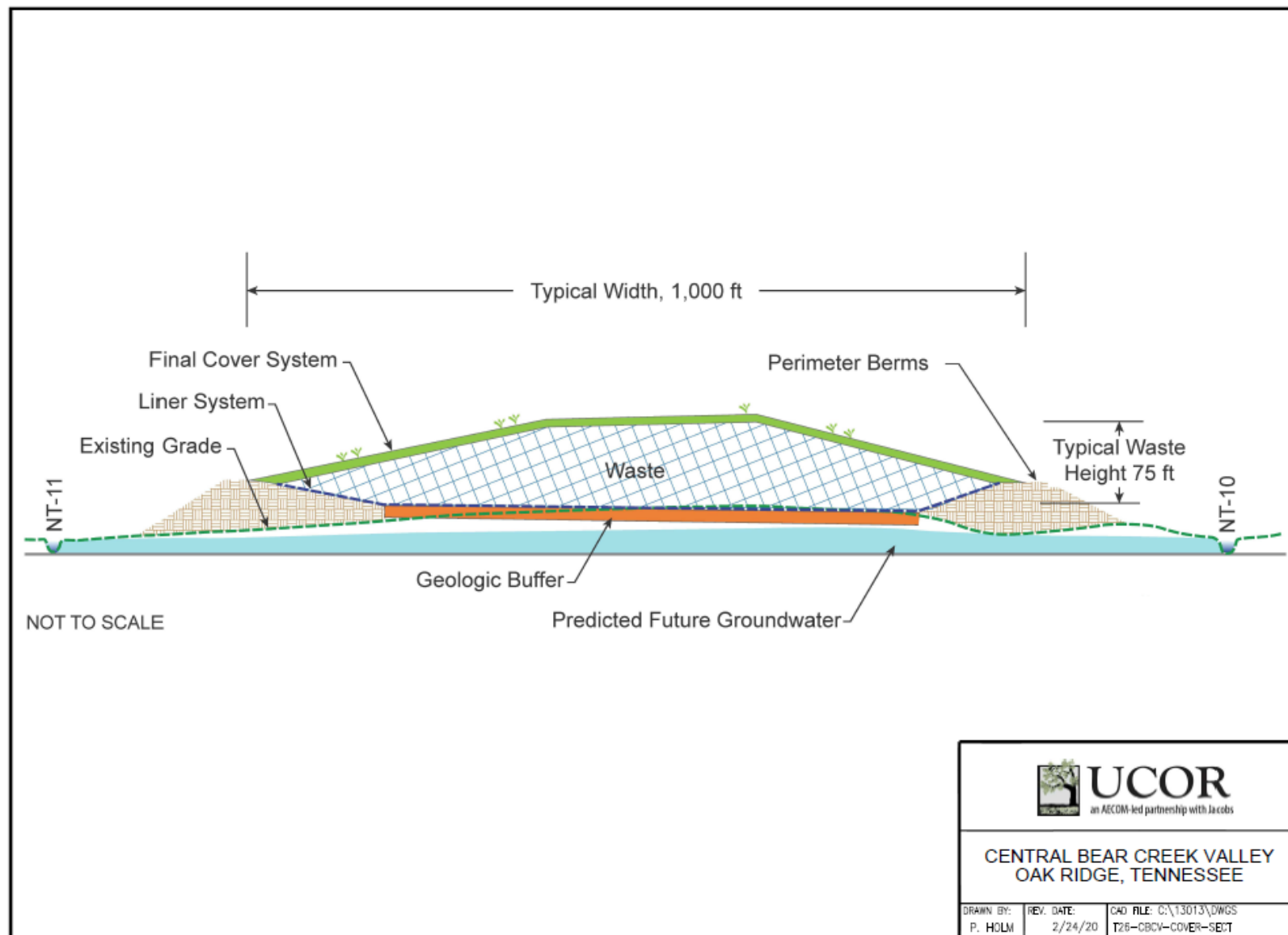
Fig. ES.5. Typical cross-section of EMDF

EMDF Disposal System Components

Safety Functions

Surface Processes: *Precipitation ↓ , Runoff & Erosion→, Infiltration↓, Evapotranspiration↑*

Cover System (surface, biointrusion & drainage layers, synthetic membrane, clay infiltration barrier)	- **Prevent or reduce infiltration into waste zone** - **Deter Inadvertent Human Intrusion and large animal intrusion** - **Prevent radionuclide release to EMDF surface**	
Waste Zone (volume, material characteristics, activity levels) *Radionuclide Release*	- **Waste treatment and packaging reduces mobility of radionuclides in waste** - **Waste placement practices and void filling limit waste subsidence and potential post-closure cover system degradation**	
Liner System (leachate collection and leak detection systems, clay liner)	- **Intercept leachate for treatment** - **Limit contaminant release & extend time for decay of short-lived radionuclides**	
Geologic Buffer Zone (low permeability, unsaturated material)	- **Retard contaminant transport & extend travel time for decay of short-lived radionuclides**	
Native vadose materials (saprolite and fractured bedrock)	- **Retard contaminant transport & extend travel time for decay of short-lived radionuclides**	
Shallow Aquifer (saturated saprolite and fractured sedimentary rock)	- **Retard contaminant transport & extend travel time for decay of short-lived radionuclides** - **Limit contaminant transfer to deep aquifer**	
Deep Aquifer (saturated, fractured sedimentary rock)	-**Retard contaminant transport, isolate radionuclides from the shallow subsurface and allow time for decay**	

Left side labels: Vadose Zone / Saturated Zone; Engineered Barrier Systems / Natural Barriers

Fig. ES.6. EMDF disposal system schematic profile and safety functions

Waste Stream Characteristics and Estimated Radionuclide Inventory

LLW disposed at EMDF will originate primarily from facility deactivation and decommissioning (D&D) or environmental remediation projects at Y-12 and ORNL. The waste will include facility demolition debris (including structural steel and concrete), contaminated equipment and soil, and other soil-like wastes. EMDF will accept both containerized LLW and bulk (uncontainerized) waste for disposal. Waste quantities are based on the estimates provided in the OREM Waste Generation Forecast. Waste stream characteristics are estimated from a variety of information sources and are described in more detail in Sect. 2.3 and Appendix B. More detailed characterization of waste streams for disposal at EMDF will be the responsibility of the waste generator(s) once EMDF is operational.

Wastes derived from CERCLA cleanup at Y-12 and ORNL will contain a wide range of radionuclides. The primary radioactive contaminants in Y-12 waste streams are uranium isotopes, whereas ORNL waste streams will contain a greater variety of radionuclides, including relatively large quantities of some fission products (e.g., Cs-137 and Sr-90), lower quantities of other fission products (e.g., Tc-99 and I-129), and trace quantities of transuranic radionuclides (e.g., plutonium and americium). This difference is important for estimation of the EMDF radionuclide inventory because Y-12 waste accounts for approximately 70 percent of the forecast waste volume and ORNL waste accounts for the remaining 30 percent. Due to these differences in waste volume and radiological characteristics, Y-12 waste accounts for the majority of uranium activity in the estimated EMDF inventory, whereas ORNL waste accounts for the majority of the total radionuclide inventory.

The method for estimating radionuclide profiles for specific EMDF LLW streams is to apply the available data to capture the differences between ORNL and Y-12 wastes and between remedial action wastes (primarily soils) and facility D&D wastes (primarily debris). Average, decay-corrected radionuclide activity concentrations for each waste stream are estimated from a combination of data sources, including EMWMF waste characterization data for previously generated and disposed (historical) Y-12 and ORNL waste lots, data from detailed facility and environmental characterization studies, and data from the OREM SORTIE 2.0 facility inventory database, which includes radionuclide activity quantities derived from various types of facility safety analyses and other data sources.

Uncertainty in the EMDF estimated inventory includes uncertainty in the underlying characterization data, as well as uncertainty associated with the assumption that the radionuclides and activity concentrations in the selected data source are representative of all future EMDF waste. In general the approach to managing the uncertainty in the estimated EMDF radionuclide inventory is to bias the inventory estimates toward higher values. For example, the use of the SORTIE data should lead to overestimation of average waste activity concentrations because the facility inventories developed for safety analysis tend to be bounding (maximum likely) estimates.

For each EMDF waste stream identified, the estimated average radionuclide activity concentrations are applied to the projected total waste quantity (mass) to derive the total estimated inventory at EMDF closure. For use in model calculations, the estimated EMDF average as-generated waste activity concentrations are adjusted (Sect. 3.2.2.5) to account for the addition of clean fill during disposal operations (to fill voids and increase stability). In addition, operational period losses of highly mobile radionuclides (H-3, C-14, Tc-99, and I-129) are estimated and used to adjust (decrease) the assumed post-closure inventory for those nuclides. The assumptions and modeling applied to estimate these operational losses and reductions in mobility resulting from treatment of collected leachate are described in Sect. 3.2.2.5.

Radionuclide Screening

There are 70 radionuclides included in the screening-level inventory (Sect. 2.3.2 and Appendix B). For the EMDF PA, a two-step approach was used for screening out radionuclides that do not contribute significantly to the total dose. The first step involved screening based on radionuclide half-life. Any parent isotope in the EMDF inventory with a half-life of less than 5 years was screened out from further analysis because during the first 100 years of post-closure institutional control, the engineered barrier systems (cover and liner, including the leachate collection system) will prevent cover infiltration and leachate release. During this 100-year time period, over 20 half-lives will have elapsed, resulting in decay of short-lived radionuclides to very low concentrations.

Additional justification for using the 5-year half-life as a cutoff is related to the anticipated travel time from the waste to the underlying groundwater. Vadose zone Subsurface Transport Over Multiple Phases (STOMP) model simulations (Appendix E) indicate that for a highly mobile radionuclide such as C-14, the average travel time from waste to the water table is greater than 200 years (approximately 40 or more half-lives for the short-lived radionuclides screened in the first step). Screening of inventory based on half-life was not performed for any isotopes that are also progeny of other parent isotopes included in the inventory. In summary, for Phase 1 screening, a total of 61 radionuclides passed and a total of nine radionuclides were screened from further consideration. Seven radionuclides were screened out based on their half-life, and two radionuclides were screened out for other reasons.

The second screening step involved implementation of a computer model (RESidual RADioactivity [RESRAD]-OFFSITE, refer to Sect. 3.3.4 and Appendix G) used to screen individual radionuclides based on a peak dose criterion of 0.4 mrem/year, which is 10 percent of the 4 mrem/year national primary drinking water standard for beta-gamma emitters (40 *Code of Federal Regulations 141*). The 0.4 mrem/year screening criterion is applied to all radionuclides, including alpha emitters, for the all-pathways dose analysis (refer to Sect. 2.3.2). The screening model implemented for the EMDF site assumes exposure via groundwater ingestion only and incorporates pessimistically biased assumptions regarding inventory levels (screening level estimates), disposal conditions (no engineered barriers to limit water infiltration), and mobility of radionuclides (distribution coefficients decreased by a factor of 10 or 100 from base-case values [see Sect. 3.2.2.6; and Appendix G, Sects. G.4.3.6 and G.4.4.1]). Out of the 70 radionuclides in the waste inventory, a total of 42 were retained for analysis (Table ES.2). For analysis of IHI, only radionuclides with half-lives less than 5 years were screened from consideration.

Based on the EMDF estimated inventory, anticipated operational conditions, and design features of the EMDF cover system, post-closure release of radionuclides in the vapor-phase is expected to be negligible. The estimated inventory of potentially volatile radionuclides is limited to H-3, C-14, Kr-85, and I-129. Small quantities of Cl-36 could be present in future EMDF LLW, associated with irradiated graphite or metals from ORNL research reactor facilities; however, Cl-36 has not been a radionuclide of concern for LLW disposed at the EMWMF, and identification of Cl-36 in environmental samples from the ORR is extremely rare. Additional discussion of the limited potential for radionuclide release through the EMDF final cover, including results of a quantitative screening model, is provided in Sect. 3.2.2.2.

Table ES.2. Screening source concentrations and radionuclide screening results

Radionuclide	Half-life (years)	Screening source concentration (pCi/g)	Phase 1: Half-life > 5 years?	Phase 2: Peak Groundwater Dose > 0.4 mrem/year for 10,000-year simulation?	Retain for dose analysis?
Ac-227	2.18E+01	4.89E+04	Yes	Yes	Yes
Am-241	4.32E+02	2.30E+03	Yes	Yes	Yes
Am-243	7.38E+03	2.29E+01	Yes	Yes	Yes
Ba-133	1.07E+01	2.71E+01	Yes	No	Intruder
Be-10	1.50E+06	7.16E+05	Yes	Yes	Yes
C-14	5.73E+03	6.27E+05	Yes	Yes	Yes
Ca-41	1.00E+05	4.11E+06	Yes	Yes	Yes
Cd-113m	1.36E+01	1.11E+05	Yes	No	No[a]
Cf-249	3.51E+02	3.92E-04	Yes	No	Intruder
Cf-250	1.31E+01	1.70E-02	Yes	No	Intruder
Cf-251	8.98E+02	7.36E-05	Yes	No	Intruder
Cf-252	2.60E+00	1.25E+03	No	NS[b]	No
Cl-36[e]	3.01E+05	1.00E+00	Yes	Yes	No[a]
Cm-243	2.85E+01	4.37E+01	Yes	Yes	Yes
Cm-244	1.81E+01	5.26E+05	Yes	Yes	Yes
Cm-245	8.50E+03	9.80E+01	Yes	Yes	Yes
Cm-246	4.73E+03	1.97E+00	Yes	Yes	Yes
Cm-247	1.56E+07	2.35E+01	Yes	Yes	Yes
Cm-248	3.39E+05	2.29E+01	Yes	Yes	Yes
Co-60	5.27E+00	1.93E+06	Yes	No	Intruder
Cs-134	2.10E+00	1.39E+05	No	NS[b]	No
Cs-135	2.30E+06	2.46E+06	Yes	Yes	No[a]
Cs-137	3.00E+01	3.82E+08	Yes	No	Intruder
Eu-152	1.33E+01	5.84E+05	Yes	No	Intruder
Eu-154	8.80E+00	7.85E+05	Yes	No	Intruder
Eu-155	4.80E+00	9.98E+05	No	NS[b]	No
Fe-55	2.70E+00	4.71E+07	No	NS[b]	No
H-3	1.24E+01	4.84E+06	Yes	Yes	Yes
I-129	1.57E+07	4.86E+05	Yes	Yes	Yes
K-40	1.28E+09	5.65E+01	Yes	Yes	Yes
Kr-85	1.10E+01	1.16E+08	Yes	NS[c]	No
Mo-93	3.50E+03	4.99E+03	Yes	Yes	Yes
Mo-100	8.50E+18	2.55E-03	Yes	NS[c]	No
Na-22	2.60E+00	5.96E-01	No	NS[b]	No
Nb-93m	1.36E+01	3.00E+03	Yes	No	Yes[d]
Nb-94	2.03E+04	1.90E+05	Yes	Yes	Yes
Ni-59	7.50E+04	1.55E+06	Yes	Yes	Yes
Ni-63	9.60E+01	1.03E+07	Yes	No	Intruder
Np-237	2.14E+06	5.63E+01	Yes	Yes	Yes

Table ES.2. Screening source concentrations and radionuclide screening results (cont.)

Radionuclide	Half-Life (years)	Screening source concentration (pCi/g)	Phase 1: Half-life > 5 years?	Phase 2: Peak Groundwater Dose > 0.4 mrem/year for 10,000-year simulation?	Retain for Dose Analysis?
Pa-231	3.28E+04	3.17E+00	Yes	Yes	Yes
Pb-210	2.23E+01	4.48E+02	Yes	No	Yes[d]
Pd-107	6.50E+06	3.34E+06	Yes	Yes	No[a]
Pm-146	5.50E+00	1.24E-01	Yes	No	Intruder
Pm-147	2.60E+00	2.67E+06	No	NS[b]	No
Pu-238	8.77E+01	7.15E+03	Yes	Yes	Yes
Pu-239	2.41E+04	1.85E+05	Yes	Yes	Yes
Pu-240	6.54E+03	8.44E+03	Yes	Yes	Yes
Pu-241	1.44E+01	2.83E+05	Yes	Yes	Yes
Pu-242	3.76E+05	4.98E+01	Yes	Yes	Yes
Pu-244	8.26E+07	1.11E+01	Yes	Yes	Yes
Ra-226	1.60E+03	1.35E+01	Yes	Yes	Yes
Ra-228	5.75E+00	3.46E+00	Yes	No	Yes[d]
Re-187	4.12E+10	1.94E-03	Yes	No	Intruder
Sb-125	2.80E+00	1.37E+06	No	NS[b]	No
Se-79	6.50E+04	2.47E+06	Yes	Yes	No[a]
Sm-151	9.00E+01	5.75E+06	Yes	No	No[a]
Sn-121m	5.50E+01	6.41E+01	Yes	No	No[a]
Sn-126	1.00E+05	1.89E+06	Yes	Yes	No[a]
Sr-90	2.91E+01	3.93E+08	Yes	Yes	Yes
Tc-99	2.13E+05	1.35E+06	Yes	Yes	Yes
Th-228	1.90E+00	1.14E+05	No	No	Yes[d]
Th-229	7.34E+03	3.48E+03	Yes	No	Yes[d]
Th-230	7.70E+04	1.48E+02	Yes	Yes	Yes
Th-232	1.41E+10	2.67E+06	Yes	Yes	Yes
U-232	7.20E+01	8.43E+05	Yes	Yes	Yes
U-233	1.59E+05	5.49E+05	Yes	Yes	Yes
U-234	2.45E+05	1.67E+03	Yes	Yes	Yes
U-235	7.04E+08	2.57E+03	Yes	Yes	Yes
U-236	2.34E+07	4.87E+02	Yes	Yes	Yes
U-238	4.47E+09	2.07E+09	Yes	Yes	Yes
Zr-93	1.53E+06	5.56E+05	Yes	Yes	No[a]

[a]Radionuclide not simulated because insufficient inventory data were available
[b]Radionuclide not simulated due to screening in Phase 1
[c]Radionuclide not simulated due to other reasons
[d]Isotope has half-life less than 5 years or screening dose less than 0.4 mrem/year, but was retained for further analysis because it is progeny of another isotope in the inventory. Intruder identifies isotopes simulated for IHI models, but not retained for further analysis.
[e]Cl-36 is not included in the inventory but was simulated in the screening model provide information for future waste management decisions.

IHI = inadvertent human intrusion
NS = not simulated

KEY ASSUMPTIONS

Key technical assumptions for the EMDF performance analyses are listed below. Proposed activities, new regulatory requirements, or other new information that could challenge key assumptions for the EMDF performance analysis will be evaluated in accordance with the EMDF change control process to assess the potential for such changes to require a Special Analysis or revisions to the PA.

Key parameter assumptions for EMDF compliance include:

1) Iodine-129 partition coefficient (K_d) values for the engineered barriers and geologic materials below the EMDF liner are greater than 1 cm^3/g.

2) IF the I-129 K_d value is less than 1.5 cm^3/g, THEN the values for the input parameters that determine cover infiltration, vadose zone thickness, and saturated zone flux (Darcy velocity) satisfy one or more of the following conditions:

   a) Average annual cover infiltration is less than or equal to 0.88 in./year.

   b) The average thickness of the unsaturated zone below the waste is greater than or equal to 31 ft.

   c) The Darcy velocity characterizing long-term average conditions within the saturated zone along the flow path from the waste to the well is greater than or equal to 4.75 ft/year.

3) The estimated post-closure EMDF average I-129 activity concentration is less than 0.41 pCi/g.

Uncertainty in these three key model input parameter assumptions will be addressed with laboratory measurements of iodine K_d for CBCV site materials and by future refinements in the estimated I-129 inventory.

Conceptual models of the evolution of engineered barrier performance and radionuclide release are important for understanding the implications of selecting one conceptualization versus another, and for integrating model codes that apply different conceptual models or levels of detail. Key assumptions related to conceptual models adopted for the PA analysis include:

1) **Failure of engineered barriers.** Post-closure degradation of the EMDF cover and liner systems occurs gradually and results in increasing cover infiltration and leachate release.

2) **Cover system performance.** The EMDF final cover will prevent significant release of radionuclides to the cover surface. Infiltration barriers in the cover fail completely within 1000 years and cover infiltration increases gradually to a maximum average annual long-term value of 0.88 in./year at 1000 years post-closure.

3) **Liner system performance.** The liner system will release leachate at a rate sufficient to prevent waste saturation and overtopping of the liner (bathtub conditions).

4) **Radionuclide release.** EMDF waste is conceptualized as homogeneous, soil-like material in which the estimated radionuclide inventory is uniformly distributed. Radionuclide release from the waste is modeled as equilibrium desorption from a soil-like material.

5) **Uniform release to groundwater.** Radionuclide release from the waste and liner system to the vadose and saturated zones is spatially uniform. Non-uniform release does not result in earlier or larger peak concentrations at the POA locations.

Model sensitivity and uncertainty analyses in the PA (Sect. 5) are completed to assess and manage uncertainty in key parameter and conceptual model assumptions. Several important pessimistic assumptions regarding the exposure scenario, radionuclide inventories, long-term cover performance, and waste

characteristics are incorporated in the PA to account for uncertainty in future human behavior, waste volumes, and waste management practices (e.g., waste treatment and containerization). These pessimistic assumptions bias the analysis toward larger estimated all-pathways dose (refer to Sect. 1.7.3).

CONCEPTUAL MODELS, MODEL CODES, AND QUALITY ASSURANCE

The EMDF site characteristics and facility features described in the preceding paragraphs are incorporated into the conceptual models and performance analyses of the PA. It is assumed in the PA modeling that the effectiveness of engineered barriers decreases over time, leading to the release of radionuclides through the liner system. A detailed description of the natural processes that degrade design features and limit safety functions over time and a generalized conceptual model of EMDF performance evolution is provided in Sect. 3.2.1 and Appendix C.

Conceptualization of the EMDF disposal system for performance analysis and modeling is organized around four related components as shown in Table ES.3.

Table ES.3. EMDF disposal system components, conceptual model elements, and model codes

Disposal system component	Conceptual model elements	Model codes
Water Balance and Performance of Engineered Barriers (Sect. 3.2.1)	- Facility water balance - Performance of engineered systems - Degradation of synthetic and earthen barriers - Assumed evolution of EMDF cover infiltration and leachate release	HELP RESRAD-OFFSITE
Radionuclide Release and Vadose Zone Transport (Sect. 3.2.2)	- EMDF radionuclide inventory - Disposal practices and waste forms - Facility design geometry - EMDF cover performance evolution - Vapor phase release and radon flux - Aqueous phase release from waste - Transport through waste and liner system, including chemical retardation - Vadose zone transport below liner	STOMP RESRAD-OFFSITE
Saturated Zone Flow and Radionuclide Transport (Sect. 3.2.3)	- Vadose zone flux to saturated zone - CBCV site geology and topography - CBCV site geology and topography - CBCV hydrogeology - CBCV surface water features - CBCV saturated zone flow and transport, including chemical retardation	MODFLOW MT3D RESRAD-OFFSITE
Exposure Pathways and Scenarios (Sect. 3.2.4) (analysis of the inadvertent human intrusion scenario is presented in Sect. 6)	- Resident farmer exposure scenario - Groundwater POA (well location) - Surface water POA - Exposure pathways, abiotic and biotic - Dose analysis	RESRAD-OFFSITE

CBCV = Central Bear Creek Valley   POA = point of assessment
EMDF = Environmental Management Disposal Facility   RESRAD = RESidual RADioactivity
HELP = Hydrologic Evaluation of Landfill Performance   STOMP = Subsurface Transport Over Multiple Phases

Conceptual models of post-closure and long-term performance of engineered barriers are incorporated in the assumed evolution of the EMDF water balance as controlled by the safety functions of engineered cover and liner system features. These conceptual models include pessimistic biases intended to lead to increased infiltration versus what is expected as a means to address uncertainty in cover performance and are described in Sect. 3.2.1 and in the cover system analysis presented in Appendix C.

The base case EMDF performance scenario assumes full design performance (zero infiltration through the cover and into the waste) for a period of 200 years post-closure. A period of increasing cover infiltration and leachate release due to degradation of engineered barriers is assumed to occur between 200 and 1000 years post-closure, followed by a long-term performance period of indefinite duration. A generalized conceptual model of changes in cover infiltration and leachate release assumed to result from natural processes and events that can impact cover and liner performance over time is presented in Sect. 3.2.1. The purpose of the model is to integrate and generalize the impact of multiple events and processes on safety functions and EMDF performance over time, incorporating uncertainty in timing and degree of degradation and the occurrence of severe events. Implementation of this general model of increasing cover infiltration over time for each of the PA models is described in Sect. 3.3. Uncertainty in the timing and degree of performance degradation (relative to the base case performance evolution scenario) is addressed in the probabilistic RESRAD-OFFSITE analysis presented in Sect. 5.4.

Conceptual models of post-closure radionuclide release from the EMDF disposal system include analysis and screening of radionuclide release through the cover to the atmosphere or biosphere, diffusive transport and release of radon through the cover (refer to Appendix H), and radionuclide release and transport in the aqueous phase (Sect. 3.2.2). Conceptual models for aqueous release incorporate the assumed changes in cover infiltration over time (Sect. 3.2.1) and include waste zone radionuclide release and unsaturated vertical flow and radionuclide transport through the waste, liner system, and underlying vadose zone. These conceptual models are based on the estimated EMDF radionuclide inventory (Appendix B), assumed waste disposal practices and waste forms (Sect. 3.2.2.5), sorptive properties of EMDF materials (Sect. 3.2.2.6), the vertical sequence of vadose zone materials (Sect. 3.2.2.4), and the analysis of cover performance presented in Sect. 3.2.1 and Appendix C.

Conceptual models of saturated zone flow and radionuclide transport are based on the hydrogeologic conceptual model for BCV (Sect. 2.1.5.1), including the lithology and stratigraphy of the EMDF site, major topographic and structural controls on groundwater movement, surface water features, and chemical retardation properties of the saprolite and bedrock. Conceptualization of the saturated zone for purposes of EMDF performance analysis is described in Sect. 3.2.3.

Conceptual models of post-closure public exposure to radionuclides include the general resident farmer scenario considered for the analysis, as well as detailed assumptions for abiotic (e.g., water ingestion, inhalation) and biotic (e.g., ingestion of contaminated fish and produce) exposure pathways. The exposure pathways assumed for the all-pathways dose analysis are shown on Fig. ES.7. The exposure scenario and pathway assumptions which form the basis for the dose analysis are described in Sect. 3.2.4.
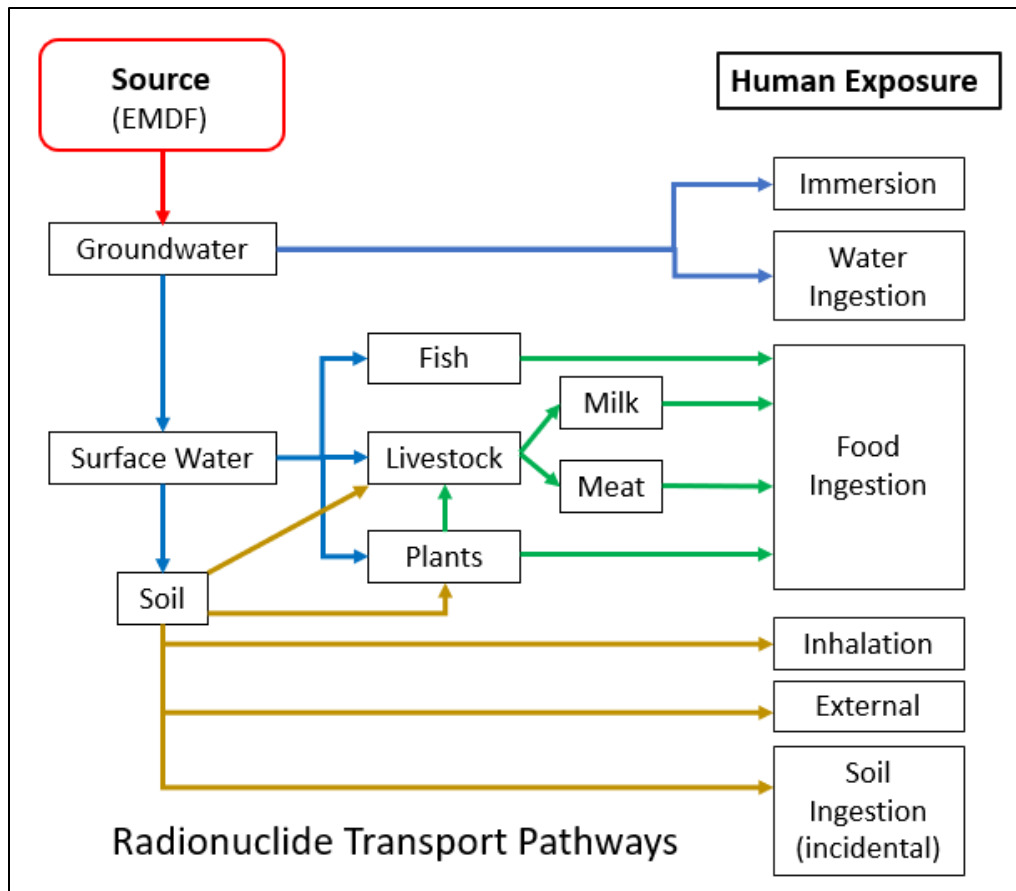
Fig. ES.7. Flow chart of environmental transport and exposure pathways for the all-pathways analysis

PA Model Implementation and Integration

Implementation of EMDF system conceptual models with computer modeling codes is structured around the four conceptual components (Table ES.3 and Fig. ES.8) and includes detailed process model codes for the components that encompass engineered facility performance and abiotic transport elements. Also included is a total system model code that encompasses all four conceptual components, including the exposure scenario and biotic pathways for radionuclide transfer. The PA model codes include: the Hydrologic Evaluation of Landfill Performance model for simulating the EMDF water balance; the STOMP model for simulating radionuclide release and vadose zone transport; MODFLOW, MODPATH, and MT3D model codes for saturated zone groundwater flow and radionuclide transport simulation; and RESRAD-OFFSITE for holistic simulation of radionuclide release and transport, as well as exposure scenarios and dose analysis. Table ES.4 identifies the PA appendices that fully describe the implementation of each of the models.

The more detailed process models (STOMP, MT3D) were used for modeling the complexities of primarily abiotic environmental transport pathways to predict concentrations of key radionuclides at the POA, while the total system model (RESRAD-OFFSITE) uses simplified representations of transport pathways along with biotic transformations and scenario-specific exposure factors to identify which radionuclides are likely key dose contributors and to quantify total dose for comparison to performance objectives.

RESRAD-OFFSITE

HELP

STOMP

Bear Creek Surface Water

Farm

Well

Cap

Waste

Liner

Dike   Buffer   Dike

Saprolite

Water Table

Bedrock

MODFLOW, MODPATH & MT3D

MODEL Domains:

HELP: Water Balance and Performance of Engineered Barriers (Section 3.2.1)

STOMP: Radionuclide Release and Vadose Zone Transport (Section 3.2.2)

MODFLOW, MODPATH, MT3D: Saturated Zone Flow and Radionuclide Transport (Section 3.2.3)

RESRAD-OFFSITE: Total system model, including radionuclide release, vadose zone radionuclide transport, saturated zone flow and transport, exposure pathways, and dose analysis. (Section 3.2.4)

UCOR
an AECOM-led partnership with Jacobs

CENTRAL BEAR CREEK VALLEY
OAK RIDGE, TENNESSEE

DRAWN BY:	REV. DATE:	CAD FILE: C:\13013\DWGS
P. HOLM	4/9/20	T26-CBCV-RESRAD

Fig. ES.8. Schematic illustration of EMDF disposal system conceptual models and modeling tools used for implementation

Implementation of the more detailed component-level EDMF PA models and the total system model proceeded concurrently, with iterative development and refinement of model assumptions, cover performance and source release approaches, and parameter value selections for each of the model tools. Some model outputs serve as inputs for other modeling tools. The primary model output-to-input linkages and the key comparisons of model outputs (presented in Sect. 3.3.5) are shown on Fig. ES.9 and Table ES.4. Inputs common to all model codes include radionuclide inventories, EMDF design specifications, and CBCV site characteristics. Selection, implementation, and integration of these model codes for EMDF performance analysis is explained in Sect. 3.3.
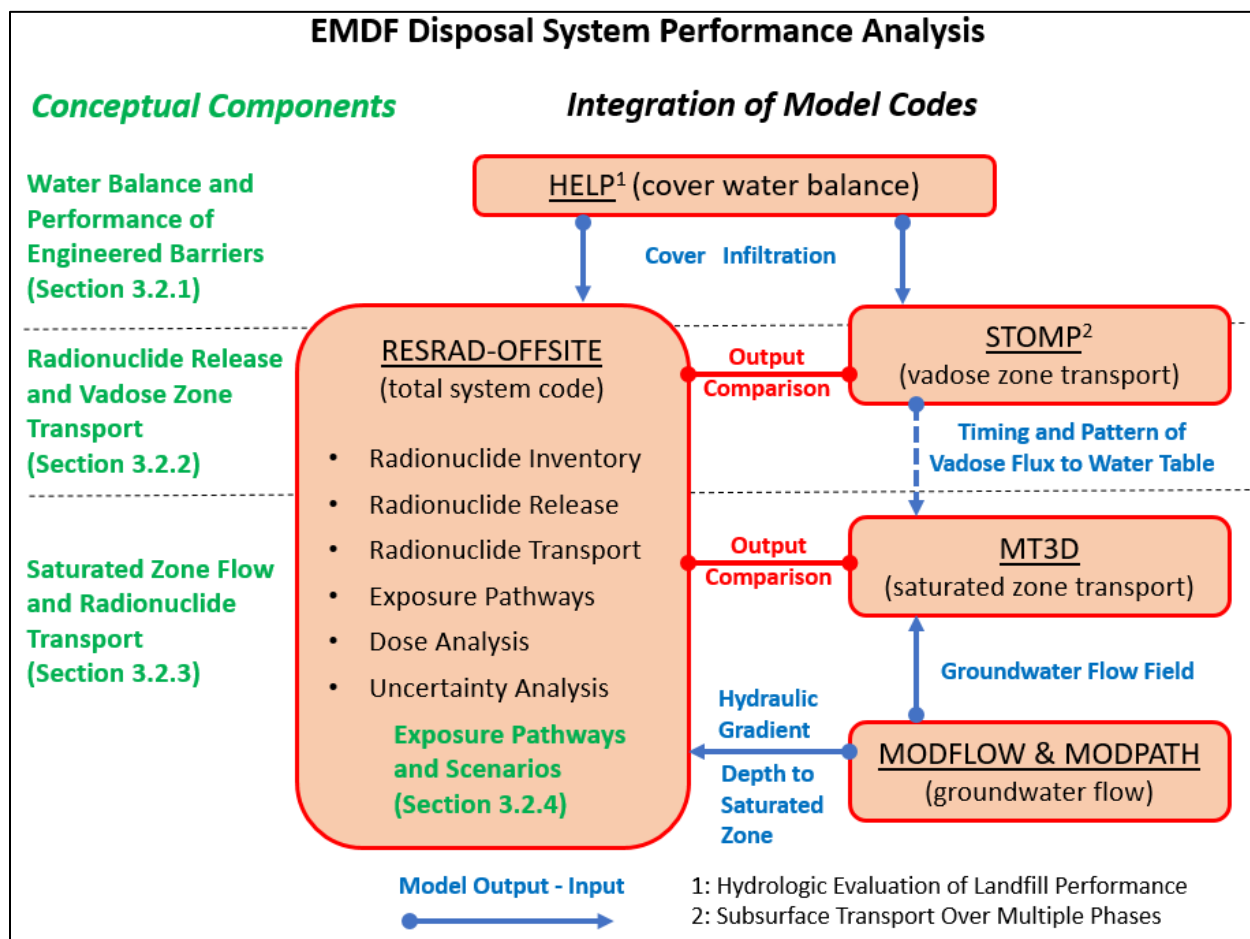
Fig. ES.9. EMDF disposal system conceptual components and integration of model codes for performance analysis

Table ES.4. EMDF PA model input parameters and linkages among models

Model and purpose	Primary model inputs	Primary model output (used as input to or compared with other PA models)
HELP Water balance and engineered barrier performance (Appendix C)	• Local climate data • EMDF preliminary design (geometry and material specifications)	• Cover infiltration rates
MODFLOW Saturated zone flow (Appendix D)	• EMDF preliminary design • Bear Creek Valley topography, geology, and surface water features • Conasauga group hydraulic conductivities • EMDF cover infiltration • Estimated natural recharge rates	• Flow directions • Hydraulic gradients • 3-D groundwater flow field • Depth to groundwater
STOMP Unsaturated flow and transport (Appendix E)	• EMDF radionuclide inventory • EMDF preliminary design • Estimated natural recharge rates • EMDF cover infiltration • Conasauga group hydraulic conductivities and porosity • Solid-aqueous partition coefficients	• Radionuclide release • Vadose zone flux • Water table flux • Water table time of arrival (vadose delay times)
MT3D Saturated zone transport model (Appendix F)	• EMDF radionuclide inventory • EMDF preliminary design • EMDF cover infiltration • Effective porosities • 3-D groundwater flow field • Solid-aqueous partition coefficients • Radionuclide flux from vadose zone	• Plume location, evolution and maximum extent • Peak groundwater concentration and time of peak at well • Contaminant discharge to Bear Creek surface waters
RESRAD-OFFSITE Radionuclide release and transport; exposure and dose analysis (Appendix G)	• EMDF radionuclide inventory • EMDF preliminary design (material specifications) • EMDF cover infiltration • Hydraulic gradients • Effective porosities • Solid-aqueous partition coefficients • Biotic transfer factors • Dose conversion factors • Exposure scenario and exposure factors (ingestions rates, etc.)	Outputs for evaluating compliance with performance objectives: • Peak total dose during compliance period • Dose contributions by exposure pathway • Key radionuclide contributions to total dose • Well water and surface water concentrations

D = dimensional
EMDF = Environmental Management Disposal Facility
HELP = Hydrologic Evaluation of Landfill Performance

PA = Performance Assessment
RESRAD = RESidual RADioactivity
STOMP = Subsurface Transport Over Multiple Phases

Quality Assurance

The *Quality Assurance Report for Modeling of the Bear Creek Valley Low-level Radioactive Waste Disposal Facilities, Oak Ridge, Tennessee* (QA Report) (UCOR 2020b) was prepared to document the QA activities for this Revision 2 PA and the companion Revision 2 CA (UCOR 2020a).

The salient components of the QA program that were implemented during the preparation of this PA include the following:

- Software QA procedures for code verification and documentation for each model code per *Software Quality Assurance Program* (PPD-IT-6007).

- Formal independent checking and review of calculation and data packages that document input parameter values and other model assumptions, model implementation, model output data, and post-processing activities for each PA model.

- Documentation of PA model development, implementation, sensitivity-uncertainty analyses, and PA model integration contained in the EMDF PA report and report appendices.

- Configuration management for PA documents and calculation packages per UCOR procedures for document control.

- Maintenance of the digital modeling information archive of PA documents, model codes, model input and output files, formal QA documentation, and reference materials in compliance with requirements of the UCOR QA Program (UCOR 2019), DOE QA Program (DOE 2012, Attachments G and H), and DOE O 414.1D (DOE 2013b).

The QA procedures and documentation for the EMDF PA are described in Sect. 9.

RESULTS OF BASE CASE ALL-PATHWAYS DOSE AND UNCERTAINTY ANALYSES

This section summarizes the results of the base case dose analysis using the total system model code RESRAD-OFFSITE. A summary of the sensitivity and uncertainty evaluations performed for the PA modeling and a brief presentation the probabilistic uncertainty analysis are also included in this executive summary. Detailed presentations of PA model results are included in Sect. 4 and Appendices C, D, E, F, and G. Results of the radon flux analysis and RESRAD-OFFSITE results used to demonstrate water resources protection are presented in the Evaluation of Performance section of this executive summary.

All-pathways dose analysis

Total system simulations were run for a post-closure period of 10,000 years to provide dose estimates for comparison with EMDF performance objectives, with a focus on predicted peak total dose within the 1000-year compliance period. Potential future release of less mobile radionuclides with significant estimated inventories (e.g., radionuclides of uranium) was evaluated with a separate 100,000-year RESRAD-OFFSITE simulation to saturated zone concentrations at the 100-m POA. These model predictions for the period beyond 10,000 years are highly uncertain and are presented only to indicate very long-term trends, rather than for comparison to regulatory standards. Results for the 100,000-year simulation are presented in Sect. 4.8.

Predicted total dose over time for the base case model is presented in Fig. ES.10. The peak total dose (i.e., all-pathways dose from all simulated radionuclides summed) within the 1000-year compliance period occurs at 490 years post-closure and is 1.03 mrem/year. The peak compliance period dose is associated with C-14. Total dose then decreases through 750 years and remains less than 0.2 mrem/year from that time to the end of the compliance period. After the compliance period, the total dose increases to a peak of 0.95 mrem/year associated with Tc-99 at approximately 1700 years. After the Tc-99 peak, the total dose increases to a maximum of 9.13 mrem/year at approximately 5084 years and then gradually decreases through 10,000 years to a predicted total dose at 10,000 years of 0.114 mrem/year. The primary isotopic contributors to the total dose are C-14, Tc-99, and I-129 (Fig. ES.11).
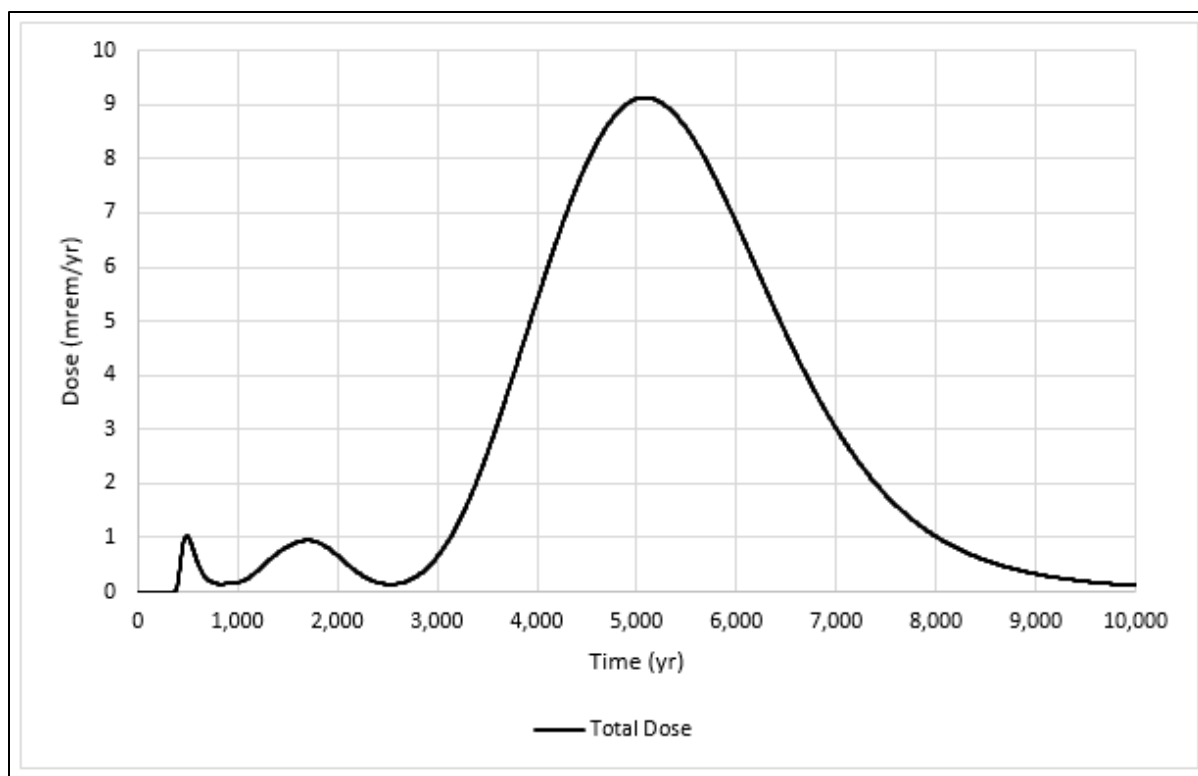
Fig. ES.10. Base case predicted total dose (all pathways, 0 to 10,000 years)
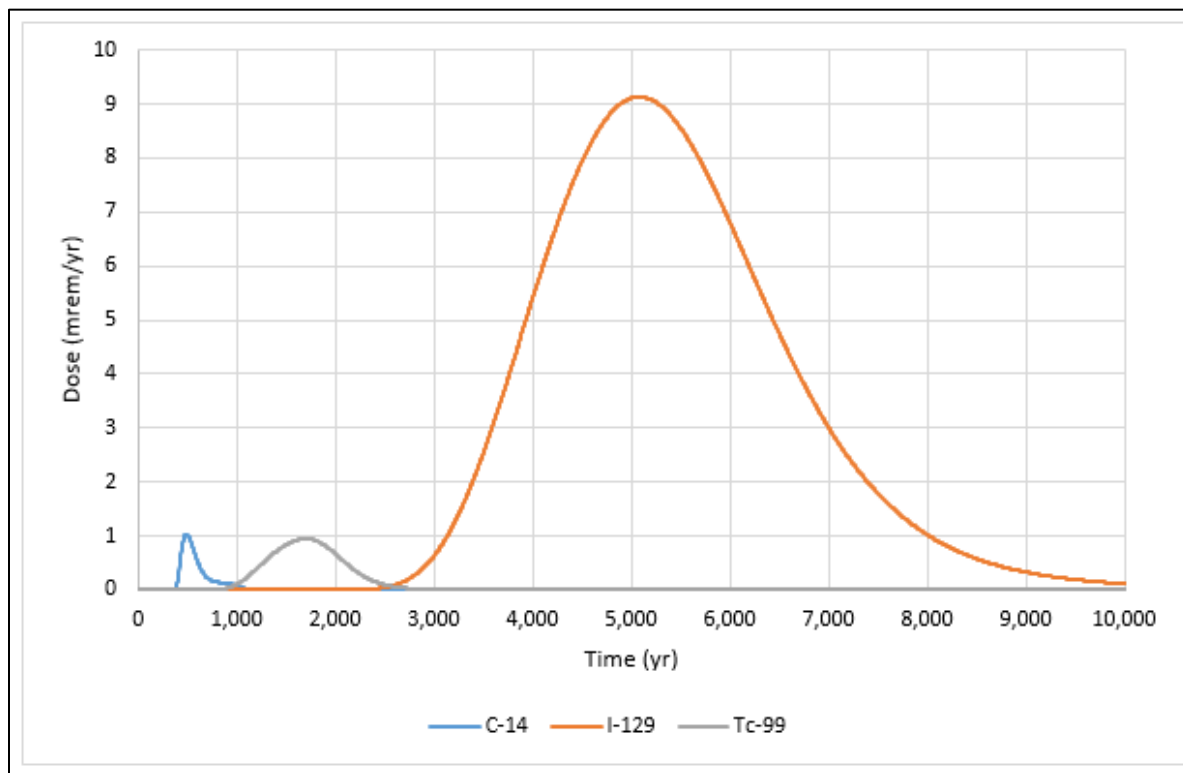
Fig. ES.11. Base case predicted total dose by isotope (0 to 10,000 years)

The three distinct peaks in total dose are each associated with one of these three radionuclides. Overall, the predicted maximum total dose during the compliance period of 1.03 mrem/year is less than 5 percent of the performance objective (25 mrem/year).

The groundwater ingestion pathway (ingestion of well water) is the dominant contributor to total dose (Fig. ES.12). Note that the dose axis on Fig. ES.12 is logarithmic to facilitate comparison of pathway dose contributions. In addition to the drinking water exposure pathway, the pathways contributing most of the remaining dose are ingestion of fish (during the compliance period) and, after about 1200 years, meat ingestion, which includes beef, poultry, and eggs (refer to Sect. 3.4.3 for additional detail).
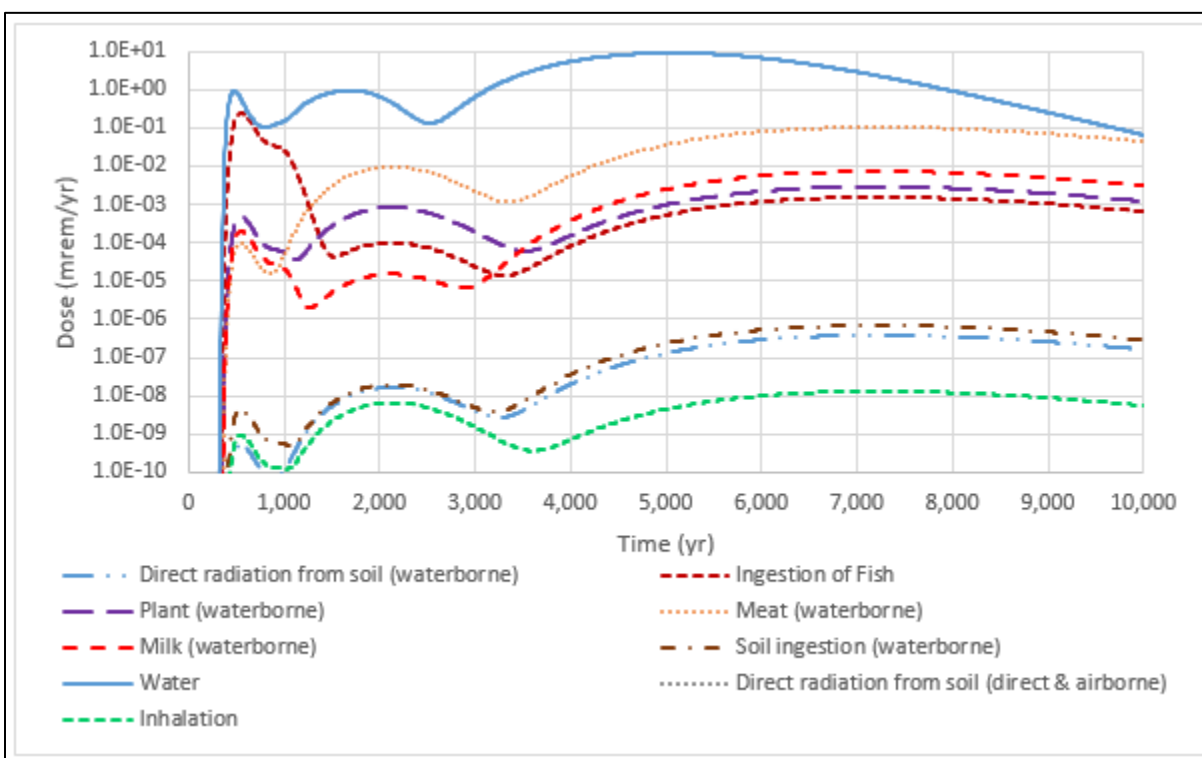
Fig. ES.12. Predicted base case dose by exposure pathway (0 to 10,000 years)

Sensitivity and Uncertainty Analysis

The goal of sensitivity-uncertainty analysis for the EMDF PA is understanding sensitivity of model predictions to uncertainty in input parameter values for those radionuclides and transport pathways that are the primary contributors to the all-pathways dose during the 1000-year compliance period. The focus is on uncertainty in long-term cover performance, partition coefficient values for dose-significant radionuclides, and hydrogeologic parameters that affect environmental transport pathways. Detailed presentation of sensitivity-uncertainty analyses is provided in Sect. 5.

The analysis includes selected sensitivity cases (what-if scenarios) for the detailed vadose and saturated zone transport models, single factor (increasing and decreasing one parameter at a time from the assumed base case value) sensitivity evaluations of the total system model predictions, and an uncertainty analysis to address the importance of key uncertainties relative to evaluation of compliance with the all-pathways dose performance objective. The uncertainty analysis involves assigning probability distributions to selected input parameters and running multiple simulations with different sets of input values, and statistical analysis of the results. The sensitivity and uncertainty evaluations undertaken for the EMDF PA are

summarized in Table ES.5. Results from model sensitivity cases and single-factor evaluations (Sect. 5 and Appendices C, D, E, F, and G) were used to inform the selection of input parameters and parameter distributions for the probabilistic analysis.

Table ES.5. Summary of sensitivity-uncertainty analyses for the EMDF PA

Type of sensitivity-uncertainty analysis	Subsystems and models evaluated	Parameters selected for analysis (related uncertainty)
Model sensitivity cases (what-if analysis)	Saturated Zone Flow – MODFLOW	• Increased recharge (climate)
	Vadose Zone Transport – STOMP	• Increased cover infiltration (climate, cover performance) • Increased waste K_d (materials and geochemistry) • Decreased non-waste K_d (materials and geochemistry)
	Saturated Zone Transport – MT3D	• Increased layer 2 hydraulic conductivity value (materials) • Non-uniform source release (uniform source release assumption)
Single factor sensitivity	Total System – RESRAD-OFFSITE	• Refer to Table 5.2
Probabilistic input parameter uncertainty analysis	Total System – RESRAD-OFFSITE	• Refer to Appendix G, Attachment G.3

EMDF = Environmental Management Disposal Facility   RESRAD = RESidual RADioactivity
PA = Performance Assessment   STOMP = Subsurface Transport Over Multiple Phases

The sensitivity cases evaluated for the STOMP and MT3D models are detailed in Sect. 5.1 and 5.2, respectively. The RESRAD-OFFSITE model single factor sensitivity evaluations are presented in Sect. 5.3. The results of the more detailed process models and model sensitivity to input assumptions were compared to RESRAD-OFFSITE model predictions to guide the RESRAD-OFFSITE model saturated zone parameter inputs and to ensure that the simplified total system model results were broadly consistent with the more detailed models. This model integration process is described in Sect. 3.3.5.

The RESRAD-OFFSITE model uncertainty analysis is summarized in Sect. 5.4 and described in detail in Appendix G, Sect. G.6.3. The probabilistic analysis addresses input parameter uncertainty by assigning probability distributions to key input variables, randomly sampling sets of input parameters values, and running multiple simulations to obtain the predicted peak dose for each realization of the EMDF disposal system. Distributions of predicted dose are used to understand the range and likelihood of peak dose related to uncertainty in input parameters. Multiple regression analysis of peak dose as a function of the probabilistic input variables is used to determine which input parameters have the greatest impact on model results. Separate RESRAD-OFFSITE uncertainty analyses were completed for the 1000-year compliance period and for the longer 10,000-year period.

To simplify the analysis, only C-14, Tc-99, and I-129 were included in the compliance period probabilistic evaluation. Selection of input parameters for probabilistic analysis focused on uncertainty in future precipitation and cover performance, K_d values for EMDF materials, and other properties of the vadose and saturated zone media that influence radionuclide transport. Assigned probability distribution parameters and assumed correlations between input parameters are summarized in Appendix G, Attachment G.3.

Figure ES.13 shows the variation of median, mean, and 95th percentile dose during the compliance period for each of 10 repetitions of 300 simulations. The deterministic base case model all-pathways dose curve

for the compliance period is also shown on Fig. ES.13 for comparison to the probabilistic results. The peak of the mean probabilistic dose (i.e., the maximum value of the mean dose over time for each repetition) occurred at 1030 years for all 10 repetitions, ranging from 0.92 to 1.2 mrem/year, which is a range that includes the deterministic base case compliance period peak dose of approximately 1 mrem/year (Fig. ES.10). The 95th percentiles of the probabilistic total dose also reached maximum values at 1030 years, with a range from 1.7 to 2.1 mrem/year among the 10 repetitions.
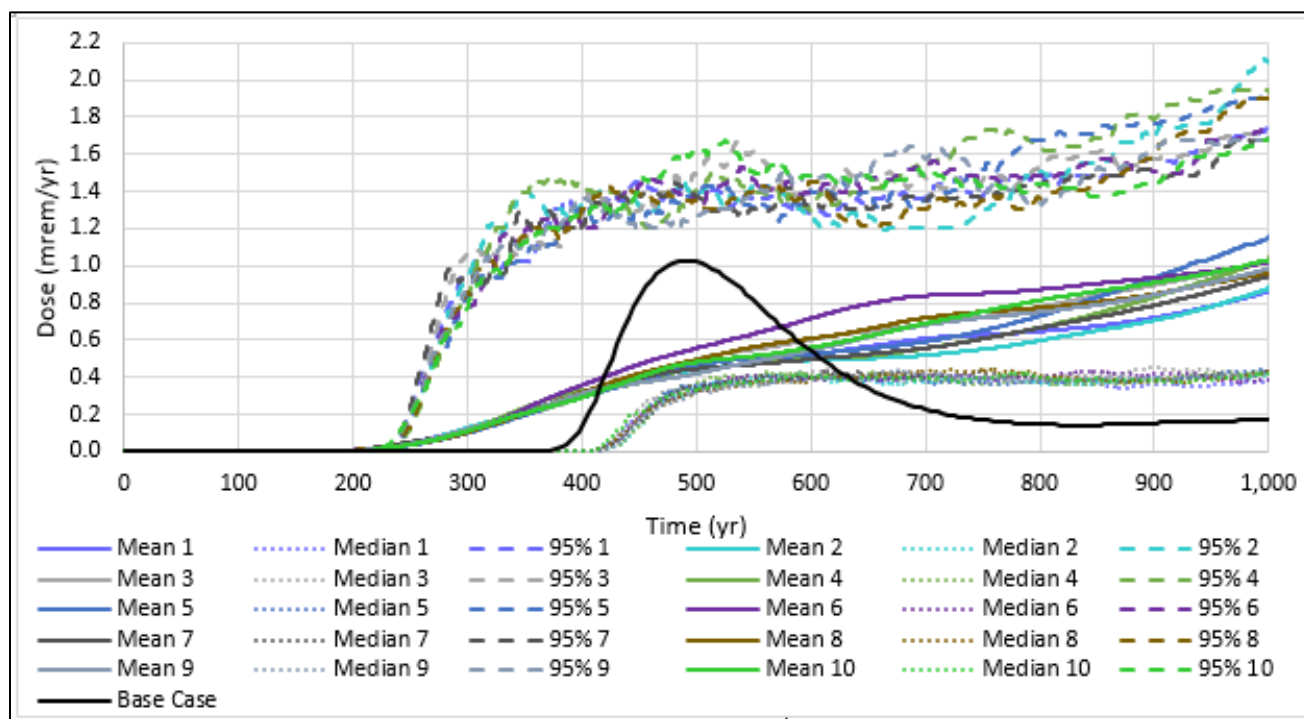
Fig. ES.13. Probabilistic all pathways dose summary for RESRAD-OFFSITE probabilistic uncertainty analysis

The difference between the deterministic base case dose curve and the probabilistic results (percentiles of the total dose distribution as a function of time) occurs because the time of peak total dose for any single probabilistic simulation varies widely (230 to 1030 years) due to variable sampling of input parameters that control release timing (particularly K_d values) among the 3000 realizations. The differences between the deterministic and probabilistic results also reflect the likelihood of much larger dose contributions from Tc-99 and I-129 toward the end of the compliance period probabilistic simulations. Carbon-14 is the primary dose contributor for times prior to about 800 years. After 800 years, I-129 and Tc-99 have mean dose contributions equal to or greater than mean C-14 contributions. Additional detail on variation of radionuclide dose over the compliance period is provided in Sect. G.6.3.3 of Appendix G. For I-129 and Tc-99, compliance period peak doses that occur at the end of the simulation period are cases in which higher long-term radionuclide peaks will occur well after 1000 years in the longer simulations. The uncertainty analysis results for the 10,000 year simulation period are presented in Sect. 5.4.2.

Regression analysis of the compliance period probabilistic peak dose output suggests that among the 33 input parameters for which probability distributions were assigned, the five most influential variables are:

- Runoff coefficient (cover infiltration rate)

- Release duration (affects release rate)

- Hydraulic conductivity of the saturated zone (saturated zone mixing)

- Mean residence time in the surface water body (C-14 fish ingestion dose)

- Depth of aquifer contributing to well (exposure factor, affects well water concentrations).

These results are consistent with results from the single parameter sensitivity analysis presented in Sect. 5.3, which show that total dose and timing of peaks are sensitive to changes in these parameters. The results of the uncertainty analysis suggest that the uncertainty in key input parameter values does not affect the conclusion that the all-pathways dose performance objective will be met during the 1000-year compliance period, and that the 25mrem/year limit is unlikely to be exceeded within timeframes of several thousand years post-closure.

INADVERTENT HUMAN INTRUSION

This section presents a brief summary of the results of the analysis of IHI for EMDF; the IHI analysis is described in more detail in Sect. 6 of the PA. Selection of IHI scenarios was guided by consideration of EMDF site characteristics and facility design as well as review of IHI analyses performed for other historical and proposed LLW disposal facilities on the ORR. Additional details on this IHI analysis, the scenarios evaluated, and the other PAs that were reviewed are provided in Appendix I. The IHI analysis for EMDF considers an acute discovery scenario that involves attempted excavation into the final cover and an acute drilling and chronic post-drilling (agricultural) scenario that involve direct contact with the waste. A summary of the three IHI scenarios analyzed for EMDF is provided in Table ES.6.

Table ES.6. Summary of IHI scenarios analyzed for EMDF and corresponding DOE performance measures

Scenario type/name	DOE Order 435.1 performance measure	Exposure scenario description
Acute exposure –discovery (excavation)	500 mrem	Intruder initiates excavation into EMDF cover, but stops digging before exposing waste; exposure to external radiation
Acute exposure – drilling (water well)	500 mrem	Intruder drills irrigation well through waste and is exposed to waste in exhumed drill cuttings; exposure to external radiation, inhalation and incidental ingestion of contaminated soil
Chronic exposure – post-drilling (subsistence garden)	100 mrem/year	Intruder uses contaminated drill cuttings to amend soil in a vegetable garden; exposure to external radiation, inhalation, and ingestion of contaminated food and soil

DOE = U.S. Department of Energy IHI = inadvertent human intrusion
EMDF = Environmental Management Disposal Facility

The IHI analysis assumes that intrusion is an accidental occurrence resulting from a temporary loss of institutional control. The occurrence of accidental intrusion also presumes a loss of societal memory of the ORR and radioactive waste disposal facilities in the area, despite existing long-term stewardship commitments of the DOE and the likelihood of legal controls such as property record restrictions and notices. For each IHI scenario, active institutional controls are assumed to preclude intrusion for the first 100 years following closure of the disposal facility.

Several key assumptions for the intruder analyses (e.g., cover and waste thickness) are based on the specifics of the EMDF design that are described in Sects. 1.3 and 2.2 and in Appendix C. The estimated EMDF radionuclide inventory (Appendix B) was used with the RESRAD-OFFSITE code to model doses resulting from these unlikely future intrusion scenarios. The results are used to establish compliance with DOE O 435.1 dose performance measures for IHI (Table ES.6).

The results of the IHI analyses are summarized in Table ES.7. The model results for the three IHI scenarios suggest the chronic post-drilling scenario is the bounding scenario (largest predicted dose). Predicted dose over time for the chronic post-drilling scenario is presented in Fig. ES.14. The total dose (all radionuclides and pathways summed) at 100 years post-closure is 3.56 mrem/year. Total dose decreases to a minimum of 2.95 mrem/year at approximately 340 years, and then gradually increases through the compliance period. After 1000 years, the dose increases more rapidly as concentrations of radioactive progeny (uranium decay products) increase. Total dose at 10,000 years is 8.24 mrem/year. The maximum predicted dose is a factor of 10 times lower than the chronic IHI performance measure of 100 mrem/year.

Table ES.7. Summary of IHI analysis results for the EMDF

EMDF IHI scenario	DOE O 435.1 IHI performance measure	Maximum dose during the 1000-year compliance period
Acute exposure – discovery (excavation)	500 mrem	1.3E-04 mrem
Acute exposure – drilling (water well)	500 mrem	0.38 mrem
Chronic exposure – post-drilling (subsistence garden)	100 mrem/year	3.56 mrem/year

DOE O = U.S. Department of Energy Order   IHI = inadvertent human intrusion
EMDF = Environmental Management Disposal Facility
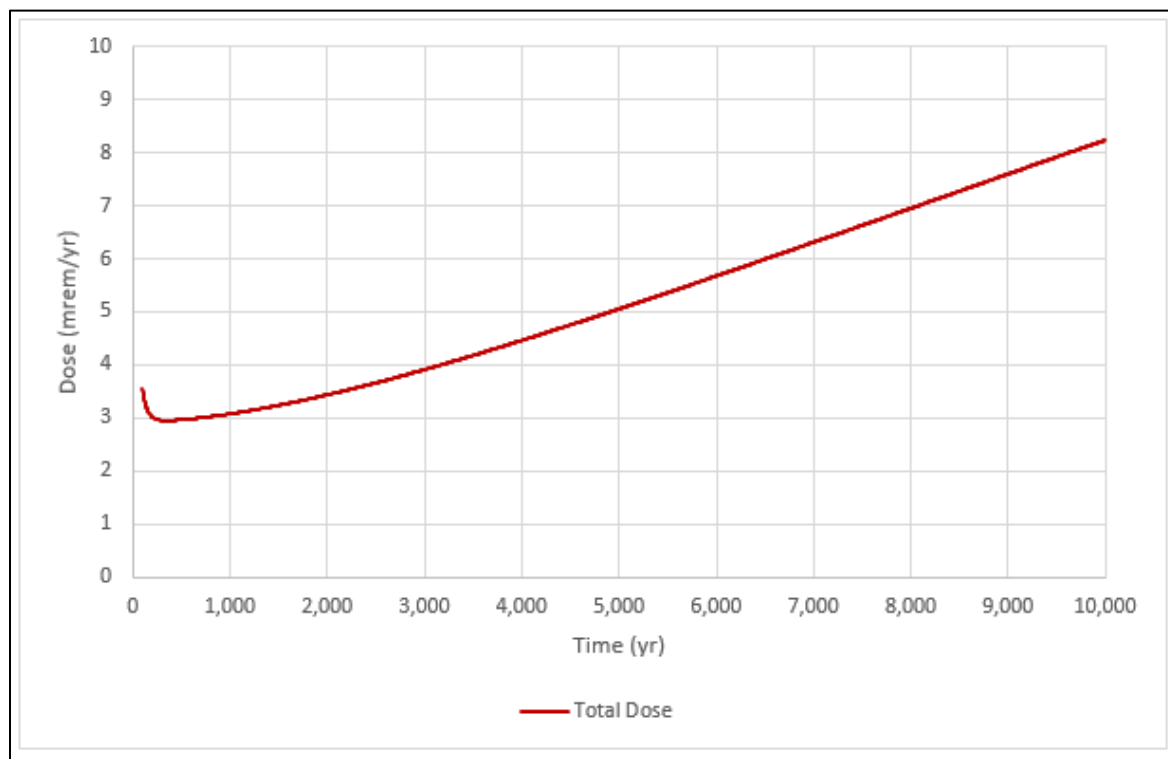
Fig. ES.14**. Chronic post-drilling scenario total dose (all radionuclides and pathways summed)**

EVALUATION OF PERFORMANCE

The base case analysis and sensitivity-uncertainty analysis performed for the EMDF PA demonstrate that there is a reasonable expectation that the facility will meet the established all-pathways dose performance objective during the 1000-year compliance period and within the first several thousand years post-closure. Analytical results are summarized in Table ES.8.

Table ES.8. Exposure scenarios, performance objectives and measures, and base case results for the EMDF PA

Exposure scenario	Performance objective or measure	EMDF PA results
All pathways	25 mrem/year	Base case maximum dose during compliance period: 1.03 mrem/year Base case peak dose through 10,000 years: 9.13 mrem/year (at 5100 years)
Air pathway[a]	10 mrem/year[b]	Pathway screened from analysis (Sect. 3.2.2)
Radon flux	20 pCi/m^2/sec	EMDF cover surface: 5.0E-08 pCi/m^2/sec EMDF waste surface (no cover): 0.80 pCi/m^2/sec
Water resources (groundwater) • Ra-226 + Ra-228 • Gross alpha activity[c] • Beta/photon activity • H-3 • Sr-90 • Uranium (total)	5 pCi/L 15 pCi/L 4 mrem/year 20,000 pCi/L 8 pCi/L 30 µg/L	Groundwater during compliance period: • Ra-226 + Ra-228: 0.0 pCi/L (negligible) • Gross alpha activity: 0.0 pCi/L (negligible) • Beta/photon activity: 1.03 mrem/year • H-3: 0.0 pCi/L (negligible) • Sr-90: 0.0 pCi/L (negligible) • Uranium (total): 0.0 µg/L (negligible).
Water resources (surface water)	DOE DCS[d]	Bear Creek peak concentration less than DCS standard for all radionuclides in EMDF inventory (Sect. 4.7.2)
Inadvertent human intrusion • Chronic exposure • Acute exposure	100 mrem/year 500 mrem	IHI dose at 100 years (compliance period maximum): Chronic post-drilling: 3.56 mrem/year Acute discovery: 1.30E-04 mrem Acute drilling: 0.38 mrem

[a]Air pathway is screened from the EMDF PA.
[b]Excluding radon in air.
[c]Including Ra-226, but excluding radon and uranium.
[d]DOE 2011b.

DCS = Derived Concentration Standard   IHI = inadvertent human intrusion
DOE = U.S. Department of Energy   PA = Performance Assessment
EMDF = Environmental Management Disposal Facility

Results of the radon flux analysis are shown in Table ES.8, discussed in Sect. 4.4, and presented in detail in Appendix H. The results suggest that EMDF can meet the 20 pCi/m^2/sec radon flux performance objective even if the cover is severely eroded. Also included in Table ES.8 is a summary of the results of RESRAD-OFFSITE modeling to demonstrate protection of water resources during the 1000-year compliance period. Modeled well water and surface water concentrations are compared to maximum contaminant levels for drinking water systems and to the DOE *Derived Concentration Technical Standard* (DOE 2011b), respectively. The results suggest there is a reasonable expectation that the EMDF disposal system will be protective of water resources during the compliance period.

With respect to performance measures for IHI, the EMDF analysis suggests that, based on the current estimated EMDF radionuclide inventory, there is a reasonable expectation that the engineering design for EMDF will protect a future inadvertent human intruder for the specific IHI scenarios considered.

USE OF PERFORMANCE ASSESSMENT RESULTS

The primary uses of this EMDF PA are to support issuance of a DAS by demonstrating the likelihood of meeting performance objectives based on the expected EMDF waste forms, estimated radionuclide inventory, preliminary facility design, and site characteristics, and to identify key site, waste, and facility uncertainties that can be prioritized for further work prior to the start of operations.

FURTHER WORK

Near-term priorities for research and development activities to support PA maintenance include the following:

- Perform laboratory evaluations of EMDF materials to reduce uncertainty in the assumed K_d values for Tc-99 and I-129

- Monitor EMDF design evolution through final design and assess changes through the EMDF change control process.

In parallel with these near-term PA maintenance activities, the FFA parties will approve operating limits, including WAC, and will issue a WAC compliance document prior to EMDF operations. Review of proposed activities, new regulatory requirements, or other new information that could challenge key assumptions for the EMDF performance analysis will be evaluated in accordance with the EMDF change control process to assess the potential for such changes to require a Special Analysis or revisions to the PA.

This page intentionally left blank.

1.   INTRODUCTION

This report documents the Performance Assessment (PA) for a proposed solid low-level (radioactive) waste (LLW) disposal facility at the U.S. Department of Energy (DOE) Oak Ridge Reservation (ORR). A new facility is required to ensure sufficient future LLW disposal capacity for environmental cleanup activities on the ORR performed under the ORR Federal Facility Agreement (FFA) (DOE 1992a).

This section of the Environmental Management Disposal Facility (EMDF) PA report provides general background information, including a facility description, a summary of the EMDF regulatory framework and need for the PA, and a summary of key assumptions. Information provided in subsequent sections of the report includes the following:

- Sect. 2 – detailed information on EMDF site characteristics and design features and the estimated radionuclide inventory used in the PA modeling analysis

- Sect. 3 – EMDF analysis of performance, including conceptual models, modeling tools, model implementation, and dose analysis

- Sect. 4 – results of the performance analysis

- Sect. 5 – sensitivity of the results to uncertainty in model inputs

- Sect. 6 – results of the analysis of (hypothetical) inadvertent human intrusion (IHI)

- Sect. 7 – integration and interpretation of results

- Sect. 8 – overall evaluation of EMDF performance

- Sect. 9 – quality assurance (QA) procedures

- Sects. 10 and 11 – information on the preparers of the PA and references

- Appendix A – PA review criteria

- Appendix B – radionuclide inventory for wastes disposed in EMDF

- Appendix C – analysis of EMDF cover system

- Appendix D – groundwater flow modeling (MODFLOW)

- Appendix E – Subsurface Transport Over Multiple Phases (STOMP) modeling

- Appendix F – MT3D modeling

- Appendix G – RESidual RADioactivity (RESRAD)-OFFSITE modeling

- Appendix H – radon flux analysis

- Appendix I – IHI analysis.

The remainder of Sect. 1 reviews the basis and programmatic context for the EMDF PA, including related analyses (Sect. 1.1), and provides general facility information and design features (Sects. 1.2 and 1.3); facility life-cycle assumptions, including closure planning (Sect. 1.4); regulatory context for the EMDF PA (Sect. 1.5); expectations regarding future land use and institutional controls (Sect. 1.6); and a summary of key assumptions that underlie the conclusions of the PA (Sect. 1.7).

1.1 BASIS FOR PERFORMANCE ASSSESSMENT

This EMDF PA has been developed to support DOE approval of a Disposal Authorization Statement (DAS) to support design and construction of EMDF. Development of the EMDF PA and early facility design activities are being conducted in parallel with activities required for approval of the EMDF for onsite LLW disposal under the FFA. Remaining documentation to support a final Disposal Authorization Statement to support operations of the landfill will occur in parallel with the final design of the facility.

1.1.1 Programmatic Background

DOE is responsible for sitewide waste management and environmental restoration activities on the ORR under its Office of Environmental Management Program at the national level and locally under the Oak Ridge Office of Environmental Management (OREM). OREM is responsible for minimizing potential hazards to human health and the environment associated with contamination from past DOE practices and addressing the waste management and disposal needs of the ORR. Under the requirements of the FFA established by DOE, the U.S. Environmental Protection Agency (EPA), and the Tennessee Department of Environment and Conservation (TDEC), environmental restoration activities on the ORR are performed in accordance with the Comprehensive Environmental Response, Compensation, and Liability Act of 1980 (CERCLA).

The major focus of the OREM Program has been remediation of facilities within the installations that are contaminated by historical Manhattan Project and Cold War activities. This cleanup mission is projected to take approximately three decades to complete and will result in large volumes of radioactive, hazardous, and mixed waste requiring disposal. The focus of CERCLA cleanup since the early 1990s has been the remediation of existing waste disposal sites and deactivation and decommissioning (D&D) of excess facilities at the East Tennessee Technology Park (ETTP), the Y-12 National Security Complex (Y-12), and the Oak Ridge National Laboratory (ORNL). Timely and effective ORR cleanup is essential to facilitate reindustrialization of the ETTP site and to ensure worker safety and the success of DOE missions at Y-12 and ORNL.

A 1999 Record of Decision (ROD) (DOE 1999a) authorized construction of a facility located in Bear Creek Valley (BCV) on the ORR to provide permanent disposal for radioactive, hazardous, and mixed wastes resulting from cleanup of facilities and media that present unacceptable risks to human health and the environment in their current setting at ORR and associated sites. This facility, the Environmental Management Waste Management Facility (EMWMF), has been constructed and is accepting CERCLA cleanup wastes. The capacity of EMWMF is 2.3 million cy as authorized by the ROD and a subsequent Explanation of Significant Difference (DOE 2010a).

The scope of the OREM cleanup effort has expanded since EMWMF began operations in 2002. Approximately 1.6 million cy of additional CERCLA waste is expected to be generated and require disposal after EMWMF has reached maximum capacity in the mid-2020s.

1.1.2 EMDF Performance Assessment Development and Related Analyses

The anticipated need for additional LLW disposal capacity is the basis for a second ORR CERCLA waste disposal facility. The associated Remedial Investigation/Feasibility Study (RI/FS) analyzed the feasibility of siting a new disposal facility at several alternative sites in BCV (DOE 2017b). The FFA parties issued a Proposed Plan (DOE 2018a) for disposal of future ORR CERCLA waste for public comment in 2018. A conceptual design for the Central Bear Creek Valley (CBCV) site contained in the EMDF RI/FS is the basis for the EMDF Proposed Plan. Since the proposed plan was issued, the design of the EMDF has been advanced to a preliminary design (60 percent) stage and is the basis for technical analyses in this PA.

The EMDF PA analysis incorporates an extensive body of environmental data drawn from over two decades of RI and monitoring in BCV. In addition, CBCV site characterization activities, including surface water and groundwater monitoring, have been completed to support FFA approval of the proposed site and development of the preliminary engineering design. Information from the CBCV site characterization was used in revising the PA models used in this revision of the document. Following the issue of a DAS for EMDF, proposed activities, new regulatory requirements, or other new information that could challenge key assumptions for the PA will be reviewed and evaluated with the EMDF change control process to assess the potential for such changes to require a Special Analysis or revisions to the PA.

Two other ORR LLW disposal facility PAs that may be of interest for comparison to the EMDF PA include the analyses performed for Solid Waste Storage Area (SWSA) 6 in Melton Valley near ORNL (ORNL 1997a) and for EMWMF (DOE 1998a) in BCV near the west end of the Y-12 site. The SWSA 6 and EMWMF PAs differ from the EMDF PA primarily in terms of facility design, conceptual models, and selection of computer codes for analysis. Table 1.1 provides a summary of the differences in facility design, release pathway and exposure assumptions, model codes, and partition coefficient (K_d) values. The EMDF and EMWMF facilities and performance analyses are very similar, whereas the SWSA 6 PA encompassed a number of different LLW disposal units within a common area (Melton Valley) on the ORR, and applied several model codes developed at ORNL. For assumed partition coefficients, the EMDF PA draws upon the currently available data for Conasauga Group materials (Sect. 2.1.6.3), whereas the SWSA 6 and EMWMF analyses used a combination of semi-empirical derivation of partition coefficients for waste forms and assumed higher mobility for technetium and iodine in the natural environment (K_d=0 in the vadose and saturated zone) than does the EMDF analysis.

Both the SWSA 6 and EMWMF analyses included derivation of performance-based radioactivity concentration limits. The EMWMF analysis applied a unit concentration approach to developing activity concentration limits (analytical waste acceptance criteria [WAC]). The EMDF RI/FS identified a preliminary range of concentration limits for radionuclides and included a discussion of the WAC development and compliance process that will be developed under the FFA (DOE 2018a, Sect. 6.2.3, pages 6-85 to 6-91, Table 6.5). The EMDF PA includes calculated site-specific Single Radionuclide Soil Guidelines (SRSGs) that can be used to evaluate proposed limits on radionuclide inventories or concentrations.

A Composite Analysis (CA) has been prepared to evaluate cumulative impacts of potential releases from historical waste disposal sites, the existing EMWMF, and the future EMDF in BCV (UCOR, an Amentum-led partnership with Jacobs, 2020a). The CA for EMWMF and EMDF summarizes modeling activities to estimate peak radiological dose at a downgradient point of assessment (POA) on Bear Creek. The resident farmer exposure scenario assumed for the EMWMF/EMDF CA differs from the EMDF PA in that surface water rather than groundwater is assumed as the source for drinking and domestic use. The CA concludes that cumulative dose will not exceed DOE Manual (M) 435.1-1 (DOE 2011a) performance objectives.

This page intentionally left blank.

Table 1.1. Comparison of EMDF, EMWMF, and SWSA 6 performance assessments

	Site, disposal facility, and waste characteristics; Exposure scenarios			
PA Characteristic	**EMDF**	**EMWMF**	**SWSA 6**	**Comments**
Location and conceptual site model	BCV	BCV	Melton Valley	Identical geological sequence (Cambrian Conasauga Group sedimentary formations), very similar conceptual site model for Melton Valley and BCV
Type of facility	Above-grade Subtitle C Landfill	Above-grade Subtitle C Landfill	Various disposal units: tumulus facility – waste in B-25 containers	SWSA 6 PA encompassed a variety of adjacent disposal units (including trenches and wells) in Melton Valley
Cover system	11-ft-thick multicomponent	11-ft-thick multicomponent	Tumulus: 4-ft-thick multicomponent	
Liner system	RCRA-compliant	RCRA-compliant	Above-grade concrete pads with gravel drainage	RCRA-compliant liners contain HDPE flexible membranes and 3-ft-thick clay layer
Facility failure – degradation assumptions	HDPE and clay degrades from 200 to 1000 years post-closure	HDPE non-functional, clay degrades at end of institutional control	Complete cover and pad failure at end of institutional control	Recent research on geosynthetics supports longer cover performance for EMDF and EMWMF; refer to Appendix C, Sect. C.1.
Cover infiltration rate(s)	Linear increase from zero at 200 years to 0.88 in./year at 1000 years	0.43 in./year at closure	Natural recharge	
Waste types	LLW, mixed, TSCA	LLW, mixed, TSCA	LLW – CH and RH	
Waste form	Soil and demolition debris from CERCLA response actions	Soil and demolition debris from CERCLA response actions	Various- from ORNL operations and legacy wastes	EMWMF and projected EMDF waste is a combination of compacted bulk waste, containerized waste, and various types of treated or stabilized waste forms (e.g., equipment grouted in place)
Radionuclide inventory	Estimated (Appendix B of this PA)	Unit concentrations approach to develop analytical WAC	Estimated	The EMWMF dose analysis for the BCV CA uses a current radionuclide inventory estimate
Exposure scenario	Resident farmer- drinking water well, surface water agricultural use	Resident farmer- drinking water well, surface water agricultural use	Resident farmer groundwater- drinking, milk, and meat; surface water- drinking, milk, meat, and fish	
Hypothetical receptor location	100 m from waste edge @ plume centerline	Bear Creek at NT-5 confluence (about 300 m from edge of facility)	100 m from edge of cover	EMWMF receptor well location selected onsite with TDEC and EPA representatives

	Assumed K$_d$ values (cm^3/g)			
Element	**Waste K$_d$, vadose zone K$_d$, saturated zone K$_d$**	**Waste K$_d$, vadose zone K$_d$, saturated zone K$_d$**	**Waste K$_d$, soil and environmental transport K$_d$**	**Comments**
Carbon	0, 0, 0	1.09, 0, 0	1.09, 0	
Hydrogen	0, 0, 0	0.199, 0, 0	0.199, 0	
Iodine	2, 4, 4	0.199, 0.199, 0	0.551, 0	
Technetium	0.36, 0.72, 0.72	1.29, 0, 0	3.18, 0	
Uranium	25, 50, 50	40, 20, 7	3820, 40	

	Model codes applied to release, transport, and dose analysis			
Medium or Transport Pathway	**EMDF**	**EMWMF**	**SWSA 6**	**Comments**
Groundwater flow	MODFLOW	MODFLOW	USGS MOC	
Surface water flow	No model	No model	UTM	
Radionuclide release	STOMP, MT3D, RESRAD-OFFSITE	PATHRAE-RAD	SOURCE1, SOURCE2	
Radionuclide transport	MT3D, RESRAD-OFFSITE	PATHRAE-RAD	PADSIM, HOLSIM	
Air pathway	RESRAD-OFFSITE (atmospheric loading for irrigated areas and cover release pathway screening model)	No model; atmospheric pathway eliminated from consideration	ISCLT3	
Dose analysis	RESRAD-OFFSITE	PATHRAE-RAD	No model code identified, dose analysis is detailed in Appendix G of ORNL 1997a	For EMWMF, performance objectives were based on risk metrics rather than dose
Reference documents	This document	DOE 1998a, DOE 1998b	ORNL 1997a	

BCV = Bear Creek Valley
CA = Composite Analysis
CERCLA = Comprehensive Environmental Response, Compensation, and Liability Act of 1980
CH = contact handled
DOE = U.S. Department of Energy
EMDF = Environmental Management Disposal Facility
EMWMF = Environmental Management Waste Management Facility
EPA = U.S. Environmental Protection Agency
HDPE = high-density polyethylene
LLW = low-level (radioactive) waste
NT = North Tributary

ORNL = Oak Ridge National Laboratory
PA = Performance Assessment
RCRA = Resource Conservation and Recovery Act of 1976
RESRAD = RESidual RADioactivity
RH = remote handled
STOMP = Subsurface Transport Over Multiple Phases
SWSA = Solid Waste Storage Area
TDEC = Tennessee Department of Environment and Conservation
TSCA = Toxic Substances Control Act of 1976
WAC = waste acceptance criteria

This page intentionally left blank.

1.2　GENERAL FACILITY DESCRIPTION

The proposed site for the EMDF in BCV is southwest of the city of Oak Ridge, Tennessee, and Y-12 (Fig. 1.1). The LLW disposal concept and preliminary design are similar to EMWMF (i.e., an engineered near-surface disposal facility for solid LLW derived from CERCLA response actions on the ORR). Given the humid-temperate climate and shallow groundwater conditions prevailing in East Tennessee, long-term performance of engineered barriers, including the composite final cover and liner systems, is critical to the overall performance of the EMDF disposal system. Sections 1.3 and 2.2 provide additional details on EMDF preliminary design features.

The proposed CBCV site for EMDF lies in an area currently designated in the Phase I BCV ROD (DOE 2000) to require cleanup levels that would be protective for future public recreational use in the near term and unrestricted use in the future. The Y-12 facility is located approximately 3 miles to the northeast. The currently operating onsite waste disposal facility (EMWMF), as well as other former waste disposal and waste management facilities, are located between Y-12 and the CBCV site, within the area with cleanup levels for DOE-controlled industrial use (i.e., Zone 3). Section 1.6 provides additional discussion of future land-use assumptions for BCV.

LLW disposed at EMDF will originate primarily from facility D&D or environmental remediation projects at Y-12 and ORNL. The waste will include facility demolition debris (including structural steel and concrete), contaminated equipment and soil, and other soil-like wastes. EMDF will accept both containerized LLW and bulk (uncontainerized) waste for disposal. Some in situ waste stabilization (grouting) may occur. Waste quantities are based on the OREM Waste Generation Forecast. Waste stream characteristics are estimated from a variety of sources and are described in detail in Sect. 2.3 and Appendix B. Detailed characterization of waste destined for EMDF will occur at the cleanup project level and is the responsibility of the waste generator(s).

EMDF operations will include waste receipt and placement, water management, and environmental monitoring of facility performance. EMDF waste certification practices are expected to be carried over from current EMWMF WAC attainment and tracking systems (DOE 2001a). Each waste lot/stream will be certified and approved for disposal at EMDF by the WAC Attainment Team before shipments of waste to EMDF are scheduled. A WAC Compliance Plan, similar to that used at EMWMF, will specify the processes to be used for certification of waste streams for disposal at EMDF. Additional discussion of the FFA process for developing EMDF WAC and waste acceptance practices is provided in Sect. 1.5.5.

EMDF waste receipt operations will include unloading and placing waste into the landfill, spreading and compacting bulk waste using heavy equipment, and placing fill materials and filling void spaces, as required. Void filling and compaction are performed to reduce the potential for post-closure waste settlement that could affect the long-term performance of the cover system. Current EMWMF waste receipt, staging, and placement practices are detailed in UCOR procedure *Waste Placement* (PROC-EMWMF-OP-003); similar procedures will be developed and approved for EMDF prior to operations.

Water management operations and performance monitoring protocols for EMDF also will be similar to those in effect for EMWMF. The potential significance of these operational activities for long-term EMDF performance is addressed in Sect. 1.3.
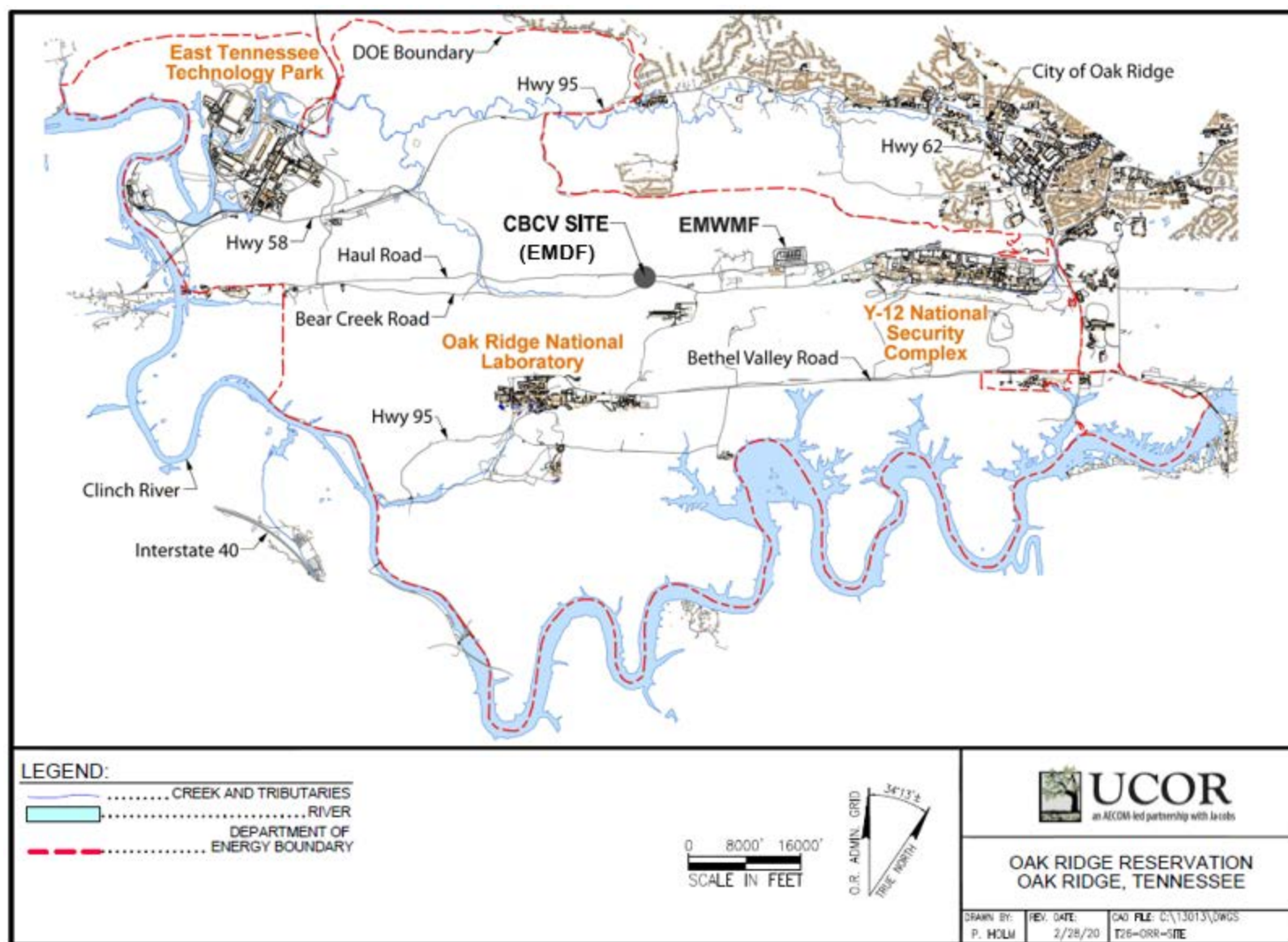
Fig. 1.1. Location map for EMDF on the ORR.

1.3   DESIGN FEATURES AND DISPOSAL SYSTEM SAFETY FUNCTIONS

The EMDF disposal system encompasses the natural features of the CBCV site, design features of the engineered disposal unit, and the operating limits (e.g., WAC) and other waste and safety management practices that ensure worker protection and post-closure facility performance. A CBCV site map showing key EMDF disposal system features and safety function is provided on Fig. 1.2. A simplified profile schematic of EMDF design and natural features and associated safety functions is provided on Fig. 1.3.

Natural features of the CBCV site important for disposal system function include the topography and geologic materials that influence groundwater flow and subsurface geochemistry. Natural topographic and hydrologic boundaries are fundamentally important to the isolation of EMDF waste from potential receptors outside of the Bear Creek watershed. These natural surface and subsurface boundaries limit the potential for short- and long-term contaminant migration via surface and groundwater pathways to the nearest populations in the city of Oak Ridge, located north of the EMDF site. The natural characteristics of the EMDF site, as well as the fact that DOE is required to maintain control of the site as long as there is a potential risk from the waste, represent important safety functions that are factored into site selection.

Selection of the small knob at the foot of Pine Ridge (Fig. 1.2) for construction of EMDF is based on the objective of hydrologically isolating the waste from natural drainage systems. The facility has been designed to maintain vertical separation of the waste from groundwater in the saturated zone beneath the disposal facility and will include a low-permeability multilayer liner and a 10-ft-thick layer of geologic buffer material between the waste and the water table. Under a long-term performance scenario, contaminant retardation in the vadose zone beneath EMDF and within the saturated matrix of the fractured rock at the CBCV site serve safety functions by delaying and attenuating impacts of radionuclide release at potential groundwater and surface water exposure points.

The EMDF preliminary design satisfies Resource Conservation and Recovery Act of 1976 (RCRA) and Toxic Substances Control Act of 1976 design requirements for hazardous and toxic waste disposal units. The engineered disposal unit consists of a multilayer liner, leachate collection and treatment systems, lined embankments for lateral containment and stability, and a multilayer final cover that completely encapsulates the waste in the post-closure period. The engineered barriers of the cover and liner systems are designed to impede the percolation of water into the waste and to retard (post-closure) the release of radionuclides through the bottom liner and into the surrounding environmental media. Perimeter berms and the cover system also serve to deter biointrusion and/or IHI that could lead to direct exposure to the waste. Engineered surface drainage systems outside of the liner footprint serve to maintain groundwater drainage and to limit increases in water-table elevation below the liner in the event of cover and/or liner system failure. A detailed description of the EMDF design features and safety functions is provided in Sect. 2.2 and Appendix C.
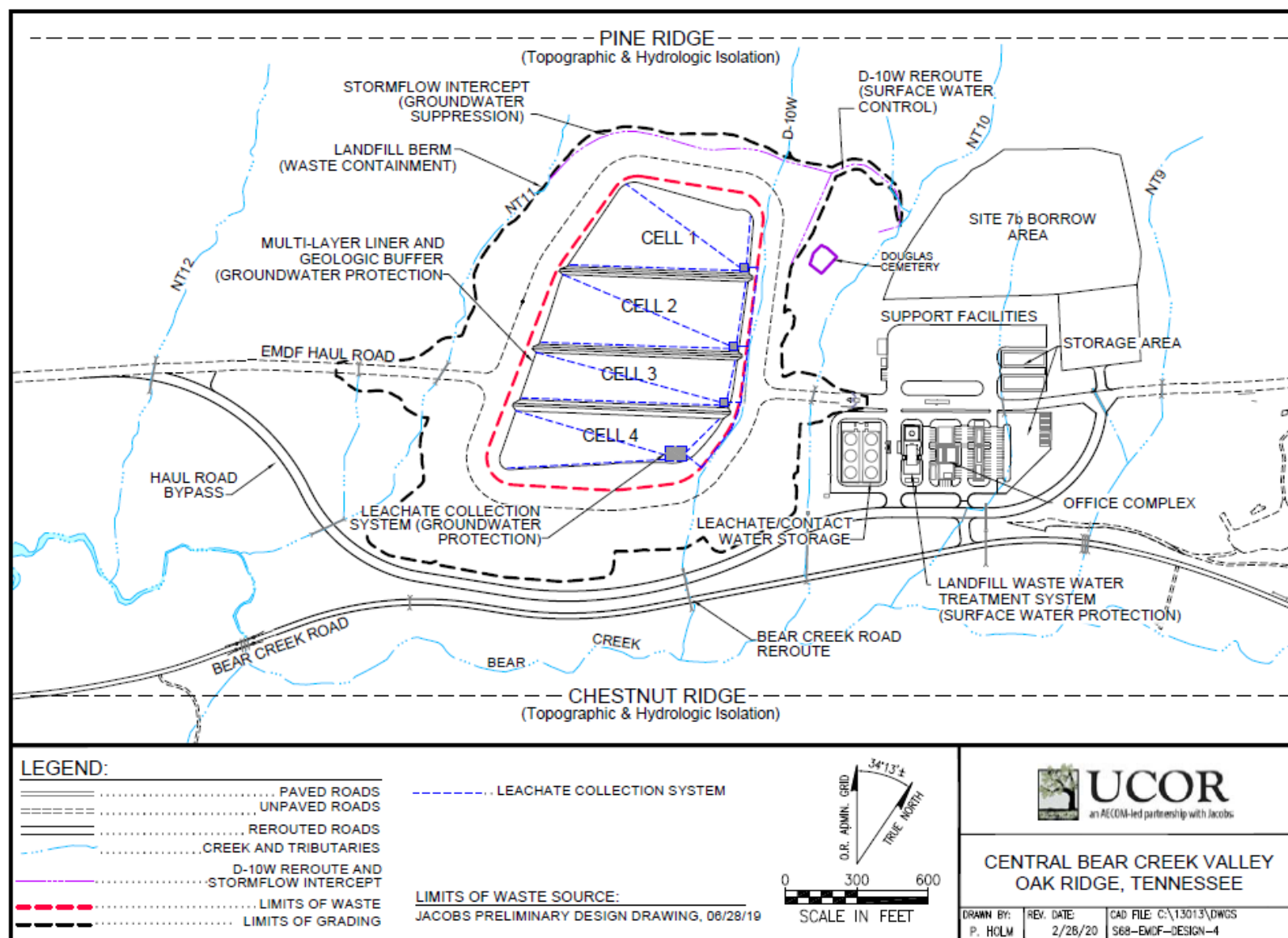
Fig. 1.2. EMDF site and design features and safety functions.

EMDF Disposal System Components	Safety Functions
Surface Processes: *Precipitation ↓, Runoff & Erosion→, Infiltration↓, Evapotranspiration↑*	

	EMDF Disposal System Components	Safety Functions
Cover System (surface, biointrusion & drainage layers, synthetic membrane, clay infiltration barrier)		- Prevent or reduce infiltration into waste zone - Deter Inadvertent Human Intrusion and large animal intrusion - Prevent radionuclide release to EMDF surface
Waste Zone (volume, material characteristics, activity levels) *Radionuclide Release*		- Waste treatment and packaging reduces mobility of radionuclides in waste - Waste placement practices and void filling limit waste subsidence and potential post-closure cover system degradation
Liner System (leachate collection and leak detection systems, clay liner)		- Intercept leachate for treatment - Limit contaminant release & extend time for decay of short-lived radionuclides
Geologic Buffer Zone (low permeability, unsaturated material)		- Retard contaminant transport & extend travel time for decay of short-lived radionuclides
Native vadose materials (saprolite and fractured bedrock)		- Retard contaminant transport & extend travel time for decay of short-lived radionuclides
Shallow Aquifer (saturated saprolite and fractured sedimentary rock)		- Retard contaminant transport & extend travel time for decay of short-lived radionuclides - Limit contaminant transfer to deep aquifer
Deep Aquifer (saturated, fractured sedimentary rock)		- Retard contaminant transport, isolate radionuclides from the shallow subsurface and allow time for decay

Left-side labels: Vadose Zone / Saturated Zone; Engineered Barrier Systems / Natural Barriers

Fig. 1.3. EMDF disposal system schematic profile and safety functions.

The EMDF site and facility features are incorporated into the conceptual models and performance analyses of the PA. In general, it is assumed in the PA modeling that the effectiveness of engineered barriers decreases over time, leading to release of radionuclides through the liner system. A detailed description of natural processes that degrade design features and limit safety functions over time, and a generalized conceptual model of EMDF performance evolution, is provided in Sect. 3.2.1 and Appendix C.

EMWMF operations monitoring, including monitoring of the leachate collection and leak detection systems, provides a basis for understanding disposal system behavior during the operational period. The collection and treatment of contaminated landfill wastewater (leachate and contact water) are important safety functions of the EMDF design which can reduce the inventory of more mobile radionuclides (e.g., H-3) prior to closure, when the flux of water in contact with waste is high. For radionuclides that are assumed to be highly mobile in the PA modeling (H-3, C-14, Tc-99, and I-129), the estimated EMDF radionuclide inventory at closure (Sect. 2.3) is reduced to account for operational period losses and/or reduced mobility of contaminants in leachate treatment residuals that could be disposed in the facility. (Sect. 3.2.2.5).

Remedial investigation of historical waste disposal sites in BCV and elsewhere on the ORR and ongoing CERCLA remedial effectiveness monitoring (DOE 2017c) have provided extensive insight into the likely behavior of the EMDF system in the decades following closure, once the performance of engineered systems begins to degrade. Detailed discussion of BCV hydrology, geology, and studies of contaminant transport phenomena on the ORR is provided in Sect. 2.1.

For purposes of modeling radionuclide release, waste disposal practices that are not credited explicitly in the PA analysis include the use of waste containers (e.g., metal drums and boxes) and waste treatment prior to disposal (e.g., grouting of waste containers, macroencapsulation, etc.). Enforcement of EMDF inventory limits, activity concentration limits, and other WAC (to be developed) will provide defense-in-depth to facility performance.

Another aspect of the EMDF disposal system not credited in the PA analysis is long-term commitments of OREM and the other FFA parties to maintaining land use controls, post-closure monitoring, and facility maintenance to ensure future performance and mitigate the risk of public exposure to radionuclides. The conceptual model of EMDF performance evolution and the exposure scenarios assumed for the PA modeling do not incorporate the likelihood that DOE and successor agencies will retain control of the CBCV site well into the future. Under DOE Order (O) 458.1, requirements for public protection and CERCLA requirements for monitoring remedial performance essentially in perpetuity, loss of institutional control and/or societal memory of the disposal facility are unlikely to occur, and future release of radionuclides or other public exposure risks are likely to be identified and addressed.

1.4 LLW DISPOSAL FACILITY LIFE CYCLE AND CLOSURE PLAN

EMDF will begin accepting waste after the first phase of construction is completed, projected for the late-2020s timeframe. The current scope of ORR cleanup work is projected to be completed by approximately 2050; therefore, the expected period of EMDF operations is approximately 25 years. Construction of the EMDF is planned in three phases, proceeding from the upper (northern) to lower (southern) disposal cell. As each of the four individual disposal cells is filled to design capacity, an interim cover will be put in place to limit infiltration and leachate generation from that portion of the disposal facility. The EMDF interim cover design is assumed to be similar to that implemented for the EMWMF, which consists of a geotextile separator layer and an approximately 1-ft-thick contouring soil layer on top of the waste, overlain by a temporary flexible geomembrane to minimize infiltration into the waste zone.

EMDF closure activities will involve construction of the final cover system and removal of any unneeded infrastructure. Post-closure activities will involve cap maintenance, continued leachate collection and management, and site environmental monitoring. Final closure plans will be detailed in approved documents required under DOE orders and manuals and by the FFA (DOE 1992a). Post-closure performance monitoring will include CERCLA 5-year reviews of remedial effectiveness.

1.5 REGULATORY CONTEXT

The regulatory context for the EMDF PA is primarily set by DOE M 435.1-1 performance requirements. Additional regulatory requirements that could influence the EMDF PA analyses may be included in future documents required for authorization of EMDF operations under the FFA, including, but not limited to, the EMDF ROD, remedial design documentation, and WAC development and compliance documentation. The EMDF RI/FS includes remedial action objectives (DOE 2017b, Sect. 4) and a preliminary set of applicable or relevant and appropriate requirements (ARARs) for the disposal facility (DOE 2017b, Appendix G). Final FFA determination of the remedial action objectives, ARARs for EMDF, and a general framework for WAC development will not be available until the EMDF ROD is approved.

1.5.1 Performance Objectives

EMDF performance objectives for the PA analysis are summarized in Table 1.1. The performance objectives are taken directly from DOE M 435.1-1 and do not reflect any site-specific regulatory requirements other than the application of drinking water maximum contaminant levels (MCLs) for water resources protection objectives. EMDF performance with respect to the performance objectives or performance measures is based on PA model results for specific environmental media, transport pathways, and exposure scenarios. The period during which compliance with performance objectives must be demonstrated is 1000 years post-closure.

All Pathway: Meeting this performance objective provides a reasonable expectation that representative members of the public will not receive more than 25 percent of the primary dose limit of 100 mrem in a year from the disposal of LLW. The requirement addresses the annual total effective dose, inclusive of all potential exposure pathways except for dose from radon and its decay products in air. For the EMDF PA, the all-pathways dose considers exposures resulting from releases to groundwater and surface water only.

Air Pathway: Meeting this performance objective provides a reasonable expectation that representative members of the public will not receive, from the disposed waste, via the air pathway alone, more than 10 mrem in a year, excluding the dose from radon and its progeny. For the EMDF PA, the engineered cover system is credited for eliminating exposure via the air pathway. Justification for this assumption is provided in Sect. 3.2.2.2.

Radon Release: Meeting this performance objective provides a reasonable expectation that radon, either as a constituent of waste at the time of disposal or produced by radioactive decay following disposal, is not released from the disposal facility at a rate that would exceed the limit established in 40 *Code of Federal Regulations* (*CFR*) Part 61, Subpart Q, *National Emission Standards for Radon Emissions from Department of Energy Facilities*. The limit on ground emanation of radon (radon flux per area) is applied to the EMDF cover surface.

Water Resources Protection: Site-specific application of regulatory standards for groundwater resources is limited to assessment of compliance with MCLs for drinking water specified by EPA in the Radionuclides Final Rule (EPA 2000), promulgated in 40 *CFR* 141.66, for which the State of Tennessee has primary enforcement responsibility. Limits are specified for combined Ra-226 and Ra-228 activity concentration,

gross alpha activity concentration, total annual dose from beta decay and photon emission, and total uranium (Table 1.2). The EMDF PA demonstrates that groundwater at 100 m from the waste boundary meets these limits.

Table 1.2. Exposure scenarios, performance objectives and measures, and POAs for the EMDF PA

Exposure scenario	Performance objective or measure	POA
All pathways	25 mrem/year	Groundwater: 100 m from waste margin at the point of maximum concentration (plume centerline)
		Surface water: Bear Creek downstream of NT-11
Air pathway[a]	10 mrem/year[b]	100 m from waste margin
Radon flux	20 pCi/m^2/sec	EMDF cover surface
Water resources (groundwater)		Groundwater at 100 m
• Ra-226 + Ra-228	5 pCi/L	
• Gross alpha activity[c]	15 pCi/L	
• Beta/photon activity	4 mrem/year	
• H-3	20,000 pCi/L	
• Sr-90	8 pCi/L	
• Uranium (total)	30 µg/L	
Water resources (surface water)	DOE *Derived Concentration Technical Standard*[d]	Bear Creek at NT-11 tributary junction
Inadvertent human intrusion		
• Chronic exposure	100 mrem/year	At EMDF
• Acute exposure	500 mrem	At EMDF

[a]Air pathway is screened from the EMDF PA.
[b]Excluding radon in air.
[c]Including Ra-226, but excluding radon and uranium.
[d]DOE 2011b.

DOE = U.S. Department of Energy   PA = Performance Assessment
EMDF = Environmental Management Disposal Facility   POA = point of assessment
NT = North Tributary

In the absence of local radiological standards for surface water protection, *Derived Concentration Standards* (DCS) (DOE 2011b) are adopted for purposes of evaluating impacts to surface water resources. The impact of any future regulatory agreements regarding surface water protection standards will be evaluated.

1.5.2   POA and Timeframes for Analysis

POAs are provided for each exposure scenario shown in Table 1.2. For the EMDF PA, the POAs are identical to DOE M 435.1-1 requirements and consistent with the Disposal Authorization Statement and Tank Closure Documentation standard (DOE 2017a). The POAs do not vary with the post-closure time period, even though expected future land use and institutional controls (refer to Sect. 1.6) would preclude public exposure at the 100-m buffer zone boundary for as long as waste remains above unrestricted use criteria in the area (as required under CERCLA). Institutional controls limiting site access are assumed to be effective for 100 years following closure. These assumptions are pessimistic given that DOE is required to maintain control over land containing radionuclide sources until the land can be safely released pursuant

to DOE O 458.1, *Radiation Protection of the Public and the Environment*, and CERCLA. Additional consideration of land use and institutional controls is provided in Sect. 1.6 of this report.

Compliance with performance objectives and measures is based on PA results for the period from EMDF closure to 1000 years post-closure, with the exception of the IHI analysis for which compliance is assessed beginning at the assumed end of institutional control (100 years). Quantitative dose estimates are presented for a period of 10,000 years post-closure to provide perspective on the potential impacts beyond the 1000-year compliance period. For long-lived, relatively immobile species (e.g., radionuclides of uranium) that are significant components of the estimated EMDF inventory, PA model saturated zone concentration results beyond 10,000 years are also provided. These model predictions for the period beyond 10,000 years are highly uncertain and are presented only to indicate very long-term trends, rather than for comparison to regulatory standards.

1.5.3   Inadvertent Intrusion

Analysis of performance relative to hypothetical future IHI at EMDF is based on the performance measures for acute and chronic exposures specified in DOE M 435.1-1 and listed in Table 1.2. The EMDF PA considers two acute exposure scenarios (excavation and discovery, and well drilling) and one chronic scenario (post-drilling agricultural) consistent with the guidance in *Disposal Authorization Statement and Tank Closure Documentation* (DOE 2017a). IHI is assumed to occur after 100 years post-closure as a result of a temporary loss of institutional control of the CBCV site. IHI at EMDF is highly unlikely given that DOE is required to maintain control over land containing radionuclide sources until the land can be safely released pursuant to DOE O 458.1 and that CERCLA requires remediated sites be monitored until shown to be acceptable for unrestricted use. The extremely pessimistic biases in the IHI analysis assumptions are discussed in Sect. 6 and Appendix I.

A compliance period of 1000 years post-closure is considered for purposes of assessing EMDF performance relative to IHI performance measures. To provide perspective on potential impacts to human intruders beyond 1000 years, IHI model results are presented for a period of 10,000 years post-closure.

1.5.4   As Low As Reasonably Achievable Analysis

The as low as reasonably achievable (ALARA) process (DOE 2013a) is used to optimize EMDF performance and maintain doses to members of the public (both individual and collective) and releases to the environment as low as reasonably achievable. DOE M 435.1-1 includes a requirement for an ALARA analysis as part of the PA. The scope of ALARA considerations for the EMDF includes design optimization, disposal protocols for worker and public protection during operations, and the development of WAC by the FFA parties. These three aspects are not included in this ALARA analysis for the EMDF PA, although insights gained from the PA modeling may be relevant to design optimization or to worker protection in the post-closure period. The scope of this ALARA analysis is restricted to: (1) presenting evidence to support the finding that only a qualitative ALARA analysis is required; and (2) describing the CERCLA process for identifying LLW disposal options for the ORR CERCLA cleanup, the basis for the EMDF preliminary design and selection of the CBCV site for EMDF.

The ALARA handbook (DOE 2014) describes a graded approach to implementing the ALARA process, including the use of reference doses for determining the level of analysis required for a given project. The reference dose for a maximally exposed individual (MEI) and the reference collective dose below which only qualitative ALARA analysis is sufficient are 1 mrem/year and 10 person-rem/year, respectively. For a LLW disposal project, the timeframe of consideration for an ALARA analysis of any level should be no greater than 1000 years (DOE 2014, pages 5–8), so estimated EMDF peak dose within 1000 years is compared to the reference values. The EMDF PA modeling predicts a base case all-pathways maximum

individual dose within the 1000-year compliance period of 1.0 mrem/year (Sect. 4.5.1). The results of the probabilistic uncertainty analysis (Sect. 5.4 and Appendix G, Sect. G.6.3.3) suggest a median peak all-pathways dose of 1.0 mrem/year and a mean all pathways dose of 1.0 mrem/year at 1000 years. Based on the guidance in the ALARA handbook, these results for individual exposure indicate that a semi-quantitative ALARA analysis could be considered. However, the ALARA guidance also states that "it is the collective dose that is utilized in the ALARA analysis to select a radiation protection alternative".

Collective exposure was not modeled for the EMDF all-pathways analysis, but, given the likelihood that BCV and the CBCV site will remain under DOE control indefinitely, there are a limited range of collective exposure scenarios that are credible. Based on the assumed resident farmer scenario for the EMDF all-pathways dose analysis, a resident family of four would receive a collective dose of four persons times 1.0 mrem/year, or 4.0E-3 person-rem/year, which is far below the 10 person-rem/year reference value. Assuming a wider area of exposure would increase the potential number of exposed individuals but would decrease the number of significant exposure pathways and the maximum individual dose. The most likely scenario leading to significant collective dose would be a number of recreational fishers eating contaminated fish from Bear Creek. The EMDF PA modeling predicts a peak individual fish ingestion dose (based on a recreational rate of catch and consumption) of 0.25 mrem/year (Sect. 4.5.3). Based on this estimate, 100 recreational fish consumers would receive a collective dose of 2.5E-02 person-rem/year.

Based on the 10 person-rem/year reference value for collective dose, these model-based quantitative estimates indicate that a qualitative ALARA analysis for EMDF design and operations is sufficient. The remainder of the analysis focuses on the process for identifying LLW disposal options for the ORR CERCLA cleanup, the basis for the EMDF preliminary design, and selection of the CBCV site for EMDF.

The EMDF RI/FS includes an analysis of alternatives for disposition of LLW from CERCLA actions on the ORR. The RI/FS includes identification and screening of disposal technologies and process options (DOE 2017b, Sect. 5) and considers broader social, economic, and public policy aspects in the analysis of remedial alternatives (DOE 2017b, Sect. 7). The disposal technology screening and conceptual facility design for the CBCV site (DOE 2017b, Sect. 6) served as the foundation for preliminary engineering design (UCOR 2020b) of the RCRA-type disposal facility at the CBCV site.

The EMDF Proposed Plan (DOE 2018a) describes the remedial action objectives for CERCLA waste disposal and presents onsite disposal at the CBCV site as the preferred (optimal) alternative based on the range of considerations required under CERCLA and the FFA. CERCLA alternative evaluation threshold criteria for remedial actions include overall protection of human health and the environment and compliance with ARARs. Balancing criteria include long-term effectiveness and permanence; reduction of toxicity, mobility, or volume through treatment; short-term effectiveness; implementability, and cost. Considerations of state and community acceptance are incorporated following public review of the Proposed Plan. Thus, the FFA remedy selection process has addressed key considerations for an ALARA analysis and the disposal options considered and conclusions presented in the EMDF RI/FS and Proposed Plan are considered to meet the intent of the DOE ALARA requirements for the EMDF PA.

1.5.5 Other Requirements

1.5.5.1 DOE safety basis requirements for EMDF design

DOE expects safety to be fully integrated into the design process for new facilities. DOE O 413.3B, Chg4 (DOE 2010b) identifies the safety design basis documentation that must be developed to support each stage of a facility design effort. The safety design basis documentation provides a preliminary identification of the required engineered safety design features early in the design process. Hazard categorization and classification is performed in accordance with the methodology described in *Hazard Categorization and*

Accident Analysis Techniques for Compliance with DOE Order 5480.23, Nuclear Safety Analysis Reports (DOE 1997a). The current safety design basis documentation for EMDF includes the *Safety Design Strategy for the Environmental Management Disposal Facility, Y-12 National Security Complex, Oak Ridge, Tennessee* (UCOR 2018a) and a Conceptual Safety Design Report (UCOR 2018b) that provides the initial hazard analysis. Progressively more detailed hazard analysis documents will be developed as the EMDF design process proceeds.

1.5.5.2 Non-DOE requirements

Non-DOE regulatory requirements for design, construction, operation, and closure of EMDF derive from the FFA and CERCLA. Landfill water radiological discharge limits for EMWMF and EMDF are being determined in consultation with the FFA parties and are currently in dispute. Once finalized, the discharge limits could be applied as surface water resources protection objectives for the EMDF.

The EMDF RI/FS contains a listing of potential ARARs (DOE 2017b, Appendix G) for EMDF and analysis of potential compliance with ARARs. The final set of ARARs will be included in the EMDF ROD. Land Disposal Restrictions (LDRs) per 40 *CFR* 268 will be an ARAR for EMDF disposal of waste containing hazardous constituents above regulatory limits (e.g., for mercury). Requirements for treatment to reduce the concentration or mobility of hazardous constituents to meet LDRs will apply to some EMDF waste.

Post-ROD FFA documents will establish additional design and operational requirements for the EMDF based on collaborative discussions among the FFA parties. Future EMDF annual summary reports will include external regulatory requirements that are relevant to PA assumptions and/or the modeling approach. As part of the development of annual summary reports for the EMDF, proposed activities, new ARARs, or other new information that could challenge key assumptions for the EMDF performance analysis will be evaluated in accordance with the EMDF change control process to assess the potential for such changes to require a Special Analysis or revisions to the PA.

1.6 LAND USE AND INSTITUTIONAL CONTROLS

The EMDF site is near existing DOE waste disposal facilities and mission-critical operational facilities at Y-12 and ORNL. BCV will remain under DOE control and within DOE ORR boundaries for the foreseeable future.

Post-closure land use designations and other institutional controls are included in RODs for cleanup actions on the ORR. These controls include property record restrictions, property record notices, and access controls to limit physical access to the EMDF site (Table 1.3). A modification to the Phase I BCV ROD or some other decision document will be needed to extend the area of DOE-controlled restricted industrial use to include the CBCV site. The future land use designations in the ROD are defined solely for the purpose of setting target cleanup levels (acceptable risk criteria) and do not reflect DOE's future land use plans. The EMDF Proposed Plan (DOE 2018a) includes discussion of land use controls for BCV that would apply to the EMDF.

Assumed POAs for the EMDF PA do not take credit for the existence of land use or other institutional controls beyond 100 years post-closure. As such, the likelihood that DOE or successor federal agencies will maintain control of closed waste management facilities in BCV is considered as an aspect of defense-in-depth for the EMDF disposal system.

Table 1.3. Land use controls for EMDF

Type of control	Purposes of control	Implementation	Affected areas[a]
1. Property record restrictions[b]	Restrict use of certain property by restricting soil and groundwater use in perpetuity	Drafted and implemented by DOE upon closure of EMDF and/or transfer	EMDF landfill and site
2. Property record notices[c]	Provide information to the public about the existence and location of waste disposal areas and applicable restrictions in perpetuity	General notice of Land Use Restrictions recorded in Roane County Register of Deeds office upon completion of the remedial activity	EMDF landfill and site
3. Access controls (e.g., signs, fences, gates, portals, etc.)	Control and restrict access to the public in perpetuity	Maintained by federal government and its contractors	EMDF landfill and site

[a]Affected areas – Specific locations will be identified in the completion documents where hazardous waste has been left in place.

[b]Property record restrictions – Includes conditions and/or covenants that restrict or prohibit certain uses of real property and are recorded along with original property acquisition records of DOE and its predecessor agencies.

[c]Property record notices – Refers to any informational document recorded that alerts anyone searching property records to important information about residual contamination/waste disposal areas on the property (TCA requirement).

DOE = U.S. Department of Energy   TCA = Tennessee Code Annotated
EMDF = Environmental Management Disposal Facility

1.7   KEY ASSUMPTIONS AND MANAGING UNCERTAINTY

This section presents eight key assumptions underlying the results of the PA analyses and the compliance conclusions drawn from those results, and addresses the need to manage uncertainty in those assumptions. Section 1.7.1 presents key assumptions concerning model input parameters that could alter the conclusions of the PA concerning EMDF compliance with performance objectives. Section 1.7.2 is a description of key assumptions associated with the conceptual models that underlie the PA analyses. Section 1.7.3 presents a summary of pessimistic biases built into the PA to make the analysis conservative by over-predicting public exposure and dose. Section 1.7.4 summarizes the eight key assumptions in the context of managing uncertainties in the PA analysis.

The key assumptions presented in Sects. 1.7.1 and 1.7.2 comprise the set of critical assumptions against which new information must be reviewed to assess the need for a Special Analysis or revision of the PA. Examples of new information requiring screening or evaluation under the EMDF change control process include proposed design changes, new data relevant to key parameter uncertainties, changes in disposal practices, new regulatory requirements, new waste streams or updated inventory estimates. This summary of assumptions does not encompass specific preliminary design specifications for the EMDF. Any new information that could challenge key assumptions for the EMDF performance analysis will be evaluated in accordance with the EMDF change control process.

1.7.1   Key Parameter Assumptions

Based on the particular conceptual models (Sect. 3.2) and model codes (Sect. 3.3) adopted for the EMDF performance modeling, the assumed range of values for a few key input parameters determines the likelihood of peak all-pathways dose exceeding the 25 mrem/year performance objective during the 1000-year compliance period. Results from the probabilistic uncertainty analysis for the compliance period (Sect. 5.4.1) show peak total doses that exceed 25 mrem/year are associated with I-129 contributions that

occur at the end of the simulation period. Those extreme peaks are rare (< 1 percent of 3000 simulated peaks) and result from lower than average sampled K_d values for I-129 in combination with other factors that favor earlier release and rapid radionuclide transport. Uncertainty in the estimated inventory of dose-significant, mobile radionuclides (C-14, Tc-99, and I-129) is also important to consider in judging the likelihood of EMDF compliance from the results of the compliance period performance modeling. The key parameter assumptions are listed below, and the remainder of Sect. 1.7.1 provides additional detail and context:

1) Iodine-129 partition coefficient (K_d) values for the engineered barriers and geologic materials below the EMDF liner are greater than 1 cm^3/g.

2) IF the I-129 K_d value is less than 1.5 cm^3/g, THEN: the values for the input parameters (refer to following paragraph) that determine cover infiltration, vadose zone thickness, and saturated zone flux (Darcy velocity) satisfy one or more of the following conditions:

    a) Average annual cover infiltration is less than or equal to 0.88 in./year.

    b) The average thickness of the unsaturated zone below the waste is greater than or equal to 31 ft.

    c) The Darcy velocity characterizing long-term average conditions within the saturated zone along the flow path from the waste to the well is greater than or equal to 4.75 ft/year.

3) The estimated post-closure EMDF average I-129 activity concentration is less than 0.41 pCi/g.

K_d for I-129 > 1 cm^3/g. Compliance period peak total doses greater than 25 mrem/year were associated exclusively with sampled I-129 K_d values ≤ 1 cm^3/g, whereas the assumed value for the base case deterministic model run is 2 cm^3/g for the waste and 4 cm^3/g for all other materials. However, not all simulations with sampled I-129 K_d values ≤ 1 cm^3/g are associated with very large peaks because other input parameter also affect the timing and rate of I-129 release or how quickly radionuclides arrive at the groundwater POA. The RESRAD-OFFSITE model input parameter values that favor very large peak doses (for I-129, K_d ≤ 1 cm^3/g) include waste zone properties (large b-parameter and small dispersivity), high cover infiltration (> 0.88 in./year) small (< 800 year) release duration, small (< 16 ft) thickness of unsaturated zone 5, and a combination of small (< 4.75 ft/year) saturated zone Darcy velocity and shallow (< 131 ft) well depth. Uncertainty in most of these input parameters is difficult to quantify or reduce, whereas the uncertainty in I-129 K_d values is essentially a data gap in the PA analysis. Laboratory measurements of Tc-99 and I-129 sorption on Conasauga Group samples have been planned to eliminate this data gap (Sect. 8.3). For the present EMDF performance modeling, adopting an I-129 K_d value > 1 cm^3/g is a key parameter assumption that supports a reasonable expectation of compliance with the 25 mrem/year performance objective during the 1000-year compliance period.

Estimated inventories for mobile radionuclides. There is considerable uncertainty in the estimated activity inventories of C-14, Tc-99, and I-129, which are the three more mobile dose drivers for the performance analysis. The estimated radionuclide inventory for EMDF waste (Appendix B) is biased high (overestimated activity concentrations) to manage uncertainty in future waste characteristics. Carbon-14 and I-129 inventories in particular may be overestimated due to inclusion of some non-representative, high activity data in the analysis. However, operational period losses of mobile radionuclides are estimated (Sect. 2.3) and used to adjust (reduce) the modeled inventories of H-3, C-14, Tc-99, and I-129, which introduces additional uncertainty in the post-closure average concentrations assumed for the highly mobile dose-drivers. For C-14 and Tc-99 the estimated operational losses are high (81 percent and 44 percent respectively), but model sensitivity analysis (Sect. 5.3) and the compliance period distribution of peak total dose (Sect. 5.4.1) suggests that this uncertainty is unlikely to challenge the conclusion that C-14 and Tc-99 dose contributions combined will not exceed the all-pathways performance objective. For I-129, estimated operational losses are small (< 13 percent) due to the assumed K_d value for the waste (2 cm^3/g), so the assumed I-129 activity inventory is still biased high relative to more realistic expectations. The likelihood

that I-129 inventory is overestimated also decreases the probability that a lower than assumed I-129 K_d value will result in the peak compliance period dose exceeding 25 mrem/year. The conclusion is that although post-operational inventory uncertainties for C-14, Tc-99, and I-129 are high, only the assumed EMDF average I-129 activity concentration value applied in the PA models constitutes a key parameter assumption that supports determination of EMDF compliance with the all-pathways performance objective.

1.7.2   Key Conceptual Model Assumptions

Conceptual models for the evolution of EMDF hydrologic performance (Sect. 3.2.1), radionuclide release as engineered barriers degrade (Sect. 3.2.2), and transport of radionuclides upon release to the natural environment (Sects. 3.2.2 and 3.2.3) are the basis for the selection and implementation of computer software (model codes) to simulate EMDF performance. Simplifying assumptions associated with particular conceptual models and codes can constrain the range of PA model results produced to support compliance conclusions. There are a few simplifying assumptions that apply to the EMDF performance analyses for which alternative conceptualizations (different assumptions) could affect the PA results, if not the conclusions concerning EMDF compliance. The PA model sensitivity and uncertainty evaluations (Sect. 5) are performed to address uncertainty in conceptual models.

1) **Failure of Engineered Barriers**. The PA modeling assumes that post-closure degradation of the EMDF cover and liner systems occurs gradually due to the cumulative effect of environmental processes (e.g., cover erosion, waste settlement, oxidation and stresses on the high-density polyethylene [HDPE] layer) on the properties of engineered materials (Sect. 3.3.1). Progressive failure of engineered barriers results in increasing cover infiltration and leachate release. The assumed rate of degradation (see item #2 below) is highly pessimistic based on reasonable expectations for the performance of HDPE membranes and clay infiltration barriers. The EMDF preliminary engineering design (including seismic stability evaluations) is assumed to prevent sudden EMDF failure due to extreme (very low probability) seismic or weather events.

2) **Cover System Performance.** The EMDF final cover design is assumed to effectively prevent significant release of radionuclides through the cover to the atmosphere and biosphere (Sect. 3.2.2). Failure of the cover (increasing infiltration) due to HDPE and clay barrier degradation begins at 200 years post-closure. Cover infiltration increases gradually to a maximum average annual long-term value of 0.88 in./year at 1000 years post-closure. Sensitivity to uncertainty in the potential impacts of release through the cover was evaluated to support screening of that release pathway from the PA analysis (Sect. 3.2.2.3). Sensitivity to uncertainty in the timing and duration of cover performance degradation and the magnitude of long-term cover infiltration was evaluated for the PA models (Sect. 5).

3) **Liner System Performance.** The base case EMDF performance scenario assumes that during the post-closure period after leachate collection ends, the liner system will release leachate at a rate sufficient to prevent waste saturation and overtopping of the liner (bathtub conditions). The potential impact of a persistent bathtub condition leading to leachate release at the cover surface is analyzed in Appendix C, Sect. C.3.

4) **Radionuclide Release.** In the PA models, the EMDF waste volume is conceptualized as a homogeneous, soil-like material in which the estimated radionuclide inventory is uniformly distributed. This conceptual model includes an assumption about the mass of clean fill material that is required to minimize void space and limit post-closure waste settlement. Estimated waste average activity concentrations are adjusted (reduced) to account for this mass of clean fill (Sect. 3.2.2.5). Radionuclide release from the waste is based on equilibrium partition between the solid and aqueous phases and assumes that a concentration-independent K_d adequately captures the desorption process (Sect. 3.2.2.6). To account for uncertainty in waste geochemistry and release kinetics, the waste K_d values are reduced

by a factor of two from the assumed base case values; this is a pessimistic approach because it is likely that sorption by the clean fill emplaced with the waste will be substantial. This conceptual model does not account for the variety of different waste forms (e.g., contaminated demolition debris and equipment) or the effect of waste containers, waste stabilization (grouting), or treatment to reduce the mobility of radionuclide in EMDF waste (Sect. 1.7.3, item #5). The sensitivity of RESRAD-OFFSITE model results to assuming alternative release models (Sect. 5.3) was evaluated to account for the possibility that these waste forms would tend to delay and/or retard the release of radionuclides.

5) **Uniform Release to Groundwater**. The sloping geometry of the EMDF liner system, heterogeneity in activity concentrations, and the possibility of spatially variable failure (leakage) of the cover and liner systems over time could cause non-uniform radionuclide release from the waste to the underlying vadose zone. The STOMP model (Sect. 3.3.2) is used to capture the impact of the sloping liner and variable waste thickness on the release pattern, but assumes homogenous activity concentrations in waste and uniform cover infiltration. The MT3D saturated zone radionuclide transport model (Sect. 3.3.3.2) is used to evaluate the difference between a uniform release conceptual model and a simplified non-uniform release conceptualization. Those results (Sect. 5.2.2) and the STOMP model release simulations are compared to total system model (RESRAD-OFFSITE) results that assume uniform radionuclide release and incorporate less detailed, semi-analytical models of transport through the vadose and unsaturated zones. The comparison of model results (Sect. 3.3.5) is the basis for ensuring that the RESRAD-OFFSITE uniform release model and simplified representation of the transport pathways do not under predict peak radionuclide concentrations at the groundwater POA. This model integration process served to manage uncertainty about the uniformity of release by demonstrating that the uniform release assumption would lead to earlier and higher peak concentrations at the POA.

1.7.3   Pessimistic Biases Intended to Make the Analysis Conservative

There are a number of important assumptions made that are intended to bias the analysis to predict higher potential exposure and dose. These assumptions are adopted to manage the uncertainty in future waste characteristics and public exposure scenarios.

1) **Institutional control of the EMDF**. The PA analyses assume loss of institutional control by DOE or successor agencies at 100 years post-closure. DOE O 458.1 requires that DOE maintain control over sites until they can be released, and public knowledge of the activities at the Oak Ridge site would be expected to persist well into the future. Thus, it is more likely that institutional and societal knowledge of the facility and radiation risks would persist over multiple centuries and that efforts to maintain facility performance to protect the public will continue.

2) **Early cover system failure.** The PA base case modeling pessimistically assumes that significant degradation of the EMDF cover system begins 100 years after the loss of institutional control (i.e., 200 years post-closure). The conceptual model also assumes that complete degradation (maximum long-term cover infiltration) occurs by 1000 years post-closure. These assumptions result in relatively early peak concentrations at the POA locations. Based on the potential for long-term institutional control (refer to item #1 above) and extended performance of cover components (> 1000 years; Appendix C, Section C.1.2), it is likely that the cover system performance will be much better over the 1000-year compliance period than is assumed for the PA. Radionuclide release over a period longer than 800 years could also reduce peak environmental concentrations and dose impacts compared to the base case assumption.

3) **Exposure scenario**. The exposure scenario for the all-pathways dose analysis assumes an MEI rather than a more representative future member of the public. The receptor is assumed to be a farming household member (residential farmer) that drinks contaminated groundwater from a well at 100 m

from the waste at the location of maximum radionuclide concentration. The receptor also consumes plant and animal foods grown onsite using contaminated Bear Creek water for irrigation and watering livestock. The assumed proximity of the groundwater POA (100 m) and surface water POA (approximately 300 m) to the facility is extremely pessimistic, even in the absence of institutional controls on site access (refer to item # 1 above). These MEI and POA assumptions result in higher dose predictions than would similar public exposure scenarios with equally likely assumptions regarding human behaviors and exposure locations.

4) **Estimated radionuclide inventory.** Modeled radionuclide inventories are based on the full EMDF waste volume capacity (2.2 million cy), and average activity concentrations for EMDF waste streams are likely over-estimated. The EMDF design capacity incorporates an added 25 percent to the projected CERCLA waste volume (DOE 2017b, Appendix A) to account for volume uncertainty. The approach to estimating activity concentrations in waste is intended to overestimate concentrations to account for uncertainty in the characteristics of future remediation waste (Appendix B). As a result, the activity inventories used in the PA models are higher than inventories likely to be present at EMDF closure.

5) **Waste containers and stabilization.** The conceptual model of radionuclide release from waste disposed in EMDF (Sect. 1.7.2, item #4) incorporates no assumptions to account for (credit) the use of waste packaging (containers), waste stabilization (e.g., grouting in the disposal facility), or treatment to reduce the mobility of contaminants. It is likely that these waste disposal practices would delay and/or retard the release of radionuclides, and possible that peak concentrations at the POA locations would be delayed and/or decreased relative to the results of the PA modeling.

1.7.4 Summary of Key Assumptions in the PA

Key parameter assumptions for EMDF compliance include:

1) Iodine-129 partition coefficient (K_d) values for the engineered barriers and geologic materials below the EMDF liner are greater than 1 cm^3/g.

2) IF the I-129 K_d value is less than 1.5 cm^3/g, THEN: the values for the input parameters (refer to following paragraph) that determine cover infiltration, vadose zone thickness, and saturated zone flux (Darcy velocity) satisfy one or more of the following conditions:

   a) Average annual cover infiltration is less than or equal to 0.88 in./year.

   b) The average thickness of the unsaturated zone below the waste is greater than or equal to 31 ft.

   c) The Darcy velocity characterizing long-term average conditions within the saturated zone along the flow path from the waste to the well is greater than or equal to 4.75 ft/year.

3) The estimated post-closure EMDF average I-129 activity concentration is less than 0.41 pCi/g.

Uncertainty in these three key assumptions will be addressed with laboratory measurements of iodine K_d for CBCV site materials and by future refinements in the estimated I-129 inventory.

Conceptual models of the evolution of engineered barrier performance and radionuclide release are important for understanding the implications of selecting once conceptualization versus another, and for integrating model codes that apply different conceptual models or levels of detail. Key assumptions related to conceptual models adopted for the PA analysis include:

1) **Failure of engineered barriers.** Post-closure degradation of the EMDF cover and liner systems occurs gradually and results in increasing cover infiltration and leachate release.

2) **Cover system performance.** The EMDF final cover will prevent significant release of radionuclides to the cover surface. Infiltration barriers in the cover fail completely within 1000 years and cover infiltration increases gradually to a maximum average annual long-term value of 0.88 in./year at 1000 years post-closure.

3) **Liner system performance.** The liner system will release leachate at a rate sufficient to prevent waste saturation and overtopping of the liner (bathtub conditions).

4) **Radionuclide release.** EMDF waste is conceptualized as homogeneous, soil-like material in which the estimated radionuclide inventory is uniformly distributed. Radionuclide release from the waste is modeled as equilibrium desorption from a soil-like material.

5) **Uniform release to groundwater.** Radionuclide release from the waste and liner system to the vadose and saturated zones is spatially uniform. Non-uniform release does not result in earlier or larger peak concentrations at the POA locations.

Model sensitivity and uncertainty analyses in the PA (Sect. 5) are completed to assess and manage uncertainty in key parameter and conceptual model assumptions. The potential for new information to challenge PA key assumptions will be evaluated in accordance with the EMDF change control process. Several important pessimistic assumptions regarding the exposure scenario, radionuclide inventories, long-term cover performance, and waste characteristics are incorporated in the PA to account for uncertainty in future human behavior and waste management practices (e.g., waste treatment and containerization). These pessimistic assumptions bias the analysis toward larger estimated all-pathways dose.

This page intentionally left blank.

2.   SITE AND FACILITY CHARACTERISTICS

This section provides detailed descriptive information and data for the EMDF site, the local environment, and the disposal facility to provide the basis for the conceptual model(s) of the disposal system. A total systems perspective is provided, recognizing the interrelationship of site characteristics and the conceptual facility design, including reasonably foreseeable natural processes (e.g., climate impacts) that might disrupt natural and engineered barriers.

2.1   SITE CHARACTERISTICS

2.1.1   Geography, Demographics, and Land Use

2.1.1.1   Site description

The proposed EMDF site is located on the 33,542-acre ORR within the city limits of Oak Ridge, Tennessee, approximately 12.5 miles west-northwest of Knoxville, Tennessee, in Roane and Anderson counties. The regional setting is shown on Fig. 2.1, including the Lower Clinch and Tennessee Rivers and the locations of the three DOE sites (ETTP, ORNL, and Y-12) within the ORR. The proposed EMDF will be located on DOE property approximately 3 miles southwest of Y-12. BCV between Y-12 and the CBCV site (Fig. 2.2) is a historical waste management area that contains several closed disposal facilities, contaminant source areas, and groundwater contaminant plumes, in addition to the currently operating EMWMF.

The ORR is located in the western portion of the Valley and Ridge physiographic province, which is characterized by long, parallel ridges and valleys that follow a northeast-to-southwest trend. The ground elevations within the ORR range from a low of 750 ft above mean sea level (MSL) along the Clinch River to a high of over 1300 ft above MSL on Copper Ridge. The Valley and Ridge physiographic province developed on thick, folded, and thrust-faulted beds of sedimentary rock deposited during the Paleozoic era. Thrust fault patterns and the strike and dip of the beds control the locations, shapes, and orientations of the ridges and intervening valleys. The topography of the BCV watershed and surrounding areas along with underlying geologic units is illustrated in Fig. 2.2. Additional detail on the local topography in relation to geologic features is provided in Sect. 2.1.3.1.

BCV is approximately 10 miles long and extends from the topographical divide near the west end of the Y-12 industrial area to the Clinch River. The valley is bounded by Pine Ridge on the northwest and Chestnut Ridge on the southeast. Bear Creek drains to the southwest along the lower elevation southeast margin of the valley. Elevations range from highs near 1260 ft along the crest of Pine Ridge to around 800 ft where Bear Creek exits BCV through the water gap in Pine Ridge at State Route (SR) 95. The topographic relief between valley floors and ridge crests is generally on the order of 300 to 350 ft. Several smaller tributaries, designated as the North Tributaries (NTs) (numbered sequentially as NT-1, -2, etc. from northeast to southwest) drain southward into Bear Creek from Pine Ridge across the geologic strike of the valley. The proposed EMDF site is located between Bear Creek tributaries NT-10 and NT-11 on the discontinuous ridge that lies between Pine Ridge and Bear Creek (Fig. 1.2).
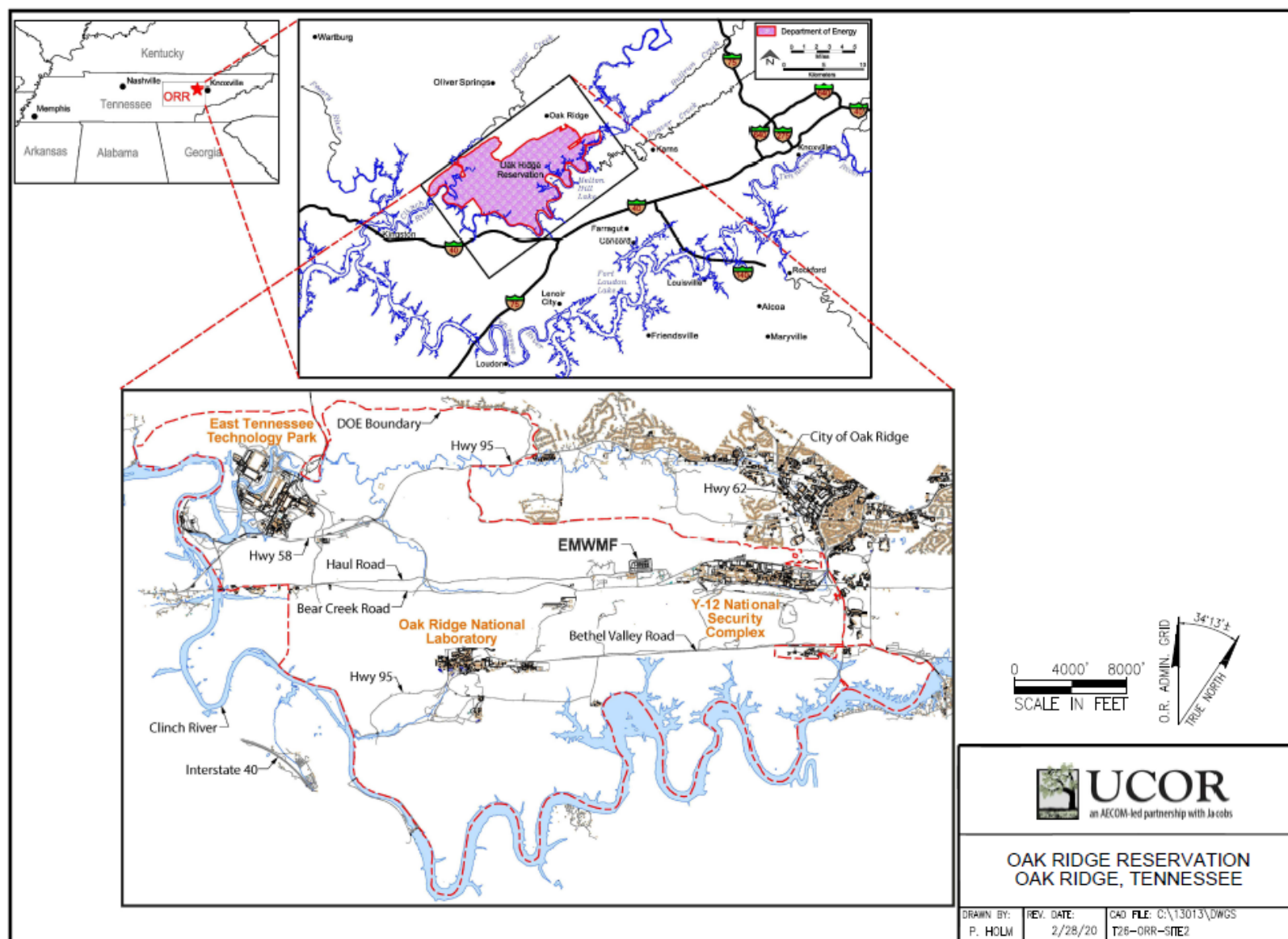
Fig. 2.1. ORR, EMWMF and nearby population centers

N
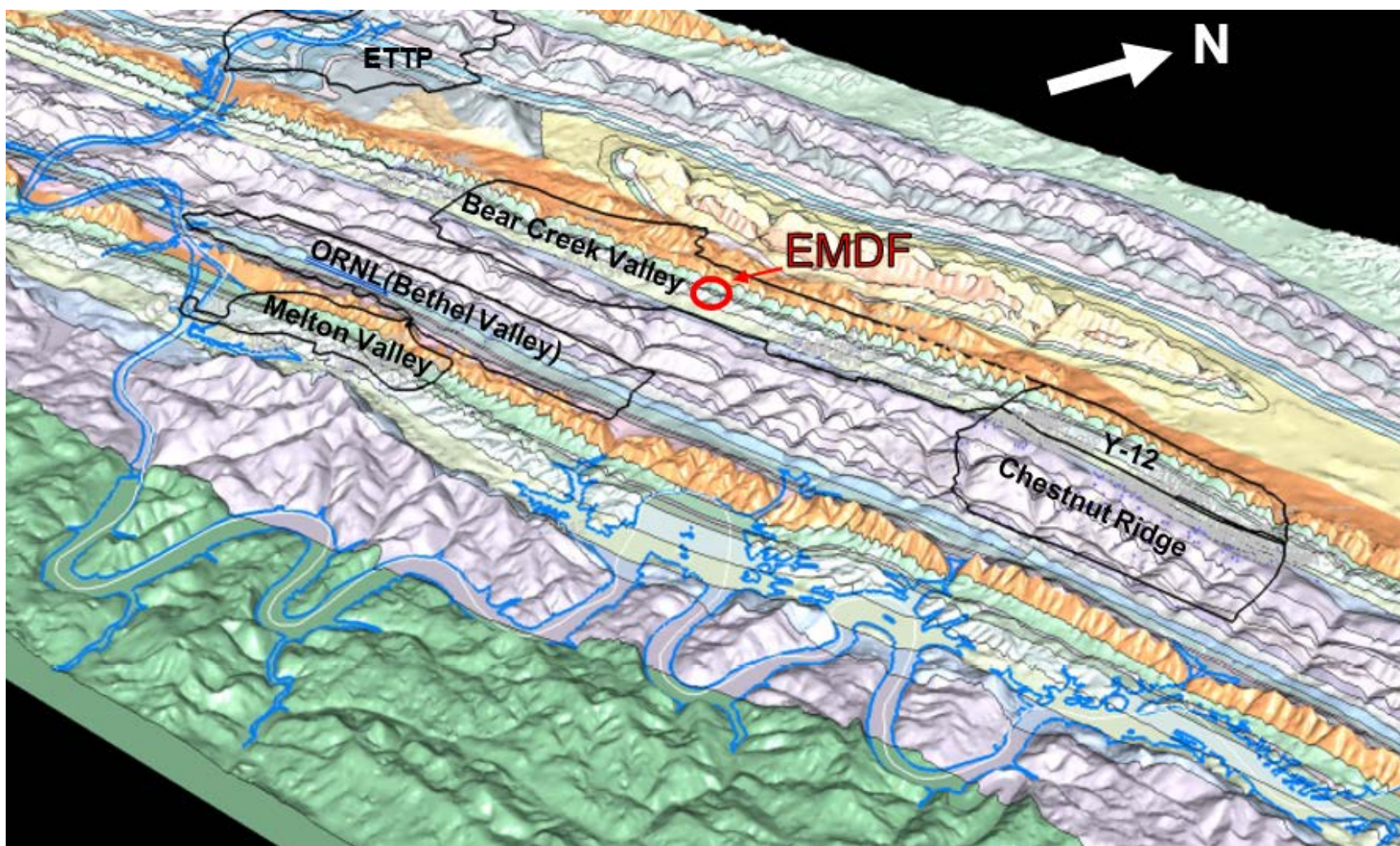
Fig. 2.2. Perspective view of topography and geologic units underlying the ORR, with CERCLA administrative watershed boundaries and EMDF location

2.1.1.2   Population distribution

The five Tennessee counties surrounding the proposed EMDF site (Anderson, Knox, Loudon, Morgan, and Roane) have a total 2010 census population of 632,079 and over 286,000 housing units. The basic demographic data for the five-county area is summarized in Table 2.1.

**Table 2.1. Total 2010 population
in five nearest counties**

County	Population	Housing units
Anderson	75,129	34,717
Knox	432,226	194,949
Loudon	48,556	21,725
Morgan	21,987	8,920
Roane	54,181	25,716
TOTALS	**632,079**	**286,027**

Source: U.S. Census Bureau, 2010 Census.

Oak Ridge, the nearest city, has a population of 29,330 (2010 census), of which 3059 reside in Roane County and the remaining 26,271 reside in Anderson County (Fig. 2.3). The proposed EMDF site lies in Roane County census tract 9801, which has no residential population. Populations of adjoining census tracts are provided in Tables 2.1 and 2.2. Roane County census tract 301 is closest to the proposed EMDF site and had a 2010 population of 3224. This tract includes the entire west end of Oak Ridge east of the Clinch River. Tract 301 had a population density of 459 persons/sq mile in 2010. Anderson County census Tract 201 is closer to the EMWMF site and had a population of 3111 in 2010. The 2010 population density for tract 201, which includes much of the center of Oak Ridge, is 585 persons/sq mile. Tract 9801 includes the DOE property in Anderson and Roane counties and has a residential population of zero. The U.S. Census Bureau projected that Anderson County population would grow by 19 percent from 2010 (75,129) to 2064 (89,814), and that Roane County population (54,181) would decline by about 10 percent over the same period (53,373).

The age distribution for Oak Ridge is skewed towards an older population than for the state of Tennessee as a whole, with slightly lower percentages in the age groups from birth to age 44 and slightly greater population in the age groups from age 45 to over age 85. The gender distribution for Oak Ridge is similar to that of the rest of Tennessee. The estimated 2017 racial composition of Oak Ridge is 78.2 percent white, 7.0 percent Hispanic, 6.8 percent black, 3.5 percent Asian, and 0.4 percent other races. About 4.4 percent of the population identifies as mixed race (City Data 2020).

Population Density in Persons per Square Mile
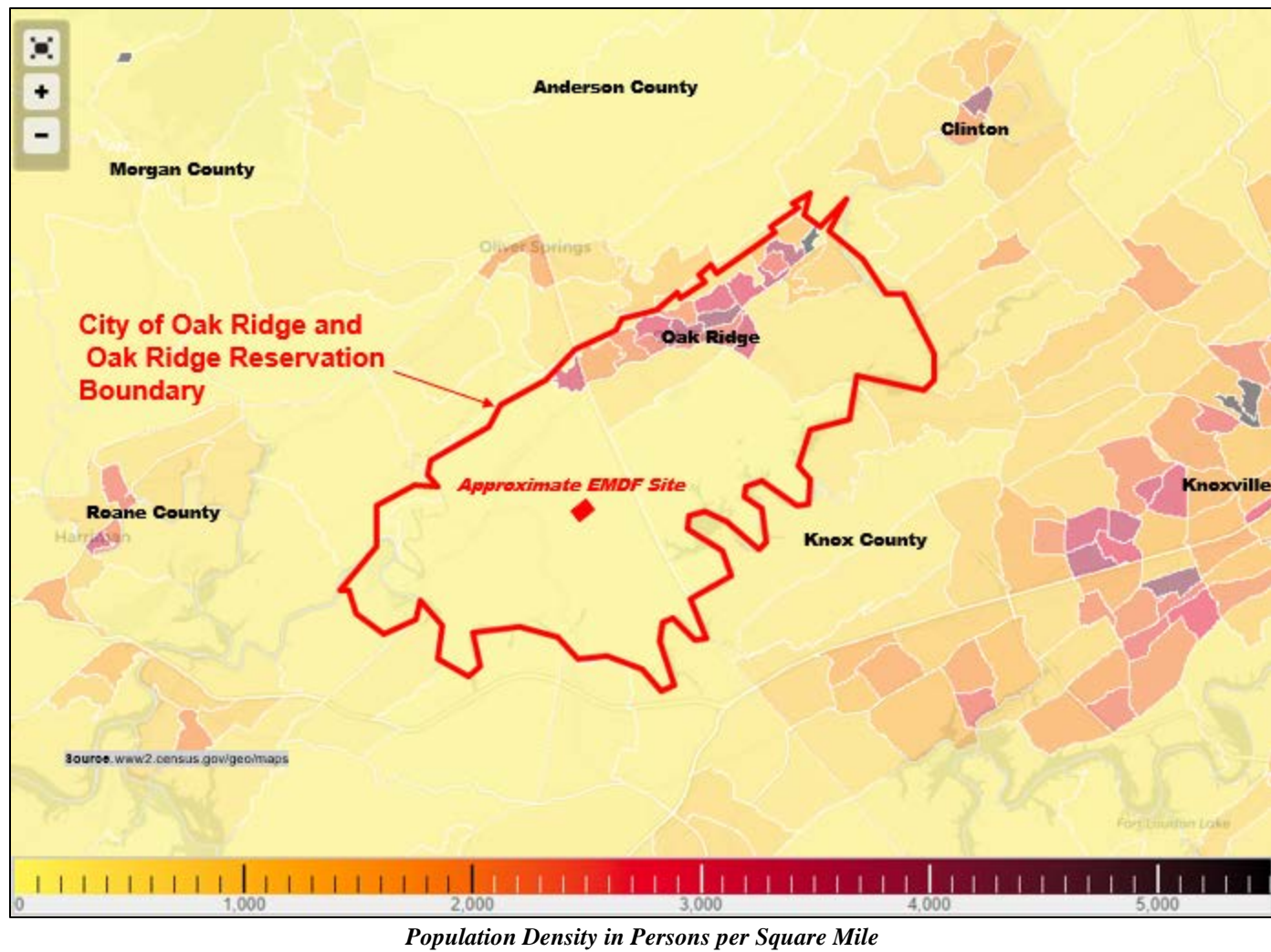
Fig. 2.3. Population density by census block group in the vicinity of the ORR

**Table 2.2. Population data for adjacent census tracts
in the 2010 census**

County	Tract	2010 population
Anderson	201	3111
	202.01	3670
	202.02	4507
	9801	0
Roane	9801	0
	301	3224
Knox	59.06	1671
	59.07	2970

Source: U.S. Census Bureau, 2010 Census.

DOE and DOE contractors employ a large proportion of the local work force. The number of employees involved in DOE OREM work during 2009 was 13,621. This total includes both federal and contractor employees. Employees reside in over 20 counties (Fig. 2.4). Knox, Anderson, and Roane counties together are home to about 82 percent of these employees. The top five counties account for 89 percent of employees and 92 percent of the 2009 DOE payroll. Payroll data for the top five counties in 2012 are provided in Table 2.3.
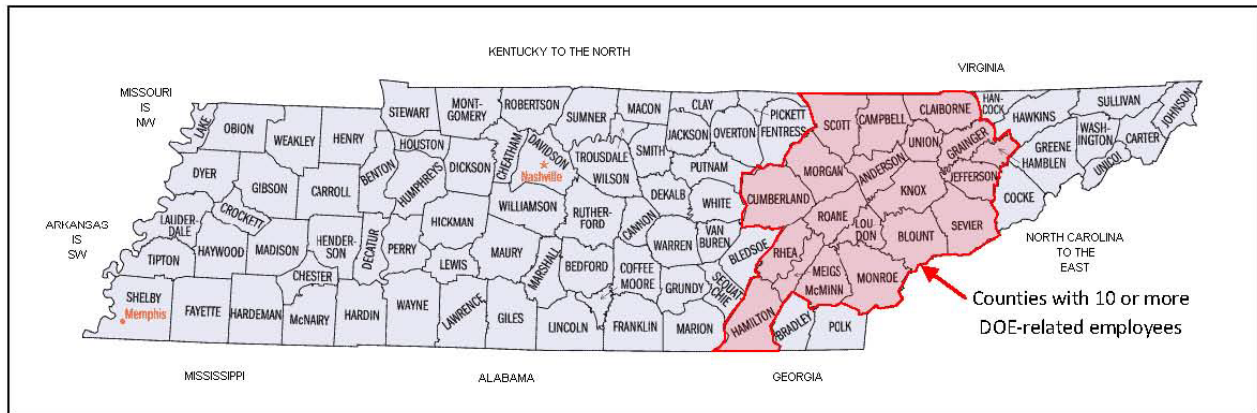
Fig. 2.4. Tennessee counties in which 10 or more OREM employees lived during 2012

**Table 2.3. DOE OREM employees and payroll
for the top five counties in 2012**

County	2012 employees	2012 payroll
Knox	5721	$511,329,075
Anderson	3065	$246,469,051
Roane	1978	$157,088,580
Loudon	669	$56,489,413
Blount	405	$31,332,173

Source: http://www.oakridge.doe.gov/external/portals/0/hr/12-31-12%20payearoll%20&%20residence.pdf.

DOE = U.S. Department of Energy
OREM = Oak Ridge Office of Environmental Management

2.1.1.3 Use of adjacent lands

DOE Land Use Near the EMDF Site. The land on the ORR is used for multiple purposes to meet the mission goals and objectives of DOE, and approximately one-third of the land (11,300 acres) is thoroughly developed for research and operations (ORNL 2002) as ETTP, ORNL, and Y-12. Uses of the land area surrounding the developed DOE facilities include national security activities, site safety and security operations, and emergency planning; research and education; environmental cleanup and remediation; environmental monitoring; wildlife management; biosolids land application; protection of cultural and historic resources; wildland fire prevention; land-stewardship activities; use and maintenance of reservation infrastructure; and activities in public areas (DOE 2008). Biological and ecological research also occurs within in the large-scale Oak Ridge Environmental Research Park (ORERP), which encompasses the majority of the ORR's 20,000 acres (DOE 2011c). The ORERP, established in 1980, is used by the nation's scientific community as an outdoor laboratory for environmental science research on the impact of human activities on the eastern deciduous forest ecosystem.

The EMDF site is near existing waste disposal facilities, the operational area of Y-12, and the Spallation Neutron Source at ORNL (SNS on Fig. 2.5), and will remain under DOE control and within DOE ORR boundaries for the foreseeable future. The Phase I BCV I ROD (DOE 2000) divides the BCV watershed into three zones to set cleanup goals and define residual risks following remediation. The proposed EMDF site is located in Zone 2, which requires cleanup levels that meet future recreational use in the near-term and unrestricted use in the future. The EMDF ROD will modify the land use to extend Zone 3 (designated future cleanup to a land use of "Controlled Industrial Use" in the Phase I BCV ROD) to encompass the EMDF site.

Existing source areas and groundwater contaminant plumes from the S-3 Ponds and former Boneyard/Burnyard, Oil Landfarm, and Bear Creek Burial Grounds (BCBG) disposal sites are all hydraulically upgradient of the proposed EMDF site. Implications of this historical contamination into the protectiveness assessment are presented in the CA and will be considered when designing future EMDF performance monitoring.

Non-DOE Land Use Near the EMDF. Land uses nearby, but outside of ORR, are predominantly rural, with agricultural and forest land dominating, and urban development within adjacent portions of the city of Oak Ridge. The residential areas of the city of Oak Ridge that abut the ORR are primarily along the northern and eastern boundaries of the reservation (Fig. 2.3). Some Roane County residents have homes adjacent to the western boundary of the ORR.

The EMDF site in relation to the nearest residential areas bordering the DOE property boundary to the north (areas to the south of BCV include non-residential DOE controlled land) is shown in Fig. 2.5. The nearest Oak Ridge communities include Country Club Estates (0.8 mile away on the north side of Pine Ridge) and the historic Scarboro community (3.5 miles away), as well as isolated homes located across the more rural intervening area. Pine Ridge separates these residential areas from Y-12 and BCV. Groundwater and surface water flow directions and prevailing wind patterns would move any EMWMF or EMDF releases away from these residential areas. Future development in these areas may increase populations near the EMDF site, but residential use of the adjacent property will not be impacted by EMDF operations.
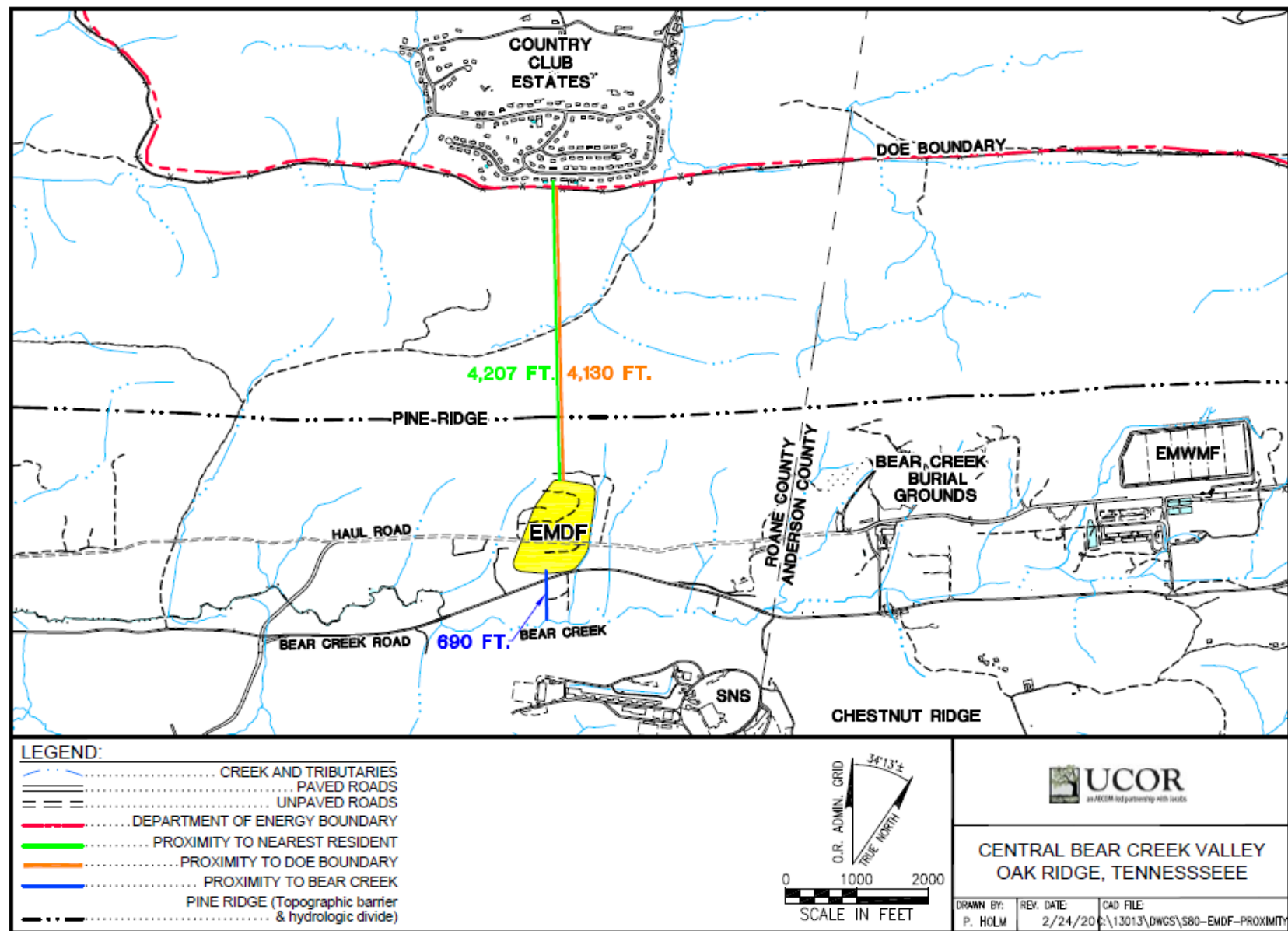
Fig. 2.5. DOE boundary and residential land use near the EMDF site in Bear Creek Valley

2.1.2   Meteorology and Climatology

The Oak Ridge area climate may be broadly classified as humid subtropical (Parr and Hughes 2006). The region experiences warm to hot summers and cool winters. Abundant climate data are available from the National Oceanic and Atmospheric Administration stations in Oak Ridge and ORNL, which operates seven meteorological towers scattered over the ORR. The summary of climate information provided in this section is limited to precipitation records to support hydrologic model inputs for the EMDF PA.

Current climate normal values (1981 to 2010) from the National Weather Service (NWS) for the Oak Ridge area are 50.91 in. for annual precipitation and 58.8°F for mean annual temperature. Precipitation is distributed uniformly through most of the year, with normal monthly precipitation for August through October averaging about 1 in. lower than during other months (Fig. 2.6). These 3 months of lower precipitation and high temperatures tend to comprise a seasonal dry period in which evapotranspiration losses are large relative to inputs of rainfall.
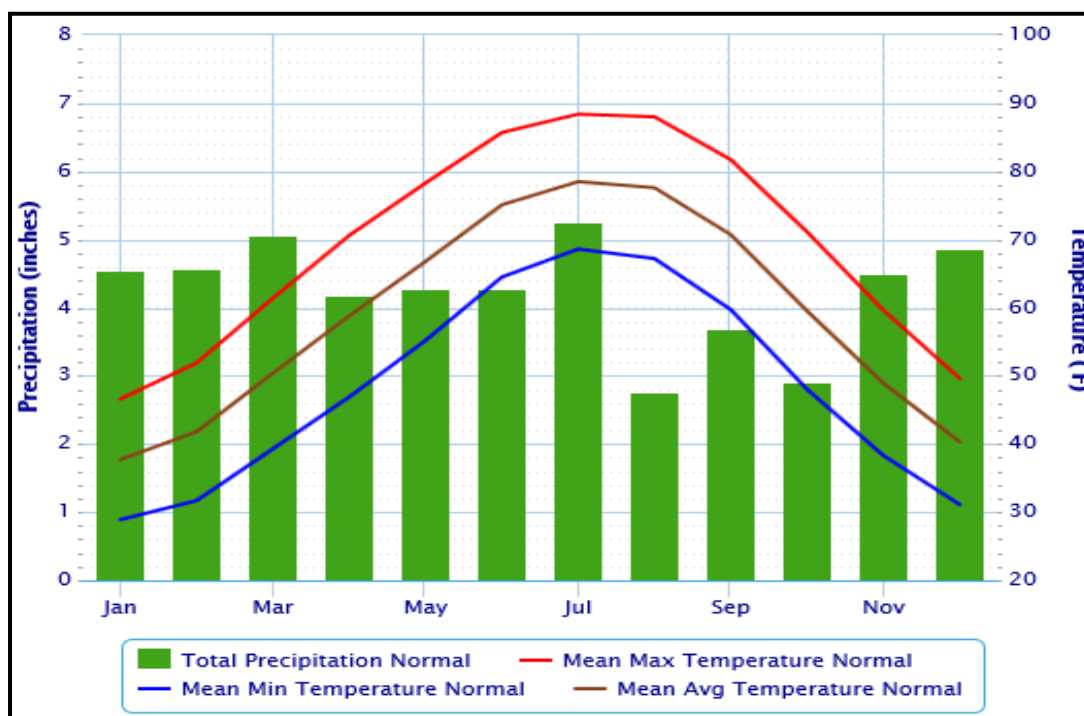
(Source: National Atmospheric and Oceanic Administration – NWS)

Fig. 2.6. Monthly climate normals (1981 to 2010), Oak Ridge area, Tennessee

Local inter-annual variability in precipitation is significant. For the NWS meteorological station in Oak Ridge (KOQT), precipitation records from 1999 through 2013 show a range in annual totals from 34.9 in. (2007) to 71.1 in. (2011), with the average annual total of 54.7 in. (Fig. 2.7). Precipitation records assembled from Oak Ridge and nearby stations for the 68-year period from 1948 to 2015 indicate minimum, average, and maximum annual precipitation totals of 35.9, 52.64, and 76.3 in., respectively (ORNL 2014). These data do not suggest any trend or cyclic variation in annual total precipitation on the time scale of the period of record (Fig. 2.8). Longer term records (1895 to 2013) assembled for the East Tennessee region indicate a similar average and range in annual total precipitation.

Rainfall intensity varies widely on seasonal, monthly, and shorter timescales (Fig. 2.9). Oak Ridge monthly total precipitation for the period 1990 to 2014 ranged from less than 0.1 in./month to over 14 in./month, with an average monthly total of 4.6 in. Monthly values of 24-hour maximum precipitation for the same period range from less than 0.1 in./24 hours to over 6.5 in./24 hours, with an average of 1.7 in./24 hours.
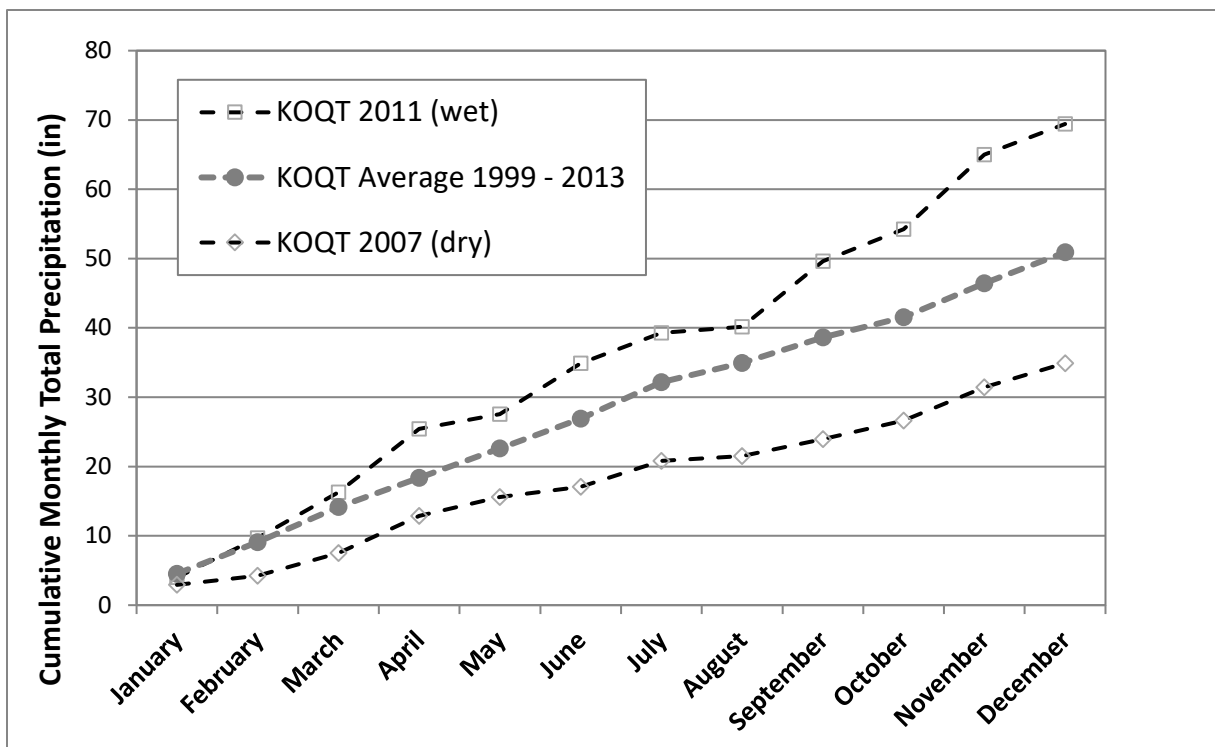
Fig. 2.7. Cumulative monthly precipitation for the NWS meteorological station (KOQT) in Oak Ridge
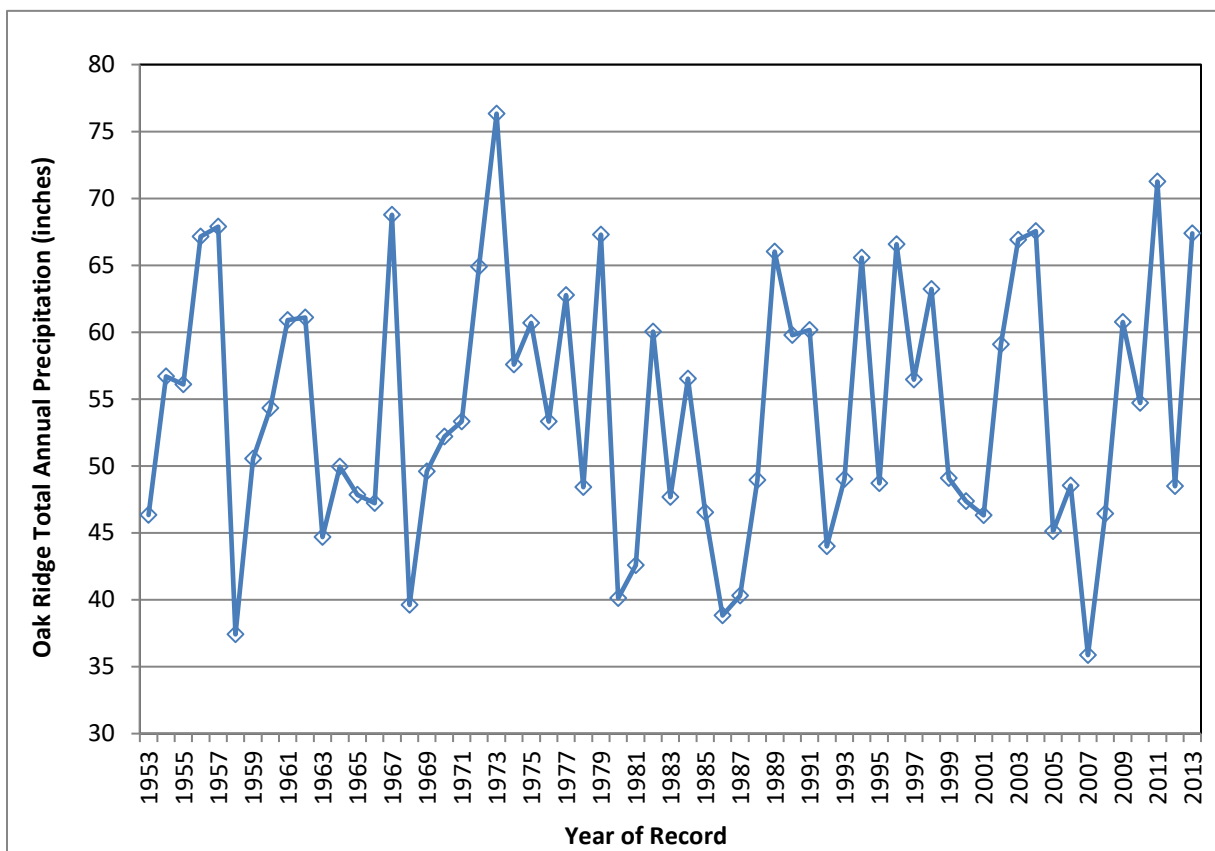
Fig. 2.8. Annual total precipitation for Oak Ridge (1953 to 2013)
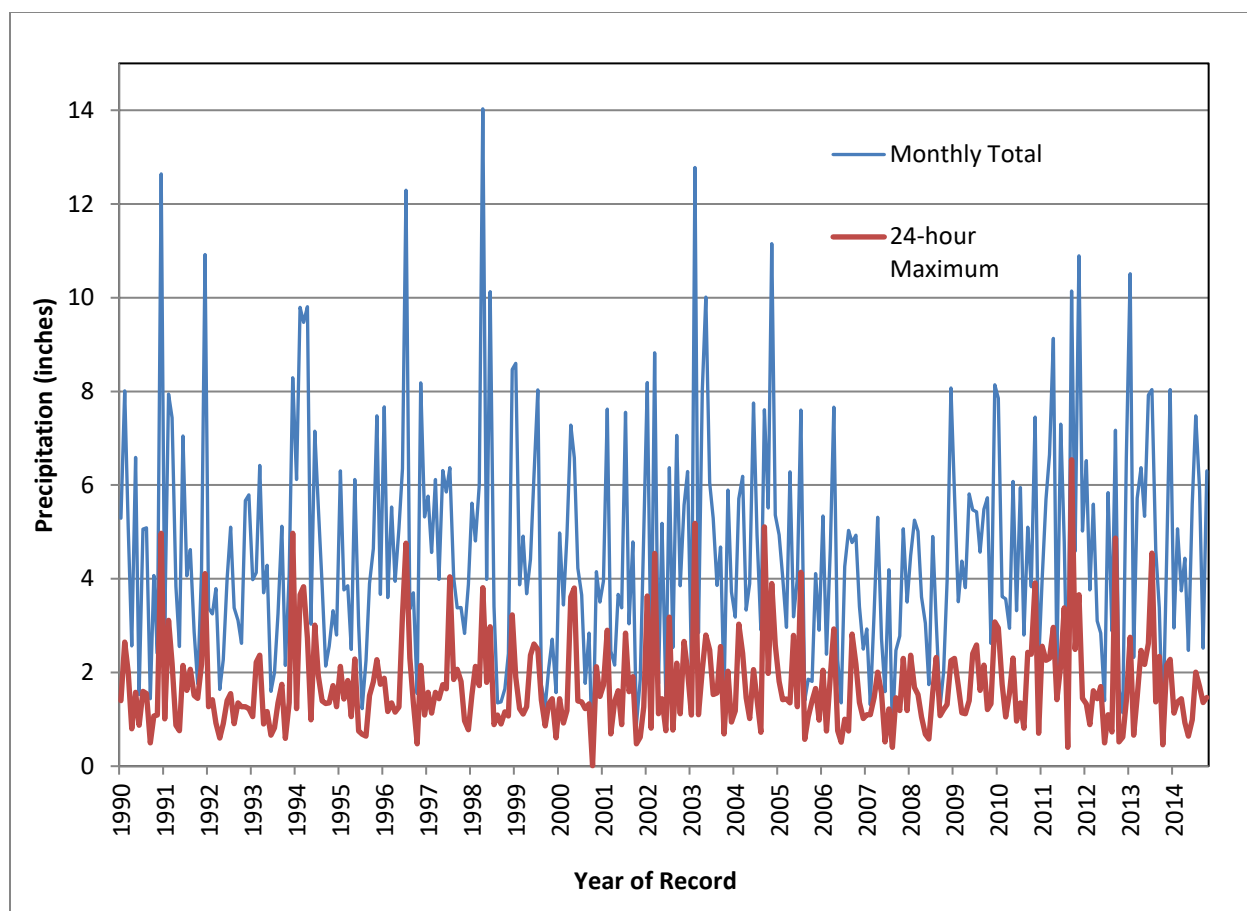
Fig. 2.9. Monthly total and 24-hour maximum precipitation and for Oak Ridge (1990 to 2014)

Precipitation intensity at hourly timescales is much larger than intensities averaged over longer periods. At the National Oceanic and Atmospheric Administration Atmospheric Turbulence and Diffusion Division station (near the Y-12 site), the point precipitation frequency estimate for hourly rainfall intensity (annual maximum series) at a 1-year average recurrence interval is 1.14 in./hour. This meteorological statistic indicates that precipitation in excess of 1 in./hour is likely to occur at least once each year.

Climate data and related assumptions about variability in annual precipitation used in hydrologic modeling for the EMDF PA are drawn from these local records and are described in Sect. 3.3. The possible impact of extreme precipitation events on EMDF performance is addressed in Sect. 3.2.1 and Appendix C. Consideration of potential future increases in average annual precipitation (climate uncertainty) is provided as part of the sensitivity-uncertainty analysis in Sect. 5.

2.1.3   Geology, Seismology, and Volcanology

The following sections address the regional geology, local geology in and around BCV, and the site-specific geology as inferred from investigations to date at similar locations in BCV. Recent characterization of the CBCV site to support EMDF site selection and preliminary design has provided additional information on groundwater and surface water hydrology, including field estimates of hydraulic conductivity (Sect. 2.1.5.4).

2.1.3.1   Regional geology

Following is a summary description of the regional geological setting for EMDF. A comprehensive and detailed report on the geology of the ORR, including a review of the regional and local structural geology,

was prepared by a panel of researchers from the ORNL Environmental Sciences Division. The *Status Report on the Geology of the Oak Ridge Reservation* (ORNL 1992a) contains detailed descriptions of soils, bedrock lithologies and stratigraphy, and geological structures within BCV at and near EMDF.

The ORR is located in the southwestern portion of the Valley and Ridge physiographic province (Fig. 2.10), which is characterized by a series of long, parallel ridges and valleys that follow a northeast-to-southwest trend. The Valley and Ridge physiographic province developed on thick, folded, and thrust-faulted beds of sedimentary rock deposited during the Paleozoic era. Thrust fault patterns and the strike and dip of the beds control the shapes and orientations of a series of the ridges and intervening valleys. The topographically high ridges are underlain by more resistant geologic formations with broad intervening valleys underlain by less resistant formations (Fig. 2.11).

The ORR lies within a classic foreland fold-thrust belt, characterized by a number of northeast/southwest striking, southeast dipping imbricate thrust sheets (ORNL 1992a). Ten major imbricate thrust faults, in which thrust sheets overlap somewhat like roof shingles, have been mapped in East Tennessee. Two of these thrust sheets, defined by the Copper Ridge and Whiteoak Mountain thrust faults, cross the ORR (Lemiszki 2000, ORNL 1992a). The cross-section in shown in Fig. 2.12 illustrates the Whiteoak Mountain thrust fault outcropping north of Pine Ridge and passing below BCV in the very deep subsurface. The Whiteoak Mountain thrust fault, along with other similar thrust faults in the Valley and Ridge province, are ancient faults inactive since the close of the Alleghanian orogeny at the end of the Paleozoic era around 250 M years ago.

The ORR and BCV are underlain by thick sequences of early Paleozoic sedimentary rocks that are stacked within adjacent thrust sheets and that generally strike northeast-southwest around N50°E. Bedding planes mostly dip to the southeast, with dip angles averaging around 45° (Fig. 2.12), but dips may vary widely on a local scale. Strike and dip measurements within BCV taken along the north tributary stream paths near EMDF (Lemiszki 2000) vary from 23° to 80° southeast to vertical.

Bedrock on the ORR consists of a variety of interbedded clastic and carbonate sedimentary rocks. The rocks are variably fractured and weathered, resulting in significant vertical and horizontal subsurface heterogeneity. The differing degrees of resistance to erosion of the shales, sandstones, and carbonate rocks that comprise the regional bedrock influence local relief. Carbonate units (limestone/dolostone) are commonly extensively weathered with massive clay overburden with dispersed residual chert nodules and pinnacled bedrock surfaces. The more resistant clastic rocks (sandstone, siltstone, mudstone/shale) generally weather to an extensively fractured residuum (saprolite) with highly interconnected fracture networks overlying less weathered to unweathered more intermittently fractured bedrock.
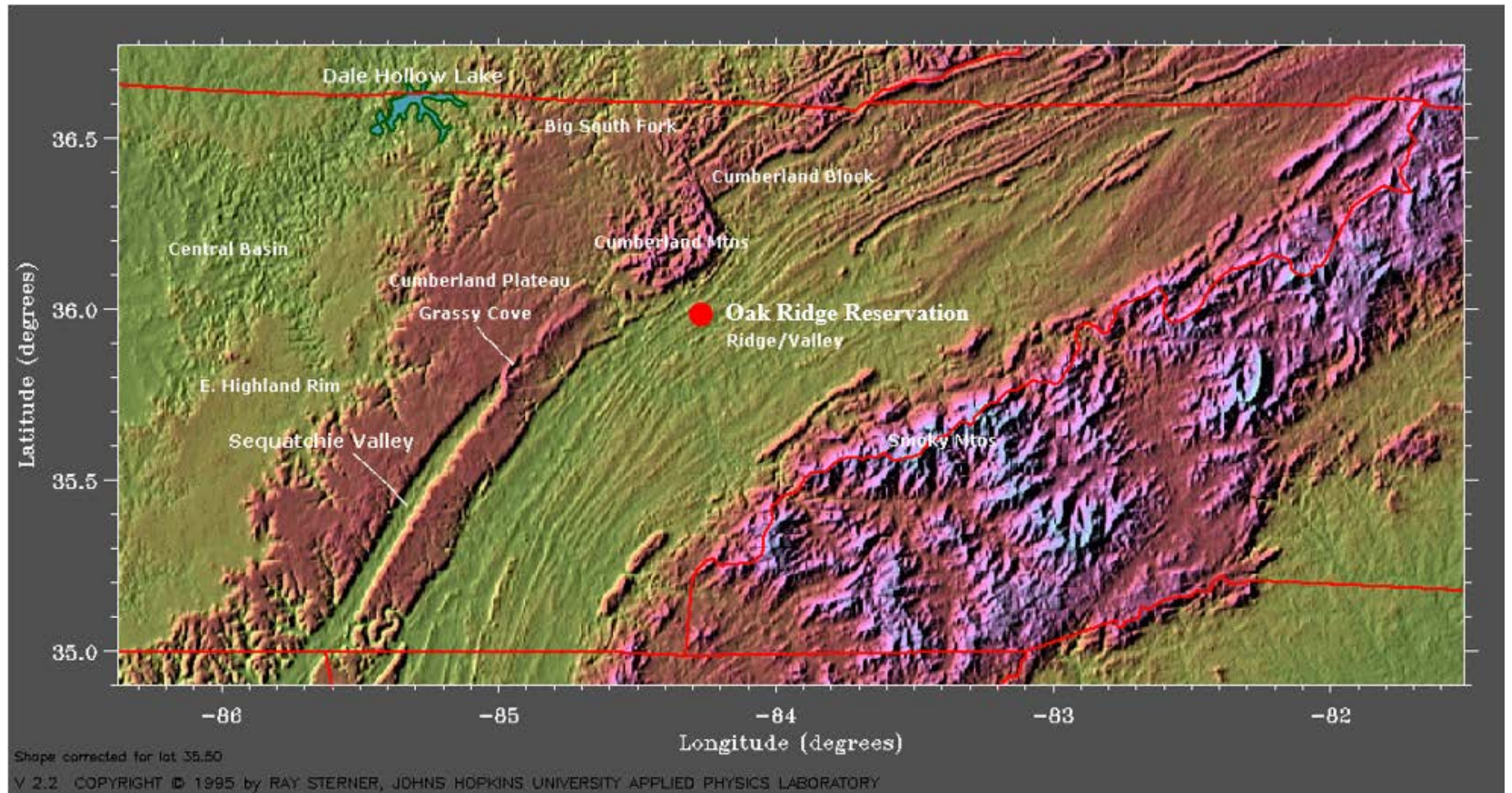
Fig. 2.10. Regional topography of Central and East Tennessee, including the southern portion of the Valley and Ridge physiographic province
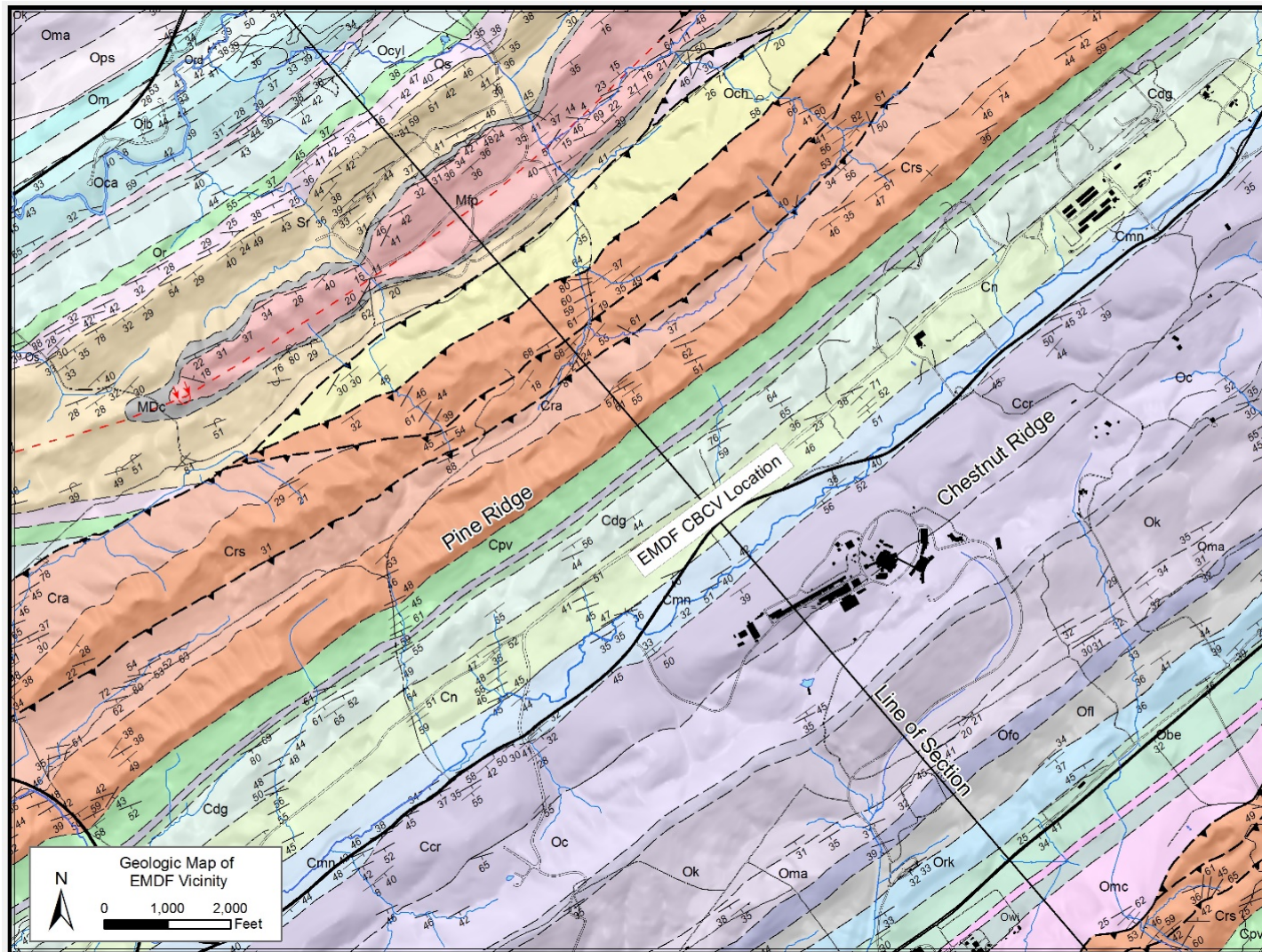
Source: Lemiszki 2000.

Note: Map shows geologic formations at and near BCV, the outcrop trace of the Whiteoak Mountain thrust fault, strike and dip measurements along BCV, and the approximate location of the proposed EMDF site.

Fig. 2.11. Geologic map of the Bethel Valley Quadrangle

NW

SE

ENVIRONMENTAL MANAGEMENT
DISPOSAL FACILITY (EMDF)

Location of cross section is shown on Fig. 2.11

WHITEOAK
MOUNTAIN FAULT

COPPER CREEK
FAULT

EAST FORK RIDGE

PINE RIDGE

BEAR CREEK
VALLEY

CHESTNUT RIDGE

BETHEL VALLEY

MDc   MDc

Olv

Oma Ofo

Obw Owi

€pv

Or Os   Mfp

€rs €rs

Och

Sr

€rs   €rs   €rs

Off Ork Obe

Omc

Cra

€cu

€mn

€cr

Oc

Ok

Ocncy

Omc

€cr

Ord

O€k

Omc

Orb

CROSS-SECTION
(No Vertical Exaggeration)

€ra/€rs - Lower Cambrian Rome Formation; Apison Shale Member and Sandstone Member.
€cu - Middle Cambrian Conasauga Shale Undivided (including the Nolichucky Shale).
€mn - Upper Cambrian Maynardville Limestone.
€cr - Upper Cambrian Copper Ridge Dolomite.

Source:

Lemiszki 2000. *Geologic Map of the Bethel Valley Quadrangle, Tennessee*, Geologic Quadrangle Map 130-NE, Lemiszki, P.J., Tennessee Division of Geology, Nashville.

UCOR
an AECOM-led partnership with Jacobs

**CENTRAL BEAR CREEK VALLEY
OAK RIDGE, TENNESSEE**

DRAWN BY:	REV. NO./DATE:	CAD FILE: C:\13013\DWGS
P. HOLM	0— 9/26/19	T04—CBCV—GEO—XSEC

Fig. 2.12. Northwest-southeast cross-section across the ORR

2.1.3.2   Stratigraphy of Bear Creek Valley

The sequence of geologic formations underlying BCV from Pine Ridge southward to Bear Creek includes the Rome Formation of lower Cambrian age and formations of the Middle Cambrian Conasauga Group (Figs. 2.11, 2.12, and 2.13). Resistant sandstone beds of the upper Rome Formation form the crest of Pine Ridge. The Conasauga Group is overlain by the Knox Group formations that outcrop along the southern border of BCV. Cherty dolomite beds of the Knox Group form the crest of Chestnut Ridge along the south side of the valley. Within the Conasauga Group, only the Maynardville Formation consists predominantly of carbonate rocks. The remaining formations of the Conasauga Group are predominantly clastic rocks composed mostly of fine-grained shales, mudstones, and siltstones. Limestones are interbedded with fine-grained rocks in portions of the Rutledge Formation and the Maryville Formation, but the only well-documented karst dissolution features in BCV are primarily associated with the Maynardville Limestone and the Copper Ridge Dolomite (Knox Group).

The stratigraphic sequence of formations in the Conasauga Group in BCV (Table 2.4) consists from bottom to top of the Pumpkin Valley Formation, the Rutledge Formation, the Rogersville Formation, the Maryville Formation, the Nolichucky Formation, and Maynardville Limestone (Lemiszki 2000, ORNL 1992a). The Rutledge and Maryville Formations consist mostly of insoluble clastic on the ORR relative to the original type sections designated at locations outside the ORR, where limestone beds are more predominant. Among the Conasauga Group formations, only the Maynardville Limestone has been recognized as containing significant conduit flow and karst features associated with limestone dissolution along the strike path of the Maynardville subcrop. That subcrop belt runs roughly parallel with the axis of Bear Creek draining toward the southwest along the margin of Chestnut Ridge.

The stratigraphic column for BCV is presented in Table 2.4 and more detailed lithologic descriptions for the geologic formations underlying BCV are provided in Table 2.5. The tables and descriptions are adapted from *Geology of the West Bear Creek Site* (Lee and Ketelle 1989). Detailed descriptions of the geologic formations for the entire ORR also are described in the *Status Report on the Geology of the Oak Ridge Reservation* (ORNL 1992a), but the descriptions and thicknesses from the Lee and Ketelle report are specific to BCV and the Whiteoak Mountain thrust sheet. The descriptions, thickness determinations, and other geologic characteristics described by Lee and Ketelle are based on hundreds of feet of bedrock cores at the West Bear Creek site used to thoroughly define the entire stratigraphic sequence across BCV. An additional report, *Subsurface-Controlled Geological Maps for the Y-12 Plant and Adjacent Areas of Bear Creek Valley* (King and Haase 1987), presents geologic maps and cross-sections for BCV that identify the contacts between and thicknesses for each of the individual Conasauga Group formations. This report addresses bedrock geology based on several additional valley-wide transects with deep boreholes and extensive bedrock cores located at the east end of BCV near Y-12, near the center of BCV at the BCBG site (Fig. 2.13), and at the West Bear Creek site. Each of these three reports, along with many others referenced in those reports, provide additional details on bedrock geology and geological structures underlying BCV.
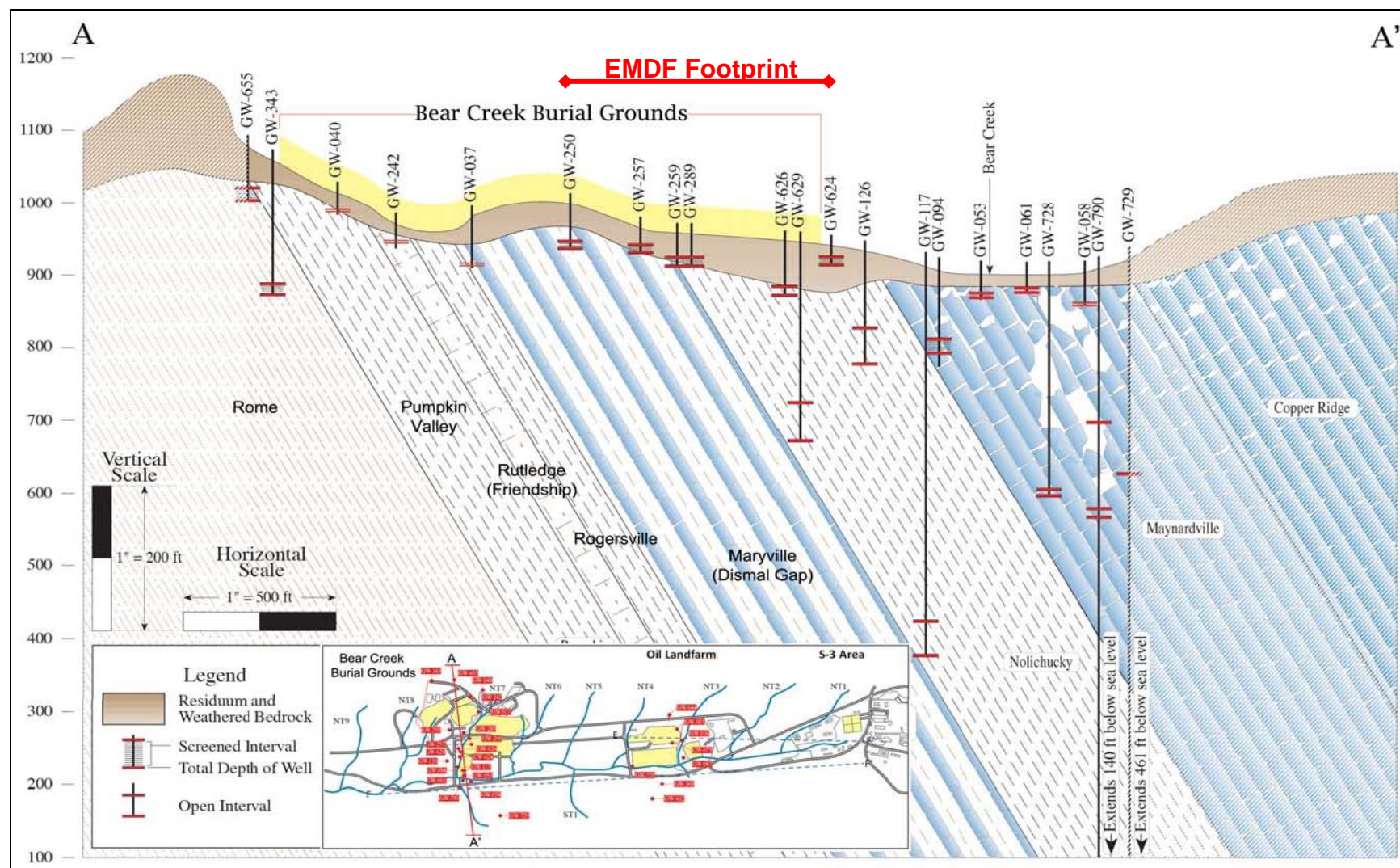
Source: ORR groundwater strategy (DOE 2013c).

Fig. 2.13. Stratigraphic cross-section for Bear Creek Valley near the Bear Creek Burial Grounds

Table 2.4. Stratigraphic column for bedrock formations in BCV

Age	Group	Formation/Unit	Description	Thickness (ft)
MIDDLE CAMBRIAN	CONASAUGA (Cc)	MAYNARDVILLE Fm.	Upper (Chances Branch Mbr.) – limestone and dolomitic limestone in thick massive beds.	140
			Lower (Low Hollow Mbr.) – dolomitic limestone in thick massive beds. Light gray to buff.	200
		NOLICHUCKY Fm.	Upper – shale and limestone in thin to thick beds. Shale dark gray or maroon. Limestone light gray, oolitic, wavy-bedded, or massive.	60–140
			Lower – shale and limestone in medium to thick beds. Shale dark gray, olive gray or maroon. Limestone light gray, oolitic, glauconitic, wavy-bedded, and intraclastic.	430–450
		MARYVILLE Fm.	Limestone and shale or siltstone in medium beds. Limestone light gray, intraclastic, or wavy-bedded. Shale or siltstone dark gray.	320–410
		ROGERSVILLE Fm.	Shale and argillaceous limestone. Laminated to thin bedded, maroon, dark gray, and light gray.	80–110
		RUTLEDGE Fm.	Limestone and shale in thin beds. Limestone light to olive gray. Shale gray or maroon.	100–120
		PUMPKIN VALLEY Fm.	Upper – shale and calcareous siltstone. Laminated to very thin-bedded. Shale reddish brown, reddish-gray, or gray. Calcareous siltstone light gray or glauconitic.	130–150
			Lower – shale and siltstone or silty sandstone. Thin-bedded. Shale reddish-brown or gray to greenish gray. Siltstone and silty sandstone light gray.	175
LOWER CAMBRIAN		ROME Fm. (Cr)	Sandstone with thin shale interbeds. Sandstone fine-grained, light gray or pale maroon. Shale maroon or olive gray.	Unknown

Source: Lee and Ketelle 1989.

42

Table 2.5. Lithologic descriptions and thicknesses of geologic formations in BCV

Geologic formations	Downhole thickness (ft)	Equivalent true thickness assuming 45° dip to SE (ft)	Lithologic and contact descriptions[a] (based on extensive rock cores collected at the proposed low level waste disposal demonstration and development site in WBCV)
Maynardville Formation - Єmn	Not reported	Not Reported	The Maynardville is divided into lower and upper members (Low Hollow and Chances Branch members). The Low Hollow member is generally a ribbon-bedded or mottled, fine-to-medium-grained dolomitic calcarenite with stylolites and irregularly spaced beds of oolitic calcarenite. Thin beds and shaley partings occur commonly within the ribbon-banded lithology. Basal portions include several laterally continuous dark gray shale beds roughly 0.5 to 2 ft thick. The Chances Branch member consists of bioturbated and thin-laminated, fine-to-medium-grained dolomicrite and dolomitic calcarenite in massive beds.
Єn/Єmn Contact			Abrupt Contact: The contact was located at the base of massive ribbon-bedded or mottled limestone of the Maynardville and uppermost thick (> 2 ft) shale in the Nolichucky.
Nolichucky Formation - Єn	Not reported	Not Reported	The lower Nolichucky is generally medium-bedded shale and limestone or calcareous siltstone resembling the underlying Maryville. The upper part of the lower Nolichucky is thick-to-very-thick-bedded maroon or olive gray shale and oolitic, coarse grained, or intraclastic limestone. The upper Nolichucky is lithologically diverse, consisting dominantly of dark gray shale with planar and wavy-laminate or ribbon-bedded micrite in thin beds (< 1 to > 2 in. thick).
Єmr/Єn Contact			Gradational Contact: The contact was placed above a 6-in.- to 2-ft-thick intraclastic limestone bed in the upper Maryville and at the base of the first clean dark gray or maroon shale bed > 2 ft thick.
Maryville Formation - Єmr	430	304	The Maryville consists of oolitic, intraclastic (flat pebble conglomerate), and thin-bedded limestone interbedded with dark gray shale that typically contains thin, planar, and wavy-laminated, coalesced lenses of light gray limestone and calcareous siltstone. Fine-grained glauconite often occurs at the tops of the thin-laminated limestone lithology. Several isolated dark maroon shale beds typically occur in both the upper and lower Maryville. Although considerable mixing of limestone lithologies is noted, the upper Maryville generally contains greater amounts of intraclastic limestone, while thin-laminated and oolitic limestone is more prevalent in the lower portion. The contact separating these two upper and lower portions is gradational over tens of feet of section. Limestone intraclasts are randomly oriented and roughly 2 to 10 cm in length. In roughly the lower 40 ft of the Maryville, a variable number of prominent, coarse-grained, pinkish limestone beds occur, which contain coarser and more abundant glauconite pellets than those higher in the section.
Єrg/Єmr Contact			Abrupt Contact: The Rogersville is terminated abruptly by the occurrence of the comparatively thick limestone beds of the overlying Maryville, with the contact placed at the bottom of the first such limestone.
Rogersville Formation - Єrg	90 and 150	64 and 106	The lower Rogersville consists dominantly of dark gray shale containing thin- laminated and bioturbated argillaceous limestone lenses less than 1 in. thick. When maroon shales occur in the lower portion, they are thinner and more chocolate brown than the maroon shales in the upper portion. Glauconite partings are commonly interlaminated with the limestones but also occur as bioturbated beds several inches thick. The Craig Member, recognized elsewhere in East Tennessee, is not present at the WBCV site. In the approximate position of the member are a few thin limestone beds which may represent the Craig Member at the site. The beds are 4 to 6 in. thick and composed of interlaminated, light gray, silty limestone and dark gray shale. These beds differ from those in the lower Rogersville principally in thickness and may be more appropriately considered the uppermost portion of the lower Rogersville at the site. The upper Rogersville consists dominantly of maroon shale containing thin (less than 1 in. thick), wavy, light gray, calcareous siltstone or argillaceous limestone lenses in varying amounts. Thin glauconitic partings are liberally incorporated within the siltstone and limestone lenses. The interlamination of these variably colored lithologies gives the upper Rogersville an overall thinly laminated appearance. Thicker beds (more than 1 ft thick) of clean, maroon-to-brownish-maroon shale are occasionally interspersed within the thin-laminated lithology.
Єrt/Єrg Contact			Abrupt Contact: The contact with the Rogersville is abrupt and recognized by the absence of 1-ft-thick limestone beds and the introduction of maroon shale. The contact is placed at the top of the uppermost such limestone bed.
Rutledge Formation - Єrt	124 and 126	88 and 89	The Rutledge consists of light gray, bedded limestone, often containing shaley partings interbedded with dark gray or maroon thin-bedded or internally clean shale in beds from 2 to 5 ft thick. Limestones are generally evenly divided between wavy laminated and bioturbated. Horizontal burrows are frequently observed. Maroon shale is more common in the lower Rutledge, and two distinctive beds on the order of 3 ft thick occur at the bottom of the formation and are separated by three limestone beds of similar thickness. These limestones are referred to as the "three limestones" of the lower Rutledge, but their lithologic similarity with limestones in the bulk of the Rutledge makes them less distinctive than the two maroon shales. The relatively clean, dark maroon shales in the lower Rutledge give way to dark gray shale with thin calcareous siltstone interbeds. Upper Rutledge interbeds are generally thinner than those below and more coalescing of lithologies is recognized. Limestone beds are often ribbon or wavy bedded and some are heavily bioturbated with abundant glauconite pellets. Glauconite stringers also occur commonly within the calcareous siltstone interbeds.
Єpv/Єrt Contact			Abrupt Contact: The contact with the overlying Rutledge is abrupt and placed at the top of generally uninterrupted, thin-bedded, reddish-brown shale and below the interbedded limestone and dark maroon shale of the Rutledge.
Pumpkin Valley Formation - Єpv	376 and 398	266 and 281	The Pumpkin Valley Formation is readily divisible into upper and lower units of nearly equal thickness. The lower Pumpkin Valley consists of reddish brown and gray-to-greenish-gray shale with thin interbeds of siltstone and silty, fine-grained sandstone. Shales typically contain thin, wavy laminated siltstone drapes and discrete laminate of fine-grained glauconite. Silty sandstone interbeds are typically wavy laminated to thin bedded, but are often heavily bioturbated. High concentrations of large glauconitic pellets occur in the bioturbated lithology. Decreasing silty sandstone content upward within the lower Pumpkin Valley attests to its transitional nature above the Rome. The upper Pumpkin Valley is laminated to thin-bedded, dominantly reddish-brown, reddish-gray, and gray shale with thin, wavy, and planar-laminated siltstone lenses. Shales are generally fissile and may be massive or thin laminated. Thin partings of fine-grained glauconite pellets are ubiquitously interlaminated within the siltstone lenses.
Єr/Єpv Contact			Gradational Contact: The contact with the overlying Pumpkin Valley Formation is gradational and placed at the top of the uppermost thick, clean, planar laminated, 8- to 12-in.-thick, sandstone bed of the Rome.
Rome Formation - Єr	>>195	>>138	The Upper Rome consists of thick beds of gray or pale maroon, fine-grained arkosic to subarkosic sandstone with occasional interbeds of maroon shale that often contain thin siltstone bands. Sandstones are typically planar to wavy-laminated or current-rippled. Vertical burrows are in great abundance in the interbedded lithology, but are also recognized in the sandstone-dominated lithology. Burrows diminish in abundance down section. Upper Rome sandstone/shale interbeds occur non-uniformly at the two site locations from which the core was acquired. The common occurrence of such interbeds on the western portion of the site is almost entirely replaced in the center of the site by gray or pale maroon sandstone couplets with a total absence of shale. Such lateral facies changes within roughly 1000 ft suggest the Upper Rome was subject to locally variable clastic influx in a low-relief paleodepositional setting.

[a]Lee and Ketelle 1989.

BCV = Bear Creek Valley

SE = southeast

WBCV = West Bear Creek Valley

This page intentionally left blank.

2.1.3.3   Conasauga Group bedrock fractures in Bear Creek Valley

Descriptions and data on bedrock fractures applicable to the EMDF site are available from site investigations and research reported from Conasauga Group sites in BCV and elsewhere on the ORR. The RI completed for BCV (BCV RI) (DOE 1997b) addresses bedrock fractures in BCV (DOE 1997b, Appendix C, Sect. C.3.3). The report notes that because of the large-scale faulting and folding characteristic of ORR geology, all bedrock lithologic units in BCV are highly fractured, consisting of extensional, hybrid, and shear fractures. Core hole studies of fractures in bedrock along a transect across BCV near the head of Bear Creek (Dreier et al. 1987, Dreier and Davidson 1994) demonstrate the existence of several major fracture sets that are dominated by a strike-parallel set. Most fractures in ORR bedrock constitute a single cubic system (three orthogonal sets) of extension fractures (Dreier et al. 1987, Sledz and Huff 1981). One fracture set is formed by bedding planes dipping to the southeast. Two other fracture sets generally parallel strike and dip. At shallow depths, these sets are commonly angled 50° to 60° below the horizon. These three fracture sets may occur in any locality and other extensions and shear fractures may also be present (DOE 1997b).

In general, fracture spacing is a function of lithology and bed thickness. Fractures in more massively bedded formations tend to have longer trace lengths and are more widely spaced. An average fracture density of approximately 60/ft was measured in saprolite of the Maryville Formation and Nolichucky Formation (Dreier et al. 1987). At the other extreme, a minimum of five fractures per meter (1.5/ft) in fresh rock was documented in the Sledz and Huff (1981). Fewer open fractures occur at deeper levels. As described in Haase et al. (1985), fracture frequency is variable, but most fractures observed in cores occur within limestone or sandstone layers > 1.6 ft thick and many are filled or partly filled with secondary minerals.

Most fractures are short, a few centimeters to approximately 3.3 ft in length (longest dimension). Fracture length at outcrops is relatively uniform (approximately 5 in.) in shale, but increases with bed thickness in siltstone (Sledz and Huff 1981). There are numerous fractures approximately 0.3 to 5 ft long in limestone and sandstone units of the Conasauga Group and Rome Formation (Haase et al. 1985). In limestone, typical fracture spacings range from < 2 in. for very thin beds to > 10 ft for very thick to massive beds.

Detailed logging of core material from wells at the BCBG site (located southwest of the EMWMF and along strike with the EMDF) has provided information on the relative changes in densities of open (hydraulically active) fractures in the Nolichucky Formation compared to depth and lithology (Dreier and Davidson 1994). This information was supported by estimates of spacings for hydraulically active fractures from resistivity, temperature, and flow meter logs of the same borings. The resulting estimates ranged from approximately 3 ft in the shallow intervals to more than 20 ft in the deep intervals.

2.1.3.4   Geologic units at the EMDF site

The CBCV site is underlain by the moderately to steeply dipping beds of the Maryville Formation on the northern end and by Nolichucky Formation on the southern end of the site (Fig. 2.13). The Maryville Formation includes limestone interbedded with fine-grained clastic rocks. Based on the inferred location of the contact between the Nolichucky Formation and the Maynardville Limestone at the EMDF site, the distance from the southernmost margin of the facility to the karstic Maynardville unit is approximately 350 ft. Field mapping of the surficial geologic unit contacts is included as part of the initial CBCV site characterization effort.

2.1.3.5   Surficial geology

In the humid subtropical climate of the southeast, the rocks have weathered over time to create a surficial regolith that includes topsoil, clayey residual soil, and highly weathered rock (saprolite) covering the

unweathered (competent) bedrock below. Unconsolidated mixtures of mud, sand, and gravel deposits (alluvium) occur along stream valleys, and relatively thin surficial deposits of colluvium may occur, generally along the lower portions of steeper slopes.

A simplified conceptual model of surficial geology in BCV is adopted for describing the natural components of the disposal system (Fig. 2.14). The saprolite zone includes all materials that overlay unweathered (competent) bedrock, corresponding to the overburden in engineering terminology. Depending on the site topography and local conditions, the saprolite zone at the EMDF site may include surficial soils (organic-rich topsoil and clayey residual subsoils), colluvium and alluvium along flanks and floors of the NT valleys, and the underlying saprolite, which is bedrock that has been completely chemically weathered but remains otherwise undisturbed. Saprolite can generally be drilled using a hollow-stem auger rig to the depth of auger refusal where the transition to less weathered or unweathered bedrock occurs. For practical purposes, the depth of the saprolite zone may be considered as auger refusal drilling depth, which typically ranges from 10 to 30 ft, but can exceed 50 ft in some locations. Saprolite retains the fabric and structure of the parent sedimentary rocks, including fracture sets (Sect. 2.1.3.3). Beneath the saprolite zone lies a bedrock zone that comprises less weathered and fractured bedrock. In general, the degree of weathering, average aperture and density of fractures, porosity, and permeability decrease with increasing depth below the surface. Materials near the saprolite-bedrock boundary are transitional and can include less weathered rock fragments (mostly shale and siltstone) in a fine-grained saprolite matrix.

The thin topsoil layer of organic rich soil varies from a few inches to < 1 ft thick. The zone of fine-grained residual soil varies from < 2 ft to 10 ft in thickness. The thickness of these intervals and the underlying saprolite varies and downward transition from one to the next may be rapid or gradual depending on the topographic position and history of profile development. Pore structure within the clayey residuum reflects surface soil formation processes, including macropore structures related to root growth and bioturbation (e.g., earthworm activity). Structural features of the underlying saprolite reflect the bedding and fracture geometry of the parent sedimentary rocks. As documented in Driese et al. (2001), there is extensive filling in saprolite fractures at the base of the residual soil due to translocation of clays. These clays and associated iron and manganese deposits contribute to the decrease in permeability with depth within the regolith.

Along the valley floors of Bear Creek tributaries, the soil-and saprolite upper portion of the subsurface profile may be replaced with alluvial sediment deposits that vary in width and thickness (Fig. 2.15). Colluvial deposits may occur along the lower slopes of these valleys. A thicker belt of alluvial deposits occurs within the floodplain of BCV. Colluvial or alluvial deposits also may occur in places outside of the current stream valleys as demonstrated by detailed site soil surveys completed for a waste disposal demonstration project in West Bear Creek Valley (WBCV) (Lietzke et al. 1988).

Saprolite Zone

➢ Chemically weathered but otherwise undisturbed (saprolitic) fine-grained sedimentary rock

➢ Saprolite retains the fabric and structure of the parent rock, including facture sets

➢ Saprolite is variably overlain by clay-rich residual soil, alluvium, and/or colluvium depending on position in the landscape.

➢ Saprolite zone also corresponds to the terms *regolith* or *overburden*

➢ Water table (top of the saturated zone) generally occurs within the saprolite zone

Gradational Transition from Saprolite to Bedrock Zone
(Depth of auger refusal indicates local top of unweathered bedrock)

Bedrock Zone

➢ Fractured and weakly weathered to unweathered sedimentary rocks (Paleozoic marine and nearshore sediments)

➢ Generally saturated conditions, except during dry periods at higher elevation locations

Fig. 2.14. Simplified conceptual model of geologic material types in Bear Creek Valley
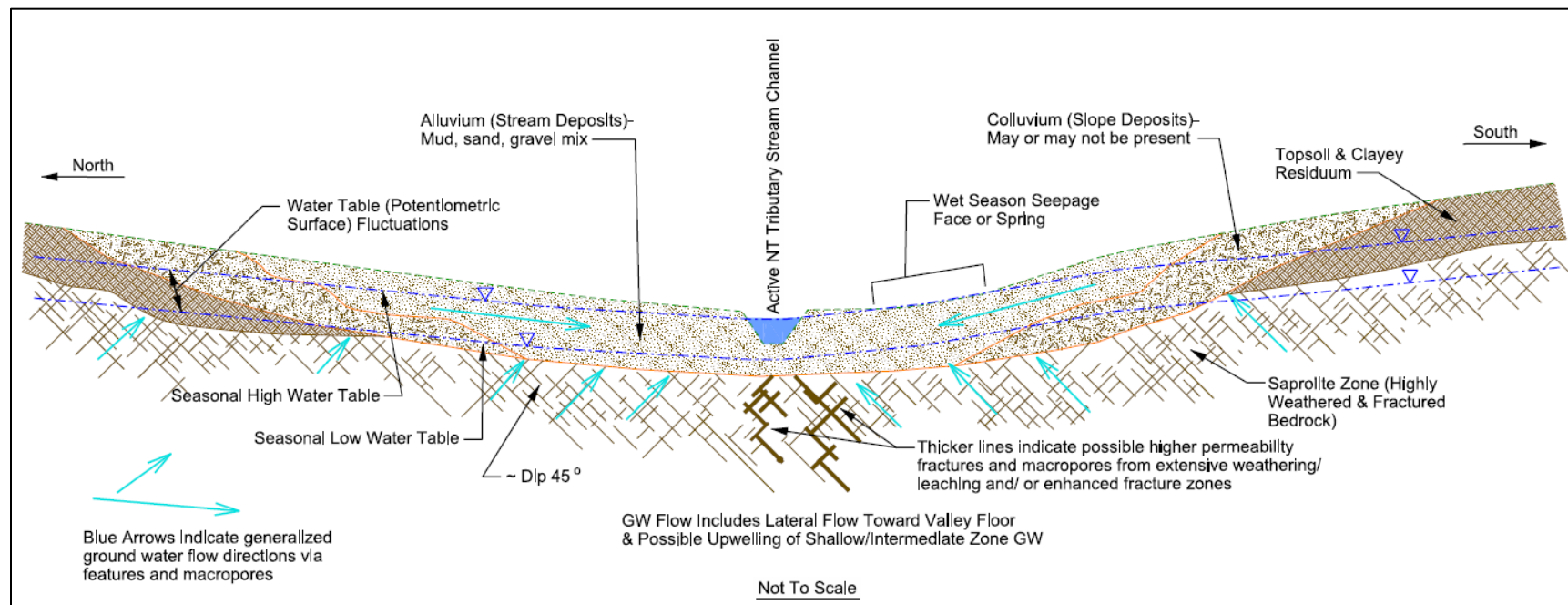
Fig. 2.15. Typical subsurface profile expected across Bear Creek tributary valleys

2.1.3.6   Seismology

Oak Ridge and the EMDF site are located within a broad zone of elevated activity of historically low-magnitude seismicity known as the East Tennessee Seismic Zone (ETSZ), a narrow zone of seismicity east of the New York-Alabama magnetic lineament (Fig. 2.16). Although there is a higher rate of seismic activity in the ETSZ, the largest documented historical earthquake in the region was approximately magnitude 4.6 (Tennessee Valley Authority [TVA] 2016).

Studies at Douglas Reservoir (Hatcher et al. 2012) concluded that at least two moment magnitude 6.5 or greater earthquakes could be associated with the ETSZ within the last approximately 73,000 to 112,000 years. However, these results are preliminary, and timing of proposed earthquake events and recurrence intervals are not established. Therefore, a reoccurring large magnitude event source zone is not defined based on the Douglas Reservoir features (TVA 2016).

There is no evidence of active, seismically capable faults in the ORR area (DOE 2011c). The Oak Ridge area lies in Uniform Building Code seismic zones 1 and 2, indicating that minor to moderate damage could typically be expected from an earthquake. Although there are a number of inactive faults passing through the ORR, there are no known or suspected seismically capable faults. As defined in 10 *CFR* 100, Appendix A, a seismically capable fault is one that has had movement at or near the ground surface at least once within the past 35,000 years, or recurrent movement within the past 500,000 years. The nearest capable faults are approximately 300 miles west-northwest of the ORR in the New Madrid (Reelfoot Rift) Seismic Zone (DOE 2011c). Historical earthquakes occurring in the ETSZ are not attributable to fault structures in underlying sedimentary rocks, but rather occur at depth in basement rock (Powell et al. 1994).

Historic earthquakes in the ETSZ typically are of small magnitude and mostly go unfelt by people. However, a number of historic earthquakes have had magnitudes greater than 4.0 and were, therefore, capable of producing at least some surface damage. Between 1844 and 1989, East Tennessee experienced 26 earthquakes that were widely felt, seven causing at least minor damage (Stover and Coffman 1993). An earthquake that shook Knoxville in 1913 was estimated to have a moment magnitude of about 5.0. Another earthquake that occurred in 1930, with an epicenter approximately 5 miles from Oak Ridge, had a Mercalli intensity of V to VII. Table 2.6 presents a description of scales. The largest recent seismic event was a moment magnitude 4.7 earthquake that had an epicenter near Alcoa, Tennessee, 21.6 miles southeast of Oak Ridge, in 1973. The intensity of this earthquake felt in Oak Ridge was estimated to be in the range of V to VI (light).

The Oak Ridge region continues to be seismically active, with 50 earthquakes recorded within a radius of 62 miles of the ORR since 1973. Approximately 60 percent of the 50 earthquakes within this radius occurred at depths greater than 6 miles. The closest of those events occurred on June 17, 1998, with an epicenter within ORR near ETTP, registering a magnitude 3.3 (U.S. Geological Survey [USGS] 2013). Two other earthquakes with epicenters beneath the ORR have been recorded since 1973. These occurred on May 2, 1975 (magnitude of approximately 2.6) and April 11, 2013 (magnitude of approximately 2.2).
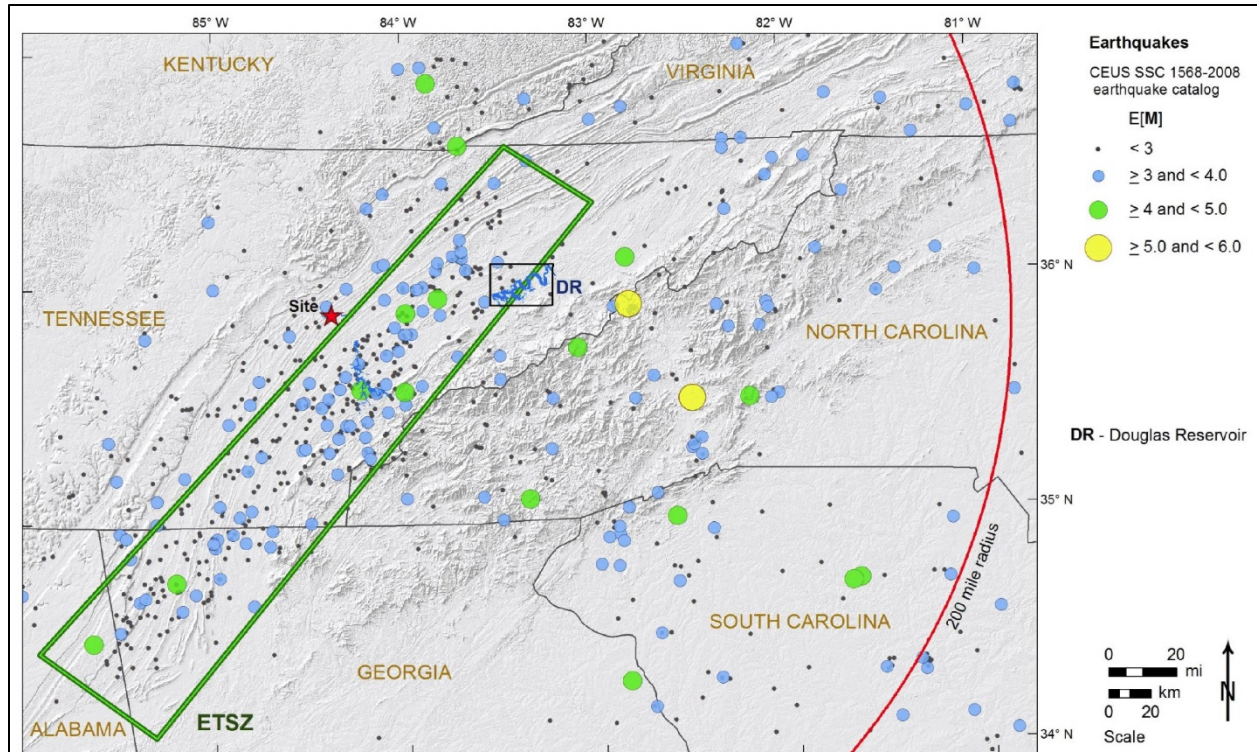
Source: TVA 2016.

Fig. 2.16. Eastern Tennessee Seismic Zone Location - U.S. Geological Survey

Table 2.6. Earthquake magnitude and intensity scales

Moment magnitude scale	Modified Mercalli scale	Intensity descriptor	Peak ground acceleration (g)
< 2.0	I	Minor	< 0.0017 to 0.039
2.0 – 2.9	I - II		
3.0 – 3.9	II – IV		
4.0 – 4.9	IV - VI	Light	0.039 to 0.092
5.0 – 5.9	VI - VII	Moderate	0.092 to– 0.18
6.0 – 6.9	VII - IX	Strong	0.18 to 0.34
7.0 and up	VIII - XII	Major to catastrophic	0.34 to > 1.24

Source: USGS 2020.

USGS = U.S. Geogolical Survey

2.1.3.7   Volcanology

Active volcanoes, lava flows, and other features of geologically recent volcanic activity do not occur in the southeastern United States anywhere near the EMDF site. Based on tectonic plate boundaries and the great distance of the site from any hot spots or plate subduction zones, volcanic activity would not be expected to occur within any future timeframes of concern relevant to the EMDF site.

2.1.4 Ecology and Natural Areas of Bear Creek Valley

The following subsections review the general ecological conditions and natural resource areas of BCV. Implications of potential impacts of biological processes on long-term changes in EMDF performance are considered in Sects. 3.2.1 and 3.2.2.1. Section 2.8.1 describes the results of ecological surveys recently completed at the CBCV site to satisfy applicable regulatory requirements for the protection of natural resources.

Ecological conditions in BCV were described in Southworth et al. (1992). This report presented results of biological monitoring for the 1984 to 1988 monitoring period, including habitat evaluation, toxicity monitoring, and surveys of fish and benthic macroinvertebrates, within the context of impacts from historical waste sites located in the central and upper parts of BCV. Extensive biological monitoring of Bear Creek for the 1989 to 1994 period was presented in the ORNL 1996. This report presented detailed descriptions of the Bear Creek watershed and results and analyses of toxicity monitoring, bioaccumulation studies, and instream ecological monitoring of fish and benthic macroinvertebrates. The BCV RI (DOE 1997b) subsequently presented results of ecological characterization and a baseline ecological risk assessment for BCV in a comprehensive assessment of risks to fish, benthic invertebrates, soil invertebrates, plants, wildlife from chemicals, and terrestrial biota from exposure to radionuclides.

Several more recent reports document ecological monitoring in BCV, including the Annual Site Environmental Report for the ORR (DOE 2015a), the annual Remediation Effectiveness Report (RER) for the ORR (DOE 2018c), and the Y-12 Biological Monitoring and Abatement Program reports (Peterson et al. 2009). The ecological monitoring includes surface water and biota sampling and analysis at stations along Bear Creek and several north tributaries in BCV. The RER aquatic biomonitoring of streams in BCV includes bioaccumulation (contaminant accumulation in fish) monitoring, fish community surveys, and benthic macroinvertebrate community surveys.

2.1.4.1 Terrestrial and aquatic natural areas in Bear Creek Valley

Outside of the Y-12 area, BCV is designated as part of the ORERP and the Oak Ridge Biosphere Reserve (Parr and Hughes 2006). In two separate but related reports, an ORR-wide analysis, evaluation, and ranking of terrestrial natural areas (NAs) (Baranski 2009) and aquatic natural areas (ANAs) (Baranski 2011) were presented. These reports compiled information from several previous reports into a comprehensive review of NAs and sensitive habitats for the ORR. The purpose of these studies "*was to evaluate and rank those specially designated areas on the Reservation that contain sensitive species, special habitats, and natural area value. Natural areas receive special protections through established statutes, regulations, and policies.*" As shown in Fig. 2.17, a swath along almost the entire length of Bear Creek and some tributaries within BCV are designated as ANA2. In the vicinity of the proposed EMDF, terrestrial NA13 and habitat area (HA) 2 are recognized. The NA13 and HA2 areas are confirmed habitats for rare plant and animal species (state and/or federal candidate and/or listed) and include terrestrially and aquatically sensitive habitats (Parr and Hughes 2006, Fig. 13). The ANA2 area (Bear Creek), NA13, and HA2 areas coincide with areas given a highest biological significance ranking of BSR-2 (very high significance) in a Nature Conservancy Report of biodiversity on the ORR (Parr and Hughes 2006).
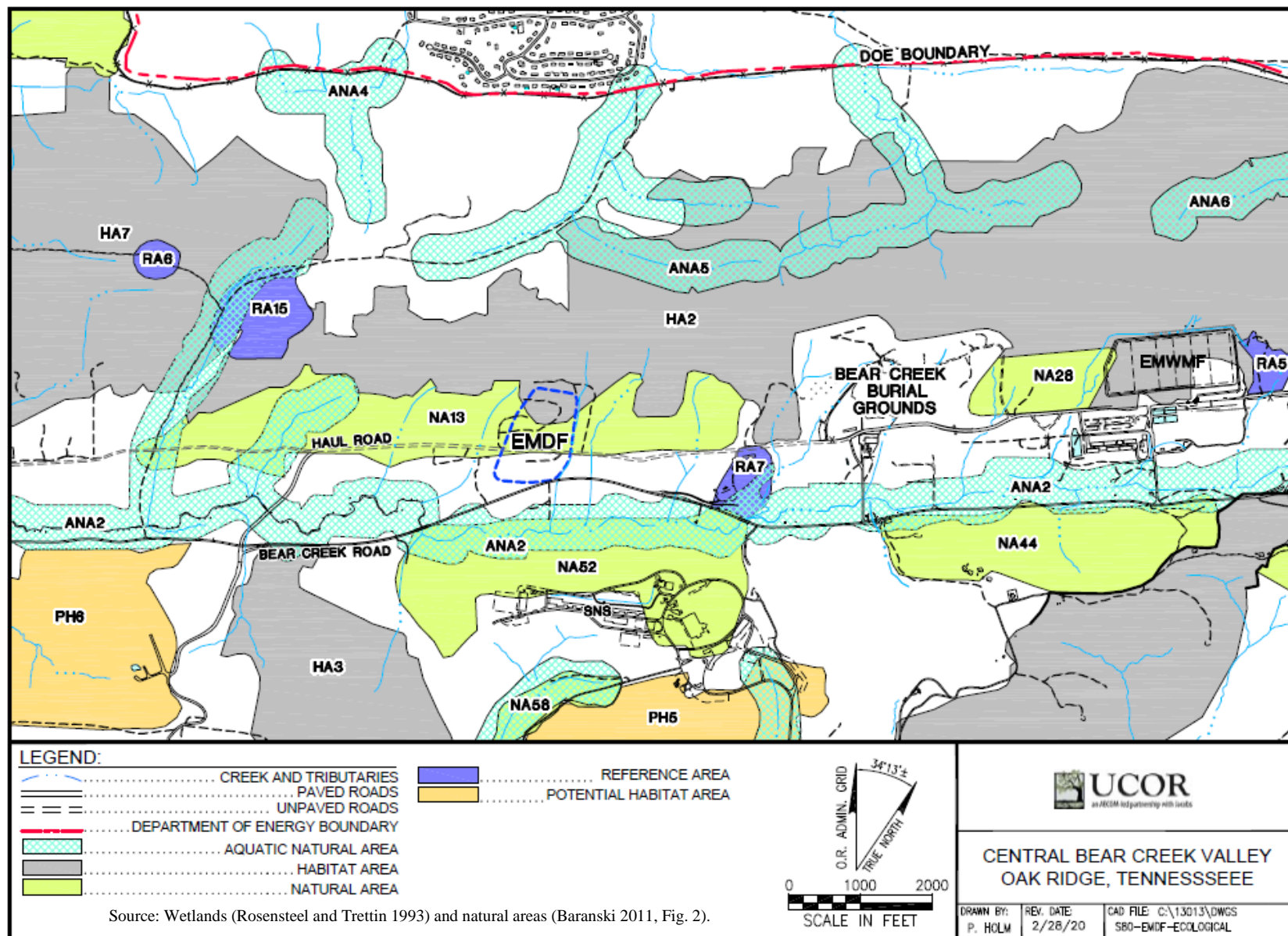
Fig. 2.17. Officially recognized special and sensitive areas near BCV

LEGEND:
.... CREEK AND TRIBUTARIES
.... PAVED ROADS
.... UNPAVED ROADS
.... DEPARTMENT OF ENERGY BOUNDARY
.... AQUATIC NATURAL AREA
.... HABITAT AREA
.... NATURAL AREA
.... REFERENCE AREA
.... POTENTIAL HABITAT AREA

CENTRAL BEAR CREEK VALLEY
OAK RIDGE, TENNESSSEEE

Source: Wetlands (Rosensteel and Trettin 1993) and natural areas (Baranski 2011, Fig. 2).

2.1.4.2   Wetlands and sensitive species surveys in Bear Creek Valley

Results of wetland surveys for the entire BCV watershed were presented in Rosensteel and Trettin (1993). Wetlands were delineated along the valley floors of local tributaries. The wetland locations suggest the influence of strike-parallel shallow groundwater flow from the uplands toward the adjacent tributary valley floors.

An environmental survey was conducted in 2004 and 2005 to assess sensitive natural resources that would be impacted by the Haul Road corridor between ETTP and EMWMF. The Haul Road generally follows the strike of BCV along the power line right of way north of and roughly parallel with Bear Creek Road. The survey evaluated rare plants and vegetation assemblages, rare wildlife and their habitat, rare aquatic species, and wetland/floodplain areas along BCV. The survey concluded that "*the most significant natural resource disturbance associated with the Haul Road's construction is undoubtedly the potential aquatic and wetland impacts near Bear Creek and its major tributaries. Bear Creek and its major tributaries contain the rare Tennessee dace, and forested wetlands adjacent to these streams were generally found to be of high natural quality. Fragmentation of interior forest was also a concern as road construction was deemed a potential impact on forest-interior neotropical migrant birds. However, a thorough review of past records as well as the present surveys found no evidence of rare, T&E wildlife species or plants present within the Haul Road corridor*" (Peterson et al. 2005).

An ORR-wide survey of bat species was conducted and reported on in late 2015 (McCracken et al. 2015). That survey confirmed Indiana and gray bats (endangered species) and the northern long-eared bat (threatened) make their home on the ORR. Additional endangered species were identified acoustically by the study, but their presence was not confirmed through capture.

2.1.4.3   Biological monitoring in Bear Creek

Virtually all of Bear Creek within BCV is designated as ANA2 within the ORERP (Baranski 2011, and Fig. 2.17). The stream habitats of upper Bear Creek and its tributaries have been impacted from headwater contamination originating from Y-12 waste disposal sites in East Bear Creek Valley (EBCV) (Southworth et al. 1992) and support small populations of benthic macroinvertebrates that are relatively intolerant to pollution. Although segments of the upper Bear Creek stream channel are periodically dry from karst stream flow capture in the summer/fall dry season, portions of the stream support a rather healthy community of benthic macroinvertebrates. During dry periods, much of the benthic fauna may migrate to the hyporheic zone of the stream.

In general, the diversity and abundance of aquatic fauna were found to increase with distance from the contaminated headwaters (Southworth et al. 1992). This also may be due, in part, to increases in stream depth and continuity of flow. A total of 126 benthic invertebrate taxa were recorded in Bear Creek, including crustaceans, aquatic worms, snails, mussels, and insects. Representatives of 11 orders of insects were collected. Mayflies, highly sensitive to heavy metal pollution, were almost totally absent in all but the lower reaches of Bear Creek. Upstream areas were numerically dominated by midge larvae, which is typical of polluted streams.

Nineteen species of fish were recorded in Bear Creek during surveys in 1984 and 1987, and data provide evidence of ecological recovery in Bear Creek since 1984 (Southworth et al. 1992, Ryon 1998). Studies concluded that much of Bear Creek contains a limited number of fish species that appear to have robust populations (high densities and biomass). Fish surveys reported over two decades ago near the headwaters demonstrated a stressed condition without a stable, resident fish population (Southworth et al. 1992). However, headwater streams often do not support very diverse fish fauna. Four fish species were found to

predominate in the upper reaches of Bear Creek (above Bear Creek kilometer [BCK] 11); by comparison, 14 fish species occur downstream from SR 95.

Biological monitoring of stream sites in BCV watershed has been conducted since 2004 to measure the effectiveness of watershed-scale remedial actions (DOE 2015b). Biological monitoring includes contaminant accumulation in fish, fish community surveys, and benthic macroinvertebrate community surveys. Fish communities in Bear Creek have generally been stable or slightly variable in terms of species richness.

The Tennessee dace, a major constituent of the fish population above the weir at BCK 4.55, is a Tennessee-listed in-need-of-management species and its habitat is protected by the state of Tennessee. No federal- or state-listed threatened and endangered aquatic species have been observed in Bear Creek or its tributaries (Southworth et al. 1992).

2.1.4.4 Terrestrial habitats in Bear Creek Valley

The CBCV site and surrounding areas are largely forested. Regional plant communities within BCV typify those found in Appalachia from southern Pennsylvania to northern Alabama.

Terrestrial flora. Much of the natural upland forest on the ORR, including much of BCV, is a mixed mesophytic forest dominated by oaks, hickories, and yellow poplar, with co- or subdominant beech and maples. Evergreens such as shortleaf pine, Virginia pine, and loblolly pine are intermixed in deciduous-dominated forests and are found in more or less pure stands, especially on recovering disturbed land and in plantations. Other trees that may be present as secondary or understory species include black cherry and dogwood (Kitchings and Mann 1976). Much of the forest is open, with little herbaceous undergrowth. Some areas may have moderate to dense undergrowth composed of rhododendron or laurel, but these are confined to relatively small niche areas. The herbaceous layer includes ferns, plantains, groundsel, and vines.

Bottomland and wetland sites are characterized by sweet gum, sycamore, and black willow, with red maple, black walnut, and boxelder. The herbaceous layer may contain sedges, rushes, cattails, and bulrushes.

Terrestrial fauna. Predators, including the coyote, red and gray fox, bobcat, and weasel, are widespread throughout the ORR. Black bears have occasionally been reported on the ORR, but these appear to be animals in transit, not permanent residents. White-tail deer, the only ungulate currently known to frequent the area, inhabit upland and bottomland forests throughout the ORR. Elk also are occasionally sighted on the ORR.

Striped skunk, opossum, raccoon, eastern cottontail rabbit, and groundhogs are small omnivores and herbivores common to both forest and field. Numerous members of the order Rodentia are present, including chipmunks, eastern grey squirrel, and flying squirrel, as well as several species of mice. Shrews and voles also are common throughout the ORR.

Streams and lake banks offer suitable habitat for muskrats and beaver. Marsh rice rats may live in wet areas along open waters that have a dense herbaceous growth of grasses and sedges.

Avifauna. The upland forest provides habitat for a large number of resident and migratory bird species. Resident woodpecker species common to mature deciduous forests include yellow-shafted flickers, redbellied woodpeckers, hairy woodpecker, downy woodpeckers, and pileated woodpeckers. The common crow and blue jay also are present in the deciduous forest.

Songbirds found in ORR forests are represented by the Kentucky warbler, pine warbler, and yellow-breasted chat; however, the ovenbird, Carolina chickadee, scarlet tanager, mourning dove and tufted titmouse are considerably less selective. Game birds include turkey and ruffed grouse.

Red-tailed hawk and sharp-shinned hawk are raptors common year-round on the ORR. Turkey vultures and black vultures also are common on the ORR. The Northern harrier and broad-winged hawk are migratory visitors.

2.1.5 Hydrogeology

Due to the abundant precipitation and shallow water tables in BCV, surface and groundwater hydrology are closely related. The information below is tailored toward the most relevant to modeling the long-term performance of the disposal facility.

2.1.5.1 Bear Creek Valley hydrogeologic framework

The BCV RI (DOE 1997b) provided the first comprehensive assessment of the environmental setting and hydrogeological conceptual model encompassing the entire length of BCV. The report incorporates the hydrologic framework for the ORR developed by ORNL researchers (ORNL 1992a, ORNL 1992b, Moore and Toran 1992), includes a comprehensive assessment of historical waste sites and groundwater contaminant plumes, and presents human health and ecological risk assessments for BCV. Section 2 of the BCV RI presents a summary presentation of the BCV conceptual model, but a more detailed presentation of the model is presented in Appendix C of that report and draws upon data from over three decades of investigations and reporting.

Most relevant to the PA and CA for the EMDF site, the BCV RI addresses details of the surface water hydrology and hydrogeology across the entire length and width of BCV, covering the broader area surrounding the EMDF site. The site-specific hydrogeologic conceptual model for EMDF (Sect. 3.2.3) is largely based on the synthesis of the large body of information on BCV surface hydrology and hydrogeology that is contained in the BCV RI.

The BCV hydrogeologic conceptual model differentiates between the surface water and groundwater flow within and across the predominantly clastic lithology underlying most of the valley floor and the flow along Bear Creek, including groundwater flow within the karstic carbonate rocks along the southern margin of BCV. This configuration of the clastic and carbonate rocks is illustrated conceptually in Fig. 2.13. Across the clastic outcrop belts, groundwater at shallow to intermediate depth tends to flow south to southwest, whereas flow within the Maynardville and along Bear Creek tends to more closely parallel the geologic strike toward the southwest. Hydraulic gradients mirror the topography and are much higher within the clastic rocks north of Bear Creek than gradients along the valley floor and Maynardville Formation outcrop. The cross-section shown on Fig. 2.13 is located near the center of the BCV watershed across the BCBG (as shown on the inset map). The proposed EMDF footprint at the CBCV site is centered across outcrop belts of the Maryville Formation and the lower portion of the Nolichucky Formation, corresponding to the lower half of the BCBG footprint shown in yellow on Fig. 2.13.

Hydrologic subsystems for areas underlain by predominantly clastic (non-carbonate) rocks (sometimes referred to on the ORR as aquitards) were defined in ORNL status report (ORNL 1992b); likewise, the technical basis for these subsystems are described in detail in the status report and in Moore and Toran (1992). The subsystems include a shallow subsurface stormflow zone, the vadose zone, three intervals within the saturated zone (water table, intermediate, and deep intervals), and an aquiclude at great depth where minimal water flux is presumed to occur. The stormflow and vadose zones and the uppermost saturated zone (water table interval) generally occur within materials of the saprolite zone presented in

Fig. 2.14. A majority of the estimated subsurface water flux occurs within these uppermost parts of the subsurface hydrogeologic profile (ORNL 1992b). In general, the seasonal range of water table elevations tends to span the transition between the saprolite zone and the underlying bedrock, suggesting that the weathering profile reflects the complexity of variably-saturated flow dynamics in space and time.

Subsurface flow within the saprolite zone is directed downward and laterally from higher elevations toward stream valleys where shallow groundwater discharge occurs. Water flux through the lower part of the vadose zone is primarily vertically downward. The vertical component of flow below the water table varies according to topographic position (recharge versus discharge areas). Shallow subsurface flux in the uppermost saprolite zone and lateral flux near the saprolite-bedrock interface respond rapidly to heavier precipitation events and contribute much of the quickflow component of storm-period runoff. At increasing depths (on the order of 100 ft or more), flow within the saturated zone contributes proportionally less to the overall subsurface flux, reflecting the decrease in porosity and permeability with increasing depth. A complete description of research methods, locations, interpretations, and findings completed in the headwaters areas of Melton Branch underlain by the same Conasauga Group formations present in BCV is documented in an ORNL status report (ORNL 1992b, pages 3-5 through 3-28). Subsequent watershed studies (Clapp 1998) indicated the proportion of flux via the uppermost saprolite zone may be less than reported by ORNL (1992b), but generally confirmed that most of the active groundwater flux occurs in the saprolite zone.

Another important aspect of the conceptual model relates to groundwater flow paths and rates that are dominant along fractures that trend parallel to geologic strike. Tracer tests and investigations of groundwater contaminant plumes on the ORR and in BCV demonstrate that groundwater tends to move more rapidly along fracture flow paths that are parallel to geologic strike versus flow paths that are perpendicular to strike. This is particularly true for the shallower portions of the saturated zone where most groundwater flux occurs.

The distinction between the shallower parts of the saturated zone and deeper levels is based on variation in groundwater chemical composition with depth thought to be related to water residence time. The approximate boundary between mixed-cation-bicarbonate (HCO_3) water and Na-HCO_3 water was defined at depths ranging from 30 to 50 m (approximately 100 to 165 ft) for the predominantly clastic rocks on the ORR such as those at the EMDF site. The deep "aquiclude," composed of saline water having total dissolved solids ranging from 2000 to 275,000 mg/L lies beneath the deep interval at depths in portions of BCV believed to be greater than 300 m (approximately 1000 ft) (ORNL 1992b). Additional information on groundwater geochemical zones is presented in Sect. 2.1.6.1.

2.1.5.2   Groundwater hydrology overview

The depth to the water table or unsaturated zone thickness varies across a relatively wide range from upland to lowland areas. Vadose zone thickness is greatest below upland areas such as those along Pine Ridge and along the subsidiary ridges underlying the Maryville outcrop belt. In these topographic positions, the water table can lie within the bedrock zone (Fig. 2.14), at depths exceeding 30 ft below the surface. Away from these upland areas of groundwater recharge, the vadose zone thins along the transition to groundwater discharge areas in valley floors where the water table is at or near the ground surface. In most lower elevation areas, the water table lies within the saprolite zone materials at depths less than 20 ft below the surface.

Groundwater within the saturated zone converges and discharges into stream channels along the tributary valley floors, supporting dry-weather base flow, primarily during the wetter portions of the year. During drier periods, groundwater may support little or no stream base flow, but may continue to slowly migrate southward toward Bear Creek along the tributary valley floor areas within alluvium, saprolite, and bedrock

fractures below the active stream channels. Deeper groundwater that does not discharge to the tributaries moves southward toward Bear Creek along pathways through the bedrock zone. Most of the groundwater flux within the saturated zone has been demonstrated to occur via the saprolite zone with progressively less flux occurring at greater depth. The flux decreases in proportion to a general decrease in saturated hydraulic conductivity (K_{sat}) with depth that is associated with smaller fracture apertures and an overall decrease in the number and density of interconnected fractures capable of transmitting groundwater.

Shallow groundwater also discharges to springs in narrow headwater ravines of Pine Ridge and across broader seepage faces along portions of the tributary valleys. Groundwater from these discharge locations contributes to stream channel base flow, particularly during the wet season. Water level hydrographs indicate that recharge to the water table occurs rapidly in response to significant rainfall events in most areas, but the response may be subdued and delayed in wells below upland areas where the water table is at greater depth and recharge rates are slower (DOE 2019). In general, water table elevations are several feet higher, on average, during the wet season (approximately December through March or April) compared to the remainder of the year.

The following subsections address hydraulic characteristics of materials and flow systems within the unsaturated (vadose) and saturated zone.

2.1.5.3   Unsaturated zone hydraulic characteristics

Unsaturated flow in undisturbed areas will migrate to the water table through the typical sequence of topsoil, silty/clayey residuum, and saprolite as described in Sect. 2.1.3.5, which may also include veneers of alluvial and colluvial materials along the flanks and floors of the tributary valleys. According to research (ORNL 1992b, Moore and Toran 1992), most of the water infiltrating the surface during and immediately after storm events travels laterally and relatively quickly through the uppermost part of the soil profile to discharge along stream channels.

Research on the ORR (ORNL 1992b, Moore and Toran 1992, Clapp 1998) has demonstrated that recharge through the unsaturated zone in undisturbed natural settings is episodic and occurs along discrete permeable features that may become saturated during storm events, even though surrounding macro and micropores remain unsaturated and contain trapped air. During recharge events, flow paths in the unsaturated zone are complex, controlled to a large degree by the nature and orientation of structures such as relict fractures in saprolite (ORNL 1992b). It is important to note that much of the surficial material of the saprolite zone at the CBCV site will be removed during site preparation for EMDF construction, and that highly permeable vadose pathways will be less prevalent in the remaining saprolite, geologic buffer, and structural fill materials below the disposal unit.

Virtually all efforts to determine hydraulic conductivity (i.e., slug tests, packer tests, borehole flow meter tests, and pumping tests) reported from sites in BCV have been conducted in the saturated zone or using laboratory tests on soil samples designed to determine K values under saturated conditions. Saturated K measurements have been made in the vadose zone using infiltration tests and packer tests (ORNL 1992b, page 3-13) and the data are lognormally distributed with a geometric mean K_{sat} of 1.9E-03 m/day (2.2E-06 cm/sec) and a range (± one standard deviation) of 1.74E-07 cm/sec to 1E-04 cm/sec.

Previous investigations of waste sites and proposed waste management/disposal sites in BCV provide considerable engineering and hydrogeological data on saprolite zone materials in the EMWMF footprint and at an adjacent site east of the EMWMF footprint (Golder Associates, Inc. [Golder] 1988a; Ogden Environmental and Energy Services Co., Inc. [Ogden] 1993a, Ogden 1993b; Bechtel Jacobs Company LLC [BJC] 1999; Waste Management Federal Services, Inc. [WMFS] 2000; CH2M-Hill 2000). With regard to K_{sat} measurements in the vadose zone, bulk soil samples from two test pits (TP12 and TP16)

excavated in the unsaturated zone at the EMWMF site were submitted for laboratory analysis of permeability (per American Society for Testing and Materials [ASTM] Method D5084) from depths of 4 ft and 8 ft below surface, respectively. TP12 was located within the outcrop belt of the Rutledge Formation and the sample was classified as silt. TP16 was located in the outcrop belt of the upper Maryville Formation and the sample classified as clay. Permeabilities ranged between 1E-06 and 1E-08 cm/sec for four tests conducted on remolded and compacted samples (two tests per sample were conducted at 5 and 30 psi confining pressures with lower permeabilities associated with the 30-psi tests). Characterization of a previous EMDF candidate site just east of EMWMF included collecting five Shelby tube samples for laboratory analysis (ASTM Method D5084) of K_{sat} (DOE 2017c). Two samples were collected from the unsaturated zone at depths of 2 to 4 ft and 10 to 11 ft below the surface. Hydraulic conductivity values were 3.5E-06 cm/sec and 5.0E-06 cm/sec, respectively, and both samples were described as silty clay (decomposed shale). These results, based on a small sample size and remolding of bulk soil materials, are not representative of bulk K_{sat} values for natural in situ soils and saprolite, but they may be applicable to overburden material (soil and saprolite) that is selected for engineered fill/geobuffer materials.

Information on vadose material characteristic curves for moisture retention or relative permeability relationships for variably saturated flow conditions is limited. Laboratory measurements of moisture characteristic curves were obtained for vadose zone soils samples at seven locations at a site in Melton Valley underlain by formations of the Conasauga Group (Rothschild et al. 1984). The samples were collected from the upper 2 m of the soil profile. The K_{sat} values were estimated in the field using a constant head technique, and hydraulic conductivity relationships were derived based on the K_{sat} estimates and the measured characteristic curves (Rothschild et al. 1984, pages 18–30 and Appendix C). The applicability of these measurements to vadose zone materials at the EMDF site is difficult to assess, but the estimates of K_{sat} obtained are generally on the upper end of the range of other laboratory estimates of K_{sat} described in the preceding paragraphs. Although geotechnical data collection to support EMDF design and construction is being conducted, unsaturated material characteristic curves are not typically measured in such investigations. Section 2.1.11 summarizes the results of recently completed characterization activities at the CBCV site.

2.1.5.4   Saturated zone hydraulic characteristics

Hydraulic characteristics of the saturated zone in BCV have been determined by numerous investigations at sites in BCV. The following subsections review the findings from site investigations and research in BCV most relevant to the hydraulic characteristics of saturated subsurface materials at the proposed EMDF site.

Porosity, effective porosity, and matrix diffusion in the saturated zone. Estimates of porosity and effective porosity reported for subsurface materials in BCV vary along the vertical subsurface profile (Fig. 2.14) and among geologic units. This variation is closely correlated with variability in hydraulic conductivity measurements that are available.

While total porosity can be high (> 0.4) in fine-grained (silty clay), porous materials of the upper saprolite zone in BCV, the drainable porosity is typically lower because the small pore size and high capillarity of the fine-grained materials prevent water from freely draining from the bulk of the material. Effective porosity (the fraction of total porosity associated with fluid advection) under hydraulic gradient conditions other than gravity-driven drainage can be higher than the drainable fraction of the total porosity.

Below the clay-rich upper portion of the saprolite zone, the highly weathered and fractured saprolite and the upper bedrock zone materials are associated with higher total and effective porosities than the deeper, less weathered and fractured bedrock at depth. Within the saprolite, porosity also varies between fragments of less-weathered rock that are embedded in the highly weathered matrix material. These general features

and downward transitions are evident in tube samples and test pits of soils and saprolite, and in bedrock cores. Local variations in porosity also reflect variability in the density and size of fractures in both saprolite and less weathered bedrock.

Total porosity values have been rarely presented in the ORR literature. A mean porosity of 0.50 for shaley saprolite in trench walls at ORNL Waste Area Grouping (WAG) 6 has been reported based on bulk density calculations (Moore and Toran 1992, page 15). The majority of porosity estimates from the ORR are presented as effective porosities or closely related quantities, such as storativity. The effective porosity and related data from various reports and research conducted on the ORR and in BCV is summarized in Table 2.7. The values for effective porosity range over several orders of magnitude depending on the methods, assumptions, and calculations applied for their determination.

Table 2.7. Effective porosity estimates (percent) from various ORR sources

Paper/report source	Mean effective porosity (%)	Range - effective porosity (%)	Notes
Dorsch et al. 1996	9.9	4.58-13.00	Bedrock cores - GW-132, 133, 134 EBCV transect shales from various Conasauga Group Formations in BCV, cores from 40 to 1156 ft bgs
Dorsch and Katsube 1996, GW-821, -822, -833 WBCV transect; Mudrock saprolite from Nolichucky Formation	39.0		Saprolite groundmass
	16.1		Less weathered saprolite mudrock fragments
		26.2-51.3	Calculated effective porosities, larger volumes of saprolite and mudrock fragments
Moore as reported in ORNL 1992b	3.2	3.2-3.6	Stormflow zone (topsoil/near surface)
	0.23		Groundwater zone (shallow water table interval)
ORNL 1992b, ORR Hydro Framework	4.0		Stormflow zone
	0.42		Vadose zone
		0.25-0.33	Groundwater zone (shallow water table interval)
		0.1-0.001	Groundwater zone appears to include entire saturated zone from shallow water table interval through intermediate to deep intervals
	Mean storativity (%)	**Range - effective porosity (%)**	
	0.084	0.58-0.0048	Storativity from field tests (10^{-3} to 10^{-5})
Moore and Toran 1992, Supplement to Hydrologic Framework for the ORR (see descriptions and Table 1, page 38-39)	**Mean effective porosity (%)**		
	3.5		Stormflow zone
	0.23		Groundwater zone
	Effective fracture porosity (%)		
	0.035		Groundwater zone
	Total matrix porosity (%)		
	0.96		Groundwater zone
	Fracture porosity (%)		
	0.05		Groundwater zone
	Storativity (%)		
	0.076		Groundwater zone
	Mean effective porosity (%)	**Range - effective porosity (%)**	
Lee et al. 1992, Tracer test/modeling at WBCV site	3	1-10	Wells screened in regolith (saprolite) and unweathered bedrock of Maryville Formation

Table 2.7. Effective porosity estimates (percent) from various ORR sources (cont.)

Paper/report source	Calculated effective porosity (%)	Estimated matrix porosity (%)	Notes
McKay et al. 1997, EPM Modeling/Tritium Tracer Test	9	8-40	ORNL Burial Ground 4 in saturated fractured weathered shale saprolite of Pumpkin Valley Formation similar to EMDF/BCV, but in different fault block
	Mean Effective Porosity (%)		
ORNL 1997b, Performance Assessment for WBCV Site	5		Values based on field tests at Engineering Test Facility in similar geology at ORNL/Melton Valley
Law Engineering 1983	0.3		OLF/BCBG pumping test
Lozier et al. 1987	0.06		OLF/BCBG pumping test
Geraghty and Miller 1986	0.01-0.04		S-3 Ponds site pumping test
Golder Associates 1988a	0.01		WBCV site (near EMDF Site 14)

BCBG = Bear Creek Burial Grounds
BCV = Bear Creek Valley
bgs = below ground surface
EBCV = East Bear Creek Valley
EMDF = Environmental Management Disposal Facility

EPM = equivalent porous medium
OLF = Oil Landfarm
ORNL = Oak Ridge National Laboratory
ORR = Oak Ridge Reservation
WBCV = West Bear Creek Valley

The values reported in Dorsch et al. 1996 and Dorsch and Katsube 1996 are based on laboratory analysis of cores from saturated portions of bedrock and saprolite, respectively. Values of effective porosity were obtained using petrophysical methods on bedrock core samples of mudrock specimens from Conasauga Group formations (Dorsch et al. 1996). Two hundred specimens were analyzed from among the Nolichucky, Maryville, Rogersville, Rutledge, and Pumpkin Valley Formations. A mean value of 0.099 ± 0.0261 was obtained using the immersion-saturation method (judged as the most reliable of the three methods used) based on a total of 56 measurements. The authors noted that the values were significantly higher than those previously reported to range between 0.001 and 0.034.

In a separate study (Dorsch and Katsube 1996), effective porosities of saprolite were determined using Rotasonic core samples collected in the saprolite zone of the Nolichucky Formation at the WBCV site. Calculated (averaged) effective porosities for larger volumes including both saprolite matrix and mudrock fragments were determined to range from 0.51 to 0.26. These results suggest considerably higher effective porosity values for saprolite versus fractured bedrock (determined by the same author using similar methodologies) and much higher values than those noted above (ORNL 1992b) for materials within the range of water table fluctuations, typically within the saprolite zone. The calculated effective porosity data for larger volumes displayed a smooth decrease with depth, mirroring the saprolite weathering profile. The calculated effective porosities were noted as probably best suited for the task of modeling and evaluating matrix diffusion as a transport mechanism within the saprolite mantle.

The values reported by Dorsch et al. (1996) and Dorsch and Katsube (1996) are at least one to two (or more) orders of magnitude higher than those reported by ORNL (1992b) and Moore and Toran (1992) for the saturated zone, which were partly derived from analysis of groundwater level recession curves. In general, estimates based on laboratory measurements of porosity or based on other bulk sample characteristics range from a few percent to around 30 percent. Estimates of effective porosity based on pumping tests or other hydraulic analyses are generally less than 1 percent. This dependence on analytical

methods highlights the difference between the porosity associated with hydraulically efficient fracture networks and the larger porosity associated with the geologic matrix materials, which may be effective, but have much lower permeability than the factures. The values shown on Table 2.7 and used in Lee et al. 1992, McKay et al. 1997, and in the ORNL PA for the proposed Class L-II Disposal Facility (C2DF) disposal facility in WBCV (ORNL 1997b) are values assumed for the purposes of groundwater and contaminant transport modeling.

The uncertainty and analytical variability in estimating effective porosity highlights the potential importance of contaminant mass transfer between highly conductive hydraulic pathways and less permeable zones. Contaminant mass transfer between highly mobile and less mobile domains is commonly referred to as matrix diffusion, though both advective and diffusive transport may occur between flow in more permeable and less permeable material zones. A summary of relationships between matrix diffusion and effective porosity in relation to the clastic "mudrock" saprolite and bedrock of BCV that dominates the subsurface environment in BCV is provided in Dorsch et al. (1996). Figure 2.18 conceptually illustrates the partitioning of contaminants by matrix diffusion to or from groundwater fracture flow paths into the adjacent pores and micropores of the surrounding host rock "matrix". The availability and permeability of highly weathered matrix materials decreases with depth below the water table in the clastic rocks of BCV. As discussed in the review of tracer tests below, matrix diffusion is thought to play a critical role in attenuating the migration rates and concentrations of contaminants from source areas to downgradient locations. Depending on the rate of contaminant decay or degradation processes, diffusion of dissolved contaminants from more transmissive zones into less mobile micropores and microfractures can result in enhanced attenuation along flow paths.
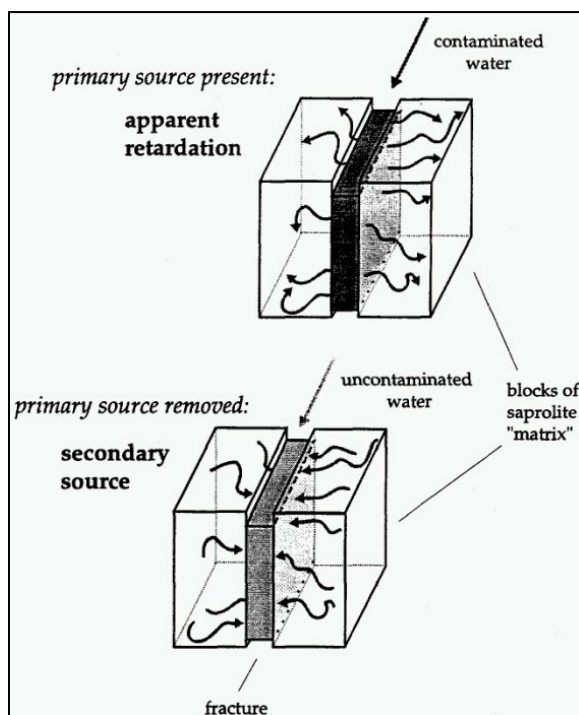
Source: Dorsch et al. 1996, Fig. 3

Fig. 2.18. Schematic diagram illustrating matrix diffusion in a fractured saprolite

61

Hydraulic conductivity of the saturated zone. The most recent compilation of K_{sat} values reported for BCV (UCOR 2014, Appendix C, page C-36) span seven orders of magnitude ranging from a minimum of 5E-05 ft/day (Nolichucky Formation) to a maximum of 164 ft/day (Maynardville Limestone). The values range from low K values determined from packer tests in deep core holes to relatively high values measured in wells completed in karst conduits in the Maynardville Limestone. The K_{sat} varies by lithology, degree of weathering and fracturing, and depth. The K_{sat} values are influenced by the test method, borehole or well completion interval tested, number and vertical spacing among permeable fractures/fracture intervals and intervening relatively impermeable rock matrix intervals, and other factors.

One of the earliest compilations and statistical analyses of K_{sat} data was reported in Connell and Bailey (1989). Pre-1985 K_{sat} data was evaluated from 10 investigation reports with 338 single-well aquifer tests from BCV and Melton Valley at ORNL. Results were segregated and evaluated by regolith and bedrock tests and by geologic formations. In BCV, 232 tests were selected from 153 wells for statistical analysis; 63 in regolith (saprolite zone), 164 in bedrock, and five in deep bedrock. Within BCV, the tested wells were located at the BCBG, Oil Landfarm, and S-3 Ponds waste sites near EMWMF, and from the proposed Exxon Nuclear site between SR 95 and the Clinch River. These results include wells completed in the same geologic formations underlying and downgradient of the CBCV site and are, therefore, representative of the range of K_{sat} values that may be expected at and near EMDF. The BCV data is summarized in terms of the distributions of K_{sat} values within and among the geologic formations spanning the width of BCV in Fig. 2.19. The median K_{sat} values for the clastic rock formations underlying the EMDF site (i.e., Maryville Formation and Nolichucky Formation) are roughly an order of magnitude lower than the median K value of the Maynardville Limestone.
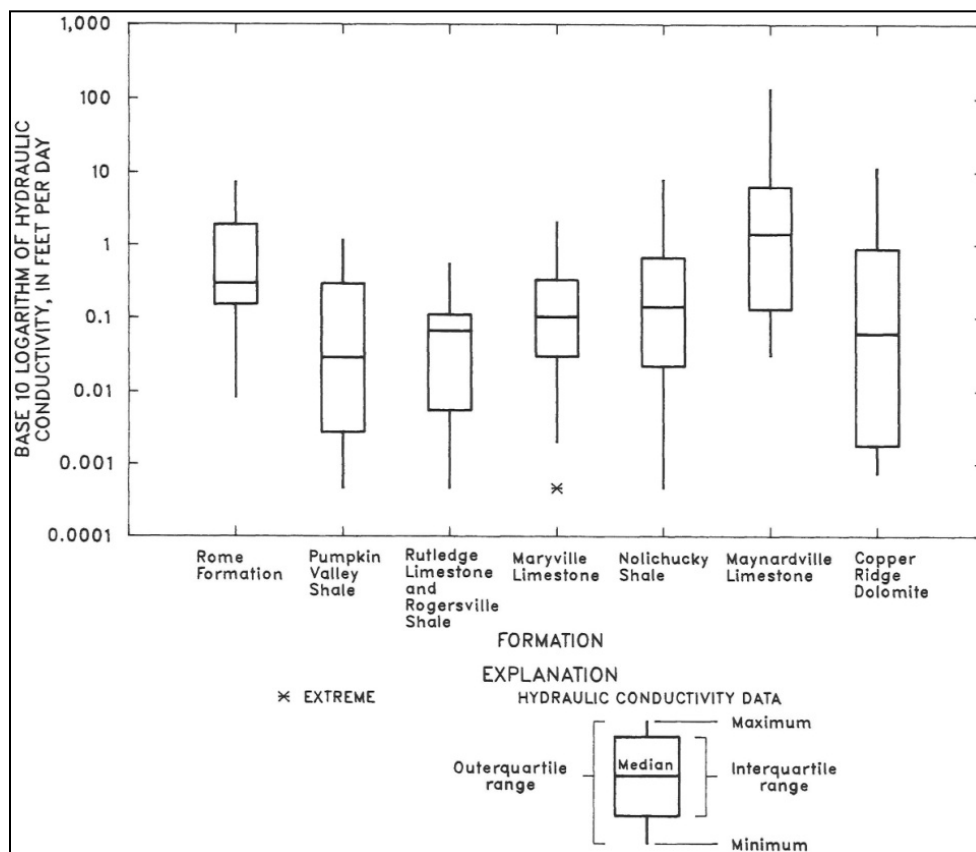
Source: Connell and Bailey 1989, based on pre-1985 wells.

Fig. 2.19. Results of statistical analysis of hydraulic conductivity of 232 tests in BCV wells

62

In addition, BCV specific information included K_{sat} data from a total of 120 packer tests, 66 slug tests, and four pumping tests across a broad area of WBCV in support of the planning for the proposed C2DF (Golder 1988b). In this report, the K_{sat} results were plotted and analyzed by test method, geologic formation, and depth. The K_{sat} data was subdivided into three depth horizons (0 to 50 ft, 50 to 300 ft, and > 300 ft) and was provided frequency distribution plots of log K data according to these three depth levels. It was concluded that "*there does not appear to be a strong relationship between K and geologic formation. However, K is clearly depth dependent.*" The 0- to 50-ft interval was considered the most permeable and most representative of saprolite or shallow bedrock, with progressive decreases in K with depth for the lower horizons. From shallow to deep, geometric mean K_{sat} values were assigned for the three horizons of 1E-04 cm/sec, 1E-05 cm/sec, and 1E-07 cm/sec.

A linear regression analysis performed of the K_{sat} data with depth as the independent variable is shown in Fig. 2.20, with a correlation coefficient of 0.46. This data set was considered too limited to conduct multivariate analysis to assess the effects of test type, test scale, and geologic formations. It was also noted that a "significant emphasis" was placed on testing the Nolichucky Formation and Maryville Formation.
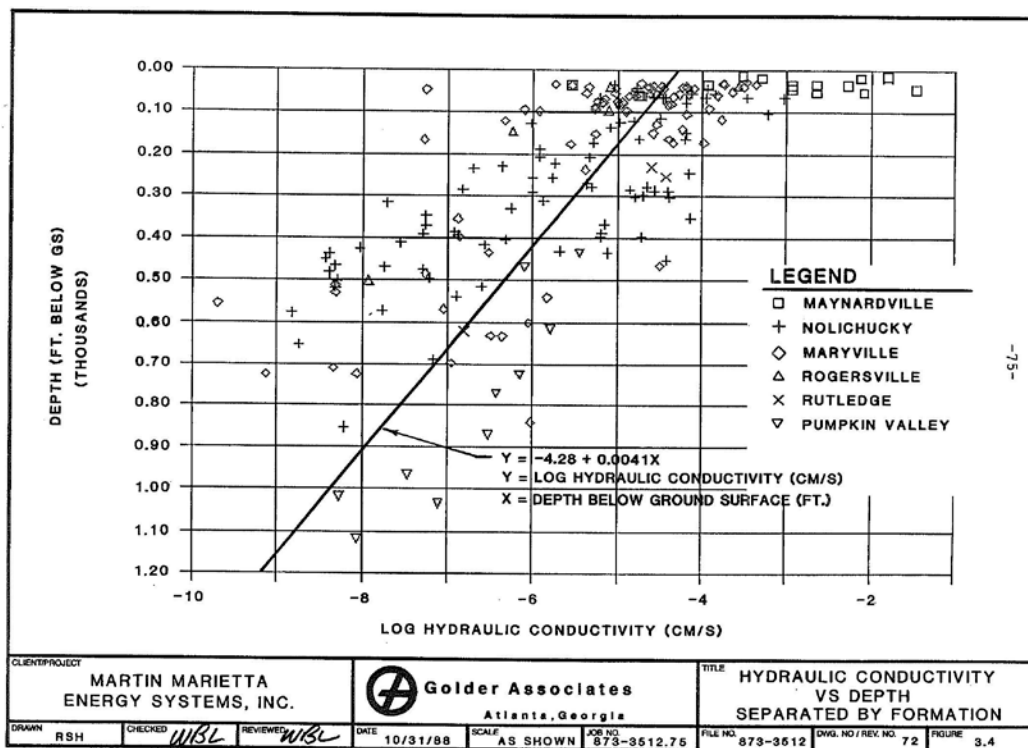
Source: Golder 1989

Fig. 2.20. Linear regression plot of hydraulic conductivity at depth at WBCV (Site 14)

A more recent comprehensive compilation, summary, and analysis of K_{sat} data from multiple sites in BCV (including other groundwater hydraulic characteristics) were presented in the BCV FS (DOE 1997c). More than 200 test results from wells completed in BCV up through 1997 are included in Appendix F of the BCV FS, Sect. 3.5. The data were derived from slug tests/bailer recovery tests, packer tests, and pumping tests, including packer test intervals conducted in deep core holes between depths of approximately 250 to 950 ft. The results were used in support of the construction and calibration of the original 3-dimensional (3-D) regional groundwater flow model for BCV used for evaluating remedial actions at the hazardous waste sites and contaminant plumes in EBCV.

The results of the K_{sat} tests presented in the BCV FS are summarized in Table 2.8 and Figs. 2.21 and 2.22. The relationship between log K_{sat} values and depths for the predominantly clastic (shaley) formations in BCV from the Rome through the Nolichucky Formation is illustrated in Fig. 2.21, while results for the carbonate formations of the Maynardville and Knox Group along the south side of BCV are illustrated in Fig. 2.21. The plots illustrate the larger number of wells and test results available for relatively shallow wells (< approximately 100 ft) versus results available for intermediate and deep levels of the saturated zone (> approximately 100 ft). The plots and regression lines also illustrate that while there is considerable scatter in the range of K_{sat} values by depth, the data suggest an overall general tendency toward reduced K_{sat} values with depth that is consistent with less weathering and fracturing evident in subsurface samples/rock cores, and a general reduction in transmissive fractures with depth.

Table 2.8. Summary statistics compiled by for K data in BCV

Hydrogeologic unit	K (min) (ft/day)	K (max) (ft/day)	K (avg) (ft/day)	Count
Knox	0.0002	3.67	0.511	27
Maynardville Limestone	0.000027	99.0	8.132	41
Nolichucky Formation	0.000009	7.1	0.723	109
Maryville Formation/Rutledge Formation/Rogersville	0.00003	2.08	0.192	33
Pumpkin Valley/Roane	0.00086	1.156	0.223	18

Source: DOE 1997c.

BCV = Bear Creek Valley   K = hydraulic conductivity
DOE = U.S. Department of Energy
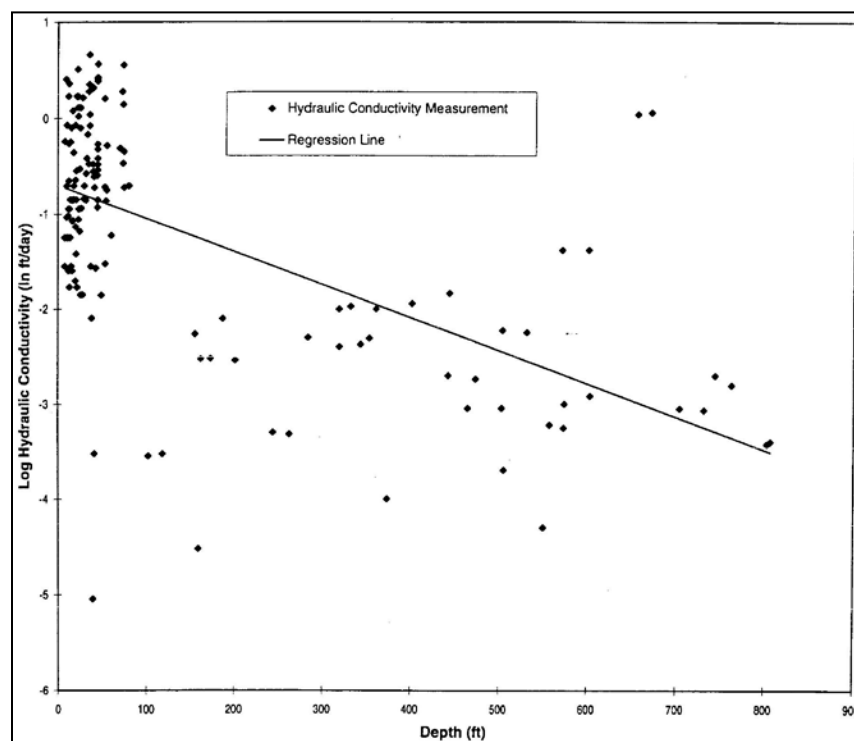
Source: DOE 1997c, Fig. F.20.

Fig. 2.21. Relationship between Log K_{sat} and depth in the clastic formations underlying BCV
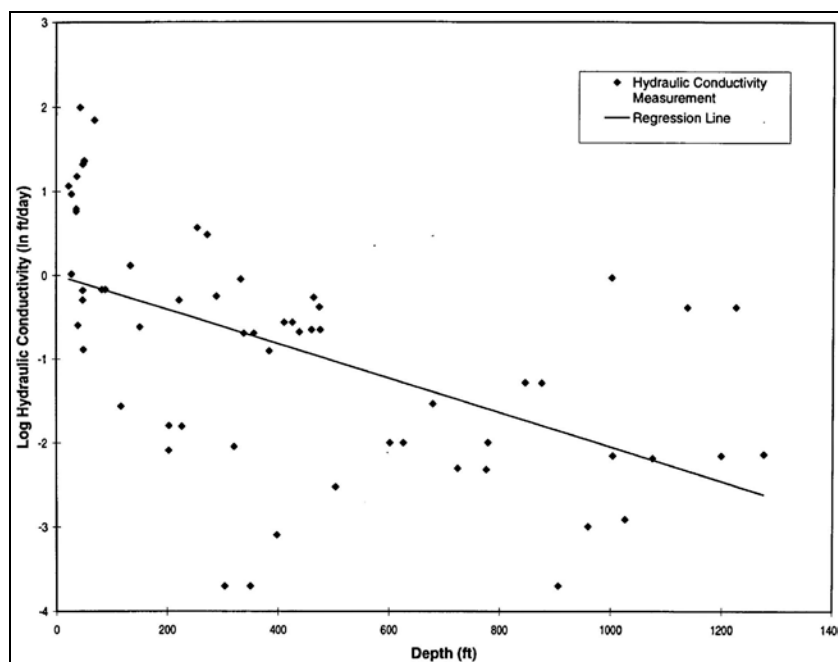
Source: DOE 1997c, Fig. F.19.

Fig. 2.22. Relationship between log K$_{sat}$ and depth in predominantly carbonate formations, BCV

In addition to these earlier efforts, UCOR completed an effort to summarize and statistically evaluate hydraulic properties of BCV units by geologic formation (UCOR 2014, Appendix C). This effort was developed for a Y-12 centered test case of a larger-scale regional groundwater flow model for the entire ORR (UCOR 2015, DOE 2016a).

Field and laboratory measurement of hydraulic conductivity at the CBCV site. Recent characterization of the CBCV site to support EMDF site selection and preliminary design has provided additional information on groundwater and surface water hydrology, including field estimates of hydraulic conductivity. The K$_{sat}$ data are summarized in the following paragraphs, and the surface water flow measurements are summarized in Sect. 2.1.7.2. Section 2.1.11 provides a general summary of the CBCV characterization activities and references to reports that summarize the results.

Hydrologic tests, including Flexible Liner Underground Technologies, LLC (FLUTe™) tests in the deeper bedrock intervals (open boreholes) and slug tests in shallow piezometers, were conducted to provide information of the in situ hydraulic properties.

FLUTe™ testing was performed within the open, uncased boreholes at the CBCV site (GW-978, GW-980R, GW-982, GW-986, GW-988, GW-992R, GW-994, and GW-998) to determine transmissivity (and/or hydraulic conductivity) values within the bedrock (DOE 2019). The results from the FLUTe™ testing and interpretation of the borehole logs, relative to identifying target intervals of permeable water-bearing bedrock, were used to determine screen and sand-pack intervals for both the intermediate and shallow piezometers at each location. During FLUTe™ testing, a flexible borehole liner made of a water-tight, urethane-coated, nylon fabric is lowered into the borehole. The rate at which water is added to the liner is governed mostly by the rate at which the water can escape into the permeable features in the open hole below the descending liner as it forces the water out into the permeable zones in the formation. The liner descent-rate or velocity is a measure of transmissivity of the entire borehole. As the liner continues

down the borehole and seals each permeable feature, changes in the liner velocity indicate the position of each feature and an estimate of transmissivity is provided.

As seen in Table 2.9, total borehole transmissivity ranged from 0.052 sq cm/sec at GW-982, located on the knoll in the Maryville, to 0.198 sq cm/sec at GW-998, located in the Nolichucky south of the proposed disposal facility. The average total borehole transmissivity for the tested boreholes was 0.118 sq cm/sec. Also of importance in Table 2.9 is the "length of the borehole remaining" column. The FLUTe™ liner is inserted into the borehole as water is added inside the liner, driving it downward. If the borehole has a very low transmissivity, the liner will not reach the bottom (water within the borehole below the liner cannot be pushed out into the geologic formation). GW-982 was nearly impermeable below 54 ft below ground surface (bgs) with 71.5 ft of borehole remaining and GW-980R had a permeability too low to conduct profiling. The results generally indicated a decreasing hydraulic conductivity with depth.

Table 2.9. FLUTe™ measurements in Phase 1 piezometers

Well ID	Depth of FLUTe™ profile (ft bgs)	Total borehole transmissivity (cm²/sec)	Length of borehole remaining (ft)	Transmissivity of remaining borehole (cm²/sec)	Average hydraulic conductivity for remaining borehole (cm/sec)	Geologic formation
GW-978	76.85	0.16164	5.24	0.02705	1.30E-04	Rutledge
GW-980R	--	--	--	--	--	Maryville
GW-982	53.74	0.05181	71.56	0.0045	2.06E-06	Maryville
GW-986	49.17	0.09862	10.25	0.01538	1.02E-04	Maryville
GW-988	75.37	0.10648	3.64	0.056714	5.12E-04	Maryville
GW-992R	51.12	0.10757	3.71	0.04239	3.75E-04	Nolichucky
GW-994	52.02	0.09845	2.73	0.06932	8.34E-04	Nolichucky
GW-998	39.92	0.19806	5.16	0.05684	3.62E-04	Nolichucky

-- = not available/applicable

bgs = below ground surface.

FLUTe™ = Flexible Liner Underground Technologies, LLC

Hydraulic conductivity (horizontal) was measured by performing slug tests for piezometers completed in the upper bedrock and residuum (DOE 2019). Slug tests were performed in shallow piezometers GW-979, GW-981, GW-983, GW-987, GW-989, GW-993, GW-995, and GW-999. Slug-test data were analyzed using the Bouwer-Rice method (Bouwer and Rice 1976, Bouwer 1989) with the AQTESOLV™ software. The results indicate that hydraulic conductivity ranged from 4.6E-05 to 5.0E-03 cm/sec in the shallow piezometers. The average/mean hydraulic conductivity determined for the two individual tests for each piezometer ranged from 5.5E-05 to 5.0E-03 cm/sec.

Anisotropy of hydraulic conductivity. Hydraulic conductivity tends to be anisotropic in BCV, with higher K_{sat} associated with bedding planes and joints in the strike-parallel direction relative to joint sets oriented at right angles to geologic strike. Expressed in general terms of the relationship of strike-parallel, dip-parallel, and cross-strata fracture flow pathways, $K_{strike} \gg K_{dip} > K_{cross-strata}$ on a whole-rock basis. Anisotropy has been observed and estimated in BCV and elsewhere on the ORR by the tendency of tracers and contaminant plumes to elongate in the direction of strike, and by elongations in the cone of depression during pumping tests. Some estimates of the degree of anisotropy in BCV, presented in Table 2.10, range from 1:1 to 38:1, but most fall between 2:1 and 10:1.

Table 2.10. Permeability anisotropy ratios determined for predominantly clastic formations of the Conasauga Group

Ratio of strike-parallel versus dip-parallel hydraulic conductivity	Test method	Analytic method	Reference
1:1	Groundwater flow model calibrated to actual conditions in portions of EBCV	Finite-difference model	Bailey and Lee 1991
2:1	Pumping tests at depths of 3 m and 33 m in Maryville Formation, BCV	Gringarten & Witherspoon Fractured Aquifer Solution	Lee et al. 1992
38:1		Papadopulos Infinite Aquifer Solution	
4:1	Pump test in Conasauga Group, Melton and BCV	Gringarten & Witherspoon Fractured Aquifer Solution	ORNL 1984
8:1	Pump test	Various analytical methods developed for use with pumping tests	Golder Associates 1989
10:1	Groundwater flow model calibrated to actual conditions in EBCV	MODFLOW	Evans et al. 1996
5:1	Pump test in Conasauga Group	Gringarten & Witherspoon Fractured Aquifer Solution	Smith and Vaughn 1985
3:1	Model Calibration; Conasauga Group, UEFPC	Numerical model	Geraghty and Miller 1990
30:1	NaCl tracer test in BCV	Papadopulos Infinite Aquifer Solution	Lozier et al. 1987
5:1	Nitrate plume and head modeling, Conasauga Group, BCV	Numerical model	Tang et al. 2010

BCV = Bear Creek Valley
EBCV = East Bear Creek Valley

ORNL = Oak Ridge National Laboratory
UEFPC = Upper East Fork Poplar Creek

A sensitivity analysis of anisotropy was conducted in Bailey and Lee (1991) by varying K_{sat} values for strike and dip flow and comparing the actual groundwater head at numerous wells with that predicted by their model. The analysis found that anisotropy of 1.1 to 1.25:1 provided the best matches between modeled and actual groundwater head and that preferential flow along strike is not indicated in BCV, except in the Maynardville Limestone. However, results of tracer tests conducted in the predominantly clastic formations of the Conasauga Group also exhibit anisotropy. A particle tracking model was used to investigate anisotropy in BCV in "Application of particle tracking and inverse modeling to reduce flow model calibration uncertainty in an anisotropic aquifer system" (Evans et al. 1996). They found empirically that particle tracks best mimic the S-3 Ponds contaminant plume at an anisotropy ratio of 10:1. Sensitivity analysis indicated that anisotropy ratios lower than 10:1 provided better fits to the contaminant plume than did ratios higher than 10:1.

Hydraulic gradients. Potentiometric surface contour maps (Fig. 2.23) developed prior to the construction of EMWMF show horizontal hydraulic gradients and generalized groundwater flow paths across the upper part of BCV. Similar patterns are present farther down valley, closer to the EMDF site. The upper half of Fig. 2.23 illustrates the shallow water table interval in saprolite zone materials, and the lower half illustrates the shallow to intermediate depths of the bedrock zone. Hydraulic head patterns show convergent flow to the Maynardville Limestone in the valley floor aligned with the southwesterly flow along Bear Creek and indicating that it serves as the hydraulic drain for BCV. The anisotropy associated with strike-parallel fracture pathways tends to modify local flow directions from the more general pattern of flow directions indicated on the maps in Fig. 2.23.

Horizontal gradients tend to vary in proportion to the local topography so that steeper gradients occur along the steeper south flanks of Pine Ridge and adjacent to the subsidiary ridges underlain by the Maryville Formation. An average horizontal gradient of 0.05 for the ORR aquitards (i.e., predominantly clastic rock formations of the Conasauga Group) was reported in Moore and Toran (1992). Measured and model-simulated hydraulic heads and cross-valley/vertical hydraulic gradients in BCV are shown in Figs. 2.24 and 2.25. Hydraulic head data obtained from discrete multiport well intervals in a series of deep core holes along a north-south transect near the S-3 ponds at the west end of the Y-12 site is presented in Fig. 2.24 (Dreier et al. 1993). The multiport depths where head data were obtained are shown as black squares down the length of each borehole in Fig. 2.24. The figure illustrates horizontal gradients from north to south (left to right on Fig. 2.24), with an upward vertical component extending across the Conasauga Group formations toward the Maynardville Limestone. The figure also illustrates mostly downward and lateral gradients below Chestnut Ridge from south to north converging toward the Maynardville. An isolated high pressure zone in the Nolichucky Formation appears to be a relic of higher density fluids flowing down dip from the S-3 Ponds. The lowest hydraulic heads around 990 ft converge within the Maynardville Limestone from higher heads below Chestnut Ridge and southward from Pine Ridge, supporting the concept that the Maynardville, along with Bear Creek, serves as the principal hydrologic exit pathway for BCV as a whole (Dreier et al. 1993). Flow in BCV was modeled and found to have a similar head distribution as shown in Fig. 2.25 (Bailey and Lee 1991).
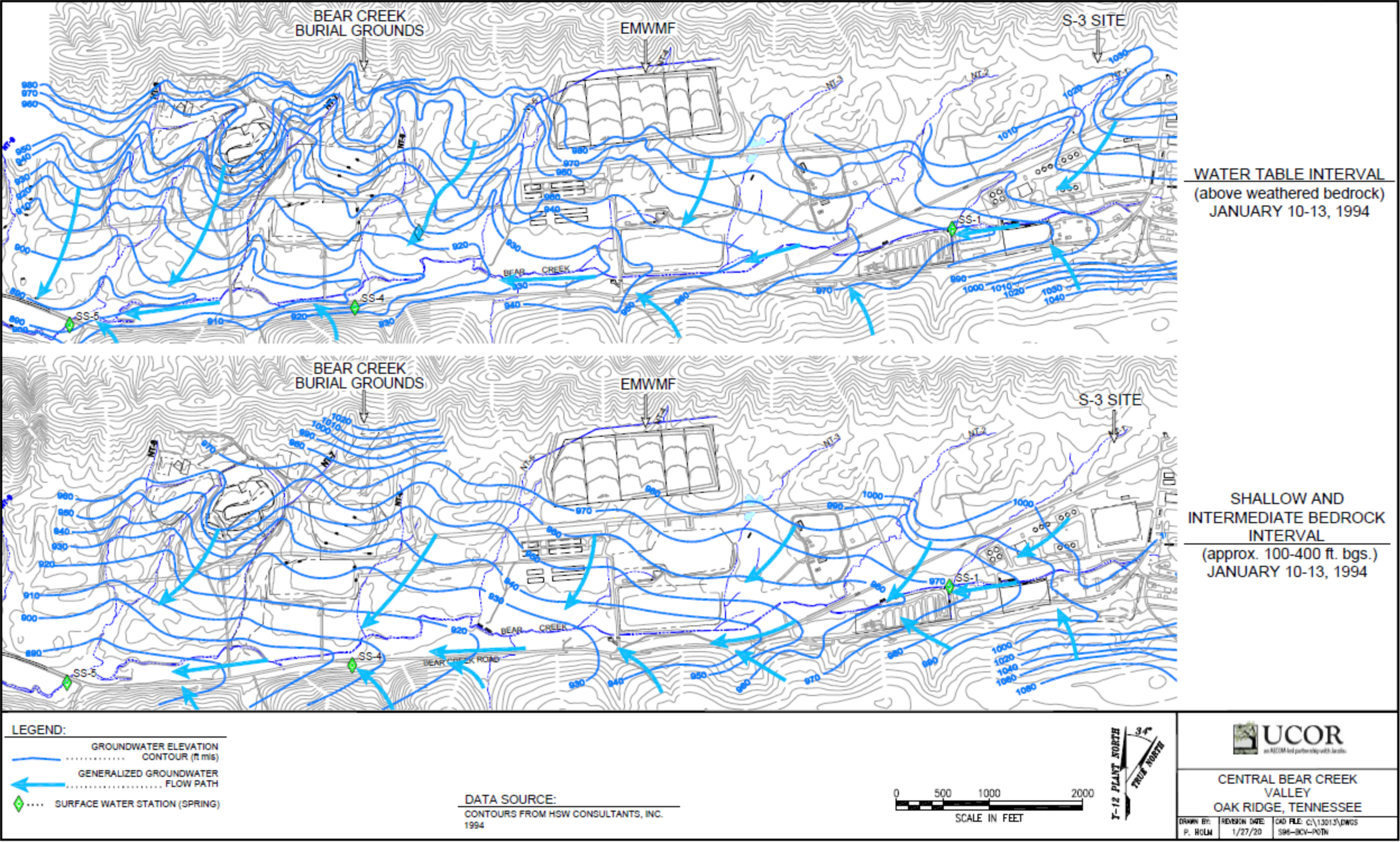
Fig. 2.23. Potentiometric surface contour maps and generalized groundwater flow directions for Upper BCV

This page intentionally left blank.
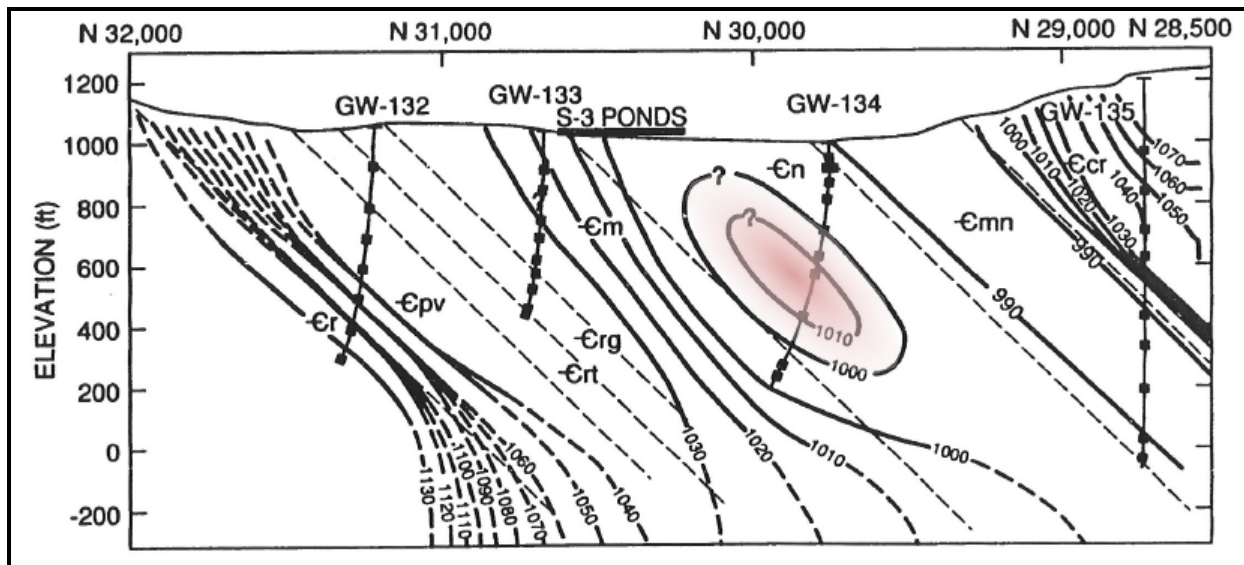
Fig. 2.24. Hydraulic head distribution across Bear Creek Valley along a deep transect near the S-3 Ponds
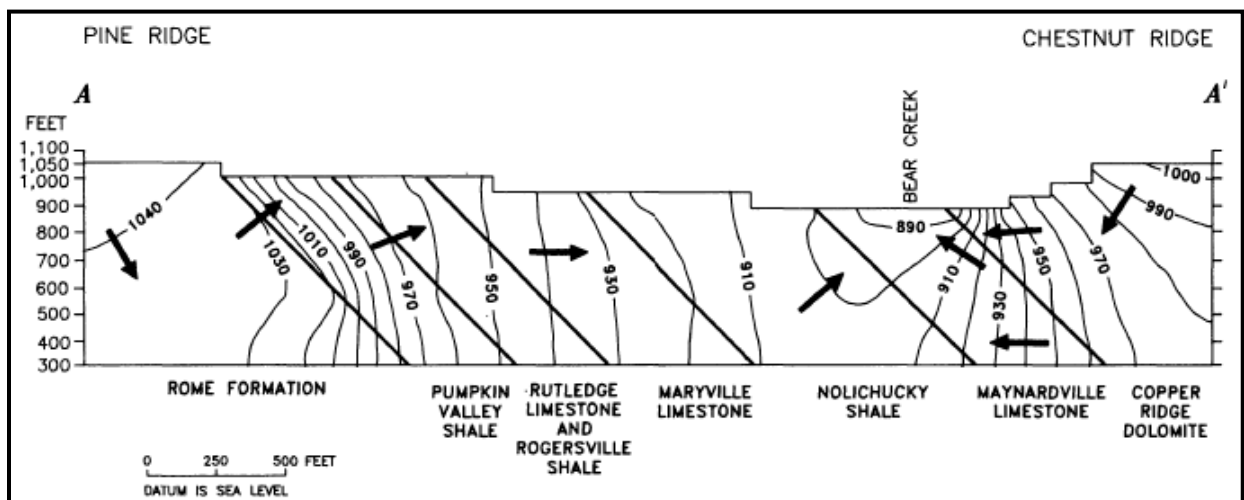
Source: Bailey and Lee 1991.

Fig. 2.25. Cross sectional representation from a computer model of groundwater hydraulic head and flow patterns in EBCV

2.1.6 Groundwater Geochemistry and Radionuclide Transport Processes

2.1.6.1 Groundwater geochemical zones and deep groundwater circulation

The boundaries between the shallow, intermediate, and deep groundwater zones defined in the hydrologic framework for the ORR and BCV (ORNL 1992b) are transitional and not precisely defined. The boundaries vary with changes in local topography, vadose zone thickness, degree and depth of saprolite zone and bedrock zone weathering, and bedrock stratigraphy. The zones occur at different levels in different parts of the ORR (Moore and Toran 1992) and field identification is commonly based on vertical changes in groundwater chemistry. Hydrogeochemical processes involving exchange of cations on clays and other minerals result in a change from calcium bicarbonate to sodium bicarbonate (Na-HCO$_3$) and ultimately to

71

a sodium chloride (Na-Cl) type water at depth. These geochemical zones reflect groundwater residence times and reduction of water flux with depth.

The top of the intermediate groundwater zone is marked by a change in the dominant cations from calcium, magnesium, and Na-HCO$_3$ to predominantly Na-HCO$_3$, and extends from approximately 100 ft to over 275 ft, where the transition to the deep zone is marked by a gradual increase in Na-Cl (Haase et al. 1987, Bailey and Lee 1991). The intermediate and deep groundwater zones are distinguished from the shallow (water table) zone by a change from a calcium-magnesium-bicarbonate (Ca-Mg-HCO$_3$) chemistry to a chemistry dominated by Na-HCO$_3$ (Moore and Toran 1992). The transition from Ca-Mg-HCO$_3$ to Na-HCO$_3$-dominant water is abrupt, occurring between depths of 80 to 200 ft in the Nolichucky Formation underlying BCV, which suggests a well-defined flow boundary (Haase 1991).

This groundwater type is common to all Conasauga Group formations (Dreier et al. 1987) at intermediate and deep depths except in the Maynardville Limestone, and appears to be unrelated to stratigraphic changes. The Maynardville Limestone and adjacent Copper Ridge Dolomite both exhibit a Na-HCO$_3$ water type with distinct zones of Ca-Mg-Na-sulfate (SO$_4$) water. These sulfate-rich water zones appear to be related to the presence of gypsum beds in the carbonate units. Table 2.11 summarizes this geochemistry information for the Conasauga Group.

Table 2.11. Geochemical groundwater zones in predominantly clastic rock formations of the Conasauga

| Interval or zone | Bear Creek Valley[a] | | | Bear Creek Valley[b] | | | Melton Valley[c,d] | | |
	Depth (ft)	Type	pH	Depth (ft)	Type	Depth (ft)	Type	pH
Shallow	75	Ca, Mg-HCO$_3$	NA	< 50	Ca, Mg-HCO$_3$ or SO$_4$	< 75	Ca, Mg-HCO$_3$ or SO$_4$	6.5 – 7.5
Intermediate	NA	NA	NA	50–500	Na-HCO$_3$ (with some Na-Cl and Na-SO$_4$)	75-275	Na-HCO$_3$	6.0 – 8.5
Deep	NA	NA	NA			75-530	Na-HCO$_3$ to Na-Cl	8.0 – 10.0
Brine (aquiclude)	> 530	Na-Cl	NA	NA	NA	590 (GW-121)	Ca-Na-Mg-Cl + SO$_4$	11.6

[a]Haase 1991.
[b]Bailey and Lee 1991.
[c]Haase et al. 1985.
[d]Nativ et al. 1997a.

NA = not applicable

The change in groundwater chemistry with depth is interpreted to be the result of rock-water interactions and diagenesis of minerals. The rate at which the groundwater reaches chemical equilibrium with source minerals is important in the diagenetic evolution of Na-HCO$_3$, indicating that the groundwater is reaching equilibrium with the host rock. If clay alteration is an important control on groundwater geochemistry, then Na-HCO$_3$ type water may mark the transition between the actively circulating shallow zone and stagnating groundwater in deeper zones (ORNL 1992b).

Studies of deep boreholes in the Conasauga Group and the Copper Creek Dolomite of the Knox Group in EBCV indicate that deep groundwater chemistry trends from Na-HCO$_3$-dominated water to increasing Na-Cl content between 550 ft below grade near Pine Ridge to over 1150 ft below grade in the Maynardville Limestone on the south side of BCV (Dreier et al. 1993). This trend is associated with an

increase in total dissolved solids and pH that appears to be related to long-term rock-water reactions. These deep transitional waters are saturated with calcite and dolomite as stated in Haase (1991).

The aquiclude zone is so named because the extremely high salinity of this water indicates that little or no groundwater movement occurs. The aquiclude is well defined in the Conasauga Group of Melton Valley, but is less well documented in BCV. Detailed water chemistry data has been provided for four wells positioned across strike in EBCV and drilled to depths between 557 ft and 1196 ft below grade (Dreier et al. 1993, Haase 1991). Both reports noted an abrupt increase in total dissolved solids to about 28,000 ppm, increase in pH to the 8.5 to 10.0 range, and change from $Na\text{-}HCO_3$ as the dominant ion pair to dominance of Na-Cl below 1150 ft. This increase occurred just below a major fracture zone. The deep Na-Cl groundwater in four deep wells sampled for this study was saturated with respect to calcium and magnesium, and contained barium at near-saturation concentrations, which is indicative of long residence time and little or no recharge by fresher water (Haase 1991).

The presence of tritium[1] and modern C-14 in some deep brine samples from the Conasauga of Melton Valley suggests that some meteoric water commingles with the brine at depths (Nativ et al. 1997a). Groundwater flow has been measured by down-hole flow meter in various deep boreholes below 750 ft. Based on these considerations, it is postulated that flow occurs in the deep brine, and that at least some meteoritic water is transported to depth (Nativ et al. 1997b). This interpretation is refuted in Moline et al. (1998) noting that the persistence of brine over geologic time provides a strong indication that deep groundwater circulation is minimal and that deep rocks exhibit very low K_{sat} values, on the order of 1E-07 to 1E-09 cm/sec, which suggests either an absence of or minimal number of permeable fractures.

The presence of shallow water signatures (comparatively low total dissolved solids, tritium, and relatively high percentages of modern carbon) may be induced by drilling, well installation and development, open borehole circulation, or purging prior to sampling. Development and purging of deep wells is hampered by extremely low flow rates and long recovery times (Moline et al. 1998).

While some groundwater exchange may occur between the halocline and shallower groundwater zones, it is volumetrically very minor and does not appear to play a significant role in regional flow patterns. As noted above, there is a significant difference in density between the shallow groundwater and the brine. The density of uncontaminated water, or water contaminated at low concentrations by dissolved constituents, is around 1.01 g/cm^3; in comparison, the density of sea water is 1.022 g/cm^3, and brine is over 1.20 g/cm^3. A great deal of hydraulic head would be required to drive fresh water into the brine zone. The S-3 Ponds nitrate plume, which extends to depths of more than 400 ft is acknowledged as a density-driven plume, with a density range between 1.06 and 1.12 g/cm^3 (DOE 1997b). This density difference is sufficient to drive the plume below the uppermost fresh water zone, but not into the brine zone. Thus, density differences also prevent deeper downward penetration of shallow groundwater. This is analogous to the fresh water – sea water boundary that develops in coastal aquifers.

2.1.6.2   Tracer tests in Conasauga Group formations

Tracer tests are conducted by introducing a locally distinct tracer (dye, chemical, radionuclide, or particulates) into groundwater and monitoring along possible flow paths or discharge points to determine if and when the tracer first arrives, when the peak concentration occurs, and how long it takes the tracer to recede. Tracer tests are commonly used in fractured and karst systems because they are often strongly anisotropic, heterogeneous, and have complex flow paths and travel times that may be difficult to

---

1 Although some tritium is produced in the atmosphere by cosmic rays, it is mostly the result of atomic testing, and its presence in deep groundwater suggests that there have been recent additions of shallow water. Tritium has a half-life of 12.3 years and it would, therefore, be expected to have decayed to undetectable concentrations if groundwater migration times were very long.

determine. Tracer tests conducted in the saturated zone in Conasauga Group formations in BCV and/or in similar geologic formations elsewhere on the ORR are reviewed below along with key findings from the tests most relevant to saturated zone contaminant transport at the EMDF site.

Tracer tests have been conducted at field sites in WBCV and at field sites in Melton Valley at ORNL near burial ground (BG) Sites BG4 and BG6 and WAG 5. The tests were all conducted under natural gradients in shallow groundwater in areas underlain by predominantly clastic formations of the Conasauga Group. The tracers were all introduced at or near the water table in highly weathered and fractured shaley saprolite. The monitored plume areas were all relatively small in areal extent (less than approximately 20 ft to 100 to 200 ft in any direction) and involved a variety of tracers: (1) fluorescent dyes, (2) tritiated water, (3) noble gases (helium, neon) and bromide, and (4) colloids. Among all the tracer tests conducted on the ORR, the WBCV field site is the most intensively studied with the largest network of downgradient monitoring wells. The longest duration tests were those conducted at the BG4 and BG6 sites in Melton Valley. The other tests vary in terms of monitoring duration and/or the configuration of the network of wells used for monitoring.

Tracing studies also have been conducted in the karstic carbonate rocks on the south side of BCV and Chestnut Ridge. In general, those studies are less relevant to the release of radionuclides to the near-field environment at the EMDF site, which is situated on Conasauga Group formations north of Bear Creek.

Tests at the WBCV tracer site. The most intensively tested tracer site within predominantly clastic rock formations on the ORR is located in WBCV southwest of the proposed EMDF site. The test site is located along the contact between the Maryville Formation and the Nolichucky Formation with subsurface conditions similar to those of the EMDF site. The WBCV tracer study area is approximately 150 ft long by 70 ft wide. The first tracer tests were conducted there in 1998 by Golder. Seventy-two monitoring wells (single and nested) were installed at 45 locations along several transects roughly perpendicular to topographic and hydraulic gradients. General shallow groundwater flow direction is toward the southwest and the nearby valley of NT-15.

The Golder scope of work also included drilling and logging of regolith materials and rock cores, packer tests, slug tests, pumping tests, and groundwater solute transport modeling. The collective data were used to calibrate and refine model results. The results of the initial tracer tests, in situ hydraulic tests, and preliminary modeling were presented by Golder in a Task 5 report for the WBCV site (Golder 1988b). The results of subsequent tracer work and modeling at the same site were published in an ORNL report (Lee and Ketelle 1989) and journal article (Lee et al. 1992) authored by an ORNL and university research team.

Findings from the 1992 summary article are summarized below. The results provide insight into the complexities associated with characterization, monitoring, and modeling contaminant releases in areas of BCV underlain by predominantly clastic rock formations (i.e., Conasauga Group formations north of the Maynardville).

The tracer plume configuration at the 3- and 12-month time periods after the initial dye injection (10 L of 40 percent rhodamine-WT dye solution) on April 20, 1988, are illustrated on Figs. 2.26 and 2.27. The dye was introduced at the water table in GW-484. Tracer analysis at 1 ppb resolution was performed using fluorimetric techniques. A longitudinal cross-section through the tracer test site (Fig. 2.28) illustrating some of the main subsurface conditions (water table within saprolite; southeasterly dipping bedrock of interbedded shale, siltstone, and limestone of the Maryville Formation; and upward vertical gradients across the site measured among nested monitoring wells).

~10 ppb plume tips at 12 months vs 3 months

CREEK

+ DETECTION WELL LOCATIONS

⊞ INJECTION WELL LOCATION

∕ DIRECTION OF MAXIMUM GRADIENT FROM INJECTION WELL

⊤ GEOLOGIC STRIKE AND DIP
45

WATER TABLE CONTOUR INTERVAL 1.0 ft

TRACER OUTLINE 3 MONTHS AFTER INJECTION
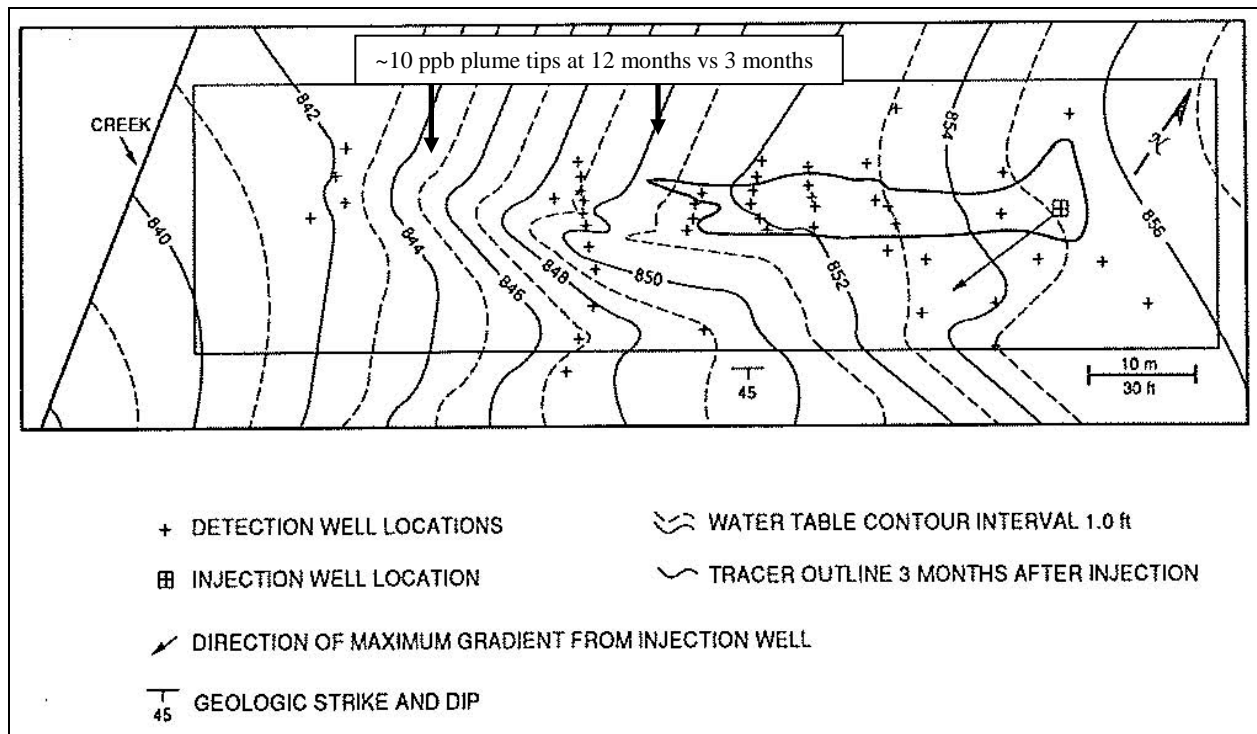
Source: adapted from Lee et al. 1992.

**Fig. 2.26. WBCV tracer test site plume map (10 ppb concentration contour
[~40 m or 131 ft long] 3 months after injection).**
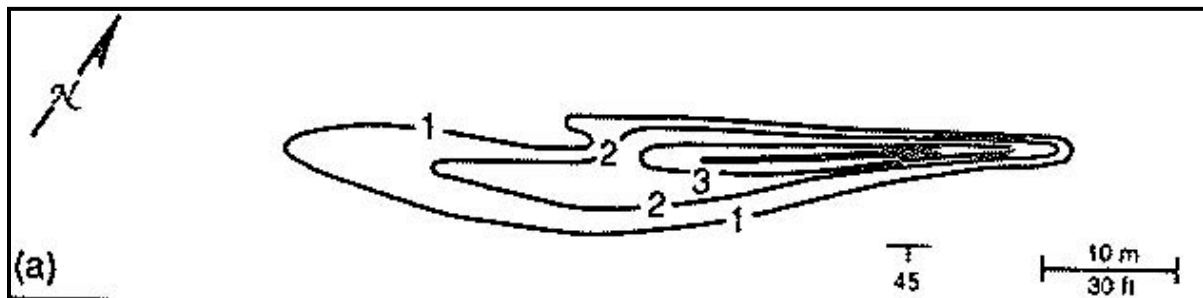
Source: adapted from Lee et al. 1992.

**Fig. 2.27. WBCV tracer test site plume map (log concentration contours
[10 ppb extent ~60 m or 197 ft long] 12 months after injection).**
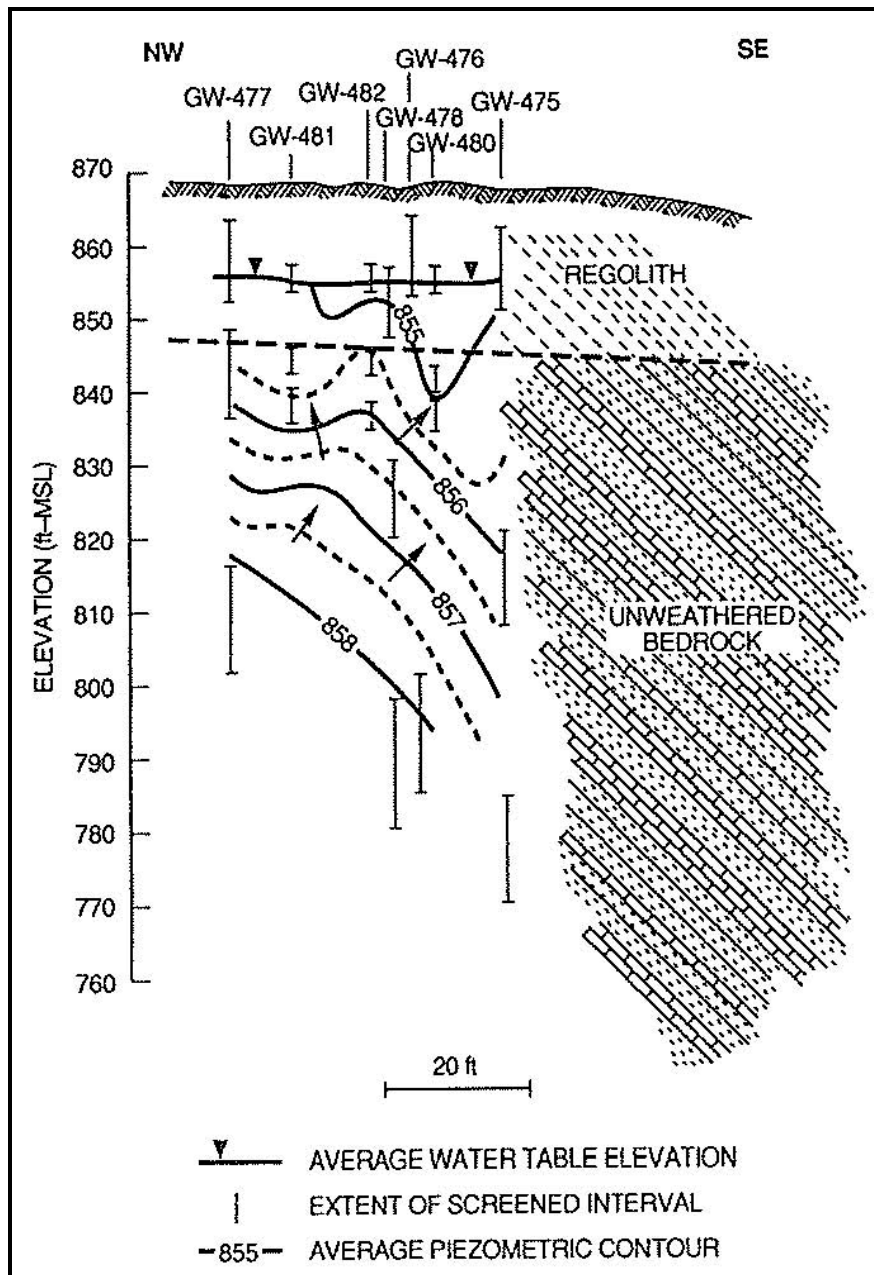
Fig. 2.28. Potentiometric contours for a northwest-southeast cross-section through the WBCV tracer test site.

Water table contours indicate horizontal groundwater flow directions toward the southwest to the local discharge zone along the valley floor of NT-15, parallel to subparallel with the geologic strike. Tracer movement at the WBCV site was found to be predominantly strike-parallel; however, at local scales on the order of inter-well distances (i.e., 10 to 30 m), plume migration was not always consistent with the local direction of maximum horizontal hydraulic gradients measured in the test wells (Fig. 2.26). The tracer plume was monitored for a period of more than 1 year and was found to remain within the water table interval throughout its length. Upward vertical gradients measured at the site were identified as the most probable factor preventing the tracer plume from deeper migration along its downgradient flow path (Fig. 2.28). The authors describe the evolution of the plume configuration over time (Lee et al. 1992):

"In the first two weeks, a high concentration plume migrated as rapidly as 1.0 m/day for about 14m in the near-field, but another 9m of migration in the mid-field required an additional 230 days (0.04 m/day). Total migration distance of 33 m (the far-field) for the 100 ppb front required 370 days (0.09 m/day average).

Data analysis could not attribute the erratic rate of migration to the presence of a concentration gradient induced by the slug dye injection, and no consistent correlation could be found with changes in the water table gradient profile or with precipitation. Rather, the migration rate, narrow overall plume shape, and slightly meandering and fingering plume all suggested the presence of lithologic and/or fracture-related pathways of preferred flow.

The general upward vertical gradient observed at the site explains the observation of tracer only in the water table zone of the aquifer. Tracer was never detected at depth despite long-term monitoring at various depths in bedrock within the tracer pathway and in stratigraphically correlative core holes downdip and downslope of the tracer injection zone. Tracer detection and observed vertical gradients at the site demonstrate that neutral density solutes introduced at the water table mix in a thin zone below the water table and migrate through the bedding plane dominated fracture system. This thin mixing zone which is recharged by local precipitation infiltration from above and by upward leakage from below approximates a two-dimensional solute mixing domain."

Analysis of "broad" and "narrow" tracer test plumes at BG4 and the WBCV site. In conjunction with simulations of fractured-rock flow using a dual permeability model (Stafford et al. 1998) and a 2-D equivalent porous medium (EPM) model (McKay et al. 1997), researchers at ORNL and the University of Tennessee contrasted the broad plume from a tracer test at the BG4 site at ORNL with the narrow tracer test plume at the WBCV site described above. The analyses noted that the orientation of shallow horizontal groundwater gradients with respect to geologic strike strongly influences the rate and direction of groundwater flow and contaminant transport. Broad plumes develop where the average water table gradient is perpendicular to the geologic strike (in the direction of lower permeability) (Fig. 2.29). Narrow, elongated groundwater contaminant plumes in the water table interval develop where the average water table gradient is roughly parallel with the geologic strike (in the direction of greater permeability) (Fig. 2.30).

As described in the article "Influence of fracture truncation on dispersion: A dual permeability model" (Stafford et al. 1998), the BG4 plume:

"…exhibited an unusually large transverse spreading, with the width of the plume approximately equal to its length. The experiment is unique due to the high levels of tritium injected (50 curies) and the long monitoring period (16 years to date). The water table gradient from the injection well to monitoring well 7 (directly downslope) averages 0.15. The migration of the plume is characterized by a fast moving, low concentration front (10's of cm/day), a slower moving center of mass (< 1 cm/day), a very long (up to 16 years) low concentration tail, and an unusually large degree of transverse spreading."
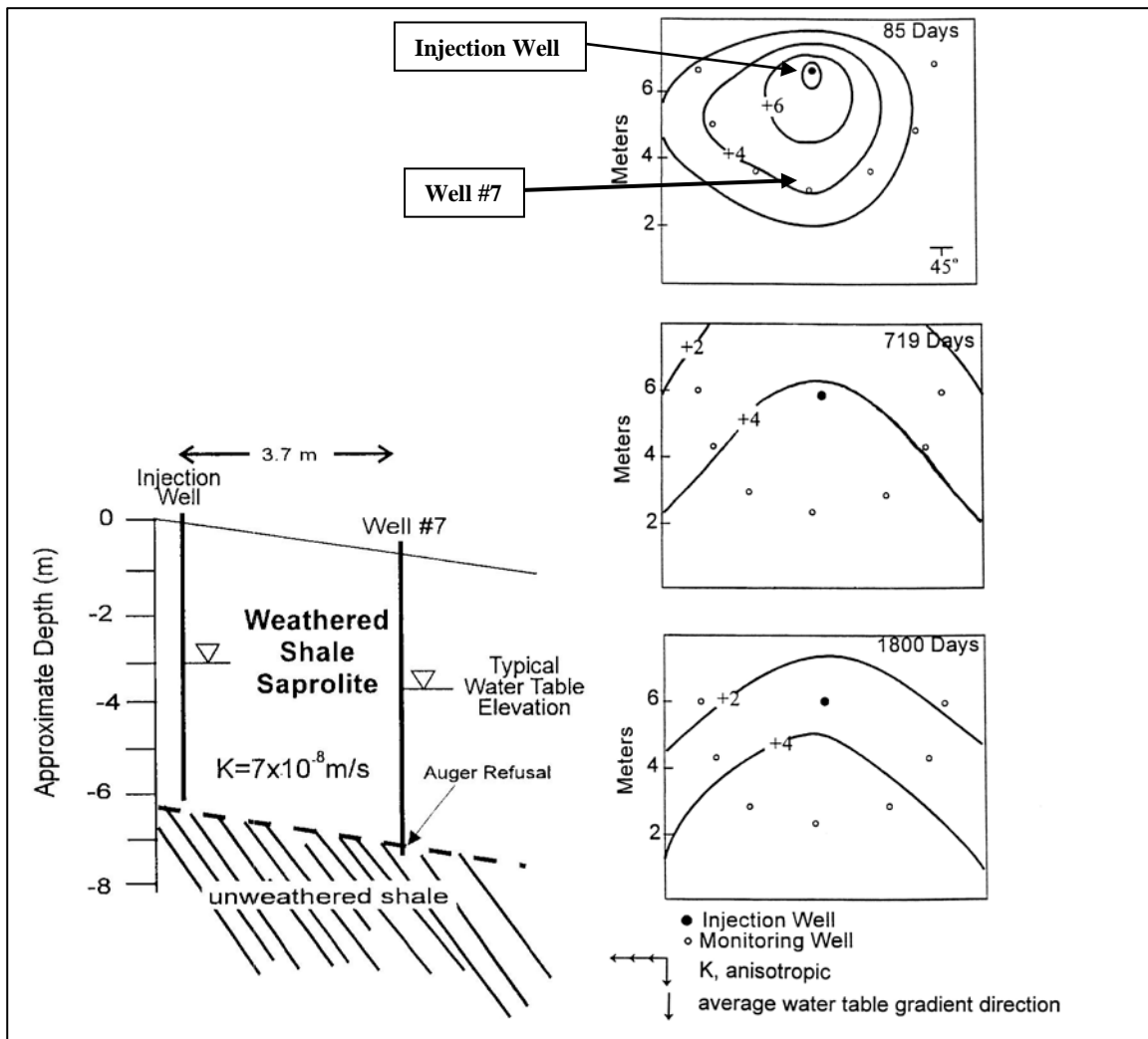
Sources: Stafford et al. 1998, McKay et al. 1997.

Fig. 2.29. Schematic cross-section and contours of tritium concentration (log [pCi/mL]) over time for the "broad" plume at the BG4 tracer test site.
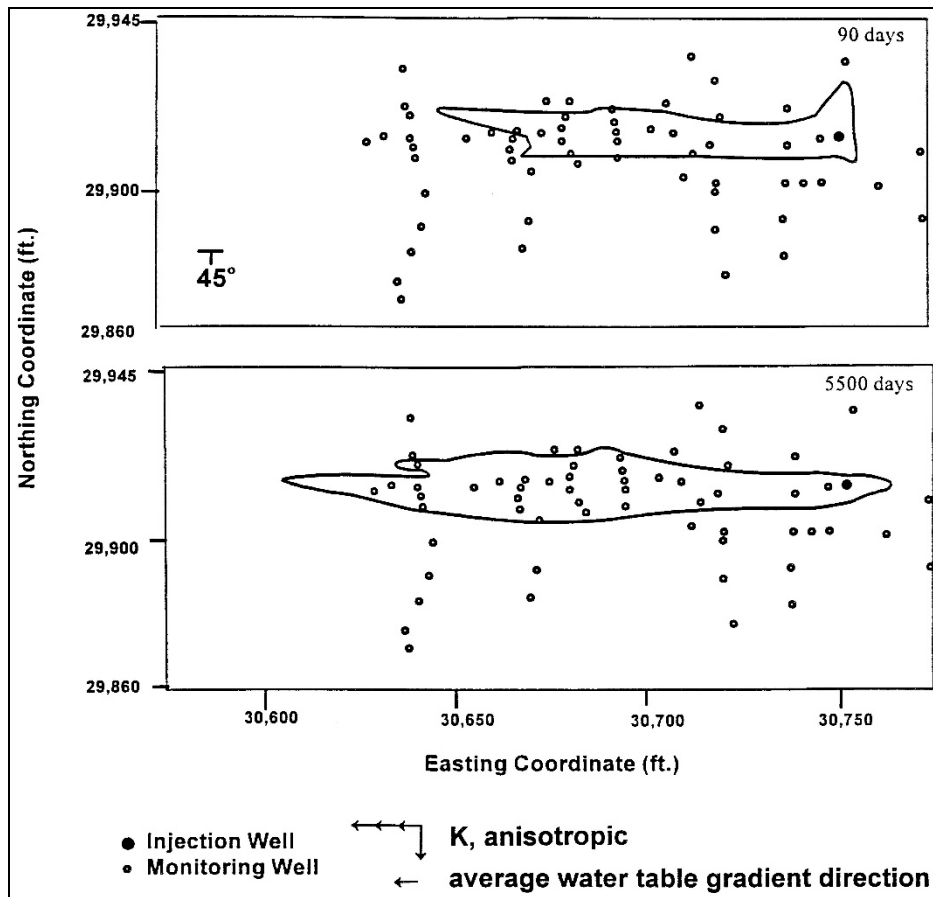
Source: Stafford et al. 1998.

Note: For the 5500-day (15-year) test period shown in the lower map, the scale indicates a total plume length of ~160 ft, less than the ~197 ft illustrated in Fig. 2.26 at 12 months (Lee et al. 1992). Dye breakdown is one possible explanation for this difference.

Fig. 2.30. Contours of 10 ppb dye concentration for the "narrow" plume at the WBCV tracer test site

At the WBCV site, the article continues:

"The geologic material at this site is similar to that at the BG4 site in terms of porosity, hydraulic conductivity, and fracture spacing and orientation. However, the shape of the plume was very narrow (Figure 3-31) as compared to the wide shape of the BG4 plume (Figure 3-30). The major difference between the two sites is that the average water table gradient direction at the WBCV site is approximately parallel to strike of the bedding plane, and at the BG4 site it is nearly perpendicular to strike. The orientation of the water table gradient with respect to the fracture planes likely contributed to the difference in plume shapes. The hydraulic conductivity is expected to be higher in the direction of strike at both locations due to bedding plane partings or fractures (Solomon et al. 1992). With this in mind, transverse spreading at the WBCV site, where there is a strike-parallel gradient, would not be strongly influenced by fluctuating water table direction and secondary fractures perpendicular to strike because of the lower hydraulic conductivity in the transverse direction. Conversely, at the BG4 site, where the average hydraulic gradient is in the direction of the lower hydraulic conductivity (perpendicular to strike) fluctuating water table direction and fractures perpendicular to bedding are expected to have more of

79

an influence on transverse spreading. It is likely that at other locations, where water table slope is neither parallel nor perpendicular to bedding strike, the shape of the plumes would be intermediate between these two extremes."

In the dual permeability model developed in Stafford et al. (1998), the discrete fracture approach was combined with an EPM approach to investigate the influence of a few widely spaced, larger-aperture fractures in a highly fractured matrix (e.g., that found in saprolite and shallow bedrock in the clastic rock formations of BCV). The simulations demonstrated that a limited number of truncated fractures within a permeable matrix can create nearly circular plumes, with about the same degree of spreading in the direction transverse to the average hydraulic gradient as in the longitudinal direction. By comparison, continuous fractures in the direction of flow tend to produce elongated plumes, similar to those typically seen in granular materials. The following conclusions were also noted (Stafford et al. 1998):

"The combined discrete-fracture/equivalent porous media (DF-EPM) approach is useful for looking at possible causes of features such as the observed transverse spreading, but in the absence of detailed data on the fracture network, it is likely that it would be no more effective than the EPM approach in predicting future behavior of the plume."

The main conclusions from the 2-D EPM modeling of the BG4 site (McKay et al. 1997) that are relevant in the context of EMDF modeling include the following:

"1) This study shows that a relatively simple EPM modeling approach can be successfully applied to a complex, highly fractured system, for describing general plume behavior and future concentration trends, **provided that** [bold added] there is sufficient monitoring data available for calibration of the model. This indicates that, at least for this type of fractured clay-rich material, the time span over which monitoring data are collected is a critical factor in model calibration and may even be more important than the number of monitoring wells or the frequency of sampling.

2) The study also illustrates the importance of using tracers that are measurable over a wide concentration range…. where the regulatory limit for the contaminant of interest is many orders of magnitude below the source concentration.

3) The model calibration may be very site- or direction-specific, as indicated by the large difference in transverse dispersivity values or ratios of longitudinal and transverse dispersivity, observed between the BG4 site and another experiment in similar materials in WBCV. This could strongly influence application of models calibrated to small-scale tracer experiments for simulating behavior at a larger scale, or at different sites.

4) Finally, the results of the tracer experiments and the modeling indicate that in cases where extensive contamination has occurred in fractured, porous materials such as shale saprolite, it may take many tens if not hundreds of years of natural flushing to remove dissolved contaminants. Because of the influence of matrix diffusion, attempts to remove dissolved contaminants by pumping would also take a very long time."

Tracer plume evolution at the BG4 site. D. A. Webster of the USGS presented the original detailed documentation of the BG4 and BG6 tracer tests (Webster 1996). The tests were conducted using tritiated water injected at the water table in shaley saprolite of the regolith in July 1977. Monitoring results were reported for the 5-year period from 1977 through 1982, but continued after 1982 (Stafford et al. 1998, McKay et al. 1997). The BG4 test site is located in the Pumpkin Valley Formation and the BG6 site is located in the Nolichucky Formation. The BG tracer tests were designed to examine the hypothesis that groundwater in regolith can flow transverse to the bedding. The layout of the injection well and downgradient monitoring wells was, thus, established so that the horizontal gradients and flow directions

of the water table interval would be perpendicular to the geologic strike (i.e., water table/potentiometric contours are parallel with the strike of the beds, in contrast to the WBCV site where the opposite occurs). At the BG4 site, seven monitoring wells were installed along a 12-ft radius downgradient of the injection well (with a 30-ft radius at the BG6 site, where plume configurations over time were similar to those at BG4). The wells at site BG4 were numbered clockwise from right to left as 4-4 through 4-10, with similar numbering at the BG6 site.

The wells with the highest tritium concentrations were located directly downgradient and strike-normal relative to the injection well. Plots of concentrations over time for several of the BG4 wells show variations in the rate of change over the first two years (Fig. 2.31) and three additional single-point observations over the longer 5-year time frame (Fig. 2.32). Note the concentration scale changes from log to arithmetic.

The BG4 plume maps show that, over time, the initial elongated plume expands laterally and downgradient into a more circular plume that widens and decreases in concentration as the center of mass moves slowly downgradient away from the injection well (Fig. 2.33). Similar plume maps and plots are illustrated for the BG6 tracer test site in Webster 1996. The annual point concentrations in 1980, 1981, and 1982 illustrate the long-term progressive decline in concentrations in downgradient wells (Fig. 2.32).
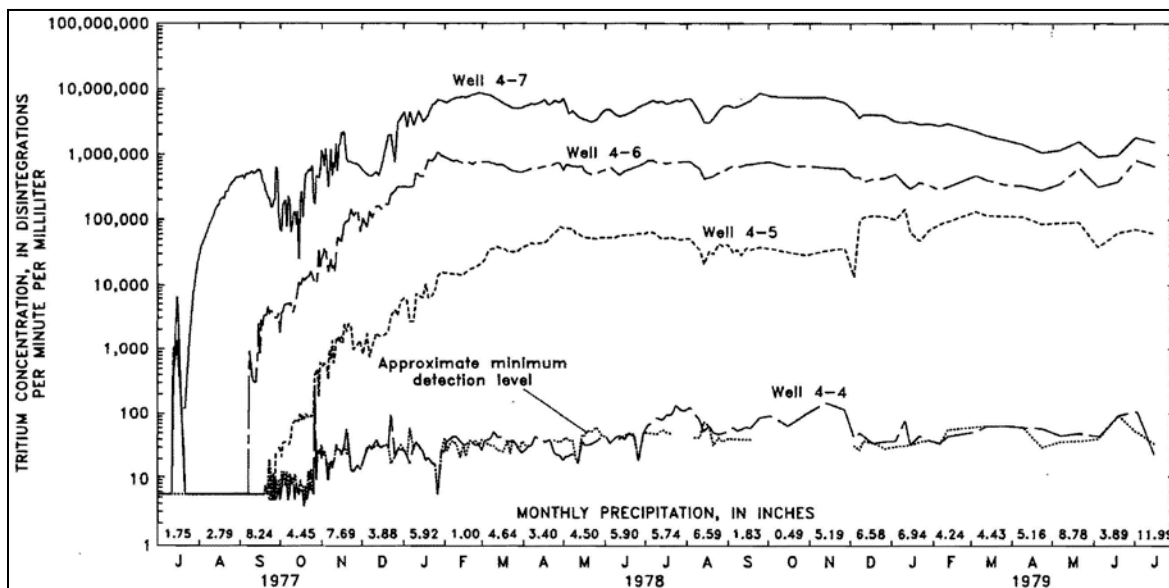
Note: From observation wells at BG4 tracer test site, 1997 to 1979 (Webster 1996).

Fig. 2.31. Tritium concentrations in groundwater over 2 years, BG4 tracer tests

81
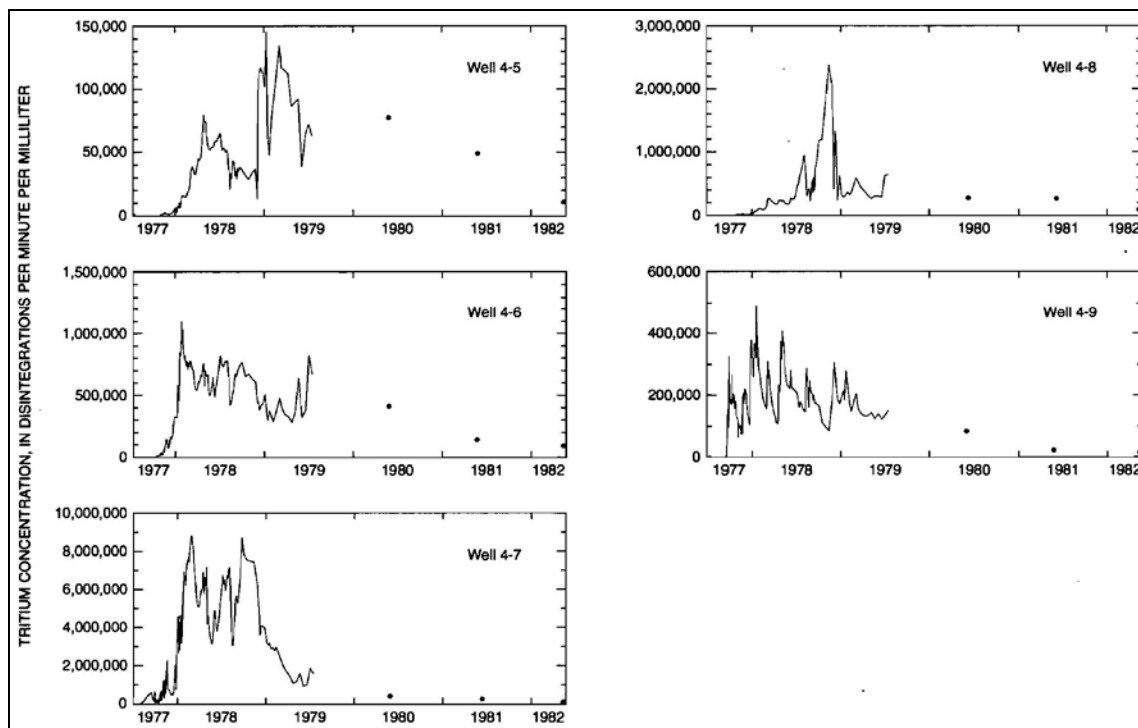
Note: From observation wells at BG4 tracer test site, 1997 to 1979 (Webster 1996).

Fig. 2.32. Tritium concentrations in groundwater over 5 years, BG4 tracer tests
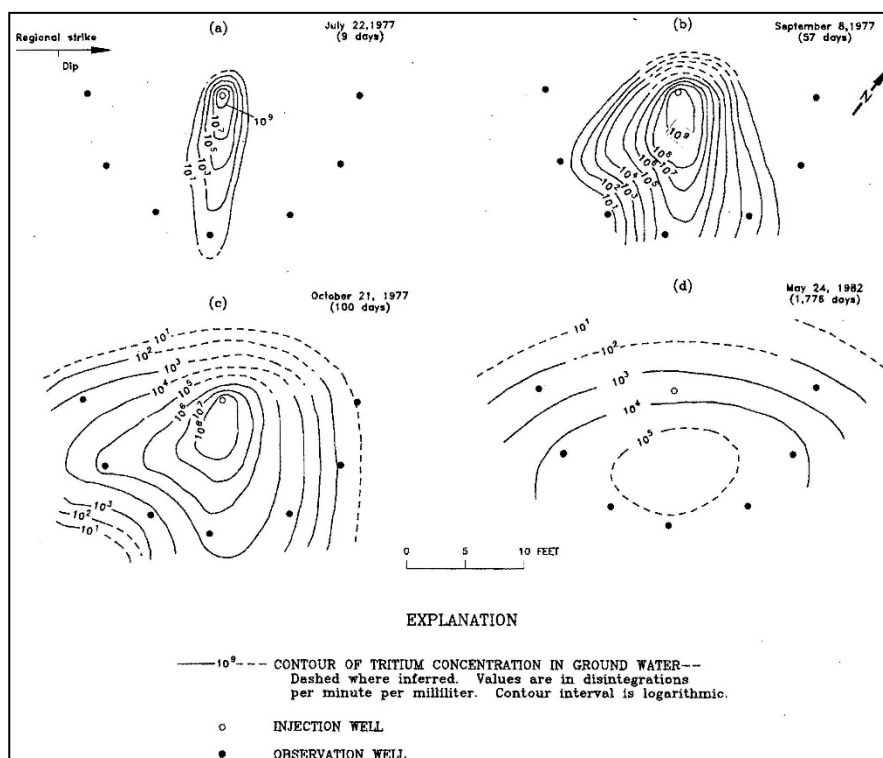
Data from the BG4 tracer site at 9 days, 57 days, 100 days, and 1776 days (4.9 years)
after tracer injection on July 13, 1977 (Webster 1996).

Fig. 2.33. Contours of tritium groundwater concentrations in tracer tests

For the BG4 site, Webster states:

> "…although the leading edge of the plume arrived within 9 days, 5 to 6 months elapsed
> before concentrations began their rapid increase to maximum values, signaling arrival of
> the main part of the plume."

For the BG4 test, the travel rate for first arrival equates to 1.3 ft/day (12 ft in 9 days). The peak concentration in well 4-7 occurred 229 days after the test began. Therefore, the average travel rate to reach peak concentration would be 0.05 ft/day.

For the BG6 site, the fastest first arrival time of 112 days was significantly slower than that at the BG4 site. This equates to a first arrival travel rate of 0.27 ft/day (30 ft/112 days). At the BG6 site, the peak concentration in well 6-7, where the highest concentrations occurred, was reached during the 16th month of the test (around 465 days). Therefore, the average travel rate to reach peak concentration would be 0.06 ft/day.

Matrix diffusion may have played an important role in these tests by acting as a mechanism for retarding transport (Webster 1996). Evidence for matrix diffusion includes the following:

- Length of time that large tracer concentrations were detected at many observation wells

- Persistence of residual concentrations at the injection wells and observation wells

- Relatively rapid movement of the leading edge of the plumes, but very slow movement of the centers of mass

- Reoccurrence of large concentrations of tritium in water of the BG4 injection well shortly after each of several flushings.

At injection well 4-11, the observed loss in tritium activity during the 5 years was seven orders of magnitude. To examine the possibility of matrix diffusion effects, the concentration data for well 4-11 were incorporated into a simple model simulating matrix diffusion. The observed concentrations were generally found to conform with the model simulations. Webster also noted the implications of matrix diffusion on limiting groundwater cleanup. Pumping would quickly remove contaminated water from joints and fractures, but only slowly remove contaminated water from the interstices or pores of the fine-grained saprolite material.

Colloidal tracer tests at the WBCV site. The results of tracer tests at the WBCV tracer site using colloidal tracers (latex microspheres and three bacteriophage strains) were presented in "Field-Scale Migration of Colloidal Tracers in a Fractured Shale Saprolite" (McKay et al. 2000). Colloidal tracers were introduced in well GW-484 and samples were collected from the downgradient well field. All tracers were detected at distances of at least 44 ft, and two of the tracers were found in all downgradient wells. The authors summarize the test results as follows.

> "In most wells the colloidal tracers appeared as a "pulse", with rapid first arrival
> [corresponding to 5 to 200 m/d transport velocity], one to six days of high concentrations,
> and then a rapid decline to below the detection limit. The colloids were transported at
> velocities of up to 500 times faster than solute tracers (He, Ne, and rhodamine-WT) from
> previous tests at the site. This is believed to be largely due to greater diffusion of the
> solutes into the relatively immobile pore water of the fine-grained matrix between
> fractures.

Peak colloid tracer concentrations in the monitoring wells varied substantially, with the microspheres exhibiting the highest relative concentrations and hence the least retention. Rates of concentration decline with distance also varied, indicating that retention is not a uniform process in this heterogeneous material."

The reported trace test results (McKay et al. 2000) summarizes key findings from the rhodamine dye tests reported above (Lee and Ketelle 1989, Lee et al. 1992) and similar tests using dissolved helium and neon (Sanford and Solomon 1998, Sanford et al. 1996).

"Important findings from these two tracer tests include: (1) solute tracer plumes tend to develop that are elongated along strike, with little transverse dispersion; and (2) solute transport rates are strongly influenced by matrix diffusion. In both tracer tests, transport rates (for a given relative concentration contour) decreased with time and distance from the injection well, and the low concentration "front" of the plumes tended to migrate at rates hundreds of times faster than the high concentration region. Both of these types of behavior indicate a high degree of longitudinal dispersion, which is typical of systems in which matrix diffusion is dominant."

These reports note that although this difference in transport rates may be "*partly attributable to physical heterogeneity, it is also consistent with greater losses of the tracer pulse with increasing time due to diffusion into the matrix.*"

Dissolved gas tracer tests at WAG 5 (ORNL). Results of dissolved noble gas (helium, neon) and bromide tracer tests initiated in October 1994 at WAG 5 in Melton Valley, south of the main ORNL campus, are presented in "Dissolved gas tracers in groundwater: Simplified injection, sampling, and analysis" (Sanford et al. 1996). The site is described as the shallow aquifer in fractured weathered shale, similar to conditions at the EMDF site. Water table contour maps were not included in the paper, but surface topographic slopes are roughly parallel with the geologic strike (similar to the configuration at the WBCV tracer site), so shallow groundwater flow directions would be anticipated to follow the geologic strike. Unlike the "slug" injections of tracers such as fluorescent dyes, the gases in these tests are injected into the well bore over a sustained period of time at a relatively constant source concentration. Breakthrough curves for the first 155 days of the test show initial breakthrough occurring at about 15 days at a well located along strike 75 ft downgradient of the injection well. This would indicate a groundwater flow rate for first arrival of 5 ft/day. The relatively low concentrations of the tracers in the breakthrough curves were explained by "*diffusion of the tracers into the less mobile matrix*".

Bromide/helium tracer tests at GW-462 site in WBCV. Tracer tests using helium and bromide were conducted at a WBCV location approximately 1500 ft southwest of the intensively studied tracer test site described above (Schreiber 1995, Moline and Schreiber 1996, Schreiber et al. 1999). This test site is hydraulically separated from the other WBCV tracer test site by the valley of NT-15 and is located near the center of the outcrop belt of the Nolichucky Formation. The Schreiber helium/bromide test site covered a small area (approximately 50×50 ft) and included only three shallow/deep observation well clusters with various locations relative to the maximum water table gradient toward the southwest. The relationships between the injection well (GW-462), three shallow/deep observation well clusters (GW-456 through GW-461), and average water table contours are shown on Fig. 2.34. The three shallow/deep cluster wells were originally placed at right angles up-dip, down-dip, and along strike from GW-462 for pumping tests (Schreiber et al. 1999). One of the well clusters is located over 30 ft upgradient to the injection well, while the remaining two clusters are located at angles cross gradient to the average maximum water table gradients (the three multilevel discrete interval monitoring wells, GW-821, -822, and -823, were not part of the tracer testing). Hydraulic gradients were at oblique angles with respect to geologic strike/dip directions (Fig. 2.34). Detailed topographical maps of the site area show an entrenched ravine located about 300 ft

southwest of the test site that apparently influenced shallow flow directions and local discharge toward the southwest.

Note: Multilevel wells GW-821, -822, and -823 were not used in tracer monitoring.
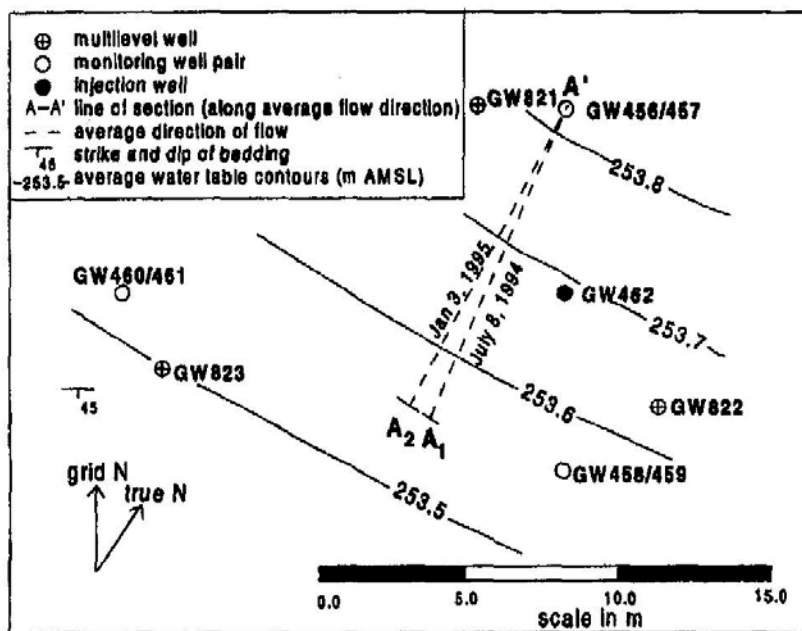
Fig. 2.34. Well locations and water table contours for the helium/bromide tracer test site in WBCV (approximately 1500 ft west of NT-15)

Due to limitations in the numbers and placement of the tracer test monitoring wells, test results were presented with qualified interpretations. Both tests indicated the highest concentration ratios of helium and bromide in the shallow GW-461 well located southwest and along geologic strike of the injection well (GW-462). A slug of bromide was introduced in GW-462 on April 11, 1994, and was monitored for approximately 6 months in the well pairs. Bromide breakthrough was only consistently detected in the water table well (GW-461) located along strike from the injection well. First arrival of low concentrations occurred on June 15, 1994, indicating a first arrival velocity of 0.75 ft/day.

The helium test involved a helium injection and sampling method (Sanford et al. 1996) and was used in the WAG 5 tracer test. The method involved sustained diffusion of helium to saturation levels through injection tubing over a period of several months from March 25 through December 12, 1994. As with the bromide test, the highest concentration ratios were detected in GW-461 along geologic strike. But concentration ratios several orders of magnitude below those in GW-461 were detected in shallow and deep wells up and downgradient of the injection well. The occurrences in upgradient wells were attributed to storm-related changes in flow conditions. Fracture pathways across the strike-parallel bedding were cited to explain helium transport to GW-458 in the downgradient (normal to strike) direction (Schreiber et al. 1999). First arrivals in the along-strike GW-460(deep)/GW-461(shallow) cluster occurred on May 15, 1994, corresponding to a first arrival velocity of 0.9 ft/day, similar to that for bromide.

Summary of key findings from tracer tests in Conasauga Group formations

- The orientation of tracer plumes and average velocities of tracers vary according to the orientation of the strike and dip of the beds with respect to the maximum hydraulic gradient:

  — Relatively narrow elongated plumes develop where shallow groundwater flow gradients are parallel to geologic strike (e.g., WBCV tracer test field)

  — Broader more diffuse plumes develop more slowly where shallow groundwater flow gradients are perpendicular to geologic strike (e.g., BG4/BG6 sites)

  — Plumes intermediate between these extremes appear likely to develop in areas with intermediate flow gradients relative to geologic strike.

- Tracer concentration contour maps and breakthrough curves for the WBCV and BG4/BG6 sites illustrate that most of the injected tracer mass lags far behind the advancing low concentration front, indicating significant longitudinal dispersion and attenuation of peak concentrations.

- Tracer transport velocities, based on first arrival times and distances for very low concentration fronts, vary and can be much higher than velocities based on arrival times of higher or peak concentration levels.

- Groundwater tracer velocities based on first arrival times vary significantly with distance from the injection well and orientation of water table gradients with respect to geologic strike:

  — Dye tracer velocities based on first arrival times at the WBCV site ranged from 3.3 ft/day in the near field (46 ft in about 14 days) to 0.3 ft/day to reach the far field (108 ft in 370 days) where flow paths and gradients were parallel to geologic strike.

  — Tritiated water velocities based on first arrival were 1.3 ft/day (12 ft in about 9 days) at BG4 and 0.27 ft/day (30 ft in about 112 days) where flow paths and gradients were perpendicular to geologic strike.

- Groundwater tracer velocities based on time-to-peak concentration are much less than velocities based on first arrival times. At BG4 and BG6, velocities based on time to peak concentrations were as follows:

  — 0.05 ft/day (12 ft in about 229 days) at BG4 versus a first arrival rate of 1.3 ft/day

  — 0.06 ft/day (30 ft in about 465 days) at BG6 versus a first arrival rate of 0.27 ft/day.

- Tracer plumes introduced at the water table in saprolite at the WBCV site remained within the shallow water table interval and did not migrate vertically to greater depths (i.e., intermediate/deep intervals).

- Matrix diffusion into the pores and microfractures of the fine-grained matrix between fractures transmitting groundwater flow (and contaminants) appears to play a major role in groundwater tracer movement and variation in concentration over time.

2.1.6.3   Laboratory measurements of solid-aqueous partition coefficients for Bear Creek Valley geologic materials

Results of laboratory evaluations of solid-aqueous K_d values for clay-rich soils, saprolite, and less weathered rock from the geologic units that underlie the EMDF site are available in several reports (Table 2.12). These references are summarized in this section along with references where potential liner and geologic buffer materials at the EMWMF site and other nearby areas were tested to determine K_d results. Several of these studies were based on samples from existing and potential waste management areas in Melton Valley (south of ORNL), which are located on the same Conasauga Group units as the EMDF site, specifically the Maryville Formation and the Nolichucky Formation. Two geotechnical investigations

were completed in support of final EMWMF design and construction (CH2M-Hill 2000, WMFS 2000). Both investigations involved test pit sampling and laboratory testing of low-permeability soils as potential liner and/or cover material for EMWMF.

Table 2.12. Sources of laboratory data on K_d values for Conasauga Group samples and local clay-rich soils

Data source	Radionuclides or elements evaluated	Geologic units and source of materials tested
Rothschild et al. 1984. *Characterization of Soils at Proposed Solid Waste Storage Area (SWSA) 7*	Am-241, Co-58, Cs-134, I-125, Sr-85	Melton Valley soils, proposed SWSA 7 site on Conasauga Group units (Maryville Formation or Nolichucky Formation)
Davis et al. 1984. *Site Characterization Techniques Used at a Low-Level Waste Shallow Land Burial Field Demonstration Facility*	Am-241, Co-58, Cr-51, Cs-134, Fe-59, I-125, Sr-85, Ca+Mg	Melton Valley SWSA 6 site near surface soils (0 to 2 m), Maryville Formation boring, depth 2 to 35 m (saprolite and rock)
ORNL 1987. *Geochemical Behavior of Cs, Sr, Tc, Np, and U in Saline Groundwaters: Sorption Experiments on Shales and Their Clay Mineral Components*	Cs-137, Np-235, Sr-85, Tc-95m, U-233	Nolichucky and Pumpkin Valley Formations, Joy-2 well (location unknown) Nolichucky 181- to 128-m depth Pumpkin Valley 604- to 605-m depth
Friedman et al. 1990. *Laboratory Measurement of Radionuclide Sorption in Solid Waste Storage Area 6 Soil/Groundwater Systems*	Co-60, Cs-137, Eu-55, Sr-89, U-233	Melton Valley SWSA 6 saturated zone saprolite, (Maryville Formation or Nolichucky Formation), coarse materials screened
DOE 1992b. *Site Characterization Summary Report for Waste Area Grouping 1 at Oak Ridge National Laboratory, Oak Ridge, TN,* Appendix A	Co-60, Cs-137, Ra-226, Sr-90, Tc-99	Bethel Valley clay-rich soils developed on Chickamauga Group units, three locations, boring intervals range from 5 to 30 ft below ground, sampled intervals at or near water table
CH2M Hill 2000. *Phase IV Final Site Investigation Report*	U, Pb	Near surface, low-permeability soils from the EMWMF site and nearby sites on Chestnut Ridge and in Union Valley (Rogers Quarry)
BJC 2000. *Final Site Investigation Report*	U, Pb	Near surface, low-permeability soils from the EMWMF site and nearby sites on Chestnut Ridge and in Union Valley (Rogers Quarry)

BJC = Bechtel Jacobs Company LLC   ORNL = Oak Ridge National Laboratory
DOE = U.S. Department of Energy   SWSA = Solid Waste Storage Area
EMWMF = Environmental Management Waste Management Facility

All laboratory studies utilized a batch-contact method to estimate the fraction of solute partitioned to the solid phase. These K_d data for local materials were utilized in combination with data from other sources in the selection of assumed K_d values and ranges for the base-case release to groundwater scenario (Sect. 4.5) and for selecting K_d probability distributions used in the uncertainty analysis (Sect. 5.4). Detailed explanation of assumed base-case K_d values is provided in Sect. 3.3.2.4.

2.1.7   Surface Water Hydrology

The surface water hydrology for BCV is well documented based on both valley-wide and smaller-scale investigations. The results indicate the close interrelationships among precipitation, runoff, and surface water/groundwater flux. The following sections review the results of previous surface water investigations in BCV, surface water features of the watershed, important relationships between streamflow and groundwater, and results of water budget analyses conducted for BCV.

2.1.7.1   Previous surface water investigations

USGS prepared an inventory of spring and seep locations and single measurements of flow at spring, seep, and selected stream locations across the entire length of BCV in 1994 that included all of the north Bear Creek tributaries (NTs) in BCV (Robinson and Johnson 1995, Robinson and Mitchell 1996). The single event measurements were made during March 1994 to represent wet season base flow conditions and again in September 1994 to represent dry season base flow conditions. The measurements were made during periods at least 72 hours after rainfall events when base flow runoff was relatively low and stable. The lowest USGS measureable flow rates were 0.005 ft^3/sec or 2.2 gpm. Flow rates below that level were designated as zero (or dry) on their report drawings.

Additional stream flow and contaminant monitoring has been completed at several flume/weir locations in BCV associated with site-specific investigations and valley-wide assessments of contaminant migration and flux. Stream flow and contaminant monitoring has been conducted for a decade or more and continues at many locations along various NTs and along the main channel of Bear Creek as part of ORR-wide CERCLA monitoring of surface and groundwater contamination. Many of the locations are equipped with weirs/flumes and data loggers to provide continuous data on flow rates and water quality parameters.

2.1.7.2   North Tributaries of Bear Creek

The lengths and watershed areas of the NTs tend to be roughly similar along the length of BCV, with a few exceptions such as NT-14, which cuts all the way through Pine Ridge and drains a larger tributary watershed. While stream flow along Bear Creek increases incrementally with flow from each of the NTs, the stream flow conditions along each of the NTs tend to be similar due to their similarity in length and size. The many springs, seeps, and wetland areas within the NT watersheds reflect the relatively shallow water table that intersects with the surface in the ravines and valleys of the tributary channel networks (Fig. 2.35).

Springs, seeps, and wetland areas. The USGS inventory identified hundreds of springs and seeps along the NT tributaries and sub tributaries throughout the BCV watershed. These springs and seeps represent the point locations of shallow groundwater discharge that supports base flow for the NT stream channels. The locations occur where the water table or potentiometric surface intersects the ground surface. Flows at these locations increase during the wet season when evapotranspiration is lowest and groundwater recharge and flux are highest, and decrease during the hotter drier summer and fall seasons when evapotranspiration is highest and recharge and rainfall are typically lowest. Headwater springs with low flows (< 1 gpm) are common near the base of some of the narrow incised valleys heading into the south flank of Pine Ridge. Other springs and seeps commonly occur along or adjacent to lower flatter areas of valley floors farther downstream along the NT tributary paths. Many of the seep/spring areas fall within wetland boundaries that have been delineated and mapped during assessments of BCV and during specific projects where wetlands have been disturbed. The locations of many springs and seeps in the vicinity of the CBCV site are shown on Fig. 2.35.
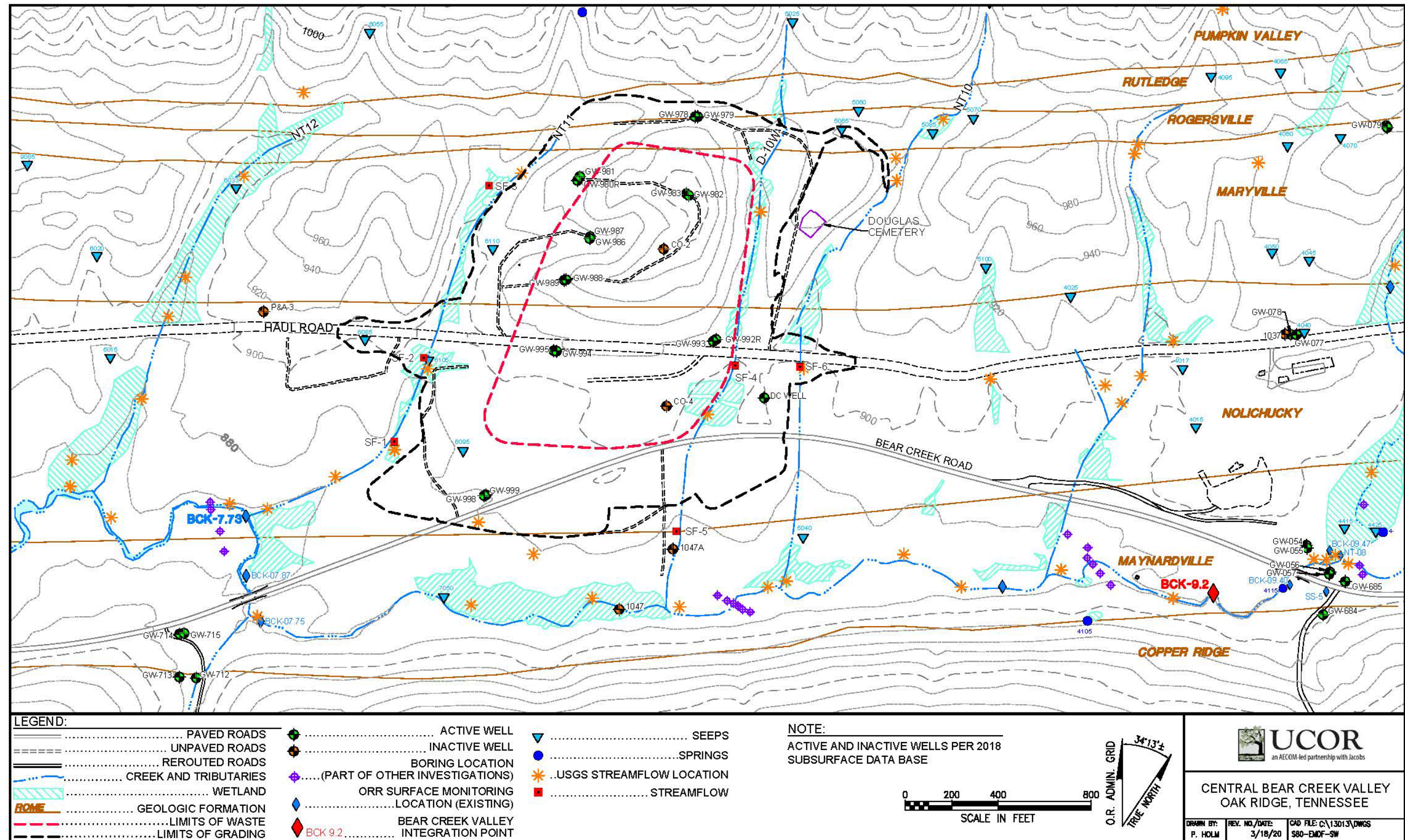
Fig. 2.35. Surface water features near the EMDF site in Central Bear Creek Valley

This page intentionally left blank.

Tributary stream flow. Stream flow along the relatively small channels of the NTs varies seasonally and in response to precipitation events. Hydrographs from continuous monitoring of NT stream flows and rainfall demonstrate that runoff occurs relatively quickly in peak episodes of a few hours or more during and immediately after storm events. The regression phases of the hydrographs show that the rapid peak runoff tapers into a stage of soil drainage and base flow conditions spanning one to several days depending on location within the watershed, antecedent conditions, and other environmental factors.

The USGS inventory data were used to map reaches of the NTs and Bear Creek that were subject intermittent periods of low to zero flow under wet and dry season base flow conditions represented by the March and September 1994 data, respectively. The results of the USGS analysis for the upper half of the BCV watershed between NT-1 and NT-8 is summarized on Fig. 2.36. These results are based on data from Robinson and Mitchell (1996) as reported by UCOR (2013). The bottom portion of the figure illustrates representative dry conditions that commonly prevail across much of the NT stream channels during the warm season, particularly during the late summer and fall seasons. In contrast, winter/early spring base flow in the upper NTs is continuous during the wet season when evapotranspiration is low, soil moisture conditions are high, and steady rainfall more common.

Period flow measurements and continuous stream flow monitoring of the NTs have been conducted in BCV in relation to site-specific investigations and for overall monitoring within BCV as a whole. The locations of ongoing stream flow monitoring across the BCV watershed are shown on Fig. 2.37. Stream flow (and water quality) is measured at weir/flume locations at stations along the lowermost sections of NT-1, NT-2, NT-3, NT-7, and NT-8, and at several locations along Bear Creek from BCK 4.55 near SR 95 upstream to the integration point at BCK 9.2, and farther upstream to BCK 12.47 near NT-1. Some of these stations provide longer-term multiyear historical stream flow data.

Flow data collection was conducted for 1 year at NT-10 and NT-11, adjacent to the EMDF site. A total of six surface water flow measurement stations (flumes) were installed at the CBCV site at locations identified during a surface water walkdown survey (Fig. 2.35). The flumes were located in the Nolichucky Formation and Maryville Formation outcrop areas in NT-10, D-10W, and NT-11. Surface water flow data collected from April 2018 to April 2019 at the flow measurement stations at the CBCV site are documented in a pair of technical memoranda (DOE 2018b, DOE 2019). Table 2.13 provides a summary of the flow rates recorded during this time at the CBCV flumes. As expected, flow rates increase downstream, from north to south, and increase quickly in response to rainfall.

The stream channels crossing the site are small and site reconnaissance indicates that there are no upstream dams or ponded structures that would release flood waters across the site. The NT-10 and NT-11 watersheds are relatively small, so extreme precipitation events could cause significant flooding near the disposal unit boundary. However, flooding under this circumstance would be limited to the tributary valleys along the perimeter of the site and would not be likely to cause significant erosional damage to the EMDF perimeter berms. Another potential cause of tributary flooding over geologic time is the occurrence of landslide deposits that dam narrow valleys and alter drainage patterns or create impounded water bodies susceptible to catastrophic release. Field observations in the Bear Creek tributary valleys have yielded no evidence of significant landslide deposits.
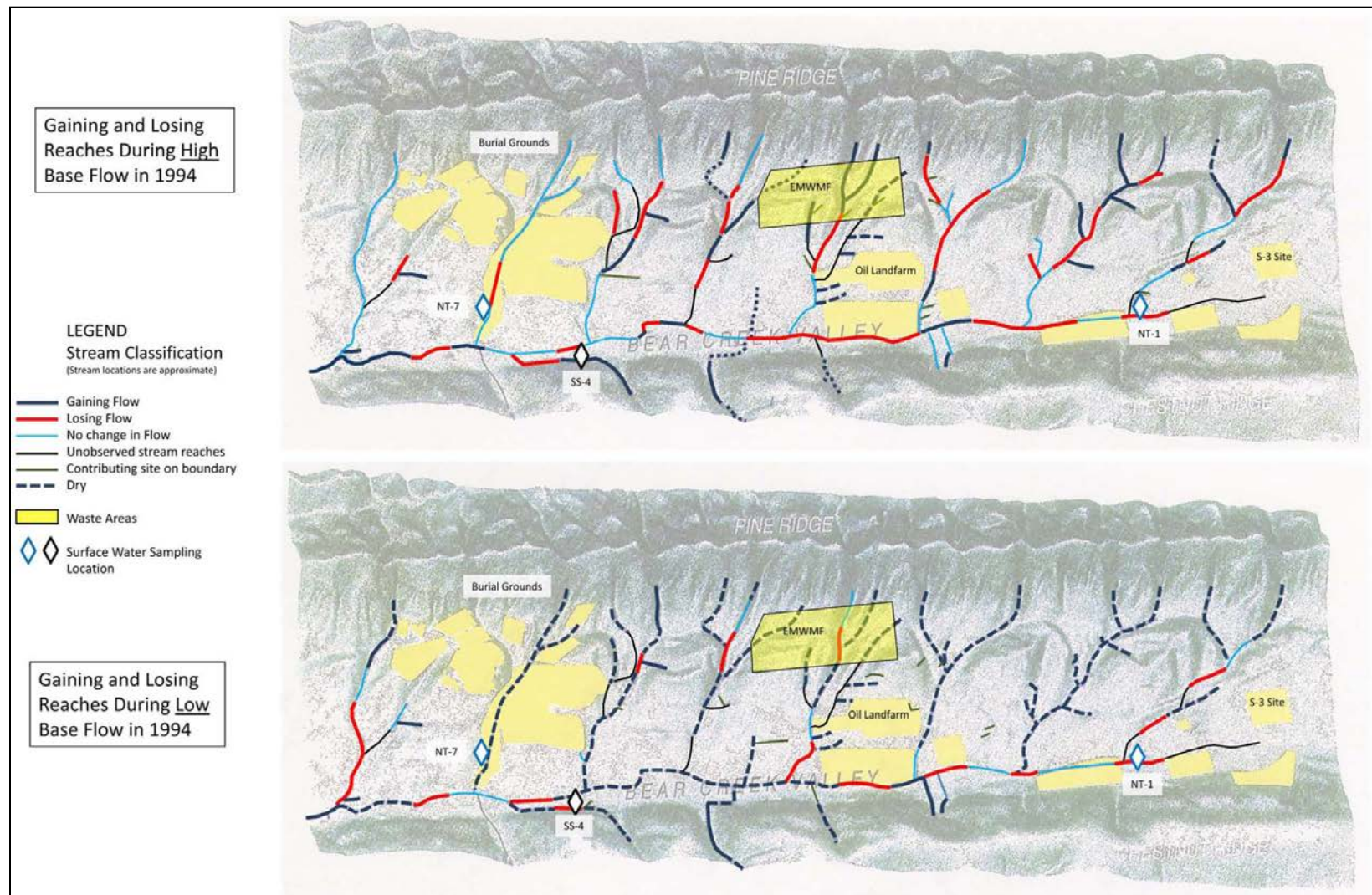
Source: UCOR 2013, Robinson and Mitchell 1996.

Note: Dry indicates flows were at immeasurable rates < 0.005 ft³/sec (2.2 gpm), not necessarily completely dry.

Fig. 2.36. Measured base flow conditions for NT streams and Bear Creek
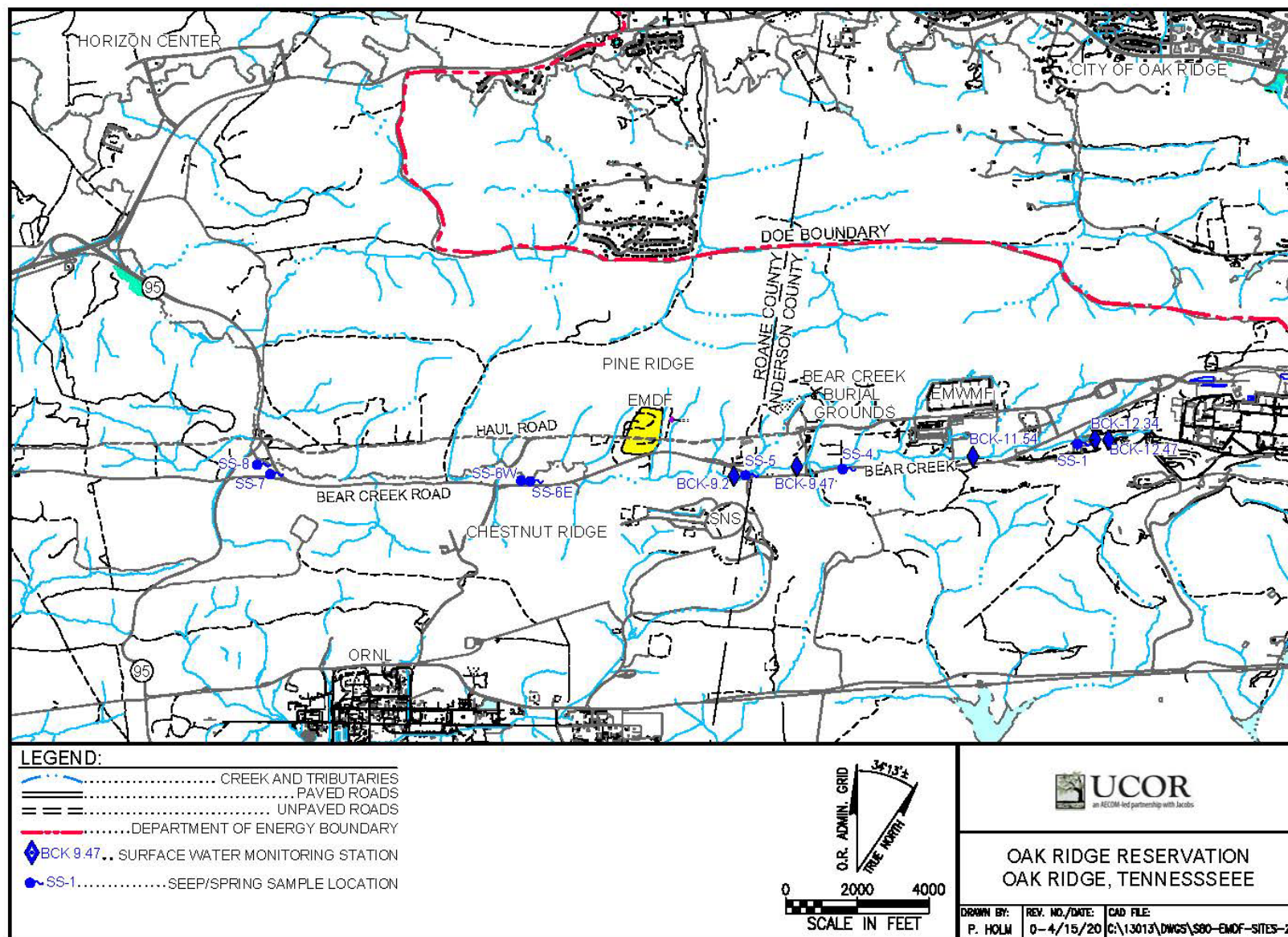
Fig. 2.37. Surface water monitoring locations in Bear Creek Valley

Table 2.13. Minimum and maximum flow rates for the CBCV site flumes, April 2018 to April 2019

Tributary measured	Flume	Minimum flow rate (gpm)	Date of minimum flow rate	Maximum flow rate (gpm)	Date of maximum flow rate
NT-11	SF-1	0.3	9/18–19/2018	5612	2/23/2019
NT-11	SF-2	0.7	9/05/2018 9/09/2018 9/12/2018	6810	2/23/2019
NT-11	SF-3	0.1[a]	9/01/2018 9/03/2018 9/05–09/2018 9/12–16/2018 9/18–19/2018 9/22–23/2018	2678	2/23/2019
D-10W	SF-4	0.1[a]	9/01–10/2018 9/13–24/2018	3042	2/23/2019
D-10W	SF-5	0.1[a]	9/10/2018 9/13/2018 9/24–25/2018	5273	2/23/2019
NT-10	SF-6	0.1[a]	9/01/2018 9/10/2018 9/14/2018 9/17/2018 9/24/2018 9/28/2018	4426	2/23/2019

[a]Essentially no flow periods.

CBCV = Central Bear Creek Valley
D = Drainage
NT = North Tributary

2.1.7.3 Bear Creek

Bear Creek provides the main surface water drainage pathway for the entire BCV watershed, following the axis of the valley toward the southwest from its head waters near the S-3 Ponds to the point near SR 95 where the channel turns north, exiting BCV through a water gap in Pine Ridge. Bear Creek follows the outcrop belt of the Maynardville Limestone along the entire length of the valley and is intimately linked with karst conduit groundwater flow in the Maynardville. Several relatively large springs (SS-1 through SS-8, Fig. 2.37) also occur at several locations along the lower slopes of Chestnut Ridge south of Bear Creek that drain groundwater from the carbonate rock formations and regolith mantle of the Knox Group. These springs interact hydraulically with groundwater and surface water flow in Bear Creek and the karst conduits of the Maynardville. Groundwater from these springs drains mostly fromuncontaminated areas along Chestnut Ridge, although dye tracing and contaminants in some of these springs demonstrate connections with surface/subsurface flow along Bear Creek and groundwater in the Maynardville Limestone.

Except for its uppermost sections near NT-1/NT-2, stream flow along Bear Creek is perennial. However, because of the karst conduit system in bedrock underlying Bear Creek, stream flow disappears along stretches of the channel between NT-3 and NT-8 during low flow periods. The lower half of Fig. 2.36 illustrates the two main portions of Bear Creek where stream flow is diverted underground into karst conduits. The primary section is approximately 3800 ft long and extends from about 600 ft west of the NT-3 confluence downstream to near SS-4. The second smaller dry section extends for approximately 1500 ft upstream from NT-8. Downstream from NT-8 and BCK 9.47, Bear Creek flow is perennial. Conduit flow

continues in bedrock below that point, but the subsurface conduits remain saturated preventing complete capture of stream flow from the surface channel. The BCV RI (DOE 1997b), Appendices C and D, includes a much more detailed presentation and analysis of the surface and subsurface flow system along Bear Creek, including supporting data, figures, and references that substantiate the karst flow system and the existing contaminant plumes along Bear Creek.

Stream flow data for the continuous monitoring stations along Bear Creek are available from the DOE web-based Oak Ridge Environmental Information System. The station nearest to the EMDF site is at BCK 9.2 (Fig. 2.37). The flow record at BCK 9.2 shows winter season average daily flows over 10,000 gpm in wetter years and typical dry season flows less than 10 gpm over the 13-year period from 2001 to early 2014 (Fig. 2.38). Given the important role played by the Maynardville Formation in transmitting the subsurface component of runoff in the watershed, large magnitude floods on Bear Creek are probably rare. The EMDF RI/FS (DOE 2017b) shows that the EMDF does not lie within the estimated limits of the 100-year floodplain.
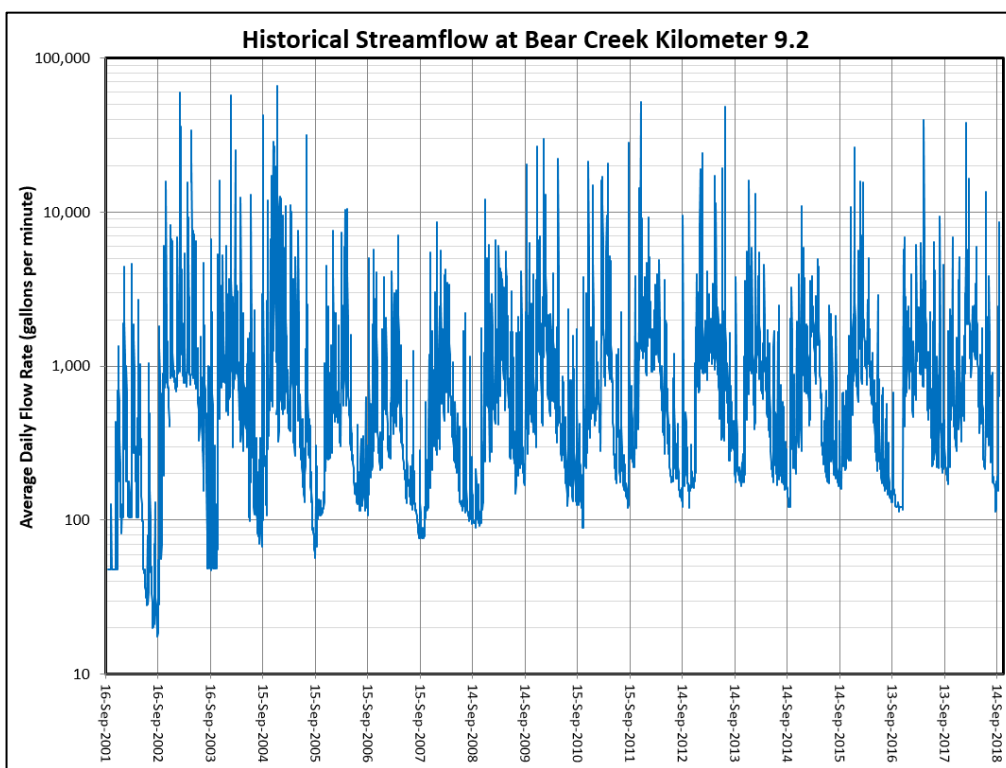
Fig. 2.38. Average daily stream flow at BCK 9.2 (2001 to 2013)

2.1.7.4 Bear Creek water quality

Table 2.14 summarizes basic water quality parameters measured at several stations along Bear Creek in the eastern part of BCV between the BCBG and S-3 ponds sites. The pH of water in the upper reaches of Bear Creek averages close to 8 standard units based on 135 measurements at six stations (BCK 9.47, BCK 11.54, BCK 11.84, BCK 12.34, BCK 12.38, and BCK 12.47; refer to Fig. 2.37 for monitoring locations) at various times between 1998 and 2009. Specific conductivity, a measure of total dissolved solids, is highly variable, ranging from < 1 μS/cm to 2738 μS/cm in samples taken at the same locations and times. In general, the average specific conductivity by measurement station decreases downstream, and the exception, BCK 12.34, is near the former S-3 Ponds possibly affected by S-3 site contaminants.

95

Table 2.14. Summary of Bear Creek water quality parameters

Station[a]	N	Period	pH	Specific conductivity (μS/cm)	Temperature (°C)	Dissolved oxygen (ppm)	Redox potential (mV)
BCK 9.47	21	2/98 – 8/06	8.06	395	15.7	10.2	132.1
BCK 11.54	10	3/02 – 8/06	7.96	552	17.5	8.2	109.1
BCK 11.84	9	3/02 – 8/06	7.98	675	16.2	8.9	106.7
BCK 12.34	66	10/01 – 9/09	7.47	994	16.7	8.4	134.6
BCK 12.47	26	3/98 – 9/03	7.6	653	16.5	8.1	102.7
Upper BCV	21	2/98 – 9/09	7.65	801	16.5	8.6	125.8
Uncontaminated river water[b]			6.5 – 8.5	50 – 50,000	NA		

[a]Station 12.38 had only two measurements and was not included in the summary table.
[b]USGS 1989.

BCK = Bear Creek kilometer   N = number of measurements
BCV = Bear Creek Valley   USGS = U.S. Geological Survey

2.1.8   Ecology and Natural Resources of the CBCV site

Ecological surveys have been completed at the CBCV site to satisfy applicable regulatory requirements for the protection of natural resources. This field work included stream surveys to define conditions (hydrologic classification), wetland delineation surveys, and aquatic and terrestrial surveys to identify threatened and endangered species. Results of these surveys are presented in a Natural Resource Assessment for the proposed EMDF(ORNL 2018). The following summarizes results of that assessment:

- Wetland surveys in the area of the proposed EMDF found extensive acreage of jurisdictional wetland. Seventeen separate wetlands are located within or partially within the EMDF study area, comprising 11.81 acres of wetland, some of which may be near or outside of the actual area used for the EMDF. The wetlands are largely found in conjunction with Bear Creek and its tributary streams, including NT-9, NT-10, NT-11, D-10W, and an unnamed tributary stream located between NT-10 and NT-9.

- Stream surveys identified five separate tributary stream sections within the EMDF study area covering 3303 m of stream. Fish communities within the five tributaries to Bear Creek that lie within the proposed area for the EMDF are typical of other first and second order streams in this watershed. No Tennessee dace, a species listed in need of management by the state of Tennessee, were observed in these surveys; however, they do occur throughout the watershed and are known to migrate in small streams annually.

- The timber assessment documented 36 species of trees within the EMDF study area. Tulip poplar is the single most common species of mature tree by quantity and volume. There is ample merchantable timber on the site. Merchantable trees are real estate assets and DOE has a mechanism in place for their disposal. EMDF access, egress and terrain are favorable for safe logging.

- Rare species surveys found rare plant and animals using the EMDF site. Four rare plant species identified within the EMDF study area include: tubercled rein orchid (*Platanthera flava var. herbiola*), American ginseng (*Panax quinquefolius*), pink lady's-slipper (*Cypripedium acaule*), and Canada lily (*Lilium canadense*). Of these, tubercled rein orchid is the rarest species. This species was found in every tributary and along Bear Creek, but the largest populations were found along NT-9 and drainage channel D10-W. These populations are the largest on the ORR and are considered large for the state.

- The bat acoustic monitoring was performed at 12 locations on the EMDF site in both 2017 and 2018. Analysis of recorded bat calls at all sites indicate that the open forested portions of the proposed EMDF

site are used as summer habitat by state and federally-listed bat species. Large numbers of calls from one state and federally listed endangered species, gray bat (*Myotis grisescens*), indicate usage across the forested areas of the proposed EMDF site. Foraging habitat and/or travel corridors to foraging grounds exist within the proposed EMDF site. Calls from the little brown bat (*Myotis lucifugus)* and tri-colored bat (*Perimyotis subflavus*) were also recorded in large numbers across the EMDF site. Both species are state-listed threatened, and both species likely roost and forage within the site. Other state or federally listed endangered bat species were recorded in small numbers, indicating minimal presence on the site.

- Drainages and wetlands on the site support relatively diverse amphibian populations. During informal site reconnaissance in 2019, biologists observed four-toed salamanders (*Hemidactylium scutatum*) on the site, a species listed as "In Need of Management" by the state.

- The area is on the southern edge of the largest area of contiguous interior forest on the ORR. Several forest bird species that can be impacted by forest fragmentation were recorded on the site, including the wood thrush (*Hylochichla mustelina*), listed by the state as "in need of management", and the American woodcock (*Scolopax minor*), blue-winged warbler (*Vermivora cyanoptera*), chuck-will's widow (*Antrostomus carolinensis*), and Kentucky warbler (*Geothlypis formosa*), which are listed federally as being of "management concern". Other bird species were observed that are in decline on the ORR.

2.1.9   Geologic Resources

No geological resources (e.g., ores, fossil fuel sources, industrial mineral deposits, geothermal resources, etc.) are known to be present at or near the EMDF site that would affect the performance of the proposed disposal facility. The Maynardville Limestone is a source of limestone aggregate in the local area and is mined from an open face quarry located about 5 miles northeast of and along geologic strike with the EMDF. However, DOE property controls preclude any use of the Maynardville near EMDF in the foreseeable future, and other local outcrop areas ensure the availability of ample source locations elsewhere over the long term.

2.1.10   Water Resources

2.1.10.1   Surface water resources and use

The city of Oak Ridge relies on surface water for its municipal water supply, but the intakes on Melton Hill Lake are miles above the surface water exiting Bear Creek, which ultimately drains into East Fork Poplar Creek and the Clinch River several miles downstream of Melton Hill Dam.

TDEC is responsible for management and protection of surface waters in Tennessee as a natural resource for human recreation and for fish and aquatic life. According to TDEC regulations (TDEC Rule 1200-40-04-.09, *Clinch River Basin – Use Classification for Surface Water*), Bear Creek, as well as East Fork Poplar Creek, Poplar Creek, and the Clinch River downstream, is classified for fish and aquatic life, recreational use, livestock watering and wildlife, and irrigation.

The EMDF site and surrounding areas are located within the DOE property boundaries. Future land use, including use of water resources, would be restricted to industrial use by DOE. Surface water use at and near the EMDF site in BCV and within the DOE property boundary as a whole is prohibited, although public access is possible in limited areas where public roads pass through the DOE property. These areas are actively patrolled.

The intermittent surface water flow and small stream channels within east BCV and along the NTs at and near EMDF will not support populations of large fish, so that fishing and fish consumption are only likely

several miles below the site where the Bear Creek contributing area is larger. The future exposure scenario adopted for the EMDF PA includes use of Bear Creek surface water to support agriculture (for irrigation and livestock water needs) and fish ingestion consistent with recreational fishing in Bear Creek; both surface water uses are highly unlikely given the anticipated actual land use and hydrologic characteristics of the watershed.

2.1.10.2   Groundwater use

The location of EMDF on DOE property and DOE property ownership and controls for areas downgradient of EMDF preclude any domestic use of groundwater in the foreseeable future. However, no water supply wells are located in BCV anywhere near the current downgradient margins of contaminant plumes originating from sources in BCV. Groundwater flow at and downgradient of the EMDF site is constrained within the groundwater divides below Pine Ridge and Chestnut Ridge. Based on the predominance of relatively shallow groundwater discharge pathways in BCV (Sect. 2.1.5.1), BCV water wells for domestic supply would have to be in relatively close proximity (i.e., within < 0.5 to 1 mile) to EMDF for release from the site to pose a measurable risk to a future hypothetical user.

TDEC well construction standards and typical well construction. TDEC is responsible for management and protection of groundwater in Tennessee. The TDEC Water Resources Division has established requirements for water well construction in Tennessee (TDEC Rule 0400-45-09, *Water Well Licensing Regulations and Well Construction Standards*). The primary requirement relevant to the PA for EMDF states that the source of water for any well shall be at least 19 ft bgs. Exceptions can be made for shallower water sources provided that other minimum requirements are met (e.g., casing and sealing off of the upper 10 ft of the subsurface). Water wells may be completed in unconsolidated materials (e.g., sand/gravel), in overburden materials above bedrock, or in bedrock, but the minimum depth of watertight casing is established at least 19 ft bgs, unless an exception is granted. Bedrock wells must be cased at least 5 ft into the top of bedrock, and the top of well slots or screens placed in overburden wells at or above bedrock must be at least 20 ft bgs. The overriding depth standard for surface isolation casing is therefore normally set at a minimum depth of 19 ft bgs.

2.1.11   Recently Completed CBCV Site Characterization

Characterization of the EMDF site began in February 2018 and was conducted in two major phases. Phase 1 characterization was intended to demonstrate the suitability of the site for onsite CERCLA waste disposal. The primary goal of the Phase 1 site characterization was to provide initial data on groundwater elevations and surface water flows to support site selection and the overall waste disposal decision. Secondary Phase 1 goals were to obtain geotechnical data to support preliminary design activities. The Phase 2 characterization effort was conducted to develop additional hydrogeologic and geotechnical information to support EMDF preliminary design.

The Phase 1 and Phase 2 subsurface hydrogeologic investigations (DOE 2018b, DOE 2019) included borehole drilling to obtain representative lithologic data, collect subsurface geotechnical samples, conduct geophysical logging, estimate hydraulic conductivities, and to support groundwater monitoring and seismic investigations. Phase 2 characterization also included digging test pits for additional geotechnical sampling. The results for Phase 2 efforts have not yet been documented. A total of 32 piezometers were installed (26 paired shallow and intermediate depth, and six single piezometers) for monitoring groundwater levels within the disposal facility boundary and on the periphery of the site. In addition, six surface water flow measurement stations (flumes) were established to document streamflow in Bear Creek tributaries.

Figure 2.39 shows the current site topography, hydrogeologic investigation locations, and key groundwater and surface water features in the proposed EMDF area. In addition to hydrogeologic characterization and monitoring, there was additional field work to delineate wetland areas and locate geologic contacts as well

as civil surveying to refine topographic data for design and to document the locations of flumes, piezometers, soil borings, and test pits.

The general observations and conclusions based on the Phase 1 characterization effort were:

- Geology is typical of BCV with steeply dipping, fractured bedrock, and there are no major karstic features in the Maryville, Nolichucky, or Rogersville Formations underlying the CBCV site.

- The contact with the Maynardville Limestone is located south of the proposed CBCV footprint. The observed locations in the field were approximately 50 ft further south than represented on geologic maps prior to the field mapping effort (DOE 2018b).

- Precipitation primarily runs off as surface water and shallow groundwater in the stormflow zone. This is consistent with the BCV conceptual site model.

- Potentiometric surface elevations are typical of other BCV wells in similar topographic and geologic settings.

Information from the Phase 1 field activities (DOE 2018b, DOE 2019), including surface water records and groundwater data that had been collected from the 16 Phase 1 piezometers over the first year of monitoring (March 2018 through early March 2019), was used in the development and calibration of the CBCV groundwater flow model (refer to Sect. 3.3.3.1 and Appendix D for details).

The Phase 1 (DOE 2018b, DOE 2019) and 2 piezometer monitoring results show that the average potentiometric surfaces are primarily influenced by topography and local recharge. There is subdued mounding of the potentiometric surface under the knoll. Generally, piezometer levels respond quickly during precipitation events then decrease rapidly to average conditions within days. Groundwater levels vary seasonally, with maximum elevations generally occurring in the interval between December and April or May, and annual low elevations occurring in drier parts of the year (which can include months from May to November).

Comparison of the piezometer pairs monitoring the shallow and intermediate groundwater zones demonstrates that in most cases, a downward-to-zero vertical gradient exists in the knoll area and slight upward vertical gradients exist away from the knoll nearer to the surface water drainages. Most of the recharge to the groundwater moves quickly to adjacent surface water bodies with limited replenishment of the deeper underlying groundwater. In general, groundwater moves from the ridges toward Bear Creek and its tributaries. The results of EMDF site characterization efforts are consistent with the general BCV hydrogeologic framework presented in Sect. 2.1.5.

This page intentionally left blank.
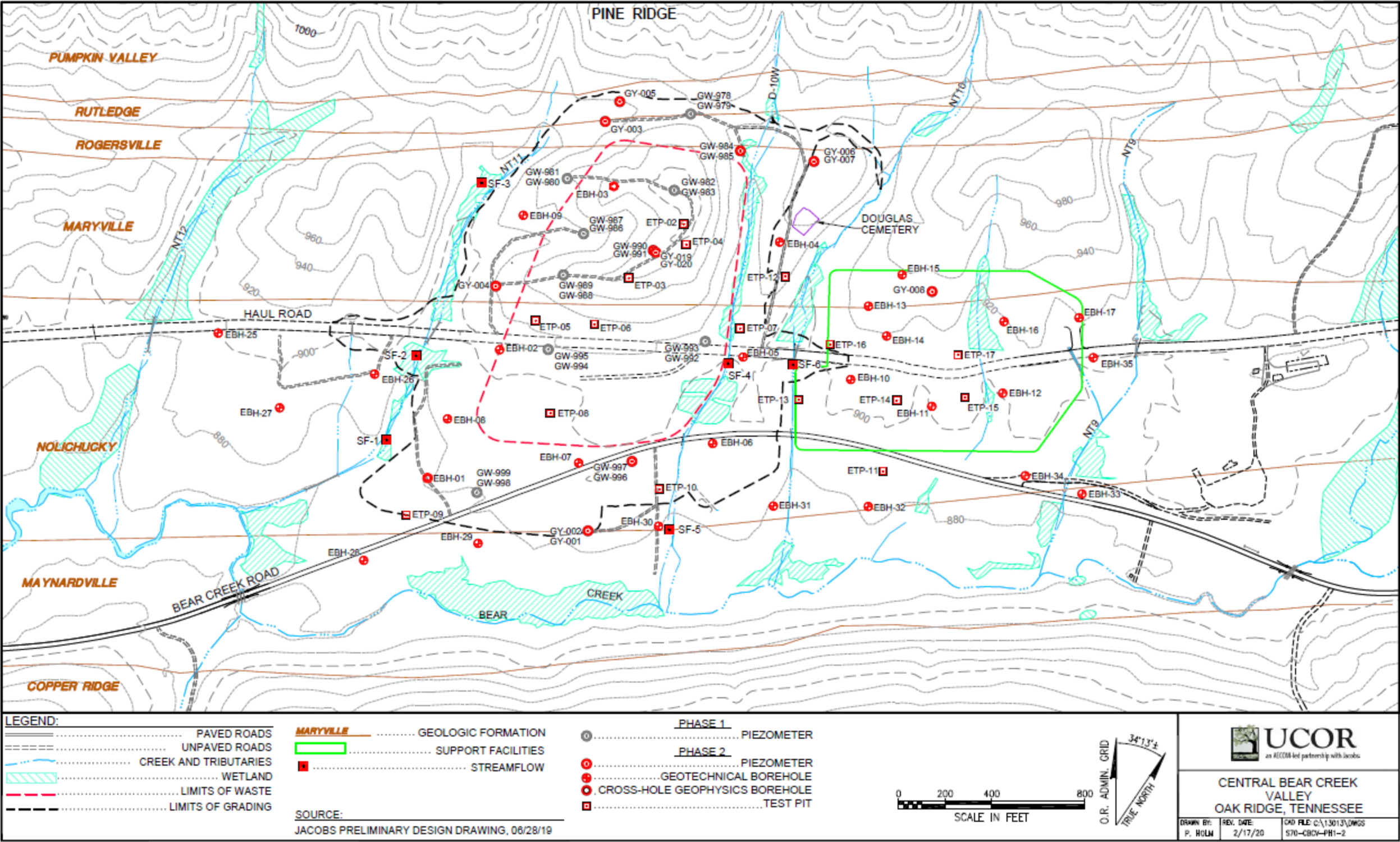
Fig. 2.39. EMDF site characterization map

This page intentionally left blank.

2.2   PRINCIPAL FACILITY DESIGN FEATURES

The EMDF Preliminary Design consists of four individual disposal cells covering a footprint of approximately 50 acres situated between the southern flank of Pine Ridge and Bear Creek and between tributaries NT-10 and NT-11. The upper portion of another surface drainage channel (D-10W) will be rerouted to accommodate the eastern section of the landfill. A site plan for EMDF is provided in Fig. 2.40 that shows the location of the disposal facility and potential areas for the required infrastructure, including operations/support trailers, material staging/laydown areas, a stockpile area, and parking areas; wastewater storage tanks, a wastewater treatment facility, and a truck loading station; storm water basins; a haul road; electrical, water, and communications utilities; a truck weigh scale; and guard stations.
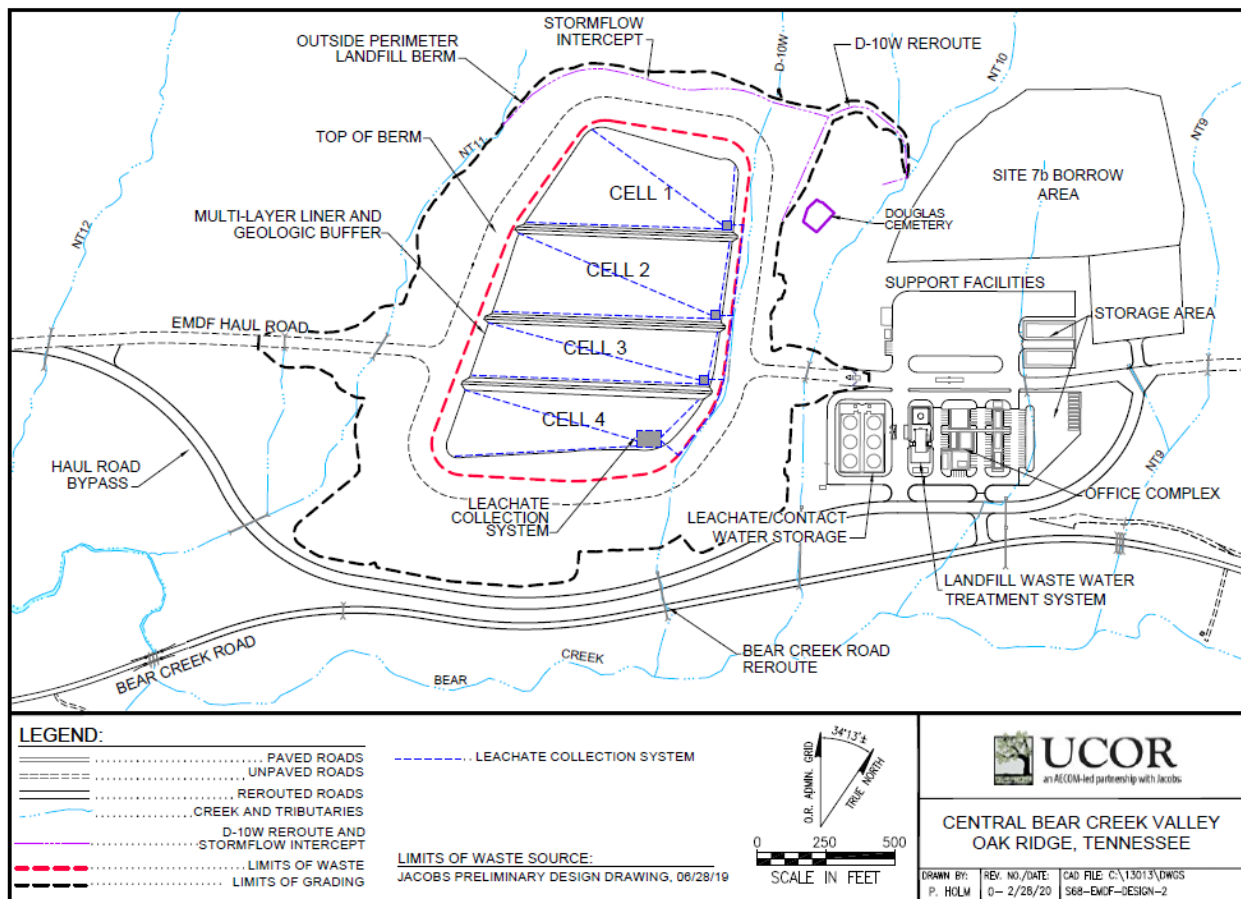
Fig. 2.40. EMDF site plan

Key engineered features of the disposal facility design include a perimeter berm to laterally contain the waste, a multilayer basal liner system along the floor of the facility with a double leachate collection/leak detection system to limit release of leachate, a 10-ft-thick geologic buffer to isolate the waste from groundwater, and the multilayer cover to reduce infiltration and isolate the waste from human and environmental receptors. Appendix C provides a detailed description of EMDF design features, associated safety functions, and natural events and processes that can limit safety functions over time. The remainder of Sect. 2.2 provides summary information on EMDF cover design features and structural stability of the disposal unit.

2.2.1 EMDF Final Cover Design

The primary waste containment feature that provides for long-term performance of EMDF is the multilayer cap. The final cover system, which is to function with little maintenance, would be designed and constructed to provide the following:

- Minimize migration of liquids through the closed landfill over the long term

- Promote efficient drainage while minimizing erosion or abrasion of the cover

- Control migration of gas generated by decomposition of organic materials and other chemical reactions occurring within the waste, if found to be necessary

- Accommodate settling and subsidence to maintain the cover integrity

- Provide resistance to rill erosion and gullying

- Provide a permeability less than or equal to the permeability of any bottom-liner system or natural subsoil present

- Resist inadvertent intrusion of humans, plants, and animals.

The final cover would be sloped to facilitate runoff and would be placed over the waste and tie into the top of the perimeter berm. It is anticipated the surface of the final cover system over the waste would be sloped at a grade of 2 to 5 percent and the sides would be sloped at a maximum grade of 25 percent. The cover is assumed to include 20-ft-wide horizontal benches spaced at maximum vertical intervals of 50 ft to reduce slope lengths, increase erosion resistance, and enhance slope stability. Actual slopes may vary and would depend on slope stability and erosion analyses performed during final design. The layers of the final cover system are depicted in Fig. 2.41. The approximately 11-ft-thick multilayer final cover system presented in the EMDF RI/FS is comprised of the following layers, starting from the top downward:

1) Erosion Control Layer: 4-ft-thick vegetated soil/rock matrix comprised of a mixture of crushed rock and native soil and constructed over the disposal facility to protect the underlying cover layers from the effects of frost penetration and wind and water erosion. This layer would also provide a medium for growth of plant root systems and would include a surficial grass cover or other appropriate vegetation with seed mix specially designed for this application.

2) Granular Filter Layer: 12-in.-thick layer of granular material graded to act as a filter layer to prevent clogging of the biointrusion layer with soil from the overlying erosion control layer. The required gradation would depend on the particle size distributions of both the erosion control layer and biointrusion layer and would be calculated using standard soil filter design criteria once these properties have been established.

3) Geotextile Separator Layer: nonwoven, needle-punched geotextile used as a separator between the granular filter layer and biointrusion layer.

4) Biointrusion Layer: 2-ft-thick layer of free-draining, siliceous coarse granular material sized to prevent burrowing animals and plant root systems from penetrating the cover system and reduce the likelihood of inadvertent intrusion by humans by increasing the difficulty of digging or drilling into the landfill.

5) Lateral Drainage Layer: 1-ft-thick layer of hard, durable, free-draining granular material with sufficient transmissivity to drain the cover system and satisfy the requirements of the infiltration analysis.

6) Geotextile Cushion Layer: nonwoven, needle-punched geotextile used as a cushion over the underlying geomembrane.

7) Geomembrane Layer: 60-mil-thick HDPE geomembrane textured on both sides to enhance sliding resistance that provides an impermeable layer to enhance water removal by the lateral drainage layer (layer 5).

8) Amended Clay Layer: 1-ft-thick (minimum) layer of native soil amended with bentonite and compacted to produce an in-place hydraulic conductivity less than or equal to 1E-07 cm/sec. It is necessary to amend native soil with bentonite for this layer to achieve the very low design hydraulic conductivity.

9) Compacted Clay Layer: 1-ft-thick (minimum) layer of native clay soil or amended soil compacted to produce an in-place hydraulic conductivity less than or equal to 1E-07 cm/sec. This layer, in conjunction with the overlying amended clay layer and geomembrane layer, would function as a composite hydraulic barrier to infiltration. Similar to the compacted clay liner for the liner system, compacted clay layer material would be selected on the basis of a borrow source assessment that would include performing a suite of geotechnical laboratory tests.

10) Contouring Layer: typically consists of a 1-ft-thick (minimum) layer of stone to serve the dual function of contour fill layer and gas vent layer (if necessary). This layer would provide a smooth, firm foundation for construction of the overlying cover layers.
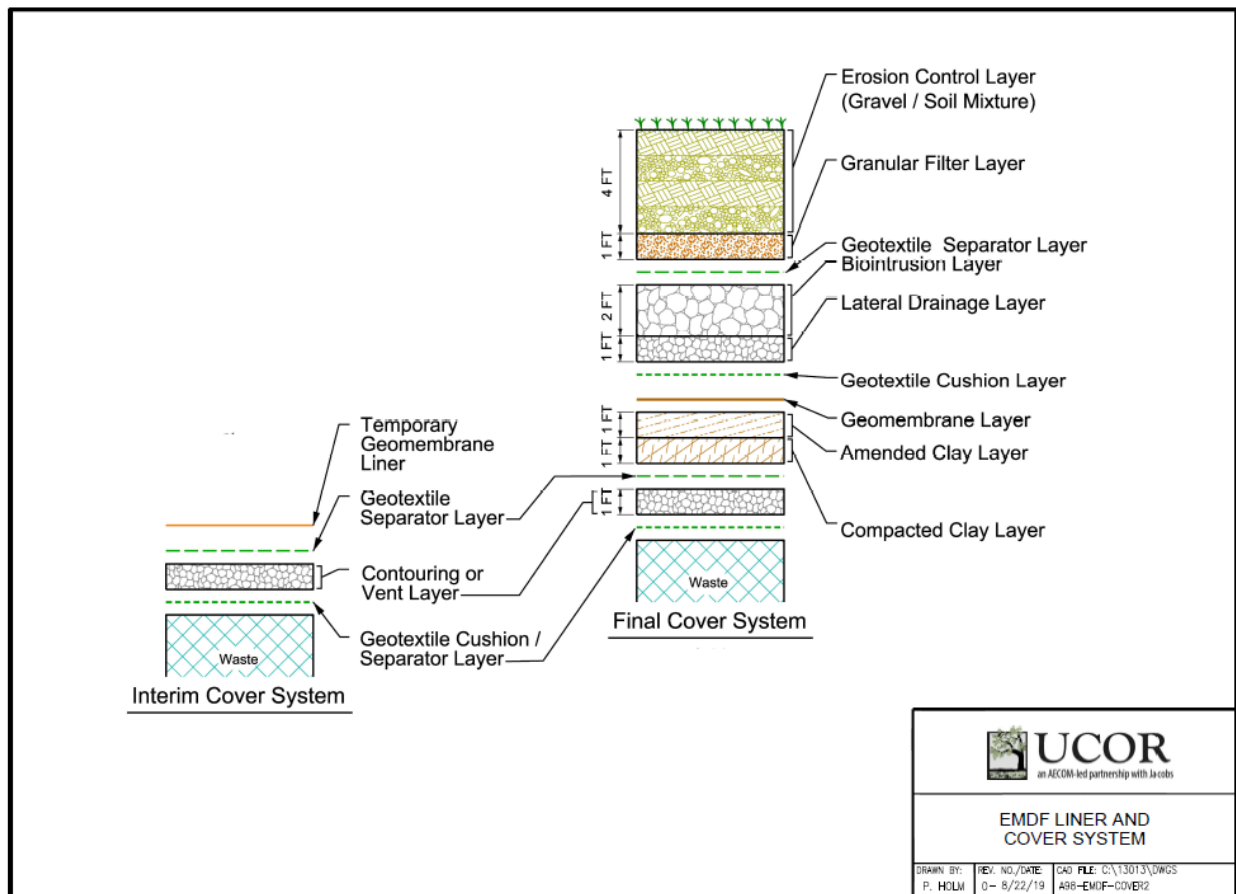
Fig. 2.41. EMDF final cover system components.

2.2.2   Biointrusion Barrier

The biointrusion layer would inhibit deep penetration by burrowing animals that could transfer radionuclides to the surface. The granular filter, biointrusion, and drainage layers will be constructed of siliceous rock that is not easily degraded by natural processes. The biointrusion layer also will limit the potential impact of cover erosion if the surface vegetation is disturbed by severe storm events. The total cap thickness in the preliminary design is 11 ft, which provides for sufficient depth-to-waste to make exposure of the waste under certain excavation scenarios (e.g., installation of a basement for a house) unlikely. However, other IHI scenarios such as well drilling may be envisioned. Section 6 and Appendix I present the IHI analysis for the EMDF.

2.2.3   Disposal Unit Cover Integrity

The overall effectiveness of the final cover system in reducing infiltration is a key long-term performance objective of the landfill. Clay layers in the final cover system are below 8 ft of engineered materials. The clay layers retain their hydraulic conductivity parameters based on their depth bgs, which ensures there is no direct exposure to freeze-thaw conditions; no cracking/tunneling due to roots or burrowing animals/insects; and limited temperature or moisture variation. High overburden pressure will maintain low permeability characteristics of the clay barrier in the cover (Boynton and Daniel 1985, Albrecht and Benson 2001). The biointrusion layer serves multiple safety functions, including preventing severe erosion that could expose the underlying clay barriers, preventing biointrusion, and serving as a redundant lateral drainage pathway. These characteristics of the cover design provide resistance to degradation mechanisms affecting the compacted clay layer. Appendix C, Sect. C.1, provides a more detailed analysis of natural events and processes that can limit the function of EMDF design features.

Long-term monitoring and maintenance actions would be conducted to control erosion, repair cap settlement/subsidence and slope erosion, repair run-on and run-off control systems, prevent rodent infestation, and prevent tree and other deep-rooted plant growth on the final cover and side slopes.

With the robust design of the cap, it is reasonable to expect that the EMDF cap will remain largely intact for many decades or centuries with little or no maintenance. The requirement for long-term cover integrity will be included in the preliminary and final design of the EMDF final cover system. For the PA analysis, the cover system is assumed to completely degrade much earlier and more rapidly (between 200 and 1000 years post-closure) than is likely given the robust engineering design.

2.2.4   Structural Stability

Detailed analysis of the structural stability, including slope stability and seismic hazard analysis, is being performed as part of the preliminary and final design. Details of the final design and associated structural stability evaluations will be evaluated with respect to their relevance to the performance analysis. Based either on applicable laws or regulations pertaining to landfills or on lessons learned from existing landfills, the final design will evaluate the following stability conditions:

- Perimeter berm stability – Site characterization data will be incorporated into design parameters to establish size and elevation of the perimeter berm necessary to ensure lateral confinement. Calculations to determine the maximum allowable slopes to ensure berm stability and requirements for compaction and lift placement parameters and appropriate slope armoring to achieve long-term stability will be part of the engineering design process.

- Waste mass stability – Operational procedures for waste placement and requirements for waste compaction and filling voids to prevent differential settlement, and best management practices to ensure proper drainage of water within disposal cells will be developed prior to EMDF operations.

- Liner stability and integrity – Calculations for maximum allowable slopes, selection of appropriate geosynthetics for predicted site conditions, and effective anchor systems at the landfill perimeter will ensure stability of the bottom liner and continued long-term performance.

- Landfill seismic stability – Using site characterization data, evaluations will be performed to determine that the landfill liner, leachate collection system, and landfill appurtenances remain functional when subjected to earthquake-induced forces. Leachate collection systems and waste cells will be designed to function with embankments that are predicted to undergo less than 6 in. of deformation.

2.3 DEVELOPMENT OF PA WASTE INVENTORY

This section summarizes the estimated radionuclide inventory for EMDF and the process for screening radionuclides for inclusion in PA analysis. Development of the estimated radionuclide inventory is documented in Appendix B. Development and application of the radionuclide screening model is documented in Appendix G, Sect. G.4.2. Discussion of waste characteristics relevant to radionuclide release modeling are presented in Sect. 3.2.2.5.

The estimated radionuclide inventory for the EMDF PA is based in part on the analysis of expected waste stream characteristics and volumes presented in the EMDF RI/FS (DOE 2017b, Sect. 2 and Appendix A). The EMDF RI/FS established the required EMDF volume capacity of 2.2 million cy based on a best estimate for the total as-generated volume of waste in the EMDF at closure of approximately 1,949,000 cy (DOE 2017b, Table 2-5). This volume was based on the OREM Waste Generation Forecast and includes a 25 percent increase from base volume estimates to allow for uncertainty in the volume of CERCLA waste generated by currently planned remedial action and facility D&D projects. The total capacity requirement reflects adjustments to the as-generated volume to account for in-cell waste compaction and addition of clean fill material (soil) to meet facility operational requirements (DOE 2017b, pages 2-8 to 2-11 and Appendix A, pages A-4 to A-5).

The approach for estimating the EMDF radionuclide inventory is based on using as-generated waste volumes without the added 25 percent uncertainty allowance to derive average activity concentrations for each waste stream (refer to Appendix B for additional detail on waste stream characteristics and waste stream inventories). The +25 percent volume uncertainty factor and added clean fill mass are incorporated into the PA analysis by adjusting the estimated average waste activity concentrations to account for clean fill (Sect. 3.2.2.5) and applying these as-disposed concentrations to the EMDF design disposal capacity of 2.2 million cy. Figure 2.42 is a flow chart depicting sources of information and the process for development of the required EMDF disposal capacity, the estimated radionuclide inventory, and the application of assumed clean fill additions to derive the as-disposed concentrations utilized in the PA modeling. For radionuclide screening, bounding activity concentration estimates (screening source concentrations) that include all maximum and upper confidence limit (UCL) data values are used as inputs to the screening model without corrections for radioactive decay or adjustments for addition of clean fill.

The procedure for adjusting the estimated as-generated activity concentrations to account for the mass of clean fill added during disposal is presented in Sect. 3.2.2.5.
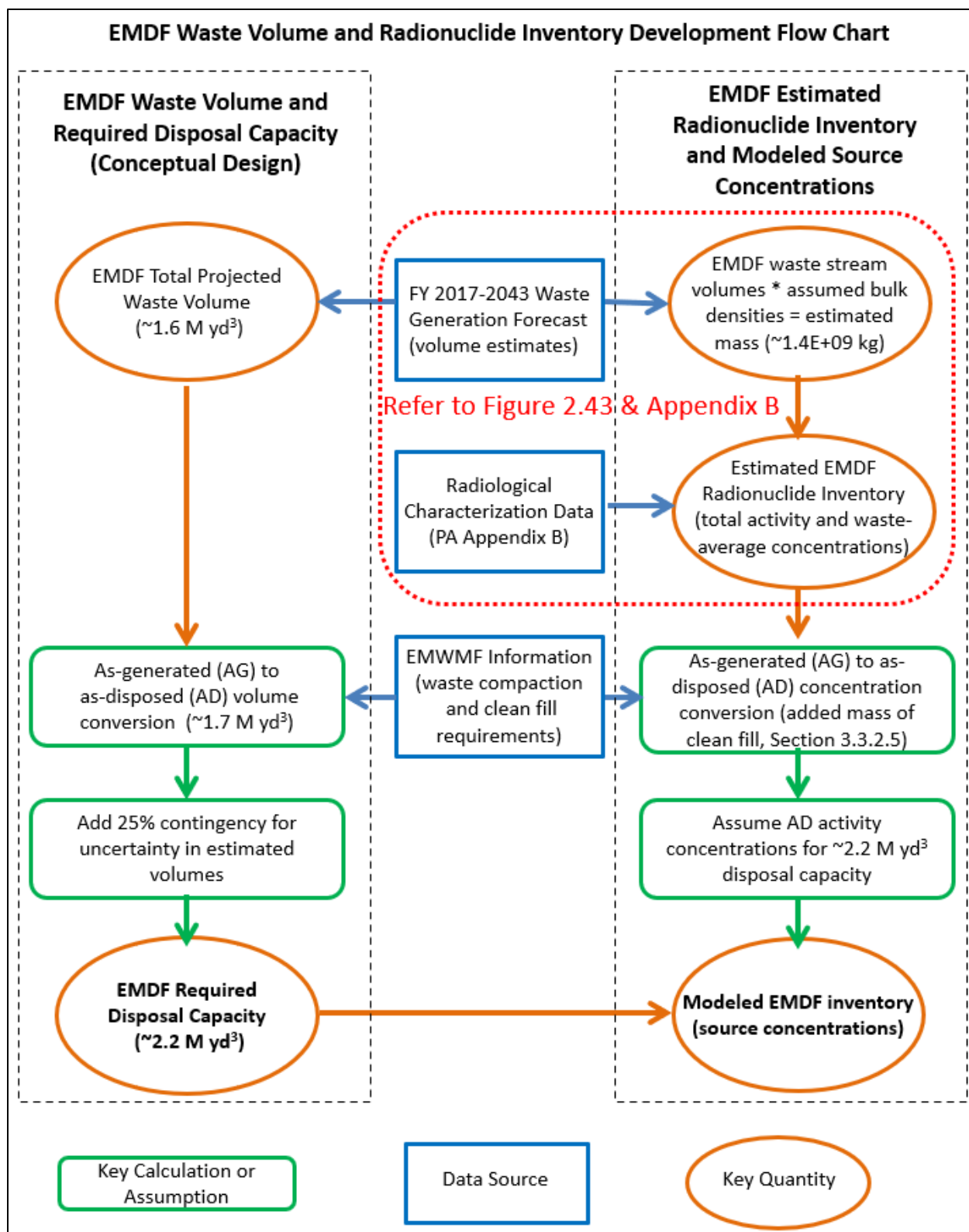
Fig. 2.42. Sources of information for development of the required EMDF disposal capacity, the estimated radionuclide inventory, and the as-disposed activity concentrations utilized in the PA modeling

2.3.1 Waste Characteristics for Screening and Inventory Estimation

Wastes derived from CERCLA cleanup at Y-12 and ORNL will contain a wide range of radionuclides that reflects the extensive duration and scope of weapons production and nuclear science activities at these two sites. The expected differences in radiological contamination reflect the different operational histories of the two DOE sites (i.e., weapons production at Y-12 versus research and development related to reactor design and the nuclear fuel cycle, radioisotope production, radioactive waste management, and biological and environmental sciences at ORNL). The primary radioactive contaminants in Y-12 waste streams are uranium isotopes, whereas ORNL waste streams will contain a greater variety of radioisotopes, including large quantities of some fission products (e.g., Cs-137 and Sr-90), lower quantities of other fission products (e.g., Tc-99 and I-129), and trace quantities of transuranic radioisotopes (e.g., plutonium and americium). This difference is important for estimation of the EMDF inventory because Y-12 waste accounts for approximately 70 percent of the forecast waste volume and ORNL waste the remaining 30 percent. Due to these differences in waste volume and radiological characteristics, Y-12 waste accounts for the majority of uranium activity in the estimated EMDF inventory, whereas ORNL waste accounts for the majority of total inventory.

For estimating EMDF radionuclide inventory, projected waste volumes for individual cleanup projects are aggregated into waste streams based on the site of origin (Y-12 or ORNL) and project type (facility D&D or remedial action). Additional differentiation of Y-12 facility D&D waste streams is based on the availability of detailed characterization data for certain Y-12 facilities. Bounding EMDF source concentrations for screening and average radionuclide activity concentrations for each waste stream were estimated from a combination of data sources, including: (1) EMWMF waste characterization data for previously generated and disposed Y-12 and ORNL waste lots, (2) data from detailed facility and environmental characterization studies, and (3) data from the OREM SORTIE 2.0 facility inventory database, which include radionuclide activity quantities derived from various types of facility safety analyses and other sources. Figure 2.43 provides a schematic overview of data sources, radiological profiles and waste quantities used to estimate EMDF radionuclide inventories.

For input to the screening model, all data including maximum and UCL-95 values were averaged without disaggregating the data by waste stream, and the resulting screening source concentrations were applied to the entire EMDF disposal volume capacity, without adjustment for addition of clean fill or radioactive decay.

To develop estimated radiological profiles the available data for specific EMDF waste streams are applied to the as-generated waste quantities (volumes and average bulk densities). Six waste streams are defined to capture the differences between ORNL and Y-12 wastes and between remedial action wastes (primarily soils) and facility D&D wastes (primarily debris). Radioisotopes having half-lives less than 1 year were not included in the EMDF estimated inventory calculations. The combination of radiological information sources provided data on 70 radionuclides having half-lives greater than 1 year. However, due to data limitations (generally the availability of only a single record for a radionuclide and/or inability to independently confirm some data from original sources), estimated waste-stream average activity concentrations (including only expected, average, and limiting value types) were developed for only 56 radionuclides. Data for nine less commonly reported fission products (Cd-113m, Cs-135, Kr-85, Pd-107, Se-79, Sm-151, Sn-121m, Sn-126, and Zr-93) could not be verified against the original data sources; therefore, these nine radionuclides are not included in the estimated EMDF inventory. EMDF waste average concentrations for five other radionuclides (Ba-133, Be-10, Ca-41, Mo-93, and Nb-93m) were estimated by applying additional assumptions to the EMDF waste quantity and radionuclide data. The assumptions made to estimate the as-generated EMDF waste average concentration values used in the EMDF PA models for these five radionuclides are presented in Attachment B.3.

Waste Volume Data (Waste Generation Forecast FY2017 - FY2043)

As-Generated Waste Volumes (yd³)		Facility D&D Projects	Remedial Action Projects	All Projects (% EMDF Total)
Y-12	Debris	599,244	167,111	766,355 (49%)
Y-12	Soil	5,069	356,789	361,858 (23%)
ORNL	Debris	250,555	55,962	306,517 (20%)
ORNL	Soil	734	123,381	124,115 (8%)
All Debris		849,799	223,073	1,072,872 (69%)
All Soil		5803	480,170	485,973 (31%)
All EMDF waste (%)		855,602 (55%)	703,243 (45%)	EMDF Total 1,558,845

Radiological Data Sources

EMDF Waste Stream	Characterization Reports	EMWMF Waste Lots	SORTIE database
Y-12 D&D Alpha 4 & 5	Alpha 5 Characterization	Alpha-5 (4)	Alpha 4
Y-12 D&D Biology	Biology Characterization	Biology D&D (2)	None Used
Y-12 D&D Remaining Facilities	None Available	Old Scrap Yard Debris (2)	Beta-1
Y-12 Remedial Action	Upper East Fork Remedial Inv.	Old Scrap Yard Soil	White Wing Scrap Yard
ORNL D&D	Isotope Row Characterization	ORNL D&D (20)	23 ORNL Facilities
ORNL Remedial Action	Bethel Valley Remedial Inv.	ORNL RA (11)	None Used

Apply average as-generated waste bulk densities (derived from EMWMF disposal operations) to waste volumes for each EMDF waste stream

Debris 773 kg/yd³

Soil 1113 kg/yd³

Adjust data to account for radioactive decay to EMDF closure in 2047. Calculate average activity concentration data (pCi/g for each radionuclide) for each waste stream

Waste Stream Estimated Mass (kg)

EMDF Waste Stream	Debris	Soil	Total
Y-12 D&D Alpha 4 & 5	1.37E+08		1.37E+08
Y-12 D&D Biology	2.25E+07	5.65E+06	2.81E+07
Y-12 D&D Remaining Facilities	3.03E+08		3.03E+08
Y-12 Remedial Action	1.29E+08	3.97E+08	5.26E+08
ORNL D&D	1.93E+08	8.17E+05	1.94E+08
ORNL Remedial Action	4.32E+07	1.37E+08	1.81E+08

Waste Stream Activity Concentration Profiles (pCi/g, Table B.5, in part)

EMDF Waste Stream	Ac-227	Am-241	C-14	U-238
Y-12 D&D Alpha 4 & 5		1.61E-02		3.43E+01
Y-12 D&D Biology		1.82E-01	4.18E+01	3.40E+02
Y-12 D&D Remaining Facilities		5.92E-02		2.91E+03
Y-12 Remedial Action		6.86E-01		1.51E+02
ORNL D&D	3.88E-02	2.10E+02	8.53E+00	6.79E+00
ORNL Remedial Action		6.14E+02	2.55E+01	2.92E+01

Multiply average activity concentration values by the total mass of each waste stream to estimate radiological inventories for EMDF waste streams and EMDF total inventory

Waste Stream Radiological Inventories (Ci, Table B.6, in part)

EMDF Waste Stream	Ac-227	Am-241	C-14	U-238
Y-12 D&D Alpha 4 & 5		2.20E-03		4.71E+00
Y-12 D&D Biology		5.11E-03	1.17E+00	9.56E+00
Y-12 D&D Remaining Facilities		1.80E-02		8.83E+02
Y-12 Remedial Action		3.61E-01		7.92E+01
ORNL D&D	7.54E-03	4.09E+01	1.66E+00	1.32E+00
ORNL Remedial Action		1.11E+02	4.60E+00	5.27E+00
EMDF Total Estimated Inventory	7.54E-03	1.52E+02	7.43E+00	9.83E+02

Fig. 2.43. Schematic overview of data sources, radiological profiles and waste stream masses used to estimate EMDF radionuclide inventories

Profile activity concentrations are calculated as the arithmetic averages of all the mean, expected, or limiting values assigned to a waste stream. Applying an arithmetic average rather than a geometric mean to radioactivity concentration data that typically span many orders of magnitude results in an intentional bias toward higher estimated concentrations. Activity concentrations for each data source are adjusted for radiological decay to the assumed year of EMDF closure (2047) based on radioisotope half-life and the year of data collection. To estimate the radionuclide inventory for each EMDF waste stream, the estimated average radionuclide activity concentrations are multiplied by the estimated waste stream mass. An average soil density of 1113 kg/cy was assumed for the soil waste volumes. An average debris density of 773 kg/cy was determined based on the bulk densities compiled for EMWMF in the Capacity Assurance Remedial Action Report (DOE 2004). Total estimated EMDF waste inventory for each radionuclide (Table 2.15) is the sum of the six waste stream inventory estimates.

Table 2.15. Total EMDF waste radionuclide inventory (Ci decayed to 2047)

	ORNL D&D	ORNL RA	Y-12 D&D Alpha-4 and Alpha-5	Y-12 D&D Biology	Y-12 D&D Remaining Facilities	Y-12 RA	EMDF Waste Total Inventory (Ci)	EMDF waste average activity concentration (pCi/g)
Waste mass (g)	1.94E+11	1.81E+11	1.37E+11	2.81E+10	3.03E+11	5.26E+11	1.37E+12	
Radio-isotope			EMDF activity by waste stream (Ci)					
Ac-227	7.54E-03						7.54E-03	5.50E-03
Am-241	4.09E+01	1.11E+02	2.20E-03	5.11E-03	1.80E-02	3.61E-01	1.52E+02	1.11E+02
Am-243	5.30E-01	7.12E+00					7.65E+00	5.59E+00
Ba-133		Refer to Attachment B.3 for basis of inventory estimate					4.14E+00	3.02E+00
Be-10		Refer to Attachment B.3 for basis of inventory estimate					6.52E-05	4.76E-05
C-14	1.66E+00	4.60E+00		1.17E+00			7.43E+00	5.43E+00
Ca-41		Refer to Attachment B.3 for basis of inventory estimate					1.09E-01	7.92E-02
Cf-249	2.80E-06						2.80E-06	2.05E-06
Cf-250	1.91E-05						1.91E-05	1.39E-05
Cf-251	5.42E-07						5.42E-07	3.96E-07
Cf-252	3.37E-07						3.37E-07	2.46E-07
Cm-243	1.01E+00	1.02E-01					1.11E+00	8.10E-01
Cm-244	3.23E+02	2.53E+00	5.39E-04				3.26E+02	2.38E+02
Cm-245	9.87E-02						9.87E-02	7.21E-02
Cm-246	4.10E-01						4.10E-01	2.99E-01
Cm-247	2.68E-02						2.68E-02	1.96E-02
Cm-248	1.44E-03						1.44E-03	1.05E-03
Co-60	4.23E-02	7.90E-03	8.87E-04			4.20E-04	5.15E-02	3.76E-02
Cs-134	5.41E-09	2.19E-08					2.73E-08	1.99E-08
Cs-137	4.11E+02	2.63E+03	2.73E-02	3.71E-03	1.42E-02	2.84E+00	3.04E+03	2.22E+03
Eu-152	7.25E+01	1.46E+00					7.40E+01	5.40E+01
Eu-154	1.65E+01	2.52E-01					1.67E+01	1.22E+01
Eu-155	1.72E-02	1.44E-04					1.74E-02	1.27E-02
Fe-55		2.31E-06					2.31E-06	1.68E-06
H-3	2.52E+01	3.56E+00		6.25E-02			2.88E+01	2.10E+01
I-129	9.56E-01	9.35E-02					1.05E+00	7.66E-01
K-40	1.07E+00	3.43E+00		6.27E-01		3.33E+00	8.46E+00	6.18E+00
Mo-100	1.08E-05						1.08E-05	7.92E-06
Mo-93		Refer to Attachment B.3 for basis of inventory estimate					1.00E+00	7.30E-01
Na-22	2.09E-06	2.63E-08					2.12E-06	1.55E-06
Nb-93m		Refer to Attachment B.3 for basis of inventory estimate					6.01E-01	4.39E-01
Nb-94	4.20E-02						4.20E-02	3.07E-02
Ni-59	7.84E+00						7.84E+00	5.73E+00

	ORNL D&D	ORNL RA	Y-12 D&D Alpha-4 and Alpha-5	Y-12 D&D Biology	Y-12 D&D Remaining Facilities	Y-12 RA	EMDF Waste Total Inventory (Ci)	EMDF waste average activity concentration (pCi/g)
Waste mass (g)	1.94E+11	1.81E+11	1.37E+11	2.81E+10	3.03E+11	5.26E+11	1.37E+12	
Radio-isotope	EMDF activity by waste stream (Ci)							
Ni-63	1.17E+02	1.62E+03		4.84E-02			1.74E+03	1.27E+03
Np-237	8.92E-02	5.08E-01	6.72E-03	6.04E-03		2.27E-01	8.37E-01	6.12E-01
Pa-231	6.15E-01						6.15E-01	4.49E-01
Pb-210	9.09E+00	4.08E-01					9.50E+00	6.93E+00
Pm-146	2.28E-04						2.28E-04	1.66E-04
Pm-147	5.49E-04	1.69E-05					5.66E-04	4.13E-04
Pu-238	1.43E+02	9.86E+01	2.52E-02		1.20E-01	4.62E-03	2.42E+02	1.77E+02
Pu-239	4.61E+01	1.04E+02			2.31E-02	3.12E-01	1.50E+02	1.10E+02
Pu-240	6.81E+01	9.18E+01	9.29E-03	5.07E-03			1.60E+02	1.17E+02
Pu-241	1.33E+01	5.12E+02					5.25E+02	3.83E+02
Pu-242	3.55E-02	4.10E-01					4.45E-01	3.25E-01
Pu-244	9.49E-03						9.49E-03	6.93E-03
Ra-226	5.68E-01	7.08E-01		2.80E-02		7.63E-01	2.07E+00	1.51E+00
Ra-228	1.27E-03	2.52E-03			5.17E-02	1.41E-03	5.69E-02	4.15E-02
Re-187	4.40E-06						4.40E-06	3.21E-06
Sb-125	7.82E-08						7.82E-08	5.71E-08
Sr-90	4.21E+02	7.50E+01		4.93E-02	5.02E-02		4.96E+02	3.62E+02
Tc-99	2.57E+00	7.11E-01	1.48E-01	1.14E+00	2.36E-01	2.43E+00	7.23E+00	5.28E+00
Th-228	2.25E-07	3.40E-10	8.14E-08	3.58E-07	4.78E-06		5.45E-06	3.98E-06
Th-229	3.36E-01	1.44E+01			1.43E-02		1.47E+01	1.08E+01
Th-230	3.30E-01	3.81E+00	5.92E-02		2.38E-02	7.20E-01	4.94E+00	3.61E+00
Th-232	2.32E-01	1.69E+00	5.14E-02	2.24E-02	1.98E-01	6.87E+00	9.07E+00	6.62E+00
U-232	1.62E-01	2.61E+01					2.63E+01	1.92E+01
U-233	5.15E+01	5.27E+01		2.71E+00	3.33E-01		1.07E+02	7.83E+01
U-234	2.15E+00	2.72E+01	1.25E+00	2.34E+00	1.58E+03	8.24E+00	1.62E+03	1.19E+03
U-235	8.15E-02	4.23E-01	1.02E-01	2.02E-01	9.57E+01	5.84E+00	1.02E+02	7.47E+01
U-236	5.14E-02	1.95E-01	5.22E-02	1.19E-01	2.26E+01	1.19E-01	2.32E+01	1.69E+01
U-238	1.32E+00	5.27E+00	4.71E+00	9.56E+00	8.83E+02	7.92E+01	9.83E+02	7.18E+02

D&D = deactivation and decommissioning   RA = remedial action
EMDF = Environmental Management Disposal Facility   Y-12 = Y-12 National Security Complex
ORNL = Oak Ridge National Laboratory

2.3.2   Radionuclide Screening

There are 70 radionuclides included in the data sources assembled for the EMDF waste inventory (Appendix B). To provide computational efficiency and enable extensive single parameter sensitivity analysis simulation and probabilistic simulations, a methodology was employed to screen (i.e., remove from further analysis) radionuclides that do not contribute significantly to the total dose. For the EMDF PA, a two-phase approach was used for screening radionuclides for further simulations (Fig. 2.44). Phase 1 involved screening based on radionuclide half-life. Any parent radionuclide in the EMDF inventory with a half-life of less than 5 years was screened out from further analysis because during the first 100 years of post-closure institutional control, the engineered barrier systems (cover and liner, including the leachate collection system) will prevent cover infiltration and leachate release, and DOE control of all property immediately surrounding the EMDF site will prevent inadvertent intrusion. During this 100-year time
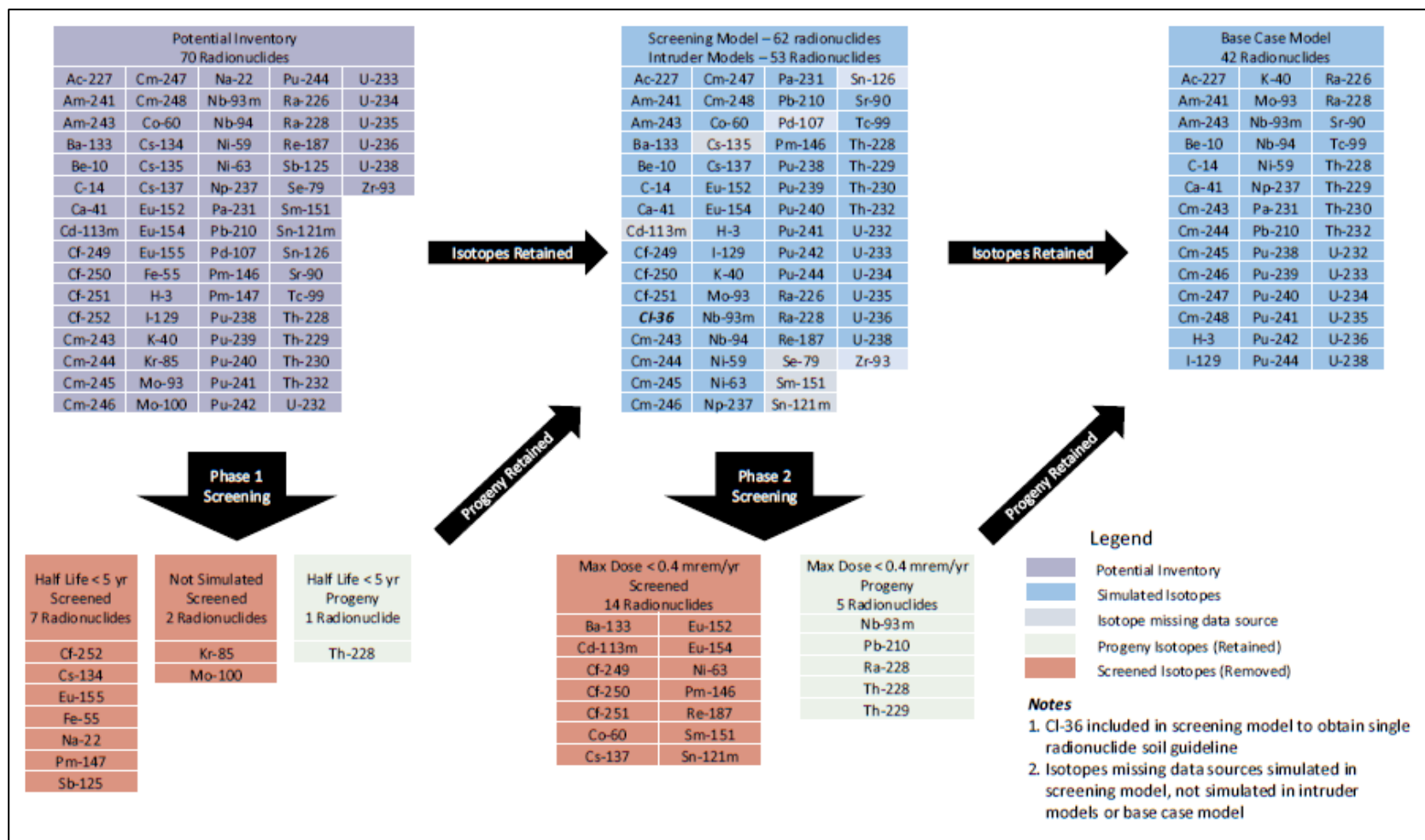
Fig. 2.44. Radionuclide screening for EMDF PA dose analysis

period, over 20 half-lives will have elapsed, resulting in decay of short-lived radionuclides to very low concentrations. Screening of radionuclides based on half-life was not performed for any nuclides that also are progeny of other parent nuclides included in the inventory. This approach avoids potential delay in progeny generation and ensures inventory progeny are accounted for in model simulations.

Additional justification for using the 5-year half-life as a cutoff for the analysis of leachate release to groundwater is the anticipated travel time from the waste to the underlying water table. STOMP model simulations (Appendix E) indicate that the average travel time from waste to the water table is greater than 200 years for a highly mobile radionuclide such as C-14 (approximately 40 or more half-lives for the screened short-lived radionuclides). Seven radionuclides were screened out in Phase 1, including: Cf-252, Cs-134, Eu-155, Fe-55, Na-22, Pm-147, and Sb-125. Thorium-228 has a half-life less than 5 years, but it was retained for the groundwater screening model because it is a progeny of several radionuclides in the inventory.

Based on the EMDF estimated inventory, anticipated operational conditions, and design features of the EMDF cover system, post-closure release of radionuclides in the vapor-phase is expected to be negligible. The estimated inventory of radioactive nuclides of noble gases and halogens is limited to Kr-85 and I-129. Other radionuclides that could be released from the EMDF waste as vapor include H-3 and C-14. Additional discussion of the potential for atmospheric release through the cover is provided in Sect. 3.2.2.2. Krypton-85 was eliminated prior to Phase 2 screening due to the expectation that significant amounts of krypton gas will not be present after waste generation, transport, placement, and in-cell compaction are complete. Molybdenum-100 is a very stable radionuclide (half-life 8.5E+18 years) that does not have a dose conversion factor in the RESRAD-OFFSITE database. The very low projected Mo-100 inventory (approximately 1.08E-05 Ci) is not expected to be a significant contributor to dose; therefore, Mo-100 was also excluded from further analysis.

In summary, for Phase 1 screening, a total of 61 radionuclides passed and a total of 9 radionuclides were screened from further consideration. Seven radionuclides were screened out based on their half-life and two radionuclides were screened out for other reasons (Fig. 2.44). For the IHI scenario, only the Phase 1 screening was applied (Sect. 6.2).

Phase 2 of the screening analysis applied a groundwater pathway screening model, which consists of a modified version of the base case model using isotope-specific distribution coefficients decreased by a factor of 10 or 100 (see Appendix G, Sects. G.4.3.6 and G.4.4.1) and other pessimistically biased assumptions that result in greater model-predicted doses regarding inventory (elevated screening source concentrations) and disposal conditions (no engineered barriers). A more detailed description of screening model simulations is provided in Sect. G.4.4.

The screening model dose is based exclusively on groundwater ingestion and applied a screening dose criterion of 0.4 mrem/year, which is 10 percent of the 4 mrem/year national primary drinking water standard for beta-gamma emitters (40 *CFR* 141). The 0.4 mrem/year screening criterion is applied to all radionuclides, including alpha emitters, for the all-pathways dose analysis. Compliance with drinking water MCLs for radionuclides, including alpha emitters, is evaluated separately from the all-pathways dose analysis (Sect. 4.7.1). Among the alpha emitting radionuclides in the estimated inventory, only Cf-249, Cf-250, and Cf-251 were eliminated from further consideration based on the Phase 2 screening criterion (Fig. 2.44). The estimated inventories of those three radionuclides are very small relative to the other alpha-emitting nuclides (Table 2.15), therefore neglecting their contributions to the estimated gross alpha activity concentration in groundwater (Sect. 4.7.1) is justified.

A total of 62 radionuclides were simulated in the groundwater screening model, which included the 61 radionuclides that passed Phase 1 of the screening process, as well as Cl-36.

Small quantities of Cl-36 could be present in future EMDF LLW associated with irradiated graphite or metals from ORNL research reactor facilities. However, Cl-36 has not been a radionuclide of concern for LLW disposed at the EMWMF, and identification of Cl-36 in environmental samples from the ORR is extremely rare. The compilation of facility inventory data, EMWMF waste profiles, and environmental characterization data used to estimate the EMDF radionuclide inventory at closure (refer to Appendix B) includes no data on Cl-36 activity. Due to this lack of information, and the likelihood that any Cl-36 will be limited to small volumes of waste, Cl-36 was included only in the Phase 2 screening model using a unit source concentration of 1 pCi/g to provide information for future waste management decisions.

Of the 62 simulated radionuclides, 43 radionuclides (42 plus Cl-36) produced a peak dose greater than 0.4 mrem/year and 19 produced a peak dose of less than 0.4 mrem/year. Out of the 19 radionuclides that produced a peak dose of less than 0.4 mrem/year, five radionuclides (Nb-93m, Pb-210, Ra-228, Th-228, and Th-229) are progeny of one of the 43 that exceeded the dose criteria. These five are retained as source concentrations for the base case groundwater pathway analysis (Fig. 2.44). The remaining 14 radionuclides removed because their individual predicted doses were less than 0.4 mrem/year were subsequently simulated together to confirm that the sum of the peak doses from the screened nuclides was less than 0.4 mrem/year. Although Cl-36 would have passed Phase 2 of the screening process, it is not simulated in the inadvertent human intruder or base case scenario simulations because there are no data available to estimate an EMDF Cl-36 inventory. A total of 47 radionuclides (42 with peak dose greater than 0.4 mrem/year plus five progeny) passed Phase 2 of the screening analysis (Table 2.16).

Table 2.16. Screening source concentrations and radionuclide screening results

Radionuclide	Half-life (years)	Screening source concentration (pCi/g)	Phase 1: Half-life > 5 years?	Phase 2: Peak Groundwater Dose > 0.4 mrem/year for 10,000-year simulation?	Retain for dose analysis?
Ac-227	2.18E+01	4.89E+04	Yes	Yes	Yes
Am-241	4.32E+02	2.30E+03	Yes	Yes	Yes
Am-243	7.38E+03	2.29E+01	Yes	Yes	Yes
Ba-133	1.07E+01	2.71E+01	Yes	No	Intruder
Be-10	1.50E+06	7.16E+05	Yes	Yes	Yes
C-14	5.73E+03	6.27E+05	Yes	Yes	Yes
Ca-41	1.00E+05	4.11E+06	Yes	Yes	Yes
Cd-113m	1.36E+01	1.11E+05	Yes	No	No[a]
Cf-249	3.51E+02	3.92E-04	Yes	No	Intruder
Cf-250	1.31E+01	1.70E-02	Yes	No	Intruder
Cf-251	8.98E+02	7.36E-05	Yes	No	Intruder
Cf-252	2.60E+00	1.25E+03	No	NS[b]	No
Cl-36[e]	3.01E+05	1.00E+00	Yes	Yes	No[a]
Cm-243	2.85E+01	4.37E+01	Yes	Yes	Yes
Cm-244	1.81E+01	5.26E+05	Yes	Yes	Yes
Cm-245	8.50E+03	9.80E+01	Yes	Yes	Yes
Cm-246	4.73E+03	1.97E+00	Yes	Yes	Yes
Cm-247	1.56E+07	2.35E+01	Yes	Yes	Yes
Cm-248	3.39E+05	2.29E+01	Yes	Yes	Yes
Co-60	5.27E+00	1.93E+06	Yes	No	Intruder
Cs-134	2.10E+00	1.39E+05	No	NS[b]	No

Table 2.16. Screening source concentrations and radionuclide screening results (cont.)

Radionuclide	Half-Life (years)	Screening source concentration (pCi/g)	Phase 1: Half-life > 5 years?	Phase 2: Peak Groundwater Dose > 0.4 mrem/year for 10,000-year simulation?	Retain for Dose Analysis?
Cs-135	2.30E+06	2.46E+06	Yes	Yes	No[a]
Cs-137	3.00E+01	3.82E+08	Yes	No	Intruder
Eu-152	1.33E+01	5.84E+05	Yes	No	Intruder
Eu-154	8.80E+00	7.85E+05	Yes	No	Intruder
Eu-155	4.80E+00	9.98E+05	No	NS[b]	No
Fe-55	2.70E+00	4.71E+07	No	NS[b]	No
H-3	1.24E+01	4.84E+06	Yes	Yes	Yes
I-129	1.57E+07	4.86E+05	Yes	Yes	Yes
K-40	1.28E+09	5.65E+01	Yes	Yes	Yes
Kr-85	1.10E+01	1.16E+08	Yes	NS[c]	No
Mo-93	3.50E+03	4.99E+03	Yes	Yes	Yes
Mo-100	8.50E+18	2.55E-03	Yes	NS[c]	No
Na-22	2.60E+00	5.96E-01	No	NS[b]	No
Nb-93m	1.36E+01	3.00E+03	Yes	No	Yes[d]
Nb-94	2.03E+04	1.90E+05	Yes	Yes	Yes
Ni-59	7.50E+04	1.55E+06	Yes	Yes	Yes
Ni-63	9.60E+01	1.03E+07	Yes	No	Intruder
Np-237	2.14E+06	5.63E+01	Yes	Yes	Yes
Pa-231	3.28E+04	3.17E+00	Yes	Yes	Yes
Pb-210	2.23E+01	4.48E+02	Yes	No	Yes[d]
Pd-107	6.50E+06	3.34E+06	Yes	Yes	No[a]
Pm-146	5.50E+00	1.24E-01	Yes	No	Intruder
Pm-147	2.60E+00	2.67E+06	No	NS[b]	No
Pu-238	8.77E+01	7.15E+03	Yes	Yes	Yes
Pu-239	2.41E+04	1.85E+05	Yes	Yes	Yes
Pu-240	6.54E+03	8.44E+03	Yes	Yes	Yes
Pu-241	1.44E+01	2.83E+05	Yes	Yes	Yes
Pu-242	3.76E+05	4.98E+01	Yes	Yes	Yes
Pu-244	8.26E+07	1.11E+01	Yes	Yes	Yes
Ra-226	1.60E+03	1.35E+01	Yes	Yes	Yes
Ra-228	5.75E+00	3.46E+00	Yes	No	Yes[d]
Re-187	4.12E+10	1.94E-03	Yes	No	Intruder
Sb-125	2.80E+00	1.37E+06	No	NS[b]	No
Se-79	6.50E+04	2.47E+06	Yes	Yes	No[a]
Sm-151	9.00E+01	5.75E+06	Yes	No	No[a]
Sn-121m	5.50E+01	6.41E+01	Yes	No	No[a]
Sn-126	1.00E+05	1.89E+06	Yes	Yes	No[a]
Sr-90	2.91E+01	3.93E+08	Yes	Yes	Yes
Tc-99	2.13E+05	1.35E+06	Yes	Yes	Yes
Th-228	1.90E+00	1.14E+05	No	No	Yes[d]

Table 2.16. Screening source concentrations and radionuclide screening results (cont.)

Radionuclide	Half-Life (years)	Screening source concentration (pCi/g)	Phase 1: Half-life > 5 years?	Phase 2: Peak Groundwater Dose > 0.4 mrem/year for 10,000-year simulation?	Retain for Dose Analysis?
Th-229	7.34E+03	3.48E+03	Yes	No	Yes[d]
Th-230	7.70E+04	1.48E+02	Yes	Yes	Yes
Th-232	1.41E+10	2.67E+06	Yes	Yes	Yes
U-232	7.20E+01	8.43E+05	Yes	Yes	Yes
U-233	1.59E+05	5.49E+05	Yes	Yes	Yes
U-234	2.45E+05	1.67E+03	Yes	Yes	Yes
U-235	7.04E+08	2.57E+03	Yes	Yes	Yes
U-236	2.34E+07	4.87E+02	Yes	Yes	Yes
U-238	4.47E+09	2.07E+09	Yes	Yes	Yes
Zr-93	1.53E+06	5.56E+05	Yes	Yes	No[a]

[a]Radionuclide not simulated because insufficient inventory data were available.
[b]Radionuclide not simulated due to screening in Phase 1.
[c]Radionuclide not simulated due to other reasons.
[d]Isotope has half-life less than 5 years or screening dose less than 0.4 mrem/year, but was retained for further analysis because it is progeny of another isotope in the inventory. Intruder identifies isotopes simulated for IHI models, but not retained for further analysis.
[e]Cl-36 is not included in the inventory but was simulated in the screening model provide information for future waste management decisions.

IHI = inadvertent human intrusion
NS = not simulated

2.3.3 Radionuclide Inventories for Further Analysis

Nine radionuclides (less commonly reported fission products) had inventory data that could not be verified from the original sources and were not included in the IHI analysis or base case models. These nine radionuclides are: Cd-113m, Cs-135, Kr-85, Pd-107, Se-79, Sm-151, Sn-121m, Sn-126, and Zr-93. Five of these nine passed the Phase 2 groundwater pathway screening; one was screened out at a noble gas. Including the removal of Mo-100, out of the 70 total isotopes considered in the EMDF waste inventory (see Appendix B), 53 isotopes were simulated in the IHI analysis models and 42 radionuclides were simulated in the base case (release to groundwater) model (Table 2.16).

As a final step in developing the estimated radionuclide inventory for the PA analysis, operational period losses of highly mobile radionuclides (H-3, C-14, Tc-99, and I-129) are estimated and used to adjust (decrease) the assumed post-closure inventory for those nuclides. The assumptions and modeling applied to estimate these operational losses and reductions in mobility resulting from treatment of collected leachate are described in Sect. 3.2.2.5.

This page intentionally left blank.

3. ANALYSIS OF PERFORMANCE

This section of the report provides detailed descriptions of the conceptual models, modeling tools, and exposure scenario used to analyze EMDF performance. The following section provides an overview of the analysis and provides summary information on the conceptual models, modeling tools, and exposure pathways in the context of the total EMDF disposal system described in Sect. 1.3 and Appendix C.

3.1 OVERVIEW OF ANALYSIS

The approach to selecting the range of potential future conditions analyzed for this PA is a top-down, total system analysis of the EMDF disposal system that is structured around the safety functions served by the engineered and natural elements of the system. An overview of safety functions for the EMDF disposal system is provided in Sect. 1.3. Appendix C provides additional detail on EMDF design features and safety functions and includes analysis of natural events and processes that can impact the safety functions of key features. Uncertainties in future environmental conditions and the long-term performance of engineered barriers are integrated and generalized in a conceptual model of EMDF performance evolution that is expressed in terms of changes in cover infiltration and leachate release over time (refer to Sect. 3.2.1 and Appendix C, Sect. C.1.3). To address these uncertainties, the PA incorporates a range of potential future conditions defined by selection of input parameter values for model sensitivity evaluations and the uncertainty analysis presented in Sect. 5. In addition, a separate analysis of the potential impact of an alternative conceptual model of EMDF failure in which cover infiltration greater than liner system release leads to waste saturation and overtopping of the liner (bathtub condition) is provided in Appendix C, Sect. C.3.

3.1.1 Conceptual Models of the EMDF Disposal System

Conceptualization of the EMDF disposal system for performance analysis and modeling is organized around four related components, as described in Table 3.1.

Table 3.1. EMDF disposal system components, conceptual model elements, and model codes

Disposal system component	Conceptual model elements	Model codes
Water Balance and Performance of Engineered Barriers (Sect. 3.2.1)	• Facility water balance • Performance of engineered systems • Degradation of synthetic and earthen barriers • Assumed evolution of EMDF cover infiltration and leachate release	HELP RESRAD-OFFSITE
Radionuclide Release and Vadose Zone Transport (Sect. 3.2.2)	• EMDF radionuclide inventory • Disposal practices and waste forms • Facility design geometry • EMDF cover performance evolution • Vapor phase release and radon flux • Aqueous phase release from waste • Transport through waste and liner system, including chemical retardation • Vadose zone transport below liner	STOMP RESRAD-OFFSITE

Table 3.1. EMDF disposal system components, conceptual model elements, and model codes (cont.)

Disposal system component	Conceptual model elements	Model codes
Saturated Zone Flow and Radionuclide Transport (Sect. 3.2.3)	• Vadose zone flux to saturated zone • CBCV site geology and topography • CBCV hydrogeology • CBCV surface water features • CBCV saturated zone flow and transport, including chemical retardation	MODFLOW MT3D RESRAD-OFFSITE
Exposure Pathways and Scenarios[a] (Sect. 3.2.4)	• Resident farmer exposure scenario • Groundwater POA (well location) • Surface water POA • Exposure pathways, abiotic and biotic • Dose analysis	RESRAD-OFFSITE

[a]Analysis of the inadvertent human intrusion scenario is presented in Sect. 6

CBCV = Central Bear Creek Valley   POA = point of assessment
EMDF = Environmental Management Disposal Facility   RESRAD = RESidual RADioactivity
HELP = Hydrologic Evaluation of Landfill Performance STOMP = Subsurface Transport over Multiple Phases

Conceptual models of post-closure and long-term performance of engineered barriers are incorporated in the assumed evolution of the EMDF water balance as the safety functions of engineered cover and liner system features become limited by natural processes of degradation. These conceptual models include pessimistic biases intended to lead to increased infiltration versus what is expected as a means to address uncertainty in cover performance (Sect. 3.2.1 and Appendix C, Sect. C.1).

Conceptual models of post-closure radionuclide release from the EMDF disposal system (Sect. 3.2.2) include analysis and screening of radionuclide release through the cover to the atmosphere or biosphere, diffusive transport and release of radon through the cover (Appendix H), and radionuclide release and transport in the aqueous phase. Conceptual models for aqueous release incorporate the assumed changes in cover infiltration over time and include waste zone radionuclide release and unsaturated vertical flow and radionuclide transport through the waste, liner system, and underlying vadose zone. These conceptual models are based on the estimated EMDF radionuclide inventory (Appendix B), assumed waste disposal practices and waste forms (Sect. 3.2.2.5), sorptive properties of EMDF materials (Sect. 3.2.2.8), the vertical sequence of vadose zone materials, and the analysis of cover performance presented in Sect. 3.2.1 and Appendix C.

Conceptual models of saturated zone flow and radionuclide transport are based on the hydrogeologic conceptual model for BCV (Sect. 2.1.5.1), including the lithology and stratigraphy of the EMDF site, major topographic and structural controls on groundwater movement, surface water features, and chemical retardation properties of the saprolite and bedrock. Conceptualization of the saturated zone for purposes of EMDF performance analysis is described in detail in Sect. 3.2.3.

Conceptual models of post-closure public exposure to radionuclides include the general resident farmer scenario considered for the analysis (Sect. 3.2.4) as well as detailed assumptions for abiotic (e.g., water ingestion, inhalation) and biotic (e.g., ingestion of contaminated fish and produce) exposure pathways. Section 3.2.4 presents the exposure scenario and pathway assumptions in detail and describes the basis for the inputs and assumptions incorporated into the dose analysis.

3.1.2 PA Model Implementation and Integration

Implementation of the EMDF system conceptual models with computer modeling codes is structured around the four conceptual components (Table 3.1 and Fig. 3.1). This implementation includes detailed process model codes for the components that encompass engineered facility performance and abiotic transport elements, as well as a total system model code that encompasses all four conceptual components including the exposure scenario and biotic pathways for radionuclide transfer. The more detailed models were used for modeling the complexities of primarily abiotic environmental transport pathways to predict concentrations of key radionuclides at the POA. The total system model uses simplified representations of transport pathways, along with biotic transformations and scenario-specific exposure factors, to identify radionuclides that are likely key dose contributors and quantify total dose for comparison to performance objectives.

Implementation of the more detailed component-level EDMF PA models and the total system model proceeded concurrently, along with iterative development and refinement of model assumptions, cover performance and source release approaches, and parameter value selections for each of the model tools. Some model outputs serve as inputs for other modeling tools. The primary model output-to-input linkages are shown in Fig. 3.2 and are described along with comparisons of model outputs in Sect. 3.3. Inputs common to all model codes include radionuclide inventories, EMDF design specifications, and CBCV site characteristics. Selection, implementation, and integration of these model codes for EMDF performance analysis is explained in Sect. 3.3. QA activities for model implementation are described in Sect. 9.

Fig. 3.1. Schematic illustration of EMDF disposal system conceptual models and modeling tools used for implementation

EMDF Disposal System Performance Analysis

Conceptual Components

Integration of Model Codes

Water Balance and Performance of Engineered Barriers (Section 3.2.1)

Radionuclide Release and Vadose Zone Transport (Section 3.2.2)

Saturated Zone Flow and Radionuclide Transport (Section 3.2.3)

HELP[1] (cover water balance)

Cover Infiltration

RESRAD-OFFSITE (total system code)

- Radionuclide Inventory
- Radionuclide Release
- Radionuclide Transport
- Exposure Pathways
- Dose Analysis
- Uncertainty Analysis

Exposure Pathways and Scenarios (Section 3.2.4)

Output Comparison

STOMP[2] (vadose zone transport)

Timing and Pattern of Vadose Flux to Water Table

Output Comparison

MT3D (saturated zone transport)

Groundwater Flow Field

Hydraulic Gradient

Depth to Saturated Zone

MODFLOW & MODPATH (groundwater flow)

Model Output - Input

1: Hydrologic Evaluation of Landfill Performance
2: Subsurface Transport Over Multiple Phases

Fig. 3.2. EMDF disposal system conceptual components and integration of model codes for performance analysis

3.2 CONCEPTUAL MODELS

The following sections present more detailed descriptions of conceptual models for EMDF system features and processes, including the facility water balance and degradation of engineered components (Sect. 3.2.1), source release and vadose zone transport (Sect. 3.2.2), and radionuclide transport in the saturated zone and discharge to surface water (Sect. 3.2.3). The assumptions regarding exposure pathways and scenarios considered for each disposal facility performance objective are described in Sect. 3.2.4.

3.2.1 Water Balance and Performance of Engineered Barriers

The basic conceptual model for the water balance of the EMDF system includes the natural environmental drivers of land surface hydrology and the engineered drainage features and barrier systems of the landfill design (Fig. 3.3). Infiltration of water through the surface layer and into the cover lateral drainage system is a function of climatic and meteorological dynamics and characteristics of the surface soil and vegetation that control local surface water and energy budgets. Subsurface percolation of water is conceptualized as predominantly vertical within the waste zone and earthen barriers of the cover and liner systems, whereas both vertical and lateral drainage are assumed to occur within the engineered drainage layers while they

122

remain functional. Water movement through the unsaturated zone beneath the liner is also conceptualized as vertically downward to the water table.
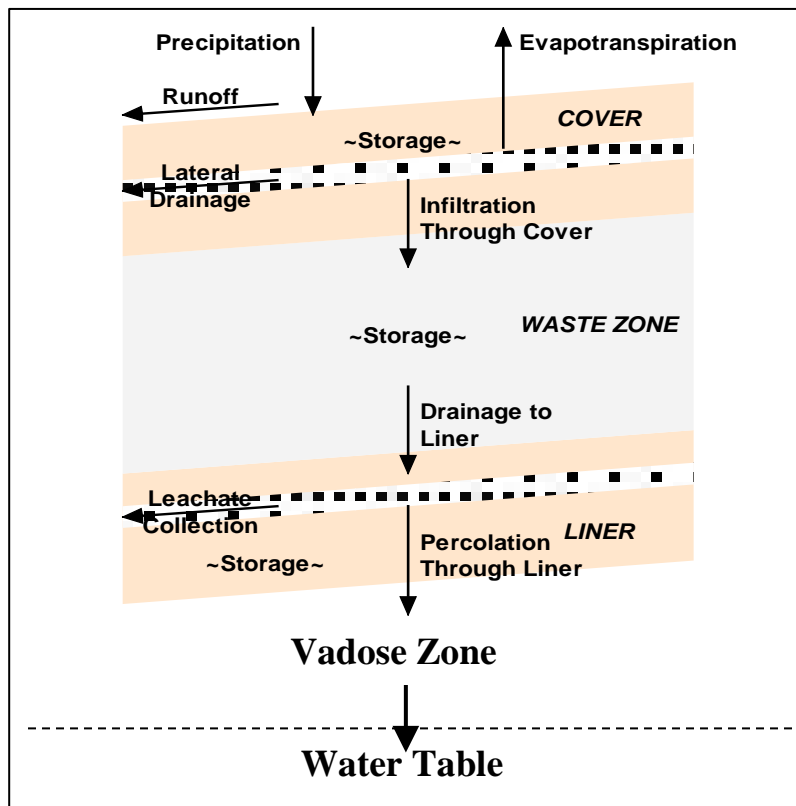
Fig. 3.3. Schematic conceptual model of EMDF water balance

EMDF design features are described in Sect. 2.2 and additional detail on the water balance model is provided in Appendix C, along with the analysis of features, events, and processes that influence system performance. The remainder of this section summarizes the information and uncertainties that are incorporated into the generalized conceptual model of EMDF system performance.

Engineered barriers of primary concern for long-term facility performance include the synthetic (HDPE) membranes and clay barrier layers of the cover and liner systems. Synthetic membrane service life and the long-term performance of engineered earthen barriers are key uncertainties. A simplified profile of the EMDF, with safety functions and events and processes important for long-term performance, is provided in Fig. 3.4. The safety functions of the various cover and liner system layers are interdependent so that the function of one layer may be limited by impaired function of one or more other layers in the system. The synthetic membranes serve as the primary short-term (decades to centuries) infiltration and leachate barriers that support the function of lateral drainage layers in the cover and liner. Thermal oxidative degradation is a primary breakdown mechanism for HDPE membranes and is highly sensitive to temperature, so that the thermal buffer provided by the overlying materials is a factor regulating the potential rate of degradation.

This page intentionally left blank.

EMDF Engineered Features	Safety Functions	Limiting Events and Processes
Cover System Components		
Vegetated erosion control layer (4 ft)	- Provides growth medium for cover vegetation - Protects underlying cover components from erosion and variability in temperature and moisture	- Surface water balance, infiltration and runoff - Vegetation and soil development, biointrusion - Surface erosion and gullying - Severe storms/flood events, landslides
Granular filter layer (1 ft)	- Prevents filling of the biointrusion layer pore space	- Biointrusion
Biointrusion layer (2 ft)	- Deters inadvertent human intrusion - Limits damage to hydrologic barriers by roots and burrowing animals - Secondary erosion control (defense-in-depth)	- Weathering and physical breakdown of cobbles/boulders - Pore space infilling and root penetration
Lateral drainage layer (1 ft)	- Provides subsurface drainage to reduce deep cover infiltration through the less permeable underlying layers	- Infilling of pore spaces with fine particulates and/or by chemical precipitation - Waste subsidence (differential settlement)
Synthetic (HDPE) membrane (60 mil)	- Primary cover infiltration barrier (initial post closure period) - Protects underlying clay barrier from desiccation and cracking	- Installation-related defects/damage - HDPE thermal oxidative degradation processes - Severe seismic event and/or rapid waste subsidence causing early membrane failure
Amended/compacted clay barriers (2 ft)	- Primary long-term infiltration barrier - Limits vapor phase release to the cover surface (radon barrier)	- Improper clay compaction - Root penetration, thermal and moisture cycles (increasing permeability) - Waste subsidence (differential settlement) - Severe seismic or storm event causing damage to cover
Contour soil layer (1ft)	- Provides a level foundation for construction of the compacted clay infiltration barrier(s)	-Improper construction impacts performance of overlying clay barrier
Waste Forms		
Waste containers	- Containers isolate waste from water and reduce radionuclide mobility	- Corrosion of metal containers - Insufficient filling of void space in waste containers
Treated and stabilized waste forms	- Provides chemical and physical stability to reduce radionuclide mobility	- Degradation of stabilized waste forms
Void filling and bulk waste compaction protocols	- Limits long-term subsidence of bulk waste and maintains cover system function	- Waste consolidation and subsidence
Liner System Components		
Protective material layer (1 ft)	- Protects underlying liner system components from damage during disposal operations.	- Improper installation - Unintentional disturbance during waste placement
Leachate collection (drainage) layer (1 ft)	- Ensures protection of human health and the environment (operations & early post-closure) - Waste mass dewatering (early post-closure)	- Damage to overlying geotextile during installation - Clogging, chemical precipitation
Primary synthetic (HDPE) membrane (60 mil)	- Ensures leachate drainage for treatment (operations) - Serves as primary leachate barrier (early post-closure period)	- Installation-related defects/damage - Chemical degradation of HDPE by leachate - HDPE thermal oxidative degradation processes
Geosynthetic clay Layer (0.02 ft)	- Reduces leachate flux through HDPE membrane holes and defects	- Installation-related defects/damage - Geochemical alteration of sodium bentonite clay (divalent cations)
Leak detection layer (0.03 ft)	- Provides performance monitoring for overlying composite leachate barrier - Provides secondary leachate removal function	- Degradation of synthetic drainage material
Secondary synthetic (HDPE) membrane (60 mil)	- Supports performance monitoring for overlying composite leachate barrier - Serves as secondary leachate barrier	- Chemical degradation of HDPE by leachate - HDPE thermal oxidative degradation processes
Compacted clay layer (3 ft)	- Serves as primary long-term leachate barrier - Provides chemical retardation of radionuclide migration	- Improper clay compaction - Physical and geochemical alteration of clay - Severe seismic event or slope failure damage to perimeter berms and clay barriers
Geologic buffer zone (unsaturated, low permeability, 10 ft)	- Isolates radionuclides from saturated zone - Provides chemical retardation of radionuclide migration	- Physical and geochemical alteration of geologic buffer material - Water table incursion into geologic buffer

Fig. 3.4. Simplified EMDF design profile, safety functions, and processes relevant to long-term performance

This page intentionally left blank.

Differential settlement (subsidence) of waste during the post-closure period can limit the safety functions of cover system components. Physical stress due to subsidence can damage the HDPE membrane and clay barrier in the cover, increasing water infiltration. Lateral drainage efficiency also can be impaired by subsidence, which will also increase infiltration. Due to the variety of expected EMDF waste forms, this degradation mechanism is an important uncertainty in the conceptual model of EMDF performance evolution. EMDF waste placement and compaction practices are developed to limit future subsidence and final cover design may incorporate features that impart resilience of the cover components to limited subsidence. In addition, post-closure monitoring and maintenance will permit timely repair of damaged cover areas that may develop due to subsidence.

For long-term (centuries to millennia) EMDF performance, function of the clay barrier layer in the cover system is essential. The cover system for EMDF has a robust configuration to protect the compacted clay layers from degrading processes in the surface environment. The vegetated surface layer serves to protect the underlying hydraulic barrier system from erosion and environmental fluctuations that can accelerate degradation of materials and impair safety functions. Site characteristics and processes that will determine the evolution of the surface layer after the cover vegetation is no longer maintained include long-term interactions among climate, soil development, vegetation, and associated successional changes in vegetation over time. These changes will affect the surface water balance, erosion of the cover surface, and infiltration of water. Eventually, severe weather events and progressive climate and vegetation changes could lead to erosion of the protective cover components and cause localized degradation of the clay barrier in the cover, increasing the potential for increased water infiltration over time. Detailed consideration of these processes and events is presented in Appendix C.

The progression of degradation of clay barrier(s) and the overlying components of the cover is contingent on the intensity and timing of multiple processes and events in the post-closure period. Although a general progression from full design performance to some long-term degraded performance condition will occur, the timing and magnitude of degradation is highly uncertain, particularly given the potential interactions among the various disposal system elements, safety functions, and degradation processes described above. One important aspect of this uncertainty is the timing of cover performance degradation (increasing cover infiltration) relative to evolution in the function of liner system components, which may be different due to the differing environments that develop in the cover and liner systems over time. There is a possibility that the cover components will degrade more rapidly than the liner components and that, after leachate collection ceases, the water (im)balance will cause accumulation of water on the liner over time (bathtub scenario). The performance implications of such a bathtub scenario for EMDF are developed in Appendix C, Sect. C.3. Uncertainty in the longevity of the engineered barriers that limit cover infiltration is addressed in the sensitivity and uncertainty analysis applied to the total system model (Sect. 5.4).

A generalized conceptual model of changes in cover infiltration and leachate release assumed as a result of natural processes and events that can impact cover and liner performance over time is shown in Fig. 3.5. The goal of the model is to integrate and generalize the impact of multiple events and processes on safety functions and EMDF performance over time, incorporating uncertainty in timing and degree of degradation and the occurrence of severe events. EMDF performance is expressed in terms of changes in cover infiltration and leachate release, beginning at the time of final cap completion and facility closure. A post-closure performance timeline (bottom of Fig. 3.5) can be divided into a 100-year institutional control period (during which facility maintenance and active institutional controls are assumed), a period during which full (or near) design performance is maintained after the end of institutional control, a period of degrading performance (increasing cover infiltration and leachate release), and a final period during which water flux into and out of the disposal unit reaches some long-term, relatively stable limit. Implementation of this general model of increasing cover infiltration over time for each of the PA models is described in Sect. 3.3.

This page intentionally left blank.
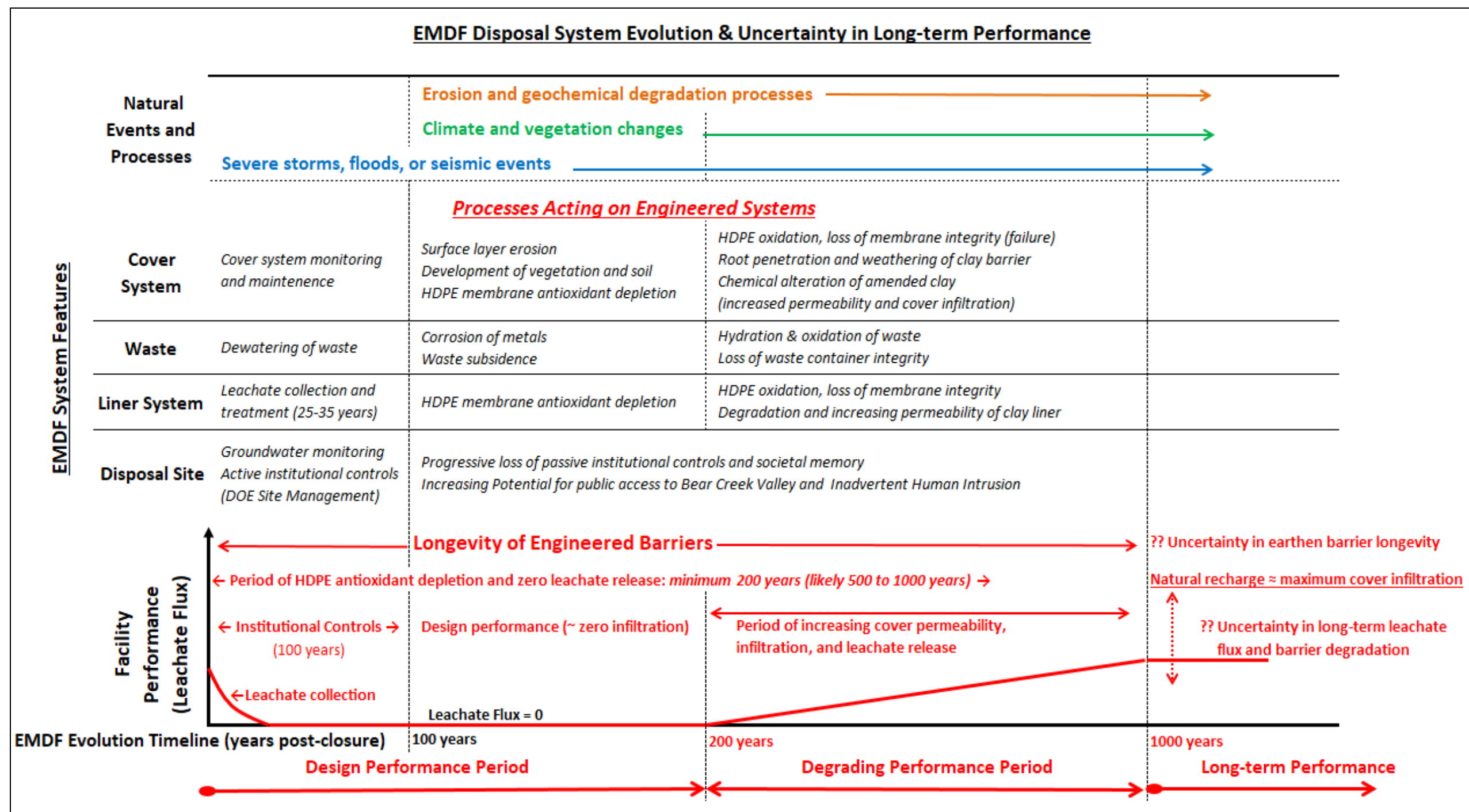
Fig. 3.5. Generalized conceptual model of EMDF performance evolution showing changes in cover infiltration and leachate release over time

129

This page intentionally left blank.

3.2.2 Radionuclide Release and Vadose Zone Transport

Conceptual models of post-closure EMDF radionuclide release include (1) upward transport through the EMDF cover system via diffusive or biologically driven transport processes that allow release to the atmosphere and biosphere, and (2) downward transport of radionuclides in solution through the variably saturated waste and liner system components and release to the vadose zone materials and groundwater underlying the disposal facility. In the humid environment of East Tennessee, the impact of upward aqueous phase diffusive transport is limited by the predominance of downward advective transport, but vapor-phase or biologically-driven upward transport of radionuclides is possible. Sections 3.2.2.1, 3.2.2.2, and 3.2.2.3 address the limited potential for significant radionuclide release through the EMDF cover system and provide the basis for screening such releases to the atmosphere or biosphere from the all pathways dose analysis of the PA. Appendix H presents model analysis of diffusive transport and release of radon gas from the EMDF cover. Sections 3.2.2.4 through 3.2.2.8. focus on the conceptual model of aqueous phase transport through to the vadose zone and release to the saturated zone, including waste forms and sorptive characteristics.

3.2.2.1 Biointrusion and biologically driven radionuclide release

Biointrusion of the EMDF cover by root systems or ground-dwelling animals is considered as a possible mechanism for release of radionuclides to the surface. Following the end of post-closure care and active institutional control, development of natural vegetation and unimpeded inhabitation of the cover system by various animals is likely. Biological intrusion by root systems, insects, and vertebrate animals will contribute to the natural evolution of the cover system components. In the absence of significant cover erosion, the five-foot thickness of the materials overlying the biointrusion layer (Fig. 3.4) is sufficient to prevent biointrusion into the waste by all but the deepest roots (Canadell et al. 1996, Jackson et al. 1996). In addition, the capillary break creased at the top of the biointrusion layer will also inhibit deeper root penetration. The potential for erosion of the cover surface is considered in detail in Appendix C, Sect. C.1.2 and the magnitude of long-term cover erosion is estimated in Appendix C, Sect. C.4.

The coarse material of the biointrusion layer is expected to be resistant to even severe erosive events and, therefore, will prevent large burrowing animals from bringing waste to the surface. Much smaller species that inhabit the subsurface (e.g., ants) would not be effectively excluded by the biointrusion layer and could potentially penetrate the cover system clay barriers in areas where erosion reduces the thickness of the material above the biointrusion barrier. Transfer of radionuclides to the cover surface by ants or other small soil-dwelling organisms would be limited to relatively small areas and is thus unlikely to produce significant airborne activity concentrations near the EMDF. Similarly, deep tree roots could penetrate the biointrusion layer and clay barrier, but typically more than 75 percent of temperate deciduous forest root systems are limited to the upper 50 cm of the soil profile (Jackson et al. 1996). Uptake of radionuclides by root systems could make radionuclides available in plant tissues at the surface, but human exposure routes originating from this transport mechanism (e.g., consumption of wild plants or animals) would make negligible dose contributions relative to the ingestion of contaminated water and farm-raised foods assumed for the resident farmer dose analysis.

Given the expectation of a relatively stable vegetated cover surface and that the coarse materials of the biointrusion barrier will prevent deep burrowing by large animals, the potential for biologically driven release of radionuclides from EMDF is small in comparison to abiotic release processes. Based on these considerations limiting human exposure to biologically-driven release of radionuclides to the cover surface, this release mechanism was eliminated from the all-pathways dose analysis.

131

3.2.2.2 Vapor-phase release through the EMDF cover

Previous risk analyses for BCV (DOE 1997b) and the original CA completed for the EMWMF (DOE 1999b, Appendix A) have identified radionuclide release to groundwater and surface water as the primary environmental transport pathways from waste disposal sites on the ORR. In 1996, a multidisciplinary technical steering committee for composite analyses was formed to develop a coherent composite analysis strategy for the EMWMF and another LLW disposal facility in Melton Valley. The steering committee analyzed site-specific conditions on the ORR and concluded that airborne contamination is not a significant public exposure pathway for waste disposal units in BCV and elsewhere on the reservation (DOE 1999b, pages A-15 to A-16). Similarly, the risk assessment and WAC development procedure for the EMWMF (DOE 1998a, Appendix E) excluded the atmospheric release pathway from consideration on the basis that the nearest public receptors were outside the DOE boundary at a significant distance from each of the sites considered.

Based on the EMDF estimated radionuclide inventory, anticipated losses of volatile chemical species during disposal operations, and design features of the EMDF cover system, post-closure release of radionuclides in the vapor-phase is not expected to result in a significant dose to nearby receptors. The remainder of this section explains the characteristics of the estimated inventory and EMDF design features that will limit vapor-phase release from the EMDF. Radon release through the cover is estimated in a separate radon analysis in Appendix H.

The estimated inventory of radionuclides that have the potential to exist in gaseous forms is limited to H-3, C-14, and I-129 (Table 3.2). Small quantities of Cl-36 could be present in future EMDF LLW associated with irradiated graphite or metals from ORNL research reactor facilities; however, these forms of Cl-36 would not be easily volatilized. Furthermore, Cl-36 has not been a radionuclide of concern for LLW disposed at the EMWMF and identification of Cl-36 in environmental samples from the ORR is extremely rare. Some ORNL facility safety documents include Kr-85 estimates in facility inventory estimates, but the utility of these data for estimating activity concentrations in demolition waste is limited. Based on the gaseous form and short half-life (11 years) of Kr-85, quantities of Kr-85 present in EMDF waste at closure are likely to be negligible; therefore, Kr-85 was screened from the PA analyses (refer to Sect. 2.3.2).

Table 3.2. EMDF waste activity concentrations and estimated radionuclide dose for RESRAD-OFFSITE cover release screening models.

Isotope	Half-life (years)	EMDF waste average activity concentration (pCi/g)	Maximum EMDF waste stream average concentration used for cover release screening (pCi/g)	Maximum estimated dose (mrem/year)
H-3	1.24E+01	2.10E+01	1.30E+02	0.023
C-14	5.73E+03	5.43E+00	4.18E+01	0.044
I-129	1.57E+07	7.66E-01	4.92E-00	4.8E-06
Total potential (bounding) dose due to release through the EMDF cover				**0.067**

EMDF = Environmental Management Disposal Facility
RESRAD = RESidual RADioactivity

For elements and compounds that commonly occur in gaseous forms, including krypton, carbon, and hydrogen, loss of more volatile chemical species during the generation, transport, and disposal of uncontainerized waste will reduce the inventory that is potentially available for vapor-phase release following closure. Similarly, exposure of soluble chemical forms of these radionuclides (e.g., as CO_2, HCO_2^-) and iodine (as I^-) to precipitation and infiltration (prior to placement of less permeable interim cover

materials) can further diminish the post-closure inventory through leaching and treatment of collected leachate. For the PA analysis, the estimated post-closure inventories of radionuclides that are highly mobile in the aqueous phase, including H-3, C-14, Tc-99, and I-129, are adjusted (reduced) based on modeling of operational period leaching (results are presented in Sect. 3.2.2.5 and in Appendix G, Sect. G.4.3.4). EMDF leachate treatment wastes (e.g., isotope exchange resins) that could be returned to the EMDF for disposal would be less likely to release these radionuclides in either the vapor or aqueous phase.

The screening analysis for radionuclide release through the EMDF cover does not, however, take credit for operational period losses of mobile species. To ensure an additional pessimistic bias for the screening analysis, the quantitative cover release screening model presented in the following section applies activity concentrations corresponding to the EMDF waste stream with the highest average concentration for each radionuclide (refer to Appendix B, Table B.5) rather than the overall as-generated EMDF waste average concentrations (Table 3.2).

Volatile forms of radionuclides remaining after final cover construction can migrate by diffusion (and potentially, biological disturbance of the cover material) toward the EMDF surface and could be available for inhalation as vapor or in suspended particulate form. The expected longevity of the cover system (provided by design features that protect the flexible geomembrane and clay barriers from degradation) will limit diffusive transport to the EMDF surface for many decades, and likely for centuries. Appendix C provides additional detail on engineered features and degradation processes for the cover system.

Transport of volatile forms to the surface will become more likely over the long-term, as cover performance declines and the hydraulic barriers of the EMDF cover become more permeable. Corrosion of waste containers and degradation of stabilized waste forms also may release previously unavailable portions of the radionuclide inventory. Vapor- or aqueous-phase diffusion can transport radionuclides toward the surface under these conditions, but other processes may be dominant. Given the abundant, year-round rainfall in the East Tennessee region, the persistent downward flux of water through the cover and underlying waste will continue to limit diffusive transport of radionuclides to the EMDF surface.

Some of the preceding arguments for limitation of vapor-phase release also apply to radon transport to the EMDF cover surface. A quantitative radon release analysis is necessary to demonstrate compliance with the DOE radon flux (or dose) performance objective (Sect. 1.5.1). Appendix H presents model analysis of diffusive transport and release of radon gas from the EMDF cover. The conceptual model of radon release incorporates the differing material layers of the cover system (Fig. 3.4; see also Appendix H, Fig. H.2). The approach does not take credit for the presence of the HDPE membrane in the cover. The method for radon flux estimation is derived from techniques for design of uranium tailings cover systems (U.S. Nuclear Regulatory Commission [NRC] 1984) and is described in detail in Appendix H. The results of the analysis suggest that radon flux at the top of the cover clay barrier is negligible as long as the clay retains a sufficient moisture content.

The limited initial quantities of potentially volatile radionuclides (Table 3.2) and likely mobility of those radionuclides in both the vapor and aqueous-phase during EMDF operations will result in very small amounts available for release as vapor after facility closure. Based on the range of operational, facility design, and environmental considerations limiting vapor-phase transport and release of radionuclides at the cover surface, this release mechanism was eliminated from the EMDF all-pathways dose analysis. To support this release pathway screening, the following section presents the results of a screening model application intended to bound the potential dose associated with the release of C-14 (as CO_2), H-3 (as water vapor), and I-129 at the EMDF cover surface.

3.2.2.3 Quantitative Cover Release Screening Model

Based on the limited inventory of potentially volatile radionuclides, the humid climate in East Tennessee, and EMDF design features that will mitigate vapor-phase diffusion, the potential dose contribution associated with release through the cover is unlikely to exceed the 10 mrem/year performance objective for the air pathway (DOE 2011a). To support the decision to eliminate cover release mechanisms from further consideration in the PA, the RESRAD-OFFSITE code was used to develop screening scenarios to bound the potential dose resulting from radionuclide release at the cover surface.

Release of volatile phases of H-3, C-14, and radon are simulated in the RESRAD-OFFSITE code with nuclide-specific submodels (Yu et al. 2001, Appendices C and L). The RESRAD-OFFSITE code also incorporates a surface mixing model that represents processes (e.g., plowing) acting to transport radionuclides from the waste zone into the overlying cover material (Yu et al. 2007). The cover is represented as a homogeneous layer above the waste that has time-varying thickness (due to erosion) and radionuclide concentrations (due to surface mixing processes). For these submodels of vapor release and upward mixing from the waste into the cover, the thickness of the cover relative to other fixed or user-specified quantities (e.g., soil mixing depth) controls the predicted radionuclide concentration in soil and air at the cover surface.

For the cover release screening model implementation, the cover thickness was assumed to be 6 ft or less, representing an extreme degraded condition in which the upper 5 ft of material (or more) has been eroded. In addition to the severely eroded cover assumption, additional pessimistic assumptions are incorporated into the screening analysis, including higher than estimated average radionuclide concentrations in the waste (waste stream maxima without adjustment for operational period loss or addition of clean fill), and assignment of zero leach rates for all radionuclides, eliminating loss to the environment below the EMDF. The exposure scenario is a human receptor that spends 50 percent of the time (e.g., 12 out of every 24 hours) on the EMDF cover. No other release mechanisms or exposure paths are included, so the modeled dose represents only inhalation of radionuclides released to the cover surface. Appendix G, Sect. G.4.4.2, provides additional detail on implementation of the RESRAD-OFFSITE code for screening of release through the EMDF cover.

Tritium and Carbon-14

For the H-3 and C-14 RESRAD-OFFSITE conceptual models, the radionuclides are released from the cover surface as water vapor and CO_2, respectively. The release of tritiated water vapor is driven by the estimated rate of evapotranspiration and occurs only when the cover thickness is less than 30 cm, whereas the evasion of CO_2 from the cover takes place over a user-specified C-14 evasion thickness. For the cover release screening model, the C-14 evasion thickness is set at 2.0 m, with the result that CO_2 loss to the surface occurs from the upper 0.18 m of the waste (cover thickness minus evasion thickness = 2.0 m – 1.82 m = 0.18 m). Loss of C-14 from the evasion thickness is based on a proportional evasion rate (22 year^{-1}); that is the highest value among the field-based measurements cited in the RESRAD-OFFSITE documentation (Yu et al. 2001, Table L.2). To provide a bounding estimate of the potential H-3 dose due to water vapor release from the cover, an extreme sensitivity case was evaluated in which the RESRAD-OFFSITE cover thickness value was reduced to approximately 0.27 m, which represents evaporative loss of tritiated water from the upper 0.03 m of the waste.

The results of the cover release screening model (Table 3.2) indicate that loss of C-14 as CO_2 from the upper 0.18 m of the waste would occur rapidly, based on the underlying assumptions of the conceptual model. The predicted C-14 dose decreases rapidly from an initial value of 0.044 mrem/year to zero dose by 25 years after closure. The rapid release of C-14 from the upper part of the waste is not representative of what is expected, even in the case of a severely eroded cover system, but the associated maximum C-14 dose

is useful as a bounding estimate for screening vapor phase release through the cover. Sensitivity analysis assuming a C-14 evasion thickness of 2.18 m, representing CO_2 loss from the uppermost 0.36 m of the waste, results in approximately twice the dose at time zero, but the value is still less than 0.1 mrem/year.

The magnitude of cover erosion represented by the sensitivity case evaluated for H-3 dose is totally unrealistic, but the result provides an appropriate bounding estimate for release pathway screening. The maximum H-3 dose is 0.023 mrem/year and occurs at time zero. During the institutional control period (100 years post-closure) the potential dose to a member of the public due to release of H-3 through the EMDF cover will never approach this bounding value. The short half-life of H-3 ensures that by the end of the 100 year institutional control period, the dose to a member of the public will be insignificant.

Iodine -129

Volatilization of iodine from soil depends on several factors including pH, total iodine concentration, and the presence of organic matter and iron oxides in the soil. Even if conditions in the EMDF waste favored production of iodine gas and diffusive transport toward the surface, the soil at the cover surface will likely be high in organic matter and at circumneutral pH, which would not favor vapor-phase release of iodine for inhalation or external exposure. Similarly, vegetation on the cover surface will limit wind-driven suspension of I-129 in particulate form.

To account for the potential vapor phase loss of I-129 that is not captured by the RESRAD-OFFSITE code, the surface mixing model was employed by setting the soil mixing depth to the maximum allowable value (1 m) and evaluating a scenario where the cover thickness is reduced to 0.97 m. In this case the soil mixing model represents uniform mixing of the upper 0.03 m of waste with the overlying cover material, which results in a cover radionuclide concentration equal to approximately 5 percent of the underlying waste concentration. This level of cover surface contamination, as an average over the whole EMDF cover surface, represents an extreme condition of cover degradation that would allow upward diffusive or biologically driven transport of all radionuclides to the surface. Exposure to surface contamination in the screening model reflects inhalation of airborne particulates suspended from the cover surface. The RESRAD-OFFSITE default value for the concentration of contaminated airborne particulates (based on a mass loading model representative of agricultural settings) is considered to be conservative (i.e., higher than expected) (Yu et al. 2001, Appendix B page B-6), so the default value (1E-04 g/m^3) is used in the screening model.

The scenario in which the cover thickness is reduced to 0.97 m (0.03 m less than the soil mixing depth) results in a constant I-129 dose of 4.8E-06 mrem/year. The invariance of the I-129 dose reflects the nature of the RESRAD-OFFSITE soil mixing model which predicts a nearly constant surface soil concentration due to the very long half-life of I-129 and the specification of zero leach rates.

The maximum annual doses for H-3, C-14, and I-129 estimated with the cover release screening model are given in Table 3.2. These doses are considered bounding as potential cover release pathway contributions to a total inhalation dose or total all-pathways dose for the resident farmer scenario, or for the total atmospheric (air) pathway dose for a receptor at 100 m from the edge of waste. The set of unrealistically pessimistic assumptions underlying the cover release screening model, including severe cover erosion, higher than estimated (base case) radionuclide inventories, and an extreme exposure scenario ensure that the predicted dose contributions, are bounding and represent unrealistically high exposures.

3.2.2.4   Aqueous-phase release and vadose transport

The conceptual model of radionuclide release and transport within the vadose zone is based on EMDF design geometry and a simplified representation of the waste as uniform and soil-like in terms of its

hydraulic and chemical retardation properties. Infiltration through the cover is assumed to occur uniformly over the area above the waste and liner system and to follow the generalized model of EMDF performance evolution over time (Fig. 3.5). Flow and radionuclide transport are assumed to be vertically downward through the waste zone, with horizontal flow components arising along the sloping surfaces of the basal liner system. The sloping geometry of EMDF liner system, heterogeneity in activity concentrations, and the possibility of spatially variable failure (leakage) of the cover and liner systems over time could cause non-uniform radionuclide release from the waste to the underlying vadose zone. The saturated zone radionuclide transport model (Sect. 3.3.3.2) is used to evaluate the difference between a uniform release conceptual model and a simplified non-uniform release conceptualization. The total system model analysis (Sect. 3.3.4) assumes homogeneous waste properties and uniform release to the vadose and saturated zones.

Radionuclide release and transport are conceptualized in terms of linear, equilibrium solid-aqueous phase partitioning via surface complexation and other sorption processes within the waste, liner, and underlying vadose zone. Equilibrium (de)sorption is assumed to govern release from the solid phase. Potential solubility limits are not incorporated into the source release representation. Flow and transport through the waste, clay barriers, and geologic buffer materials is primarily downward though vadose material zones (Fig. 3.4) that differ in moisture retention and permeability characteristics. Assumed hydraulic and physical parameters for the waste and liner system materials are presented in Sect. 3.3.2. The conceptual model of waste characteristics and the approach to calculating EMDF average activity concentrations, which accounts for the addition of clean fill and operational period losses, are described in Sect. 3.2.2.5. The basis for assumed K_d values for various hydrologic and material zones are described in Sects. 3.2.2.6, 3.2.2.7, and 3.2.2.8. Section 3.2.2.9 provides a summary of radionuclide release and vadose zone conceptual model assumptions.

3.2.2.5 Waste characteristics and modeled radionuclide concentrations

EMDF waste forms will include contaminated soil, sediment and other soil-like waste, and contaminated demolition debris, including equipment. The majority of debris generated from facility demolition activities will be concrete and masonry (walls, floors, ceilings, and building structure), steel (building structural members, piping, ductwork, and some equipment), and contaminated process equipment (gloveboxes, machining equipment, pumps, and other). Ventilation ducting, process equipment and piping, and hot-cell debris (internal surfaces, manipulators, and equipment) are expected to compose a smaller volume of more highly contaminated debris that may require decontamination or stabilization prior to waste acceptance and disposal at EMDF. Radionuclide contamination will include fixed surface contamination as well as contamination distributed within the matrix of more porous materials such as concrete and masonry. Activated metals from demolition of some facilities may be present, but the proportion of radionuclides in activated metal form is likely to be small. Waste that does not meet EMDF WAC (e.g., maximum allowable activity concentrations) will be disposed at one or more offsite disposal facilities.

The majority of EMDF waste is expected to be disposed in bulk (uncontainerized) form and transported by dump trucks to the landfill. Other volumes of waste, including mercury-contaminated debris or soil that requires treatment to meet CERCLA ARARs, may be grouted in containers or otherwise treated or stabilized prior to disposal, but no explicit assumptions regarding physical or chemical waste forms for specific waste streams are incorporated in this analysis. Additional information on particular ONRL and Y-12 waste stream characteristics are provided in Appendix B.

Due to uncertainty in the sequencing of future cleanup efforts and placement of waste streams within EMDF, the preliminary state of waste characterization (i.e., uncertainty in the physical and chemical characteristics of future EMDF LLW), and practical limitations in representing waste heterogeneity in some model codes, simplifying assumptions are adopted for representing the waste. The EMDF waste mass is conceptualized as a homogeneous, soil-like material in which the radionuclide inventory (Sect. 2.3 and

Appendix B) is uniformly distributed. Waste placement practices consistent with current EMWMF operations are assumed for future EMDF waste, including compaction of waste using heavy equipment and the use of clean fill material (generally clay-rich soil) to fill voids in bulk debris waste. Although soil and soil-like wastes comprise only approximately 30 percent of the estimated EMDF waste inventory, the volume of uncompacted clean soil added during placement of bulk debris is larger than the debris volume (DOE 2004). The requirement for additional clean fill material is the basis for adjusting estimated EMDF average waste activity concentrations (Table 2.15) to derive the source concentrations (average as-disposed EMDF waste concentrations, Table 3.3) used in the PA models. Figure 2.42 provides a schematic overview of the process.

Activity concentration adjustment to account for clean fill

The adjustment to estimated waste activity concentrations to account for the mass of clean fill is derived by taking the estimated total EMDF waste mass (refer to Fig. 2.42) and dividing that quantity by the combined mass of waste and clean fill:

Source concentration/estimated waste concentration = waste mass / (waste mass + clean fill mass)

= 1 − [clean fill mass / (waste mass + clean fill mass)]

The mass of clean fill required for disposal is based on the clean soil requirements algorithm described in DOE 2004. For purposes of estimating the average source concentrations for EMDF PA modeling, it is assumed that all the contaminated waste soil is used as fill, so the amount of clean fill required is minimized. The required clean fill volume is calculated as:

Total fill required = 2.26 × debris volume (as-disposed)

Clean fill required = total fill required − waste soil volume (as-disposed)

Based on the total volumes of debris and soil waste types (Appendix B, Table B.1), the total as-disposed volume of clean fill required is 832,488 cy. The mass of added clean fill is calculated based on the EMWMF average as-disposed soil bulk density (DOE 2004), which is a factor of 1.3 higher than the average asgenerated bulk density assumed for soil (1113 kg/cy, refer to Sect. 2.3.1). The total clean fill mass is estimated as:

832,488 cy × 1113 kg/cy × 1.3 = 1.21E+09 kg

The total waste mass is calculated based on the assumed average as-generated bulk densities for debris and soil as described in Sect. 2.3.1. Based on the estimated total waste mass of 1.37E+09 kg (Fig. 2.42 and Appendix B, Sect. B.4), the adjusted waste activity concentrations (source concentrations) are calculated as:

Source concentration (pCi/g) = waste concentration (pCi/g) × 1.37E+09 kg /
(1.37E+09 kg + 1.21E+09 kg)

= waste concentration (pCi/g) × 0.531

= waste concentration (pCi/g) / 1.88

This derivation of the source concentrations is based on EMDF total waste volume estimates that do not include the added 25 percent volume estimate uncertainty that was assumed for calculating the total disposal

capacity requirement (design capacity) for the EMDF (refer to Sect. 2.3). The +25 percent waste volume uncertainty factor is incorporated into the PA analysis by applying the calculated source concentrations (accounting for clean fill mass) to the total mass of waste and clean fill that corresponds to the EMDF design disposal capacity of 2.2 million cy. The total mass of material emplaced in the EMDF is based on an estimated average as-disposed bulk density (approximately 1480 kg/cy) that incorporates the clean fill and compaction factors (ratios of as-disposed to as-generated volumes for debris and soil). The same clean fill assumptions were used to derive both the capacity requirement and the adjusted activity concentrations.

Activity concentration adjustment to account for operational period losses

In addition to the activity concentration adjustment for clean fill, the estimated post-closure inventories of radionuclides that are highly mobile in the aqueous phase, including H-3, C-14, Tc-99, and I-129, are adjusted (reduced) based on modeling of operational period leaching. Taking credit for operational period losses is conceptually consistent with the equilibrium desorption model for radionuclide release adopted for the PA models (Sect. 3.2.2.4). The modeling approach to estimating operational period inventory reduction for mobile radionuclides is presented in Sect. G.4.3.4 of Appendix G. Removal of mobile radionuclides by the leachate collection system is assumed to effectively reduce the total inventories (and average concentrations) of H-3, C-14, Tc-99, and I-129. This is justified even for leachate treatment residuals that could be returned to the EMDF for disposal because such wastes (e.g., isotope exchange resins) would, by design, retain the target radionuclides resulting in much lower release rates than assumed for a generic waste form. The adjusted average activity concentrations for H-3, C-14, Tc-99, and I-129 are referred to as post-operational concentrations.

The activity losses due to leaching during the 25-year operational period were quantified using four RESRAD-OFFSITE models, one for each disposal cell. The four cells are assumed to be filled sequentially, with the filling duration (simulation period as a fraction of 25 years) for each cell proportional to the corresponding fraction of the total EMDF volume capacity. For each cell, leaching losses were estimated from the onset of filling until the following cell is filled to capacity, at which time enhanced operational cover is applied and leaching ceases. Estimates of the volume of leachate collected by the liner system and of contact water that moves through waste but exits as surface runoff were based on EMDF preliminary design analyses (for leachate) and EMWMF operational records (for contact water).

Activity losses estimated for each disposal cell were added to obtain the total loss during the operational period. The proportional inventory losses for the four radionuclides simulated were used to adjust the (as-disposed) source concentrations to obtain the post-operational concentrations. Estimated waste inventory values, as-generated waste average concentrations, as-disposed waste average concentrations, and post-operational waste average concentrations for the 42 radionuclides simulated in the base case model are provided in Table 3.3. For all radionuclides other than H-3, C-14, Tc-99, and I-129 the post-operational average activity concentrations are the same as the as-disposed concentrations.

Table 3.3. Waste activity concentrations used for the EMDF PA models

Isotope	Half-life (year)	Estimated waste inventory (Ci)	EMDF as-generated waste average concentration (pCi/g)	EMDF as-disposed waste average concentration (pCi/g)	EMDF post-operational waste average concentration (pCi/g)
Ac-227	2.18E+01	7.54E-03	5.50E-03	2.92E-03	2.92E-03
Am-241	4.32E+02	1.52E+02	1.11E+02	5.90E+01	5.90E+01
Am-243	7.38E+03	7.65E+00	5.59E+00	2.97E+00	2.97E+00
Be-10	1.50E+06	6.52E-05[a]	4.76E-05[a]	2.53E-05	2.53E-05

138

Table 3.3. Waste activity concentrations used for the EMDF PA models (cont.)

Isotope	Half-life (year)	Estimated waste inventory (Ci)	EMDF as-generated waste average concentration (pCi/g)	EMDF as-disposed waste average concentration (pCi/g)	EMDF post-operational waste average concentration (pCi/g)
C-14	5.73E+03	7.43E+00	5.43E+00	2.88E+00	5.40E-01[b]
Ca-41	1.00E+05	1.09E-01[a]	7.92E-02[a]	4.21E-02	4.21E-02
Cm-243	2.85E+01	1.11E+00	8.10E-01	4.30E-01	4.30E-01
Cm-244	1.81E+01	3.26E+02	2.38E+02	1.26E+02	1.26E+02
Cm-245	8.50E+03	9.87E-02	7.21E-02	3.83E-02	3.83E-02
Cm-246	4.73E+03	4.10E-01	2.99E-01	1.59E-01	1.59E-01
Cm-247	1.56E+07	2.68E-02	1.96E-02	1.04E-02	1.04E-02
Cm-248	3.39E+05	1.44E-03	1.05E-03	5.59E-04	5.59E-04
H-3	1.24E+01	2.88E+01	2.10E+01	1.12E+01	4.64E+00[b]
I-129	1.57E+07	1.05E+00	7.66E-01	4.07E-01	3.50E-01[b]
K-40	1.28E+09	8.46E+00	6.18E+00	3.28E+00	3.28E+00
Mo-93	3.50E+03	1.00E+00[a]	7.30E-01[a]	3.88E-01	3.88E-01
Nb-93m	1.36E+01	6.01E-01[a]	4.39E-01[a]	2.33E-01	2.33E-01
Nb-94	2.03E+04	4.20E-02	3.07E-02	1.63E-02	1.63E-02
Ni-59	7.50E+04	7.84E+00	5.73E+00	3.04E+00	3.04E+00
Np-237	2.14E+06	8.37E-01	6.12E-01	3.25E-01	3.25E-01
Pa-231	3.28E+04	6.15E-01	4.49E-01	2.39E-01	2.39E-01
Pb-210	2.23E+01	9.50E+00	6.93E+00	3.68E+00	3.68E+00
Pu-238	8.77E+01	2.42E+02	1.77E+02	9.38E+01	9.38E+01
Pu-239	2.41E+04	1.50E+02	1.10E+02	5.83E+01	5.83E+01
Pu-240	6.54E+03	1.60E+02	1.17E+02	6.20E+01	6.20E+01
Pu-241	1.44E+01	5.25E+02	3.83E+02	2.04E+02	2.04E+02
Pu-242	3.76E+05	4.45E-01	3.25E-01	1.73E-01	1.73E-01
Pu-244	8.26E+07	9.49E-03	6.93E-03	3.68E-03	3.68E-03
Ra-226	1.60E+03	2.07E+00	1.51E+00	8.01E-01	8.01E-01
Ra-228	5.75E+00	5.69E-02	4.15E-02	2.21E-02	2.21E-02
Sr-90	2.91E+01	4.96E+02	3.62E+02	1.92E+02	1.92E+02
Tc-99	2.13E+05	7.23E+00	5.28E+00	2.80E+00	1.56E+00[b]
Th-228	1.90E+00	5.45E-06	3.98E-06	2.11E-06	2.11E-06
Th-229	7.34E+03	1.47E+01	1.08E+01	5.71E+00	5.71E+00
Th-230	7.70E+04	4.94E+00	3.61E+00	1.92E+00	1.92E+00
Th-232	1.41E+10	9.07E+00	6.62E+00	3.52E+00	3.52E+00
U-232	7.20E+01	2.63E+01	1.92E+01	1.02E+01	1.02E+01
U-233	1.59E+05	1.07E+02	7.83E+01	4.16E+01	4.16E+01
U-234	2.45E+05	1.62E+03	1.19E+03	6.30E+02	6.30E+02
U-235	7.04E+08	1.02E+02	7.47E+01	3.97E+01	3.97E+01
U-236	2.34E+07	2.32E+01	1.69E+01	8.98E+00	8.98E+00
U-238	4.47E+09	9.83E+02	7.18E+02	3.81E+02	3.81E+02

[a]Data limited radionuclide with non-standard basis of estimate, refer to Appendix B.
[b]Post-operational waste concentration adjusted for operational period activity loss.

EMDF = Environmental Management Disposal Facility
PA = Performance Assessment

3.2.2.6　　　　Assumed partition coefficient (K_d) values

Solid-aqueous partition coefficients are key parameters that represent sorption and chemical retardation phenomena in the conceptual models of radionuclide release and transport. For modeling source release and chemical retardation of radionuclide transport, equilibrium, linear isotherm sorption is assumed and a single parameter, K_d, defines the partition between radionuclide concentrations in the aqueous phase and the concentration of the sorbed phase within the porous matrix. The validity of the equilibrium sorption assumption depends on a variety of material, geochemical and hydrodynamic factors that can vary in space and time in the subsurface (Valocchi 1985). Although laboratory determinations of K_d values for some radionuclides using samples of clay-rich soils, saprolite, and rock cores collected in the Maryville Formation and the Nolichucky Formation are available in several reports (refer to Sect. 2.1.6.3 and Table 2.12), the assignment of representative K_d values to represent sorption processes integrated over long time periods is an important uncertainty in the EMDF performance analysis. The following paragraphs outline the general approach to selecting K_d values and ranges of values for the EMDF disposal system analysis, including the waste, saprolite, and bedrock zone materials.

For the EMDF PA, a graded approach to selection of K_d values was adopted in which use of the available laboratory data for Conasauga Group materials was combined with information from previous modeling in related, comparable assessments along with other published reports and compilations of K_d data for materials similar to those of the EMDF system. Different radionuclides of a given element are assumed to have the same K_d value because sorption is a chemical phenomenon that is primarily dependent on oxidation state rather than isotopic mass. For elements that had been evaluated in sorption studies using local materials, those data sources were verified by experts and given precedence, followed by comparable ORR performance modeling K_d value assumptions. Specific experimental conditions (e.g., ionic strength, pH) in each local study were also considered in the selection of K_d value for these elements, and data from other sources were used as supporting information. On this basis, base case K_d values for the clay rich saprolitic and bedrock materials were assigned. Section 3.2.2.8 provides additional detail on the rationale for assigning K_d values to different engineered and natural materials. The waste materials will include debris, equipment, soil waste, and clean fill (Sect. 3.2.2.5). The clean fill accounts for almost half of the estimated mass in the disposal facility. Clean fill will be sourced from saprolite zone material in local borrow areas, and soil remediation waste will have similar characteristics. Given that approximately one-half of the waste mass is thus similar to saprolite zone material, the K_d values in the waste zone are assumed for the base case to be one-half the K_d values assumed for the saprolite and bedrock zone materials.

Table 3.4 summarizes the assumed base case K_d values and provides the primary and supporting references used as the basis for each value, including the material type associated with the K_d value in the primary reference. In general, for elements without data derived from local laboratory studies, values were adopted from existing performance analyses of SWSA 6 (ORNL 1997a) and the EMWMF (DOE 1998a, BJC 2010a), with a material type listed as generic soil in Table 3.4. Generic references (e.g., Sheppard and Thibault 1990) were used as primary references for those elements that were not included in the previous ORR performance analyses.

140

Table 3.4. Solid-aqueous K_d values assumed for the EMDF PA analyses

| Element | K_d, EMDF base case model (cm³/g) | | K_d, EMDF screening model (cm³/g) | Primary reference | Material/soil texture in primary reference associated with base case value | Supporting references |
	Waste zone	Saprolite and Bedrock zones				
Ac	20	40	2	ORNL 1997a (Table 2.3, p.2-18)	Generic soil	
Am	2000	4100[a]	20[b]	Rothschild et al. 1984b (Table 6, p. 38), Davis et al. 1984 (Table 7, p.40)	Silty clay (Maryville Formation)	Sheppard and Thibault 1990
Ba	28	55	3	DOE 1998a (Appendix E, p. E 71-73)	Generic soil	Baes et al. 1984
Be	400	800	40	DOE 1998a (Appendix E, p. E 71-73)	Generic soil	Sheppard and Thibault 1990
C	0	0	0	ORNL 1997a (Table 2.3, p.2-18)	Generic soil	
Ca	15	30	2	ORNL 1997a (Table 2.3, p.2-18)	Generic soil	Sheppard and Thibault 1990
Cd	100	200	10	ORNL 1997a (Table 2.3, p.2-18)	Generic soil	
Cf	20	40	2	ORNL 1997a (Table 2.3, p.2-18)	Generic soil	
Cl	N/A[c]	N/A[c]	0	ORNL 1997a (Table 2.3, p.2-18)	Generic soil	
Cm	20	40	2	ORNL 1997a (Table 2.3, p.2-18)	Generic soil	
Co	400	800	40	ORNL 1997a (Table 2.3, p.2-18)	Generic soil	Rothschild et al. 1984
Cs	1500	3000	150	Friedman et al. 1990 (Table 3.1, p.7)	Silty clay (Maryville Formation)	Davis et al. 1984
Eu	20	40	2	ORNL 1997a (Table 2.3, p.2-18)	Generic soil	Friedman et al. 1990
Fe	450	890	45	Yu et al. 2015 (Table 2.13.2, p. 67)	Loam	Davis et al. 1984
Gd	410	820	40	Yu et al. 2007 (Appendix B, Attachment A Table 2-4, p. AttA-60)	N/A	
H	0	0	0	ORNL 1997a (Table 2.3, p.2-18)	Generic soil	DOE 1998a, IAEA 2010
I	2	4	0.2	Davis et al. 1984 (Figure 14)	Silty clay (Maryville Formation)	Rothschild et al. 1984
K	15	30	2	ORNL 1997a (Table 2.3, p.2-18)	Generic soil	DOE 1998a
Mo	45	90	5	Sheppard and Thibault 1990	Clay	
Na	5	10	1	Yu et al. 2007 (Appendix B, Attachment A Table 2-4, p. AttA-60)	N/A	IAEA 2010
Nb	50	100	5	ORNL 1997a (Table 2.3, p.2-18)	Generic soil	DOE 1998a
Ni	1000	2000	100	ORNL 1997a (Table 2.3, p.2-18)	Generic soil	DOE 1998a

Table 3.4. Solid-aqueous K$_d$ values assumed for the EMDF PA analyses (cont.)

Element	K$_d$, EMDF base case model (cm^3/g)		K$_d$, EMDF screening model (cm^3/g)	Primary reference	Material/soil texture in primary reference associated with base case value	Supporting references
	Waste zone	Saprolite and Bedrock zones				
Np	20	40	2	ORNL 1997a (Table 2.3, p.2-18)	Generic soil	ORNL 1987
Pa	200	400	20	ORNL 1997a (Table 2.3, p.2-18)	Generic soil	DOE 1998a
Pb	50	100	5	ORNL 1997a (Table 2.3, p.2-18)	Generic soil	
Pd	1000	2000	100	ORNL 1997a (Table 2.3, p.2-18)	Generic soil	
Pm	410	820	40	Yu et al. 2007 (Appendix B, Attachment A Table 2-4, p. AttA-60)	NA	IAEA 2010
Pu	20	40	2	ORNL 1997a (Table 2.3, p.2-18)	Generic soil	Gil-Garcia et al. 2008
Ra	1500	3000	150	ORNL 1997a (Table 2.3, p.2-18)	Generic soil	DOE 1998a
Re	20	40	2	Sheppard and Thibault 1990	Loam	
Sb	75	150	8	Sheppard and Thibault 1990	Loam	
Se	250	500	25	Sheppard and Thibault 1990	Loam	
Sm	500	1000	50	ORNL 1997a (Table 2.3, p.2-18)	Generic soil	
Sn	50	100	5	ORNL 1997a (Table 2.3, p.2-18)	Generic soil	Sheppard and Thibault 1990
Sr	15	30	2	Friedman et al. 1990 (Table 4.1, p.21)	Generic soil	ORNL 1997a, DOE 1998a
Tc	0.36	0.72	0.04	DOE 1992b (Appendix A, Table A.4.1.8, p. 86)	Silty clay	ORNL 1987
Th	1500	3000	150	ORNL 1997a (Table 2.3, p.2-18)	Generic soil	Sheppard and Thibault 1990
U	25	50	3	Friedman et al. 1990 (Table 3.8, p.12)	Clay	ORNL 1987, ORNL 1997a, CH2M-Hill 2000
Zr	25	50	3	ORNL 1997a (Table 2.3, p.2-18)	Generic soil	Sheppard and Thibault 1990

Table 3.4. Solid-aqueous K$_d$ values assumed for the EMDF PA analyses (cont.)

---

[a] Weighted average of 14 samples from Rothschild et al. 1984 (Table 6, samples #4 and 16-18 omitted as non-representative), and 24 samples from Davis et al. 1984 (Table 7)
[b] Screening model K$_d$ value decrease by a factor of 100 from base case value based on range of data in primary and supporting references.
[c] Chlorine (Cl-36) is not included in the EMDF estimated radionuclide inventory. Cl-36 is included in the EMDF radionuclide screening model

DOE = U.S. Department of Energy
EMDF = Environmental Management Disposal Facility
EPA = U.S. Environmental Protection Agency
IAEA = International Atomic Energy Agency
N/A = not applicable

ORNL = Oak Ridge National Laboratory
PA = Performance Assessment
RESRAD = RESidual RADioactivity
SWSA = Solid Waste Storage Area

For uranium and transuranic elements, site-specific laboratory K_d measurements are used for uranium and americium, but the values for plutonium, neptunium, curium, and californium are taken from the SWSA 6 PA, which applied a value of 40 cm^3/g to uranium and all transuranics in the saturated zone (ORNL 1997a). Although the K_d of uranium species can vary over a very wide range depending on the geochemistry of the system, the uranium base case value of 50 cm^3/g is likely to be lower and of the expected range for Conasauga Group materials. Uranium sorption experiments on local clay rich soils were performed during the design phase for the EMWMF (WMFS 2000) and the results indicated that the sorptive capacity of those materials was very high, implying K_d > 1000 cm^3/g. Similarly, the uranium K_d sources and data compiled by EPA (EPA 1999, page 5.75) suggests that for pH in the 6 to 7 range, minimum uranium K_d values are > 50 cm^3/g. This evidence supports the adoption of uranium K_d = 50 cm^3/g as a pessimistic assumption for the PA modeling.

Data from supporting references were used to assess possible ranges of values for similar material types and to support selection of K_d values used for the radionuclide screening model (refer to Sect. 2.3.2 and Appendix G for description of the model used for radionuclide screening). Following an initial selection of K_d values generally chosen to be representative for medium to fine textured soils, the waste zone values were decreased by a factor of 10 or 100 to provide a pessimistic (lower than likely) assumed value for use in the screening model (Table 3.4). The K_d values were reduced by a factor of 100 in cases where a factor of 10 reduction was judged insufficiently pessimistic for use in the screening model, on the basis of the ranges of values reported in the primary and/or supporting references. Application of the screening process reduced the number of radionuclides carried forward in the all-pathways scenario from 70 to 42, representing 21 different elements. Preliminary dose modeling results (refer to Sects. 3.3.4 and 3.4) identified key radionuclides for EMDF performance (including C-14, Tc-99, and I-129) for which uncertainty in the assumed K_d value could significantly impact the magnitude or timing of the peak all-pathways dose, and additional scrutiny of the available data for these highly mobile radionuclides provided a basis for the assumed K_d values for the base case all-pathways dose analysis. Details are provided in Sect. 3.2.2.7.

3.2.2.7   Partition coefficients for I-129 and Tc-99

As two of the key radionuclides in terms of dose, I-129 and Tc-99 K_d values as determined in previous ORR studies were reviewed in detail. These studies and conclusions supporting the K_d values adopted for the PA are summarized below.

Iodine-129 partition coefficient (K_d)

Partitioning of iodine in a soil/water matrix is dependent on the iodine speciation as well as the soil and water properties. Organic content of the soil is a key soil parameter influencing iodine sorption (EPA 2004, Serne 2007, Kaplan et al. 2000). Iodine can form very strong (covalent) bonds with soil organic matter (OM) and slight increases in OM, even at trace concentrations (0.1 to 0.4 wt percent), can result in corresponding increases in iodine K_d values (Xu et al. 2015, Kaplan et al. 2014). Soil and saprolite OM concentrations are generally quite high for ORR soils. Rothschild et al. (1984) reported an average of 3.31 wt percent OM in 15 soils collected from SWSA 7 in Melton Valley, where Conasauga soils are dominant. Davis et al. (1984) reported value values of 0.37 wt percent organic matter from 3 cores and 24 samples, also from Conasauga soils in Melton Valley.

Iodine sorption by geological materials is influenced by pH and iron- and manganese-oxide content. As a general rule, lower pH and greater iron- and manganese-oxide contents result in greater iodine sorption (EPA 2004). At low pH values, mineral surfaces become protonated and have a net positive charge, whereas at higher pH values, the surfaces become deprotonated and have a net negative charge. The surface charge of iron- and manganese-oxides is comprised almost entirely of this pH-dependent charge, which promotes

greater anion exchange capacity at lower pH levels. The iron- and manganese-oxide contents in Conasauga soils, saprolite, and shale bedrock are considered high; for example, Rothschild et al. (1984) reported soil manganese concentrations of 412 ± 322 mg/kg and soil iron concentrations of 139 ± 69 mg/kg. Following the conceptual geochemical model put forth by Watson et al. (2004) for the Oak Ridge Field Research Center located in Bear Creek, the pH in the soil/saprolite above the water table is likely to be acidic, pH 4.5 to 6, while the pH in the saturated zone will be near neutral, 7 to 8. If similar pH conditions occur in the unsaturated materials below the EMDF clay liner, the vadose interval may be especially well suited for binding iodine.

Mineralogy can also play an important role in binding iodine (Kaplan et al. 2014, Kaplan et al. 2000). In an evaluation of various minerals, illite, a common mineral at the ORR and within the Conasauga soil profiles, had the greatest iodine K_d value, 15.14 cm^3/g (Kaplan et al. 2000), of the wide suite of investigated minerals. Mineralogical characterization of soils (Davis et al. 1984, page 58, Table 17) and bedrock (Davis et al. 1984, page 22, Table 3) of the Maryville Formation indicates illite to be the predominant clay mineral. Rothschild et al. (1984b, pages 53-60) also found illite to be abundant in the clay size fraction of Conasauga group soils at ORNL. Similarly, mineralogical analysis of the Nolichucky formation (ORNL 1987, page 4, Table 3.1) identified illite to be the most abundant of all minerals including quartz and feldspars. Significant iodine sorption to illite over a very wide range of pH values has been demonstrated (Kaplan et al. 2000, Table 5), reproduced below as Fig. 3.6), with K_d values > 20 cm^3/g at pH > 9.0. Laboratory K_d measurements on samples of cuttings from a 35 m deep borehole in the Maryville Formation also show significant iodine sorption (K_d > 7 cm^3/g) at pH > 7.0 for increments deeper than 5 m below the surface (Davis et al. 1984, Sect. 4.1.2.3, Fig. 14 and Table 4, pages 23 to 29), which is consistent with the predominance of illite identified in the Maryville Formation.

Iodide K_d Values on Illite as a Function of pH[a]

pH	electrical conductivity (mS/cm)	K_d (mL/g)
3.6	2.52 ± 0.03	46 ± 3.9
5.0	2.31 ± 0.03	59 ± 2.2
7.9	2.35 ± 0.04	24 ± 1.2
9.4	2.41 ± 0.04	22 ± 0.2

[a] Background electrolyte was 0.01 M CaCl$_2$; pH adjustment with NaOH and HCl, three replicates; pH equilibration period was 5 weeks; ^{125}I$^-$ contact time with the pH equilibrated sediments was 1 week.

Source: Kaplan et al. 2000.

Fig. 3.6. Laboratory measurement of iodide sorption on illite

Together the combination of pH (circumneutral to weakly acidic), OM, iron- and manganese-oxide, and mineralogical (presence of illites) conditions that are likely to exist at the EMDF site in BCV would be expected to promote the sorption of iodine. Conversely, conditions known to resist iodine binding are less likely to exist at the site, including sandy texture, low OM (< 0.1 wt percent), low iron- and manganese-oxide content, with high pH groundwater (pH > approximately 8).

Iodine K_d values measured for soils and saprolite of the Maryville Formation were reported by Rothschild et al. (1984) and Davis et al. (1984). The quality of these measurements is high because (1) the experimental conditions correspond reasonably well with those likely to exist at the EMDF; (2) they used ASTM methods; (3) they conducted replicates; (4) important attributes of the solid and aqueous phases were characterized, permitting variation in data to be assessed within a geochemical context (e.g., through regression on principles of radiochemistry and geochemistry); and (5) iodine K_d values were measured on

a large number of samples (15). Rothschild et al. (1984) collected soil samples from the SWSA 7 site and combined them with stream water spiked with I-125. The resulting K_d values and associated geochemical parameters are presented in Table 3.5, where the average iodine K_d value in is 17.1 ± 13.4 cm^3/g and the data had a range of 3.6 to 54.4 cm^3/g for 15 values (excluding results from the "stream sediment" samples because they differ from materials at the EMDF). The equilibrium pH values for these soil samples taken from the upper 2 to 3 m of the saprolite zone ranged from 4.6 to 6.2, whereas the three samples of stream sediment from the SWSA 7 site resulted in equilibrium pH of 7.2 to 7.3 (Table 3.5, samples 16-18). The K_d values estimated for the three stream sediment samples were relatively high (> 10 cm^3/g), especially given the neutral pH conditions.

Table 3.5. Laboratory iodine K_d values from geological samples collected from SWSA 7

Iodine K_d (cm^3/g)	Description	pH	Organic Matter (%)	Manganese (mg/kg)	Iron (mg/kg)	Comment
9.4	Sample 1	5	3.06	360	118	Soil
4.7	Sample 2	6.2	4.15	715	151	Soil
3.6	Sample 3	6	4.99	1160	250	Soil
54.4	Sample 4	4.7	0.4	170.5	118	Soil
12.3	Sample 5	4.5	2.06	169	120	Soil
19.9	Sample 6	5.4	3.48	390	119	Soil
14.8	Sample 7	4.7	3.43	655	245.5	Soil
11.2	Sample 8	4.9	3.8	645	209	Soil
20.1	Sample 9	4.9	2.01	153.5	78.5	Soil
16.3	Sample 10	4.6	3.4	277.5	88.5	Soil
17	Sample 11	5	2.84	367.5	112.5	Soil
10.9	Sample 12	4.6	4.61	148.5	96.5	Soil
37.7	Sample 13	4.9	3.25	28.5	41	Drainage side slopes
19.5	Sample 14	4.9	4.73	825	257	Drainage side slopes
4.4	Sample 15	4.6	3.48	109.5	83.5	Drainage side slopes
11.1	Sample 16	7.2	0.883	1910	237	Stream sediment
11	Sample 17	7.2	0.847	1575	192	Stream sediment
17	Sample 18	7.3	0.515	4950	317	Stream sediment
17.1	**Ave. #1-#15**	**5.0**	**3.31**	**412**	**139**	**Ave., excluding stream sediments**
13.4	**Stdev #1-#15**	**0.5**	**1.2**	**321.9**	**68.5**	**Stdev., excluding stream sediments**

Data taken from Tables 6 and 7 in Rothschild et al. 1984.

SWSA = Solid Waste Storage Area

Davis et al. (1984) also reported iodine K_d values for soil and saprolite that correspond with those at the EMDF. Again, the data is of high quality for similar reasons as used to describe the data from Rothschild et al. (1984). They collected Conasauga group soils from SWSA 6, and the results were intended to be relevant to the LLW disposal site, shallow land burial. They collected three profiles from three trenches. The results from these iodine K_d values are summarized in Table 3.6. The average iodine K_d value was 11.7 ± 9.0 cm^3/g and had a range of 1 to 21.4 cm^3/g. All but one of the pH values for these samples

were less than 5, and the highest pH was 5.8. The results from Davis et al. (1984) and Rothschild et al. (1984) are consistent in that they report similar average iodine K_d values for Conasauga Group soils recovered from the ORR. Both sources attributed the appreciable iodine attenuation to the low pH conditions and the presence of iron/manganese oxides and natural OM.

Table 3.6. Iodine K_d values of 24 soils collected from three cores recovered from SWSA 6

Iodine K_d (cm³/g)	Description (core ID/core depth-cm)	pH	Organic matter (wt%)
21.4	334/20	4.3	1.4
18.5	334/40	4	1.4
22.8	334/60	4.2	0.26
2.2	334/100	4.4	0.15
1.1	334/130	4.4	0.14
4.2	334/150	4.3	0.11
10.5	334/180	4.3	0.11
11.3	334/200	4.3	0.11
4.1	338/20	4.4	1.24
11.1	338/40	4.4	0.83
1	338/60	4.3	0.3
18.6	338/100	4.4	0.16
0.3	338/130	4.4	0.11
3.8	338/150	4.6	0.27
2.6	338/180	4.7	0.09
0.1	338/200	5.8	0.11
10.1	342/20	4.4	0.41
14.8	342/40	4.3	0.45
13.8	342/60	4.6	0.21
23	342/100	4.3	0.29
14	342/130	4.2	0.28
31.7	342/150	4.3	0.12
24	342/180	4.3	0.2
16	342/200	4.2	0.07
11.7	**Ave of 24 samples**	**4.4**	**0.37**
9.0	**Stdev of 24 samples**	**0.3**	**0.41**

Data taken from Table 7 in Davis et al. 1984.

ID = identification
SWSA = Solid Waste Storage Area

Importantly, the K_d values most likely to be representative are those based on experimental conditions and materials similar to those at the EMDF. The Davis et al. (1984) and Rothschild et al. (1984b) data are of high quality and used methods that approximate a geochemical environment (low pH, oxidizing) which is within the range observed at the EMWMF. For this reason, it is more reasonable to rely on these site-specific values than to include iodine K_d measurements using off site samples. Most of the available ORR data for iodine sorption reflect low pH (< 6.0) conditions, whereas the likely range of geochemical

147

environments within the EMDF system (waste, vadose zone, saturated zone) are likely to have higher pH (> 6).

Recent studies of iodine sorption on sediments from the Savannah River Site (SRS) provide a useful point of reference for evaluating the Oak Ridge data because the SRS has similar climate and deeply weathered soils, although the soils have developed from different parent materials at the two sites. Kaplan et al. (2013) evaluated radioiodine geochemistry and sorption on three different SRS sediment types. This study evaluated variation in iodine sorption related to oxidation state (iodide vs iodate) and pH conditions to support SRS performance assessments. The SRS results for the clay soil type (most similar to EMDF soils) under aerobic conditions indicate that K_d values for iodide and iodate decrease toward zero as pH approaches 6.5 (Fig. 3.7). The data for Oak Ridge Conasauga soil and saprolite samples are similar, with the highest measured iodine K_d values associated with pH < 5.0 (Fig. 3.8). Oak Ridge K_d values higher than 20 cm^3/g at pH< 5.0 are similar to SRS data for iodate sorption to clay soil, which may indicate that a portion of iodine in the Oak Ridge studies was present as iodate.

There is limited but significant evidence in the two Oak Ridge studies that iodine sorption can occur at pH > 6.0. (Fig. 3.8). The two SWSA 7 soil samples analyzed by Rothschild et al. (1984) having pH ≥ 6.0 have K_d values > 3 cm^3/g, and the three stream sediment samples analyzed had pH > 7.0 and iodine K_d > 10 cm^3/g. Similarly, the deeper (> 5m) Maryville Formation samples analyzed by Davis et al. (1984) had pH values that range from 7.3 to 8.0 and geometric mean K_d value of 8.4 cm^3/g (range 4.8 to 13.2 cm^3/g). It is possible that these nonzero K_d values at higher pH result in part from the abundance of illite present in the soils, saprolite and bedrock of the Maryville Formation.

Comparison of iodine sorption in IO_3^- and I^- amended clayey sediment suspensions under aerobic and variable pH conditions after 8 and 12 weeks of equilibration (1000 ppb I_{total}, 25 g/L sediment in 0.01 M NaCl) (values not corrected for natural iodine desorption from sediment slightly increasing reported K_d).

(graphic reproduced from Kapan et al. 2013)
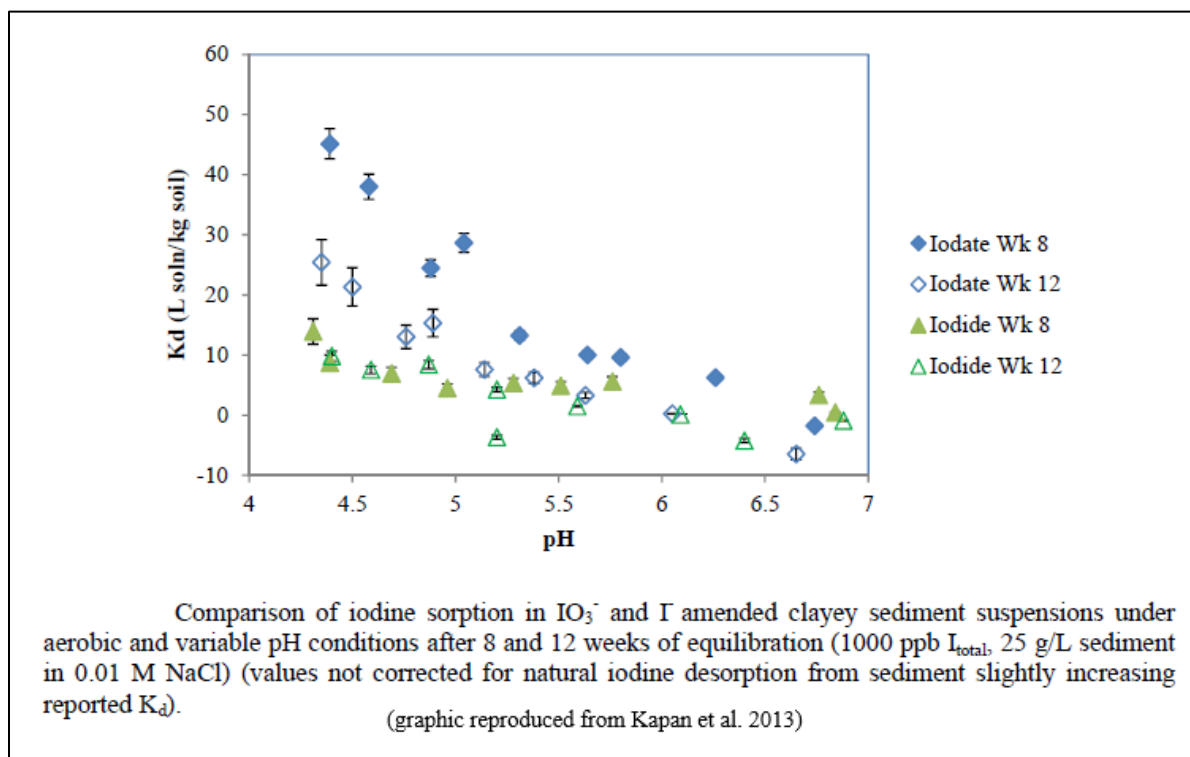
Fig. 3.7. Experimental results for iodine sorption on SRS clay sediments showing effects of pH and oxidation state
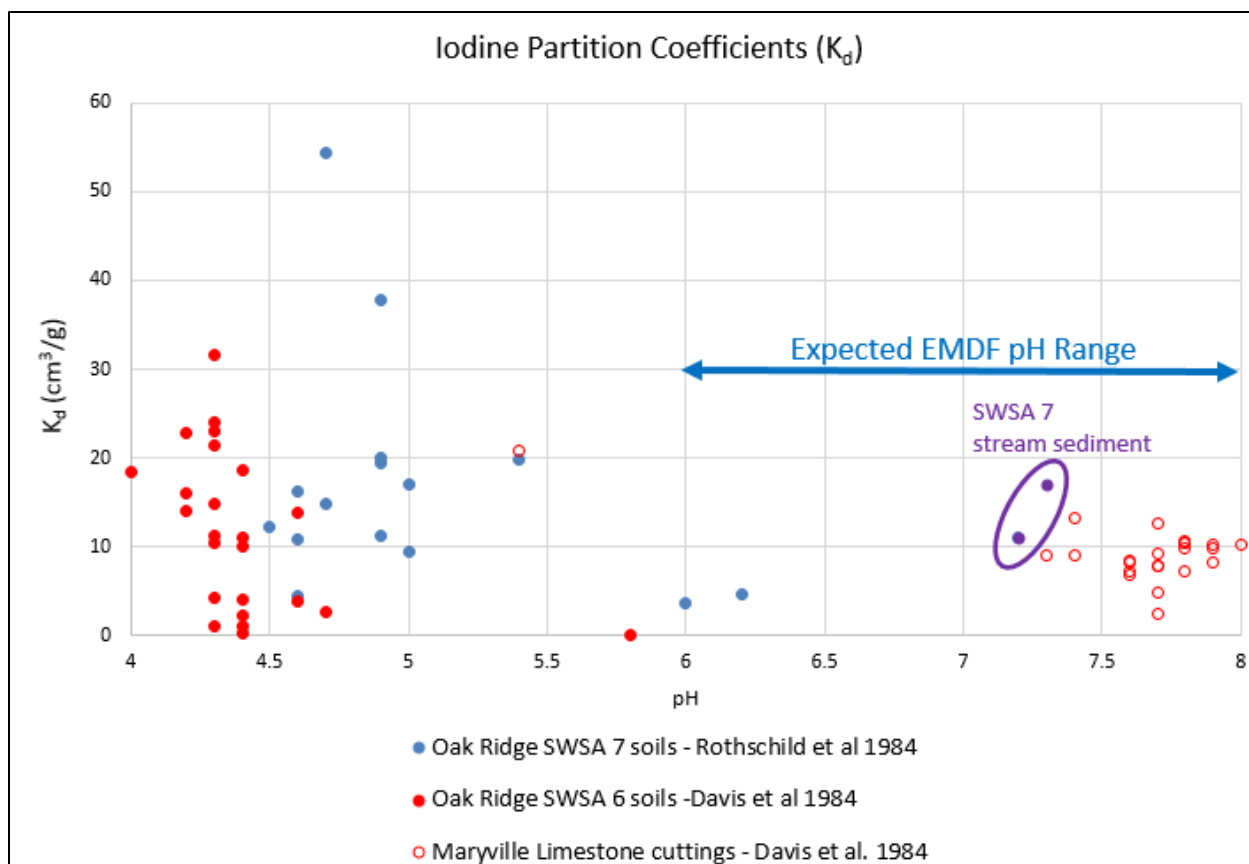
Fig. 3.8. Experimentally determined iodine partition coefficients for samples of Oak Ridge Conasauga Group soils, sediment, and bedrock

Given that the likely geochemical conditions in the EMDF disposal system are oxidizing and slightly acidic to circumneutral, adopting relatively high iodine K_d values (> 10 cm^3/g) is not justified by the available data. However, the likely abundance of the mineral illite in the soils and bedrock of the EMDF system and the possibility that the iodate oxidation state will be sustained by the expected pH and redox conditions suggest that a nonzero K_d value for iodine is reasonable and defensible. Based on the potential for iodine sorption at pH > 6.0 in material derived from the Maryville Formation (Fig. 3.8), a K_d value of 4 cm^3/g is proposed for iodine in the natural soils, saprolite, and bedrock of the EMDF system. This K_d value represents the lower end of the range of measured values for the range of pH values anticipated to exist at the EMDF site (Fig. 3.8). Additional support for the proposed K_d value for EMDF is found in a recent recommended iodine K_d value of 3.0 cm^3/g for clayey sediments at SRS (Kaplan et al. 2013), which was increased from a previous estimate of 0.9 cm^3/g. The proposed iodine K_d value for SRS PAs is relevant because it is derived over pH and oxidizing geochemical conditions that are similar to what is likely at the EMDF, and because the EMDF saprolites contain an abundance of illite (Kim et al. 2009), more so than do the clayey SRS sediments tested by Kaplan et al. (2013). The K_d value adopted for iodine in the EMDF waste zone is 2.0 cm^3/g. Adopting this lower iodine K_d value for the waste zone reflects significance of this parameter assumption for the maximum total dose that could occur during the 1000-year compliance period.

The lack of iodine K_d measurements on materials derived from the Nolichucky Formation is a source of uncertainty in the selection of a single representative K_d value for the bedrock and saprolite below the EMDF. However, field evidence of the similarity between the Maryville and Nolichucky units of the Conasauga Group in the vicinity of the ORR (ORNL 1992a, Sect. 3.3, pages 18–40) provides a reasonable

level of confidence that the iodine sorption properties of the Nolichucky Formation are similar to those of the Maryville Formation. On the ORR and at the EMDF site, the Maryville Formation is dominated (> 50 percent relative abundance) by mudstone lithologies (claystone, siltstone, and shale) rather than limestone lithologies (ORNL 1992a, Fig. 3-3). General descriptions of these two geological units in the vicinity of the EMDF site (Lee and Ketelle 1989, Sect. 4.2.5 and 4.2.6, pages 15–18) suggest that these Conasauga units comprise similarly interbedded mudstone and limestone lithologies in comparable proportions. Borehole logs obtained during recent EMDF site characterization (DOE 2018b, DOE 2019) also support this characterization of the lithology of the Maryville Formation and Nolichucky Formation at the disposal site. In addition, the two Conasauga Group units are mineralogically similar, with illite and chlorite predominant among the clay minerals (Davis et al. 1984, Table 3; ORNL 1987, Table 3.1), and have similar bulk density, grain density, and porosity characteristics (Dorsch et al. 1996, Table 3 and Fig. 23).

Previous Oak Ridge PA documents and modeling (ORNL 1997a, DOE 1998a, DOE 1998b) used lower values for the iodine K_d (0.0 and 0.199 cm^3/g, refer to Table 1.1). However, the data presented in the preceding paragraphs strongly suggests that the assumed base case value of 4 cm^3/g, is reasonable given that it is on the low end of the range of values for pH > 6 (Fig. 3.8). To increase confidence in the iodine K_d values applied in the EMDF PA, controls on the partitioning of iodine will be experimentally determined for local site materials (clayey soils and saprolite) derived from the Maryville and Nolichucky Formations. These data will evaluated through the EMDF change control process.

Technetium-99 partition coefficient (K_d)

Technetium exists in nature either as the highly mobile oxidized species, TcO$_4^-$, or the appreciably less mobile, less soluble Tc^{+4} species. Technetium at the EMDF is likely to exist primarily as dissolved TcO$_4^-$, with relatively small amounts of bound TcO$_4^-$ or Tc^{4+} species. However, the small amounts of soil-bound technetium are very important for evaluating the efficacy of the EMDF and are the focus of this discussion. The primary conditions influencing technetium geochemistry are pH, Eh (the oxidation reduction potential, or redox), and the presence or absence of iron/manganese oxides and natural OM (EPA 2004).

The primary factor controlling technetium sorption to geological media is the redox status. Under high redox conditions, the poorly sorbing species, TcO$_4^-$, exists. This oxyanion sorbs very weakly to soils, however sorption increases when groundwater pH decreases in the presences of OM and iron- and manganese-oxides. As the pH decreases, these surfaces become protonated, thereby creating more positive surface charge sites for the anionic TcO$_4^-$ species to bind. Above a critical pH value, referred to the point-of-zero-charge, the net charge becomes negative, thereby diminishing the extent of anion sorption. The point-of-zero-charge for iron oxides is about pH 7.8 and manganese oxides is pH 2.8. The point-of-zero-charge of OM varies greatly depending on its source, age, and how it is measured, but is commonly measured between pH 6 and 8 (Stumm and Morgan 1996). Especially as it applies to the EMDF, an important impact of OM on technetium mobility is not the tendency to sorb (more specifically, to complex) TcO$_4^-$, but instead the tendency for OM to convert TcO$_4^-$ into the less mobile Tc^{4+} form by chemical reduction. This was demonstrated using geological media collected from the Field Research Center on the ORR (Gu et al. 2011).

Following the conceptual geochemical model put forth by Watson et al. (2004) for the Oak Ridge Field Research Center located in BCV, the pH in the soil/saprolite above the water table can be acidic, pH 4.5 to 6.0, while the pH in the saturated zone will be near neutral, 7 to 8. Furthermore, they describe the oxidation-reduction state of the system as primarily oxidizing, but with microenvironments of reducing conditions. This acknowledgement of the presence of reducing microenvironments is especially important for technetium because the pH/Eh conditions separating TcO$_4^-$ from Tc^{4+} exists within the common domain of natural subsurface ORR conditions (Fig. 3.9). Moderately high concentrations of OM and high

concentrations of iron- and manganese-oxides likely exist at the EMDF (see data presented above from Rothschild et al. 1984 and Davis et al. 1984, and similar information in ORNL 1987; DOE 1992b). While together these geochemical conditions appear to support conditions conducive for technetium sorption, there is a great deal of uncertainty, especially regarding the redox conditions that may exist at the EMDF. Consequently, this analysis emphasizes ORR-specific measurements of technetium K_d values.
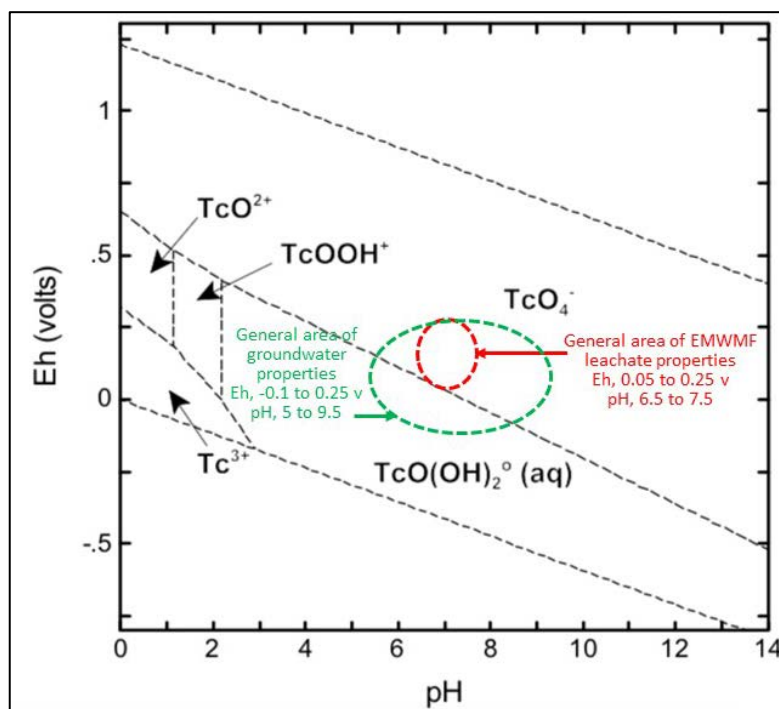
Diagram based on a total concentration of 10^{-8} mol/L dissolved technetium (from EPA 2004 VIII, Fig. 5.9).

Fig. 3.9. Eh-pH stability diagram for the dominant technetium aqueous species at 25°C

Two studies were identified that measure technetium K_d values under conditions that approximate those of the EMDF subsurface (DOE 1992b, ORNL 1987). DOE (1992b) reported K_d measurements of technetium (along with cesium, strontium, neptunium, and uranium) using soil sampled from Bethel Valley near the WAG 1. The studies followed an acceptable ASTM method and obtained an average technetium K_d value of 0.72 ± 0.16 cm^3/g, with a range of 0.53 to 1.04 cm^3/g (see Table 3.7). Also noteworthy, little time dependency of sorption with contact time was observed, suggesting that steady state conditions with respect to technetium were achieved in less than or equal to 1 day. This has important implications because flow through fractured media in the EMDF subsurface may be faster than through unfractured porous media. This data indicates that the full extent of technetium sorption, albeit quite small, is completed in a short period of time.

The data from DOE (1992b) is of high quality and the experimental conditions are largely appropriate for estimating technetium K_d values at the EMDF. The WAG 1 data (Table 3.7) provides a reasonable and defensible K_d value of 0.72 cm^3/g for technetium in the EMDF soils, saprolite, and bedrock for modeling purposes. ORNL (1987) found higher technetium K_d values in test on samples of the Nolichucky Formation (K_d=1.2 cm^3/g for dilute brine groundwater). Sensitivity analyses conducted in this PA will consider both lower and higher K_d values for Tc-99.

151

Table 3.7. Technetium K_d values measured from shales samples recovered from near the Waste Area Group 1 in Bethel Valley

Technetium K_d (cm³/g)	Sample ID	Contact Time (day)	Sample description[a]
1.04	01.SB103	1	#1
0.84	01.SB103	3	#1
0.79	01.SB103	14	#1
0.76	01.SB135	1	#2
0.67	01.SB135	3	#2
0.68	01.SB135	14	#2
0.53	01.SB184B	1	#3
0.59	01.SB184B	3	#3
0.61	01.SB184B	14	#3
0.72 ± 0.16	**Ave. ± Stdev.**		
0.53 to 1.04	**Range**		

Data taken from Table A4.1.8 and geological media descriptions from page 10 of DOE 1992b,

[a] #1 - clay texture sediment, 8 to 9 ft interval from boring 01.SB103 adjacent to Impoundment 3513

#2 - predominant clay texture sediment, red/yellow & brown color; 24 to 25.8 ft interval from boring 01.SB135 located just south of Building 3019; "Explosion 3019"

#3 - clay texture sediment; yellow-brown; 6 to 8 ft interval from boring 01.SB184B located at the southeast corner of Building 3525; "Leak 3525"

DOE = U.S. Department of Energy K_d = partition coefficient
ID = identification

Previous PA documents and modeling (ORNL 1997a, DOE 1998a, DOE 1998b) used zero values for the technetium K_d cm³/g in the vadose and saturated zones, but higher values (> 1 cm³/g) for waste forms (refer to Table 1.1 for a comparison). To increase confidence in the iodine K_d values applied in the EMDF PA, controls on the partitioning of technetium will be experimentally determined for local site materials (clayey soils and saprolite) derived from the Maryville Formation and Nolichucky Formation units. These data will be incorporated in future performance analyses as determined to necessary through the EMDF change control process.

3.2.2.8 Variations in K_d due to material characteristics and geochemical conditions

The K_d values are typically assigned to specific waste forms and earthen material components of a modeled system, and compilations of K_d values (e.g., International Atomic Energy Agency [IAEA 2010], Sheppard and Thibault 1990) include average values and ranges of values for different soil types, reflecting the significance of mineralogy and organic matter content to sorption phenomena. For different components of the EMDF system (e.g., waste materials and clean fill in the disposal unit, engineered basal liner and geobuffer clays, and native clay rich saprolite and sedimentary rocks underneath the disposal unit), the approach to representing variation in K_d values is based on several factors, including: (1) the limited availability of K_d data for EMDF waste materials, (2) the common local geologic source(s) and similar mineralogical characteristics of the materials expected to be used as clean fill and for liner and geologic buffer construction (UCOR 2018a), and (3) the variability and uncertainty in geochemical conditions present in different components of the disposal system during the post-closure period.

Previous radionuclide release and transport modeling for LLW disposal units on the ORR have applied different K_d values to different materials including waste, vadose zone materials (generally corresponding to soil and saprolite), and saturated zone materials (generally corresponding to saprolite and bedrock) (ORNL 1997a, DOE 1998b, BJC 2010b). For the EMDF waste zone material, the assumption is to assign a K_d value equal to one-half the K_d assigned to the saprolite zone material (Sect. 3.2.2.6), based on incorporating large volumes of clean fill (refer to Sect. 3.2.2.5) with textural and mineralogical characteristics similar to those of geologic materials at the EMDF site. This assumption conservatively reduces the K_d in the waste zone, based on the lack of information regarding soil waste also occupying the waste zone, and also conservatively assumes all contaminants sorbed or embedded in debris are immediately released to the surrounding soil. The locally sourced, clay-rich materials used as clean fill and the onsite materials that meet geotechnical requirements for use as EMDF liner and geologic buffer materials are derived from the underlying bedrock of the Maryville Formation and Nolichucky Formation. These materials are rich in clay minerals (e.g., illite) demonstrated to have high sorptive capacity in tests on samples from those geologic units (ORNL 1987, Friedman et al. 1990, Watson et al. 2004). Most of the available K_d measurements for Conasauga Group materials have been performed on saprolite or clayey soils, rather than bedrock samples (refer to Table 2.12). In the absence of data on differences in sorptive capacity between local saprolite and bedrock materials, K_d values for the bedrock zone are assumed to be the same as the saprolite zone values.

This simplifying assumption that all model material zones have similar K_d values (based on similarity in material characteristics) does not account for potential differences in geochemical environment (e.g., oxidation-reduction potential [Eh] and pH) within the waste zone, unsaturated zone, and saturated materials at the EMDF site, or the possibility for evolution in the geochemical conditions that control sorption and radionuclide mobility over time as the cover system degrades, cover infiltration increases, and leachate release begins. Leachate and groundwater monitoring at the EMWMF site provide a limited basis for anticipating the range of future geochemical conditions that may affect radionuclide release and transport mechanisms. Periodic field measurements of the EMWMF leachate collection system, underdrain outflow, and groundwater in monitoring wells along the facility perimeter indicate a wide range of pH and Eh conditions (Fig. 3.10).

The EMWMF leachate samples (black symbols in Fig. 3.10) span a range of pH values from 5.3 to 9.1 and a range of Eh values from -85 mV to 392 mV. Most of the leachate data fall within a pH range of 6.6 to 7.5 and an Eh value range of 50 to 250 mV (oxidizing conditions). Groundwater measurements from the EMWMF underdrain tend to have pH values and Eh values similar to leachate observations. Data from EMWMF groundwater monitoring wells span a wide range, with pH ranging from 5 to 10 and Eh values as low as -150 mV (reducing conditions).

In general, the groundwater data are most relevant to geochemical conditions in the saturated zone (Sect. 3.2.3), whereas the EMWMF leachate observations may be more representative of waste and vadose zone conditions. The data represent pre-closure, operational conditions at EMWMF and may or may not be representative of future EMDF conditions. Given that the general composition and range of EMWMF waste material types (concrete, steel, soil, etc.) is similar to the expected EMDF waste, the data are taken as the best available indication of future geochemical conditions in the EMDF waste and underlying vadose zone. The central tendency and range of pH and Eh observations for EMWMF leachate and underdrain samples (i.e., circumneutral to weakly acidic, oxidizing conditions) suggest that the K_d values within the EMDF waste zone and unsaturated zone may be similar to each other, and that adopting K_d values representing circumneutral, oxidizing conditions is appropriate. The assumption of near neutral, oxidizing conditions for the EMDF waste zone is reasonable considering the large volume of clean fill used in disposal operations that will provide buffering capacity for waste types (e.g., concrete) associated with higher pH values.
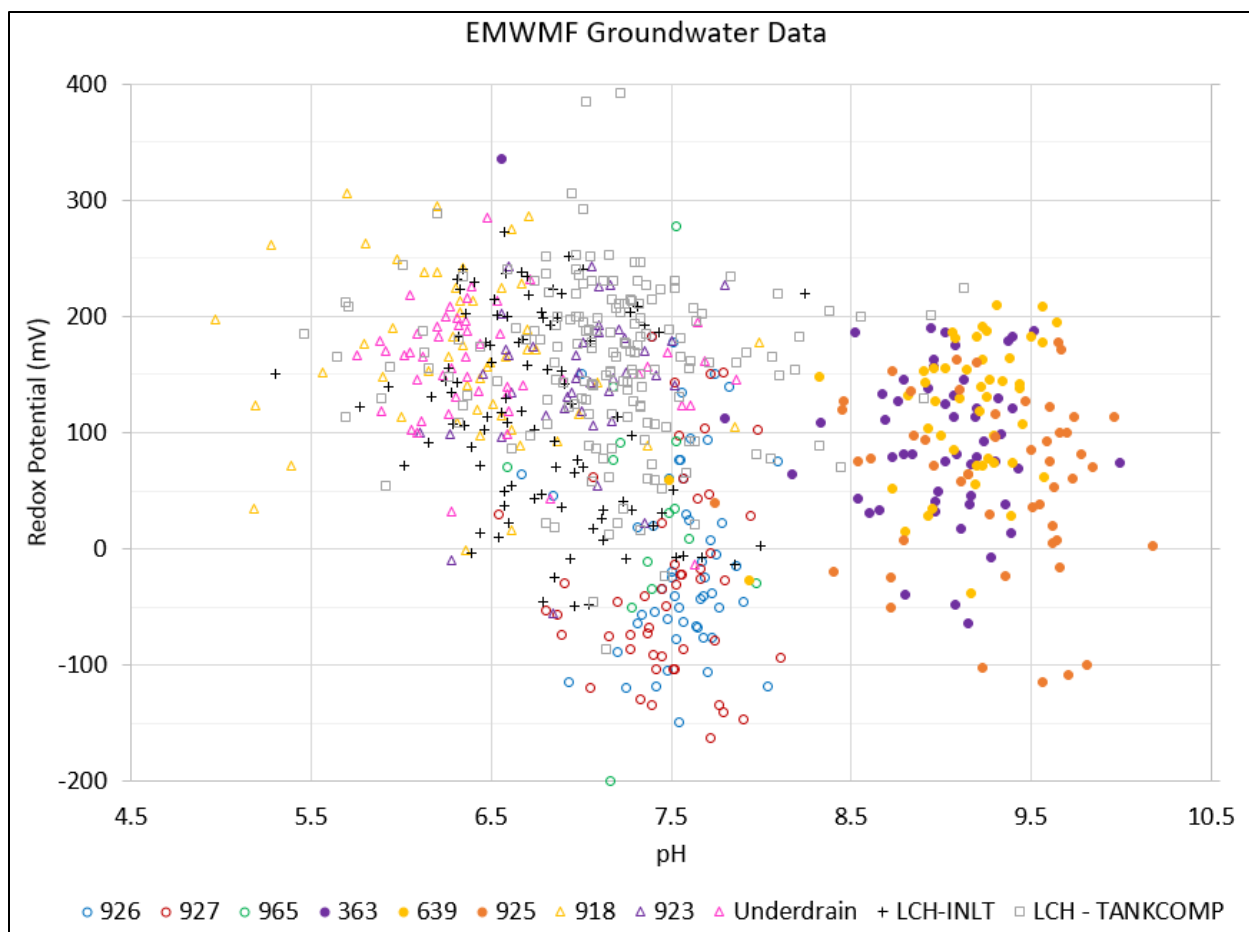
Fig. 3.10. Paired pH and redox potential observations from samples of EMWMF leachate, underdrain groundwater, and groundwater monitoring wells near the facility

While the EMWMF groundwater monitoring well data suggest that a wider range of pH and redox conditions is possible in the saturated zone, the clusters in the well data do not coincide with similarities in well location relative to the disposal unit, and so do not provide a strong basis for concluding that the geochemical environment in the saturated zone will be less acidic or less oxidizing, in general, than the overlying unsaturated and waste zones. Thus, the EMWMF leachate and groundwater data do not suggest systematic differences in pore water chemistry among the waste, vadose zone, and saturated zone.

The EMWMF field data show temporal variability in leachate chemistry that probably reflects changes in waste composition and environmental fluctuations such as seasonal cycles. However, these data from the operational period do not show any persistent trend in pH or redox conditions. Geochemical evolution of the EMDF waste and vadose zone may occur in the post-closure period as waste-dewatering and long-term changes in cover and liner system performance cause variations in the flux and chemistry of infiltrating water. However, no general model of geochemical evolution of the EMDF system that would result in progressive changes in K_d values has been assumed for the PA, in part due to limitations in specifying time-variable input parameter values.

For purposes of modeling source release and radionuclide transport, the geochemical environment is assumed to remain stable throughout the post-closure period, and the uncertainty in K_d values associated with differences in materials or geochemical conditions is addressed as part of the sensitivity and

uncertainty analysis for the each of the models (refer to Sect. 5). Assuming a single, constant K_d value for the engineered materials, saprolite, and bedrock below the waste does not capture the potential geochemical complexity of the disposal system. However, given the anticipated similarity in material characteristics and uncertainty in the variation of geochemical conditions over time, the simplified assumption is adopted for the base case model implementation and combined with a focus on model sensitivity to uncertainty in K_d values applied to different material and model zones (i.e., waste versus saprolite and bedrock, vadose versus saturated zone). In general, the all-pathways dose analysis is most sensitive to the K_d value assigned to the waste material, which governs the rate of radionuclide release from the disposal unit. From that perspective, a significant conservative step is taken in assuming these K_d values are one-half the values of the other zones. Sensitivity of PA model results to uncertainty in K_d values is addressed in Sect. 5.

3.2.2.9 Summary of radionuclide release and vadose zone conceptual model assumptions

Key assumptions for the conceptual models of radionuclide release and vadose zone transport include the following:

- Based on the EMDF estimated inventory, anticipated operational conditions, and design features of the EMDF cover system, post-closure release of radionuclides through the cover is assumed to be negligible (Sect. 3.2.2.1, 3.2.2.2, and 3.2.2.3).

- Infiltration through the cover is assumed to occur uniformly over the area above the waste and liner system (Sect. 3.2.2.4), and to follow the generalized model of EMDF performance evolution over time (Fig. 3.5).

- Equilibrium desorption is assumed to govern release from the solid phase (refer to Table 3.4 for assumed K_d values).

- Potential solubility limits are not incorporated in the source release representation.

- The EMDF waste mass is conceptualized as a homogeneous, soil-like material in which the estimated radionuclide inventory is uniformly distributed.

- Estimated post-closure inventories of radionuclides that are highly mobile in the aqueous phase (H-3, C-14, Tc-99, and I-129) are adjusted (reduced) based on modeling of operational period leaching (Sect. 3.2.2.5).

- The assumed mass of clean fill disposed with EMDF waste is based on average clean fill-to-waste ratios documented for the EMWMF. Average waste inventory concentrations are adjusted downward to account for this added mass (Sect. 3.2.2.5).

- Assumptions regarding the geochemical environment in the disposed wastes and pore water and the potential for changes over time are limited to assumed ranges in pH and Eh (Sect. 3.2.2.8).

- Geochemical conditions in the waste and vadose zone are assumed to be circumneutral and oxidizing.

- For purposes of modeling source release and radionuclide transport, the geochemical environment is assumed to remain stable throughout the post-closure period, and saturated and unsaturated material zones are assumed to have identical (invariant among zones) radionuclide-specific K_d values, while the waste zone radionuclide-specific K_d values are assumed to be equal to one-half these K_d values based on clean fill accounting for approximately one-half the mass in the waste zone (Sect. 3.2.2.6).

3.2.3 Saturated Zone Flow and Radionuclide Transport

Based on the BCV hydrogeologic conceptual model (Sect. 2.1.5) and the evidence from BCV tracer studies presented in Sect. 2.1.6.2, flow within the saturated zone near EMDF is expected to be 3-D, with

groundwater close to the water table (generally within the saprolite zone) diverging toward lower surface elevations (e.g., Bear Creek tributary channels) around the periphery of the disposal unit. With increasing depth, groundwater flow direction becomes predominantly along-strike toward the south-southwest and the vertical component of flow decreases with increasing depth into the bedrock zone. This flow pattern reflects the pronounced horizontal anisotropy associated with strike-parallel fracture pathways as well as decreasing porosity and permeability with depth. Based on evidence from several BCV saturated zone tracer studies, radionuclides reaching the saturated zone will be transported laterally toward shallow groundwater discharge areas with limited downward transport into the deeper portions of the bedrock zone. Deeper groundwater and radionuclide transport pathways will be directed down valley and toward Bear Creek, with surface discharge occurring at more distant locations relative to shallower transport pathways (Fig. 3.11).

Saturated zone groundwater flux is conceptualized as a traditional Darcian porous media system. Neither statistical nor more detailed, discrete representation of fracture networks is adopted due to limitations in the types and quantity of field data available to support parameterization of such conceptual models of flow in fractured media. The large amount of existing permeability data compiled for Conasauga Formations and applied in previous BCV modeling efforts (Sect. 2.1.5.4) is the basis for an EPM representation of the heterogeneous, anisotropic nature of the geologic media at the CBCV site. Specifically, stratigraphic variation in hydraulic conductivity and vertical variation in porosity and horizontal anisotropy in conductivity is the basis for parameterization of the 3-D complexity of the saturated zone. More detailed information on this parameterization scheme is presented in Sect. 3.3.3.

Saturated zone radionuclide transport is conceptualized as advective, chemically retarded aqueous-phase transport within the porous medium (saprolite and bedrock), with a simple equilibrium, linear isotherm sorption model assumed for retardation. This conceptual model is represented with a standard formulation (Bouwer 1991) for retarded aqueous-phase transport in porous media. The influence of discrete fracture networks and matrix diffusion on radionuclide transport are not explicitly incorporated because the site-specific data required to parameterize more detailed representations of subsurface transport are not available. Without detailed field measurements of the spatial variability in fracture size and frequency at the scale of the disposal site, even finer-resolution EPM representation of simple retarded transport in a fractured rock system is not possible. EMDF site characterization (DOE 2018b, DOE 2019) has provided a general confirmation of the hydrogeologic conceptual model adopted for the PA modeling.

The conceptual model of radionuclide flux from the vadose zone to the water table incorporates the possibility of non-uniform concentration and flux below the facility footprint. Simplified representations of both non-uniform and uniform fluxes to the water table are applied to the site-specific saturated zone transport model described in Sect. 3.3.3. A uniform flux to the saturated zone is assumed for purposes of total-system modeling (described in Sect. 3.3.4).

The conceptual model of saturated zone flow and radionuclide transport is a simplification of the geochemistry and hydrogeology of the EMDF saturated zone. However, the practical limitations on implementation of fracture-matrix type conceptual and mathematical models (i.e., lack of data for parameterization and calibration of more complex approaches) are significant constraints on the utility of such alternative conceptual models for this performance analysis. Efforts to further evaluate the data collection requirements and calibration approaches that might be applicable to fractured-rock modeling of the EMDF saturated zone may have value in the context of PA maintenance.
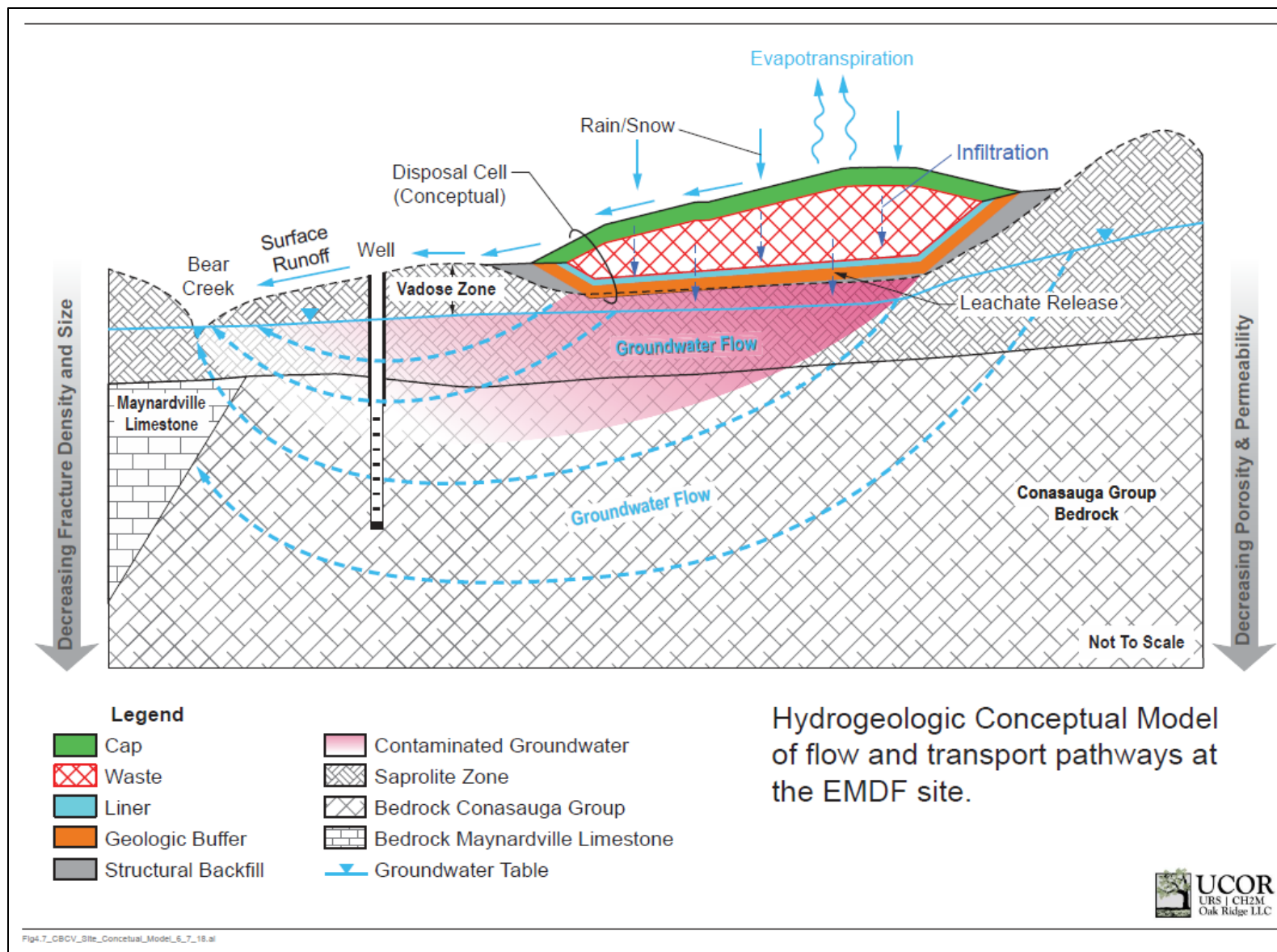
Fig. 3.11. Simplified conceptual model of flow and transport pathways at and downgradient of the EMDF site

3.2.4 Exposure Pathways and Scenarios

This section includes the descriptions of the exposure pathways and scenario(s) considered for each of the DOE M 435.1-1 performance objectives and measures, including atmospheric and all-pathways release and radon flux from the EMDF cover. Detail on key input parameters and assumptions is provided in Sect. 3.4. Exposure pathways and scenarios for IHI are presented in Sect. 6.

3.2.4.1 Atmospheric pathway and radon flux

Release of radionuclides through the EMDF cover is assumed to be negligible (Sect. 3.2.2). One of the exposure pathways included in the all-pathways analysis is inhalation of and immersion in air contaminated with radionuclides (external exposure) that are mobilized in particulate form from soil in food production plots (Fig. 3.12 and Appendix G). The performance measure for radon flux is assessed at the EMDF cover surface and does not explicitly incorporate specific exposure pathway or scenario assumptions (Appendix H).
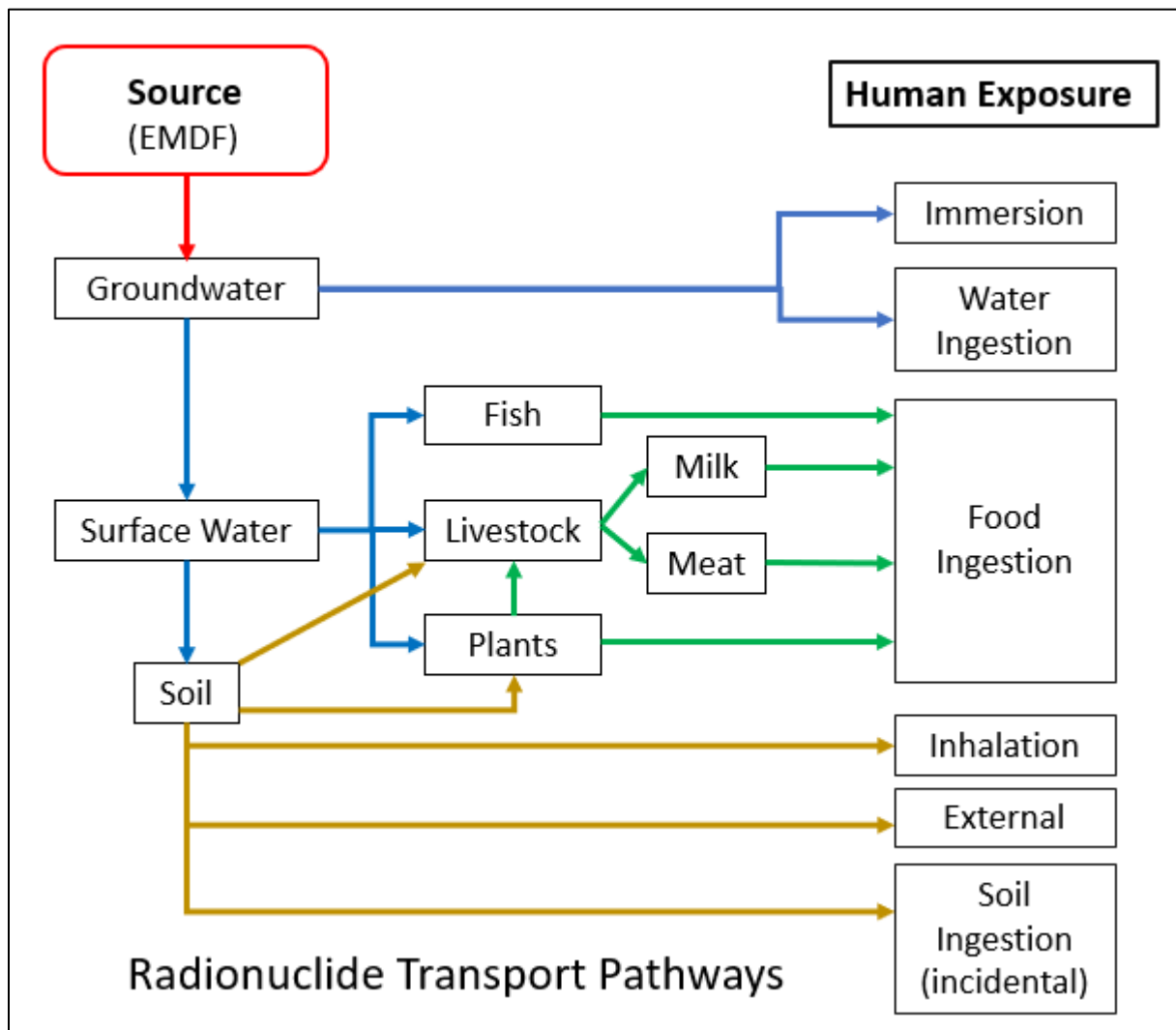
Fig. 3.12. Flow chart of environmental transport and exposure pathways for the all-pathways analysis

158

3.2.4.2 All-pathways exposure scenario

For the all-pathways exposure scenario (Fig. 3.12), radionuclide release through the EMDF cover is not included based on the screening analysis presented in Sect. 3.2.2. Release of radionuclides to groundwater and discharge of contaminated groundwater to surface streams are the environmental transport pathways modeled to estimate groundwater and surface water concentrations at the time and place of maximum concentration. The all-pathways scenario assumes that a resident farmer sets up a homestead somewhere near the disposal facility and pumps groundwater for drinking and household use from a well at the location of highest radionuclide concentration that is 100 m from the waste limit (Fig. 3.11). In addition, the farmer is assumed to draw contaminated surface water for crop irrigation and to support livestock from Bear Creek at the point where most of the contaminated groundwater is predicted to discharge. The basis for assuming use of surface water for agricultural activity is presented below.

In addition to consumption of contaminated groundwater from the well, the all-pathways scenario considers exposure due to immersion and inhalation during showering with contaminated groundwater. Contaminated surface water used to irrigate food production areas is the transport pathway that drives exposure from ingestion of contaminated agricultural products, including plant foods, meat, eggs, and milk. Working in contaminated food production areas is assumed to cause direct external exposure to radiation from contaminated soil as well as internal exposure by incidental soil ingestion and inhalation of particulates entrained from the ground surface.

Use of Water Resources

In East Tennessee, abundant rainfall and numerous surface water reservoirs support extensive use of surface water resources. Based on a recent TVA water use report, in Anderson and Roane Counties (the counties in which the Oak Ridge Reservation is located), surface water withdrawals for public water supply and crop irrigation are much greater than groundwater withdrawals for those two uses (TVA 2012). The proportion of total public water supplies withdrawn from groundwater sources in 2010 was 1.6 percent and 16 percent for Anderson and Roane Counties, respectively (Table 3.8). The residential exposure scenario adopted for the EMDF PA all-pathways analysis assumes the use of local groundwater for drinking and household use, even though facilities in BCV draw from surface water sources. The assumptions regarding the use of groundwater and surface water resources by the resident farmer are consistent with the exposure scenarios used in the evaluation of EMWMF performance and the development of the EMWMF WAC (DOE 1998b).

Table 3.8. Groundwater and surface water withdrawals in Anderson and Roane Counties for 2010

Tennessee county and water use		Surface water withdrawal (2010) in million gal/day (% of total)	Groundwater withdrawal (2010) in in million gal/ (% of total)
Anderson	Public Supply	13.2 (98%)	0.22 (1.6%)
Roane	Public Supply	6.65 (84%)	1.28 (16%)
Anderson + Roane	Public Supply	19.85 (93%)	1.5 (7%)
Anderson	Irrigation	0.45 (98%)	< 0.01 (< 2.2%)
Roane	Irrigation	0.04 (> 80%)	< 0.01 (< 20%)
Anderson + Roane	Irrigation	0.49 (96%)	< 0.02 (3.9%)

Data Source: TVA 2012, Table 2-21 (public supply) and Table 2-24 (irrigation)

TVA = Tennessee Valley Authority

In Anderson and Roane Counties, relatively little groundwater withdrawal for agriculture is required to supplement natural precipitation and surface water. For irrigation of crops, the proportions of water

withdrawals from groundwater and surface water in 2010 for Anderson and Roane Counties were similar to proportions withdrawn for public supply (Table 3.8). The predominant use of surface water for irrigation reflects its accessibility. When a source is available, reliable, and convenient, such as Bear Creek, surface water is used for irrigation rather than groundwater.

County level water use data available from USGS indicates that withdrawals of surface water to support livestock exceed groundwater withdrawals for that purpose by a factor of 2 or more (http://waterdata.usgs.gov/tn/nwis/water_use/). In the USGS database for 2010, Anderson and Roane Counties together used 0.27 million gal/day for livestock, which is less than the irrigation total for that year based on the TVA water use report (Table 3.8). However the USGS data for years 2000, 2005, 2010, and 2015 all indicate that surface water withdrawals for livestock are two to 10 times larger than total crop irrigation withdrawals, which is consistent with the abundant rainfall and ready availability of surface water sources to support agriculture in Anderson and Roane Counties. The predominant use of surface water for irrigation and livestock in the vicinity of the ORR supports the PA exposure scenario assumption that water from Bear Creek is used for agriculture.

Ingestion of Plant and Animal Foods

Selection of the types of contaminated products included in the food ingestion pathway is based on review of performance analyses for the EMWMF and other similar facilities (e.g., Portsmouth onsite waste disposal facility [DOE 2015c]). The agricultural products consumed include leafy vegetables and produce (non-leafy vegetables), as well as meat and milk from animals that drink contaminated surface water and are fed with contaminated feed grown in plots irrigated with surface water. The types of farm-raised meats could include beef, pork, and poultry. Farm-raised eggs could also be included in the range of locally grown foods. Locally obtained game (e.g., deer, turkey, geese) could also be consumed, but wild animals would not feed exclusively on contaminated agricultural products or drink only contaminated surface water; therefore, they would have lower radionuclide concentrations in muscle tissue than livestock.

For the EMDF PA, the assumed ingestion of animal foods is limited to meat and milk from cows, poultry, eggs, and fish from Bear Creek. This range of foods accounts for the most likely ingestion-based dose contributions to a resident farmer. Ingestion of fish from Bear Creek is based on an assumption for recreational catch rates because of the limited populations of large fish in the areas near the EMDF site. It is assumed there is no consumption of crustacea or mollusks, which is reasonable given the EMDF location in eastern Tennessee.

In summary the exposure pathways incorporated in the all-pathways dose analysis (Fig. 3.12) include the following:

- Ingestion of contaminated groundwater

- Immersion and inhalation during showering with contaminated groundwater

- Direct exposure to radiation from contaminated garden soil

- Inhalation of contaminated soil particles entrained from contaminated garden soil

- Incidental ingestion of contaminated garden soil

- Ingestion of plant foods irrigated with contaminated surface water

- Ingestion of meat and milk from cows that eat plants irrigated with contaminated surface water and drink contaminated surface water

- Ingestion of meat and eggs from poultry that ingestion contaminated feed and water

- Ingestion of fish caught from Bear Creek (based on recreational fishing).

While not unrealistic, the all-pathways exposure scenario is based on a local agricultural subsistence lifestyle that is uncommon in present day East Tennessee, which provides bias toward more highly exposed individuals. A subsistence farmer is specified as the receptor to incorporate a diverse set of exposure pathways. For purposes of EMDF performance analysis, the exposure at the time of peak dose is evaluated relative to the performance objective of 25 mrem/year.

3.2.4.3   Water resources protection

The performance criteria identified for protection of groundwater resources are the MCLs for drinking water specified by EPA in the Radionuclides Final Rule (EPA 2000), promulgated in 40 *CFR* 141.66, for which the State of Tennessee has primary enforcement responsibility. These radiological limits on public drinking water sources are based on drinking water ingestion only. The POA is the groundwater well at 100 m from the waste limit.

The performance criteria identified for protection of surface water resources are based on the DCS for water ingestion (DOE 2011b). The DCSs are based on total water ingestion including water as a beverage and water used in preparation of other beverages and food. The POA is Bear Creek immediately downstream of the NT-11 tributary confluence. Most of the radionuclide flux from the EMDF is predicted to discharge to surface water at or upstream of NT-11 (Sect. 3.3.3).

3.3   MODELING TOOLS AND IMPLEMENTATION

Selection of modeling tools to simulate the EMDF cover system water balance and radionuclide transport is based on the conceptual models presented above. The PA model codes include: the Hydrologic Evaluation of Landfill Performance (HELP) model for simulating the EMDF water balance; the STOMP model for simulating radionuclide release and vadose zone transport; MODFLOW, MODPATH, and MT3D model codes for saturated zone groundwater flow and radionuclide transport simulation; and RESRAD-OFFSITE for holistic simulation of radionuclide release and transport as well as exposure scenarios and dose analysis.

Simulation of transient hydrologic phenomena (i.e., variability in precipitation, runoff and evapotranspiration) is necessary for prediction of long-term cover system performance. Short-term dynamics of flow and contaminant transport within the unsaturated zone below the cover and in the saturated zone are considered less important to capture for simulation of long-term facility performance. Rather, the evolution of cover system performance and release of radionuclides over hundreds to thousands of years is the transient aspect of most significance for simulating disposal facility performance.

For cover system water balance modeling that incorporates daily and seasonal fluctuations in weather, the HELP computer code (Schroeder et al. 1994) is used to estimate post-closure rates of vertical percolation into the waste zone under different cover performance scenarios. Flow and contaminant transport in the vadose zone below the cover are modeled using the STOMP code (White and Oostrom 2000, White and Oostrom and 2006). The STOMP model is used to analyze the impact of disposal cell geometry on the timing and location of release from the engineered barriers of the liner system. STOMP results are used to guide the development of input flux boundary conditions (radionuclide release) for the saturated zone transport model, and are then compared to the simplified vadose zone representation in the total-system model.

Saturated zone groundwater flow and radionuclide transport are modeled using the MODFLOW and MT3D model codes, respectively. These 3-D flow and contaminant transport codes represent the hydrogeologic complexity of the EMDF site explicitly, incorporating a simplified EPM representation of fractured-rock characteristics that influence radionuclide transport. As with the STOMP modeling of the vadose zone, the 3-D saturated zone models provide a basis for assessment of the less complex model of saturated zone transport in the total-system model code, RESRAD-OFFSITE, which is used to integrate conceptual models of the EMDF system, including exposure pathways and scenarios. Simplified representation of environmental transport processes in the total-system model permits holistic simulation of release, transport, and exposure pathways, and facilitates a probabilistic analysis of the impact of input parameter uncertainty on dose predictions. Model sensitivity evaluations and the total system uncertainty analysis is presented in Sect. 5.

Table 3.9 presents a summary of how specific components of each model code represent the EMDF engineered materials, waste and natural geologic materials of the disposal system. The HELP model represents only the unsaturated, engineered materials and waste materials. The materials above the liner system are not included in the 3D MODFLOW and MT3D models, which simulate flow and radionuclide transport in the saturated parts of the saprolite and bedrock zones. The STOMP and RESRAD-OFFSITE models include the engineered barriers, waste, and natural material components, which are represented as variably saturated in the STOMP model. The RESRAD-OFFSITE model represents the engineered and waste materials and uppermost saprolite zone as unsaturated. The saturated zone component (aquifer) of the RESRAD-OFFSITE model is assigned porosity and permeability characteristics intermediate between the saprolite zone and the bedrock zone. Linkages among models are illustrated in Figs. 3.1 and 3.2 (Sect. 3.1.2) and summarized in Table 3.10. The remainder of this section provides summary information on each of the model codes utilized and the selection of parameter values for the EMDF system. Model results that support parameterization of other PA models are presented as necessary. More detailed information on model setup and implementation is provided in separate appendices for each model (first column of Table 3.10).

Table 3.9. Representation of material zones of the EMDF system within different PA model codes

PA Model Codes → Material Zones ↓	HELP	MODFLOW & MT3D	STOMP	RESRAD-OFFSITE
Engineered Materials and Waste	Cover, waste, liner, and geologic buffer layers	Model layer 1 (EMDF liner & geobuffer)	Material zones 1-9, 18	Cover, waste, and unsaturated zone layers UZ1 –UZ4
Saprolite Zone	Not represented	Model layer 1	Material zones 10-13	UZ5 saturated zone (aquifer)
Bedrock Zone	Not represented	Model layers 2-9	Material zones 14-17	Saturated zone (aquifer)

EMDF = Environmental Management Disposal Facility
HELP = Hydrologic Evaluation of Landfill Performance
PA = Performance Assessment

RESRAD = RESidual RADioactivity
STOMP = Subsurface Transport Over Multiple Phases
UZ = unsaturated zone

162

Table 3.10. EMDF PA model input parameters and linkages among models

Model and purpose	Primary model inputs	Primary model output (used as input to or compared with other PA models)
HELP Water balance and engineered barrier performance (Appendix C)	• Local climate data • EMDF Preliminary Design (geometry and material specifications)	• Cover infiltration rates
MODFLOW Saturated zone flow (Appendix D)	• EMDF Preliminary Design • Bear Creek Valley topography, geology, and surface water features • Conasauga Group hydraulic conductivities • EMDF cover infiltration • Estimated natural recharge rates	• Flow directions • Hydraulic gradients • 3-D groundwater flow field • Depth to groundwater
STOMP Unsaturated flow and transport (Appendix E)	• EMDF radionuclide inventory • EMDF Preliminary Design • Estimated natural recharge rates • EMDF cover infiltration • Conasauga Group hydraulic conductivities and porosity • Solid-aqueous partition coefficients	• Radionuclide release • Vadose zone flux • Water table flux • Water table time of arrival (vadose delay times)
MT3D Saturated zone transport model (Appendix F)	• EMDF radionuclide inventory • EMDF Preliminary Design • EMDF cover infiltration • Effective porosities • 3-D groundwater flow field • solid-aqueous partition coefficients • Radionuclide flux from vadose zone	• Plume location, evolution and maximum extent • Peak groundwater concentration and time of peak at well • Contaminant discharge to Bear Creek surface waters
RESRAD-OFFSITE Radionuclide release and transport; exposure and dose analysis (Appendix G)	• EMDF radionuclide inventory • EMDF Preliminary Design (material specifications) • EMDF cover infiltration • Hydraulic gradients • Effective porosities • Solid-aqueous partition coefficients • Biotic transfer factors • Dose conversion factors • Exposure scenario and exposure factors (ingestions rates, etc.)	OUTPUTS for evaluating compliance with performance objectives: • Peak total dose during compliance period • Dose contributions by exposure pathway • Key radionuclide contributions to total dose • Well water and surface water concentrations

D = dimensional   PA = Performance Assessment
EMDF = Environmental Management Disposal Facility RESRAD = RESidual RADioactivity
HELP = Hydrologic Evaluation of Landfill Performance STOMP = Subsurface Transport Over Multiple Phases

Due to limitations in representing the sequence of material layers in the cover system for radon flux modeling, the RESRAD-OFFSITE code was not utilized for the radon analysis. The tool for modeling radon flux from the EMDF cover is the 1984 NRC technique for design of uranium tailings cover systems (NRC 1984) and is described in detail in Appendix H.

QA activities that support model implementation include software QA, input data validation and checking, documentation and independent review of model outputs and post-processing procedures, and archival and configuration management of model files and supporting QA documentation. Additional detail on the QA activities for the PA is provided in Sect. 9 and model QA activities are documented in *Quality Assurance Report for the Performance Modeling of the Bear Creek Valley Low-level Radioactive Waste Disposal Facilities, Oak Ridge, Tennessee* (QA Report) (UCOR 2020b).

3.3.1   Engineered Barrier Performance Model Code (HELP)

The HELP model was selected for hydrologic modeling of EMDF performance based onsite characteristics (weather and climate) and the EMDF Preliminary Design. The HELP model helps to identify a reasonable range of cover infiltration and leachate release rates applicable to short-term and long-term post-closure performance periods, with a focus performance within the 1000-year, post-closure compliance period. Sections 1.3, 2.2, and 3.2.1 review EMDF design features and safety functions that HELP modeling integrates to represent facility hydrologic performance. Appendix C provides additional detail on EMDF system features, events, and processes relevant to performance and more detailed presentation of HELP model input parameter selection.

The HELP model was developed at the U.S. Army Corps of Engineer Waterways Experiment Station under a cooperative agreement with EPA to support RCRA and Superfund programs (Schroeder et al. 1994). The HELP model is recommended by EPA and required by most states for evaluation of closure designs of hazardous and nonhazardous waste management facilities. The HELP code has been widely used for landfill design and performance evaluation over more than two decades.

HELP is a quasi 2-D hydrologic model of water movement into and through landfill systems. The model accepts climate, soil, and design data, and uses estimation techniques that account for the effects of surface storage, snowmelt, runoff, infiltration, evapotranspiration, vegetative growth, soil moisture storage, lateral subsurface drainage, and unsaturated vertical drainage as well as leakage through soil, geomembrane, or composite liners. Landfill systems including various combinations of vegetation, cover soils, waste cells, lateral drain layers, low permeability barrier soils, and synthetic geomembrane liners may be modeled. The HELP model has been used for design and performance modeling of EMWMF and EMDF.

The HELP model uses an extensive set of submodels to represent the water and energy balance at the surface; the U.S. Department of Agriculture (USDA)-Standardized Partial Regression Coefficient Standard Curve Number method for estimating surface runoff (USDA 1986); a Dupuit-Forcheimer approximation for saturated flow in lateral drainage layers; and simplified algorithms for vertical flow and routing of water through a user-defined profile of landfill layers that may include lateral drainage layers, vertical percolation layers, soil barrier layers, and synthetic geomembranes (Schroeder et al. 1994).

The HELP model includes approximations that can affect the predicted surface water balance and vertical fluxes below the surface. Parameterization of surface soil and vegetation characteristics in particular will affect the estimated net infiltration through the surface layer (precipitation–runoff–evapotranspiration), which sets an upper bound on percolation through the cover system as a whole. HELP utilizes a soil moisture characteristic model for unsaturated flow based on moisture content at soil field capacity and at wilting point and employs a unit hydraulic gradient assumption (Darcy velocity equal to (un)saturated hydraulic conductivity) for each vertical percolation layer. Soil barrier layers are assumed to remain saturated, with flow driven by the estimated head on the top of the barrier. Depending on the predicted net infiltration, lateral drainage flux, and specified soil hydraulic characteristics, these simplifying vertical flow assumptions will tend to over predict downward vertical water movement through the modeled profile. In particular, these unsaturated flow approximations omit more complex surface tension physics such as the effect of capillary barriers designed to inhibit downward subsurface flow. Detailed presentation of the

mathematical expressions for various HELP submodels, methods of solution, and model limitations can be found in Schroeder et al. (1994). Additional discussion of HELP model limitations, reviews of previous applications of HELP, and evaluations of model results relative to other models and field data are included in Appendix C, Sect. C.2.2.2.

3.3.1.1 HELP input data requirements

HELP model inputs include climatic data, design specifications for the thickness and hydrologic characteristics of each soil layer or synthetic membrane, and parameter selections concerning the condition of vegetation on the surface layer and the quality of synthetic membrane placement.

Climatic Data. HELP requires inputs of precipitation, air temperature, and solar radiation data as well as data for estimating evapotranspiration, which includes latitude, growing season dates, wind speed, quarterly average relative humidity, evaporative zone depth, and maximum leaf area index. Daily precipitation and temperature data for Oak Ridge, Tennessee from 1961 to 1990 are input for the EMDF model runs, whereas the solar radiation and evapotranspiration data are supplied by HELP based on user specification of Knoxville, Tennessee as the landfill location. Both earlier and more recent climate data are similar to the 1961 to 1990 data set and do not justify updating the HELP model files. The average annual total precipitation based on this data set is 54.39 in. The evaporative zone depth specified for all EMDF base case model runs is the HELP-suggested value (21 in.) for the Knoxville, Tennessee area. Maximum leaf area index was set to the HELP-suggested value 3.50. Model sensitivity to climate parameter values is presented in Appendix C.

Soil and Design Data. Soil and design data inputs define the profile(s) of landfill layers simulated by HELP. In addition to total landfill area and the percent of the area that generates surface runoff (assumed 100 percent), the thickness and soil properties of each layer are the essential data inputs. There are eight discrete layers incorporated into the cover design and eight layers incorporated into the liner design below the waste (Sect. 2.2). Additional geotextile layers incorporated into the design to protect the geomembrane layers were not considered in the HELP model as they do not significantly alter or retard the movement of infiltrating water.

Necessary data on the soil material include total porosity, volumetric moisture content (VMC) at field capacity (defined as VMC at 0.33 bars capillary pressure), VMC at wilting point (defined as VMC at 15 bars capillary pressure), and saturated hydraulic conductivity. The porosity, field capacity, wilting point, and saturated hydraulic conductivity are used to estimate the soil-water evaporation coefficients and Brooks-Corey soil moisture characteristic function parameters. The HELP model code contains default soil characteristics for 42 soil texture types (Schroeder et al. 1994, pages 30-31). The selected soil texture type and corresponding default characteristics for each EMDF layer are given in Table 3.11. The HELP profile of EMDF layer thickness, layer type designations, and soil characteristics is based on the preliminary design information referenced in the QA Report (UCOR 2020b). As engineering design for the EMDF proceeds, the HELP parameter assignments for future PA evaluations will be reviewed for consistency with updated design specifications.

The HELP model input data also includes the length and slope of lateral drainage layers, and assumptions regarding synthetic membrane quality, including pinhole density, installation defect density, and membrane placement quality. Values for these parameters based on the EMDF Preliminary Design are given in Table 3.12.

Table 3.11. HELP layer soil characteristics for EMDF design

EMDF profile	Layer #	Material description	Layer type[a]	Layer thickness (in.)	Soil texture type[b]	Total porosity (vol/vol)	Wilting point (vol/vol)	Field capacity (vol/vol)	Saturated hydraulic conductivity (cm/sec)
Final cover	1	Top soil/rock mix (vegetative/erosion control layer)	1	48	11	0.464	0.310	0.187	6.40E-05
	2	Sand/gravel (granular filter/drainage layer)	1	12	3	0.457	0.083	0.033	3.10E-03
	3	Large rock/riprap (biointrusion layer)	1	24	21	0.397	0.032	0.013	3.00E-01
	4	Gravel (lateral drainage layer)	2	12	21	0.397	0.032	0.013	3.00E-01
	5	HDPE-FML (geomembrane layer)	4	0.06	35				2.00E-13
	6	Amended compacted clay (low permeability)	3	12	0	0.427	0.418	0.367	2.50E-08
	7	Cover compacted clay (low permeability)	1	12	16	0.427	0.418	0.367	1.00E-07
	8	Contour gravel (waste surface layer)	1	12	24	0.365	0.305	0.202	2.70E-06
Waste	9	Waste	1	690.45	22	0.419	0.307	0.180	1.90E-05
Liner	10	Protective soil (layer protects liner)	1	12	8	0.463	0.232	0.116	3.70E-04
	11	Drainage (leachate collection system)	2	12	21	0.397	0.032	0.013	3.00E-01
	12	HDPE-FML (geomembrane layer)	4	0.06	35				2.00E-13
	13	GCL (low permeability)	3	0.24	17	0.750	0.747	0.400	3.00E-09
	14	Geonet leak detection layer (leak detection)	2	0.3	20	0.850	0.010	0.005	1.00E+01
	15	HDPE-FML (geomembrane layer)	4	0.06	35				2.00E-13
	16	Compacted clay layer (low permeability)	3	36	16	0.427	0.418	0.367	1.00E-07
	17	Soil geobuffer (barrier layer)	1	120	0	0.419	0.307	0.180	1.00E-05

[a]1 = vertical percolation, 2 = lateral drainage, 3 = barrier soil, 4 = geomembrane
[b]Soil texture types as defined in Schroeder et al. 1994, Table 4, pages 30–31.

EMDF = Environmental Management Disposal Facility   HDPE = high-density polyethylene
FML = flexible membrane liner   HELP = Hydrologic Evaluation of Landfill Performance
GCL = geosynthetic clay liner

Table 3.12. HELP model parameters for EMDF Preliminary Design lateral drainage and geomembrane layers

Drainage layer parameters			HDPE geomembrane quality characteristics (HELP layers 5, 12, 15)
HELP layer number	Drainage length (ft)	Drainage slope (%)	
4	476.9	21.52	• Pinhole density: 1 hole/acre
11, 14	258.8	4.22	• Installation defect density: 1 hole/acre
			• Membrane placement quality: good

EMDF = Environmental Management Disposal Facility   HELP = Hydrologic Evaluation of Landfill Performance
HDPE = high-density polyethylene

3.3.1.2   Engineered barrier performance assumptions

To account for long-term degradation of engineered barrier materials, consistent with the conceptual model of EMDF performance evolution (Fig. 3.5), the following three performance conditions are considered for disposal facility performance:

- Full design performance (design performance period, EMDF closure through 200 years post-closure): All layers are functional and included in the simulated HELP profile (Appendix C, Table C.2). This period includes the 100-year, post-closure period of institutional control and the first 100 years following the assumed loss of institutional control by DOE. Every component of the cover system is assumed to perform as designed, including the HDPE membrane and engineered drainage layer.

- Partial design performance (representative of the degrading performance period from 200 to 1000 years post-closure): Geomembrane liner layers and geosynthetic clay layers are assumed to be totally ineffective (i.e., no longer function as impermeable layers in the cover and liner systems) after 200 years post-closure. Assuming 200 years for the service life of the HDPE membrane is pessimistic given that recent studies have estimated much longer periods of full HDPE membrane performance in mixed LLW facilities (Tian et al. 2017). These layers (Appendix C, Table C.2, layers 5, 12, 13, and 15) are eliminated from the simulated EMDF profile for this performance period. In addition, the lateral drainage layers in the liner system are designated as vertical percolation layers, consistent with the expectation that active leachate collection will not continue for more than a few decades. The amended clay layer (Appendix C, Table C.2, layer 6) is also assumed to be degraded from 2.5E-08 to 3.5E-08 cm/sec due to the failure of the geomembrane liner above. In the context of the generalized conceptual model of EMDF performance evolution (Appendix C, Fig. C.4), this modeled performance condition provides a reference performance level (cover infiltration rate) for the period of degrading EMDF performance. Modeling EMDF performance without the HDPE membranes and assuming slightly degraded performance of the clay barriers is consistent with the expectation that while the membranes are intact, degradation of the clay layers by natural processes is limited. Full design performance is assumed for the lateral drainage layer in the cover system due to the expectation that the cover system remains largely intact, clogging of the drainage layer is unlikely (refer to Appendix C, Sect. C.1.2.2.1), and the overlying biointrusion layer will provide effective lateral drainage capacity in the event that the drainage layer capacity is reduced.

- Long-term performance (long-term performance period, > 1000 years post-closure): Degradation of the cover system due to some combination of erosion, root penetration, soil development, damage by storms, floods, or other natural hazards or differential settlement of the underlying waste causes an increase in the permeability of the clay barriers in the cover and a decrease in the efficiency of the engineered lateral drainage layer of the cover. The degraded condition for this performance period is represented by changes in the hydraulic conductivity of the lateral drainage layer (factor of 3 decrease) and amended clay layer (factor of 2.8 increase from design specification) in the HELP model profile.

HELP model parameter values chosen to represent degraded performance conditions are summarized in Table 3.13 for the full design, partial design and long-term performance conditions.

Table 3.13. Summary of HELP model input parameter assumptions and model output representing design and degraded EMDF hydrologic performance conditions

HELP model input parameter or predicted output flux		Full design performance (0–200 years)	Partial design performance (201–1000 years)	Long-term performance (> 1000 years)
HELP inputs (cover)	Lateral drainage layer hydraulic conductivity (cm/sec)	3.0E-01	3.0E-01	1.0E-01
	HDPE geomembrane function[a]	Functional	Degraded	
	Amended clay hydraulic conductivity (cm/sec)	2.5E-08	3.5E-08	7.0E-08
HELP output flux (in./year)	Lateral drainage collected	18.50	18.07	17.62
	Infiltration through cover clay barrier and into waste zone	0.00	0.43	0.88
HELP inputs (liner)	Leachate collection drainage layer function[a]	Functional	Not functional	
	HDPE geomembrane function[a]	Functional	Degraded	
	Geosynthetic clay layer function[a]	Functional	Degraded	
	Leak detection drainage layer function[a]	Functional	Not functional	
	HDPE geomembrane function[a]	Functional	Degraded	
HELP output flux (in./year)	Leachate collection layer drainage	0.00	Degraded	
	Leak detection layer drainage	0	Degraded	
	Infiltration through liner clay barrier	0	0.43	0.88

[a]Model layer function "Degraded" indicates the layer has been removed from the HELP profile for that performance stage. For lateral drainage layers in the liner system, "Not Functional" indicates that the layer type has been changed from lateral drainage to vertical percolation in the HELP profile.

EMDF = Environmental Management Disposal Facility   HELP = Hydrologic Evaluation of Landfill Performance
HDPE = high-density polyethylene

3.3.1.3   HELP model results and sensitivity to parameter assumptions

HELP model results and sensitivity to key input parameters are presented to provide the basis for quantitative cover infiltration inputs to the PA models described in subsequent sections. Additional information on the evaluation of HELP model sensitivity is provided in Sect. 5 and Appendix C.

HELP model runs were performed for each of the three disposal facility performance conditions described above. HELP model outputs (Table 3.13) provide estimated water fluxes through the EMDF cover system into the waste and out of the EMDF liner system. The HELP-predicted values are used to guide inputs (cover infiltration rates) to the more complex models of flow and contaminant transport used for the EMDF PA. Because the HELP model is primarily intended as a design tool rather than for predictions of long-term landfill hydraulic performance, the model outputs for the two degraded performance conditions are utilized as a general indication of the magnitude of increases in cover infiltration and leachate release that could be realized. Sensitivity of the HELP model results to input parameter uncertainty also is used to define the range of cover infiltration applied to evaluate uncertainty in long-term EMDF performance evolution.

Uncertainty in using the HELP model to predict long-term hydrologic performance of the EMDF cover system is related to the difficulty of specifying representative degraded-condition hydraulic conductivity (K_{sat}) values based on very limited understanding of the long-term performance evolution of earthen barriers and engineered drainage systems. The degree of degradation of clay barrier performance that could occur (due to natural processes over hundreds of years under stable climate conditions) is plausibly bounded by the upper end of the estimated range of rates of natural annual average recharge to groundwater in BCV, estimated at 7 to 12 in./year (DOE 1997b, Volume 2, Appendix F, pages F-36 and F-40). Additional HELP

model runs were performed to evaluate the sensitivity of estimated infiltration to the degree of degradation (change in saturated hydraulic conductivity, K_{sat}, value) assumed for the lateral drainage layer and the clay barrier of the cover, and to possible increases in future precipitation. The results of the sensitivity runs are summarized in the following paragraphs.

HELP model predicted cover infiltration values associated with different values of K_{sat} for the clay barriers of the cover system are shown in Fig. 3.13. For the partial design performance and long-term performance conditions, the amended clay and compacted clay units are modeled as separate layers (layers 6 and 7 in Table 3.11). For the sensitivity cases that represent more severe cover degradation, the clay barriers are modeled as a single uniform 2-ft-thick barrier layer in the HELP model. The value of K_{sat} given on the horizontal axis of Fig. 3.13 represents the hydraulic conductivity of the amended clay layer for the partial design and long-term performance conditions.
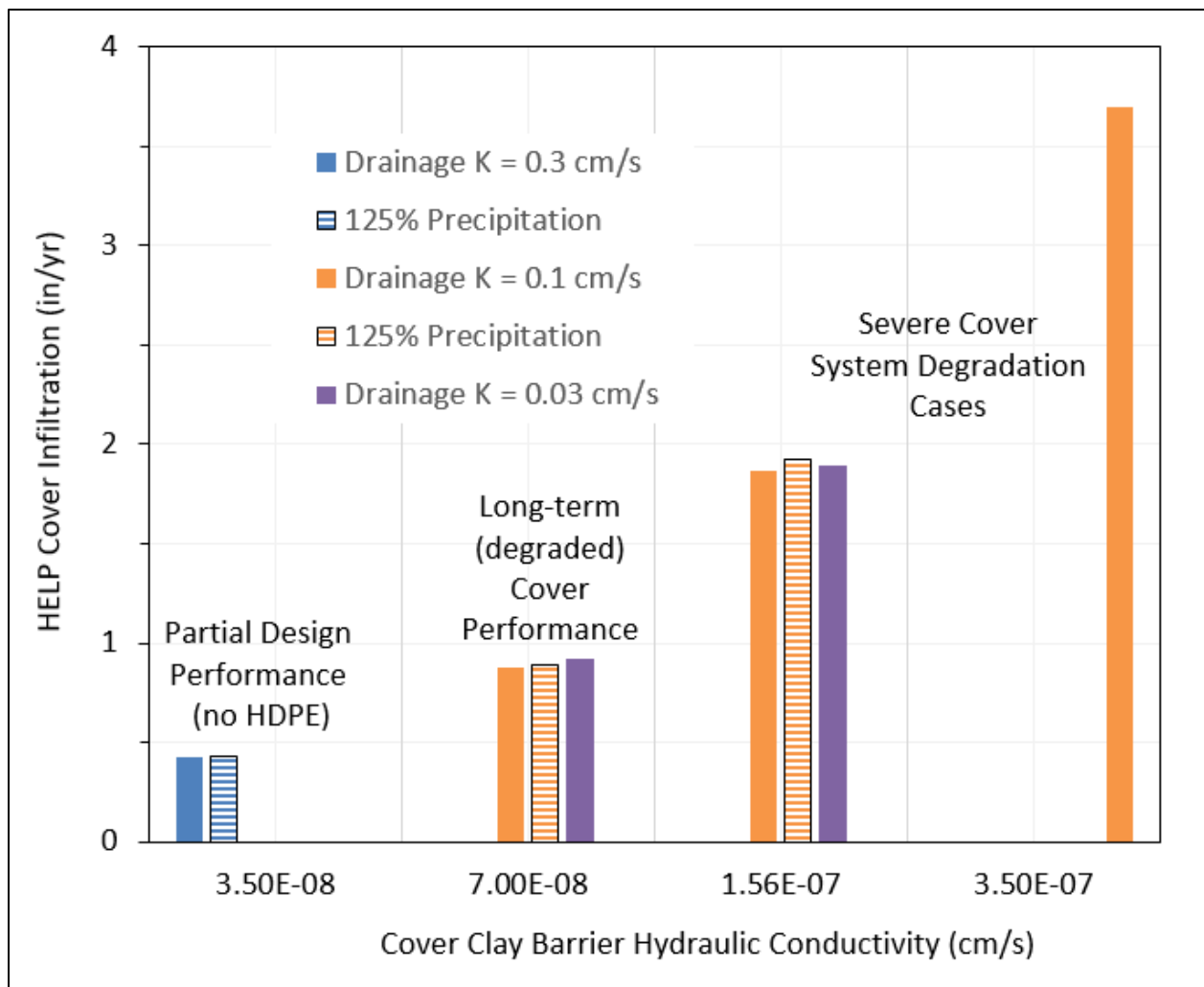
Fig. 3.13. HELP model sensitivity to cover layer parameter assumptions and precipitation inputs

The left-hand pair of bars in Fig. 3.13 represents infiltration predictions for the partial-design performance condition (without HDPE membranes) under the current average annual precipitation (approximately 54 in./year) and for a 25 percent increase in total annual precipitation. HELP-predicted infiltration sensitivity to the increased precipitation is minimal (1 percent increase) for the partial design performance

169

condition. For the long-term performance condition and the degraded cover sensitivity case with clay K_{sat} = 1.56E-07 cm/sec, a 25 percent increase in precipitation results in increases in cover infiltration of 2 percent and 3 percent, respectively (compare solid orange and striped orange bars on Fig. 3.13).

Results of HELP model sensitivity evaluation for anticipated future changes (Appendix C, Table C.4) in the clay barrier K_{sat} (increase from full design performance) and the lateral drainage layer K_{sat} (decrease from full design performance) show that sensitivity to cover drainage K_{sat} is much lower than for cover clay K_{sat} (Fig. 3.13) and that sensitivity to these two parameters is interdependent. Increases in infiltration are roughly proportional to the modeled increases in clay barrier K_{sat} (orange bars on Fig. 3.13) whereas decreases in lateral drainage K_{sat} result in much smaller increases (< 5 percent) in cover infiltration (compare the solid orange and purple bars on Fig. 3.13).

The sensitivity of the HELP model predictions to these parameter values, particularly the K_{sat} of the amended clay barrier in the cover system, indicates the importance of uncertainty in selecting parameter values to represent long-term performance conditions. HELP model parameter values selected for the EMDF long-term performance condition (Table 3.13, Fig. 3.13) result in predicted infiltration of 0.88 in./year, whereas the highest values of cover infiltration from the HELP sensitivity evaluation (3 to 4 in./year) are equivalent to approximately 50 percent of natural recharge rates estimated for geologic units at the EMDF site. The predicted fluxes are consistent with the expectation that the EMDF cover system, even in a degraded condition, will promote lateral drainage above the clay barrier and limit vertical percolation through the barrier, relative to natural conditions, for hundreds of years.

The HELP model tendency to over predict cover infiltration at humid sites (Appendix C, Sect. C.2.2.2) may mitigate some of the uncertainty in specifying degraded-condition parameter values for the HELP-modeled, long-term performance condition. In the context of EMDF performance modeling over thousands of years, using HELP to estimate EMDF performance degradation resulting from the full range of climatic and geologic processes and events is not justified, given the uncertainties at such extended time scales. For the EMDF PA, STOMP model sensitivity evaluation (Sect. 5.1) and sensitivity-uncertainty analysis for the EMDF total system model (Sects. 5.3 and 5.4) incorporates uncertainty in future precipitation and the degree of EMDF cover performance degradation consistent with the range of HELP modeled infiltration values.

3.3.2 Radionuclide Release and Vadose Zone Model Codes

Models of radionuclide release from the EMDF waste mass and vadose zone transport between the bottom of the waste and the water table are included in EMDF PA models at different levels of detail and complexity. A relatively complex numerical model, STOMP (White and Oostrom 2000, White and Oostrom 2006) has been implemented to simulate release of radionuclides from EMDF waste in the aqueous phase and to provide information on variations in the location, magnitude, and timing of radionuclide release beneath the disposal unit under different cover performance conditions and radionuclide mobility assumptions. The STOMP output provides the basis for developing a simplified representation of the pattern of release to the water table that is applied in the 3-D saturated zone transport model (Sect. 3.3.3). The STOMP model provides radionuclide flux exiting the liner and entering groundwater in the saturated zone below the facility that is compared to similar outputs from the total-system model (used for dose analysis and described in Sects. 3.3.4 and 3.4). This provides a basis for assessing the simplified radionuclide release and vadose zone representations in the total-system model.

The STOMP model was developed by Pacific Northwest National Laboratory (PNNL) for modeling variably saturated subsurface flow and transport systems. The STOMP code meets Nuclear Quality Assurance (NQA)-1-2000 software requirements and DOE O 414.1D (DOE 2013b) requirements for safety software. PNNL maintains the STOMP code in accordance with DOE contractor requirements.

Documentation of all verification and validation testing is publicly available (White and Oostrom 2000, White and Oostrom 2006, and Nichols et al. 1997).

A summary description of STOMP model inputs and implementation for the EMDF system is provided in the following subsections. Additional detail on the STOMP model architecture, governing equations, and solution schemes is provided in White and Oostrom (2000 and 2006). Detailed information on STOMP model setup and parameterization for the EMDF is provided in Appendix E of this PA.

3.3.2.1 STOMP model domain setup for EMDF

EMDF preliminary design data and existing information on stratigraphic geometry and hydrogeologic properties of rock and saprolite units in BCV (Sects. 2.1.3 and 2.1.5) were used to create two 2-D cross-section STOMP models for the EMDF site (Figs. 3.14 through 3.18). The 2-D approach to STOMP implementation is based on how the geometry of the liner system is expected to control spatial patterns and timing of leachate release. It is also based on the practical consideration of the computing resources required to develop a fully 3-D model grid with sufficiently fine resolution to capture liner design details at the scale of the facility. Because flow and radionuclide transport in the vadose zone is likely to be predominantly vertical (downward), the 2-D representation is appropriate. The results of the 2-D implementation are judged to adequately capture the effects of the sloping cell bottoms and sides (berms), variable waste thickness, and modeled variation in vadose zone thickness (water table depth below the liner bottom, refer to Sect. 4.1). A primary purpose of the STOMP simulations is to guide development of simplified uniform and non-uniform models of release to the saturated zone, for which the 2-D results are sufficient.

The Section A-A′ (Section A) STOMP model is a northwest to southeast (NW-SE) section oriented parallel to the predominant disposal facility floor slope (Fig. 3.14). Section A crosses cells 1, 2, 3, and 4 obliquely and captures the horizontal drainage impact of the liner system geometry. The northwest end of the model (A) starts at the crest of Pine Ridge while the southeast ends (A′) at Bear Creek. The Section B-B′ (Section B) STOMP model is a northeast to southwest (northeast to southwest) oriented section through the crest of the final cover surface that captures the maximum waste thickness across all four waste disposal cells.

The material type boundaries defined at each cross-section are shown on Figs. 3.15 and 3.16, based on the preliminary design and configuration of geologic materials at the site. For the STOMP modeling, the HDPE and other synthetic components of the liner system are assumed to be fully degraded. Each figure also shows the current (pre-construction) topography, estimated top of bedrock and approximate location of the post-closure water table based on the long-term performance condition groundwater flow model results (refer to Sect. 3.3.3.1 for detail on implementation of the EMDF groundwater flow model).

Model Discretization. A uniform grid spacing of 10 ft is used in the X (horizontal) direction. Each grid is assumed to have a 1 ft thickness in the Y (normal to section) direction for easy mass calculation. A refined and uniform 1-ft grid space is used to represent the lithologic and design component variation in the vertical (Z) direction in most of the section, except in the deeper bedrock zone where it transitions to 5 ft and 10 ft in thickness. The finer grid spacing in the vertical direction represents the disposal facility features and lithologic variation more precisely for predicting movement of the contaminants in the unsaturated zone beneath the facility. The same model grid design is used for both southwest to northeast and west to east cross-sections. Additional detail on STOMP model discretization is presented in Appendix E, Sect. E.2.2.
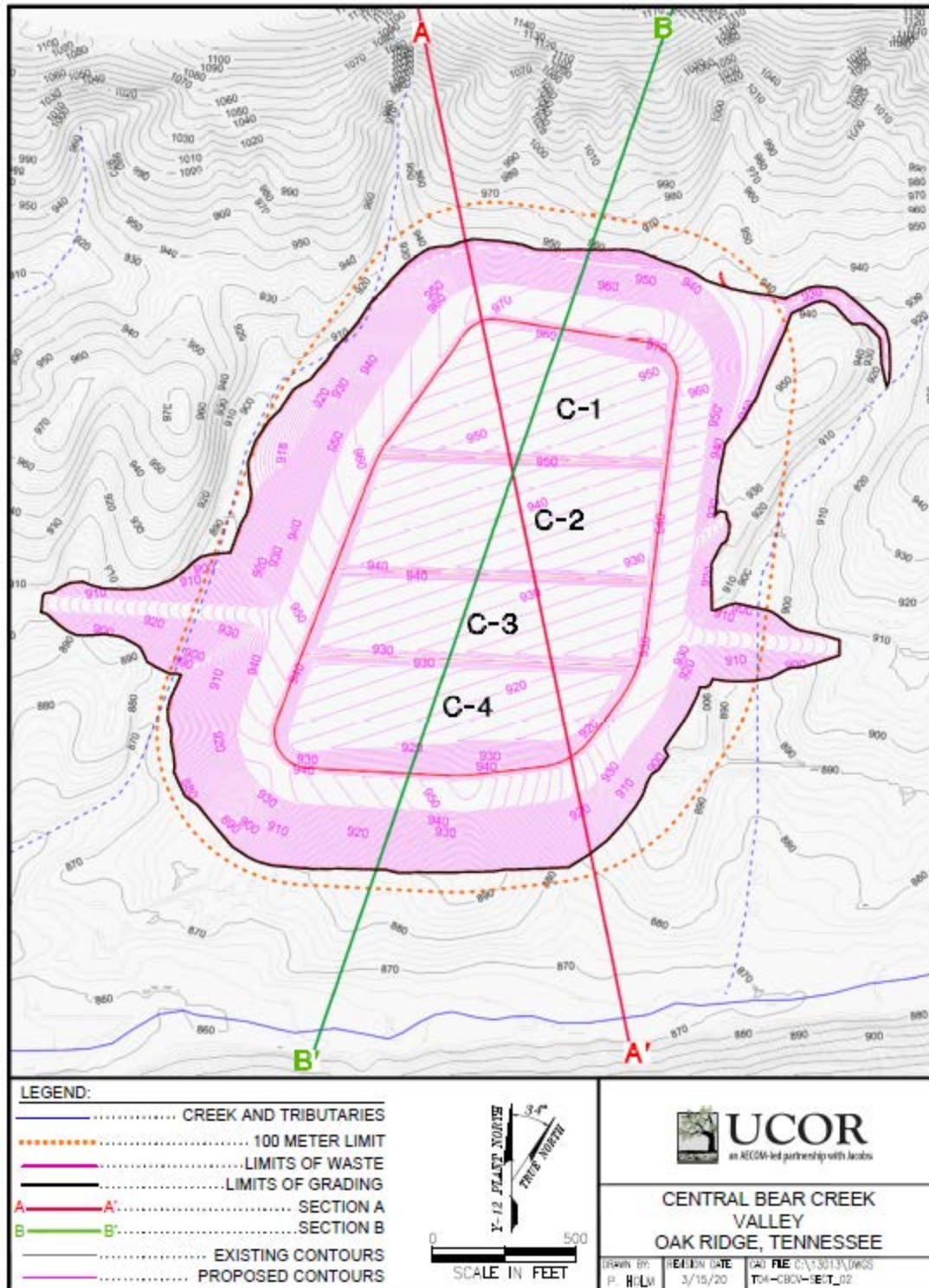
Fig. 3.14. Location of STOMP model cross-sections for EMDF
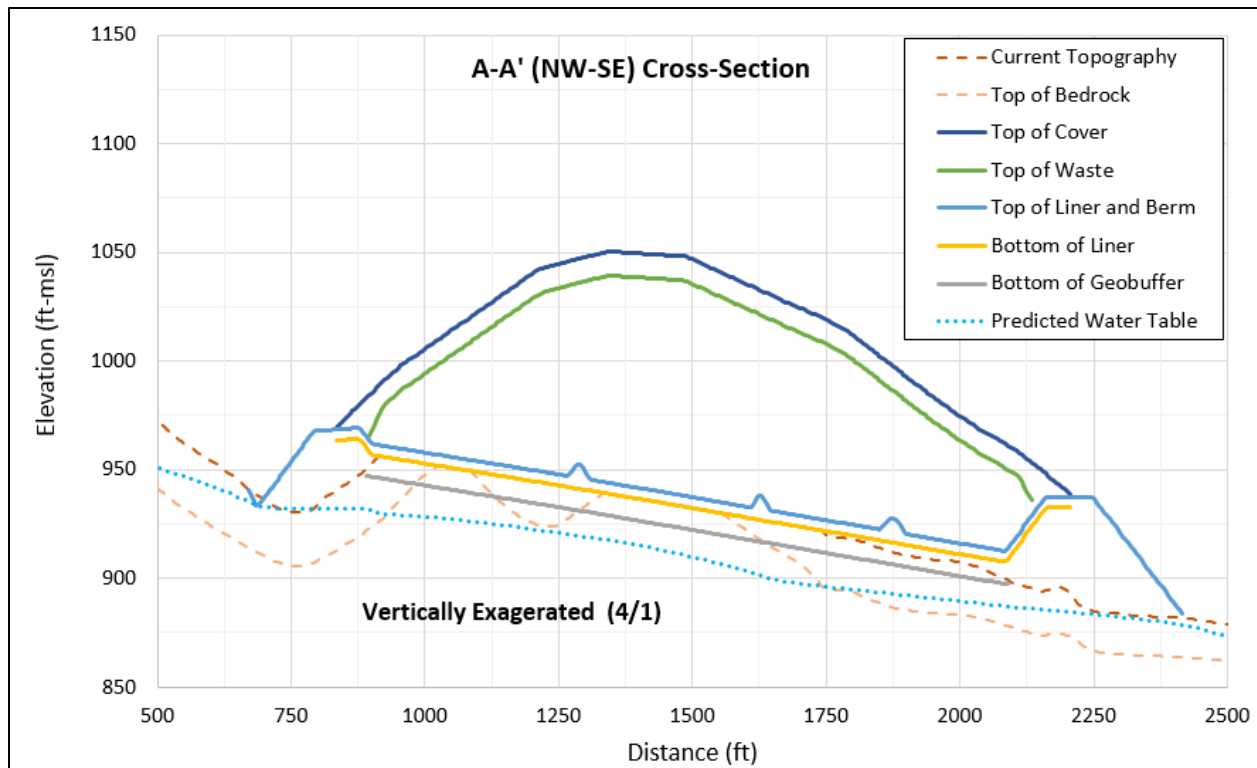
Fig. 3.15. Cross-section A-A′ material boundaries for STOMP model discretization
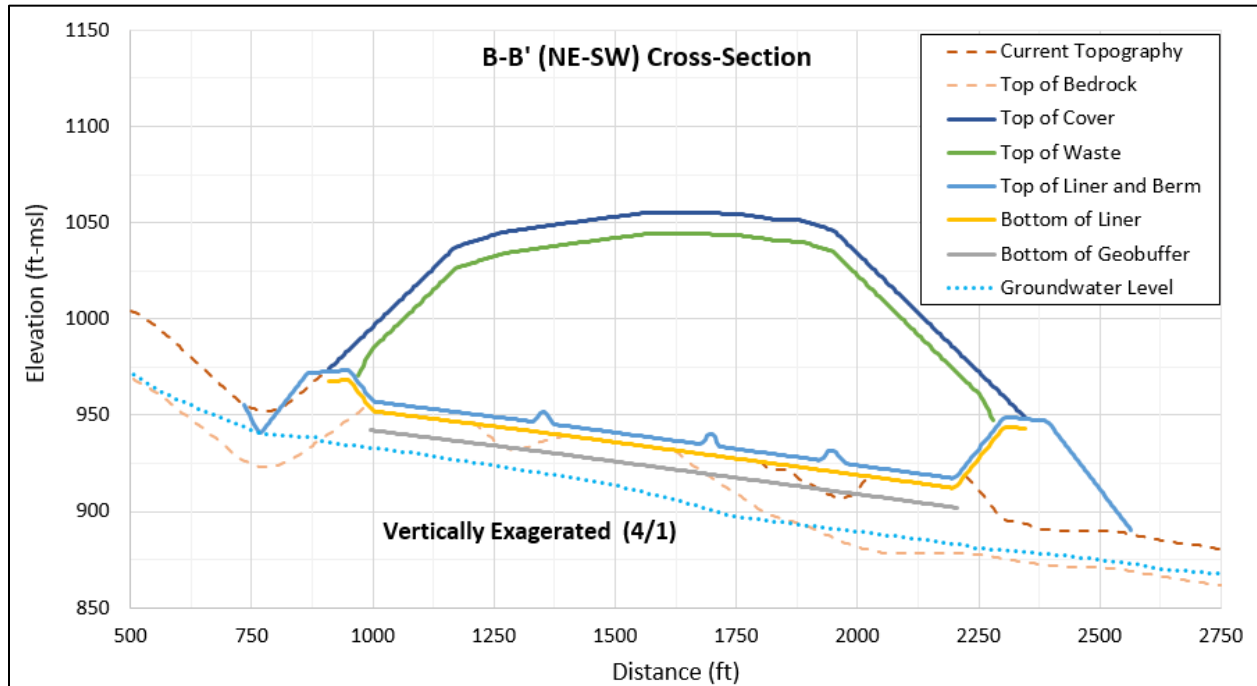
Fig. 3.16. Cross-section B-B′ material boundaries for STOMP model discretization

173
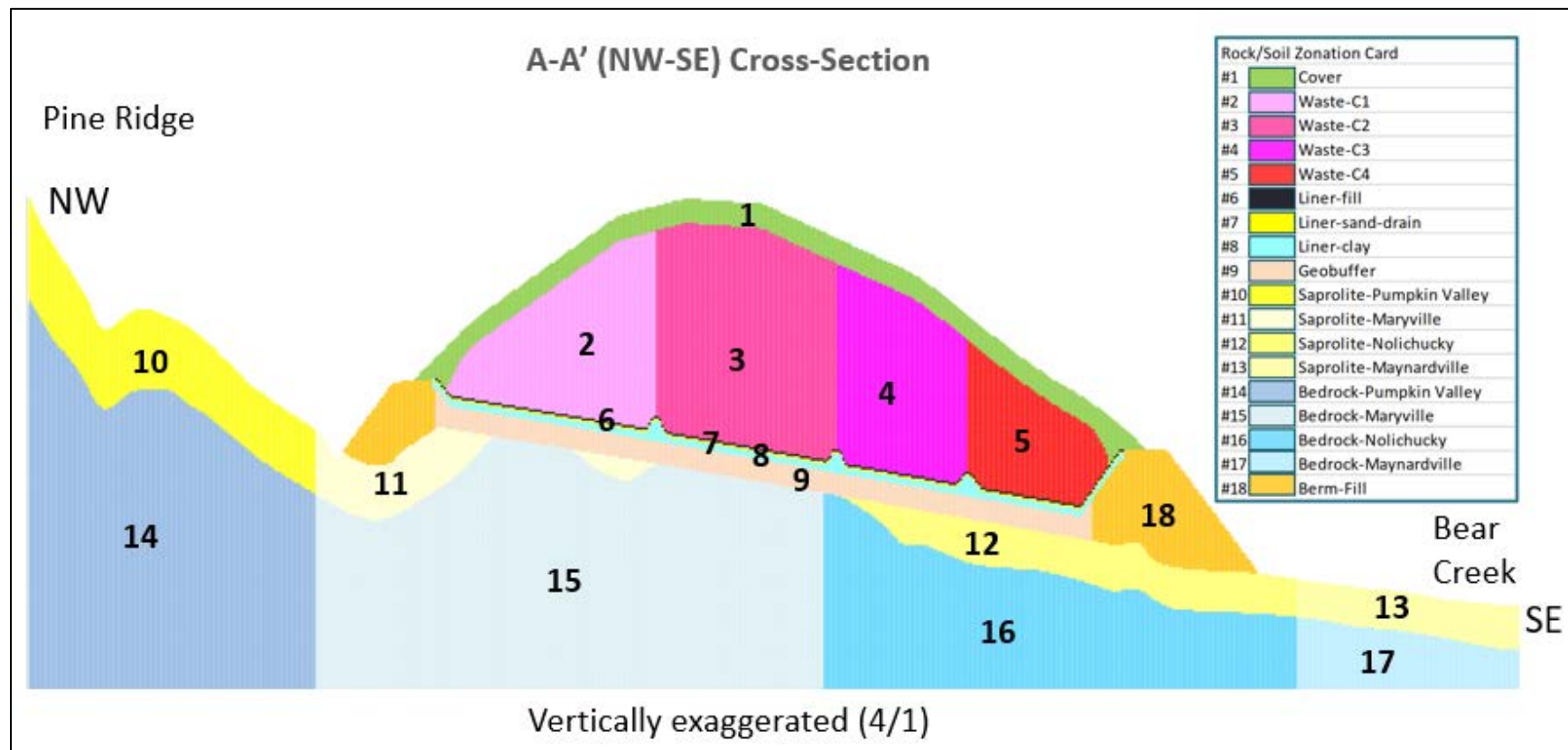
Fig. 3.17. Cross-section A-A′ material property zones
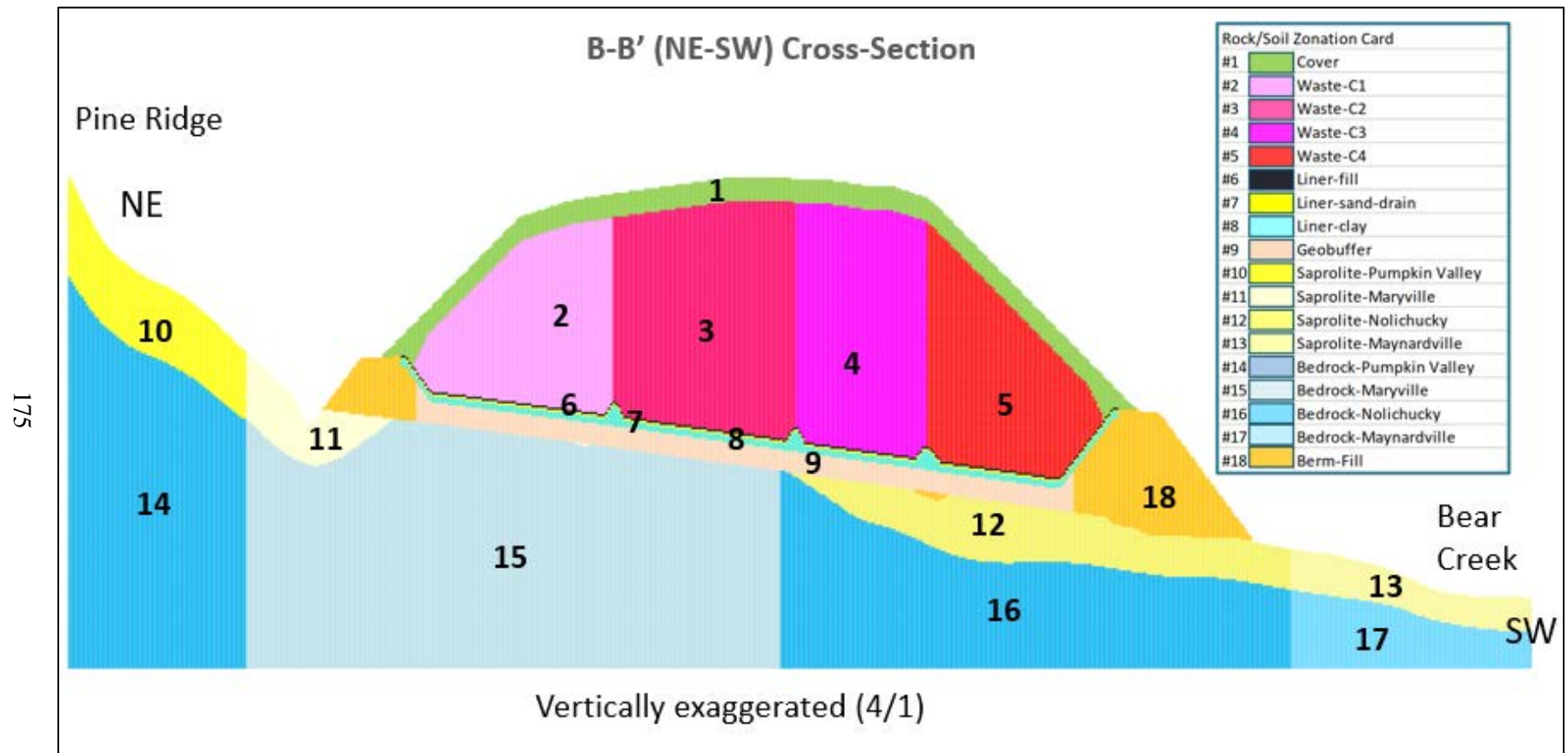
Fig. 3.18. Cross-section B-B' material property zones

Material Types. Properties of the materials in each 2-D zone of each cross-section (Figs. 3.17 and 3.18) are assigned for the following material types:

1) EMDF cover (single material type with properties derived from multilayer cover system design)

2) Waste-cell 1

3) Waste-cell 2

4) Waste-cell 3

5) Waste-cell 4

6) Liner-fill (protective material at the top of the liner system)

7) Liner-sand-drain (leachate drainage layer)

8) Liner-clay (infiltration barrier)

9) Geobuffer (geologic buffer zone)

10) Saprolite-Pumpkin Valley

11) Saprolite-Maryville (includes Rogersville and Rutledge units)

12) Saprolite-Nolichucky

13) Saprolite-Maynardville

14) Bedrock-Pumpkin Valley

15) Bedrock-Maryville (includes Rogersville and Rutledge units)

16) Bedrock-Nolichucky

17) Bedrock-Maynardville

18) Berm-fill (perimeter berms and structural fill).

The four waste material zones (2 through 5) are assigned a common set of properties, including initial radionuclide mass concentrations.

3.3.2.2   Model boundary conditions

The topographic surface for the EMDF (top of cover and berm) and the area outside of the footprint is the set of uppermost active model cells (nodes) where a free-air model boundary condition is assigned. All other boundary nodes where an unsaturated condition is present also have free-air boundary conditions that permit water discharge if the water pressure is greater than the atmospheric pressure. The bottom model boundary is assumed to be a no flow boundary. For the vertical boundaries at either end (southwest/northeast or west/east) of the model cross-sections, a hydraulic head gradient boundary condition (constant flux) is assigned for the saturated model nodes, allowing groundwater to flow in and out of the model domain at either end of the cross-section. The lower limit of the model domain was set well below the predicted long-term post-closure water table elevation (within the saturated zone) so that applied surface recharge rates and lateral flux boundary conditions do not lead to saturated conditions within the model domain above that elevation. For these 2-D model cross-sections, there is no flux into or out of the model domain in the Y direction.

Cover infiltration or (outside the cover limits) recharge boundary conditions are assigned along the top of the active model domain for each modeled cross-section. Spatial variation in the infiltration/recharge rate is assigned as shown in Fig. 3.19 for the Section A model. The same general recharge pattern is applied for

Section B. The infiltration/recharge rates applied in different areas include the natural recharge zones (6.1, 6.6, 9.6, and 13.1 in./year, depending on geologic unit), the berm side slopes (1 in./year), and the central cover/liner zone (increasing from 0 to 0.88 in./year between 200 and 1000 years post-closure). The maximum cover infiltration rate (0.88 in./year) is based on hydrologic performance model results for the long-term cover performance condition (Table 3.13), and the timing of the increase in infiltration is based on the assumed evolution of EMDF cover performance over time (Fig. 3.5). Sensitivity to the long-term cover performance assumption is addressed with a simulation assuming long-term cover infiltration increases to 1.76 in./year at 1000 years post-closure (Sect. 5.1).
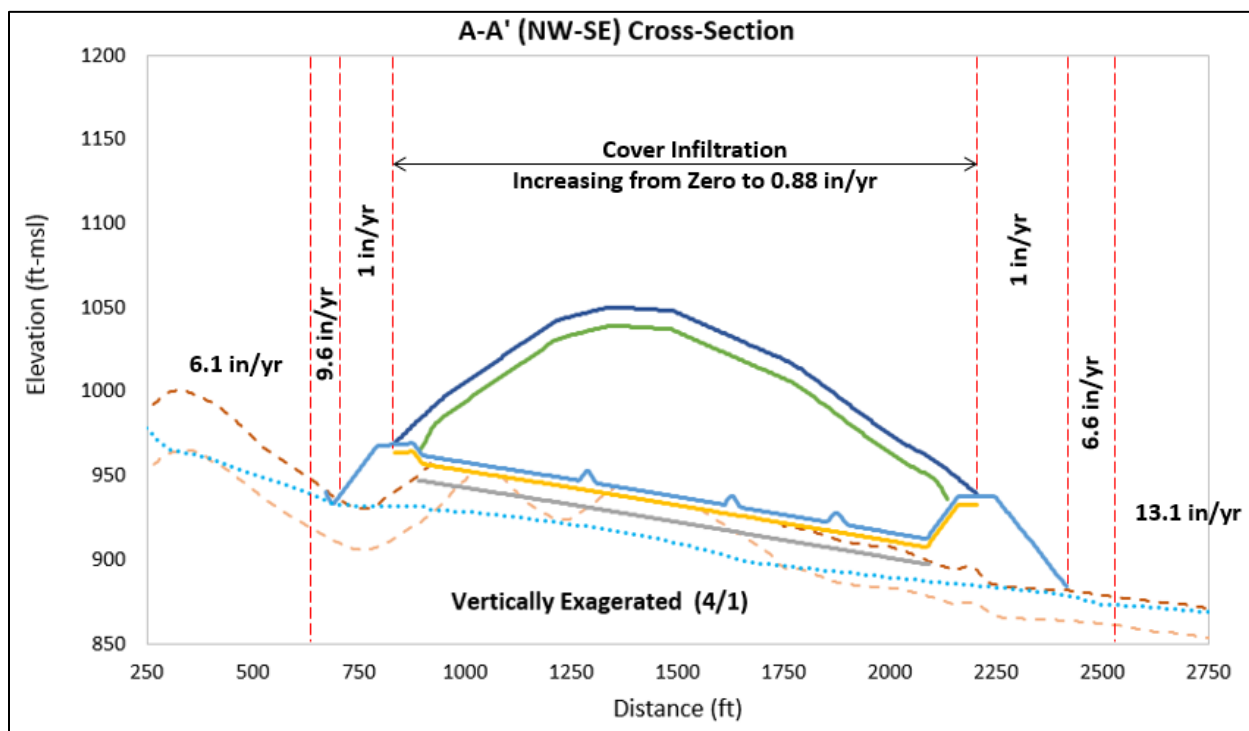
Fig. 3.19. Recharge zones applied to the STOMP Section A model

3.3.2.3   Material property inputs

The input parameter categories required to conduct a STOMP simulation include media mechanical and hydraulic properties; saturation function parameters; aqueous relative permeability relationship parameters for unsaturated flow; solute-fluid interaction; and solute-porous media interaction. These specific properties include the following:

- Mechanical properties include a particle density, porosity (total and diffusive), specific storativity, compressibility, and tortuosity function for each defined rock/soil type

- Hydraulic properties include an intrinsic permeability or hydraulic conductivities in each coordinate direction for each defined rock/soil type

- Saturation function parameters define a saturation-capillary pressure function for each defined rock/soil type

- Aqueous relative permeability parameters defines a relative permeability-saturation function for the aqueous phase for each defined rock/soil type

177

- Solute-fluid interactions define solutes, solutes, solubilities, diffusion coefficients, and solute radioactive decay path parameters (half-life)

- Solute-porous media interactions define solid-aqueous phase K_d and porous-media-dependent hydraulic dispersivities; solute-porous parameters are dependent on both the solute and rock/soil type.

Tables of STOMP input parameter values are provided in Appendix E, Sect. E.2.5. In general, the waste properties are assumed to be the same for all disposal cells, and material properties vary among the waste, cover, and liner system components as well as the geobuffer material, saprolite, and bedrock zones. The engineered materials and waste are assumed to be hydraulically isotropic, whereas the natural materials have anisotropic hydraulic conductivity values identical to those applied in the EMDF groundwater flow model (refer to Appendix D). Saturation and relative permeability functions are assumed to be similar across vadose material types except for minimum relative saturation values, which vary according to assumed material texture/pore size distribution (refer to Appendix E).

Values for all material property input parameters used in the EMDF STOMP models are based on available BCV data, design assumptions, or literature values. Values for material parameters (e.g., bulk density, porosity, saturated hydraulic conductivity, etc.) that are used in multiple EMDF models are consistent (equal values) in all cases where material zones or engineered layers were defined similarly across models. In some cases, (weighted) average values for some parameters are utilized for models with less detailed representation of system components such as cover system layers (STOMP) or saturated zone stratigraphy (RESRAD-OFFSITE). Detailed descriptions of input parameter values, data sources, and approaches for deriving average quantities are provided in the model-specific appendices (Appendix E for the STOMP model) and QA documentation (UCOR 2020b). An additional description of the QA procedures for ensuring and documenting consistency in assumptions and parameter values across models is provided in Sect. 9.

3.3.2.4 Initial radionuclide concentrations and solid-aqueous partition coefficients

Initial Radionuclide Concentrations in Waste. Based on initial simulations with the total system model (Sect. 3.3.4), a limited number of highly mobile or long-lived radionuclides were selected from the EMDF estimated inventory (Sect. 2.3 and Appendix B). These radionuclides have estimated inventories and other characteristics that result in large predicted dose contributions (relative to other radionuclides), either in the first few thousand years post-closure (C-14, Tc-99, I-129) or much later due to greater chemical retardation of transport (U-234, U-238, Pu-239). Tritium was also included in the STOMP simulations.

It is assumed that the waste has a uniform average initial radionuclide mass concentration throughout the four disposal cells. Estimated inventory concentrations are expressed in terms of activity concentrations (pCi/g) and must be converted to radionuclide mass per waste volume units (mg/L) as initial waste concentrations in the STOMP model. Table 3.14 summarizes the estimated waste average (as-generated) activity concentrations, adjusted concentrations to account for addition of clean fill (soil) and operational period losses of mobile radionuclides, and equivalent mass concentrations based on radionuclide specific activities and an assumed waste dry bulk density of 1900 kg/m^3.

Table 3.14. Initial activity and mass concentrations for the waste in STOMP model simulations

Radionuclide	As-generated waste average activity concentration (pCi/g)	As-disposed[a] waste average activity concentration (pCi/g, corrected for added clean soil mass)	Initial mass concentration (g/g)	Initial Volumetric concentration (mg/L)
H-3	2.10E+01	4.64E+00	4.73E-16	9.00E-10
C-14	5.43E+00	5.40E-01	1.20E-13	2.28E-07
Tc-99	5.28E+00	1.56E+00	9.18E-11	1.74E-04
I-129	7.66E-01	3.50E-01	1.94E-09	3.69E-03
U-234	1.19E+03	6.30E+02	1.02E-07	1.93E-01
U-238	7.18E+02	3.81E+02	1.12E-03	2.13E+03
Pu-239	1.10E+02	5.83E+01	9.25E-10	1.76E-03

[a] H-3, C-14, Tc-99, and I-129 concentrations are decreased to account for operational period losses.

STOMP = Subsurface Transport Over Multiple Phases

Solid-Aqueous Partition Coefficients. The assumed solid-aqueous partition coefficient values (K_d values, Table 3.15) for each of the radionuclides included in the STOMP model is based on available data for ORR materials and review of other data sources. Base case K_d values and data sources for all radionuclides included in the estimated EMDF radionuclide inventory are provided in Sect. 3.2.2.6. The base case K_d values in the waste zone are assumed to be one-half the base case K_d values assigned to the non-waste materials.

Table 3.15. Solid-aqueous partition coefficients for radionuclides included in STOMP modeling

Radionuclide	K_d (Waste) (cm³/g)	K_d (Other Materials) (cm³/g)	Half-life (year)	Specific Activity (Ci/g)
H-3	0	0	1.23E+01	9.80E+03
C-14	0	0	5.70E+03	4.50E+00
Tc-99	0.36	0.72	2.11E+05	1.70E-02
I-129	2	4	1.57E+07	1.80E-04
U-234	25	50	2.46E+05	6.20E-03
U-238	25	50	4.47E+09	3.40E-07
Pu-239	20	40	2.41E+04	6.30E-02

K_d = partition coefficient
STOMP = Subsurface Transport Over Multiple Phases

Model sensitivity to uncertainty in K_d values was evaluated with sensitivity runs utilizing either lower values for all non-waste media or higher values for the waste zone. For K_d value sensitivity runs, both the waste and non-waste media were assigned either the (lower) waste K_d value or the (higher) non-waste value. Results of STOMP model sensitivity runs are presented in Sect. 5.1 and Appendix E, Sect. E.3.3.

The STOMP model results are used to estimate an average vadose delay time for each radionuclide. This delay is due to the cover/liner system preventing infiltration and leachate release during the design performance period (assumed as 200 years for the PA analysis) and also results from chemical retardation of radionuclides migrating vertically through the unsaturated zone above the water table. The vadose delay time was assigned as the year at which the STOMP model total radionuclide flux reached 50 percent of the

peak simulated flux at the water table elevation. Additional detail is provided in Appendix E, Sect. E.3.4.2. The STOMP-based delay times were used in developing radionuclide-specific release models for calculating radionuclide flux to the water table in the MT3D saturated zone transport model (refer to Sect. 3.3.3.2 and Appendix F).

In addition to providing the basis for the vadose delay time estimates, the STOMP model results were used to quantify non-uniformity in volumetric leachate flux and radionuclide flux at the water table beneath the EMDF liner and geologic buffer. These STOMP results were applied develop non-uniform waste area leachate flux and recharge concentrations for the MT3D model analysis of the impact of non-uniform release on saturated zone model results at the groundwater POA. Additional details on the use of STOMP model results to support the saturated zone radionuclide transport modeling are provided in Sect. 3.3.3.2 and Appendix F.

3.3.3 Saturated Zone Flow and Transport Model Codes

Model tools utilized for the EMDF saturated zone are 3-D models of groundwater flow (MODFLOW) and radionuclide transport (MT3D). This pair of models is used to simulate the effect of the local reduction in groundwater recharge below EMDF following facility closure and to provide a fully 3-D simulation of radionuclide transport in the heterogeneous, anisotropic, fractured-rock system at the CBCV site. A separate radionuclide release approximation (release model) was developed to provide the time-varying radionuclide flux to the water table below the disposal unit.

3.3.3.1 Groundwater flow model

The groundwater model was developed based on the BCV regional groundwater flow model (DOE 1997b). This regional model forms the foundation for all the sub-regional and site-specific models developed for the Bear Creek, Y-12, and the EMWMF sites (DOE 1998a, BJC 2003, BJC 2010a). The BCV model and site-specific models were developed using MODFLOW code, a finite-difference groundwater flow code developed by USGS (USGS 1988a). MODFLOW is a modular, block-centered finite-difference groundwater flow code capable of simulating both transient and steady-state saturated groundwater flow in one, two, or three dimensions.

MODFLOW implicitly considers that the system can be characterized as a porous medium. The application of a porous media code to a fractured bedrock system such as BCV is, therefore, an EPM approach. This approach assumes the rock is fractured to the extent that it behaves hydraulically as a porous medium. Three-D representation of hydraulic properties within MODLFOW also provides flexibility to represent fracture orientations in terms of anisotropy and fracture distribution in terms of heterogeneity. This approach is applicable to BCV given the high degree of weathering near the surface, numerous bedding planes and fractures in the sedimentary rock units, presence of a very active groundwater flow system, and extensive groundwater-surface water interaction. Previous model applications in BCV show consistency with field groundwater and surface flow measurements through mass balance analyses and with contaminant plume extent and movement through particle tracking (USGS 1988b, DOE 1997b, BJC 2010a).

Groundwater flow models were developed to represent current, pre-construction conditions (CBCV model) and future, post-closure conditions (EMDF model). The CBCV model incorporates recently completed site characterization data (Sect. 2.1.11) and was calibrated against a year of groundwater and surface water monitoring data (Appendix D, Sect. D.3.3). The EMDF model incorporates preliminary design features and incorporates the assumptions regarding long-term changes in cover infiltration in the post-closure period. Setup of the model domain, vertical discretization (model layering), and parameterization are reviewed

briefly in the following subsections. Additional detail on model development, including calibration, is provided in Appendix D.

MODFLOW code setup and parameterization. The extent of the model domain for the CBCV and EMDF flow models was selected based on the EMDF location, calibration data availability, and consideration of the effects of imposed boundary conditions on model predictions close to the disposal site. The model domain (Fig. 3.20) and finite difference grid are based on a telescopic mesh refinement applied to the calibrated regional flow model originally constructed for the BCV FS (DOE 1997c). The models have a 10 ft × 10 ft horizontal grid spacing with nine vertical layers (Fig. 3.21).

Material parameters for the nine model layers are selected to reflect vertical variation in the hydraulic properties (porosity, hydraulic conductivity, anisotropy) of the geologic media and engineered materials. Model layer 1 represents the saprolite zone and engineered features (e.g., berms and liner system in the EMDF model). Model layers 2, 3, and 4 represent highly fractured bedrock, and layers 5 through 9 represent less fractured bedrock. The EMDF flow model includes modifications to the upper two model layers to represent the EMDF liner and geobuffer configuration. The top two model layers have variable thicknesses ranging from 4 to 88 ft, reflecting variation in the thickness of the saprolite zone (Fig. 3.21) and the engineered features in the EMDF model.

Six distinct hydraulic conductivity zones for each model layer (shown for model layer 1 in Fig. 3.22) were used in the flow models to represent the eight geologic units that exist in BCV (Knox, Maynardville, Nolichucky, Maryville-Rogersville-Rutledge [combined], Pumpkin Valley, and Rome Formations) based on existing field measurements (Sect. 2.1.5.4) of hydrological properties. The selection of these geologic units as distinct hydraulic units is based on the thickness of the units, the availability of hydraulic data, and lithologic and hydraulic similarity among units. For the EMDF model, additional zones for layer 1 were incorporated to represent liner/geobuffer materials and areas of structural fill (Fig. 3.22). The CBCV site is modeled as a single unconfined system, with decreasing hydraulic conductivity with depth, and the 45-degree dip in the geological strata represented by staggering hydrogeologic units (conductivity zones) with depth (Fig. 3.23, Table 3.16).

Previous BCV field observations and modeling efforts (Sect. 2.1.5.4) have established that the groundwater system is strongly anisotropic and flows preferentially along the geologic strike (model y-coordinate direction). The K_y value represents the conductivity parallel to strike, K_x is the horizontal conductivity perpendicular to strike, and K_z represents the vertical hydraulic conductivity. Anisotropy ratios [K_y vs. K_x or K_z] of 5:1 (for model layer 1) and 10:1 (for layers 2-9) were used to represent the preferred fracture/bedding orientation of the geologic units (Table 3.17). Both field data and previous modeling sensitivity analyses support the anisotropy ratios used in the model (Appendix D, Sect. D.3.2.1).
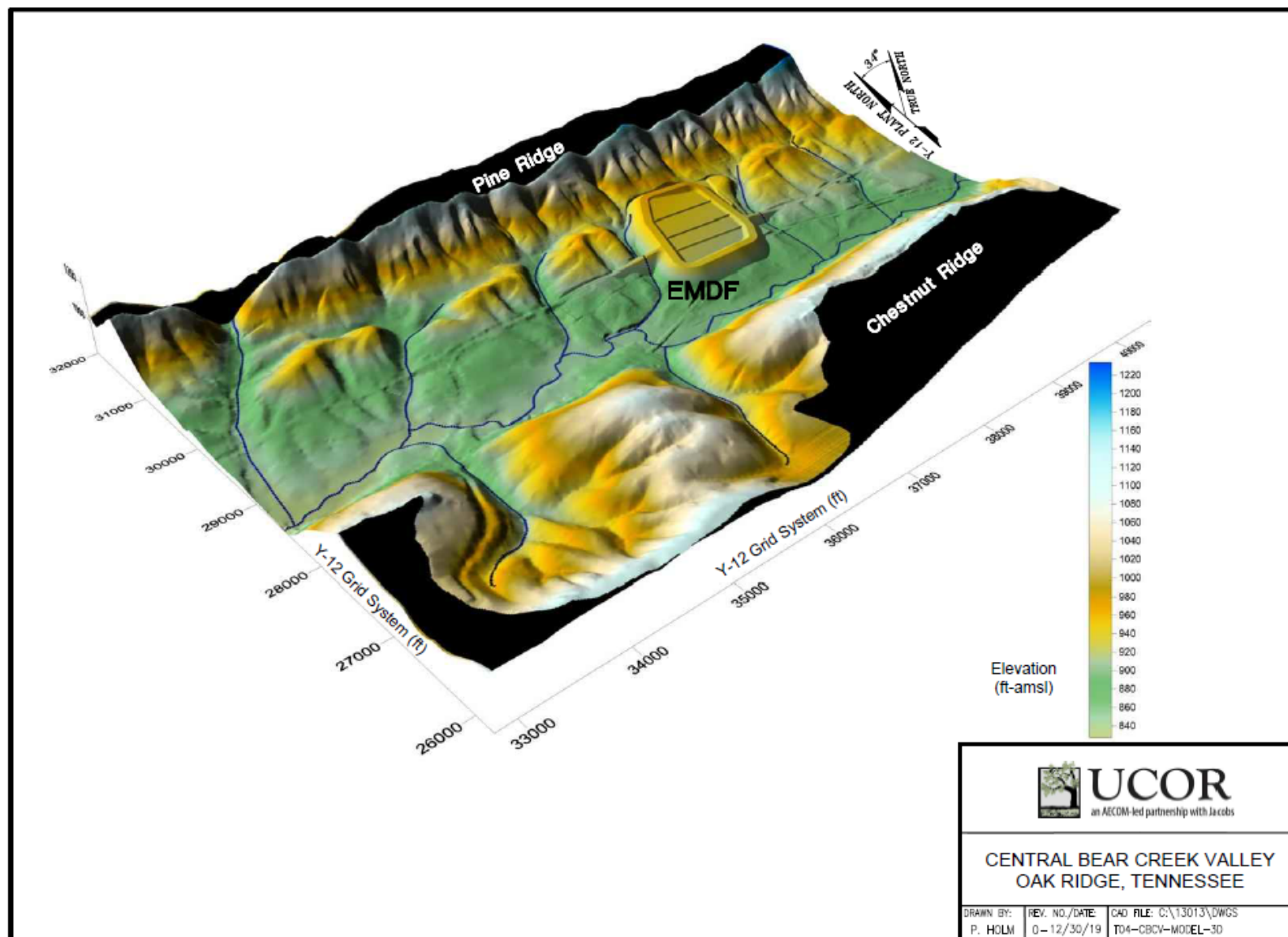
Fig. 3.20. EMDF groundwater flow model domain and topography
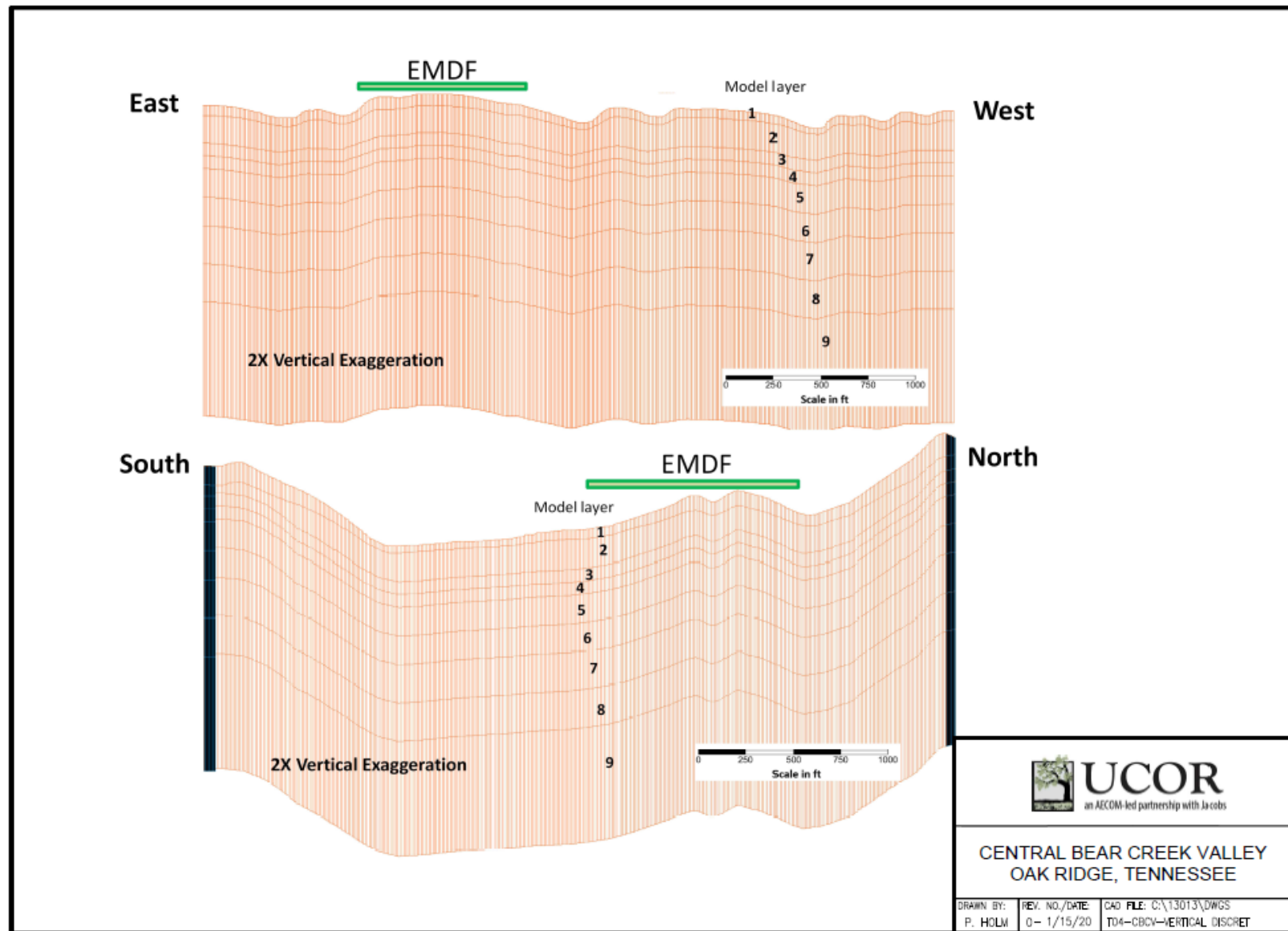
Fig. 3.21. CBCV model vertical cross-sections showing horizontal and vertical discretization
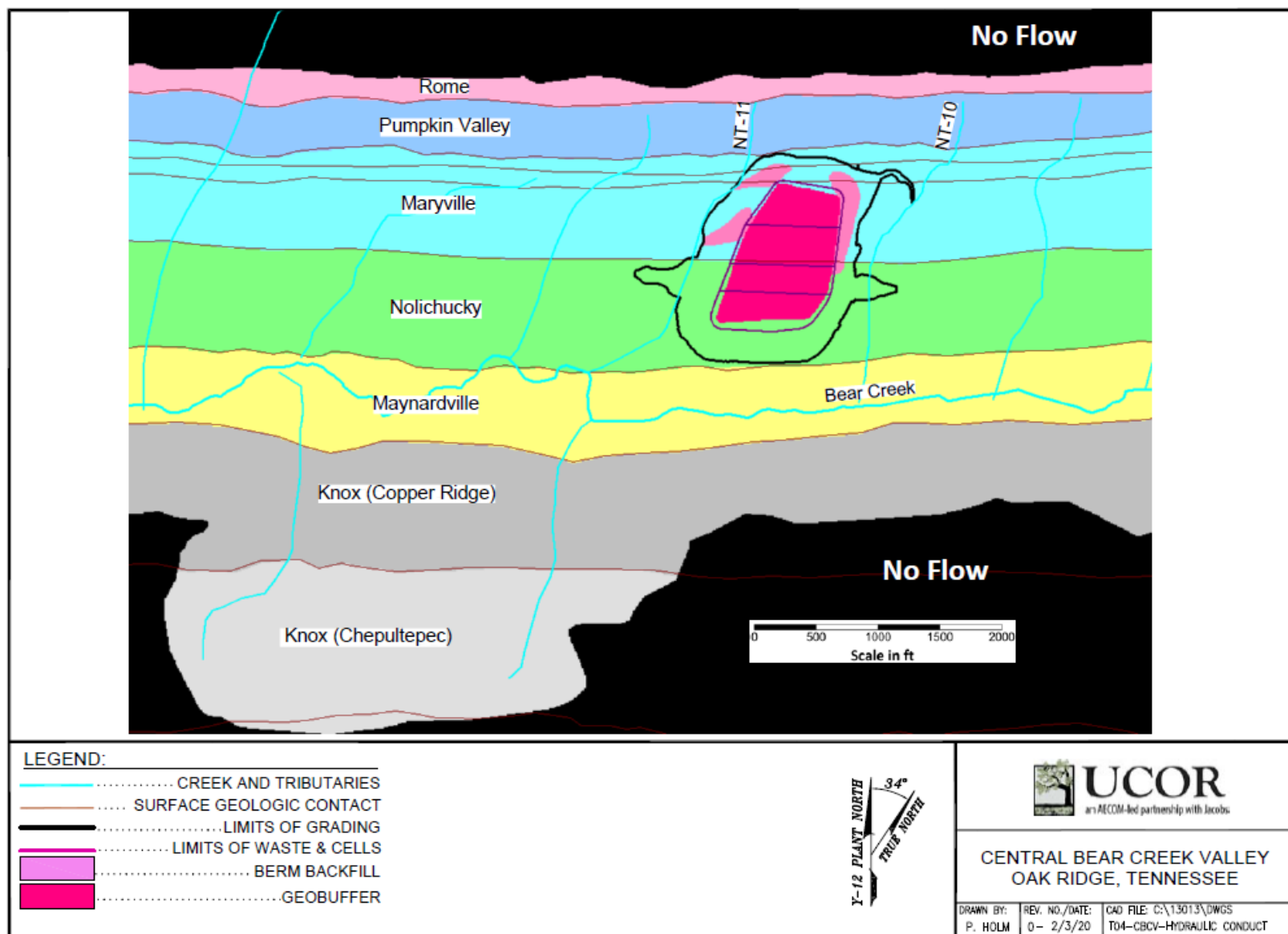
Fig. 3.22. Hydraulic conductivity zones corresponding to geological units in EMDF model layer 1
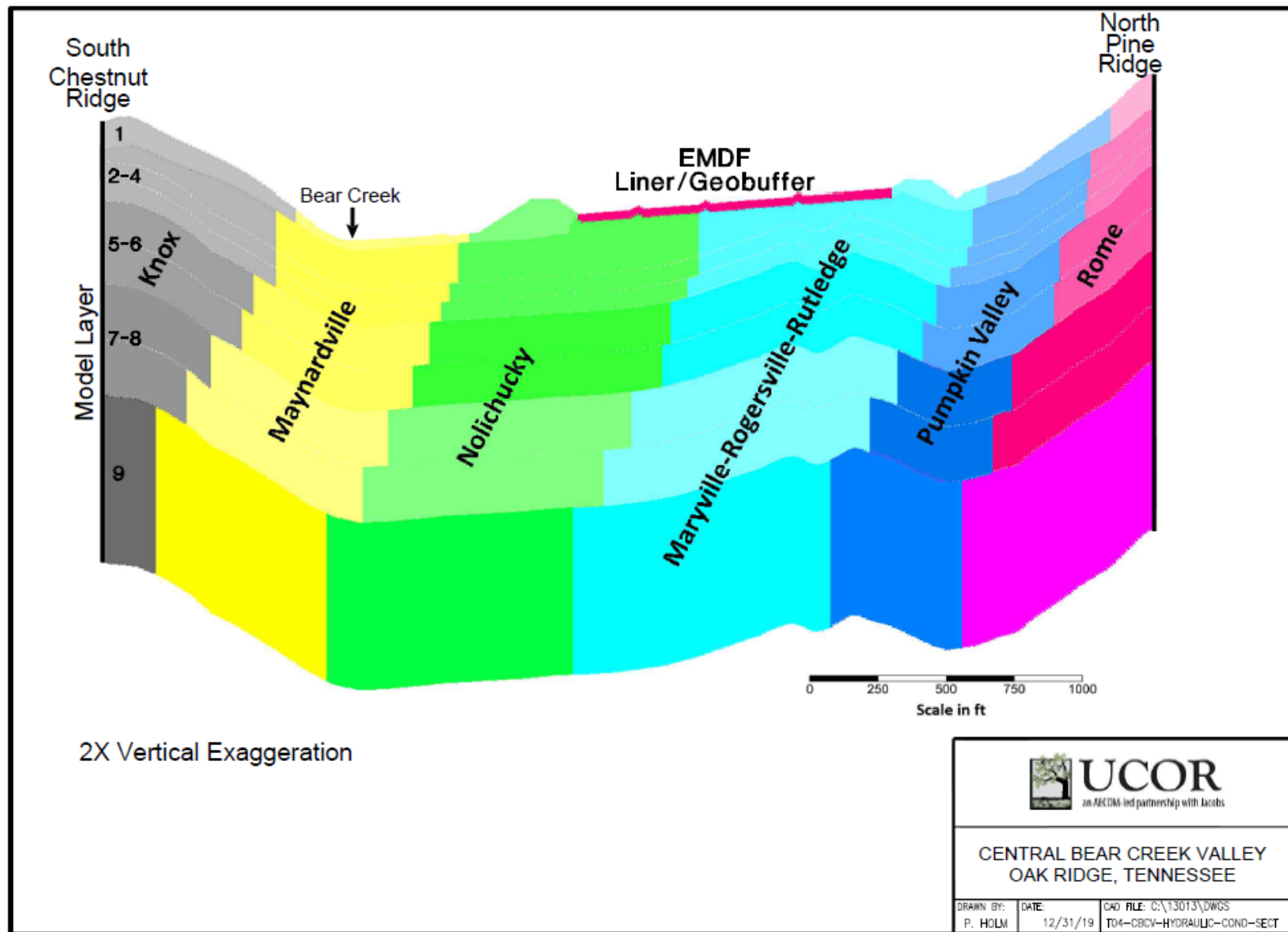
Fig. 3.23. Hydraulic conductivity field representing BCV stratigraphy and engineered features in the EMDF flow model

Table 3.16. Hydraulic conductivity values for geologic formations and model layers of the CBCV and EMDF flow models

Geologic Formation	Model Layer	Kx (ft/day)	Ky (ft/day)	Kz (ft/day)	Ky/Kx Ky/Kz	Kx (cm/sec)	Ky (cm/sec)	Kz (cm/sec)
Knox	1	1.56E+00	7.80E+00	1.56E+00	5	5.5E-04	2.7E-03	5.5E-04
	2--4	9.18E-03	9.18E-02	9.18E-03	10	3.2E-06	3.2E-05	3.2E-06
	5--6	2.54E-03	2.54E-02	2.54E-03	10	8.9E-07	8.9E-06	8.9E-07
	7--8	1.16E-03	1.16E-02	1.16E-03	10	4.1E-07	4.1E-06	4.1E-07
	9	5.00E-04	5.00E-03	5.00E-04	10	1.8E-07	1.8E-06	1.8E-07
Maynardville	1	2.13E+00	1.07E+01	2.13E+00	5	7.5E-04	3.8E-03	7.5E-04
	2--4	5.00E-02	5.00E-01	5.00E-02	10	1.8E-05	1.8E-04	1.8E-05
	5--6	3.34E-03	3.34E-02	3.34E-03	10	1.2E-06	1.2E-05	1.2E-06
	7--8	1.52E-03	1.52E-02	1.52E-03	10	5.4E-07	5.4E-06	5.4E-07
	9	4.80E-04	4.80E-03	4.80E-04	10	1.7E-07	1.7E-06	1.7E-07
Nolichucky	1	1.50E-01	7.50E-01	1.50E-01	5	5.3E-05	2.6E-04	5.3E-05
	2--4	9.50E-03	9.50E-02	9.50E-03	10	3.4E-06	3.4E-05	3.4E-06
	5--6	2.52E-03	2.52E-02	2.52E-03	10	8.9E-07	8.9E-06	8.9E-07
	7--8	6.10E-04	6.10E-03	6.10E-04	10	2.2E-07	2.2E-06	2.2E-07
	9	5.00E-05	5.00E-04	5.00E-05	10	1.8E-08	1.8E-07	1.8E-08
Maryville-Rogersville-Rutledge	1	1.00E-01	5.00E-01	1.00E-01	5	3.5E-05	1.8E-04	3.5E-05
	2--4	3.60E-03	3.60E-02	3.60E-03	10	1.3E-06	1.3E-05	1.3E-06
	5--6	1.35E-03	1.35E-02	1.35E-03	10	4.8E-07	4.8E-06	4.8E-07
	7--8	3.20E-04	3.20E-03	3.20E-04	10	1.1E-07	1.1E-06	1.1E-07
	9	4.50E-05	4.50E-04	4.50E-05	10	1.6E-08	1.6E-07	1.6E-08
Pumpkin Valley	1	1.00E-01	5.00E-01	1.00E-01	5	3.5E-05	1.8E-04	3.5E-05
	2--4	4.72E-03	4.72E-02	4.72E-03	10	1.7E-06	1.7E-05	1.7E-06
	5--6	1.75E-03	1.75E-02	1.75E-03	10	6.2E-07	6.2E-06	6.2E-07
	7--8	4.20E-04	4.20E-03	4.20E-04	10	1.5E-07	1.5E-06	1.5E-07
	9	5.60E-05	5.60E-04	5.60E-05	10	2.0E-08	2.0E-07	2.0E-08
Rome	1	4.00E-01	2.00E+00	4.00E-01	5	1.4E-04	7.1E-04	1.4E-04
	2--4	4.00E-02	4.00E-01	4.00E-02	10	1.4E-05	1.4E-04	1.4E-05
	5--6	5.00E-03	5.00E-02	5.00E-03	10	1.8E-06	1.8E-05	1.8E-06
	7--8	1.00E-03	1.00E-02	1.00E-03	10	3.5E-07	3.5E-06	3.5E-07
	9	5.00E-04	5.00E-03	5.00E-04	10	1.8E-07	1.8E-06	1.8E-07

CBCV = Central Bear Creek Valley
EMDF = Environmental Management Disposal Facility

Table 3.17. Recharge rates for the EMDF flow model

Recharge areas	Recharge rate	
	ft/day	in./year
Rome	2.20E-03	9.6E+00
Pumpkin Valley	1.40E-03	6.1E+00
Maryville-Rogersville-Rutledge	2.20E-03	9.6E+00
Nolichucky	1.50E-03	6.6E+00
Maynardville	3.00E-03	1.3E+01
Knox (Copper Ridge)	1.00E-03	4.4E+00
Knox (Chepultepec)	5.00E-04	2.2E+00
EMDF berm slope	2.28E-04	1.0E+00
EMDF lined area	2.00E-04	8.8E-01

EMDF = Environmental Management Disposal Facility

Groundwater Flow Model Boundary Conditions. The groundwater system in BCV is bounded by Pine Ridge to the north and Chestnut Ridge to the south; the two ridge crests coincide with the northern and southern no-flow boundaries of the groundwater model domain (Fig. 3.24). The vertical base (bottom) of the model also is assumed to be a no-flow boundary because minimal exchange of meteoric water with mineralized groundwater occurs below this depth (about 800 ft bgs [Sect. 2.1.6.1]). Constant head boundary conditions were assumed along the west (outflow) and east (inflow) ends of the model, based on a steady-state simulation of the calibrated regional BCV groundwater flow model (Appendix D).

Recharge from precipitation is the primary source of inflow to groundwater for the model because the domain is bounded on two sides by no-flow boundaries and two sides by the constant head boundaries. Varying recharge rates were assigned in the model for different zones corresponding to surface exposure of different geological units, hydrologic properties of soils, and assumed values for the perimeter berms (1 in./year) and the EMDF liner footprint (Table 3.17). For the EMDF flow model, cover infiltration rates representing three different performance conditions (Sect. 3.3.1.2) were applied as the recharge rate to the lined area (Fig. 3.22). Model sensitivity to higher and lower recharge rates was evaluated for both the CBCV model and the EMDF model.

The EMDF flow model results supported the development of the preliminary design and the long-term performance analysis, providing estimated water table elevations and groundwater flow fields beneath the disposal unit. For the saturated zone radionuclide transport modeling described in the following section, the EMDF model with the recharge rate that represents the long-term performance condition (0.88 in./year applied to the lined area of the disposal unit) is used to provide the flow field for the MT3D transport model. This approach over estimates EMDF recharge for the period of degrading cover performance (between 200 and 1000 years) assumed for the base case scenario, and results in quicker saturated zone transport toward the 100 m buffer during that period. This simplification in applying the recharge boundary condition to the EMDF footprint thus provides a measure of pessimistic bias to the modeling.
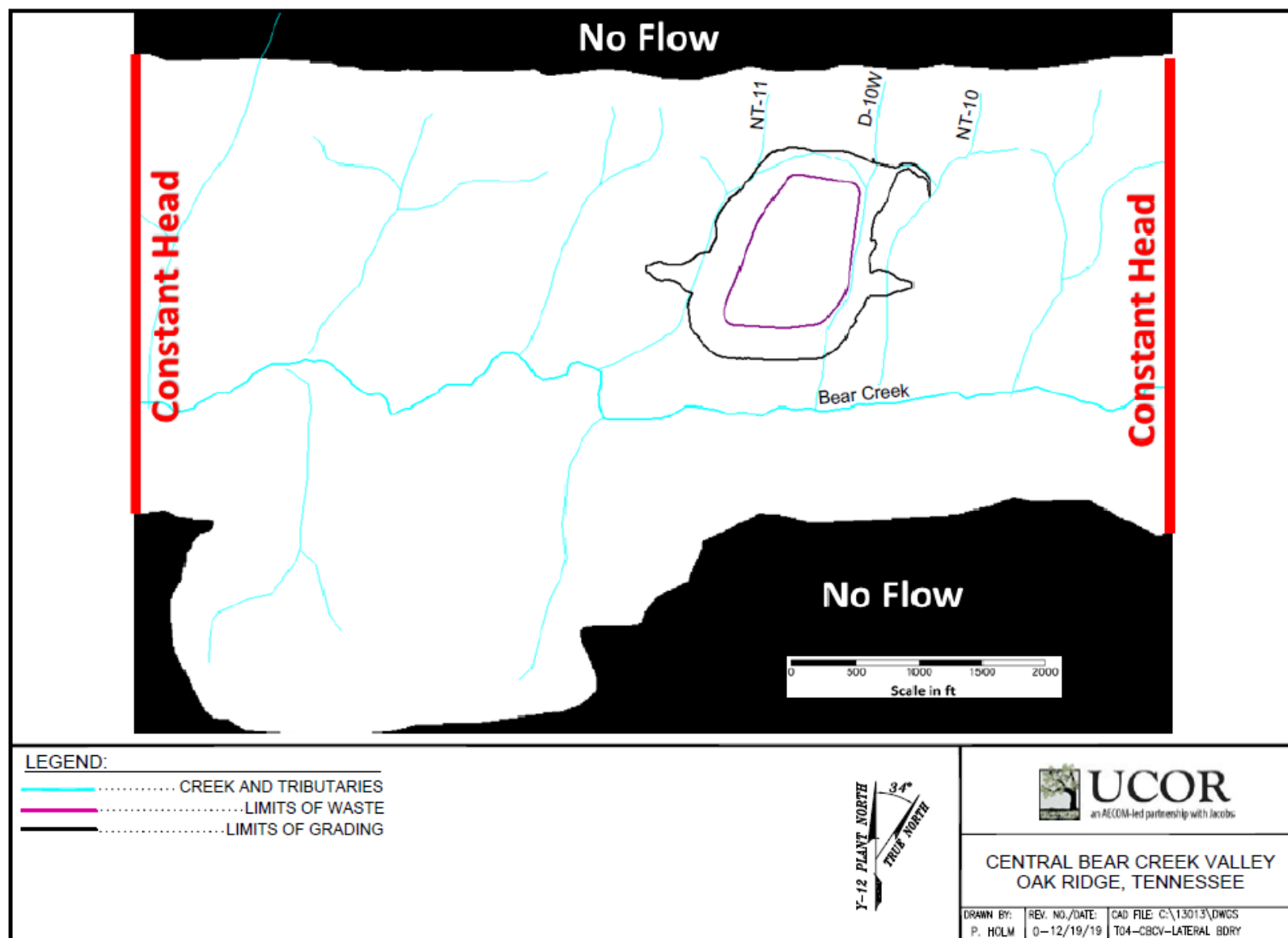
Fig. 3.24. Hydraulic boundary conditions for the EMDF flow model

Model domain interior boundary conditions represent the surface water-groundwater connections. The surface drainage features are represented in the model as either drain cells (for Bear Creek tributaries) or river cells. Both drain cells and river cells are head-dependent flux boundary conditions. Drain cells only allow groundwater to discharge at a surface water feature, whereas river cells allow both influx (gaining) and outflux (loosing) interaction with the groundwater. Section 2.1.7 presents a discussion of spatial and seasonal variations in surface water flows that reflect variability in groundwater discharge.

Appendix D provides a detailed description of the development and calibration of the CBCV model and the application of the EMDF model to the PA analyses. The primary uses of the EMDF flow model results are to provide an estimate of the average vertical interval between the bottom of waste and the water table (vadose zone thickness) for the long-term performance condition, and as the groundwater flow field for the MT3D saturated zone radionuclide transport model. These flow model results support the parameterization of the vadose zone (thickness) in the total system model (RESRAD-OFFSITE) and identifying the location of the groundwater and surface water POAs, as described in the following section. The EMDF model results are presented in Sect. 4.1.

3.3.3.2 Saturated Zone Radionuclide Transport Model

The MT3D model uses the EMDF flow model results for the long-term performance condition as the flow field for simulation of saturated zone radionuclide transport. The purposes of the MT3D modeling include the following:

1) Delimit the maximum extent of the contaminant plume

2) Determine the location of maximum concentration along the 100-m buffer zone boundary (groundwater POA)

3) Quantify the pattern of radionuclide discharge to streams and identify the surface water POA

4) Predict the peak concentrations and timing of peak for selected radionuclides at the 100-m groundwater well location

5) Evaluate the potential impact of non-uniform radionuclide release from the EMDF.

MT3D (Zheng 1990) is a comprehensive 3-D numerical simulation code that incorporates physical and geochemical processes that influence radionuclide fate and transport including advection, hydrodynamic dispersion, chemical retardation, and radioactive decay. Necessary input parameters include solute dispersivity in the three model coordinate directions, solid-aqueous phase K_d values, and radionuclide half-life. Bulk density and effective porosities of the saprolite and bedrock are also needed for parameterizing chemical retardation. The boundary condition for radionuclide flux from the vadose zone to the water table below the disposal unit, including the area and timing of release, is estimated with a simplified release model developed for each radionuclide of interest.

Based on the radionuclide release and vadose zone transport modeling results (STOMP model, Appendix E), only three of the radionuclides in the EMDF estimated inventory (Tc-99, C-14, and I-129) will be released to the saturated zone within the EMDF post-closure period before 10,000 years. The others will either decay before release (H-3) or arrive at the groundwater table after 50,000 years (uranium and plutonium isotopes). Therefore, the MT3D fate-transport modeling of saturated zone is conducted only for Tc-99, C-14, and I-129.

The MT3D model domain and discretization scheme are identical to the EMDF flow model, which provides the saturated zone flow field for the radionuclide transport simulation. Parameterization of the MT3D model and application for the five purposes listed above are reviewed briefly in the following subsections.

Additional detail on model development and parameterization, including use of STOMP model results to determine the timing of release for each radionuclide, is provided in Appendix F.

Material properties, dispersivity, and retardation parameters. Total and effective porosity values for different layers in the transport model are listed in Table 3.18. For the saturated zone, a single porosity conceptualization is adopted and only the effective porosity is used in the MT3D model (total and effective porosity were assumed to be equal). Decreased effective porosity values in deeper model layers reflect the fact that the bedrock at depth is less fractured and less weathered. Based on the total porosity, the dry bulk density values are calculated assuming average solid particle densities of 2.65 g/cm^3 for model layer 1 and 2.78 g/cm^3 for all other layers (Table 3.18). The same material properties were applied in all the PA models to the extent possible given differing levels of model detail.

**Table 3.18. Porosity and bulk density values assigned
in the MT3D model**

Model layer	Total porosity	Effective porosity	Bulk Density (g/cm^3)
1	0.27	0.27	1.93
2	0.20	0.20	2.22
3	0.15	0.15	2.36
4	0.10	0.10	2.50
5	0.05	0.05	2.64
6	0.04	0.04	2.67
7	0.03	0.03	2.70
8	0.02	0.02	2.72
9	0.01	0.01	2.75

The transport model assumes a longitudinal (Y-direction) dispersivity of 10 m, based on the 100-m distance to the groundwater well and a 10 percent rule-of-thumb (Gelhar et al. 1992) for estimating longitudinal dispersivity as a fraction of travel distance. In the absence of site specific data, horizontal (X-direction) transverse dispersivity is assumed to be one order of magnitude smaller than longitudinal dispersivity while vertical transverse (Z-direction) dispersivity is assumed to be two orders of magnitude smaller than longitudinal dispersivity (Zheng and Bennett 1995).

For chemical retardation of radionuclide transport, linear isotherm equilibrium sorption is assumed and a single distribution coefficient, K_d, defines the relationship between radionuclide concentrations in the aqueous phase and the concentration of sorbed material in the porous matrix. The assignment of an appropriate, constant K_d value to represent the retardation effect of sorption processes integrated over long time periods is an important uncertainty in the PA analysis. This key uncertainty is addressed with a probabilistic analysis (described in Sect. 5.4) using the total system model presented in Sect. 3.3.4. For the MT3D saturated zone transport simulations, a single K_d is assumed to apply to all the solid media (rock) types in the model for each radionuclide.

The base-case K_d values used for the three radionuclides evaluated in the MT3D simulations are listed in Table 3.19, along with corresponding half-lives and specific activity values. These three radionuclides were selected on the basis of predicted dose contributions in preliminary runs using the total system model. Detailed discussion of the basis for selection of base case K_d values for all radionuclides in the EMDF radionuclide inventory is provided in Sect. 3.2.2.6.

Table 3.19. Radionuclide parameter values for MT3D saturated zone transport modeling

Radionuclide	K_d (cm^3/g)	Half-life (year)	Specific activity (Ci/g)
C-14	0	5.70E+03	4.50E+00
Tc-99	0.72	2.13E+05	1.70E-02
I-129	4.0	1.57E+07	1.80E-04

Initial and boundary conditions. For the PA analyses, only EMDF contributions to groundwater contamination are considered. The initial concentration within the model domain for all radionuclides is assumed to be zero. There has been no existing radiological contamination of groundwater at the CBCV site, although there is the potential for BCV groundwater contaminants from sites higher in the watershed to extend as far as CBCV near the main channel of Bear Creek. The CA for EMDF and EMWMF (UCOR 2020a) considers the contributions of other BCV waste sites to potential future total doses assessed downstream of EMDF.

In addition to boundary conditions identified for the groundwater flow model (Sect. 3.3.3.1), boundary conditions for the transport model include recharge concentrations for each radionuclide that represent leachate emanating from the EMDF (radionuclide flux to the water table). This radionuclide flux is a function of the recharge concentration for each nuclide and the estimated volumetric recharge rate from the disposal unit to the saturated zone. For purposes of saturated zone flow and transport modeling, the volume flux of leachate from the vadose zone to the water table beneath the disposal facility (recharge) is based on the modeled EMDF cover infiltration for the long-term performance condition (0.88 in./year, Sect. 3.3.1). The recharge areas defined for the saturated zone transport model are shown in Fig. 3.25. The leachate recharge area is defined by the waste limits. The outer lined area and berm/side slope area are assigned low recharge rates (0.88 in./year and 1.0 in./year, respectively) but have zero recharge concentration and do not contribute radionuclide flux to the saturated zone.

A general application of the MT3D model (advective transport only with no retardation or decay) was used to determine the general plume extent, location of maximum concentration at 100 m (groundwater POA location), and to locate the surface water POA. For the general application a uniform, non-depleting source is modeled by assigning a constant unit recharge concentration to the waste area shown on Fig. 3.25. For modeling transport of C-14, Tc-99, and I-129 to determine peak POA concentrations and the timing of peaks, a simple model of radionuclide release is used to specify time-varying recharge concentrations for each radionuclide. The mass-balance calculation of time-varying leachate concentration is explained in the following subsection that describes the MT3D modeling to estimate peak radionuclide concentrations at the groundwater POA.

Plume extent and groundwater well (POA) location. A simplified general application of the transport model was first used to delineate the plume extent, determine the location of maximum groundwater concentration along the 100-m buffer zone boundary (groundwater POA), and estimate the pattern of mass flux to streams to locate the surface water POA. For these purposes, hydrodynamic dispersion, chemical retardation, and radioactive decay were neglected and only advective transport is simulated in the MT3D model. In addition, an infinite (non-depleting) contaminant source is assumed, and a constant recharge (leachate) concentration of 1 unit (units are arbitrary for the general application) is assigned for the waste area. These simplifying assumptions will result in the largest (relative) concentrations at the assessment locations.
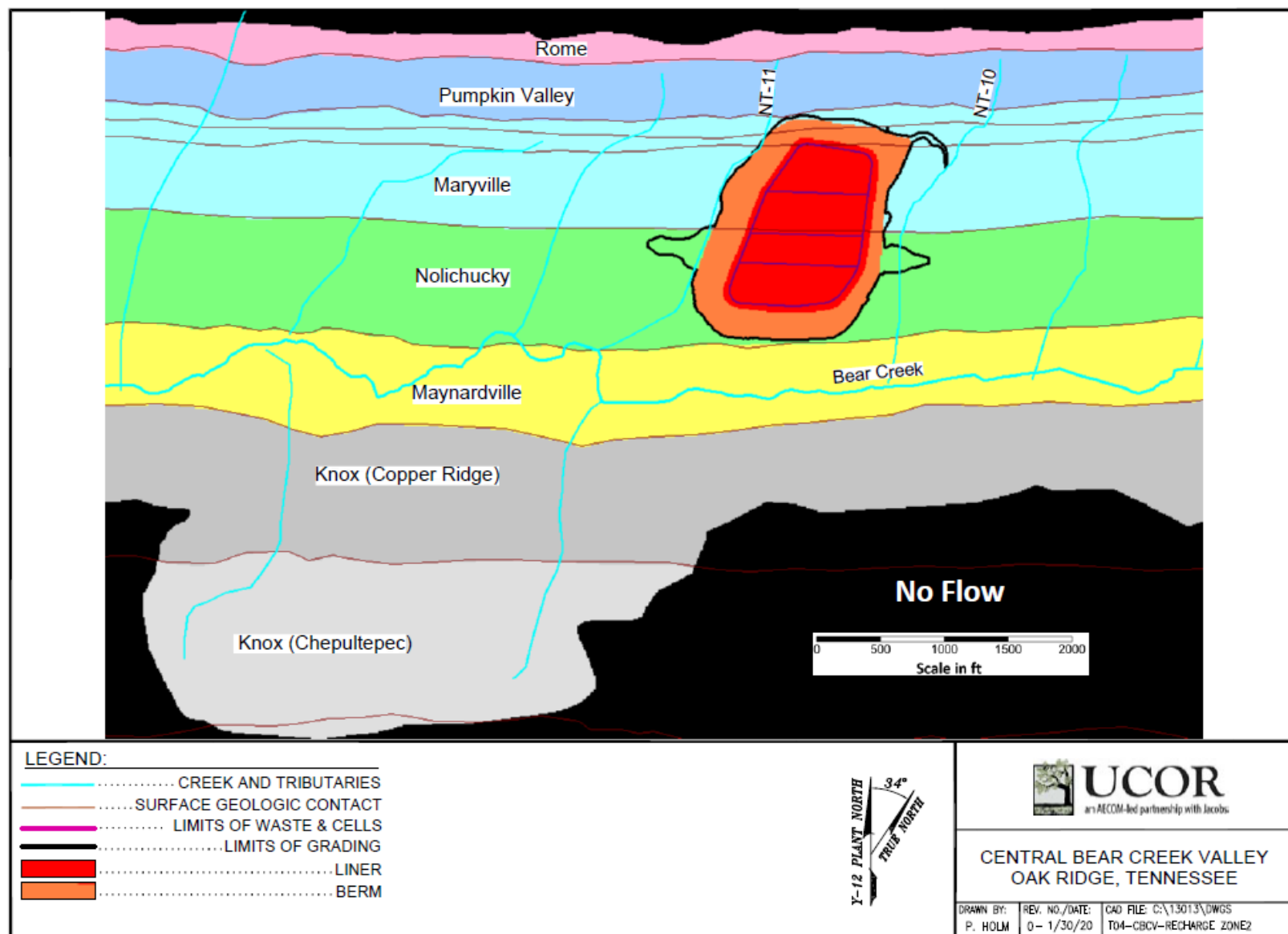
191

Fig. 3.25. EMDF disposal facility recharge zones for the saturated zone transport model

The model was run to a near steady-state plume configuration which was achieved after 2000 years of simulation. The steady-state plume configuration (maximum concentration of all model layers) is shown in Fig. 3.26. The simulation indicates that most groundwater contamination will discharge into Bear Creek and its tributaries near the EMDF site. The (minor) remaining contaminant mass will move downstream along the more permeable formations (Maynardville Limestone) below Bear Creek and discharge to the surface farther downstream. The transport model predicts that essentially all of release from the disposal facility discharges into Bear Creek surface water upstream of the Gum Branch tributary (NT-14). This pattern of predominantly shallow groundwater flow and contaminant transport is consistent with the BCV hydrogeologic conceptual model presented in Sect. 2.1.5 and with observations of plume migration from other sources in BCV.

Based on the steady-state advective transport model results representing the long-term performance condition, the maximum concentration 100-m buffer zone limit is located southwest of the disposal facility (Fig. 3.26). This location is the POA for groundwater concentrations (hypothetical drinking water well location). For the simplified transport model based on the constant, uniform source release, the location of maximum concentration does not vary appreciably over time. The steady-state vertical distribution of relative concentration at the groundwater POA (Fig. 3.27) indicates the highest concentrations in the model layers 2, 3, and 4 at the well location.

Radionuclide discharge to surface water. The general application MT3D transport model result was used to quantify groundwater and contaminant discharge to the model river cells and drain cells that represent surface water features near the EMDF. The simulated contaminant mass discharge to NT-10, NT-11, and the Bear Creek main channel segment between those tributaries was determined for corresponding areas of the model domain. The model calculates contaminant mass flux as groundwater discharge times the concentration at each model drain or river cell. Polygons identifying the areas for each of the stream channel segments and the simulated concentrations for model layer 1 (where contaminant discharge to river and drain cells occurs) are shown on Fig. 3.28.

Table 3.20 summarizes the distribution of contaminant mass discharge to the three stream channel segments. The discharge is expressed as a percentage of the total (steady-state) contaminant mass discharge from the entire model domain. Most of the contaminant mass discharge (> 87 percent) is received by NT-11, whereas NT-10 and the Bear Creek main channel segment receive only 8.2 and 2.8 percent, respectively. Together the three model channel segments account for over 98 percent of the release from the model domain. These results are the basis for selection of Bear Creek at the junction with NT-11 as the surface water POA (i.e., water for agricultural use is drawn from a single location that integrates most of the simulated release from the EMDF). It also validates that use the junction of Bear Creek and NT-11 as the point of compliance for evaluating protection of surface water resources.

Table 3.20. Contaminant mass discharge to surface water features in the MT3D model (simulation year 2000)

NT-10	Bear Creek between NT-10 and NT-11	NT-11	Total of three surface water model segments
8.17	2.80	87.12	98.09

Values in table are percent of total contaminant discharge within the entire model domain
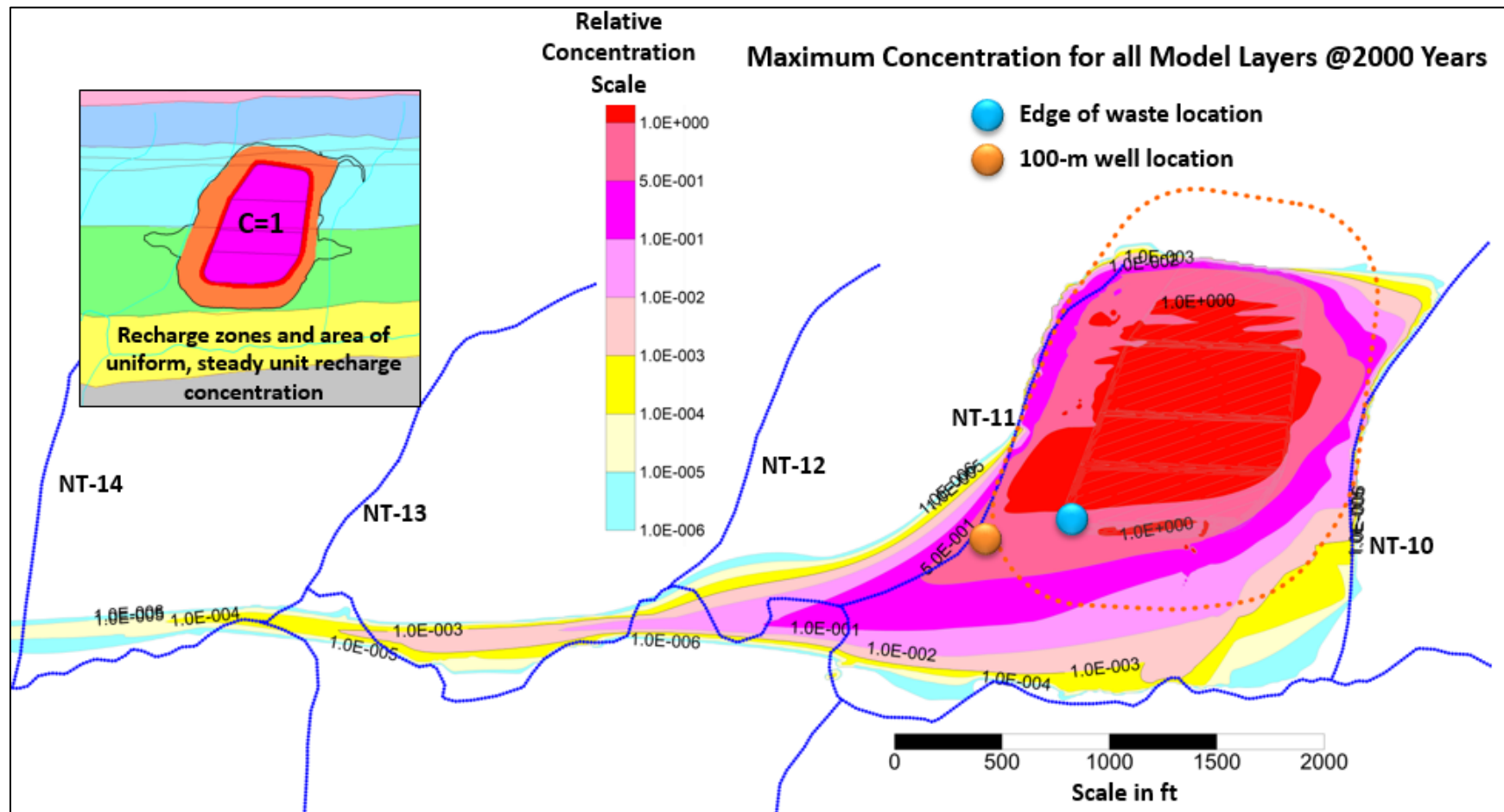
NT = North Tributary

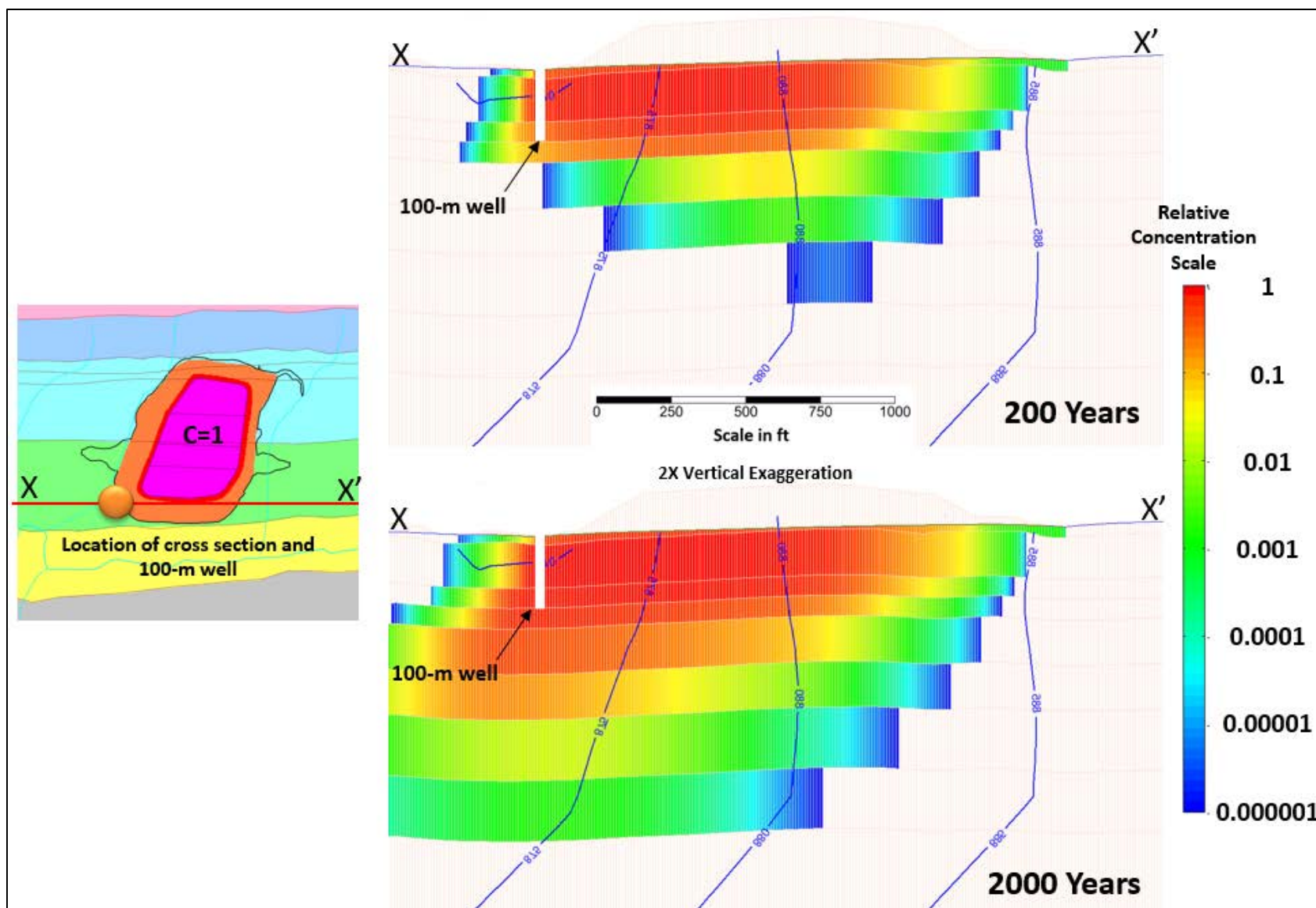**Fig. 3.26. Plume distribution (maximum concentrations) for non-depleting release from EMDF**

Fig. 3.27. Subsurface distribution of concentration for the general application of the MT3D transport model
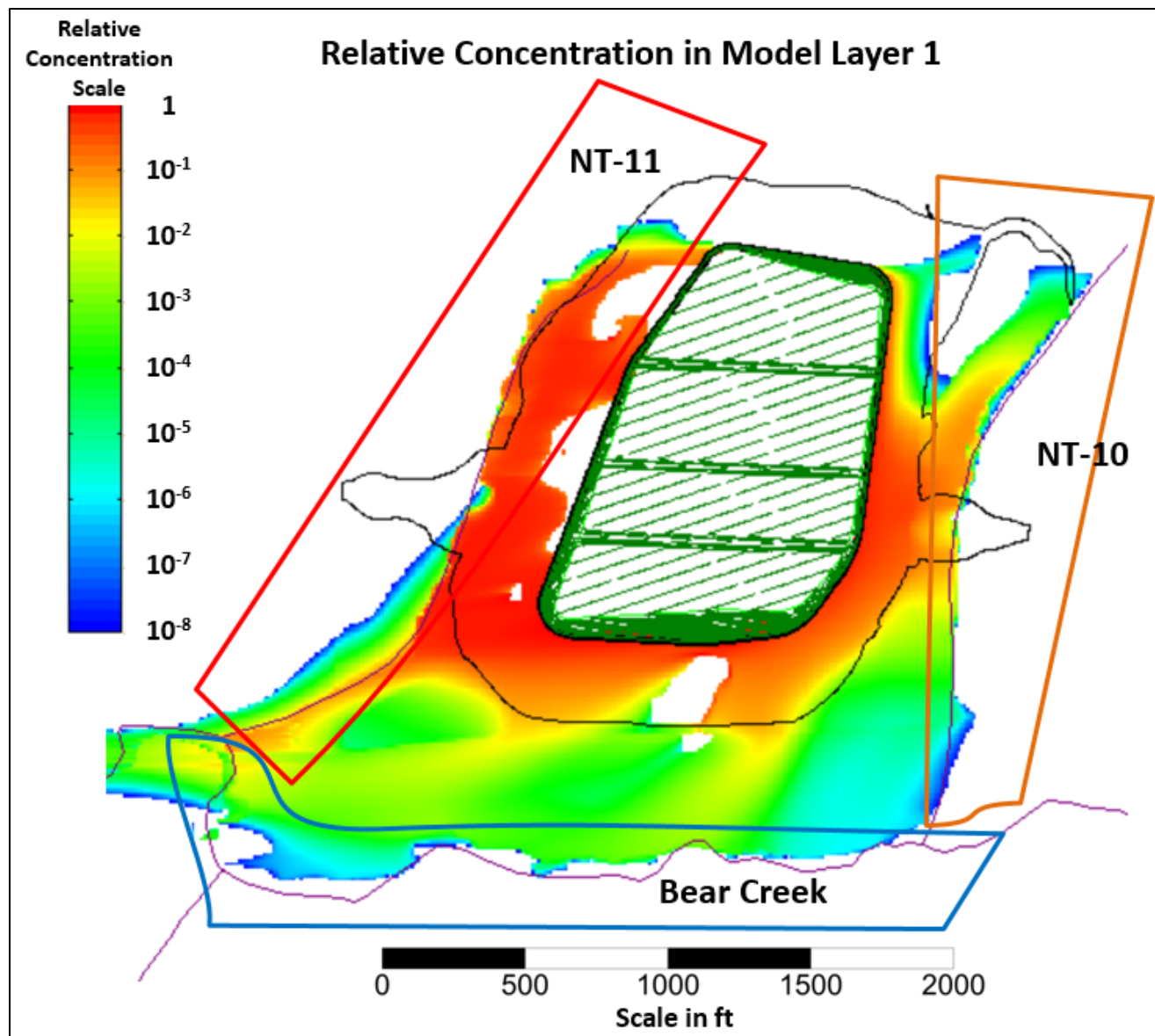
Fig. 3.28. Segments of surface water features defined for quantifying groundwater and contaminant discharge from the transport model domain

Saturated zone radionuclide transport to the groundwater POA. For simulating peak concentrations of C-14, Tc-99, and I-129 at the groundwater POA, the full implementation of the MT3D model incorporates radioactive decay, chemical retardation, and hydrodynamic dispersion in addition to advective transport. To model depletion of a finite radionuclide source, a simple radionuclide release model was developed. Based on the estimated initial radionuclide concentrations in the waste and assumed K_d values for radionuclides, initial moisture (pore water) concentrations are calculated for the waste. This approach assumes equilibrium solid-aqueous partitioning for a linear isotherm. The pore water concentration and volumetric leachate release rate based on the assumed increase in cover infiltration are used in a mass balance framework to calculate the decrease in radionuclide inventory, pore water (leachate) concentration, and radionuclide flux to the water table over time. This mass balance approach also incorporates post-closure radioactive decay and the vadose delay times derived from the STOMP model results (Table 3.21).

Table 3.21. Estimated vadose delay time for radionuclides released from the EMDF

Radionuclide	Delay time (years)
C-14	530
Tc-99	850
I-129	1750

EMDF = Environmental Management Disposal Facility

The calculated leachate concentration is applied during successive model stress periods to approximate the effect of source depletion on radionuclide flux to the water table. The recharge concentration from the release model is adjusted (decreased) as necessary for times prior to 1000 years (when the assumed leachate release is less than the constant 0.88 in./year applied to the waste area in the MT3D model) to ensure the correct mass flux to the saturated zone. The radionuclide flux to the water table applied to the MT3D model is compared to the STOMP model results and to the RESRAD-OFFSITE release model results in Sect. 3.3.5.

Estimated radionuclide flux to the water table is restricted to the waste area based on the assumption of primarily vertical transport through the vadose zone, which is generally supported by the STOMP simulations (STOMP results are presented in Sect. 4.2). For the base case simulations, the release of radionuclides was assumed to enter the saturated zone uniformly below the waste area. Because release from the disposal unit could be non-uniform, a sensitivity case simulation of non-uniform, time-varying Tc-99 recharge based on a modified release model also was performed. This sensitivity evaluation is performed to assess the significance of the simplified geometric representation of the waste and vadose zone that is assumed in the total system model.

The non-uniform release model for Tc-99 incorporates the funneling effects of the liner side slopes and sloping floors by restricting leachate recharge to the area directly below the cell floors (i.e., no leachate recharge beneath side slopes) and by assuming a higher release from the lower elevation (southeast) half of each of the four disposal cells (Fig. 3.29). The non-uniform release model also accounts for variation in waste volume between disposal cells. Additional detail on the radionuclide release model for MT3D simulations is provided in Appendix F, Sect. F.4.1.3. Development of the non-uniform sensitivity case is described in Sect. F.4.2.
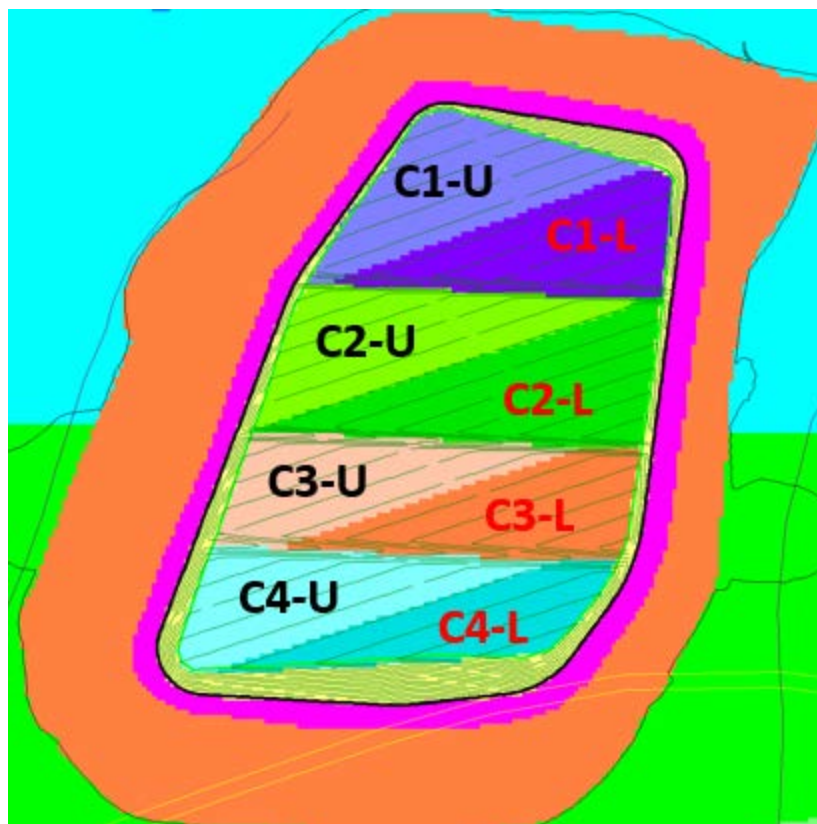
**Fig. 3.29. Disposal cell floor areas defined for
the non-uniform source release simulation
with MT3D**

MT3D model results (peak concentration and timing of peaks) for the upper four model layers at the groundwater POA location were compared to saturated zone results from the RESRAD-OFFSITE model that are used for the dose analysis. This model integration step is presented in Sect. 3.3.5.

3.3.4   Total System Model Code (RESRAD-OFFSITE)

For purposes of modeling the total EMDF disposal system, including radionuclide release, environmental transport, exposure pathways, and dose analysis, the computational code RESRAD-OFFSITE version 3.2 was selected (Yu et al. 2007, Gnanapragasam and Yu 2015). In general the detailed representations of the vadose and saturated zones that are described in the preceding sections have simplified conceptualizations and parameterizations in the RESRAD-OFFSITE model (Fig. 3.30). The advantage of the total system model is that it provides a holistic, integrated representation of the EMDF disposal system. As the total system model and detailed models were developed in parallel, predicted concentrations and fluxes in EMDF subsystems can be compared to provide confidence that simplified total system sub-model results are consistent with the more complex models of the system. The RESRAD-OFFSITE code was also used as an initial radionuclide screening tool (refer to Sect. 2.3.2) and for IHI dose analysis, which is described in Sect. 6.

198
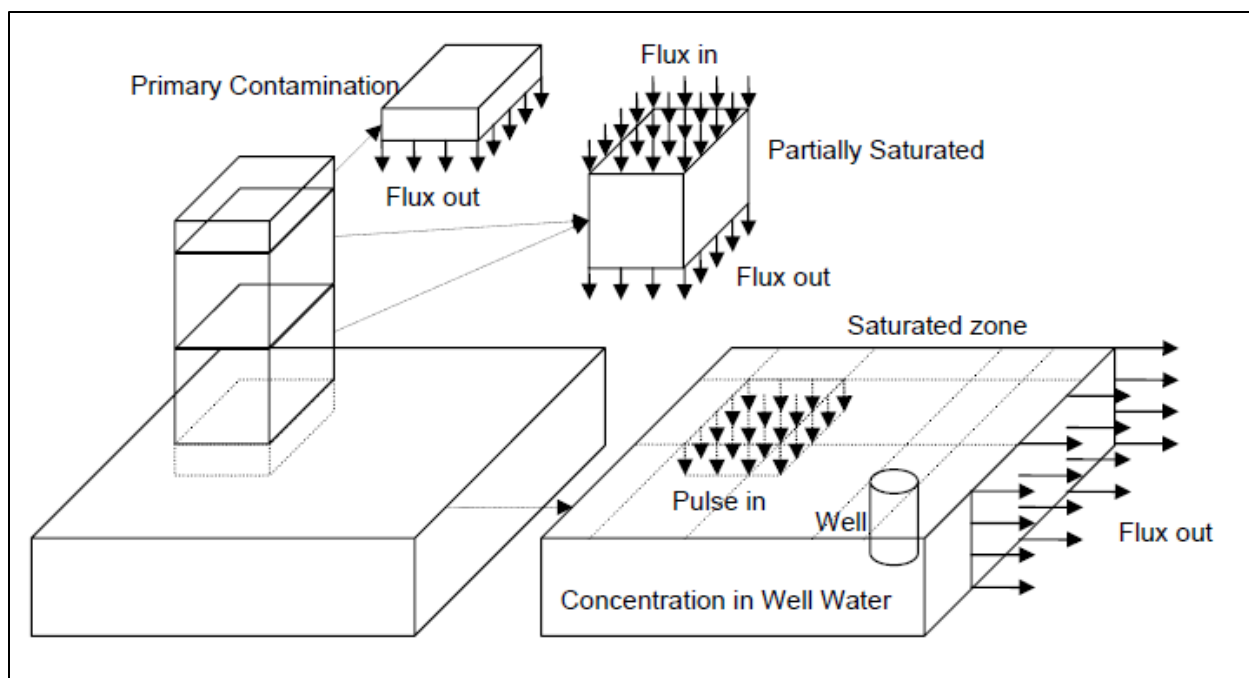
Fig. 3.30. Schematic of RESRAD-OFFSITE conceptual model of the primary contamination, vadose ("partially saturated") zone and saturated zone (Yu et al. 2007, Fig. 3.1)

Total system simulations were run for a post-closure period of 10,000 years to provide dose estimates for comparison with EMDF performance objectives, with a focus on predicted peak total dose within the 1000-year compliance period. Potential future release of relatively immobile radionuclides with significant estimated inventories (e.g., radionuclides of uranium) was evaluated with a 100,000-year RESRAD-OFFSITE simulation to estimate peak groundwater concentrations at the 100-m POA.

This section summarizes the RESRAD-OFFSITE simplified representation of the EMDF system and describes parameterization of the abiotic radionuclide transport pathways, including radionuclide release and the vadose and saturated zones. The RESRAD-OFFSITE model exposure scenario, biotic pathways, and dose analysis for the EMDF PA is described in Sect. 3.4. There are hundreds of input parameters for the RESRAD-OFFSITE model and only the most significant parameters are presented in this section of the EMDF PA report. Detailed explanation of all RESRAD-OFFSITE model input parameters and tabulation of all base case parameter values are provided in Appendix G.

The RESRAD-OFFSITE model identifies subsystems (Fig. 3.30), including the primary contamination (EMDF waste) and cover soil layer, a layered vadose zone below the waste, the aquifer (saturated zone), and dwelling and agricultural areas that can be affected by release of radionuclides from the primary contamination.

3.3.4.1   Climate parameters

Climate parameters specified in the RESRAD-OFFSITE model include annual precipitation and an evapotranspiration coefficient. Average precipitation is assumed to be 54.4 in./year and the evapotranspiration coefficient was assigned based on the average annual evapotranspiration estimated by the HELP model base case simulations, approximately 60 percent of precipitation.

3.3.4.2 Cover performance, primary contamination and radionuclide release

Thickness of the soil cover layer (11 ft) and average waste thickness (57.5 ft) are based on the EMDF Preliminary Design (Sect. 2.2). Other physical and hydraulic parameters values for the cover soil and primary contamination are provided in Table 3.22. Cover infiltration (for a given precipitation and evapotranspiration coefficient) is determined by the value of the runoff coefficient for the primary contamination, which is back-calculated to obtain the base-case long-term infiltration rate of 0.88 in./year. Evolution of EMDF cover performance is also represented in the source release parameterization described below. Erosion of the cover and upward transport of radionuclides into the clean cover by biological soil mixing or vapor phase transport are assumed to be negligible (refer to Sect. 3.2.2 and Appendix C), so erosion parameters for the cover soil are set to zero.

For modeling purposes, the 2.2 million cy of emplaced waste in EMDF was assumed to be of uniform thickness, homogenous both horizontally and vertically, and soil like (uncontainerized). The simplified representation of the primary contamination in RESRAD-OFFSITE (Fig. 3.30) as a homogeneous rectangular prism is consistent with the conceptual model of radionuclide release described in Sect. 3.2.2.4. Radionuclide concentrations in the primary contamination are based on the EMDF estimated radionuclide inventory (Sect. 2.3 and Appendix B) and adjusted to account for the addition of clean fill during waste placement and compaction (Sect. 3.2.2.5). In addition, operational period losses of highly mobile radionuclides (H-3, C-14, Tc-99, and I-129) are estimated to derive post-operational source concentrations for those for nuclides.

The RESRAD-OFFSITE code offers three options to simulate source release (Yu et al. 2013): First-Order Rate Controlled Release with Transport, Version 2 Release, and Instantaneous Equilibrium Desorption Release. All three release options were evaluated in the EMDF PA (Instantaneous Equilibrium Desorption Release in the base case and First Order Rate Controlled Release with Transport and Version 2 Release as part of the sensitivity analysis described in Sect. 5.3). An important limitation of RESRAD-OFFSITE is that the code does not account for solubility limits, which can allow for unrealistically high aqueous concentrations and predicted dose.

Instantaneous Equilibrium Desorption release assumes that equilibrium radionuclide concentrations in the solid and aqueous phases are achieved as soon as water contacts the waste and these equilibrium concentrations are governed by both the nuclide-specific K_d values in the contaminated zone and the soil/waste concentration. Additionally, the K_d determines the rate at which the radionuclides are transported by infiltration down through the primary contamination (Yu et al. 2013). In addition to the suitability of the Instantaneous Equilibrium Desorption release option for the expected waste forms and conceptual model of radionuclide release (Sect. 3.2.2.4), selection of this release option yields more rapid release of radionuclides compared to both the First Order Rate Controlled Release with Transport and Version 2 release options. Selecting this RESRAD-OFFSITE release model option is one important source of pessimistic bias toward higher release (and dose impacts) incorporated in the PA analysis.

First Order Rate Controlled Release with Transport assumes that radionuclide transfer from waste to pore water at any time is proportional to the radionuclide inventory at that time and occurs uniformly over the thickness of the primary contamination (i.e., the horizontal area does not change). The proportionality constant is the time varying leach rate. Version 2 release is a first-order exponential leaching model that accounts for radiological transformations (decay and ingrowth), but not for radionuclide transport in the waste. When Version 2 release is used, leached material is assumed to leave the contaminated zone as soon as it is leached. A time delay cannot be added when this release option is used, so all material is available for leaching at the beginning of the simulation period.

Table 3.22. Summary of material zone parameter values for RESRAD-OFFSITE modeling

RESRAD-OFFSITE zone	Layer (zone) thickness		Bulk density (g/cm³)	Total porosity (vol/vol)	Effective porosity (vol/vol)	Field capacity (vol/vol)	Saturated hydraulic conductivity	
	in.	m					cm/sec	m/year
Clean cover	132	3.35	1.5	0.400	*a*	*a*	*a*	*a*
Primary contamination (waste)	690	17.5	1.9	0.419	0.234	0.307	1.90E-05	5.99E+00
UZ1 (protective soil)	12	0.305	1.4	0.463	0.294	0.232	3.70E-04	1.17E+02
UZ2 (leachate drainage)	12	0.305	1.6	0.397	0.389	0.032	3.00E-01	9.46E+04
UZ3 (clay liner)	36	0.914	1.5	0.427	0.195	0.418	1.00E-06	3.15E-01
UZ4 (geologic buffer)	120	3.05	1.5	0.419	0.234	0.307	1.00E-05	3.15E-00
UZ5 (saprolite or bedrock)	120	4.85	1.8	0.353	0.270	0.247	5.30E-05	1.67E+01
Aquifer (saturated zone)	2400	61	2.1	0.240	0.200	NA	8.49E-05	2.68E+01

[a]Parameter not required for RESRSAD-OFFSITE.

RESRAD = RESidual RADioactivity
UZ = unsaturated zone

The Instantaneous Equilibrium Desorption release model is applied consistent with the assumed evolution of EMDF cover performance and leachate release (Sect. 3.2.1). One of the limitations of the RESRAD-OFFSITE code is that the infiltration rate cannot be varied over time, so a constant infiltration rate must be applied for the entire simulation period. The RESRAD-OFFSITE model runoff coefficient input parameter was assigned a value to produce the HELP-calculated long-term performance infiltration rate (0.88 in./year), based on the base case values for the evapotranspiration coefficient and average annual precipitation (refer to Appendix G, Sect. G.4.3.5.2).

The release model incorporates the assumed evolution in EMDF performance by assigning a release time (initially set at 200 years) and a release duration set at 800 years. As a surrogate representation of the assumed increase in cover infiltration over the release duration, and to account for the higher than assumed infiltration rate from years 200 to 1000, the release model applies a releasable fraction parameter which is increased from zero to one over the 800 year release. The model requires an initial value of the releasable fraction (set to zero at the release time, 200 years) and a final value (set to one at 1000 years) for each radionuclide.

Based on comparison of the RESRAD-OFFSITE model results to the STOMP and MT3D model results for C-14 and Tc-99, the initial release time was adjusted upwards to 300 years for all radionuclides. To adequately capture the high mobility of radionuclides with K_d = zero, increasing the initial releasable fraction from zero to 0.75 for C-14 was found necessary. This adjustment produced peak C-14 release concentrations consistent with the STOMP and MT3D model results for C-14. Initial releasable fraction was also changed to 0.75 for H-3, (also K_d = zero) for consistency. Similarly, the release duration was decreased to 500 years for C-14 and H-3 to better match MT3D model output. Comparison and integration of RESRAD-OFFSITE model results with STOMP and MT3D model results is presented in Sect. 3.3.5.

3.3.4.3 Solid-aqueous partition coefficients

The K_d values used in the RESRAD-OFFSITE modeling were based on ORR-specific values where such data are available or used generic values based on soil type (Sect. 3.2.2.6). Base case K_d values for each element in the EMDF radionuclide inventory are listed in Table 3.4. These base case values are identical to those listed for radionuclides considered in the vadose (STOMP) and saturated zone (MT3D) models. Also shown in Table 3.4 are K_d values used for the radionuclide screening model described in Sect. 2.3.2, along with references used to guide selection of the base case values. Detailed discussion of the available ORR-specific data on distribution coefficient values is provided in Sect. 2.1.6.3. Where ranges reported in general compilations of values were utilized, lower values (generally pessimistic in term of dose predictions) were selected as base case values for the EMDF PA. A more detailed presentation of the approach to selection of base case K_d values is provided in Sect. 3.2.2.6.

In the RESRAD-OFFSITE model, distribution coefficients are assigned to various disposal system components, including the waste, vadose zone layers, aquifer (saturated zone), and surface water feature sediments. The K_d values are also assigned for soils in agricultural fields and the dwelling site (Sect. 3.4). The distribution coefficient for sediment in the surface waterbody was specified as zero for all radionuclides as a pessimistic assumption in the context of bioaccumulation in fish and the fish ingestion exposure pathway.

Sensitivity of dose estimates to variation in K_d values for particular model material zones (primary contamination, vadose zone, saturated zone) is evaluated in Appendix G, Sect. G.6.2. Sensitivity of total dose to variation in the I-129 K_d values for different material zones is shown in Fig. 5.7. The sensitivity of peak dose estimates to uncertainties in K_d values for key dose-contributing radionuclides is a primary focus of the probabilistic analysis presented in Sect. 5.4 and in Appendix G, Sect. G.6.3.

3.3.4.4 Vadose zone parameterization

In addition to the clean soil cover layer and the primary contamination (EMDF waste), the RESRAD-OFFSITE model identifies the following five layers in the unsaturated zone between the waste and the water table:

- UZ1 – Protective soil (layer protects liner)

- UZ2 – Drainage layer (leachate collection system)

- UZ3 – Compacted clay liner

- UZ4 – Low-permeability geobuffer

- UZ5 – Native vadose saprolite or bedrock.

A summary of key input parameters by zone is provided in Table 3.22. The model layer thicknesses for the cover through the geobuffer (UZ4) are based on the EMDF preliminary design. The thickness of UZ5 (16 ft) is based on predicted water table elevation from the EMDF flow model (Sect. 3.3.3.1), assuming long-term performance (0.88 in./year) cover infiltration. The uncertainty in the thickness of UZ5 primarily reflects uncertainty in long-term site hydrogeologic conditions that, in combination with the effectiveness of the cover, will determine the long-term average water table elevation below the disposal unit.

Values for porosity, field capacity, and hydraulic conductivity for the waste and non-native (engineered) materials were specified to align with HELP default values for each specific material type. Waste bulk density is based on estimated average bulk densities and proportions of waste soil, clean fill, and demolition debris expected for the EMDF (Appendix B). Bulk density and porosity values for native materials in UZ5 and the saturated zone are from based on analysis of Nolichucky Formation samples (Dorsch and Katsube 1996). The EMDF preliminary design specified a K value of 1.0E-07 cm/sec, but the RESRAD-OFFSITE code would not accommodate such a low value for the imposed infiltration rate (0.88 in./year) through the vadose zone. For the RESRAD-OFFSITE model the K value for UZ3 was increased by a factor of 10 to 1.0E-06 cm/sec, to accommodate the limitation in executing the code. Hydraulic conductivity for UZ5 is based on estimates for the Nolichucky Formation vertical conductivity (refer to Sect. 2.1.5.4).

For the primary contamination, the longitudinal (vertical) dispersivity is set as 10 percent of the average waste thickness, or 1.8 m, based on the scale and likely heterogeneity of the waste zone. Each unsaturated zone unit is assigned a longitudinal dispersivity of 0.1 m.

3.3.4.5 Saturated zone parameterization

The saturated zone representation in RESRAD-OFFSITE is a simplified homogeneous, isotropic unconfined groundwater flow system (Fig. 3.30). The term aquifer is used to refer to the saturated zone submodel in RESRAD-OFFSITE. Saturated zone parameter values given in Table 3.22 are based on laboratory and field measurements, with the exception of aquifer thickness set at 200 ft. The active BCV saturated zone is much thicker than 200 ft, but the BCV hydrogeologic conceptual model and results of tracer studies in BCV and from the 3-D groundwater flow and radionuclide transport models for the EMDF site suggest that the depth to which contamination introduced at the surface penetrates the saturated zone is limited. Given the RESRAD-OFFSITE model structure, radionuclide concentrations at the receptor well can depend on the depth of the well relative to the depth of the aquifer. Preliminary sensitivity analysis suggested that given the well depth assumed for the analysis (131 ft, which is based on comparison of the RESRAD-OFFSITE and MT3D model results), the well concentration and predicted peak dose would not be sensitive to assuming a more realistic (larger) value for aquifer depth. Parameterization of the

groundwater well (well depth and location) is presented in the context of the all-pathways exposure scenario (Sect. 3.4.2).

The average horizontal hydraulic gradient (slope of the potentiometric surface) along the flow path to the groundwater well is approximately 0.036 ft/ft, based on the EMDF model results for the long-term performance condition. The hydraulic gradient to the surface water body is also assumed as 0.036 ft/ft. Due to the sensitivity of the RESRAD-OFFSITE predicted well concentrations to hydraulic gradient to the well, the value for the gradient was increased to 0.054 ft/ft. This adjustment was made to account for less saturated zone dilution in the RESRAD-OFFSITE model compared to the MT3D model (Sect. 3.3.5).

The RESRAD-OFFSITE model requires both longitudinal (horizontal) and lateral (horizontal and vertical) dispersivities for the aquifer. A longitudinal dispersivity of 10 m was initially assigned based on the 100-m distance to the groundwater well (10 percent rule-of-thumb) and for consistency with the MT3D saturated zone transport model parameterization. As assumed for the MT3D radionuclide transport model, horizontal lateral and vertical lateral dispersivities are set at 10 percent and 1 percent of the longitudinal value.

3.3.4.6   Surface waterbody

The surface water point of exposure is assumed to occur at a location that would provide flow during drier parts of the year. A surface water exposure location on Bear Creek near the junction of NT-11 was selected because year-round flow is more typically encountered there than in surface water tributaries closer to the landfill.

The dimensions of the section of Bear Creek assumed to be impacted by radionuclides are 100 m in length, 5 m in width, and 0.5 m in depth with a simulated surface area of 500 m^2 and volume of 250 m^3. A representative mean residence time in the surface waterbody of 0.0001 year was specified based on an estimated average flow rate in Bear Creek at NT-11 of approximately 1570 gpm (UCOR 2020a, Sect. 4.2).

3.3.4.7   Other applications of the RESRAD-OFFSITE model for the EMDF PA

In addition to the base case holistic system simulation for the all-pathways dose analysis, the RESRAD-OFFSITE code was used for several other applications to the EMDF analysis, including the following:

1) Operational period inventory depletion estimates – Four simulations were performed to quantify activity loss from the waste due to leaching during the 25-year operational period for the four mobile radionuclides (C-14, H-3, I-129, and Tc-99). A summary of this application is provided in Sect. 3.2.2.5.

2) Screening models for radionuclide release through the EMDF cover– Two models were developed to support screening of the cover release pathway from the all-pathways analysis and to provide bounding estimates for demonstrating compliance for the air pathway. Results of these applications are presented in Sect. 3.2.2.3.

3) IHI scenarios – Three IHI scenarios were evaluated: acute discovery, acute drilling, and chronic post-drilling. IHI development and results are summarized in Sect. 6 and presented in detail in Appendix I.

4) Long-term simulations – These extended duration simulations were performed similar to the 10,000-year base case simulation, with the simulation duration extended to 100,000 years to evaluate radionuclides, such as uranium isotopes, with peak predicted concentrations occurring after tens of thousands of years (Sect. 4.8).

5) Sensitivity and uncertainty analysis –RESRAD-OFFSITE was used to perform a comprehensive set of single-factor model sensitivity evaluations for the base case scenario and a more limited set for the long-term simulation (Sect. 5.3). Based on initial sensitivity evaluations, a probabilistic uncertainty

analysis was performed to evaluate the sensitivity of RESRAD-OFFSITE model results to uncertainty in important input parameters (Sect.5.4). The sensitivity and uncertainty analysis provides perspective on the potential range of uncertainty in modeled dose predictions and insight into which input parameter value assumptions are most important in supporting the conclusions of the PA.

3.3.5　　　　　Radionuclide Transport Model Integration

Prior to final implementation of the exposure and dose analysis using the total system model (described in Sect. 3.4), the results obtained from the more complex transport model codes (STOMP and MT3D) were compared to radionuclide release and transport output from the total system model (RESRAD-OFFSITE). This model integration step was performed to ensure that the simplified representations of the vadose and saturated zones in the RESRAD-OFFSITE model were producing results consistent with the more detailed models. Based on preliminary dose predictions from the total system model, the model output comparison was focused on C-14, Tc-99, and I-129, three radionuclides that make primary contributions to the predicted total dose at various times during the post-closure period. The model output examples in the following subsections are for Tc-99, because the examples incorporate output from sensitivity runs (e.g., MT3D non-uniform release scenario) that were only performed for Tc-99.

3.3.5.1　　　　　Vadose zone model comparison

STOMP results from the Section A model show complex non-uniform patterns of radionuclide release over time (Sect. 4.2). To compare results of radionuclide release to the vadose zone across models having different dimensionality and complexity, the total activity flux from the waste and from the vadose zone, including variation over time, was selected as the quantity of interest. The STOMP model predicted total vertical activity flux across the output surface for the waste-liner interface and the water table output surface were calculated by summing the vertical flux for all model nodes along each output surface. Because the STOMP model is a 2-D representation, the activity flux results were scaled up for comparison to the MT3D release model and the RESRAD-OFFSITE model based on the ratio of the STOMP model total initial activity to the total EMDF inventory represented in the other two models.

For the initial RESRAD-OFFSITE input parameter value selections for the release model (release time = 200 years and release duration = 800 years), the RESRAD-OFFSITE model predicted earlier Tc-99 release from the waste than the STOMP model. Based on this difference, the RESRAD-OFFSITE model release time was increased to 300 years for all radionuclides. This adjustment resulted in a better match in release timing for both flux from the waste (Fig. 3.31 solid curves) and from the vadose zone (flux to water table, Fig. 3.31 dashed curves). Technetium-99 flux from the waste shows similar peak values and timing of peak flux for the two models, with the RESRAD-OFFSITE predicted release occurring from 300 to approximately 2000 years post-closure. The (scaled) STOMP model flux from the waste occurs slightly later and extends over slightly longer (200 to 300 years) period. This difference reflects the STOMP model 2-D representation of a complex combination of faster and slower transport pathways (refer to Sect. 4.2), compared to the simpler 1-D release model. In general the results from the two models are quite consistent in terms of the timing and peak flux from the waste, providing confidence in the results.

The STOMP and RESRAD-OFFSITE model Tc-99 flux curves representing transport from the vadose zone to the saturated zone (flux to water table) are very closely aligned over the period of increasing flux from 600 to 1000 years post-closure (Fig. 3.31). The STOMP predicted flux peaks soon after 1000 years, but the RESRAD-OFFSITE model predicted flux continues to increase between 1000 and 1500 years post-closure, and peaks higher than the STOMP model output. The disparity in the predicted vadose zone Tc-99 transport reflects the difference between the more detailed 2-D STOMP model representation and the simpler RESRAD-OFFSITE 1-D vadose zone model, and suggests that RESRAD-OFFSITE under-predicts vadose zone performance (over-predicts peak flux at the water table) relative to the STOMP model.

The vadose zone flux results from the STOMP and RESRAD-OFFSITE models are compared to Tc-99 fluxes calculated from the radionuclide release model applied to the MT3D saturated zone transport model in Figs. 3.32 and 3.33. The timing of the MT3D release model (vadose delay time, Sect. 3.3.2) is based on the STOMP water table flux output. The MT3D Tc-99 release model is a simplified approximation of flux to the saturated zone beginning at 850 years post-closure, corresponding to the time when the STOMP modeled flux reaches 50 percent of its peak value (Fig. 3.32). The onset of Tc-99 release applied to the MT3D model is about 200 years later than the predicted beginning of release based on the STOMP and RESRAD-OFFSITE models. The peak Tc-99 flux applied to the MT3D model is earlier than predicted by the other two models, and the MT3D model peak flux is very close to the RESRAD-OFFSITE model peak Tc-99 flux.

Comparison of the STOMP and RESRAD-OFFSITE Tc-99 output with the MT3D Tc-99 release model input in terms of cumulative flux (Fig. 3.33) shows that in general, there is very good consistency between the model representations of Tc-99 release prior to 1500 years post-closure. After 1500 years, the rate of release for the RESRAD-OFFSITE model is unchanged and over 90 percent of the total activity release is complete by 2000 years post-closure. For the STOMP model Tc-99 output and the Tc-99 release model input to the saturated zone MT3D model, the rate of release becomes more gradual after 1500 year and the duration of release is extended compared to the RESRAD-OFFSITE results. These model similarities and differences suggest that the EMDF total system model of radionuclide release to the saturated zone is consistent with the STOMP vadose zone model results and the MT3D saturated zone model implementation for Tc-99.

Fig. 3.31. Comparison of Tc-99 flux from the waste and from the vadose zone for the STOMP and RESRAD-OFFSITE models of the EMDF
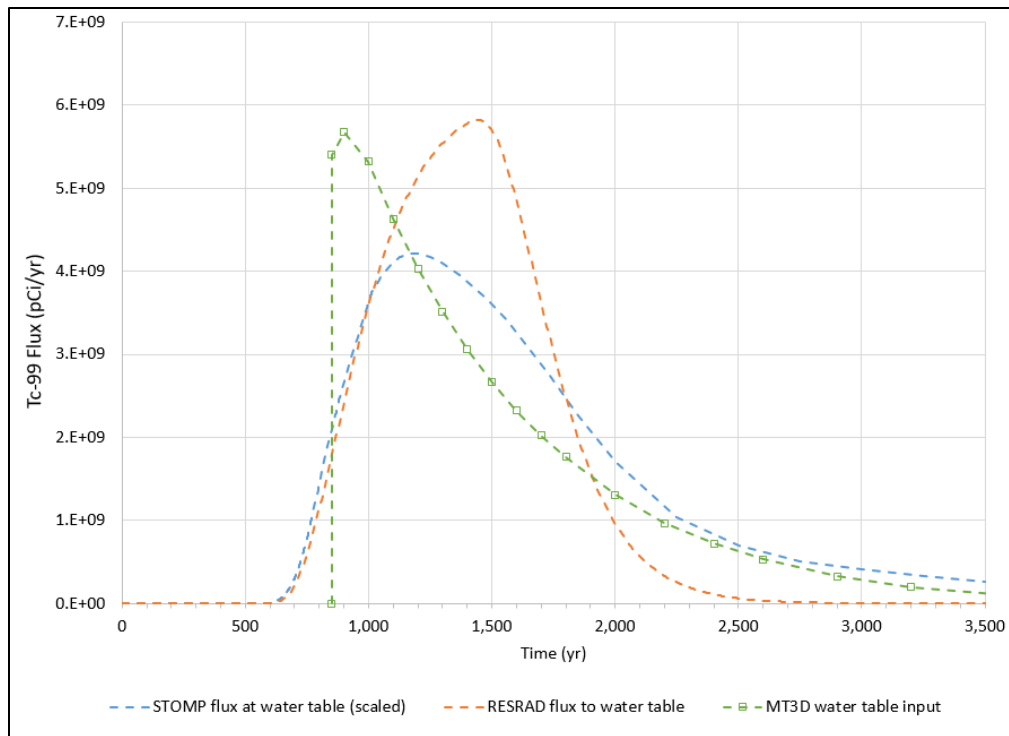
Fig. 3.32. Comparison of STOMP and RESRAD-OFFSITE predicted Tc-99 flux from vadose zone with Tc-99 release applied to the MT3D saturated zone model
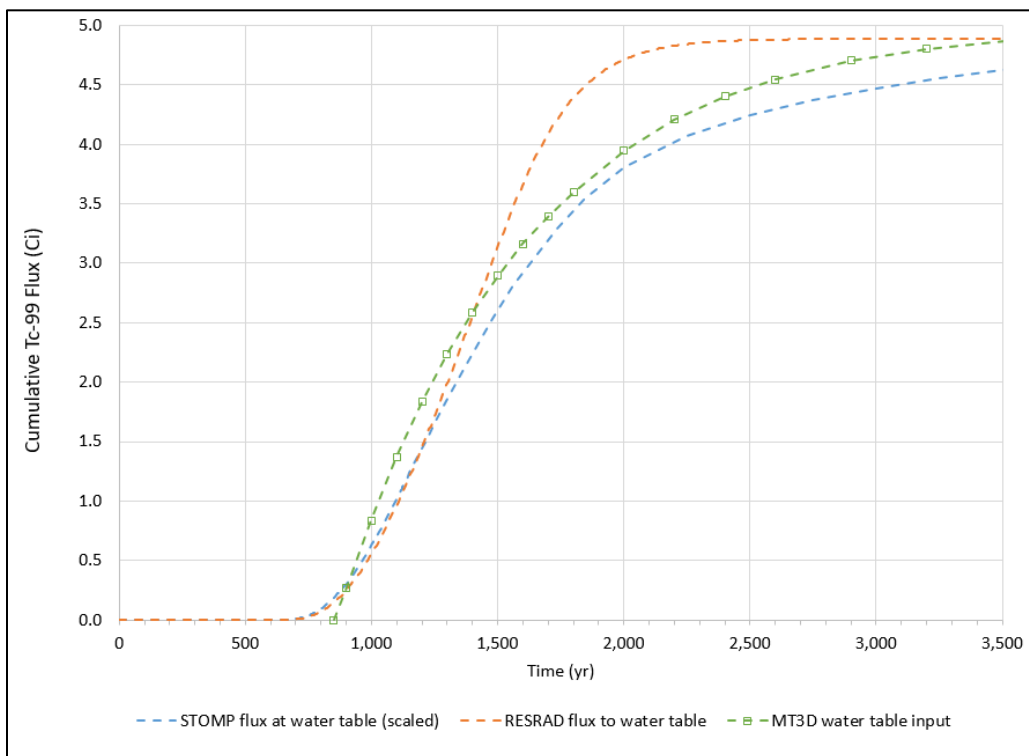
Fig. 3.33. Comparison of STOMP and RESRAD-OFFSITE predicted cumulative Tc-99 flux from vadose zone with cumulative Tc-99 release applied to the MT3D saturated zone model

207

Predicted release of I-129 and U-234 to the vadose zone and flux into the saturated zone for the STOMP and RESRAD-OFFSITE models are compared in Figs. 3.34 and 3.35. For these two radionuclides that have assumed base case K_d values greater than 1 cm^3/g (i.e., 4 and 50 cm^3/g for iodine and uranium, respectively), the instantaneous equilibrium desorption release model in the RESRAD-OFFSITE code over-predicts peak activity flux rates significantly relative to the scaled STOMP model simulations. Consistent with the model comparison for Tc-99 (Fig. 3.32) the RESRAD-OFFSITE model-predicted peak flux to the water table occurs somewhat later than the corresponding STOMP model-predicted peak, but for I-129 and U-234 the RESRAD-OFFSITE model peak flux rates are approximately 2.5 times larger than the STOMP model peaks.

The differences between the STOMP model and the RESRAD OFFSITE model predictions for the flux of Tc-99, I-129, and U-234 entering the saturated zone suggest that for K_d values greater than 1 cm^3/g, the instantaneous equilibrium desorption release model and vadose zone representation in the RESRAD OFFSITE code do not capture extent to which the EMDF design and the vadose zone below the disposal facility contribute to long-term performance of the disposal system. This limitation of the RESRAD-OFFSITE model is consistent with the simplified radionuclide release and vadose zone conceptualizations of the total system model. Use of the RESRAD-OFFSITE model predictions for the dose analysis is therefore a pessimistic approach for the less mobile radionuclides because the peak dose will be over-estimated relative to dose estimates based on the more detailed radionuclide transport models (STOMP and MT3D).
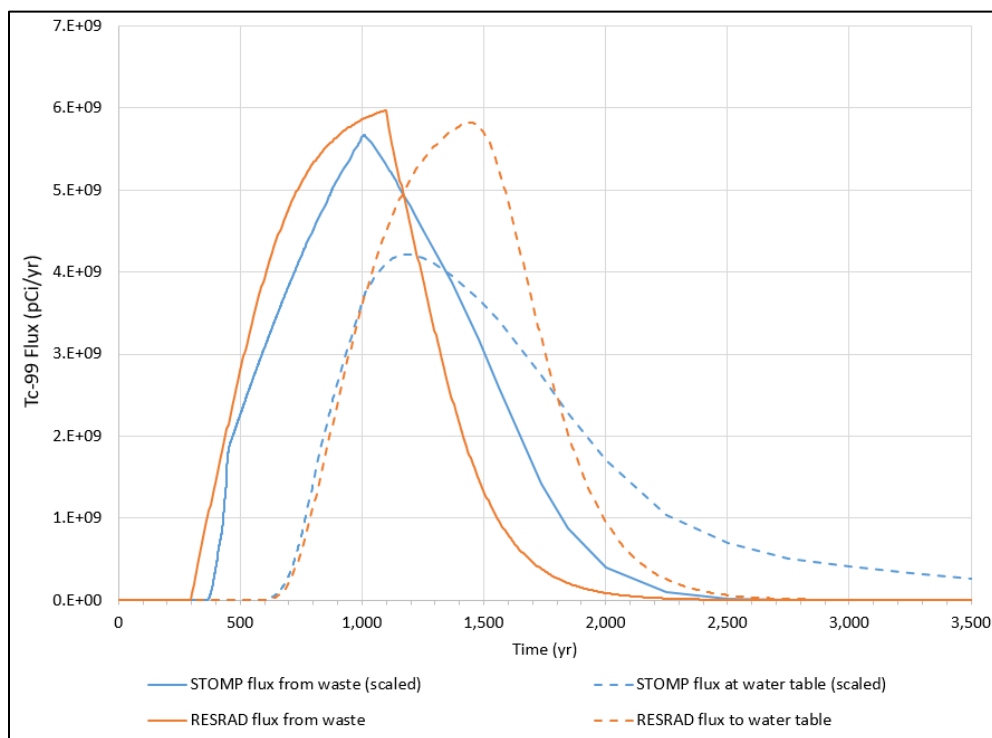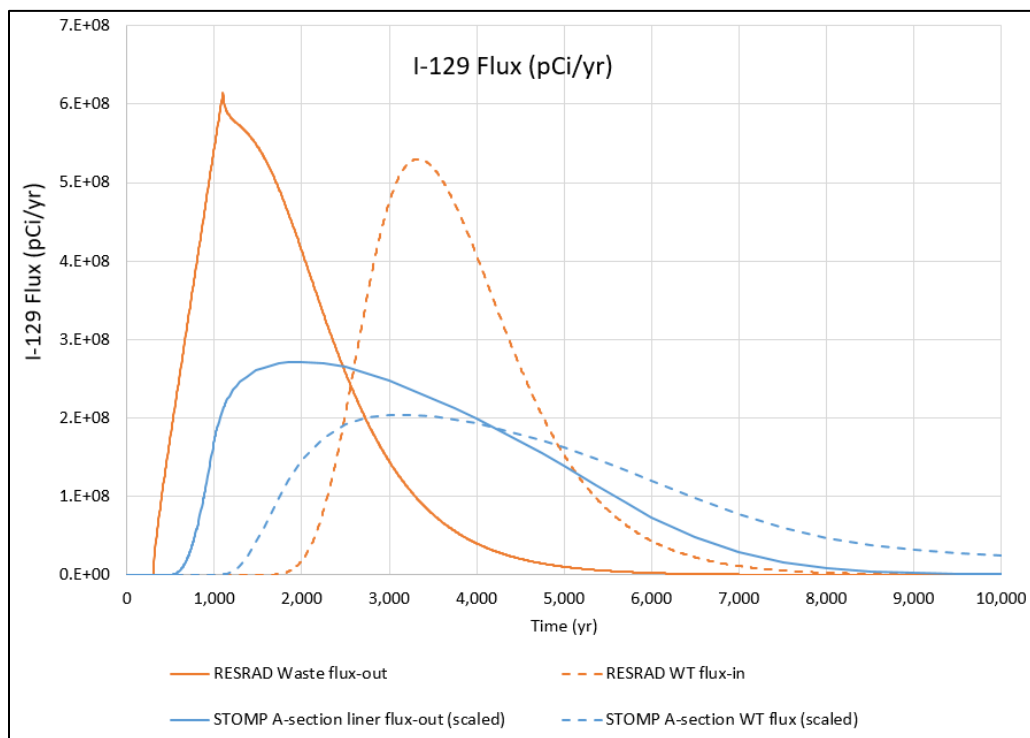

Fig. 3.34. Comparison of Tc-99 flux from the waste and from the vadose zone for the STOMP and RESRAD-OFFSITE models of the EMDF
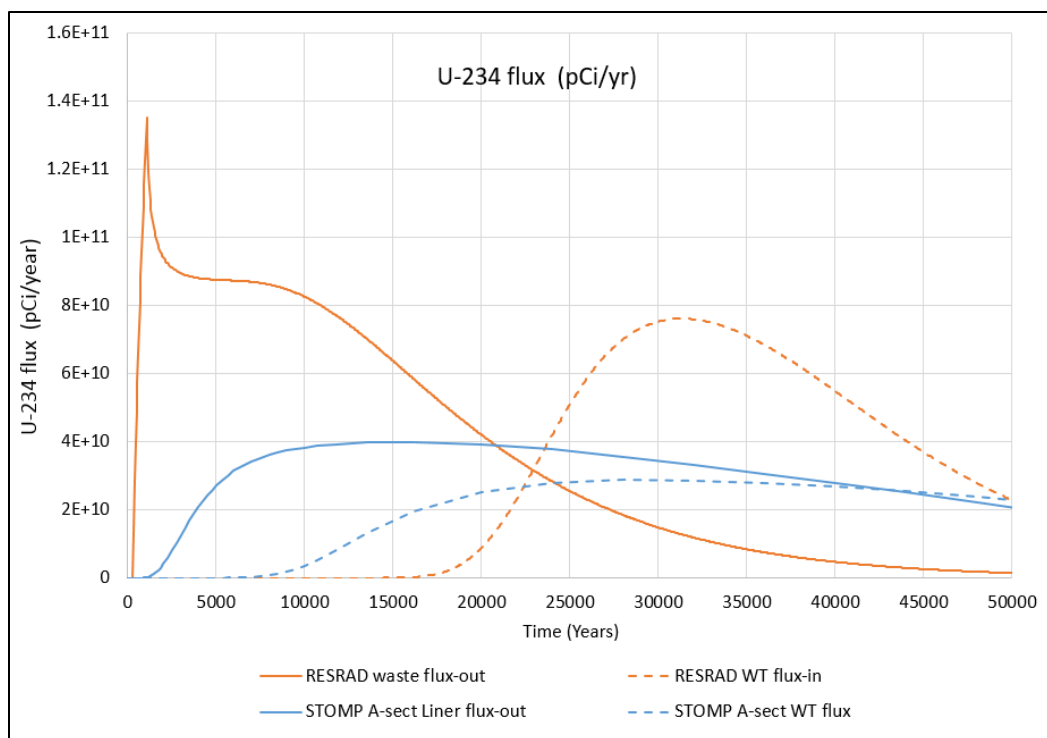
**Fig. 3.35. Comparison of Tc-99 flux from the waste and from the vadose zone
for the STOMP and RESRAD-OFFSITE models of the EMDF**

3.3.5.2 Saturated zone model comparison

Aqueous activity concentrations are the basis for comparison of the MT3D and RESRAD-OFFSITE saturated zone model results. To provide linkage between the vadose zone results reviewed in Sect. 3.3.5.1 and the saturated zone model results, the Tc-99 recharge concentrations are compared to RESRAD-OFFSITE model vadose zone concentrations at the water table, and to saturated zone concentrations at downgradient edge of waste (EOW) location along the flow path to the groundwater POA (Fig. 3.34). The RESRAD-OFFSITE model vadose Tc-99 concentrations are calculated as the model predicted flux (activity/time) divided by the assumed leachate flux (volume/time) corresponding to the (constant) 0.88 in./year infiltration rate for the long-term performance condition. The two vadose Tc-99 concentration time series shown in Fig. 3.32 (dashed curves) correspond to the MT3D and RESRAD-OFFSITE flux curves plotted in Figs. 3.36 and 3.37.

The Tc-99 saturated zone concentrations at the EOW for MT3D model layer 2 (model layer 1 is above the water table at the EOW) and for a RESRAD-OFFSITE model well at zero distance from the EOW are also shown in Fig. 3.36 (dotted curves). The RESRAD-OFFSITE model EOW well depth is 65.6 ft (specified as 20 m in model units), which is approximately the same as the thickness of MT3D model layer 2 at the EOW (70 ft). The Tc-99 saturated zone concentration curves are closely aligned during the period of increasing concentration from approximately 700 to 1100 years post-closure. After 1100 years, the RESRAD-OFFSITE model saturated zone concentrations increase faster than the MT3D model layer 2 Tc-99 concentration and reach a peak at approximately 1600 years post-closure. The MT3D model saturated zone concentration at the EOW reaches a somewhat lower peak (20 percent less than the RESRAD-OFFSITE model maximum) approximately 500 years later (around 2100 years). The difference between peak vadose zone Tc-99 concentration and peak saturated zone concentration is similar for the two models; peak saturated zone concentrations are about a factor of 4 less than peak vadose concentrations, suggesting

a similar degree of predicted saturated zone dilution. The difference in the peak Tc-99 saturated zone concentration (MT3D Tc-99 peak is smaller and occurs later) is related to the difference in release models (Figs. 3.36 and 3.37) and to the difference between the simplified analytical saturated zone model in the RESRAD-OFFSITE code and the more detailed MT3D numerical model. The RESRAD-OFFSITE model predicted well concentration is highly sensitive to the specified well depth (Sect. 5.3), but for a similar thickness of saturated zone at the EOW, the two models predict similar peak Tc-99 concentrations.
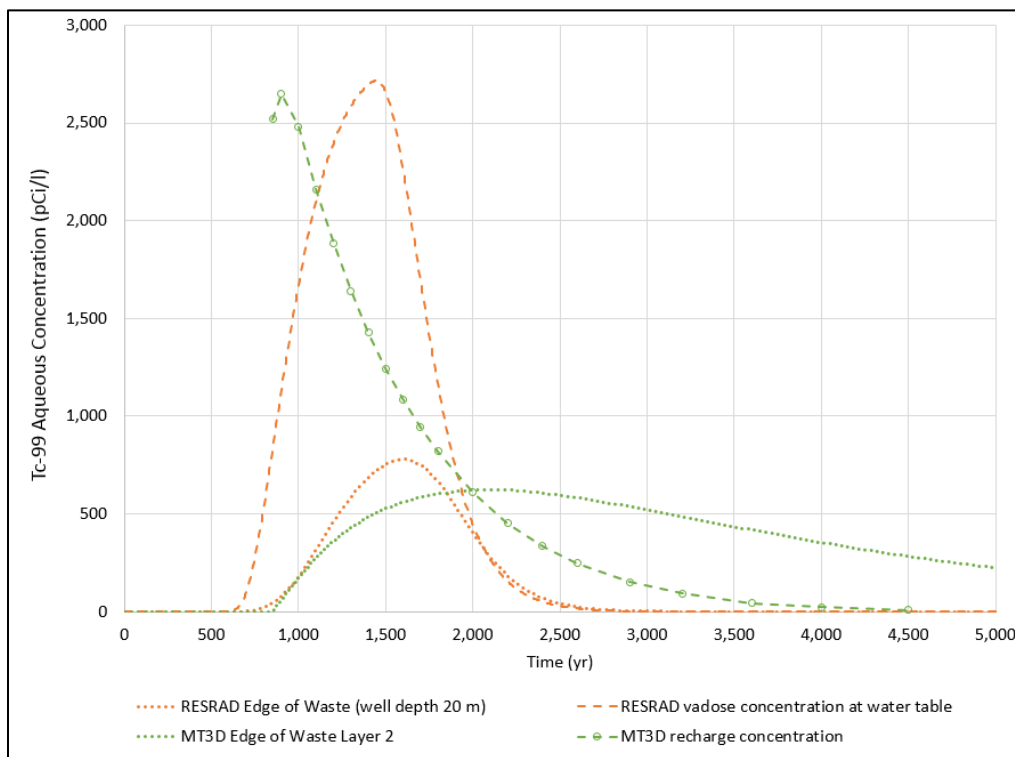
Fig. 3.36. Comparison of vadose zone (at water table) and saturated zone (at edge of waste) Tc-99 concentrations for the MT3D and RESRAD-OFFSITE models.

Predicted saturated zone Tc-99 concentrations at the EOW and at the groundwater POA located 100 m from the EOW (100-m well) for the MT3D and RESRAD-OFFSITE models are plotted in Fig. 3.37. The well depth for the RESRAD-OFFSITE model 100-m well is 131 ft (specified as 40 m in model units), which is approximately equal to the total thickness of MT3D model layers 1 to 3 at the groundwater POA. MT3D model layers 1 to 3 typically have the highest peak activity concentrations at the 100-m well location (Sect. 4.3). For the RESRAD-OFFSITE model, the saturated zone Tc-99 concentration curves for the EOW and 100-m well are similar, with the peak concentration at the 100-m well about half the peak concentration at the EOW due to the difference in the specified well depth (131 ft versus 65.6 ft for the EOW). The RESRAD-OFFSITE model Tc-99 peak at the 100-m well occurs only 100 years later than the EOW peak (1700 versus 1600 years), whereas the peak Tc-99 concentrations for the MT3D model occur later (after 2500 years) and the delay between the EOW Tc-99 concentration peak and the peak at the 100-m well is much larger for the MT3D model (Fig. 3.37). The differences in timing of the saturated zone Tc-99 concentration peaks is the result of the difference in release models (Sect. 3.3.5.1) and to the difference between the simplified analytical saturated zone model in the RESRAD-OFFSITE code and the more detailed MT3D numerical model representation.

The MT3D model results for the 100-m well show a complex pattern of saturated zone Tc-99 concentrations over time, with model layer 1 concentration increasing quickly in parallel with the RESRAD-OFFSITE

210

model results and then increasing more gradually after about 1100 years to reach a peak at approximately 3000 years post-closure. MT3D model layer 2 Tc-99 concentrations at the 100-m well increase gradually between 1500 and 3500 years post-closure, exceeding model layer 1 Tc-99 concentrations after about 2500 years and reaching a peak at approximately 4000 years. The MT3D model layer 1 and layer 2 Tc-99 peaks at the 100-m well are lower than the RESRAD-OFFSITE model peak by about 50 percent and 30 percent, respectively (Fig. 3.37).
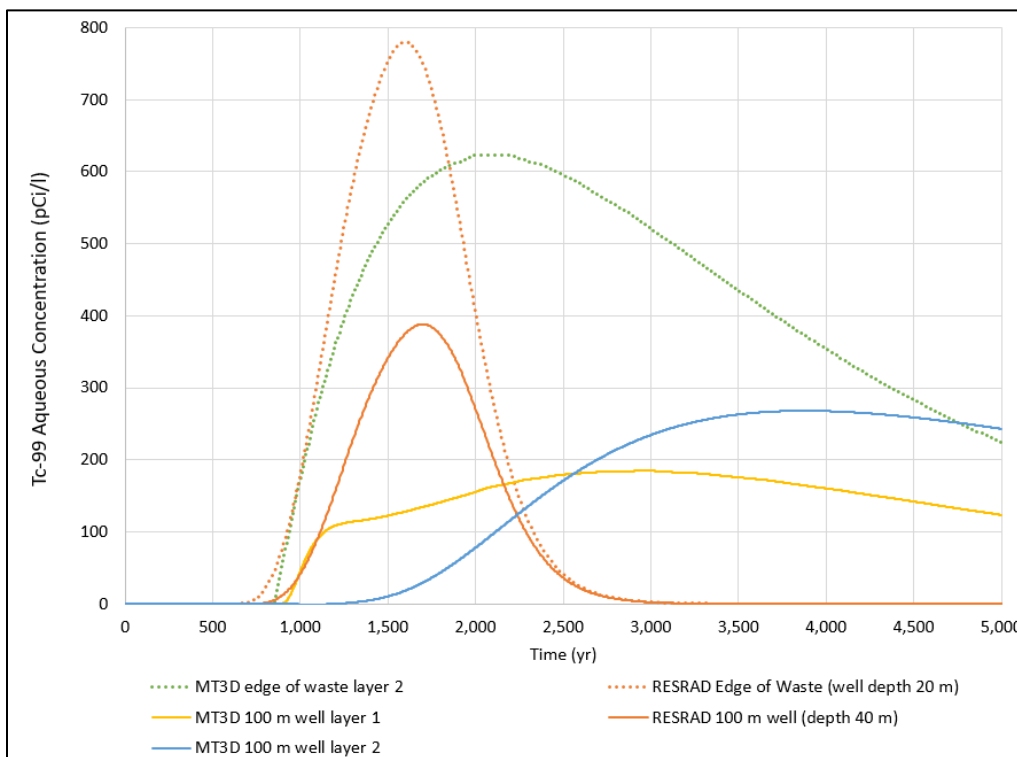
Fig. 3.37. Comparison of predicted saturated zone Tc-99 concentrations for the MT3D and RESRAD-OFFSITE models

The RESRAD-OFFSITE model tends to predict larger and earlier peak saturated zone activity concentrations than does the MT3D model due to the differences in model structure and complexity. The saturated zone concentrations from the RESRAD-OFFSITE model are sensitive to a number of saturated zone input parameters in addition to the well depth specification. The saturated zone hydraulic gradient in particular has a large impact on the predicted 100-m well concentration, as does the assumed value of saturated zone hydraulic conductivity. The product of these two input parameters is the saturated zone Darcy velocity, which determines the predicted dilution of leachate as it arrives at the water table. The hydraulic conductivity of the saturated zone assigned to the RESRAD-OFFSITE model was a transmissivity-weighted average of the K values assigned to MT3D model layers 1 and 2 for the Nolichucky Formation (Sect. 3.3.3.1). The final RESRAD-OFFSITE model input parameter values for the hydraulic gradient to the well and the well depth were selected to ensure general consistency in predicted saturated zone concentrations with the MT3D model results. The well depth of 131 ft was considered reasonable given that MT3D model layers 1 to 3 typically showed the largest peak concentrations and the total thickness of the saturated zone represented was similar. This interval is also consistent with the range of local water well depths (Sect. 3.4.2). The base case value for hydraulic gradient was specified as 0.054, which is higher than the estimated average gradient (0.036) of the water table along the flow path toward the groundwater POA derived from the EMDF flow model results for the long-term performance condition (Sect. 4.1). Applying the higher base case value of hydraulic gradient in the RESRAD-OFFSITE model

211

resulted in predicted peak saturated zone concentrations at the 100-m well that are broadly consistent (but higher than) the peak concentrations for MT3D model layers 1 and 2, although predicted MT3D model peaks occur later. The sensitivity of RESRAD-OFFSITE model dose predictions to these and other saturated zone input parameter assumptions is presented in Sect. 5.3.

Conceptual model uncertainty. The RESRAD-OFFSITE model saturated zone Tc-99 concentration results are also compared to the results of MT3D model sensitivity evaluations for the hydraulic conductivity of model layer 2 and the non-uniform radionuclide release scenario. These comparisons were made to address potential conceptual model uncertainties related to the characteristics of saprolite and bedrock along the flow path to the groundwater POA and to the assumption of uniform radionuclide release to the saturated zone.

The relatively large thickness (70 ft) of model layer 2 in the EMDF model compared to the thickness of layers 1 and 3 at the 100-m well location suggested that the hydrogeologic properties assigned to layer 2 along the flow path from the EOW to well location could have a large effect on predicted saturated zone activity concentrations. A sensitivity case was evaluated for the EMDF groundwater flow model and the MT3D model Tc-99 transport simulation in which the hydraulic conductivity of model layer 2 was increased to the value assigned to model layer 1, constituting an 8-fold increase. Applying the larger K value to model layer 2 is not an accurate representation of site conditions, based on the CBCV site characterization results (DOE 2018b, DOE 2019), but the sensitivity case does illustrate how a different configuration of material properties affects the results of the MT3D saturated zone radionuclide transport model (Fig. 3.38). Peak saturated zone Tc-99 concentrations at the 100-m well location are higher with the increase in the K values for MT3D model layer 2, reflecting the impact of reduced saturated thickness (decreased water table elevation) within model layer 2 beneath the EMDF waste footprint, and the increased transport velocity associated with the increased conductivity. The MT3D model Tc-99 concentration peaks for the increased K sensitivity case are also much earlier than the base case MT3D model Tc-99 peaks, coinciding with the earlier Tc-99 saturated zone concentrations predicted by the RESRAD-OFFSITE model (Fig. 3.36). The RESRAD-OFFSITE model Tc-99 peak concentration falls between the Tc-99 peaks for MT3D model layers 1 and 2 predicted for the increased layer 2 hydraulic conductivity. This result, for which the MT3D model sensitivity case predictions are closer to the RESRAD-OFFSITE model Tc-99 results, is expected because the increase in K for model MT3D layer 2 creates a groundwater flow system closer to the simplified RESRAD-OFFSITE analytical model of the saturated zone. The MT3D model sensitivity case results are consistent with expectations based on the differences in conceptualization and parameterization of the saturated zone between models.

The sensitivity of MT3D model Tc-99 concentration results to the assumption of uniform radionuclide release to the saturated zone was evaluated with a non-uniform release scenario (Sects. 3.3.3.2 and 5.1). The details of implementing the non-uniform Tc-99 release model for the MT3D sensitivity evaluation are presented in Appendix F, Sect. F.4.2. The non-uniform Tc-99 release scenario results indicate that the impact is greatest on early (prior to 2500 years post-closure) Tc-99 concentrations for MT3D model layer 1, which do not show the rapid increase at around 1000 years, increasing more gradually from 1200 to 3500 years to a peak Tc-99 concentration that is slightly less than the base case result for MT3D model layer 1 (Fig. 3.39). The increase in MT3D model layer 2 Tc-99 concentrations is also delayed relative to the base case result, but the layer 2 peak Tc-99 concentrations are nearly the same as the base case peak concentrations in model layer 2. These results were the basis for concluding that assuming a uniform release of leachate to the saturated zone (as applied to the MT3D model base case simulations and as the conceptual basis for the RESRAD-OFFSITE model code) does not lead to underestimating the impacts of release at the groundwater and surface water POAs because the RESRAD-OFFSITE model used for the total system simulation and dose analysis predicts earlier and larger peak concentrations.
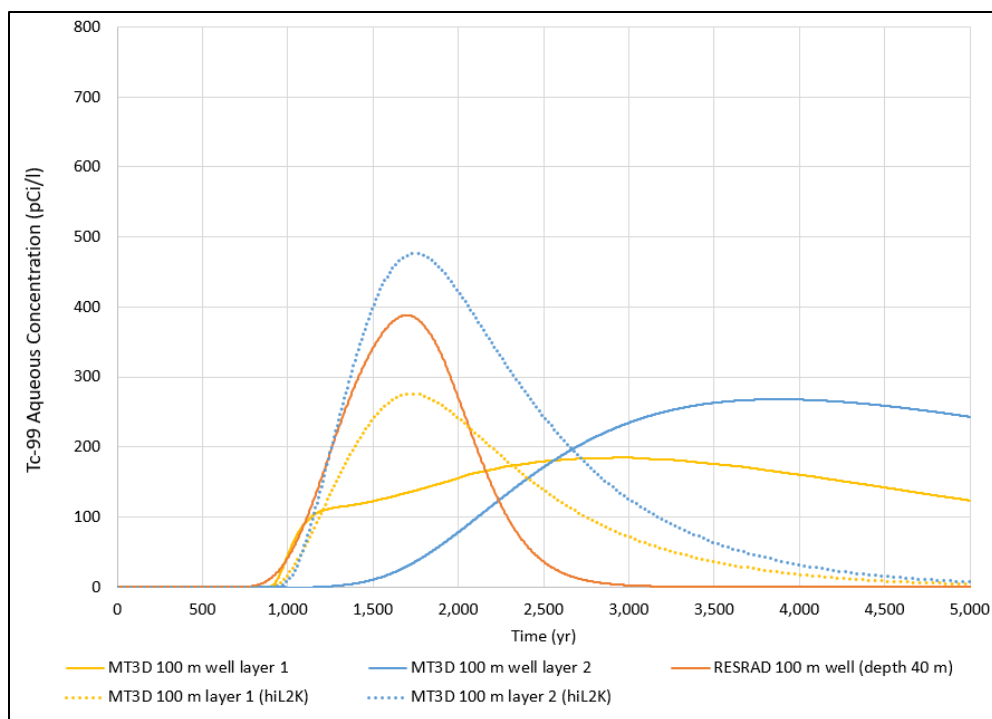
Fig. 3.38. Sensitivity of MT3D model predicted Tc-99 concentrations (groundwater POA) to increased hydraulic conductivity of MT3D model layer 2
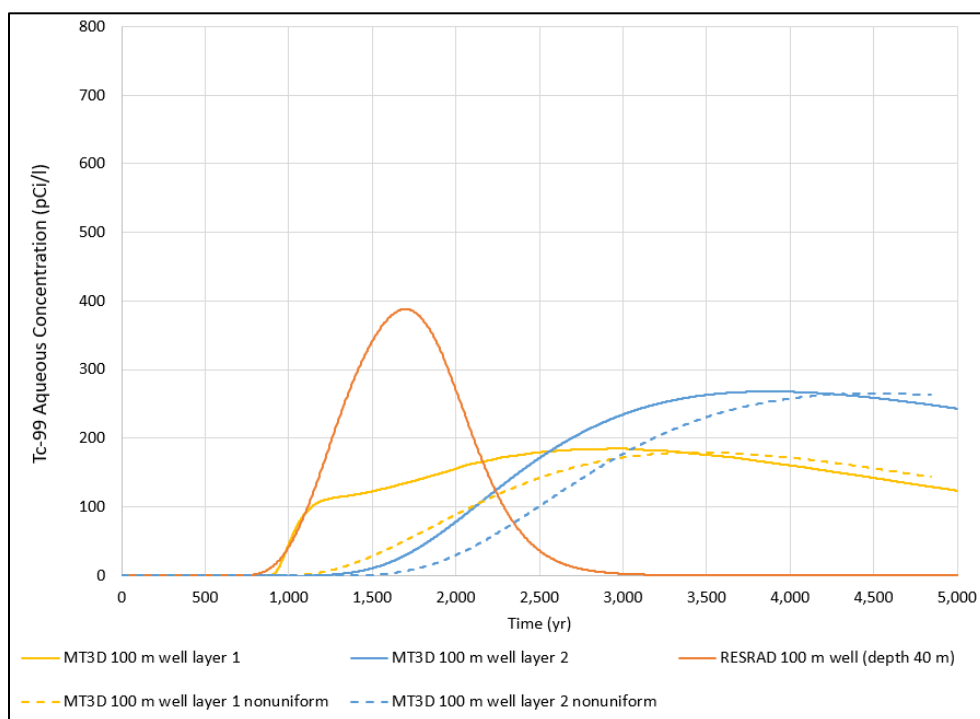

Fig. 3.39. Sensitivity of MT3D model predicted Tc-99 concentrations (groundwater POA) for the non-uniform radionuclide release scenario

213

3.3.5.3 Transport model integration − summary and conclusion

Based on the comparison of PA model results for Tc-99 flux from the waste and vadose zone (Sect. 3.3.5.1), saturated zone Tc-99 concentration results from the MT3D and RESRAD-OFFSITE models, and MT3D model sensitivity evaluations related to conceptual model uncertainties (Sect. 3.3.5.2), RESRAD-OFFSITE model base case predictions of peak concentrations at the groundwater POA are larger and earlier than corresponding predictions from the more detailed MT3D transport model. Final base case values for critical RESRAD-OFFSITE model input parameters that impact the simulated saturated zone concentrations, including the well depth and hydraulic gradient to the well, were adopted on this basis. For radionuclides with assumed base case K_d values greater than 1 cm^3/g, the instantaneous equilibrium desorption release model and vadose zone representation in the RESRAD-OFFSITE code do not capture the extent to which the EMDF design and the vadose zone below the disposal facility contribute to long-term performance of the disposal system. The conclusion is that the RESRAD-OFFSITE model saturated zone concentration estimates are pessimistically biased high relative to predictions from the more detailed models, and this bias provides a measure of conservatism to the PA dose analysis.

3.4 EXPOSURE AND DOSE ANALYSIS

This section describes implementation of the exposure pathways and scenario described in Sect. 3.2.4 using the total system simulation code RESRAD-OFFSITE.

3.4.1 Site Layout

The EMDF site layout implemented in the RESRAD-OFFSITE model (Fig. 3.40) is based on the assumed resident farmer exposure scenario and site-specific conditions including topography and surface water locations. One limitation of the RESRAD-OFFSITE model is that the primary contamination must be specified as a rectangle, which only approximates the layout of the facility as designed. The EMDF dimensions in the model were specified such that the shorter dimension (822 ft) is equal to the average east-west dimension of the EMDF preliminary design, and the longer dimension (1255 ft) is input as the value that maintains the total design waste volume of 2.2 million cy, based on the average waste thickness (57.5 ft). Sizes and locations of the dwelling site and agricultural fields shown on Fig. 3.40 are assumptions based on topography and proximity to the groundwater well and Bear Creek water supply. The receptor well is located 100 m from the southwest corner of the EMDF rectangle in the direction of groundwater flow as indicated by the EMDF flow model (Sect. 4.1). The well is assumed to be located along the centerline of the modeled plume. The distance to the surface water body in the RESRAD-OFFSITE model layout is 1035 ft, based on the distance from the edge of waste to Bear Creek downstream of NT-11.

3.4.2 Well Construction and Water Use Assumptions

The subsurface vertical interval from which groundwater is withdrawn for human consumption and domestic use is parameterized in the RESRAD-OFFSITE model as "depth of aquifer contributing to well", defined as the depth from the water table (top of the model domain for the aquifer) to the bottom of the well. This depth is set to 131 ft, consistent with the combined thickness of the MT3D model layers having the highest predicted concentrations at the groundwater POA (Sect. 3.3.3.2). Selection of the final base case value for the well depth was also influenced by the fact that the predicted concentration is highly sensitive to this input parameter and values much smaller than 131 ft produced peak concentrations much higher than saturated zone peak concentrations predicted the MT3D model. The final value selected was therefore an outcome of the comparison and integration of results obtained from different PA models (Sect. 3.3.5.2).
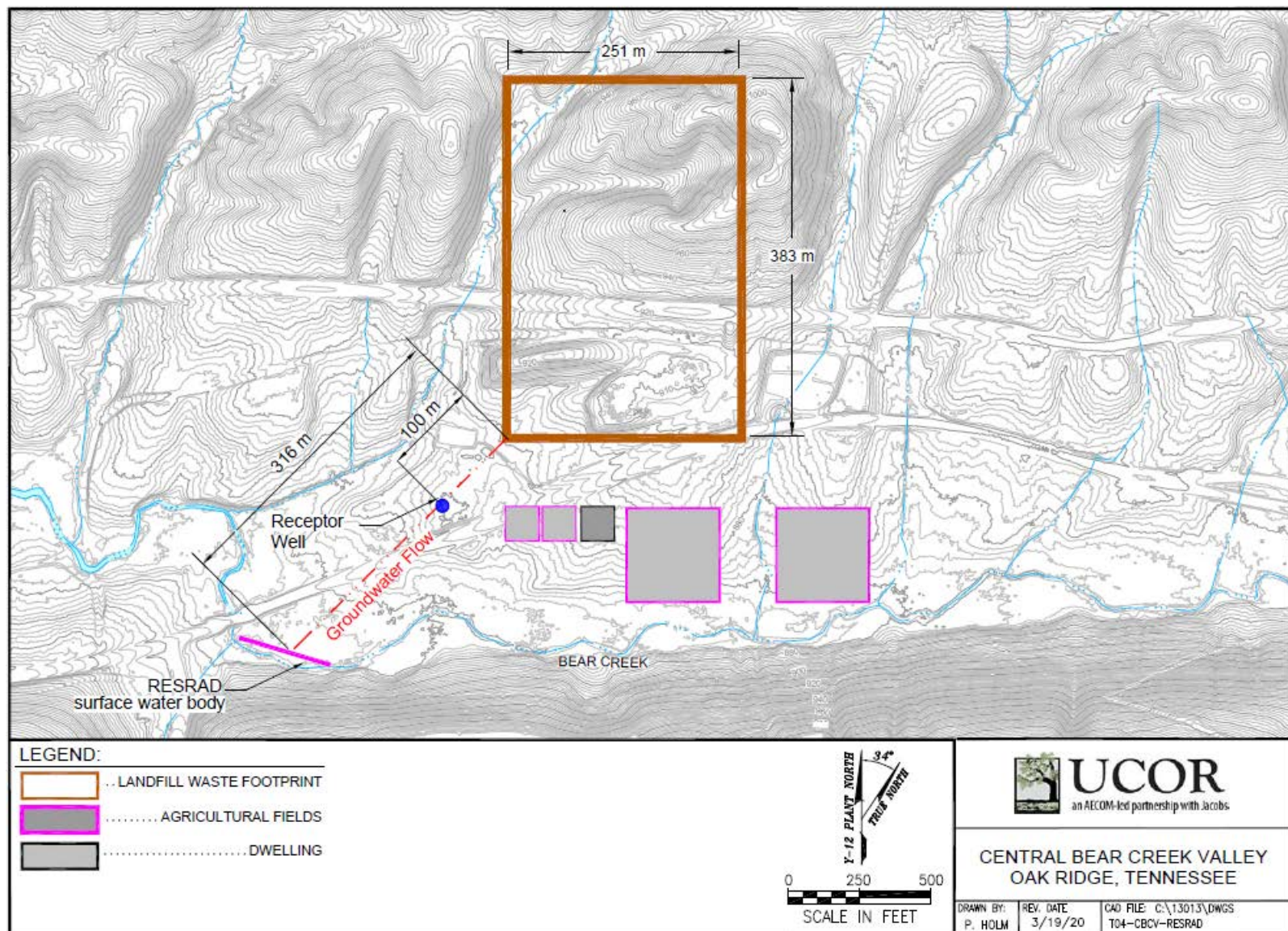
Fig. 3.40. Site map showing conceptual layout of EMDF footprint, dwelling and agricultural fields, groundwater well, and surface water body (Bear Creek)

The assumed well depth is consistent with the documented range of local water well depths in the area, which vary from less than 100 ft to more than 300 ft deep. The RESRAD-OFFSITE analytical model of the saturated zone predicts the highest concentrations at or very near the water table at the 100-m location, so that the 131-ft-deep cylindrical zone over which groundwater concentration is averaged includes the most contaminated upper part of the saturated zone, consistent with the results from the MT3D model (Sect. 3.3.3.2).

The water source assumption is that 100 percent of water that is used for drinking and to cook food and for cleaning and showering inside the dwelling is obtained from the well located 100 m from the EOW. Water ingestion for an individual was assumed to be 2 L/day. The livestock (assumed to include two beef cattle and two dairy cows) derive 100 percent of their drinking water from Bear Creek surface water that is impacted by contaminated groundwater emanating from the disposal facility. Irrigation water use for the various crop fields was assumed to be 0.15 m/year, with 100 percent of the irrigation water coming from contaminated portions of Bear Creek. The use of surface water for irrigation of crops is consistent with the predominance of surface water withdrawals for agricultural purposes in Anderson and Roane Counties (Sect. 3.2.4.2) due to the reliable nature of precipitation and surface water availability. The assumed values for key water use parameters are provided in Table 3.23.

**Table 3.23. Key water use parameter values assumed
for RESRAD-OFFSITE**

Water use or ingestion parameter	Value	Units
Human consumption	730	L/year
Indoor dwelling use	225	L/day
Beef cattle	50	L/day
Dairy cows	160	L/day
Well pumping rate	332	m^3/year

RESRAD = RESidual RADioactivity

3.4.3 Food and Soil Ingestion Rates

Assumed values for ingestion of foods and soil are presented in Table 3.24. Ingestion rates of food consumed by the receptor are based on EPA guidance (EPA 2011) for plant foods and Putnam et al. (1999) for beef, poultry, and eggs. The fish ingestion rate reflects limited recreational fishing in Bear Creek. It is assumed there is no consumption of crustacea or mollusks, which is reasonable given the EMDF location in eastern Tennessee.

Table 3.24. Simulated ingestion rate values

Parameter	Value	Units	Fraction from affected area
Fish	2.43	kg/year	1.0
Fruit, grain, non-leafy vegetables	176	kg/year	0.5
Leafy vegetables	17	kg/year	0.5
Meat	92	kg/year	0.25
Milk	110	L/year	0.5
Soil (incidental)	36.53	g/year	[a]

[a]The fraction of this intake from each contaminated area is proportional to the occupancy in that area.

Total fluid milk ingestion is given as the equivalent of 84 L/year on Table 11-12 of EPA 2011; however, the base case milk ingestion value for EMDF is set at 110 L/year. The higher milk ingestion value serves to increase the total food ingestion dose and thereby bias the dose estimate toward higher values. Values for ingestion of non-leafy produce and leafy vegetables are consistent with the data listed in Tables 9-1, 9-6, and 12-1 of EPA 2011.

The RESRAD-OFFSITE model exposure pathways do not include poultry or egg consumption explicitly. The animal food ingestion pathways represented in the model are limited to meat and milk from cows. To account for possible dose contributions from consumption of poultry and eggs, an effective meat ingestion rate (91.9 kg/year) is applied, representing the sum of beef (55.4 kg/year), poultry (21.3 kg/year), and eggs (15.2 kg/year) given in Putnam et al. (1999). Adjusted meat transfer factors are also calculated and applied in the RESRAD –OFFSITE model dose analysis (Sect. 3.4.5).

The Oak Ridge area is assumed to remain populated and urbanized in the future, with many commercial food sources (e.g., restaurants, grocery stores, farmer's markets) available in close proximity to the hypothetical BCV farm adjacent to EMDF. Food consumption is assumed to include some uncontaminated food as well as locally grown agricultural products contaminated with radionuclides released from the EMDF. For plant foods and milk, 50 percent of the food ingested is assumed to come from the contaminated agricultural areas. For meat ingestion, 25 percent is assumed to come from farm raised animals that ingest contaminated water and feed. The RESRAD-OFFSITE model sensitivity analyses include evaluating uncertainty in the fraction of food products obtained from contaminated areas (Appendix G, Sect. G.6.3).

Fish ingestion is based an EPA recommendation of 54 g/day for recreational fishing in areas with large bodies of water (EPA 1990), combined with an exposure frequency of 45 days/year, which is the value used as recreational surface water exposure frequency for the human health risk assessment in the BCV RI (DOE 1997b). Because of the limited populations of larger fish in BCV, and because the proportion of fish caught locally is set at 1.0, the fish ingestion rate of 2.43 kg/year overestimates the likely fish ingestion dose.

The incidental soil ingestion rate is based on the EPA recommended value (100 mg/day) and the fractional occupancy time in the agricultural areas (Sect. 3.4.4). The annual inhalation rate required for the inhalation pathway dose calculation (Sect. 3.2.4) was set at the RESRAD-OFFSITE default value of 8400 m^3/year.

3.4.4 Occupancy

Specified occupancy fractions represent the assumed fractional annual time period (fractional years) that the receptor spends inside or outside the specified exposure areas. For example, occupancy factors are specified for the EMDF area and for farmed areas or pasture land contaminated by irrigation. Those occupancy factors are used to compute exposure from direct external radiation from contaminated soil in irrigated fields, and internal exposure due to incidental ingestion of soil and inhalation of dust resuspended from contaminated soil. The RESRAD-OFFSITE base case model assumes that the receptor spends approximately 2.6 weeks outdoors on the primary contamination (5 percent of time), half the time inside the offsite dwelling (50 percent of time), 2.6 weeks outdoors at the offsite dwelling (5 percent of time), and 10 percent of the time at each of the four agricultural areas (40 percent of the time total). Overall, the representative receptor is assumed to spend 100 percent of the time at EMDF, thereby inducing a bias toward a greater dose from the external, inhalation, and soil ingestion pathways.

3.4.5   Biotic Transfer Factors and Dose Conversion Parameters

3.4.5.1   Biotic transfer factors

The RESRAD-OFFSITE model uses transfer factors to convert soil and/or water concentrations to concentrations in plant and animal tissues. Below are brief descriptions of the transfer factor types included in the default library:

- Soil to plant transfer factors: Represents the nuclide concentration in vegetables, fruits, and in livestock feed products at the time of harvest (fresh weight basis) due to root uptake from soil containing a unit concentration (dry weight basis) of the nuclide

- Intake to animal product transfer factors: Represents the nuclide concentration in the animal meat and milk at the time of slaughter or milking, respectively, due to a uniform intake of unit activity of radionuclide per day

- Water to aquatic food transfer factors: Represents the nuclide concentration in aquatic food products such as fish and crustacea at the time of harvest from the simulated surface waterbody containing a unit concentration of radionuclide in the aqueous phase.

The RESRAD-OFFSITE model exposure pathways do not include poultry or egg consumption explicitly. The animal food ingestion pathways represented in the model are limited to meat and milk from cows, fish, and crustaceans. To account for possible dose contributions from consumption of poultry and eggs, an effective (total) meat ingestion rate is applied (Sect. 3.4.3) and adjusted feed consumption to meat transfer factors are calculated and applied in the RESRAD–OFFSITE model dose analysis.

With the exception of transfer factors for H-3, C-14, I-129, all values are from PNNL 2003, which are reproduced in Yu et al. (2015). RESRAD default values are applied for the H-3 freshwater fish transfer factor and the I-129 soil to plant transfer factor. Transfer factors for H-3 (except fish) and C-14 (except fish) are calculated within specialized RESRAD-OFFSITE submodels for these two radionuclides. The adjusted radionuclide-specific transfer factors represent consumption rate weighted average transfer factors for beef, poultry, and eggs as follows:

$$\text{Consumption Weighted TF} = (CR_{beef}TF_{beef} + CR_{poultry}TF_{poultry} + CR_{eggs}TF_{eggs}) / (CR_{beef} + CR_{poultry} + CR_{eggs})$$

where:

CR = Consumption Rate of Specified Animal Product (kg/year)
TF = Intake-to-Animal Transfer Factor for Specified Meat Type (pCi/kg)/(pCi/day).

3.4.5.2   Dose conversion factors

The RESRAD-OFFSITE model libraries (Table 3.25) contain the dose conversion factor databases for external exposure and internal exposure as inhalation and ingestion that are applied in the dose analysis (Gnanapragasam and Yu 2015). The library of default transfer factors is used to supplement the values given in PNNL (2003).

Table 3.25. Key radiological and dose conversion factor data sources

Parameter/library	Basis
Basis for radiological transformations	ICRP 2008
External exposure library	DCFPAK3.02 database, https://www.dcfpak.org, DOE 2017a
Internal exposure dose library	DOE 2011b (reference person)
Slope factor (risk) library	DCFPAK3.02 morbidity, https://www.dcfpak.org, DOE 2017a
Transfer factor library	RESRAD default transfer factors
Calculation time points	2048

DCFPAK = Dose Coefficient File Package (database)　　　　RESRAD = RESidual RADioactivity
ICRP = International Commission on Radiological Protection

This page intentionally left blank.

4.   RESULTS OF ANALYSES

This section presents the environmental transport modeling results and the dose analysis performed for the EMDF disposal system. HELP model results for evaluating cover design performance and potential degraded performance conditions are summarized in Sect. 3.3.1 and detailed in Appendix C, Sect. C.2. Those results are the basis for the assumed evolution of cover performance and cover infiltration rates applied in the radionuclide transport models.

4.1   PREDICTED GROUNDWATER CONDITIONS

This section provides a succinct summary of the groundwater flow model results used directly or indirectly as inputs to the environmental transport modeling. Additional detail on the groundwater flow model results including particle tracking analysis and model sensitivity evaluations is provided in Appendix D.

The steady-state flow model results for the CBCV model (current conditions) and the EMDF model (long-term performance condition) are shown in Figs. 4.1 and 4.2. The EMDF model provides the flow field (Fig. 4.2) for the 3-D saturated zone radionuclide transport model. The general flow pattern for the long-term performance condition is downward flow below the disposal unit directed horizontally toward Bear Creek and the NT-10 and NT-11 tributaries. Flow farther south between disposal cell 3 and Bear Creek is directed predominantly down valley toward NT-11 and Bear Creek. The estimated water table elevation below the EMDF and average hydraulic gradient from the EMDF model are used for parameterizing the total system model (RESRAD-OFFSITE) simulation (Appendix G).

The effect of long-term cover system degradation leading to increased cover infiltration and recharge to the saturated zone below the facility is illustrated in Fig. 4.3, which shows EMDF model results for both the full design performance condition (zero cover infiltration/recharge) and the long-term performance condition (0.88 in./year cover infiltration/recharge). The predicted impact of cover degradation and leachate release on the water table is significant, with elevation differences of up to 8 ft near the center of disposal cell 2 (Fig.4.4). However, the predicted groundwater levels for the long-term performance condition are still below the base of the geobuffer zone.

For the EMDF model long-term performance condition, simulated depth to the water table below the waste ranges between 20 and 50 ft (Fig. 4.5). The average vertical interval between the bottom of waste and the water table is approximately 31 ft. This average total vadose zone thickness below the waste is used to set the base case thickness for unsaturated zone 5 in the RESRAD-OFFSITE model (Sect. 3.3.4, Table 3.22).
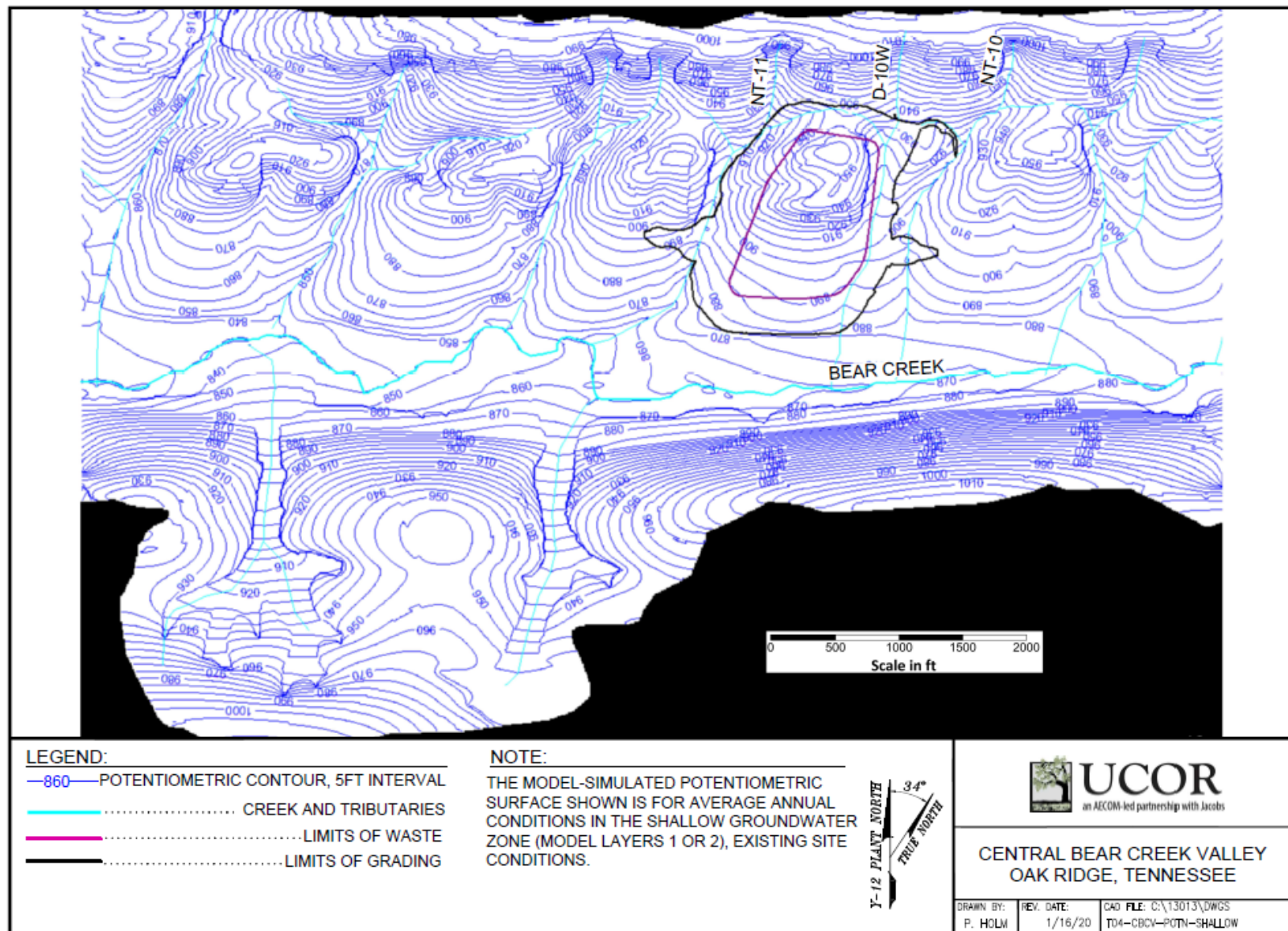
Fig. 4.1. CBCV model predicted water table elevation
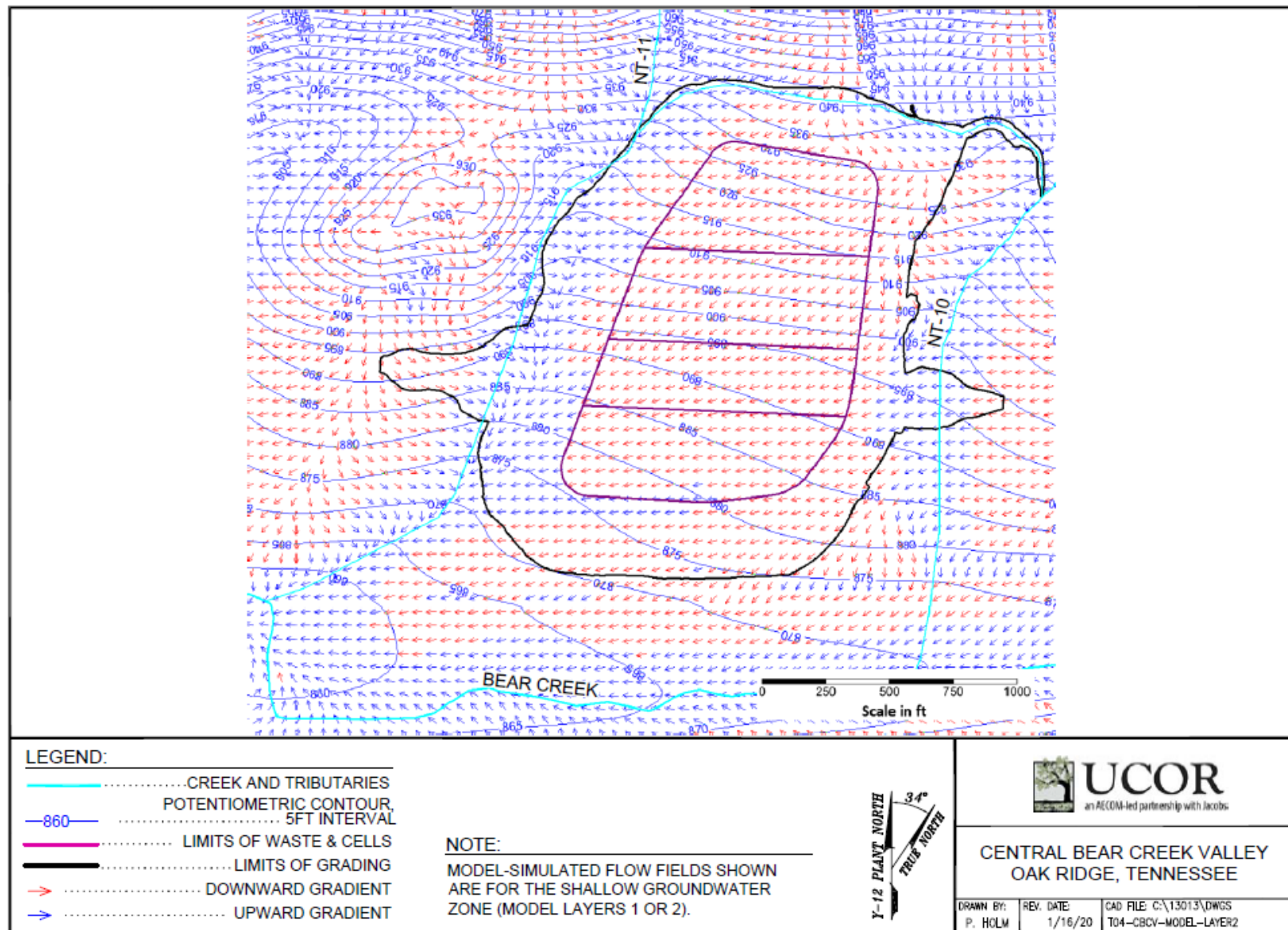
Fig. 4.2. EMDF model long-term performance condition predicted potentiometric surface and flow field for model layer 2
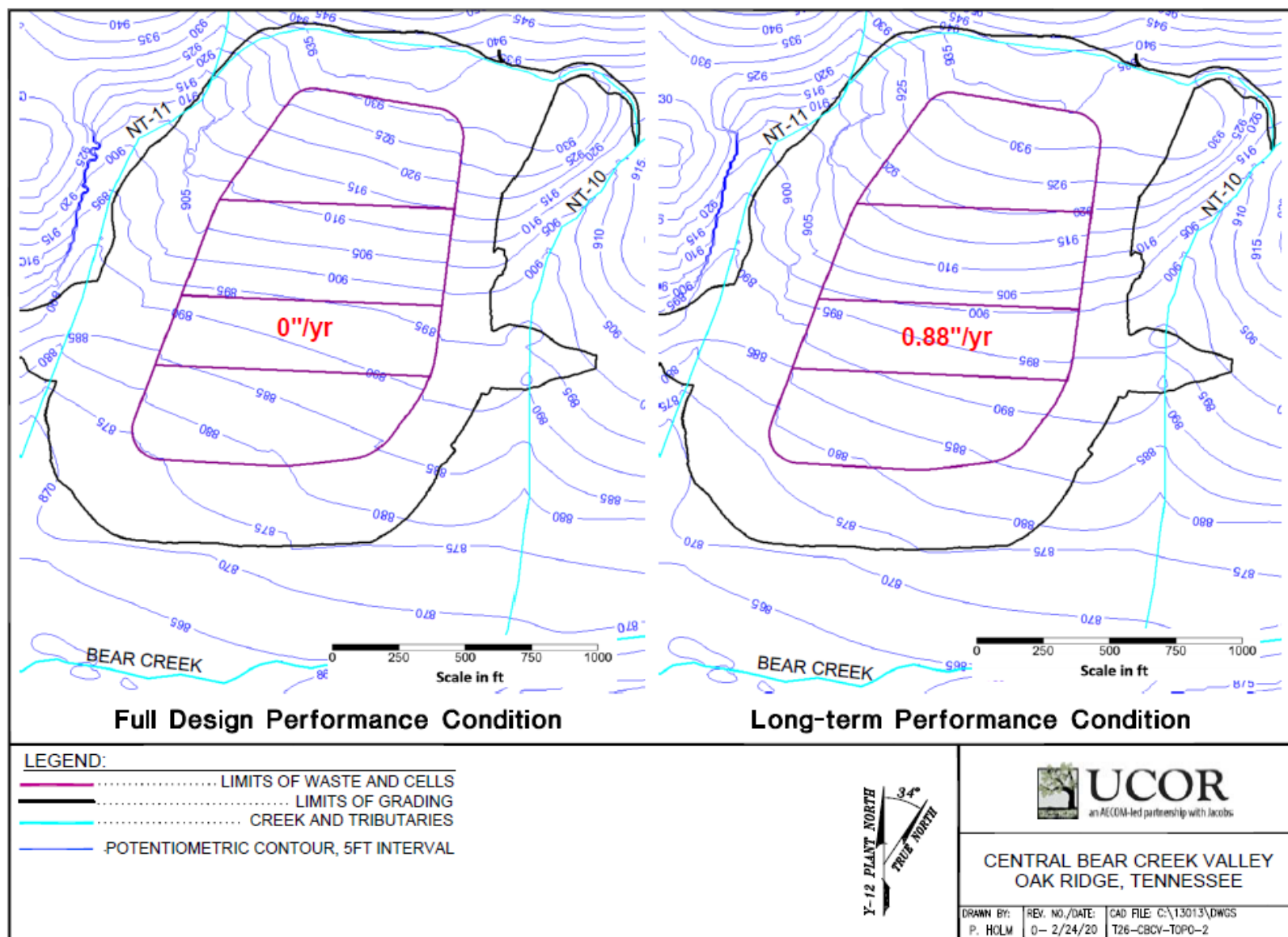
Fig. 4.3. EMDF model predicted groundwater levels for full design performance condition and long-term performance condition
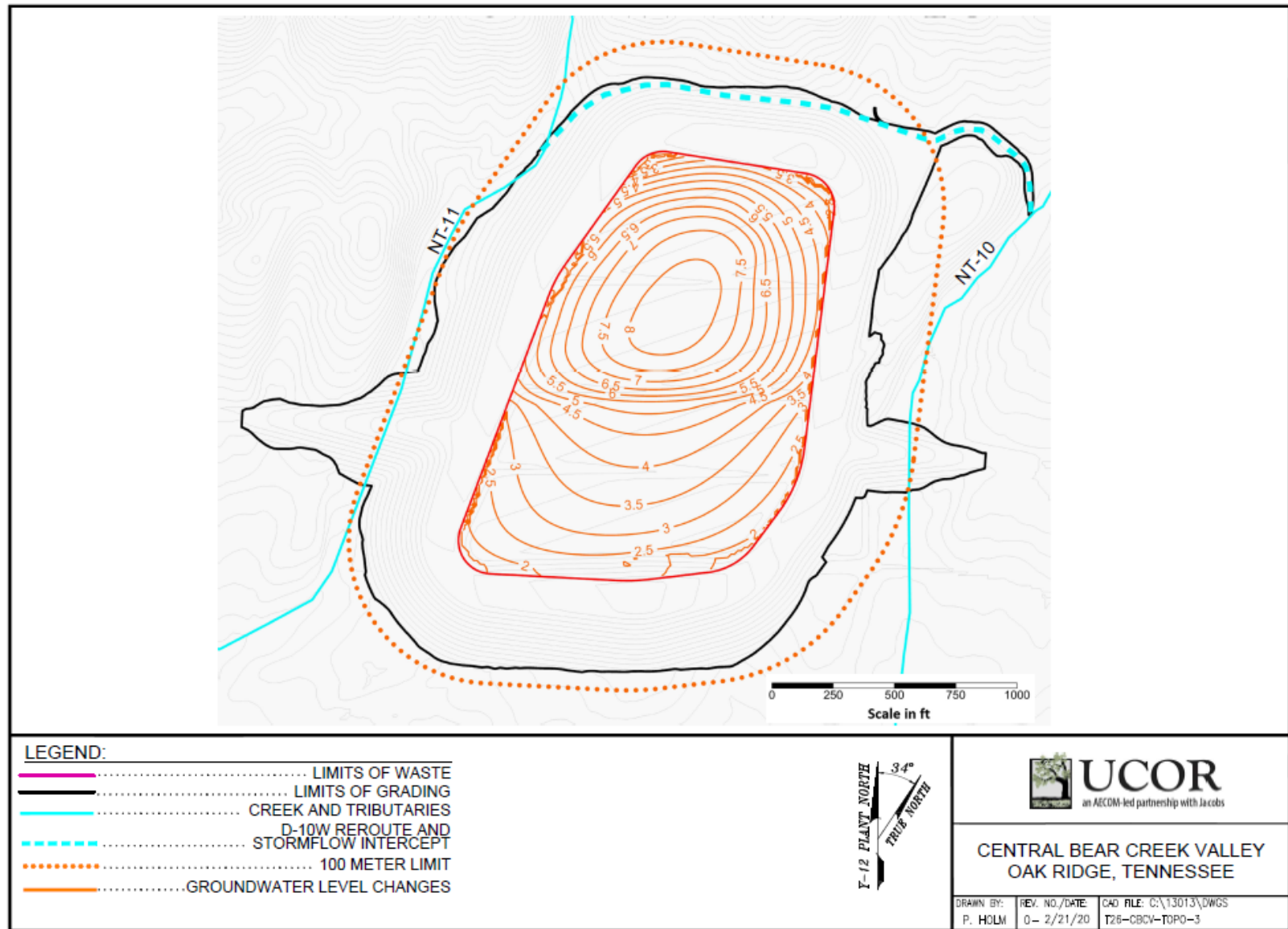
Fig. 4.4. Groundwater level changes from full design performance to long-term performance condition
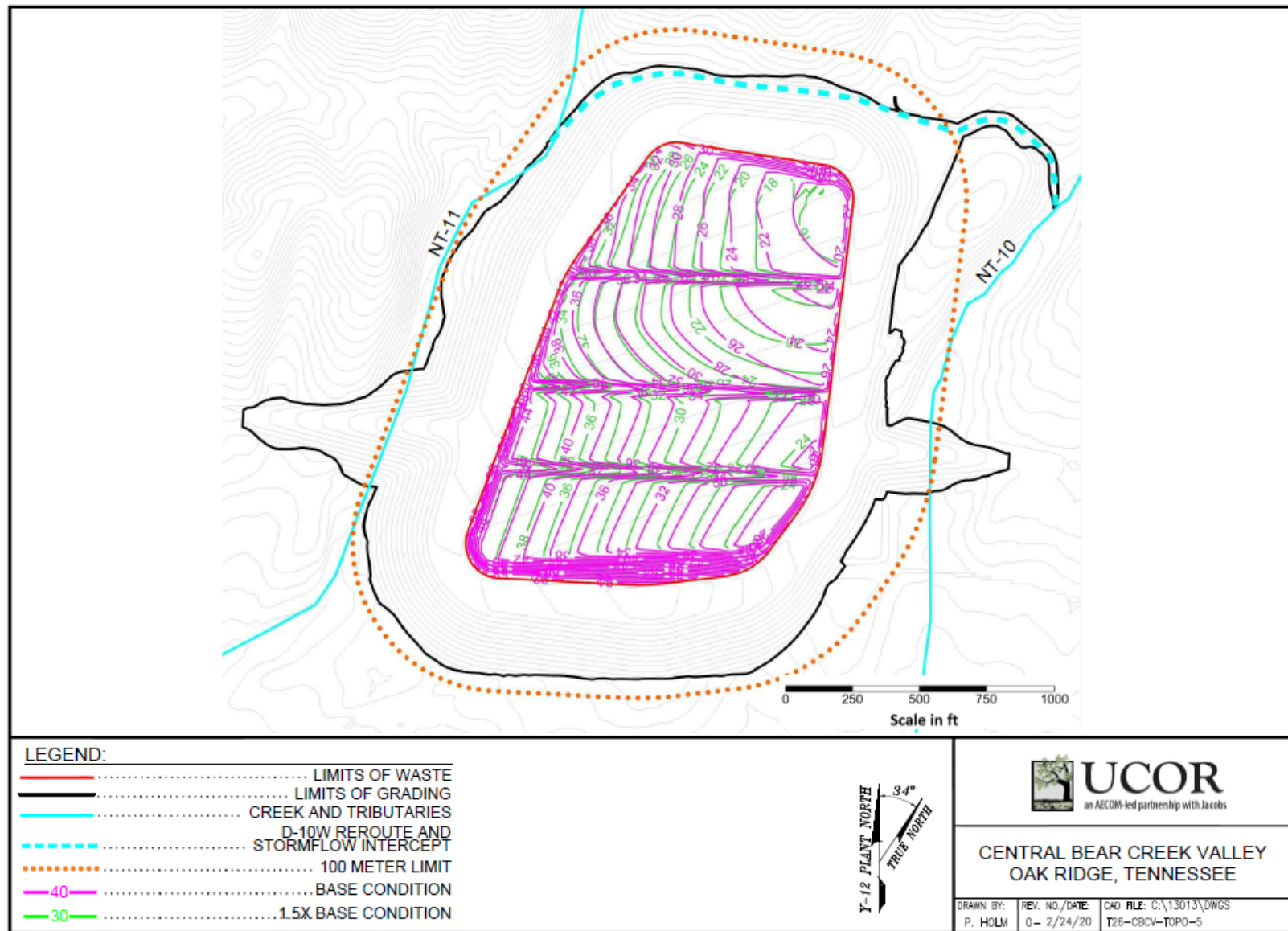
Fig. 4.5. Depth to groundwater contours for 1.5 times base recharge and the base recharge case

4.2 RADIONUCLIDE RELEASE AND VADOSE ZONE TRANSPORT

4.2.1 STOMP Model Simulations

The STOMP model simulations provided a detailed representation of patterns of radionuclide release beneath the EMDF, and were used to quantify average vadose travel times, total activity flux at particular locations, and the non-uniformity of release for seven radionuclides (H-3, C-14, Tc-99, I-129, U-234, U-238, and Pu-239). Six of these radionuclides were selected on the basis of potential dose contributions within the general 10,000-year timeframe for the PA analysis (C-14, Tc-99, and I-129), or dose impacts over much longer timespans (U-234, U-238, and Pu-239). STOMP model runs were extended to 1,000,000 years to simulate release of less mobile radionuclides such as U-234. Section 3.3.2 provides a summary of the STOMP model implementation. Detailed description of STOMP model input parameters including mechanical and hydraulic properties of materials, initial radionuclide concentrations, assumed K_d values, as well as model domain setup and assignment of boundary conditions is provided in Appendix E.

Two 2-D cross-section STOMP models were developed for the EMDF site (Section A and Section B, refer to Fig. 3.14). Due to the large number of model nodes and the extended period of simulation, and in order to streamline output data post-processing, a limited number of model outputs were specified. The STOMP output included data for selected model nodes at several vertical output profiles and along three output surfaces (Fig. 4.6), and data for all model nodes at selected model time steps. The three output surfaces comprised all model nodes along the top of the liner (bottom of waste), bottom of the liner, and along the estimated water table elevation beneath the EMDF (based on the EMDF flow model long-term performance condition output shown in Fig. 4.2). The data output surfaces were used to calculate the total vertical activity flux across the surface as a function of time. These activity flux time series were then used to estimate the average vadose delay times and to support development of the non-uniform Tc-99 release scenario for the MT3D model (Sect. 4.3). The STOMP model output was also compared to the radionuclide release model developed for the MT3D saturated zone model and the predicted release to the vadose and saturated zones from the RESRAD-OFFSITE model code (refer to Sect. 3.3.5 for description of PA model integration).

Appendix E presents detailed model output for individual STOMP model nodes, as well as total activity flux estimates and cross-sectional graphics for specific model time steps. The remainder of Sect. 4.2 provides a limited range of STOMP model output examples, including saturation and activity concentration fields, and activity flux time series used to estimate the vadose delay times applied to the MT3D model inputs and outputs.
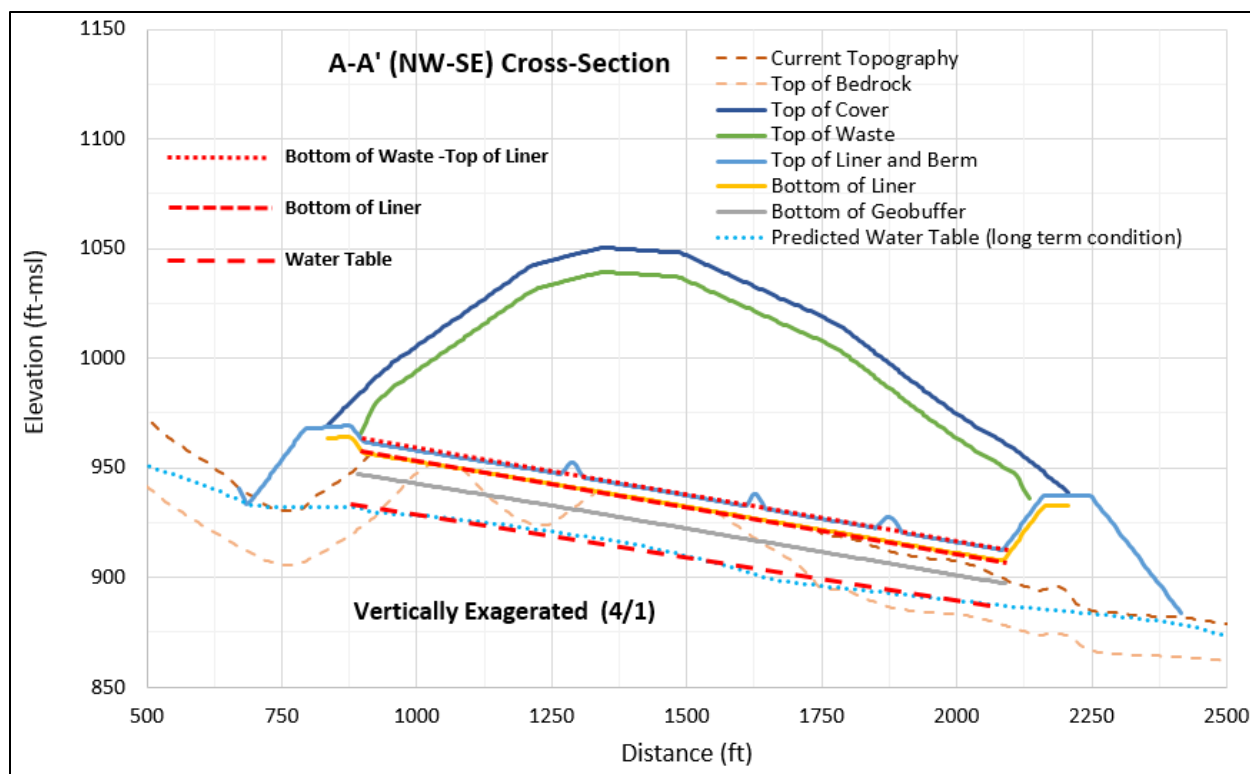
Fig. 4.6. Data output surfaces defined in the STOMP Section A model

4.2.2 Water Movement and Saturation

Water input along the top of the STOMP model domain represents the estimated natural rates of groundwater recharge (from 6 to 13 in./year depending on geologic unit) outside the perimeter berms, lower rates applied to the berm areas outside of the cover (1 in./year) and time varying cover infiltration along the central area (final cover system) of the disposal unit (refer to Fig. 3.19). The evolution of relative saturation (water content as a fraction of total available porosity) for the Section A model is shown in Fig. 4.7. Increasing cover infiltration begins at 200 years post-closure, but significant increases in saturation for most model nodes do not occur until the interval between 350 and 450 years. As early as 500 years, a strongly non-uniform pattern of saturation develops along the base of the liner system within the geologic buffer and underlying natural materials. Wetter areas develop beneath the downslope (lower) end of each disposal cell, reflecting the strong impact of the liner system geometry (sloping drainage layer above the clay barrier) in controlling the pattern of water flow. Equilibrium (steady state) saturation levels are achieved by approximately 1200 years for all materials. The progressive increase in relative saturation varies with material type and location in the cross section, reflecting the systematic pattern of leachate drainage along the liner and into the underlying materials. The liner system geometry causes non-uniformity in water flux and saturation that drive similar non-uniformity in patterns of radionuclide flux below the disposal unit.

228
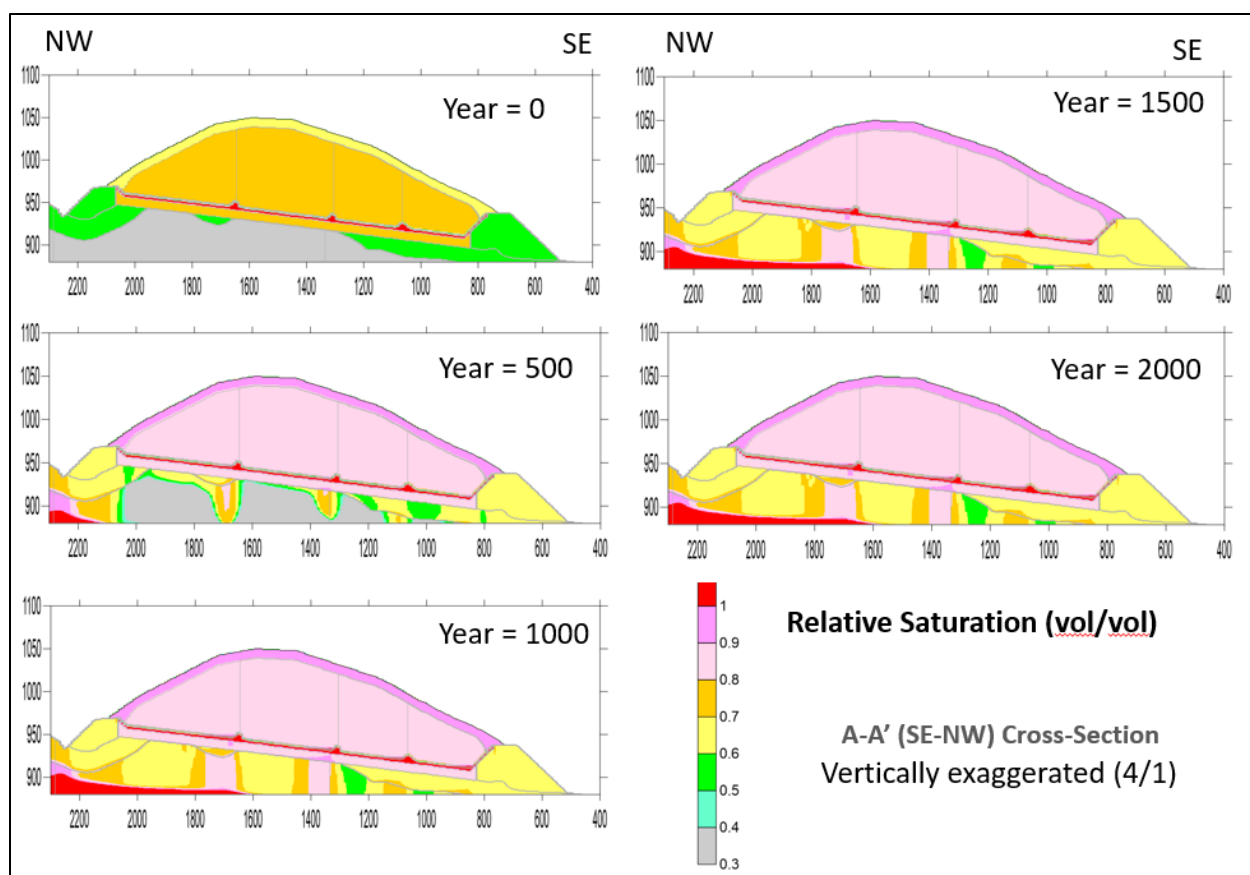
Fig. 4.7. Saturation change with time in the STOMP Section A model

4.2.3 Source Depletion and Vertical Migration of Radionuclides

STOMP model activity concentrations fields presented in this section are limited to results for C-14, Tc-99, and I-129. Results for the other radionuclides included in the STOMP modeling are presented in Appendix E. Section A modeled activity concentration fields for C-14, Tc-99, and I-129 at successive simulation times are presented in Figs. 4.8, 4.9, and 4.10. The successive radionuclide concentration fields illustrate both downward and lateral transport and highlight the strongly non-uniform pattern of release below the disposal unit. The time increments between panels in Figs. 4.8, 4.9, and 4.10 vary among radionuclides because of differences in mobility (K_d). Differences in the patterns of radionuclide depletion from the waste and migration into the vadose zone below the liner are controlled by differences in half-life and sorption (K_d value), and also reflect variation in waste thickness, disposal cell dimensions and liner system geometry.

The biggest control on the duration of radionuclide release and eventual depletion is the K_d value. Carbon-14 (K_d = zero) is completely depleted from the waste by 1500 years post-closure (Fig. 4.8), whereas depletion of I-129 (waste K_d = 2 ml/g) requires more than 5000 years (Fig. 4.10). There are different durations of radionuclide release for different disposal cells due to variable waste thickness. Disposal cells 1 and 4 have lower average waste thickness and therefore less radionuclide inventory and are depleted more quickly than the middle two cells (cells 2 and 3). The width of each cell and resulting differences in total water influx also influences this pattern. Cell 4 is relatively narrow and has a relatively small waste thickness and so is depleted most quickly (e.g., for Tc-99, cell 4 is nearly depleted by 2000 years, Fig. 4.9).

229
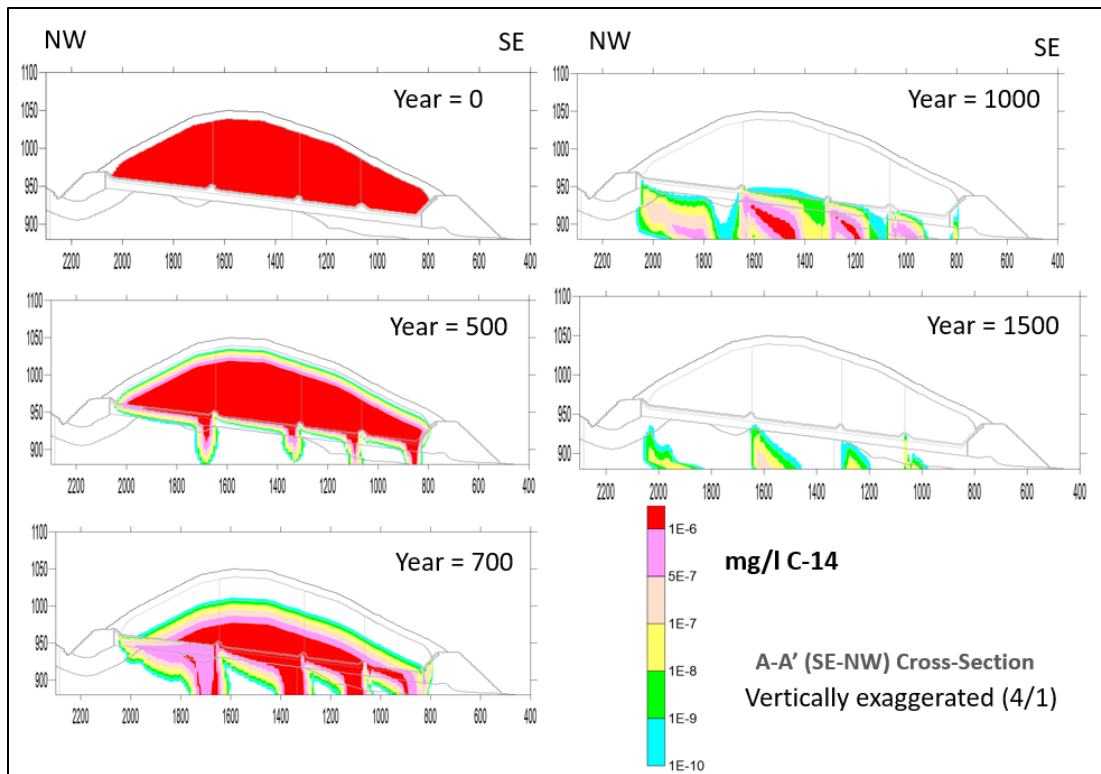
Fig. 4.8. C-14 concentration fields for the STOMP A-section model at successive simulation times
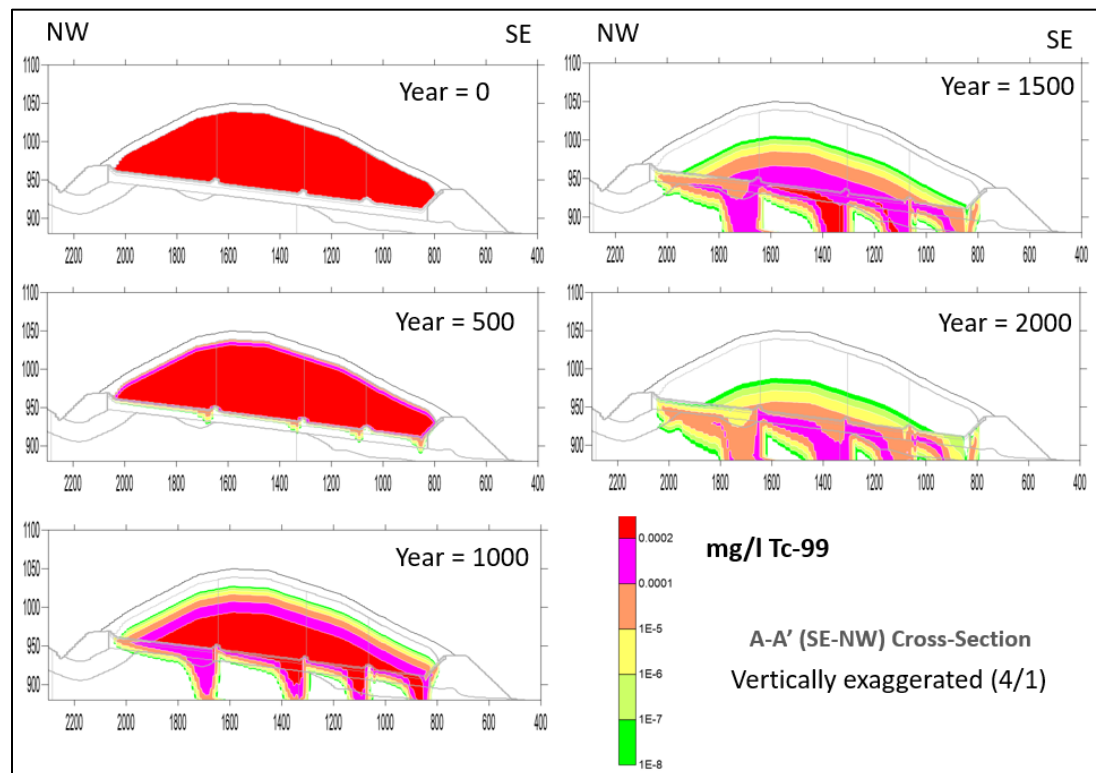
Fig. 4.9. Tc-99 concentration fields for the STOMP A-section model at successive simulation times
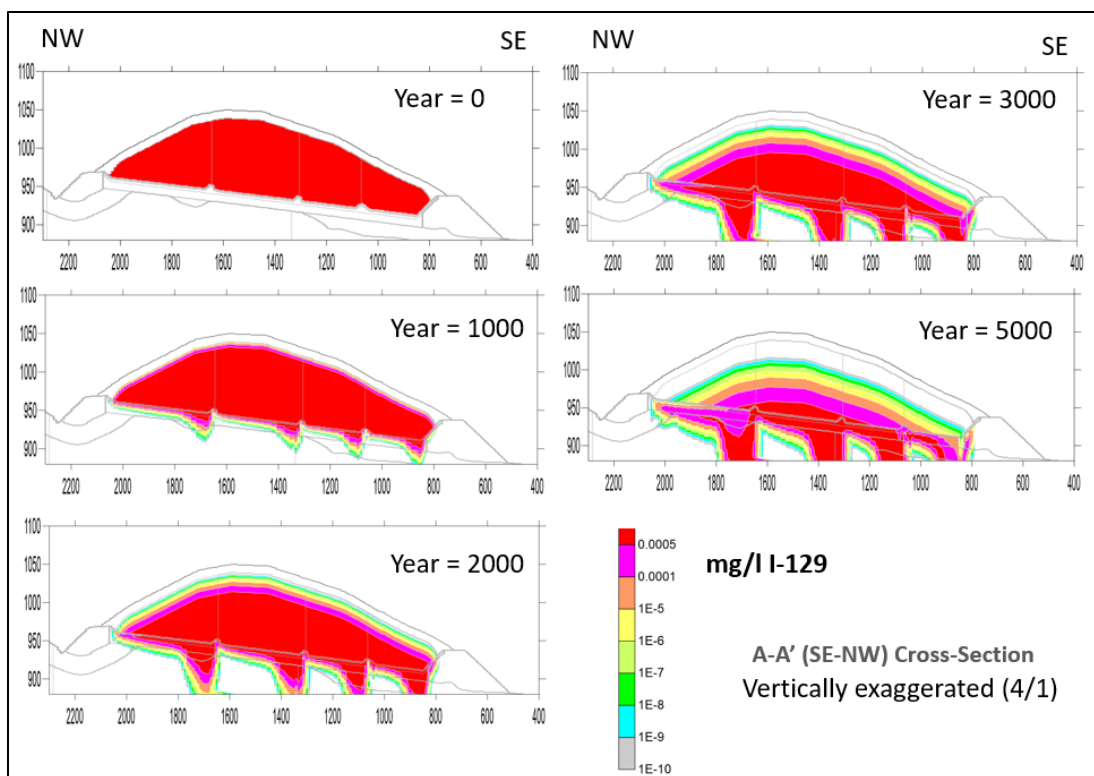
Fig. 4.10. I-129 concentration fields for the STOMP A-section model at successive simulation times

The non-uniform pattern of release beneath each disposal cell corresponds to variations in saturation and leachate concentration that results from downslope leachate movement along the liner system. The magnitude, duration, and timing of peak concentrations varies strongly along the base of each disposal cell and also varies among the four disposal cells (particularly the timing and duration of maximum concentrations; refer to Appendix E for illustrative graphics). The non-uniform release through the vadose zone to the saturated zone represented in the STOMP model simulations is summarized in terms of separate radionuclide flux curves developed for each disposal cell and presented in the following section.

These detailed modeling results show the potential complexity of contaminant movement in variably saturated and transient conditions and provide a good illustration of the value of the STOMP model in representing a complex system. The complexity of the radionuclide transport field within the vadose zone is greatly simplified for the 3-D saturated zone model (MT3D) and total system model (RESRAD-OFFSITE). An evaluation of the significance of non-uniform release to the predicted radionuclide concentrations at the groundwater well POA is presented in Sect. 5.2.

4.2.4 Radionuclide Flux at Output Surfaces

The radionuclide flux into the vadose zone below the liner and into the saturated zone were quantified based on the STOMP model results at the data output surfaces described in Sect. 4.2.1. The total flux calculations are a useful summary of STOMP model release predictions for comparison to the other release models (MT3D radionuclide input and RESRAD-OFFSITE output, refer to Sect. 3.3.5).

Figures 4.11, 4.12, and 4.13 show the activity flux rate across the three output surfaces for C-14, Tc-99, and I-129, respectively, and illustrate the progressive migration of radionuclides from waste through the liner and through the vadose zone. (Note the different time scales on the horizontal axes in these three

figures.) The increase in cover infiltration between 200 and 1000 years post-closure is also plotted on each figure. Carbon-14 has a much earlier release and shorter depletion time (Fig. 4.11) than either Tc-99 or I-129 due to the zero K_d value. The C-14 migrates quickly with water and the peak flux rate out of the waste occurs at 650 years, well before the water infiltration rate reaches its maximum rate at 1000 years. The peak flux rate at the water table for C-14 occurs at about 775 years.
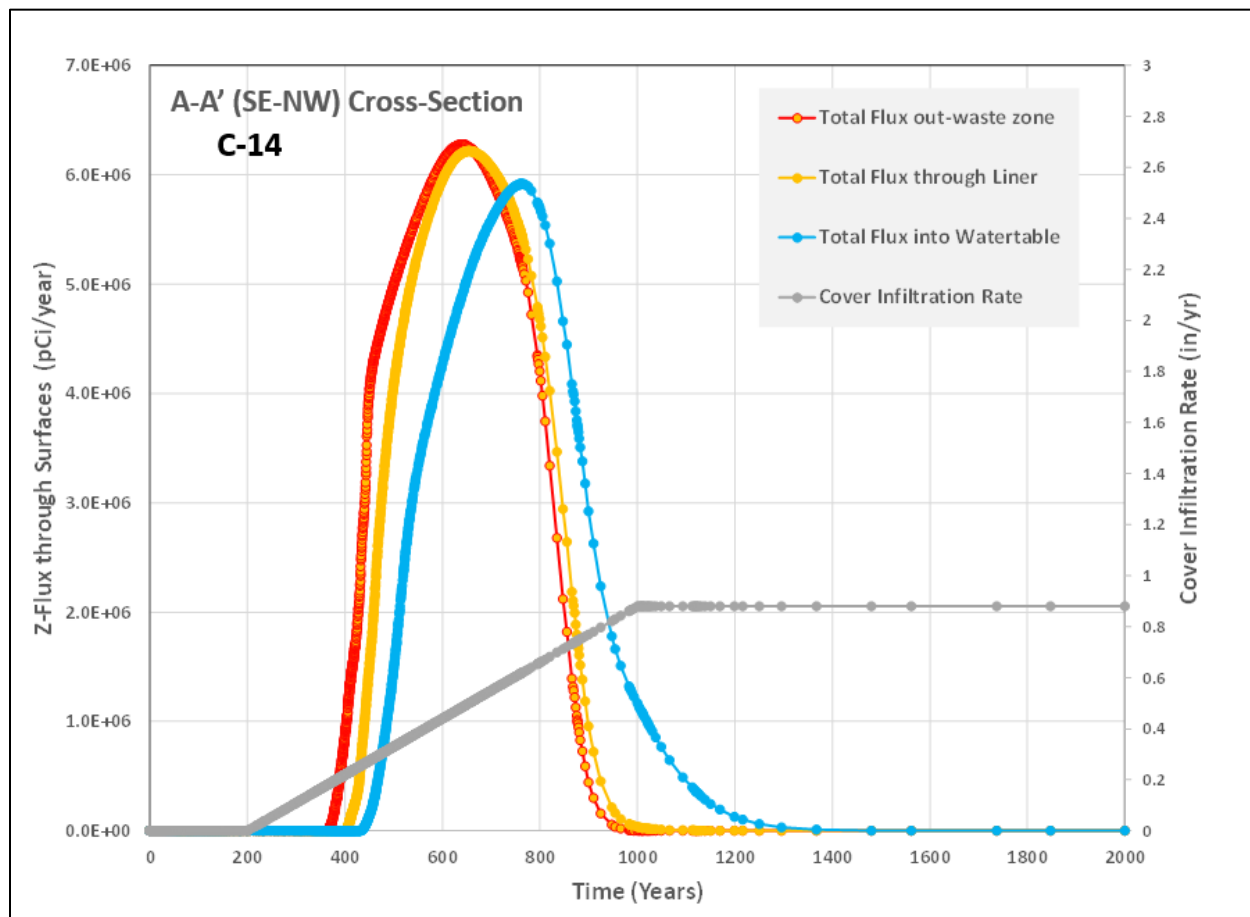
Fig. 4.11. C-14 flux in the STOMP Section A model over time

Technetium-99 starts to migrate from the waste zone into the liner system at year 400 when the infiltration of water from the cover reaches the bottom of the waste zone (Fig. 4.12). The mass flux rate increases with increased water infiltration rate until year 1000 when the water infiltration rate reaches the long-term EMDF performance condition (0.88 in./year). The mass flux rate then starts to decrease due to source depletion. The mass flux rate at the bottom of the liner system begins to increase slightly later (450 to 500 years) due to sorption in the liner and peaks at year 1000. The decline in mass flux from the waste and liner output surfaces is rapid between 1000 and 1600 years, after which the rate of decline decreases due to radionuclide depletion (refer to Fig. 4.9). The Tc-99 mass flux rate at the water table output surface increases later (600 to 1000 years) and peaks lower and later (1200 years) due to sorption and mass retention in the vadose zone. The decline in flux to the saturated zone decreases more gradually than the flux from the liner, reflecting mass depletion along faster transport paths combined with continued migration of residual contamination along slower paths in the vadose zone. This residual mass is concentrated beneath the upslope end of each disposal cell (refer to the C-14 concentrations at years 1000 and 1500 in Fig. 4.8).

Iodine-129 also starts to release from the waste zone to the liner system at year 400 (Fig. 4.13). However, due to its higher K_d, the peak flux rates at the base of the liner and the water table output surface occur 1000 to 2000 years later than for the Tc-99 simulation. Also in contrast to the Tc-99 example, the I-129 peak from the liner output surface is much later than the peak flux from the waste output surface, reflecting greater sorption and mass retention in the clay liner material. The peak flux rate at the water table for I-129 occurs at about 3225 years.
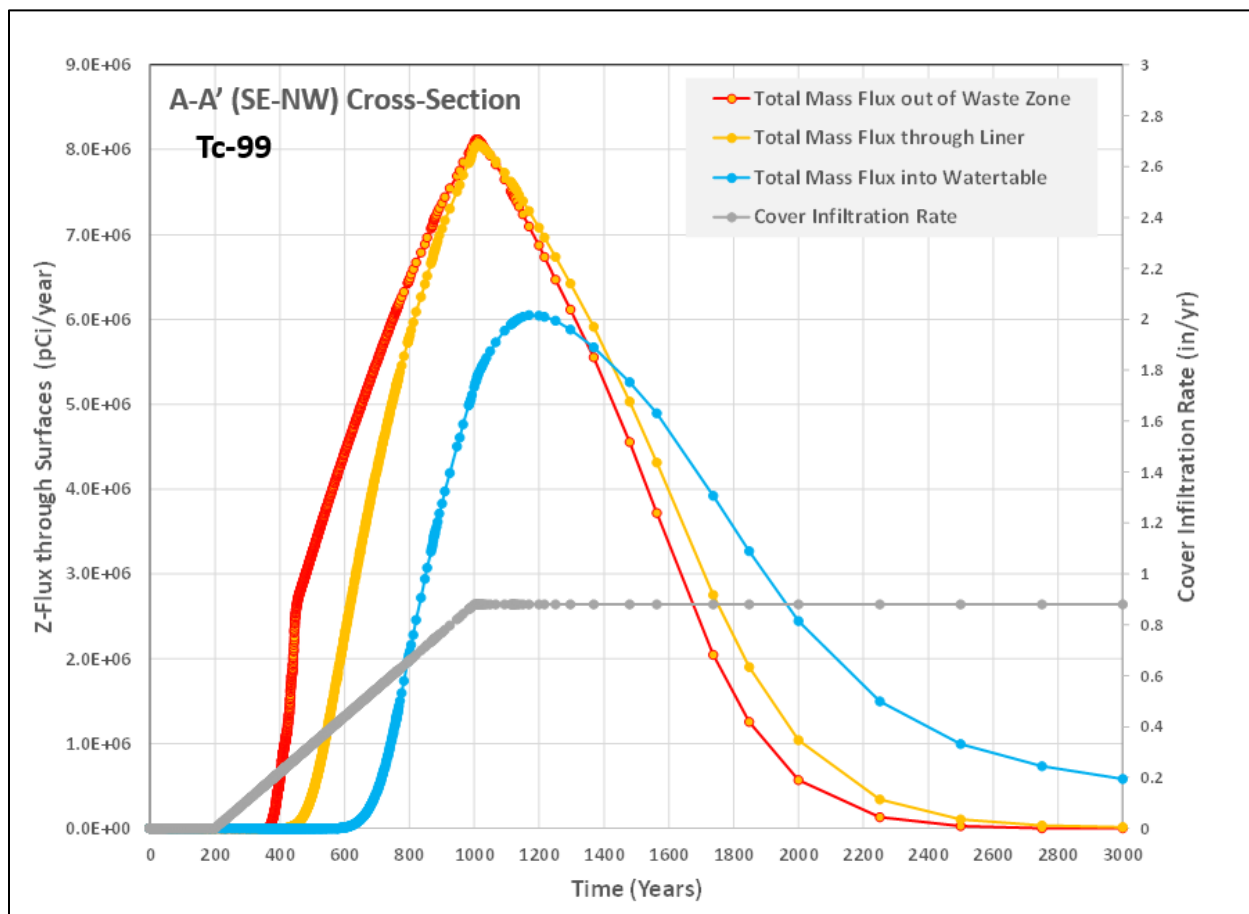
Fig. 4.12. Tc-99 flux in the STOMP Section A model over time
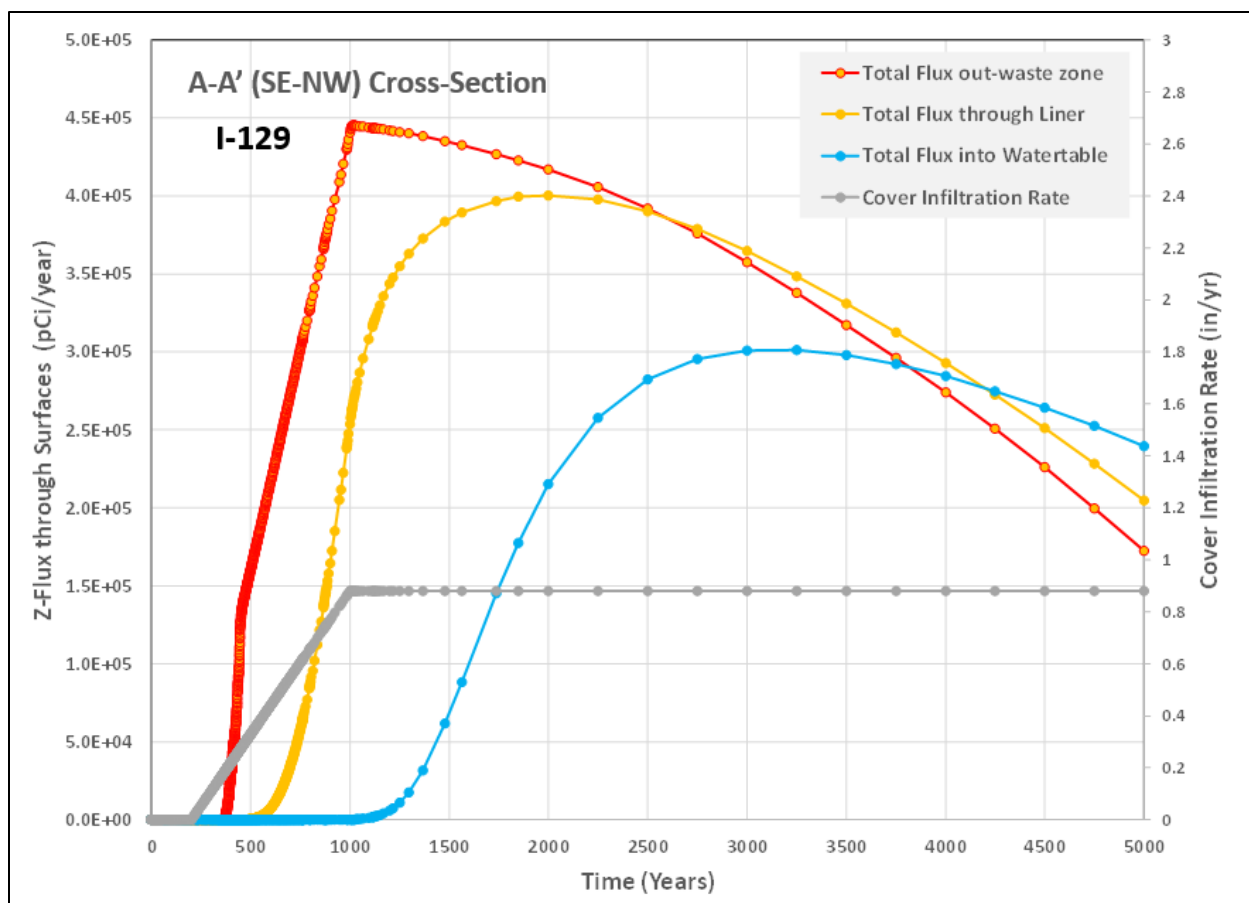
Fig. 4.13. I-129 flux in the STOMP Section A model over time

4.2.5   Estimated Vadose Zone Delay Times

As discussed above, STOMP modeling provides a detailed understanding of source depletion and the impact of liner system design on release to and transport in the vadose zone. Two key output products provided by the STOMP modeling are used to implement the other PA models. These outputs relate to the non-uniform pattern of release and the vadose zone transport time (arrival time at the water table elevation below the disposal unit). These outputs were calculated and applied to the saturated zone radionuclide transport analysis conducted using the MT3D model (see Sect. 3.3.3 and Appendix F). Use of the STOMP model output to develop the non-uniform Tc-99 release scenario for the MT3D model is summarized in Sect. 5.2.

The STOMP model results clearly show the impact of the vadose zone on the movement of the radionuclides. The vadose zone both retards transport and reduces the radionuclide aqueous concentration between the waste and saturated zone beneath the EMDF due to the sorption and desorption process. To provide an estimated average vadose delay time for the MT3D saturated zone transport model the total radionuclide flux rate at the water table output surface in the STOMP Section A model is utilized. The Section A results were selected rather than the Section B model results because the former yielded smaller delay times and earlier saturated zone arrival times.

The Tc-99 total mass flux rate at the water table surface in the Section A model is shown on Fig. 4.14. The plot illustrates the initial arrival time of approximately 600 years and peak flux time of 1180 years. The

234

time when the flux reaches 50 percent of the peak rate is approximately 850 years. (The time to 50 percent peak water table Tc-99 flux rate based on the Section B model output is approximately 910 years due to greater average thickness of the vadose zone.) Since the saturated zone transport model applies a simplified depleting source approximation for radionuclide release at the water table (Appendix F, Sect. F.4.1), using the STOMP model-based 50 percent peak mass flux time to represent the saturated zone arrival time is a reasonable approach. This STOMP model-based arrival time incorporates the assumed (base case) progression of cover degradation and maximum cover infiltration rate, as well as the simulated vadose transport time in representing the release to the saturated zone. The average arrival times were calculated for the three radionuclides that make the primary dose contributions in the performance analysis (see Table 3.21).

In addition to overall average vadose delay, the complexity of the EMDF design (multiple disposal cells with variable liner floor elevations) and the effect of non-uniform vadose zone thickness results in variable initial arrival times and peak concentrations for radionuclides entering the saturated zone. To support the non-uniform release scenario applied to the MT3D model, radionuclide-specific arrival times (refer to Appendix E, Table E.8) for each disposal cell were also calculated based on the flux output from the corresponding water table surface segments (Fig. 4.14, cell-by-cell flux curves).
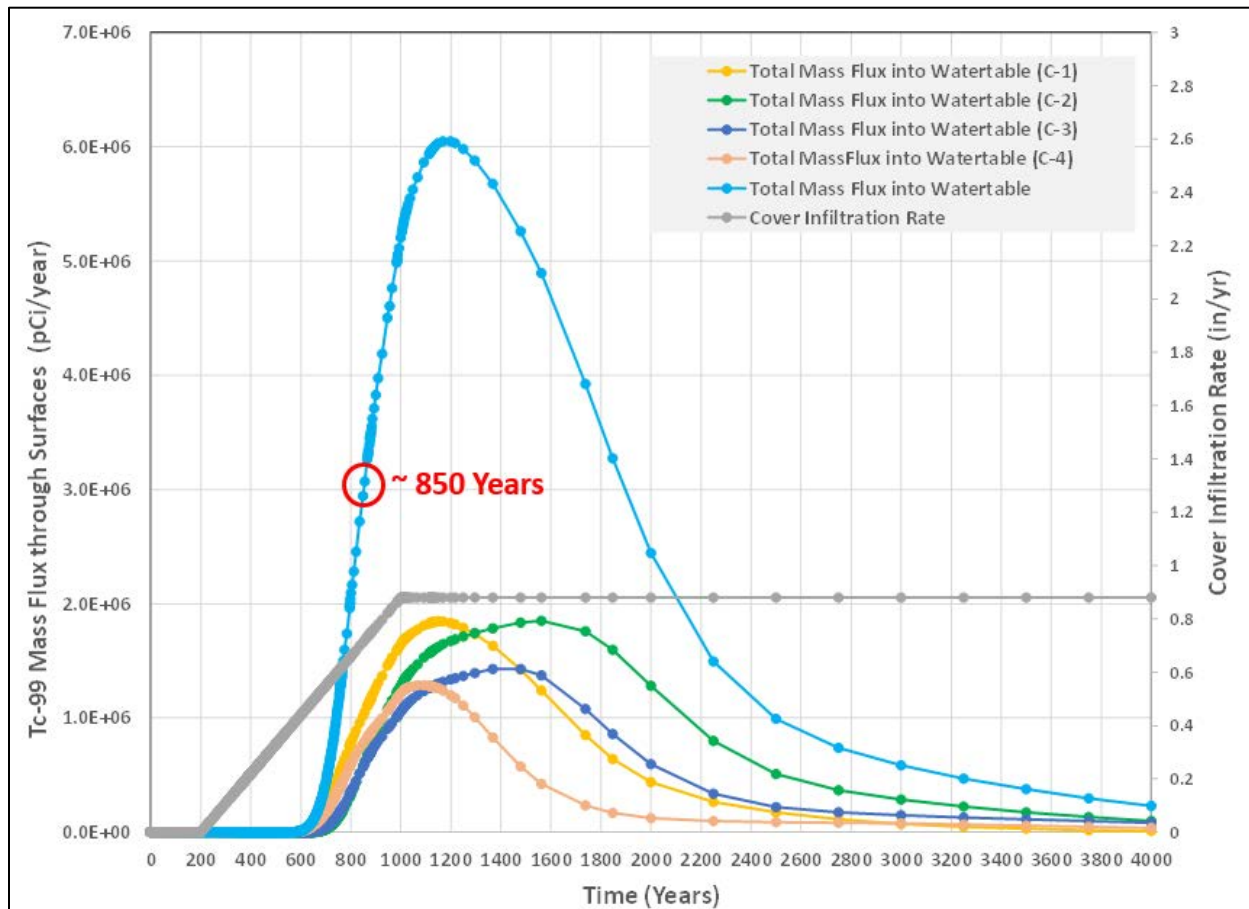
Fig. 4.14. Time to 50 percent peak Tc-99 flux at water table surface in the STOMP Section A Model

4.3   SATURATED ZONE RADIONUCLIDE TRANSPORT

This section presents the results of the 3-D saturated zone radionuclide transport modeling, focusing on results for Tc-99. Evidence from the STOMP modeling that contaminant release from the EMDF liner system may be non-uniform (even under the assumption of uniform cover infiltration) motivated the development of a simplified non-uniform representation of leachate flux to the water table to compare to model results using the uniform leachate flux boundary condition. The results of the non-uniform release MT3D model simulations are compared to the base case uniform release results in Sect. 5.2.

Model results for the base case (uniform release and leachate flux) Tc-99 simulation show the effect of the depleting source approximation (release model) used for the leachate flux boundary condition at the water table below the disposal unit. The Tc-99 plume evolution for the base case release is shown on Fig. 4.15. Technetium-99 concentration time series for individual MT3D model layers at the downgradient EOW location and the 100-m well are shown on Fig. 4.16. The modeled concentrations for each model layer at the EOW and POA locations reflect the relatively complex spatial and temporal evolution of the plume. Model layer 2 at the EOW (Fig. 4.16 upper plot) has the highest peak concentration due to proximity to the upgradient source area. At the EOW location, most of the contamination is restricted to the shallow groundwater zone (model layers 2, 3 and 4). The peak time for the model layer 2 at the EOW is 2100 years, where peak concentrations for model layers 3 and 4 occur after 4000 years. Peak concentrations at the 100-m well are lower than peaks at the EOW, and occur much later for model layer 2 (peak at 3750 years), layer 3 ($>$ 5000 years), and layer 4 ($>$ 5000 years) compared to the EOW location (Fig. 4.16 lower plot). Model layer 1 concentrations at the 100-m well increase quickly between 850 and 1200 years and then more gradually to a peak around 2700 years, whereas model layer 2 concentrations increase significantly at the 100-m well only after 1500 years. Transmissivity-weighted average concentrations at the POA for model layers 1+2 and layers 1+2+3 are calculated to provide a vertically integrated estimate of well concentrations over potential well screen intervals (Fig. 4.16 lower plot). The transmissivity-weighted concentrations peak around 2750 years at approximately 200 pCi/L.

MT3D transport model results for C-14 and I-129 show similar variations in concentration and peak timing between output locations and among model layers to the Tc-99 results, but the range of concentrations and timing reflect the difference in assumed K_d values. The model-predicted C-14 concentrations at the EOW and 100-m well locations reflect rapid release (delay time is 530 years) and transport due to the zero K_d of C-14 applied in the release model and saturated zone media (Fig. 4.17). The highest C-14 concentration for model layer 2 at the 100-m well is just over 600 pCi/L between 1100 and 1200 years post-closure, and the peak transmissivity-weighted concentrations are approximately 450 pCi/L at nearly the same time as the layer 2 peak (Fig. 4.17 lower plot). Deeper model layers 4 and 5 reach C-14 concentrations that are closer to shallow layer concentrations than for either Tc-99 or I-129, due to the higher mobility of C-14. Similarly, the difference in the timing of peak concentrations between output locations and among model layers is much less for C-14 (Fig. 4.17) than for Tc-99 (Fig. 4.16) or I-129 (Fig. 4.18), which have non-zero K_d values.

The MT3D predicted I-129 concentrations at the EOW and 100-m well locations are lower than Tc-99 and C-14 as a result of the smaller initial source inventory and higher K_d for I-129 (Fig. 4.18). The initial release (delay time 1750 years) and peak concentrations occur much later than for C-14 and Tc-99, due to the higher assumed K_d value for I-129. The I-129 concentrations in model layer 1 at the 100-m well increase rapidly between 2000 and 3000 years to about 6 pCi/L, and increase gradually to 8 pCi/L by approximately 10,000 years. Model layer 2 I-129 concentrations begin increasing just after 4000 years and reach a peak of 12 pCi/L at approximately 16,000 years post-closure.

236
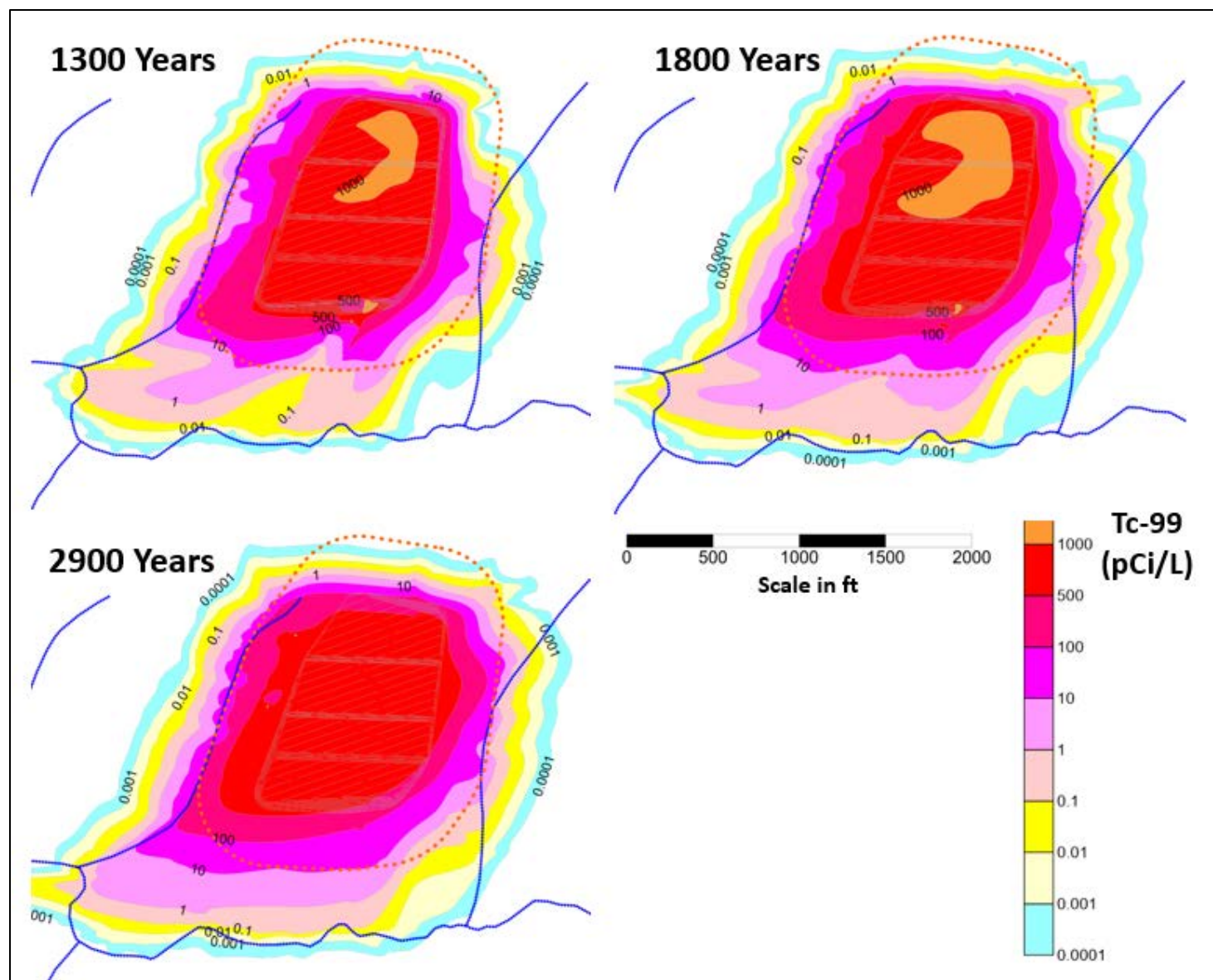
Fig. 4.15. Modeled Tc-99 plume evolution for model layer 2 of the MT3D transport model
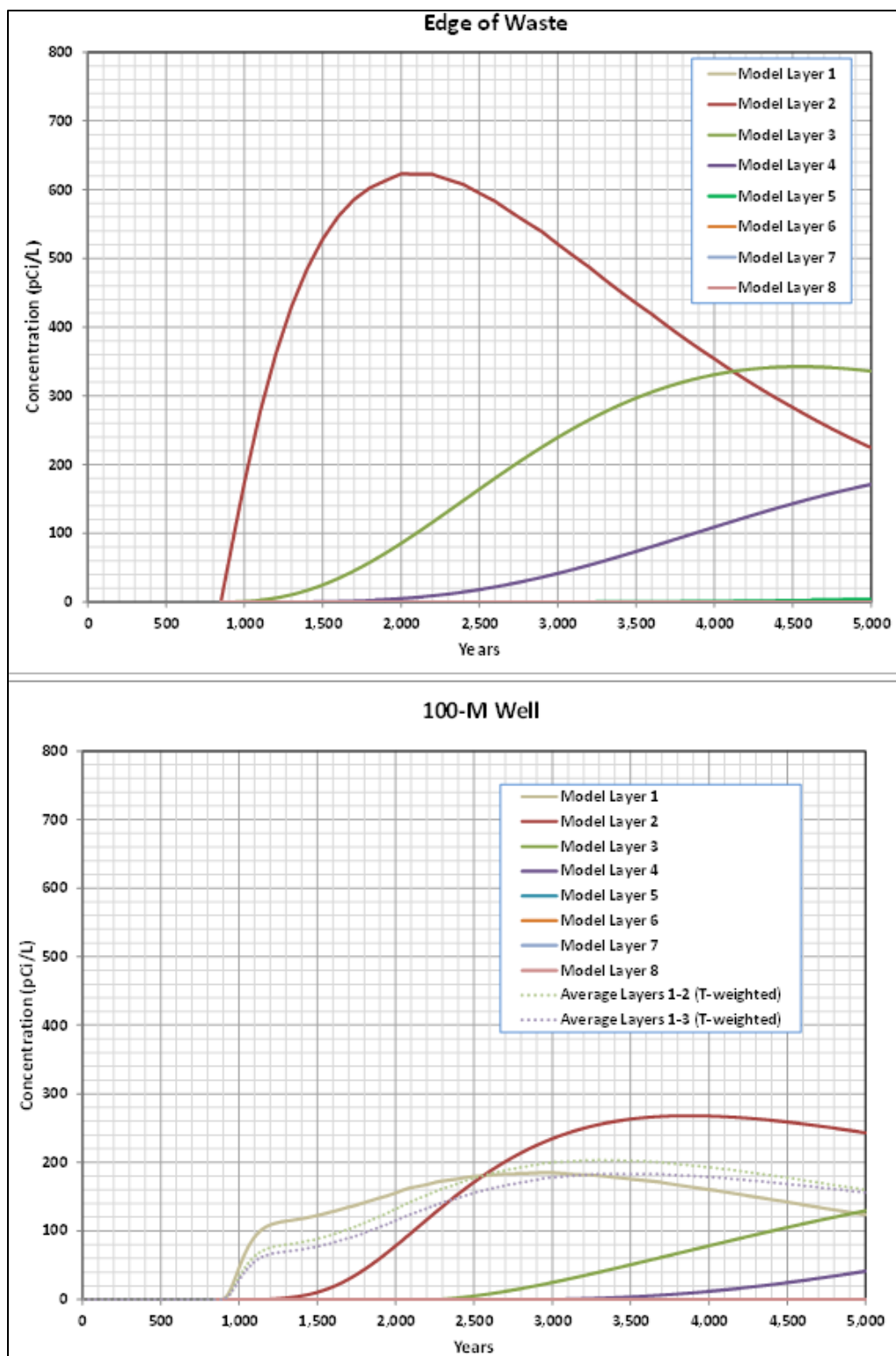
Fig. 4.16. MT3D Tc-99 concentration time series for the waste edge location and at the 100-m well

238
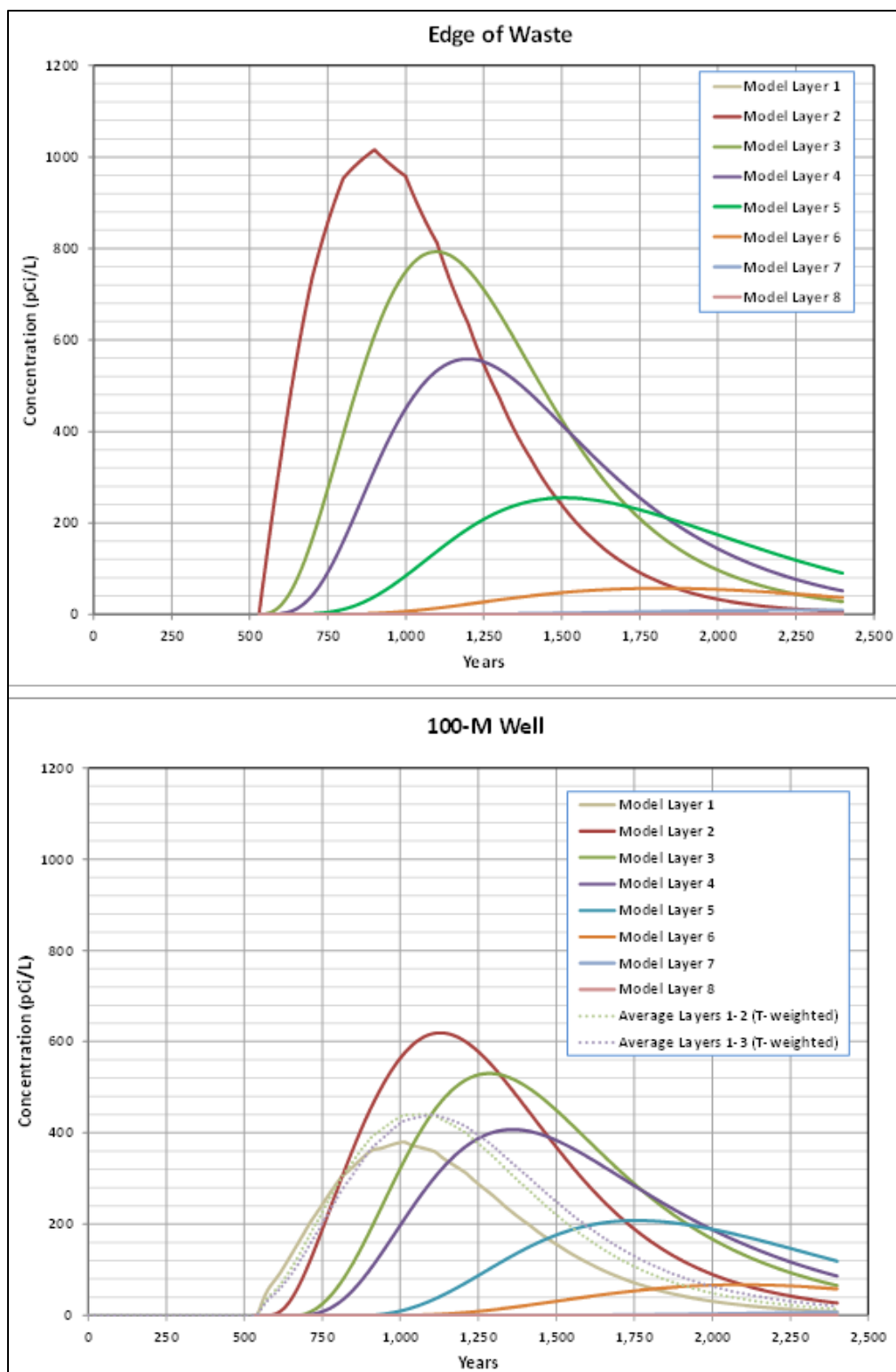
Fig. 4.17. MT3D C-14 concentration time series for the waste edge location and at the 100-m well
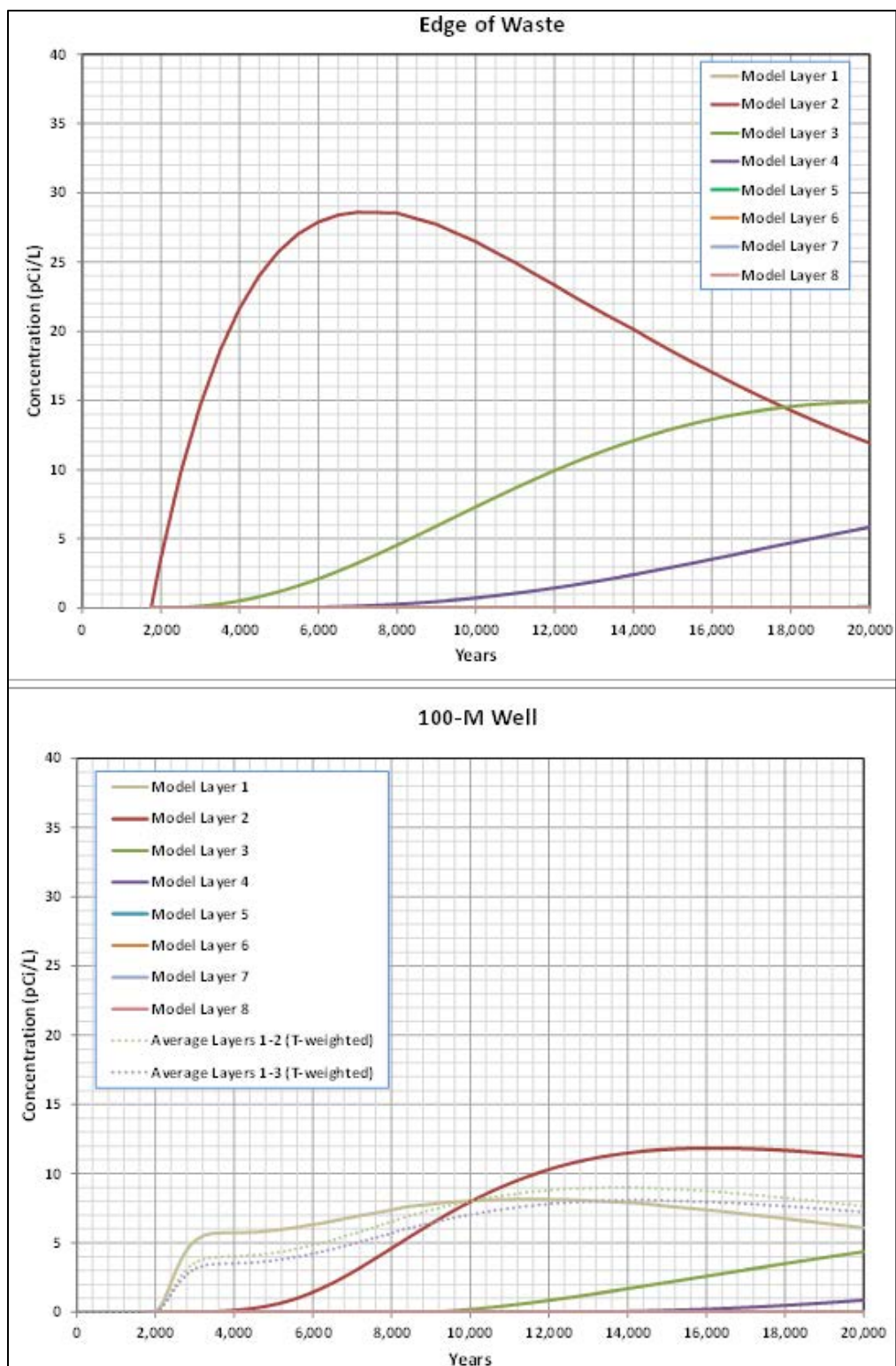
Fig. 4.18. MT3D I-129 concentration time series for the waste edge location and at the 100-m well

RESRAD-OFFSITE saturated zone model outputs were evaluated against the MT3D model results to provide confidence in the saturated zone parameterization for the total system model. Those model comparisons were presented in Sect. 3.3.5. Figure 3.37 shows the comparison of MT3D and RESRAD-OFFSITE model saturated zone results for Tc-99.

4.4   RADON FLUX ANALYSIS

This section summarizes the radon flux analysis, which is presented in detail in Appendix H. Based on the EMDF cover system characteristics and estimated Ra-226 activity, the radon flux was estimated for the design condition of the final cover and for three degraded cover scenarios: fully exposed waste, a severely eroded residual 2-ft-thick clay cover, and cover eroded to the biointrusion layer. A radon emanation coefficient of 0.25 for Rn-222, the default value in the RESRAD model (Gnanapragasam and Yu 2015) was assumed. The value is on the higher end of the reported radon emanation coefficients for Rn-222 in various soils (Yu et al. 2015, Sect. 4.2.2, page 122), which typically range from less than 0.01 to 0.30.

The radon flux is primarily controlled by clay layers that lie below the biointrusion layer. Even with some expected erosion of the cover system, the integrity of the clay layers will likely be preserved within the first 1000 years. Uncertainty in the radon release performance of the EMDF cover is minimal. The predicted radon flux at the EMDF cover surface is 5.0E-08 $pCi/m^2/sec$. The predicted radon flux for fully exposed waste at year 1000 is 0.80 $pCi/m^2/sec$. The radon fluxes for the residual clay cover and the erosion to biointrusion layer scenarios are 6.6E-06 and 5.4E-06 $pCi/m^2/sec$, respectively. Sensitivity evaluations for higher concentrations of radon parents and for potential release of Rn-222 indicate that EMDF compliance with the 20 $pCi/m^2/sec$ performance objective is not affected (Appendix H, Sect. H.7).

The radon calculation indicates that, based on the estimated radionuclide inventory and assuming a uniform distribution of contamination within the waste mass, there will be minimal post-closure radon flux from the proposed EMDF within the 1000-year compliance period, even with significant erosion of the 4-ft-thick cover surface layer (refer to Appendix C for discussion and analysis of potential cover erosion).

4.5   ALL-PATHWAYS DOSE ANALYSIS

This section includes the results of simulations using the total system model, RESRAD-OFFSITE.

4.5.1   All-Pathways Dose Analysis - Base Case Model Results

Predicted total dose over time for the base case model is presented in Fig. 4.19 for the 1000-year compliance period and Fig. 4.20 for the 10,000-year time period including the compliance period and the subsequent 9000 years. The peak total dose (i.e., dose from all simulated radionuclides summed) for the 1000-year compliance period is 1.03 mrem/year and occurs at 490 years. The peak compliance period dose is associated with C-14. Total dose then decreases through 750 years and remains less than 0.2 mrem/year from that time to the end of the compliance period. After the compliance period, the total dose increases to a peak of 0.95 mrem/year associated with Tc-99 at approximately 1700 years. After the Tc-99 peak, the total dose increases to a maximum of 9.13 mrem/year at approximately 5084 years and then gradually decreases through 10,000 years to a predicted total dose at 10,000 years of 0.114 mrem/year. The three distinct peaks in total dose are each associated with a single radionuclide, as presented in the following subsection. Overall, the predicted maximum total dose during the compliance period of 1.03 mrem/year is less than 5 percent of the performance objective (25 mrem/year).

241
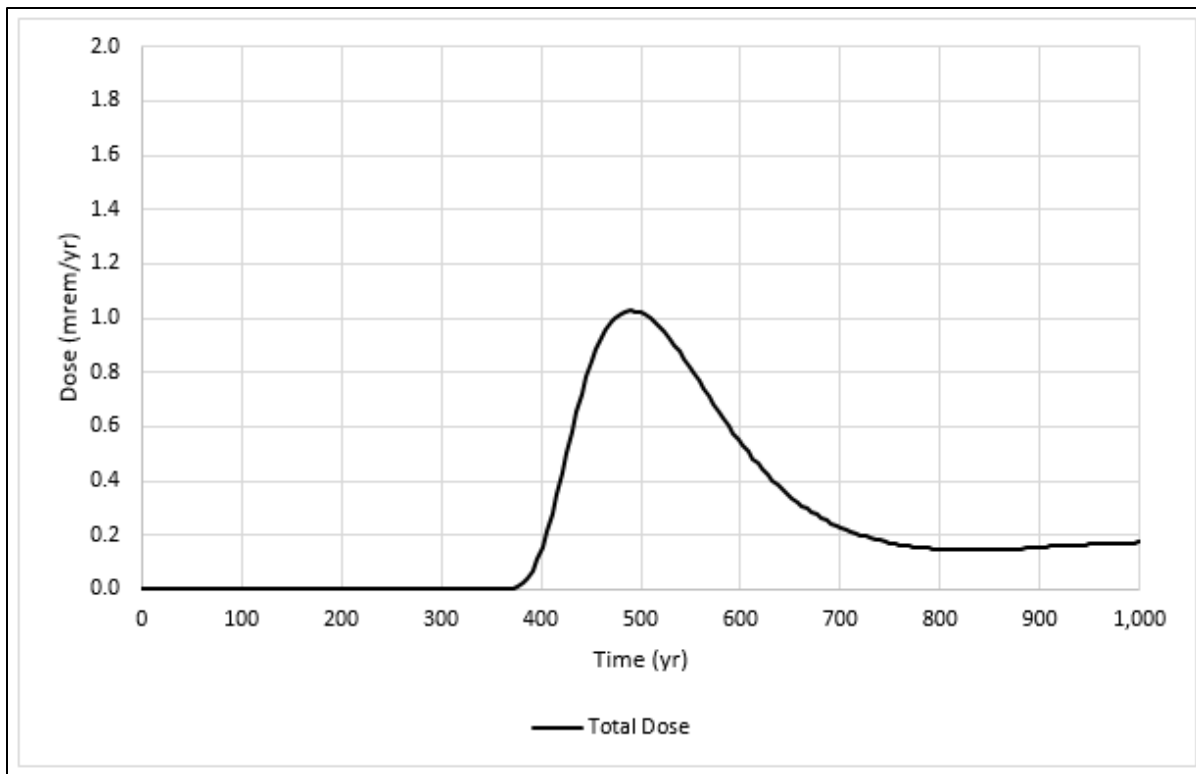
Fig. 4.19. Base case predicted total dose (all pathways; compliance period)
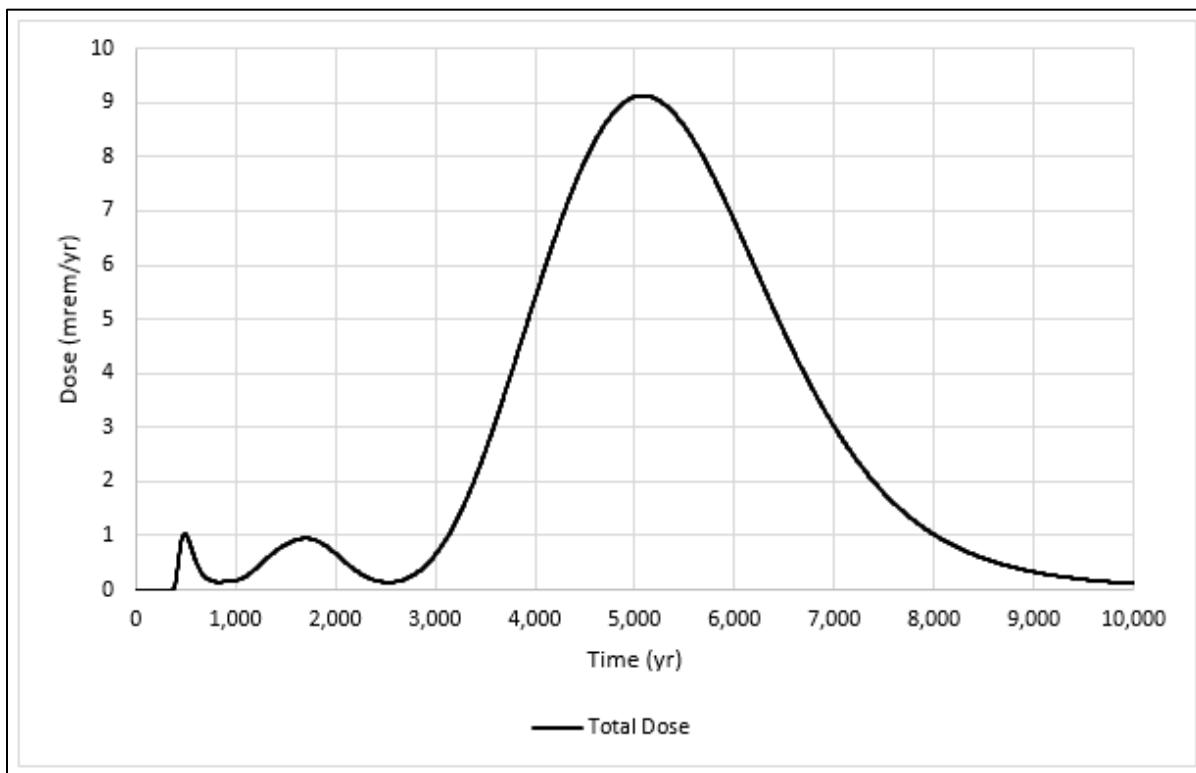
Fig. 4.20. Base case predicted total dose (all pathways; 0 to 10,000 years)

242

4.5.2 Base Case-Peak Dose for Each Radionuclide

The primary contributors to total dose consist of C-14, I-129, and Tc-99. Source concentrations input for C-14, I-129, and Tc-99 are based on the post-operational waste concentrations (Table 3.3).

For the compliance period, the greatest predicted dose is 1.03 mrem/year from C-14 contributions at 490 years (Fig. 4.21). Peak dose contributions from Tc-99 and I-129 occur after 1000 years. After the compliance period through 10,000 years, I-129 is the largest dose contributor, with a maximum predicted dose of 9.13 mrem/year at 5084 years (Fig. 4.22). The peak Tc-99 dose is 0.95 mrem/year at 1700 years.
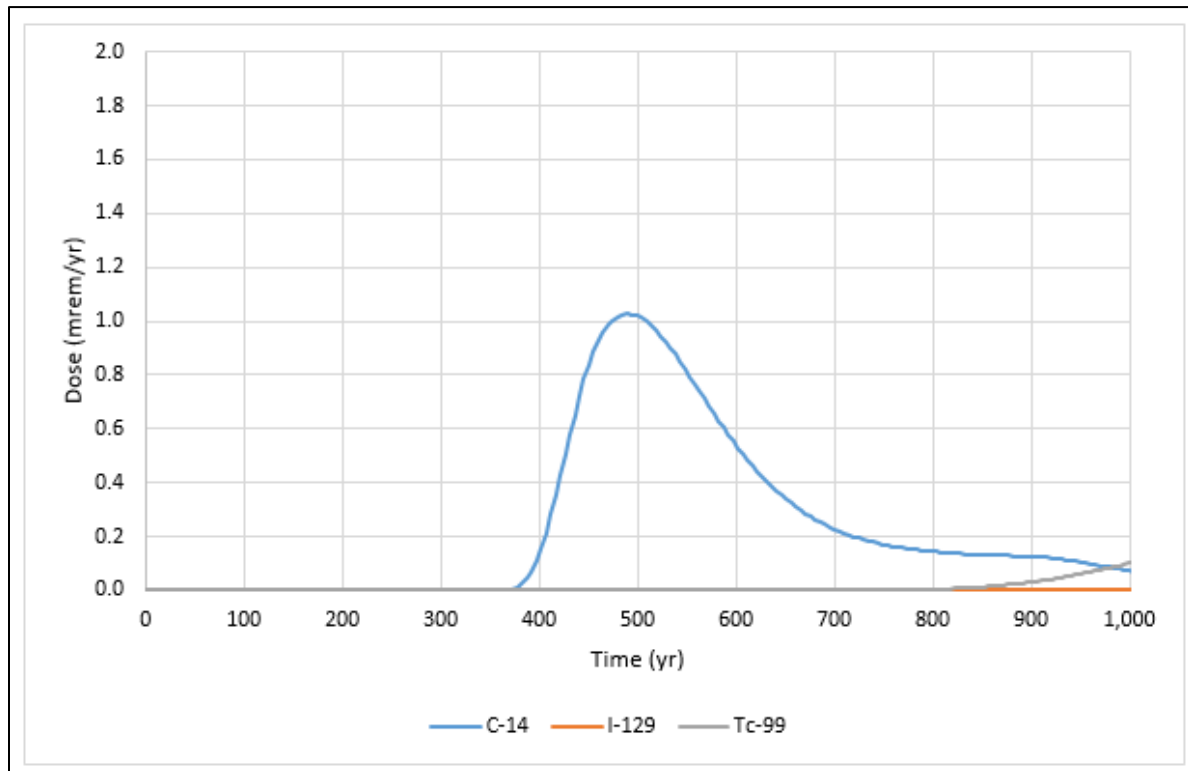
Fig. 4.21. Base case predicted dose by isotope for the compliance period
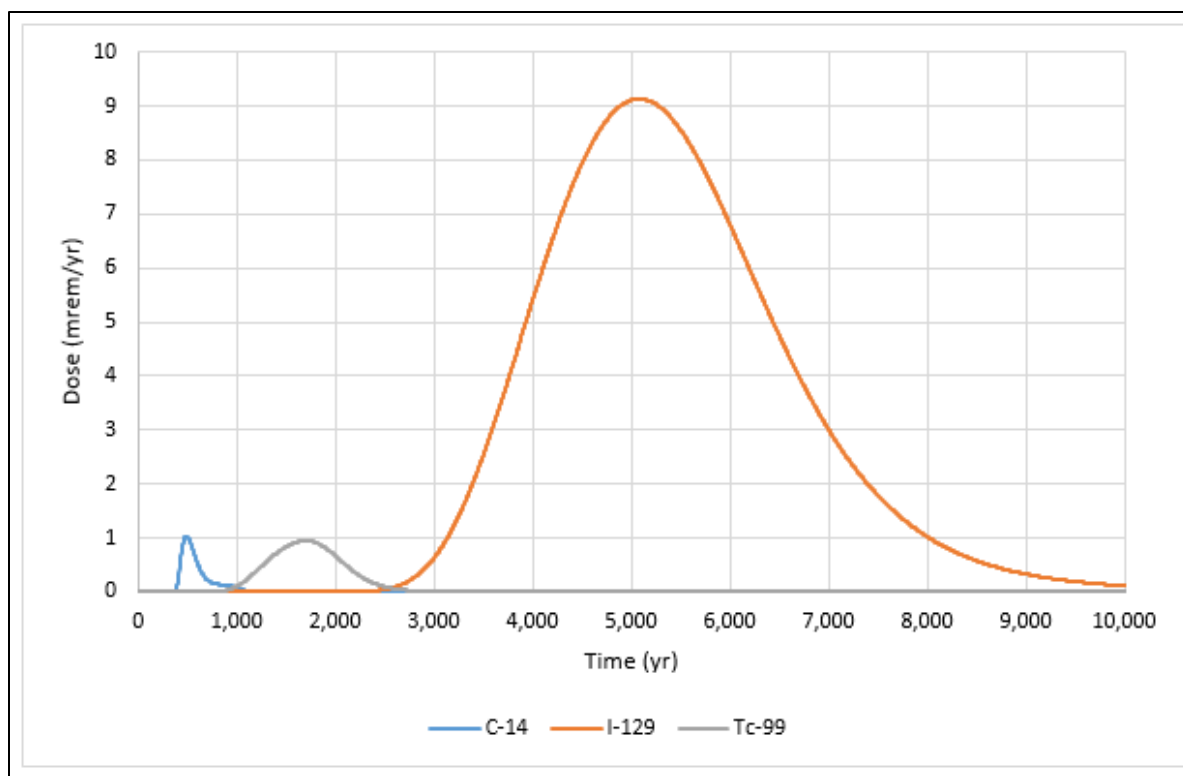
Fig. 4.22. Base case predicted total dose by isotope (0 to 10,000 years)

4.5.3 Base Case-Dose by Exposure Pathway

The groundwater ingestion pathway (ingestion of well water) is the dominant contributor to total dose. In addition to the drinking water exposure pathway, the four pathways contributing most of the remaining dose during the compliance period in order of descending dose contribution are ingestion of fish, plants (waterborne), milk (waterborne), and meat (waterborne) (Fig. 4.23). During the 10,000-year simulation period, the water pathway remains dominant with ingestion of meat (waterborne), milk (waterborne), plant (waterborne), and fish also contributing to the total dose. Because the cover system is assumed to maintain integrity and prevent waste from leaving the facility, there are no predicted dose contributions from any of the airborne (atmospheric) pathways. Doses from individual exposure pathways for the post-closure period from 0 to 10,000 years are shown in Fig. 4.24. The same output data on an altered (logarithmic) scale to highlight the very small (negligible relative to total dose) base case contributions of exposure pathways other than water and fish ingestion is shown on Fig. 4.25. Note that pathways with no calculated dose contribution, which include the direct and airborne pathway components of plant, meat, milk, and soil ingestion and the radon pathway, are not included in the plots in Figs. 4.23 to 4.25.
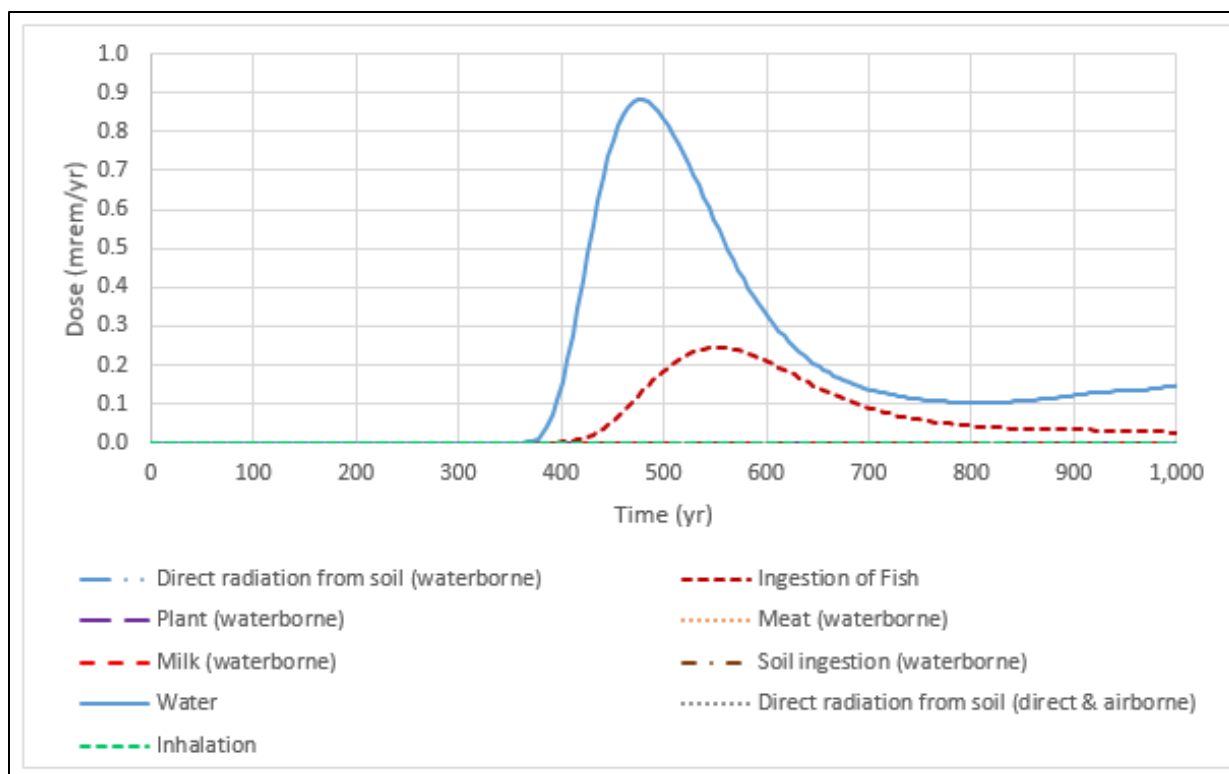
Fig. 4.23. Predicted base case dose by pathway during the compliance period
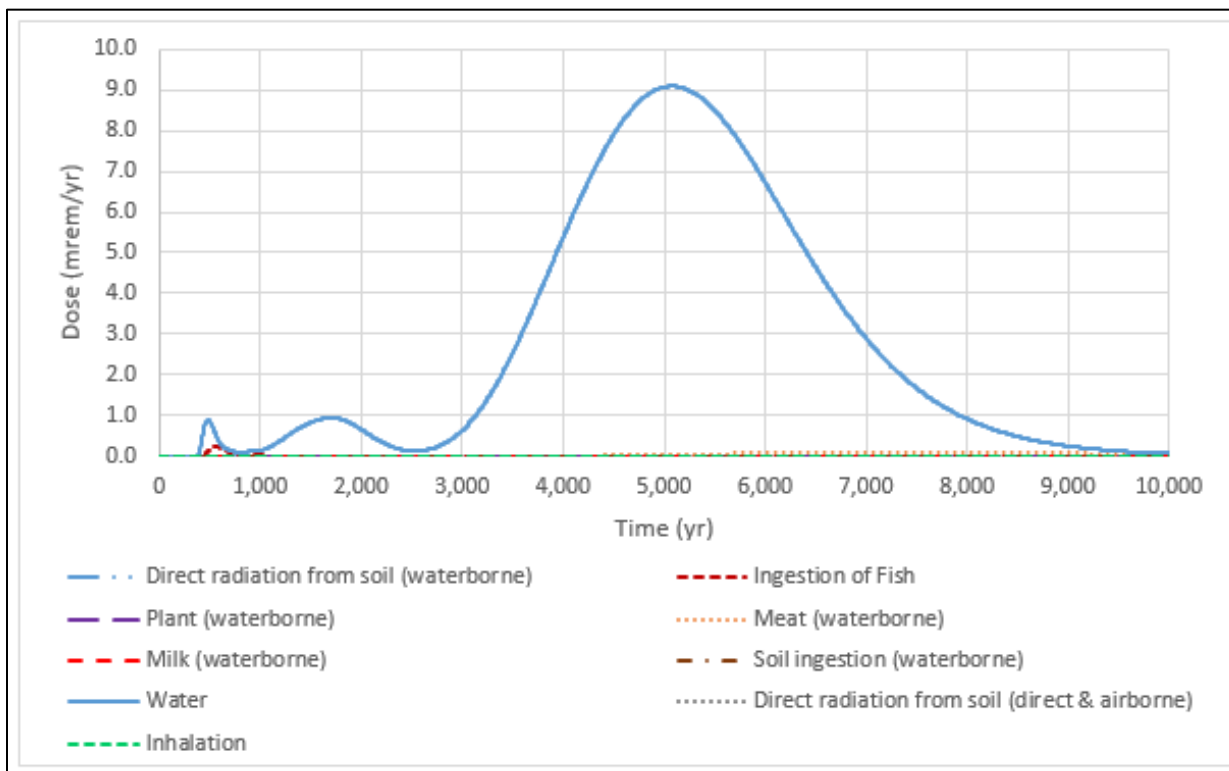
Fig. 4.24. Predicted base case dose by exposure pathway (0 to 10,000 years)
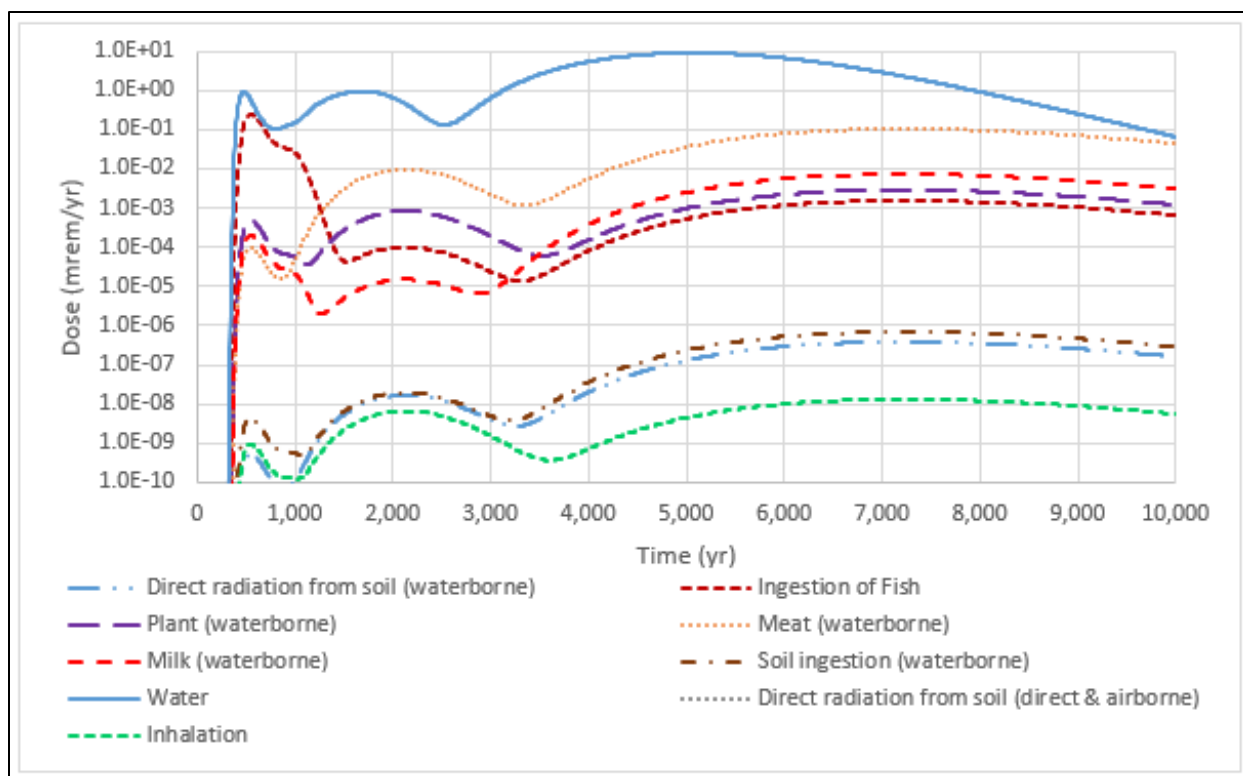
Fig. 4.25. Predicted base case dose by exposure pathway (0 to 10,000 years)

4.6 RESRAD-OFFSITE SINGLE RADIONUCLIDE SOIL GUIDELINES

Dose-based performance criteria are one basis for setting radionuclide concentration limits for LLW to ensure protection of members of the public. RESRAD-OFFSITE SRSGs are calculated waste activity concentrations that will meet a specific dose target for a single radionuclide at a specific time, based on the modeled scenario. The SRSGs do not depend on the assumed radionuclide concentrations or the corresponding modeled doses, but only on the target dose value and the specific exposure scenario considered. Thus, the SRSGs are dose-based radionuclide source concentration limits for the particular system and scenario simulated.

The RESRAD-OFFSITE SRSG values represent the source concentrations corresponding to the 25 mrem/year dose target, calculated for the base case (all pathways dose) model scenario. For most radionuclides, the minimum SRSG within the 1000-year compliance period occurs at or near 1000 years post-closure.

Table 4.1 presents the compliance period minimum SRSG values for the base case scenario, and the corresponding estimated EMDF average (post-operational) concentrations used in the dose analysis for comparison. For the suite of simulated isotopes, the modeled EMDF source concentrations are less than the model-predicted minimum SRSG values.

Table 4.1. RESRAD-OFFSITE SRSGs for the all pathways scenario
(compliance period minimum values)

Radionuclide	SRSG (25 mrem/year) (pCi/g)	EMDF post-operational source concentration (pCi/g)
Ac-227[a]	7.23E+13	2.92E-03
Am-241[a]	3.43E+12	5.90E+01
Am-243[a]	2.00E+11	2.97E+00
Be-10[a]	2.36E+10	2.53E-05
C-14	1.32E+01	5.40E-01
Ca-41[a]	8.35E+10	4.21E-02
Cm-243[a]	5.05E+13	4.30E-01
Cm-244[a]	8.09E+13	1.26E+02
Cm-245[a]	1.72E+11	3.83E-02
Cm-246[a]	3.05E+11	1.59E-01
Cm-247[a]	9.28E+07	1.04E-02
Cm-248[a]	4.14E+09	5.59E-04
H-3	8.52E+12	4.64E+00
I-129[a]	1.75E+08	3.50E-01
K-40[a]	6.98E+06	3.28E+00
Mo-93[a]	9.52E+11	3.88E-01
Nb-93m[a]	2.39E+14	2.33E-01
Nb-94[a]	1.86E+11	1.63E-02
Ni-59[a]	5.91E+10	3.04E+00
Np-237[a]	7.03E+08	3.25E-01
Pa-231[a]	4.72E+10	2.39E-01
Pb-210[a]	7.63E+13	3.68E+00
Pu-238[a]	1.71E+13	9.38E+01
Pu-239[a]	6.20E+10	5.83E+01
Pu-240[a]	2.27E+11	6.20E+01
Pu-241[a]	1.03E+14	2.04E+02
Pu-242[a]	3.94E+09	1.73E-01
Pu-244[a]	1.83E+07	3.68E-03
Ra-226[a]	9.89E+11	8.01E-01
Ra-228[a]	2.73E+14	2.21E-02
Sr-90[a]	1.37E+14	1.92E+02
Tc-99	3.80E+02	1.56E+00
Th-228[a]	8.20E+14	2.11E-06
Th-229[a]	2.13E+11	5.71E+00
Th-230[a]	2.06E+10	1.92E+00
Th-232[a]	1.10E+05	3.52E+00

**Table 4.1. RESRAD-OFFSITE SRSGs for the all pathways scenario
(compliance period minimum values) (cont.)**

Radionuclide	SRSG (25 mrem/year) (pCi/g)	EMDF post-operational source concentration (pCi/g)
U-232[a]	2.24E+13	1.02E+01
U-233[a]	9.64E+09	4.16E+01
U-234[a]	6.22E+09	6.30E+02
U-235[a]	2.16E+06	3.97E+01
U-236[a]	6.47E+07	8.98E+00
U-238[a]	3.36E+05	3.81E+02

[a]Indicates SRSG at specific activity limit

EMDF = Environmental Management Disposal Facility
RESRAD = RESidual RADioactivity
SRSG = Single Radionuclide Soil Guideline

4.7 WATER RESOURCES PROTECTION ASSESSMENT

This section presents estimated radionuclide doses and concentrations during the compliance period for comparison to regulatory standards for water resources protection.

4.7.1 Groundwater Protection Assessment

Protection of groundwater is demonstrated by comparing well water radionuclide concentrations under the base case scenario to MCLs for drinking water specified by EPA in the Radionuclides Final Rule (EPA 2000), promulgated in 40 *CFR* 141.66, for which the State of Tennessee has primary enforcement responsibility. Radionuclide MCLs are as follows:

- Radium-226/228 combined standard is 5 pCi/L.

- Gross alpha standard for all alpha emitters is 15 pCi/L (not including radon and uranium).

- Beta/photon emitters combined standard is 4 mrem/year dose.

- Strontium-90 standard is 8 pCi/L.

- Hydrogen-3 standard is 20,000 pCi/L.

- Uranium (all isotopes combined) is 30 µg/L.

The following subsections compare modeled radionuclide concentrations in well water for the base case to the MCLs given above.

4.7.1.1 Radium-226 and radium-228

The maximum activity concentration of Ra-226 + Ra-228 in well water during the compliance period is 0.0 pCi/L (negligible) compared to the MCL of 5 pCi/L for these combined isotopes.

4.7.1.2 Gross alpha activity

The radionuclides included in the gross alpha activity analysis are shown on Table 4.2. Radionuclides not simulated because they were screened from analysis include Cf-249, Cf-250, and Cf-251 (Sect. 2.3.2). The

maximum summed gross alpha activity concentration in well water during the compliance period is 0.0 pCi/L (negligible) compared to the MCL of 15 pCi/L for all alpha emitters (not including radon and uranium).

**Table 4.2. Radionuclides for water resources
protection assessment - gross alpha activity**

Am-241	Cm-246	Pu-242
Am-243	Cm-247	Pu-244
Cf-249[a]	Cm-248	Th-228
Cf-250[a]	Np-237	Th-229
Cf-251[a]	Pa-231	Th-230
Cm-243	Pu-238	Th-232
Cm-244	Pu-239	
Cm-245	Pu-240	

[a]Indicates isotope not simulated.

4.7.1.3   Beta/photon activity

The 13 radionuclides simulated for the beta/photon MCL compliance analysis are listed in Table 4.3. Sixteen radionuclides were not simulated because they either did not have a verified inventory data source, or because they were screened from the all pathways dose analysis (see Appendix G, Sect. G.4.2). The 15 radionuclides not included are: Cd-113m, Co-60, Cs-135, Cs-137, Eu-152, Eu-154, Ni-63, Pd-107, Pm-146, Re-187, Se-79, Sm-151, Sn-121m, Sn-126, and Zr-93 (see Table 2.16). The MCL for total beta/photon emitters is expressed as a water ingestion dose of 4 mrem/year (Table 4.3). RESRAD-OFFSITE simulations indicate that only C-14 and Tc-99 contribute substantially to the total beta/photon dose during the compliance period. The maximum dose over 1000 years is 1.03 mrem/year at 475 years (Fig. 4.26), which is less than the corresponding MCL for each radionuclide, yielding a dose of 4 mrem/year (Table 4.3).

Table 4.3. Water resources protection assessment –beta/photon activity

Radionuclide	Decay	MCL (pCi/L) yielding a dose of 4 mrem/year (EPA 2002a)
Ac-227	beta	15
Be-10	beta	1000
C-14	beta	2000
H-3	beta	20,000
I-129	beta	1
K-40[a]	beta	192
Nb-93m	gamma	1000
Nb-94[a]	beta	720
Ni-59	beta	300
Pb-210[a]	beta	1.6
Pu-241	beta	300
Sr-90	beta	8
Tc-99	beta	900

[a]The MCL for given isotope was not included in EPA 2002a, therefore the Derived Concentration Standard (DOE 2011b) was used to calculate the MCL at 4 mrem/year.

EPA = U.S. Environmental Protection Agency
MCL = maximum contaminant level
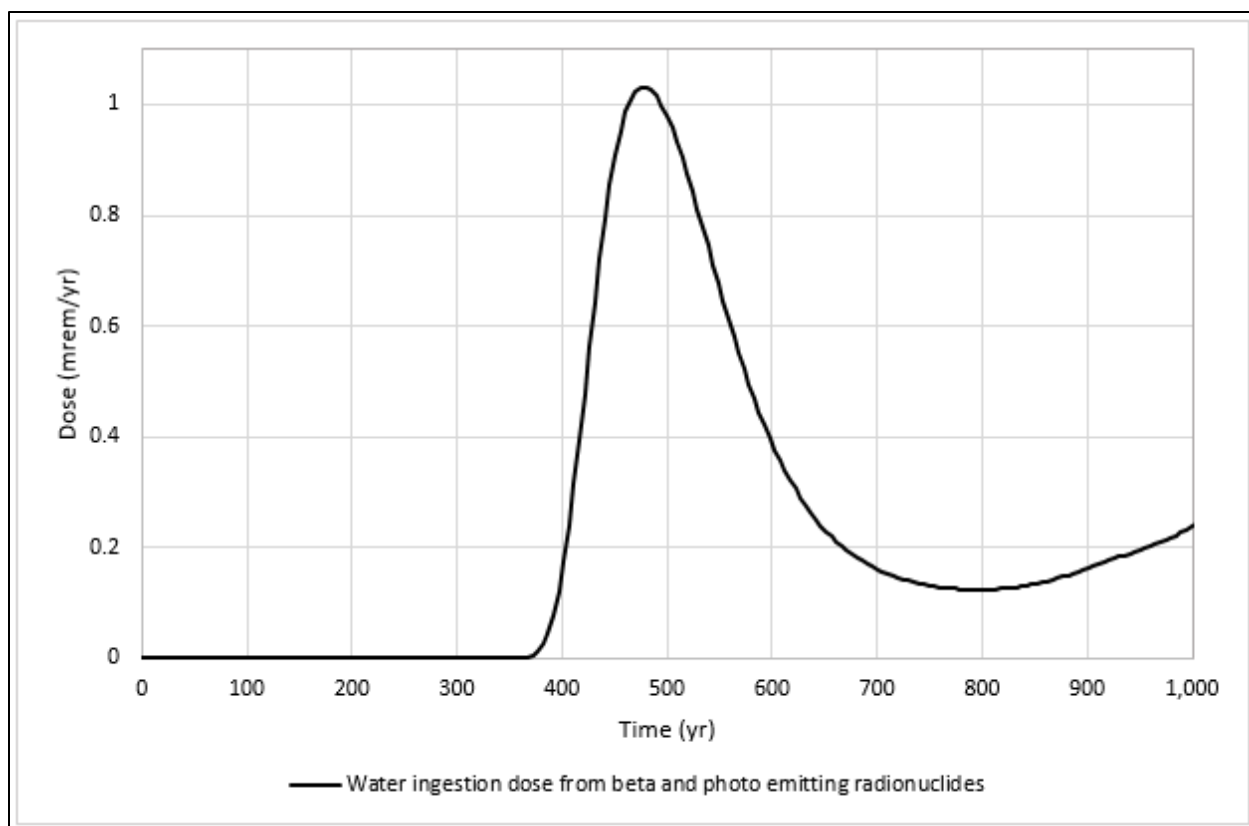
Fig. 4.26. Predicted water ingestion dose from beta/photon emitters (0 to 1000 years)

4.7.1.4 Hydrogen-3 and strontium-90

The maximum predicted groundwater well H-3 concentration during the compliance period is 0.0 pCi/L (negligible). The regulatory standard (MCL) for H-3 concentration is 20,000 pCi/L.

The maximum predicted Sr-90 groundwater well water concentration during the compliance period is 0.0 pCi/L (negligible). The regulatory standard (MCL) for Sr-90 concentration is 8 pCi/L.

4.7.1.5 Uranium (total)

The total uranium MCL is 30 µg/L. The predicted total mass concentration in well water was calculated by summing the activity concentrations for the uranium isotopes (U-232, U-233, U-234, U-235, U-236, and U-238) that RESRAD-OFFSITE predicts in the groundwater well, then converting from the total uranium activity concentration to the mass concentration using the conversion factor 1.49 µg/pCi (EPA 2002b). The maximum predicted total uranium mass concentration for the compliance period is 0.0 µg/L.

4.7.2 Surface Water Protection Assessment

Of the 42 radionuclides included in the base case (i.e., those not screened under the screening model scenario [see Sect. 2.3]), only three have predicted peak surface water concentrations greater than 1.0E-06 pCi/L within the 10,000 year simulation period. Within the 1000-year compliance period, only C-14 and Tc-99 have substantial (greater than 1.0E-06 pCi/L) predicted concentrations in the surface water body (Bear Creek). None of the predicted non-zero peak surface water concentrations for the 10,0000-year simulation period exceeds the corresponding DCS value (DOE 2011b), which serve as the regulatory basis

250

for discharge limits applied to the existing EMWMF landfill for discharge to surface waters in BCV (DOE 2016b). Table 4.4 summarizes the peak surface water concentrations for the three dose significant radionuclides within the 1000-year compliance period and the 10,000-year post-closure period and for uranium isotopes predicted to reach peak concentrations after 10,000 years. Model results for nuclides of uranium at times greater than 10,000 years post-closure are presented in Sect. 4.8.

Table 4.4. Predicted non-zero peak surface water concentrations for radionuclides compared to the DOE-STD-1196 DCS limits

Radionuclide	Peak surface water concentration, compliance period (pCi/L)	Peak surface water concentration, 10,0000-year simulation	DOE-STD-1196 DCS (pCi/L)	Time of simulated peak (year)
Tc-99	2.34E-03	6.24E-01	4.40E+04	2,130
C-14	8.61E-01	8.61E-01	6.20E+04	553
I-129	< 1.0E-06	3.53E-02	3.30E+02	7,219
U-233	< 1.0E-06	< 1.0E-06	6.60E+02	~50,000
U-234	< 1.0E-06	< 1.0E-06	6.80E+02	~50,000
U-235	< 1.0E-06	< 1.0E-06	7.20E+02	~50,000
U-236	< 1.0E-06	< 1.0E-06	7.20E+02	~50,000
U-238	< 1.0E-06	< 1.0E-06	7.50E+02	~50,000

DCS = Derived Concentration Standard

4.8 PREDICTIONS FOR TIMES GREATER THAN 10,000 YEARS

Results from simulations of tens of thousands of years are highly speculative and have limited, if any, quantitative value. However, results from very long-term simulations can be informative on a qualitative basis for long-lived, less mobile radionuclides. To assess the potential release of such radionuclides, simulations were performed for a post-closure duration of 100,000 years.

The RESRAD-OFFSITE long-term simulations indicate that peak well water concentrations of U-233, U-235, and U-236 do not exceed the DCS limits (DOE 2011b, Table G.21), but that peak concentrations of U-234 and U-238 occurring after 30,000 years are larger than the DCS limits (Fig. 4.27). The predicted peak groundwater concentrations of U-234 and U-238 are very high (> 1000 pCi/L), but the RESRAD-OFFSITE source release model does not incorporate solubility limits on the release of uranium in solution, so the model may overestimate the peak concentrations. In addition, the comparison of STOMP model simulations of U-234 release to the RESRAD-OFFSITE release predictions (refer to Sect. 3.3.5, Fig. 3.35) shows that the equilibrium desorption release model over-predicts peak U-234 release significantly relative to the scaled STOMP model simulations. The model output comparison also shows that the simplified RESRAD-OFFSITE vadose zone representation appears to match the timing of the STOMP model peak U-234 flux to the water table, but that the predicted peak RESRAD-OFFSITE U-234 flux is over twice as large as the peak STOMP U-234 flux to the water table beneath the EMDF. This difference in U-234 release model predictions suggests that the RESRAD-OFFSITE peak well water concentrations are too uncertain (probably over-estimated) to draw conclusions about the very-long-term performance of the EMDF with respect to less mobile radionuclides ($K_d > 1.0$ cm^3/g) including nuclides of uranium and possibly also I-129 (refer to Sects. 3.3.5, 5.3 and 5.4).
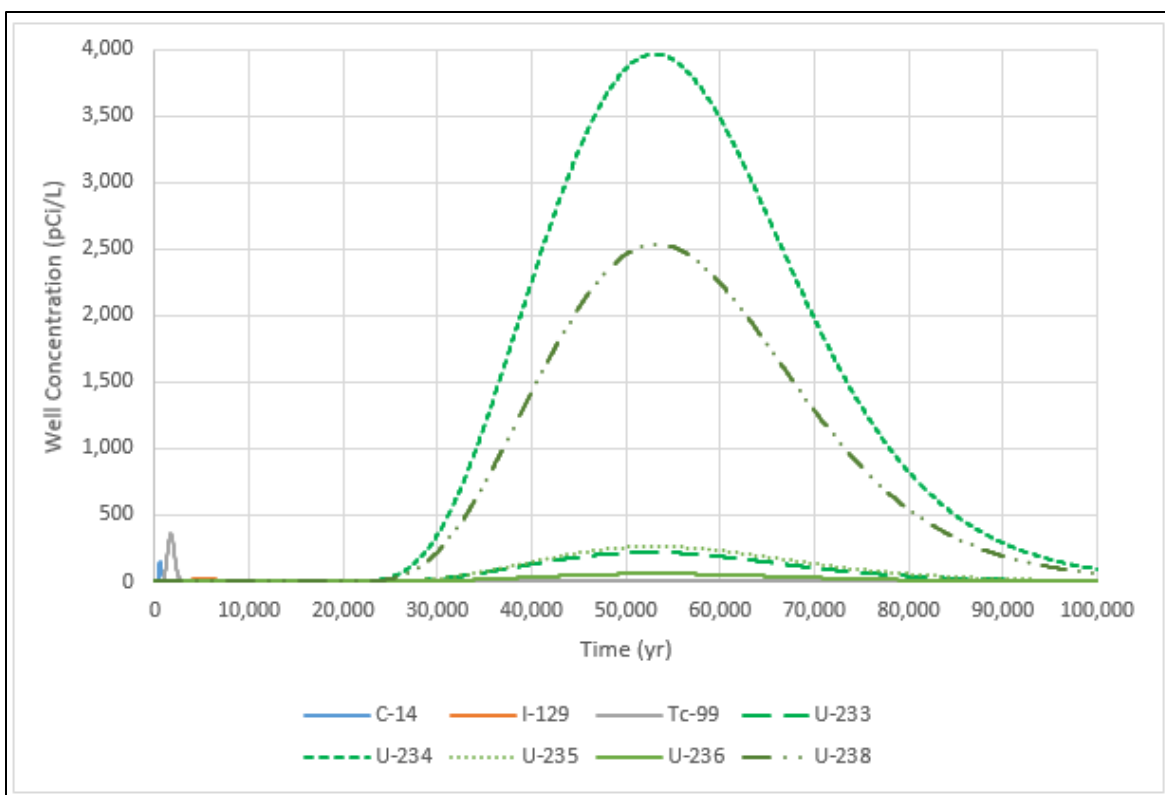
Fig. 4.27. RESRAD-OFFSITE predicted radionuclide concentrations in well water, 100,000-year simulation

5. SENSITIVITY AND UNCERTAINTY ANALYSIS

The goal of sensitivity-uncertainty analysis for the EMDF PA is understanding sensitivity of model predictions to uncertainty in input parameter values for those radionuclides and transport pathways that are the primary contributors to the all-pathways dose within the 1000-year compliance period. The base case all-pathways maximum dose during the compliance period is approximately 1 mrem/year, and the peak dose within 10,000 years is less than half of the 25 mrem/year performance objective. The focus of the analysis is on importance of uncertainty in long-term cover performance, partition coefficient values for key radionuclides, and hydrogeologic parameters for meeting DOE performance objectives. Given the pessimistic exposure assumptions incorporated in the base case all pathways scenario (Sect. 1.7), consideration of uncertainty in exposure factor assumptions (e.g., ingestion rates) was limited to the ingestion rates of fish and meat, and the depth of aquifer contributing to well (well depth).

The analysis includes selected sensitivity cases (what-if scenarios) for the detailed vadose and saturated zone transport models. For the RESRAD-OFFSITE model that analysis includes single factor sensitivity evaluations (increasing and decreasing one parameter at a time from the assumed base case value) and an uncertainty analysis to address the importance of key uncertainties relative to compliance with the 25 mrem/year performance objective. The uncertainty analysis involves assigning probability distributions to selected input parameters and running multiple simulations with different sets of input values, and statistical analysis of the results. The sensitivity and uncertainty evaluations undertaken for the EMDF PA are summarized in Table 5.1.

Table 5.1. Summary of sensitivity-uncertainty analyses for the EMDF PA

Type of sensitivity-uncertainty analysis	Subsystems and models evaluated	Parameters selected for analysis (related uncertainty)
Model sensitivity cases (what-if analysis)	Saturated Zone Flow – MODFLOW	• Increased recharge (climate)
	Vadose Zone Transport – STOMP	• Increased cover infiltration (climate, cover performance) • Increased waste K_d (materials and geochemistry) • Decreased non-waste K_d (materials and geochemistry)
	Saturated Zone Transport – MT3D	• Increased layer 2 hydraulic conductivity value (materials) • Non-uniform source release (uniform source release assumption)
Single factor sensitivity	Total System – RESRAD-OFFSITE	• Refer to Table 5.2
Probabilistic input parameter uncertainty analysis	Total System – RESRAD-OFFSITE	• Refer to Appendix G, Attachment G.3

EMDF = Environmental Management Disposal Facility RESRAD = RESidual RADioactivity
K_d = partition coefficient STOMP = Subsurface Transport Over Multiple Phases
PA = Performance Assessment

HELP model sensitivity evaluation is presented in Sect. 3.3.1.3 and Appendix C, Sect. C.2.5. The range of cover infiltration considered in the probabilistic uncertainty analysis is consistent with the uncertainty in HELP model predictions of cover performance. Sensitivity of the groundwater flow model results to increased recharge (future wet condition) is presented in Sect. 5.1 and Appendix D, Sect. D.5.6.

5.1 STOMP MODEL SENSITIVITY

Presentation of STOMP model sensitivity evaluations is limited to Tc-99 results, which are representative of the sensitivity of predicted concentrations of other radionuclides with nonzero K_d values (e.g., I-129) to the uncertainties in K_d values. STOMP model sensitivity to increased long-term maximum cover infiltration was also evaluated. The base case assumption for all radionuclides with nonzero K_d, for all PA models, is that the waste K_d value is one-half of the value assumed for all non-waste materials (refer to Sect. 3.2.2 and Table 3.4). The STOMP model sensitivity evaluations for (nonzero) K_d values included increasing the waste K_d value to the value assumed for non-waste materials (i.e., doubling the waste K_d), and decreasing the non-waste K_d value to the waste value (i.e., reducing the non-waste K_d value by half). For Tc-99, the waste K_d value was increased to 0.72 cm^3/g and the non-waste value was reduced to 0.35 cm^3/g. Sensitivity to increased maximum cover infiltration (twice the base case value), representing uncertainty in long-term cover performance was evaluated for all seven radionuclides included in the STOMP modeling. The potential for long-term cover performance to be better than assumed (lower maximum cover infiltration) is evaluated with the total system model in Sects. 5.3 and 5.4.

The sensitivity of STOMP predicted Tc-99 flux over time to the alternative K_d values and maximum cover infiltration are shown in Figs. 5.1 and 5.2. In each figure the upper plot is the base case STOMP model result and the lower plot is the sensitivity case. The K_d value controls the initial aqueous concentrations in waste materials and governs the release rate for a given inventory and cover infiltration. For the higher Tc-99 waste K_d the following differences from the base case are observed (Fig. 5.1):

- Lower peak mass flux rates at the base of the liner and the water table output surface due to lower initial aqueous concentrations

- Delayed peak flux at the water table surface (1400 years versus 1200 years for the base case)

- Longer duration of Tc-99 release from waste and flux into the saturated zone.

The results for lower K_d in the non-waste materials are shown on Fig. 5.2. Compared to the base case result the following differences are observed:

- Essentially the same Tc-99 mass flux at the liner output surface due to the same waste zone K_d value and initial aqueous concentration as the base case

- More rapid increase in mass flux at the water table output surface due to the lower K_d values in the vadose zone

- Higher and earlier peak mass flux at the water table surface (1100 years versus 1200 years for the base case).

These results are expected based on the K_d relationships to radionuclide release and transport. An increased waste K_d has a larger impact on release to the saturated zone than does a decreased vadose zone K_d.

For cover performance uncertainty, a maximum cover infiltration rate two times the base case long-term performance condition value was simulated. The linear increase between 200 and 1000 years changed from 0 to 0.88 in./year to 0 to 1.76 in./year and stayed at 1.76 in./year beyond 1000 years. Changing the maximum infiltration rate but not the assumed timing of cover degradation represents more rapid increase in cover infiltration than the base case scenario. Due to the increased amount of the water flux, there is also earlier Tc-99 mass release from the waste and a higher (nearly double) peak mass flux rate at the water table output surface (Fig. 5.3). The higher maximum infiltration also results in much faster waste zone depletion and faster migration to the saturated zone (peak flux occurs 200 years earlier) due to the larger water flux.

254
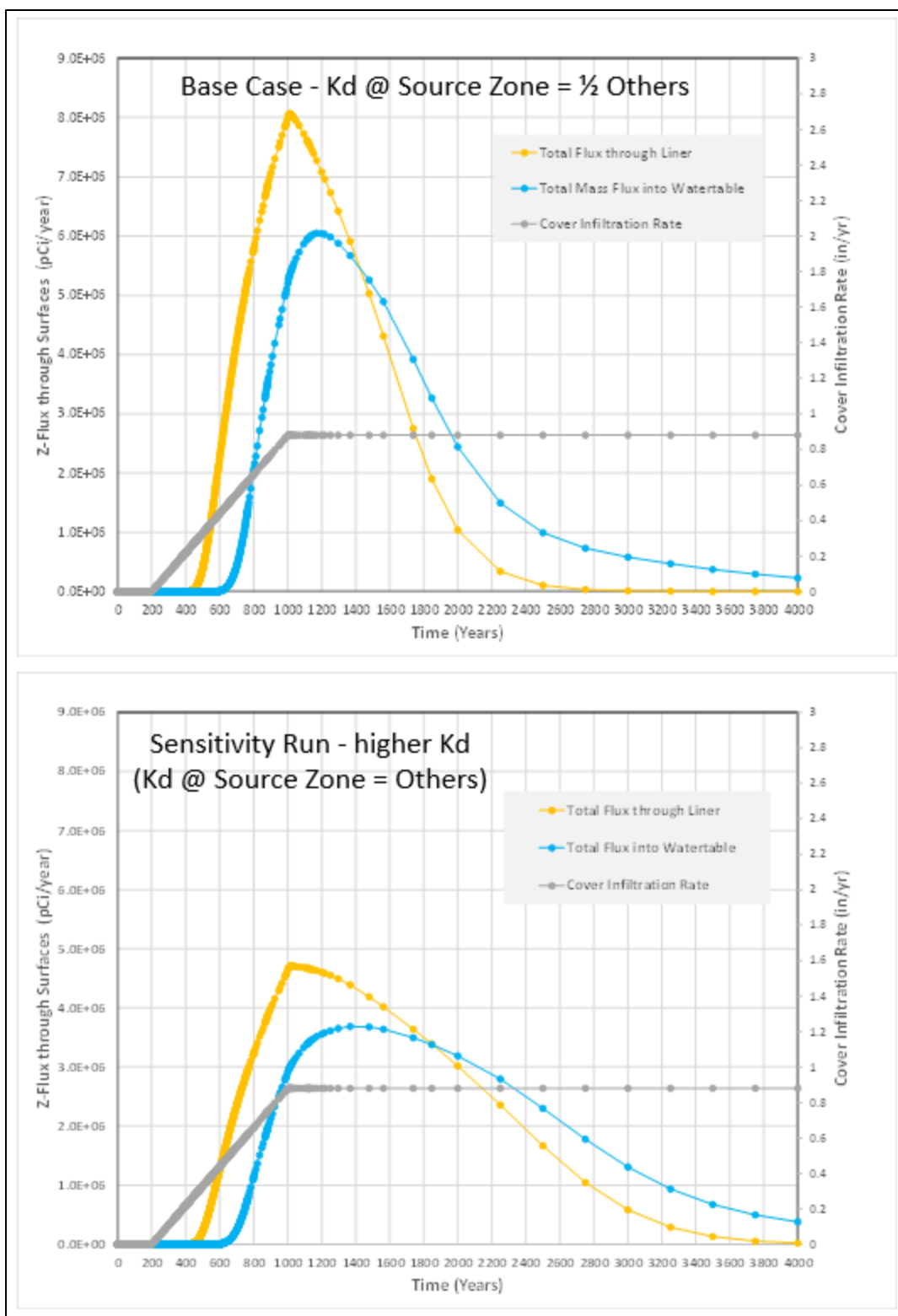
Fig. 5.1. Waste zone K_d impact on STOMP model Tc-99 flux

255
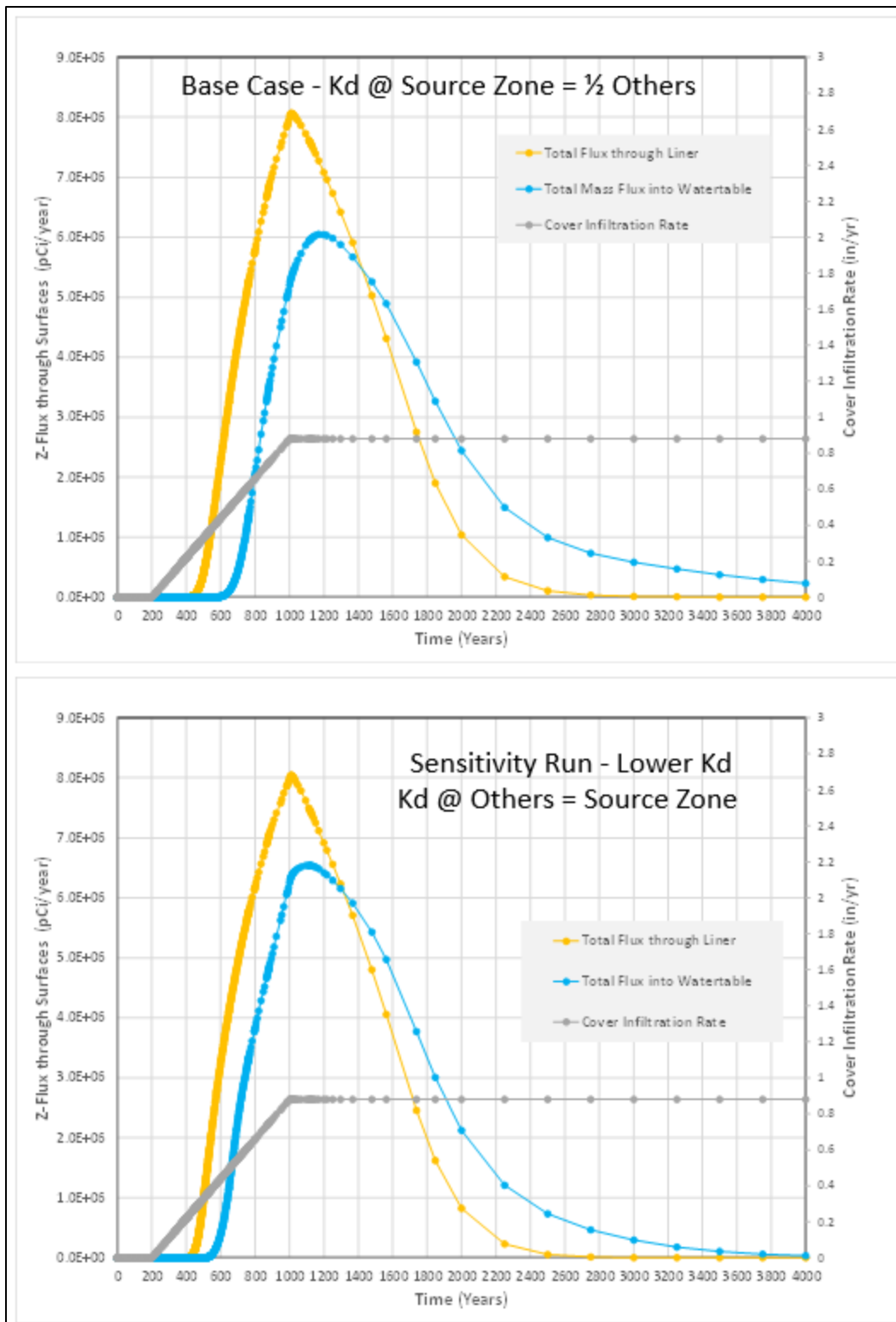
Fig. 5.2. Vadose zone K_d impact on STOMP model Tc-99 flux
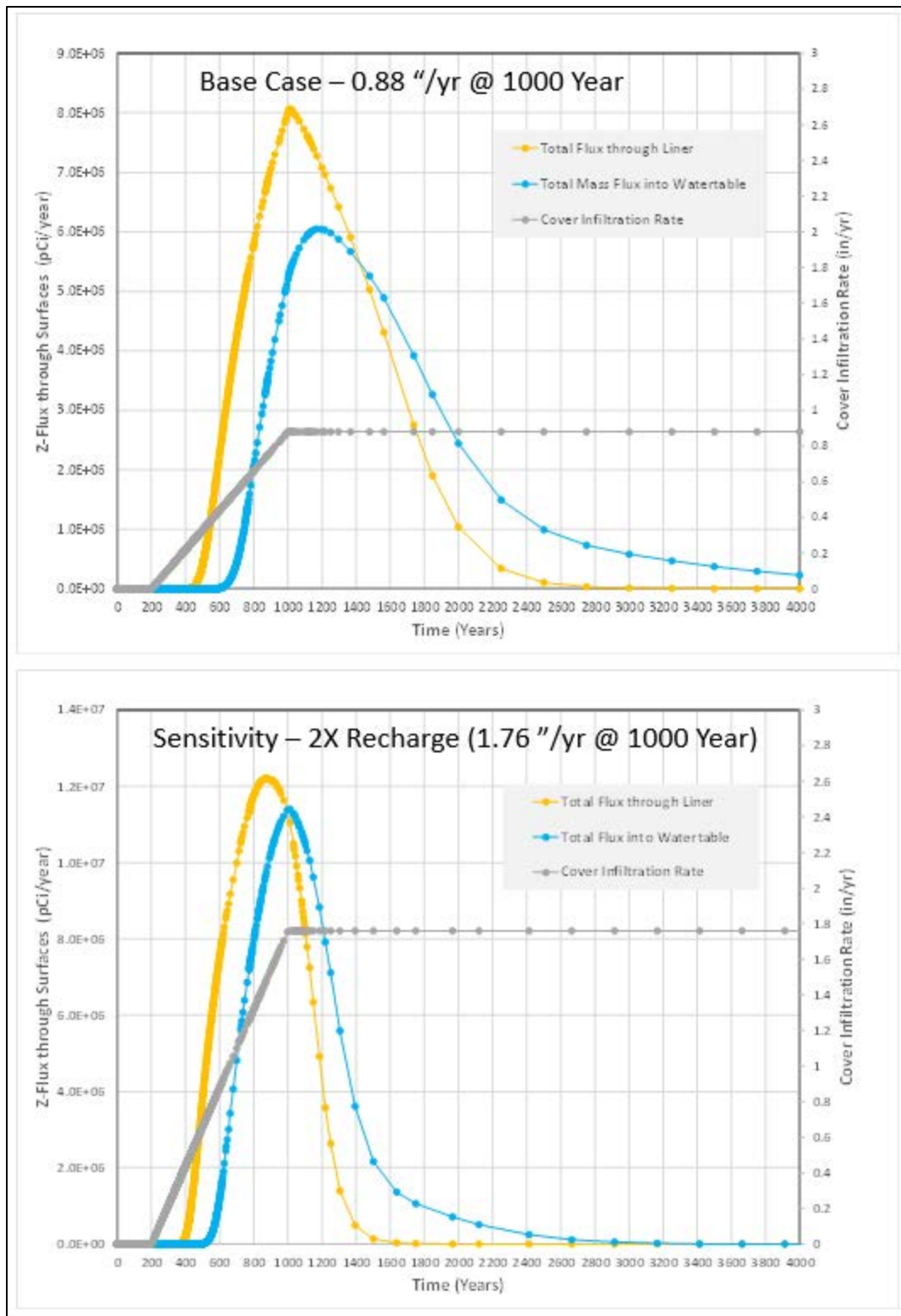
Fig. 5.3. Higher cover infiltration impact on STOMP model Tc-99 flux

257

The maximum aqueous concentrations in the waste zone and vadose zone are the same as for the base condition since K_d controls the mass partition between solid and aqueous phases. However, the resulting saturated zone concentrations underneath the EMDF would be higher than for the base case since there is more mass flux into the groundwater system from the vadose zone.

5.2   MT3D MODEL SENSITIVITY

MT3D results for two sensitivity cases are presented in this section. The sensitivity evaluations for the MT3D model included a scenario in which the hydraulic conductivity of model layer 2 was increased, and the non-uniform radionuclide release scenario. These two sensitivity cases address potential conceptual model uncertainties related to the characteristics of saprolite and bedrock along the flow path to the groundwater POA and to the assumption of uniform radionuclide release to the saturated zone. Results for these two sensitivity cases are also presented in Sect. 3.3.5 in the context of integrating the results from the different PA models.

5.2.1   Sensitivity to Hydraulic Conductivity of the Shallow Aquifer

To evaluate the impact of shallow aquifer hydraulic conductivity uncertainty and possible variation from the base case flow model assumptions, a sensitivity analysis was performed by applying higher hydraulic conductivity values in model layer 2. The relatively large thickness (70 ft) of model layer 2 in the EMDF model compared to the thickness of layers 1 and 3 at the 100-m well location suggested that the hydrogeologic properties assigned to layer 2 along the flow path from the EOW to well location could have a large effect on predicted saturated zone activity concentrations. The hydraulic conductivity of model layer 2 was increased to the value assigned to model layer 1, constituting an 8-fold increase. Applying the larger K value to model layer 2 is not an accurate representation of site conditions, based on the CBCV site characterization results (DOE 2018b, DOE 2019), but the sensitivity case does illustrate how a different configuration of material properties affects the results of the MT3D saturated zone radionuclide transport model. After the flow simulation was conducted with the higher hydraulic conductivity, impact on Tc-99 transport simulation with the MT3D model was evaluated. Additional detail is provided in Appendix F, Sect. F.4.3.

The Tc-99 concentration time series for all MT3D model layers at the 100-m well location for both base case and the layer 2 high K scenario are plotted in Fig. 5.4. Compared with base case scenario, the peak Tc-99 concentrations in different model layers are either higher or lower and occur earlier for the layer 2, high K sensitivity run. This difference is associated with the lower water table elevation and more rapid flow due to higher conductivity in model layer 2 beneath the waste and along the transport path to the 100-m well. Most of the Tc-99 movement occurs within model layer 2 due to its higher hydraulic conductivity, resulting in a very low concentration in the deeper model layers. At the 100-m well location, the model layer 1 and 2 peak Tc-99 concentrations are significantly higher and much earlier for the high K sensitivity run, peaking around 1750 years post-closure (vs peak concentrations occurring after 2500 years for the base case). The peak transmissivity-weighted average Tc-99 concentrations are approximately 50 percent higher than the base case peaks (300 pCi/L vs 200 pCi/L for the base case). The peak model layer 2 Tc-99 concentration is over 70 percent higher than for the base case.
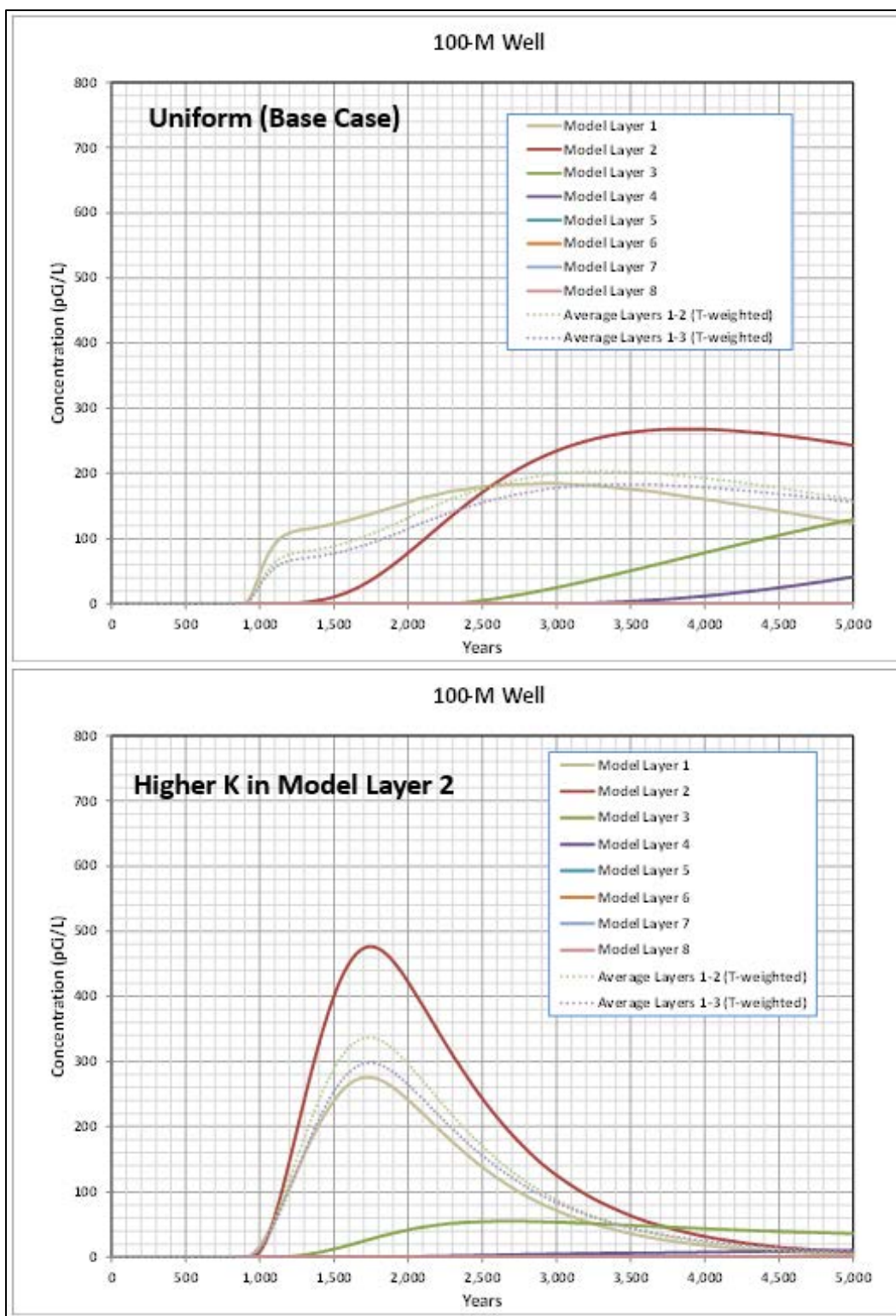
Fig. 5.4. MT3D predicted Tc-99 groundwater concentrations at the 100-m well (sensitivity to high K in layer 2)

Although the simulated Tc-99 concentrations at the 100-m well are very sensitive to the nearly 10-fold increase in the hydraulic conductivity of model layer 2, applying the higher K values representative of the saprolite zone to the deeper parts of the model domain is not an accurate representation of EMDF site conditions. The sensitivity run results suggest that uncertainty in hydrogeologic characteristics of the shallow subsurface materials in the vicinity of the disposal unit may be important for evaluating uncertainty in peak concentrations at the POA, but the uncertainty in field conditions is not as large as the applied increase in layer 2 conductivity. Due to the potential sensitivity of results to saturated zone hydraulic conductivity, the probabilistic uncertainty analysis for the PA total disposal system model (RESRAD-OFFSITE) includes a range of possible K values based on the available field data.

5.2.2   Non-uniform Release Scenario

The base condition saturated zone transport model assumes that the leachate flux from the waste area is uniform, implying that the waste volume has both a uniform radionuclide concentration and uniform thickness. The STOMP model simulation for EMDF (see Appendix E) demonstrates that there can be spatially variable (non-uniform) release rates within the facility footprint due to variation in waste thickness and liner system control of leachate drainage patterns. Variable leachate release rates will result in different radionuclide mass flux rates into the saturated zone that could have an impact on radionuclide concentrations at the 100-m well location. To evaluate this possibility, a non-uniform release scenario for the flow and transport model was developed using STOMP model results to estimate the variation in leachate flux and radionuclide concentration within the waste area. This sensitivity analysis was performed for Tc-99 transport only since it has a relatively small non-zero K_d value and the initial arrival time at the POA for the base condition falls within the 1000 year post-closure compliance period for the PA.

The non-uniform pattern of leachate flux beneath the EMDF predicted by the STOMP model was used to develop a non-uniform Tc-99 release model for MT3D based on the radionuclide release model (Sect. 3.3.3.2) developed for the uniform release scenario. The Section A STOMP model results were used to calculate the cumulative total volumetric leachate flux (volume/time) and cumulative total Tc-99 activity flux (activity/time) at the water table elevation directly below the upper half (upslope portion with lower flux) and the lower half (downslope portion with higher flux) of each disposal cell. The lower half to upper half ratios of leachate flux and Tc-99 flux represent a time-integrated measure of the non-uniformity of release from each disposal cell, derived from the STOMP Section A model results. An average Tc-99 concentration ratio is obtained by dividing the Tc-99 flux ratio by the leachate flux ratio for each cell.

The calculated leachate flux ratios were used to assign water recharge rates to each of eight cell floor sub-areas (upper and lower halves) of the floor of each cell (refer to Appendix F, Fig. F.17), accounting for the funneling effect of the outer sideslopes of each disposal cell and the pattern of water flux driven by the sloping cell floors. The individual water recharge (leachate flux) rates were applied in the MODFLOW model code to generate the flow field for the non-uniform Tc-99 release scenario MT3D transport model.

The Tc-99 mass in each disposal cell was calculated based on the cell volume and EMDF average initial (post-operational) Tc-99 concentration. Applying these initial Tc-99 masses, and utilizing STOMP model results to estimate Tc-99 vadose delay times for each disposal cell (Appendix E, Table E.8), a Tc-99 release model for each cell was created (refer to Appendix F, Sect. F.4.2.3). The Tc-99 recharge concentrations for each disposal cell were then partitioned into concentrations applied to the upper and lower half of each disposal cell on the basis of the calculated Tc-99 concentration ratio value. The resulting non-uniform Tc-99 release model accounts for variation in waste volume, water infiltration, and liner geometry among the four disposal cells. Additional detail on implementation of the non-uniform Tc-99 release model is provided in Appendix F.

The Tc-99 concentration time series for all model layers at the 100-m well location for both uniform and non-uniform release scenarios are plotted in Fig. 5.5. At the 100-m well, the model layer 1 and 2 peak Tc-99 concentrations are nearly the same for the uniform and non-uniform release scenarios, but the initial increase in layer 1 concentrations is much more gradual in the non-uniform release scenario. This difference in layer 1 concentrations directly reflects the non-uniform release to model layer 2 within the upgradient waste area, where model layer 1 remains unsaturated (i.e., recharge concentrations are applied to model layer 2). The peak transmissivity-weighted average Tc-99 concentrations occur slightly later for the non-uniform release, but are essentially the same (190 to 200 pCi/L) as the peak concentrations for the uniform release scenario.

This model sensitivity evaluation of uniformity of leachate release suggests that the base case uniform release scenario, although incorporating simplified release assumptions, does not underestimate peak concentrations relative to a more complex conceptualization and model implementation of non-uniform release. Using a more complex source representation could provide more information on variability in saturated zone concentrations in space and time, but will also introduce more uncertainty to the dose analysis associated with uncertainty in waste inventory and recharge distributions. Assuming non-uniform release would also increase the uncertainty in the selection of a groundwater POA location that will capture peak saturated zone impacts under differing sets of model input assumptions.
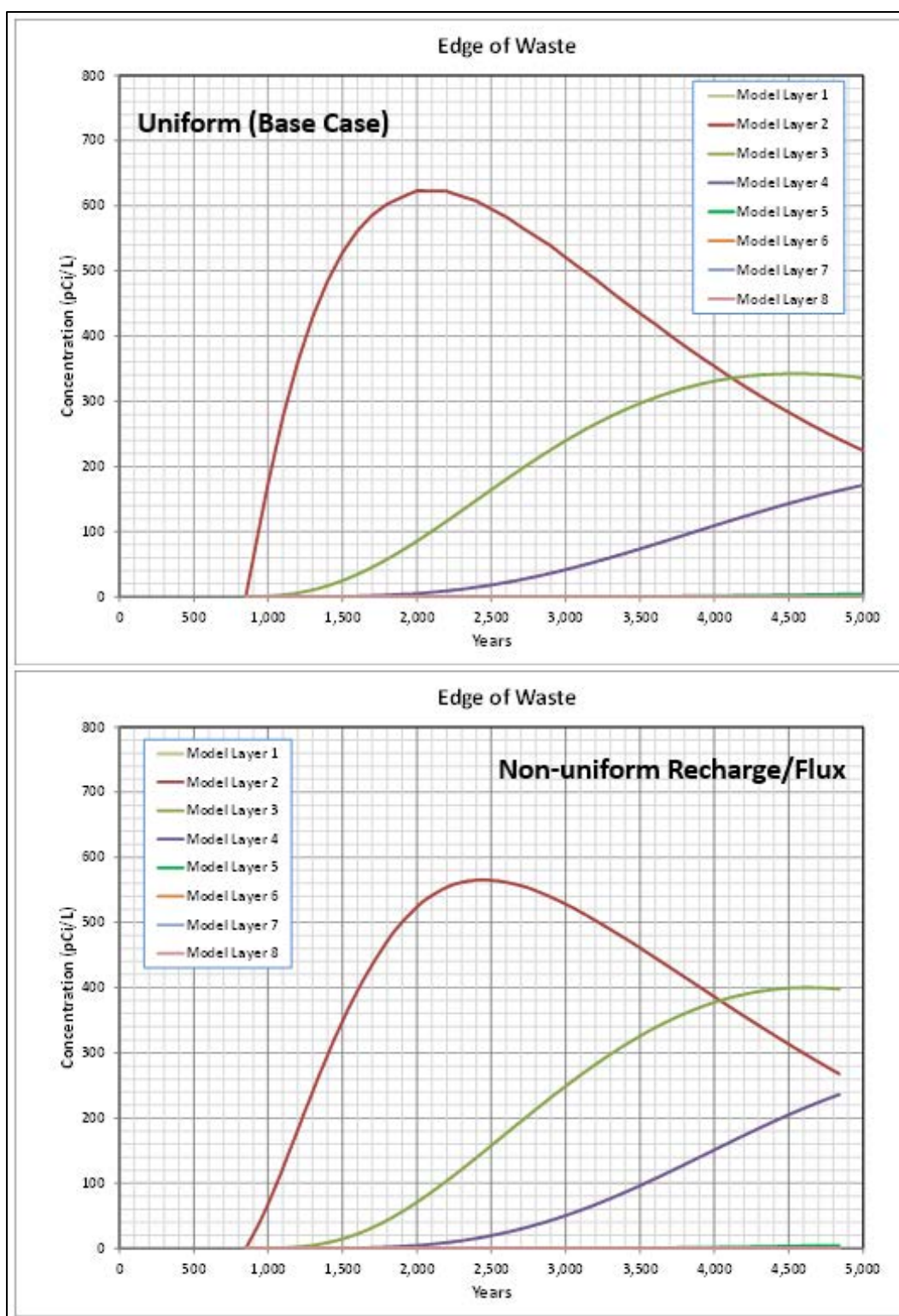
**Fig. 5.5. Comparison of MT3D base case Tc-99 concentrations
with results for the non-uniform source release simulation**

5.3 RESRAD-OFFSITE SINGLE-FACTOR SENSITIVITY

The RESRAD-OFFSITE model was used to perform a large number of sensitivity evaluations for individual model input parameters (Appendix G, Sect. G.6.2). The utility of single factor analysis is limited because potential sensitivity of modeled dose to changing multiple parameter values is not captured. The qualitative evaluation of relative dose sensitivity to input values presented in Appendix G is also influenced by the selection of the range over which individual parameters are varied. The selected range is usually based on likely ranges of natural parameter variability or judgements about the degree of uncertainty associated with the assumed base case value. The single factor analyses are used to guide the selection of input parameters for which probability distributions are assigned in the probabilistic uncertainty analysis presented in Sect. 5.4.

The RESRAD-OFFSITE code package provides convenient evaluation of sensitivity for single input parameters. Input parameters can be increased and decreased by a user-selected factor. Table 5.2 contains the input parameters for which single factor sensitivity was evaluated and presented in Appendix G, and identifies the corresponding plots from this section and from Appendix G, Sect. G.6.2. The selection of input parameters was based on preliminary evaluations performed during development of the total system model. To focus the sensitivity analysis, parameters were varied for sitewide parameters (e.g., precipitation, runoff coefficient, residence time in lake) as well as for select radionuclides. The selected radionuclides are the top three contributors to total dose: C-14, Tc-99, and I-129. Sensitivity analysis results are for total dose and include contributions from all isotopes simulated during base case modeling. Graphical output for all of the parameter sensitivities evaluated are provided in Appendix G. Five of those graphics are included in this section to highlight a few of the more sensitive parameters.

Table 5.2. RESRAD-OFFSITE sensitivity analysis parameters, base case scenario

Parameter Description	RESRAD parameter identifier	Factor applied to base case value	Total dose plot figure
C-14 K_d in contaminated zone	DCACTC(C-14)	N/A	G.18
C-14 K_d (UZ1-UZ5)	DCACTU1-5(C-14)	N/A	G.18
C-14 K_d in saturated zone	DCACTS(C-14)	N/A	G.19
I-129 K_d contaminated zone	DCACTC(I-129)	5	G.19
I-129 K_d (UZ1-UZ5)	DCACTU1-5(I-129)	5	G.19
I-129 K_d saturated zone	DCACTS(I-129)	5	G.19
Tc-99 K_d contaminated zone	DCACTC(Tc-99)	5	G.20
Tc-99 K_d (UZ1-UZ5)	DCACTU1-5(Tc-99)	5	G.20
Tc-99 K_d saturated zone	DCACTS(Tc-99)	5	G.20
Precipitation	PRECIP	1.25	5.9, G.21
Initial releasable fraction	RELFRACINIT	(C-14) = 0.998, 0.564 (I-129, Tc-99) = 0.5, 0	G.22
Time at which C-14 first becomes releasable (delay time)	RELTIMEINIT(C-14)	2	G.23
Time at which I-129 first becomes releasable (delay time)	RELTIMEINIT(I-129)	2	G.23
Time at which Tc-99 first becomes releasable (delay time)	RELTIMEINIT(Tc-99)	2	G.23
Time over which transformation to releasable form occurs (C-14)	RELDUR(C-14)	2	G.24

Table 5.2. RESRAD-OFFSITE sensitivity analysis parameters, base case scenario (cont.)

Parameter Description	RESRAD parameter identifier	Factor applied to base case value	Total dose plot figure
Time over which transformation to releasable form occurs (I-129)	RELDUR(I-129)	2	G.24
Time over which transformation to releasable form occurs (Tc-99)	RELDUR(Tc-99)	2	G.24
Runoff coefficient	RUNOFF	N/A	5.10, G.25
Source release	--	N/A	5.6, G.17
Source concentrations	--	N/A	5.8, G.26
C-14 K_d in contaminated zone	DCACTC(C-14)	N/A	G.18
I-129 K_d contaminated zone	DCACTC(I-129)	5	5.7, G.19
Tc-99 K_d contaminated zone	DCACTC(I-129)	5	G.20
Longitudinal dispersivity of contaminated zone	ALPHLCZ	5	G.27
Contaminated zone b parameter	BCZ	1.4	G.27
Hydraulic conductivity of contaminated zone	HCCZ	5	G.27
Total porosity of contaminated zone	TPCZ	1.1	G.27
Effective porosity of contaminated zone	EPCZ	1.5	G.27
C-14 K_d (UZ1-UZ5)	DCACTU1-5(C-14)	N/A	G.18
I-129 K_d (UZ1-UZ5)	DCACTU1-5(I-129)	5	5.7, G.19
Tc-99 K_d (UZ1-UZ5)	DCACTU1-5(Tc-99)	5	G.20
Bulk density of UZ3	DENSUZ(3)	1.05	G.28
Total porosity of UZ3	TPUZ(3)	1.1	G.28
Effective porosity of UZ3	EPUZ(3)	1.1	G.28
Bulk density of UZ4	DENSUZ(4)	1.05	G.29
Total porosity of UZ4	TPUZ(4)	1.1	G.29
Effective porosity of UZ4	EPUZ(4)	1.1	G.29
Bulk density of UZ5	DENSUZ(5)	1.05	G.30
Total porosity of UZ5	TPUZ(5)	1.1	G.30
Effective porosity in native vadose zone (UZ5)	EPUZ(5)	1.5	G.30
Longitudinal dispersivity of native vadose zone (UZ5)	ALPHALU(5)	2	G.30
Thickness of native vadose zone (UZ5)	H(5)	2	G.31
Thickness of native vadose zone (UZ5)	H(5)	H(5) = 0.01 m	G.31
C-14 K_d in saturated zone	DCACTS(C-14)	N/A	G.18
I-129 K_d saturated zone	DCACTS(I-129)	5	5.7, G.19
Tc-99 K_d saturated zone	DCACTS(Tc-99)	5	G.20
Dry bulk density of saturated zone	DENSAQ	1.15	G.32
Total porosity of saturated zone	TPSZ	1.5	G.32

Table 5.2. RESRAD-OFFSITE sensitivity analysis parameters, base case scenario (cont.)

Parameter Description	RESRAD parameter identifier	Factor applied to base case value	Total dose plot figure
Effective porosity of saturated zone	EPSZ	1.5	G.32
Thickness of saturated zone	DPTHAQ	1.5	G.32
Hydraulic conductivity of saturated zone	HCSZ	2	G.32
Hydraulic gradient of aquifer to well	HGW	2	5.11, G.33
Longitudinal dispersivity of aquifer to well	ALPHALOW	2	5.11, G.33
Hydraulic gradient of aquifer to surface water body	HGSW	2	G.34
Longitudinal dispersivity of aquifer to surface waterbody	ALPHALOSW	2	G.34
Depth of aquifer contributing to surface waterbody	DPTHAQSW	2	G.34
Mean residence time of water in surface waterbody	TLAKE	10	G.34
Meat ingestion	DMI(1)	1.19	G.35
Fish ingestion	DFI(1)	2	G.35
Fraction of meat from affected area	FMEMI(1)	2	G.35
Depth of aquifer contributing to well	DWIBWT	1.5	G.36

N/A = not applicable   UZ = unsaturated zone
RESRAD = RESidual RADioactivity

The conceptual model of radionuclide release from the waste is an important uncertainty in the PA. Figure 5.6 shows predicted dose sensitivity to the selection of the RESRAD-OFFSITE release model option. RESRAD-OFFSITE offers three options to simulate source release (Sect. 3.3.4.2): First-Order Rate Controlled Release with Transport, Version 2 Release, and Instantaneous Equilibrium Desorption Release. The Version 2 release model does not allow for a time delay like the other two release models, so for comparison of predicted dose from the three release models, results from the sensitivity simulation with this release option were shifted by 300 years. Dose peaks are lower for the first two release model options, which may be more representative of a release limited by containerization or treatment of some portion of the total waste, or the impact of non-uniform cover failure and infiltration that leads to preferential release and transport paths through the waste zone.
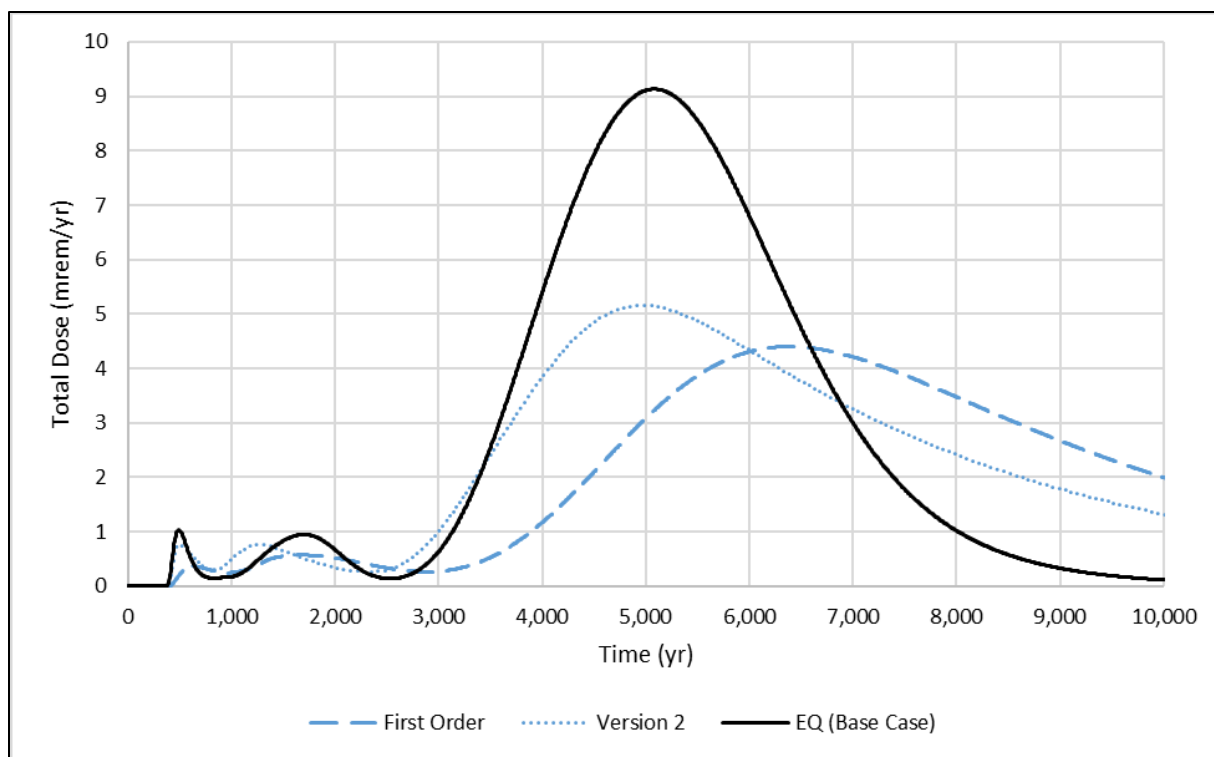
Fig. 5.6. Sensitivity analysis on RESRAD-OFFSITE release option

The factor of 5 sensitivity analysis on the specified distribution coefficient of I-129 in the contaminated zone, saturated zone, and unsaturated zones indicates that the predicted total dose is sensitive after the compliance period to variation of K_d for I-129. Increasing the K_d in each of the zones causes lower peak doses that occur later, while decreasing the K_d causes higher peak doses that occur earlier. Predicted total dose for the 10,000-year simulation period is most sensitive to the K_d of I-129 in the contaminated zone and the saturated zone and least sensitive to K_d of I-129 in the unsaturated zone. Results from the factor of 5 sensitivity analyses on the K_d of I-129 are shown in Fig. 5.7.

To evaluate the impact of radionuclide source concentrations in the waste on deterministic dose, the base case model was simulated with source concentrations higher than and lower than base case values for C-14, I-129, and Tc-99. Soil concentrations were not changed for any other simulated radionuclide, as dose contributions from all other radionuclides besides C-14, I-129, and Tc-99 are negligible. High-source concentrations evaluated are equal to as-disposed source concentrations, which do not account for operational period losses. Low-source concentrations are equal to 10 percent of the base as-disposed value (for C-14) or based on excluding the high outliers from the available radionuclide inventory data for I-129 and Tc-99.

Results from the sensitivity analysis on source concentrations are shown in Fig. 5.8. Predicted total dose for the compliance period is sensitive to varying the C-14 concentrations. Higher C-14 source concentrations cause a higher peak dose while lower source concentrations cause a lower peak dose. The high C-14 source concentrations are probably not realistic given that the estimated inventory (unadjusted for operational losses) is likely biased high. The timing of the peak dose for the compliance period is not sensitive to the C-14 source concentrations. Predicted total dose for the 10,000-year simulation period is also sensitive to varying the source concentrations. The lower I-129 source concentrations are probably a more realistic estimate of EMDF average as-disposed waste concentrations because of one particularly large I-129 data point included in the estimate used for the base case.

266
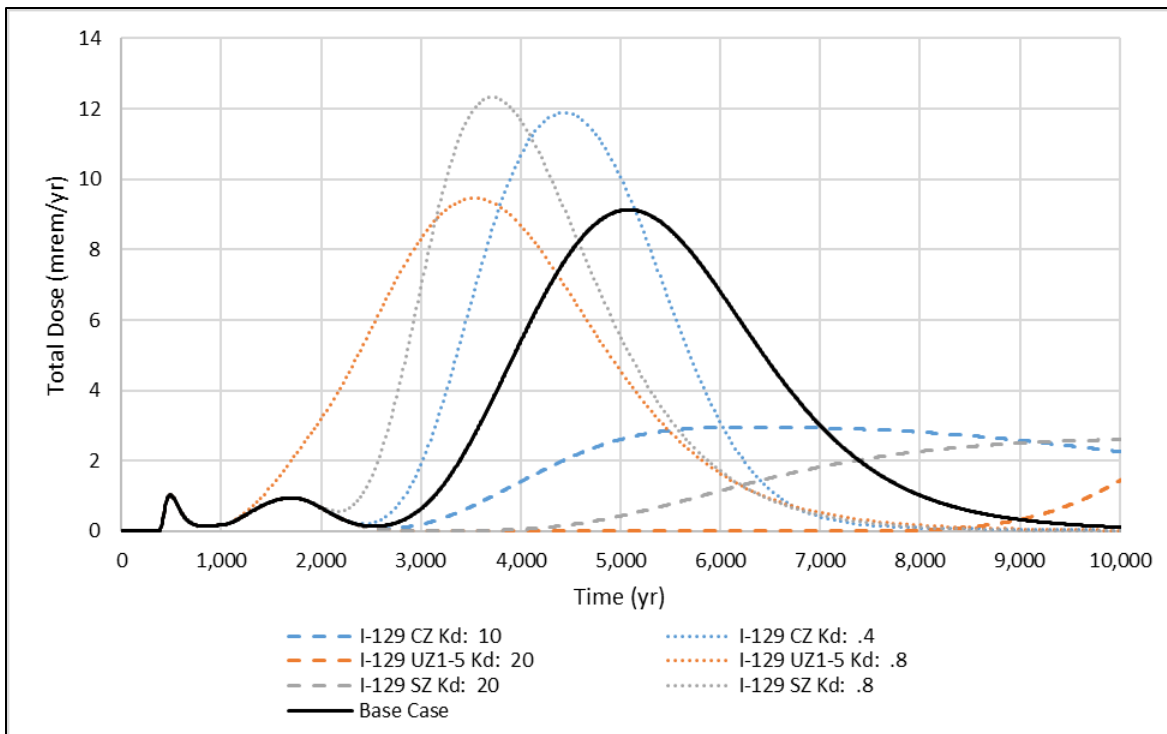
Fig. 5.7. Sensitivity analysis on I-129 distribution coefficient in the contaminated zone (CZ), saturated zone (SZ), and unsaturated zones (UZ1 - UZ5) with adjustment factor of 5
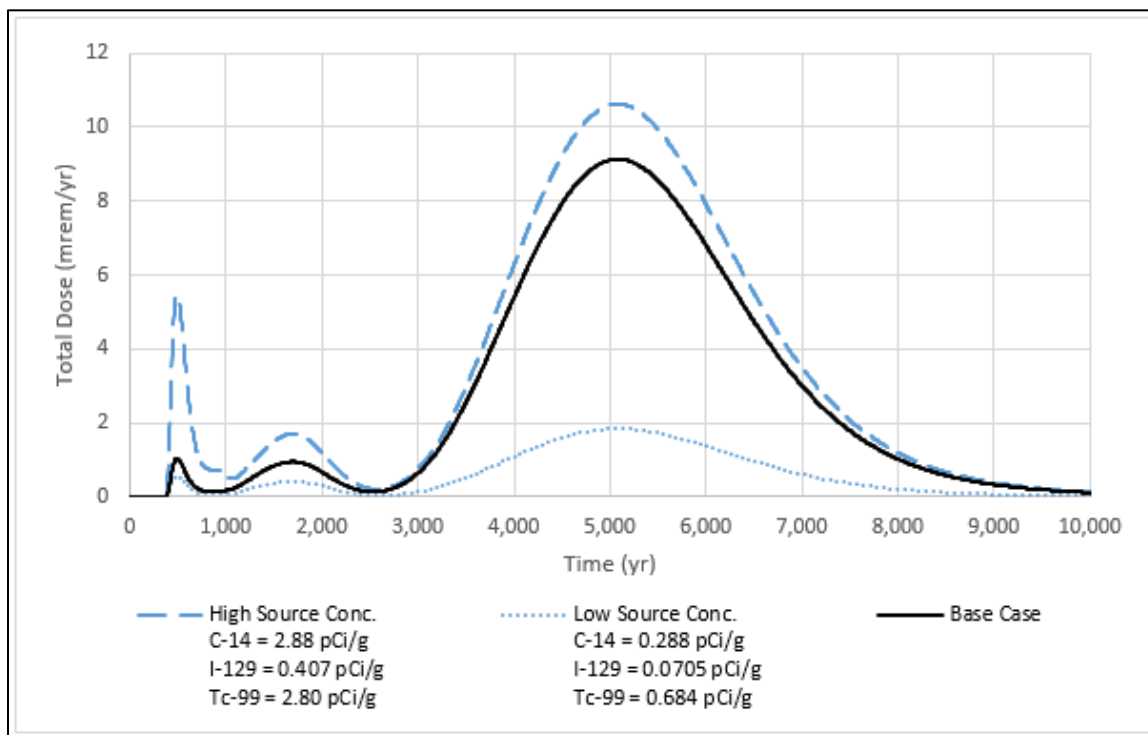
Fig. 5.8. Sensitivity analysis on radionuclide source concentrations for key radionuclides (C-14, I-129, and Tc-99)

267

Total dose sensitivity to variation in assumed values of average annual precipitation (representing climate uncertainty) and the runoff coefficient (representing uncertainty in long-term cover performance) confirms that uncertainty in future climatic conditions and cover system degradation are important for EMDF performance analysis (Figs. 5.9 and 5.10). The range in assumed precipitation evaluated corresponds to a range in modeled cover infiltration of 0.70 to 1.1 in./year (Fig. 5.9), while the range in the assumed value of the runoff coefficient corresponds to a 10-fold range in cover infiltration from 0.43 to 4.0 in./year (Fig. 5.10). The upper end of this range of modeled cover infiltration rates is much larger than rates reasonably expected for long-term EMDF cover performance.

Total dose peaks and the timing of peaks are sensitivity to varying the precipitation rate (Fig. 5.9). The factor of 1.25 is an extreme range of variation for a long-term annual average, at least on the upper end of the range (68 in./year). However the increases in total dose at the peak times are proportionally limited (about 15 percent or less). Proportional total dose increases in response to increased cover infiltration (decreased runoff coefficient) are more dramatic (Fig. 5.10). Compliance period impacts of increase cover infiltration on the C-14 dose peak are limited, but the I-129 peak is increased by 30 percent and occurs over 2000 years earlier than the based case scenario. The RESRAD-OFFSITE release model (instantaneous equilibrium release option) and one-dimensional vadose zone representation appear to over-predict the activity flux from EMDF for radionuclides having K_d values > 1 cm^3/g, including I-129 and U-234 (refer to Sect. 3.3.5 and Appendix G, Sect. G.5.6). The sensitivity evaluation on the lower runoff coefficient value (0.83) corresponding to 4 in./year cover infiltration produced extremely large doses after 5000 years that are associated with actinides (e.g., U-234 and Pu-239) in the EMDF estimated inventory. These extreme dose levels are not likely representative of future releases of uranium and plutonium for EMDF, and so the results of the sensitivity evaluation for the runoff coefficient are presented only for the total dose associated with C-14, Tc-99 and I-129 in Fig. 5.10.
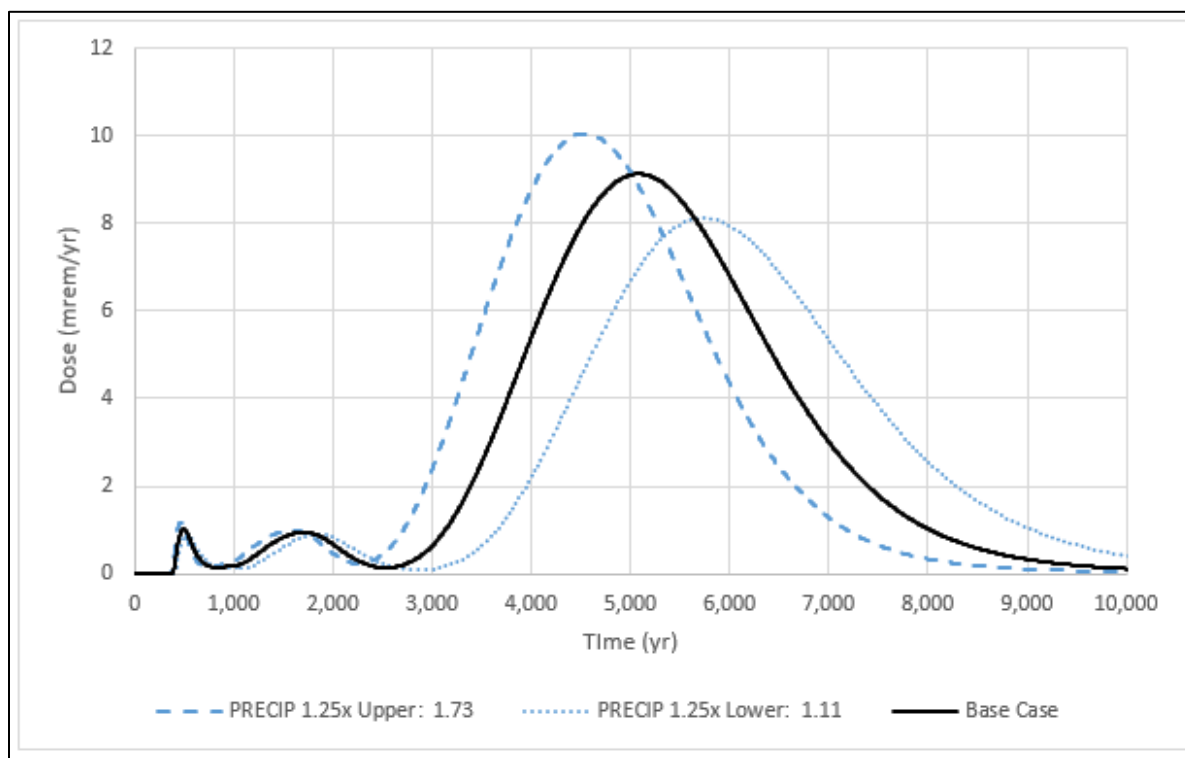
Fig. 5.9. Sensitivity analysis on precipitation rate (PRECIP) with adjustment factor of 1.25
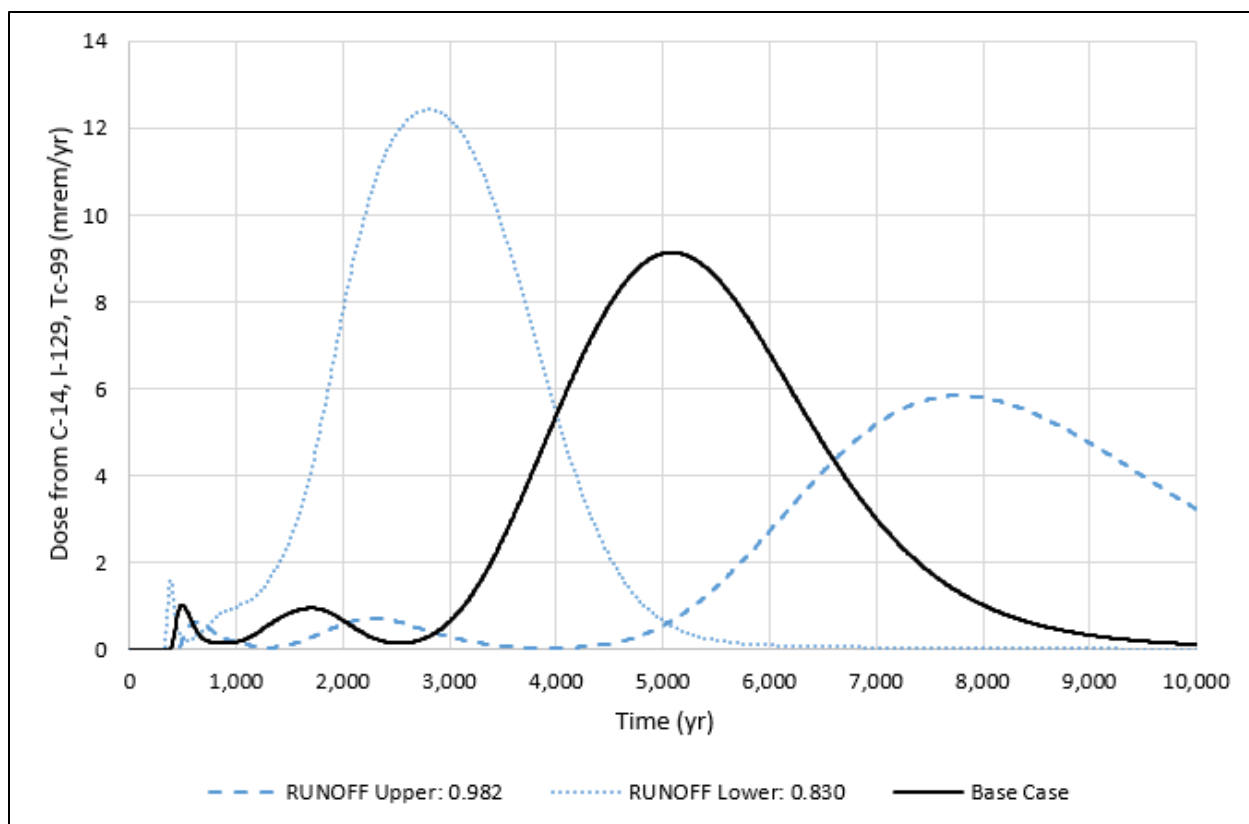
Fig. 5.10. Sensitivity analysis on runoff coefficient of the waste (RUNOFF)

Total dose sensitivity to variation in parameters that represent hydrologic controls on saturated zone radionuclide concentrations is significant for the range of parameter values evaluated (Fig. 5.11). Hydraulic gradient to the well location has relatively large impacts on total dose for the factor of 2 range of input values considered. The sensitivity appears to represent a source dilution effect that scales directly with the flux of groundwater through the aquifer. Dose sensitivity to the hydraulic conductivity of the saturated zone (Appendix G, Fig. G.32) is essentially the same as sensitivity to the hydraulic gradient because the product of those two parameters sets the Darcy velocity for the saturated zone and the magnitude of leachate dilution.
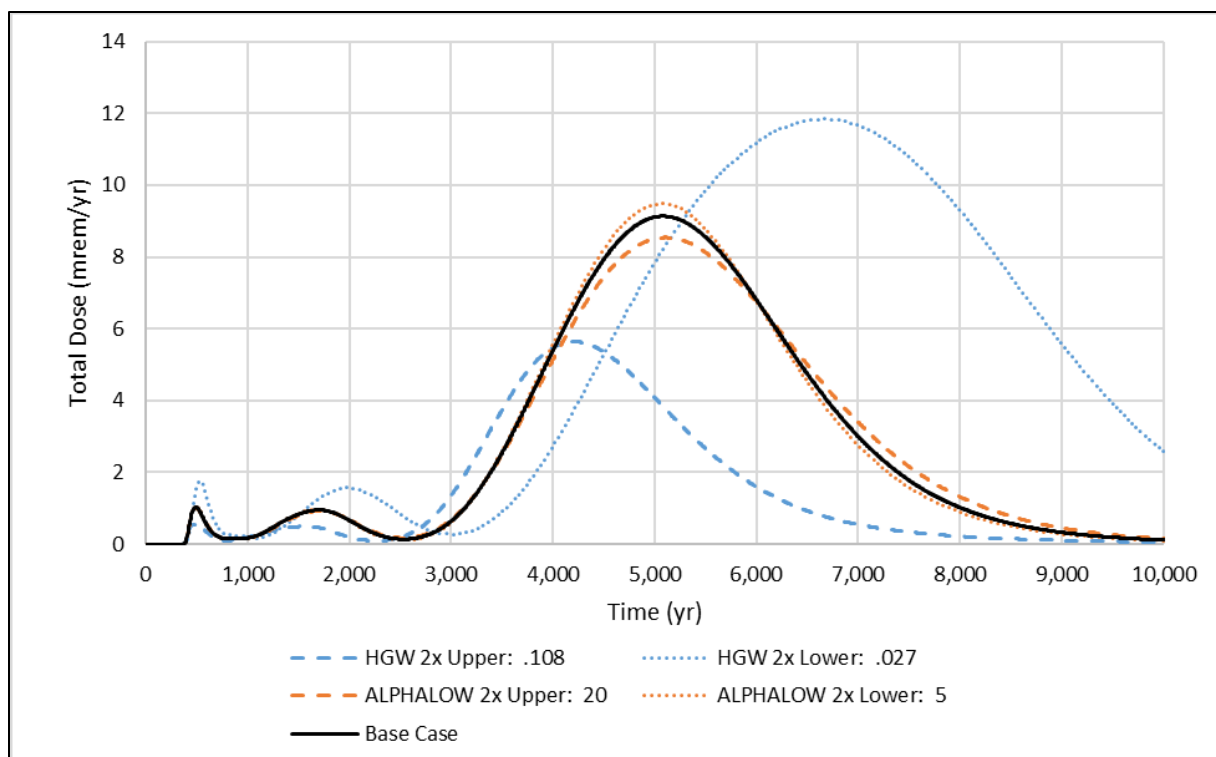
Fig. 5.11. Sensitivity analysis on hydraulic gradient of aquifer to well (HGW) and longitudinal dispersivity of aquifer to well with (ALPHALOW) and adjustment factor of 2

5.4   PROBABILISTIC UNCERTAINTY ANALYSIS

The RESRAD-OFFSITE probabilistic uncertainty analysis is described in detail in Appendix G and the results are briefly summarized in this section the EMDF PA report. The probabilistic analysis addresses input parameter uncertainty by assigning probability distributions to key input variables, randomly sampling sets of input parameters values and running multiple simulations to obtain the predicted peak dose for each of 3000 realizations of the disposal system. Distributions of predicted dose can be used to understand the range and likelihood of peak dose related to uncertainty in input parameters. Multiple regression analysis of peak dose as a function of the probabilistic input variables is used to determine which input parameters have the greatest impact on model results. Separate RESRAD-OFFSITE uncertainty analyses were completed for the 1000-year compliance period and for the longer 10,000-year period. The assignment of probability distributions for input parameters, relationships among parameters (including assigned correlations), and the sampling approach used to select input values for each simulation are described in detail in Appendix G, Sect. G.6.3. Appendix G also includes an evaluation of parameter value combinations that result in rare cases for which the simulated peak total dose exceeds 25 mrem/year.

Initially, using insights gained from preliminary model runs and sensitivity analysis simulations, key RESRAD-OFFSITE parameters for which uncertainty could have significant dose impacts were identified. C-14, I-129, and Tc-99 were identified as the radionuclides which had the most influence on total dose predictions during the compliance period; therefore, the compliance period probabilistic analysis includes only these three radionuclides. Preliminary model runs and sensitivity analysis simulations showed that Pu-239, U-234, U-235, and U-238 could potentially have dose contributions during the 10,000-year simulation period; accordingly, these radionuclides along with C-14, I-129 and Tc-99 were included in the 10,000-year probabilistic and uncertainty analysis. Both the compliance period and 10,000-year uncertainty

and probabilistic analyses focused on parameters with significant uncertainty in the assignment of deterministic base case values, which include radionuclide release parameters (initial releasable fraction, initial release time, release duration), isotope-specific K_d values, the surface runoff coefficient (cover performance uncertainty), precipitation (climate uncertainty), and parameters controlling flow in the waste, unsaturated, and saturated zones.

5.4.1 Probabilistic Results – Compliance Period

To simplify the analysis and to make total run time shorter, only C-14, Tc-99, and I-129 were included in the probabilistic evaluation for the compliance period. For the compliance period probabilistic simulations presented in this section, total dose refers to the dose resulting from C-14, Tc-99, and I-129.

The RESRAD-OFFSITE uncertainty analysis calculates statistics of the total dose distribution for each repetition at each simulation time step. Figure 5.12 shows the variation of median, mean, and 95th percentile dose over time for each of the 10 repetitions of 300 compliance period simulations. The deterministic base case model all-pathways dose curve is also shown on Fig. 5.12 for comparison to the probabilistic results. By 250 years, the mean of the simulated dose distribution begins a steady, gradual increase through 1000 years. The 95th percentile values increase rapidly between 250 and 400 years and then increase more gradually through 1000 years in parallel with the mean. In contrast, the median of the simulated dose distribution increases between 400 and 550 years and then becomes steady at approximately 0.4 mrem/year through the end of the compliance period. The difference between the deterministic base case dose curve and the probabilistic results (percentiles of the total dose distribution as a function of time) occurs because the time of peak total dose for any single probabilistic simulation varies widely (230 to 1030 years) due to variable sampling of input parameters that control release timing (particularly K_d values) among the 3000 realizations. The differences between the deterministic and probabilistic results also reflect the likelihood of much larger dose contributions from Tc-99 and I-129 toward the end of the compliance period probabilistic simulations.
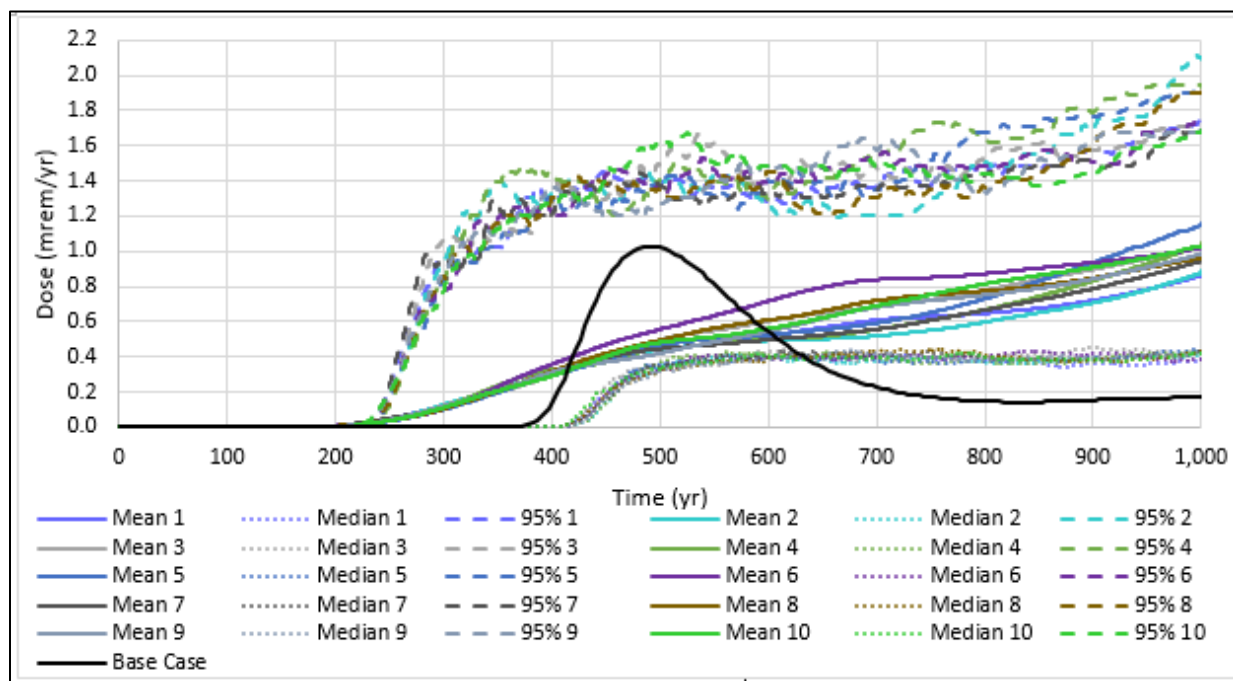
Fig. 5.12. Probabilistic total dose summary for 10 sets of 300 RESRAD-OFFSITE compliance period simulations, all pathways, all calculation points

The peak mean probabilistic dose (i.e., the maximum value of the mean dose for each repetition) occurred at 1030 years for all 10 repetitions, ranging from 0.92 to 1.2 mrem/year, which is a range that includes the deterministic base case compliance period peak dose of approximately 1 mrem/year. The 95th percentiles of the probabilistic total dose also reached maximum values at 1030 years, with a range from 1.7 to 2.1 mrem/year among the 10 repetitions.

Carbon-14 is the primary dose contributor for times prior to about 800 years. After 800 years, Tc-99 and I-129 have mean dose contributions equal to or greater than mean C-14 contributions. Additional detail on variation of radionuclide dose over the compliance period is provided in Appendix G, Sect. G.6.3.3.

The timing of peak radionuclide doses varies among simulations and radionuclides. For C-14, roughly 95 percent of the radionuclide peaks occur between 300 and 900 years, with an average peak dose of 1.03 mrem/year and average time of peak dose at 560 years. Most of the Tc-99 and I-129 peaks occur at the end of the simulation period (1030 years) as a result of the probability distributions of K_d values assigned to Tc-99 and I-129 (the C-14 K_d value was zero for all probabilistic simulations). For Tc-99, only the earliest 8 percent of radionuclide peak doses occur prior to 1030 years and the other 92 percent of peaks occur at the end of the simulation period. For I-129, only seven out of 3000 peaks (0.23 percent) occur prior to 1030 years. For Tc-99 and I-129, compliance period peak doses that occur at the end of the simulation period are cases in which higher long-term radionuclide peaks will occur well after 1000 years in the longer simulations.

Table 5.3 provides peak radionuclide dose statistics for the compliance period uncertainty analysis. For I-129, the average peak dose is larger than the 95th percentile because there are is a very large proportion of zero peak values for I-129 in the compliance period uncertainty analysis. The compliance period distributions of peak total dose for each of the ten repetitions of 300 simulations are shown in Fig. 5.13. The median (average median value of the 10 repetitions) peak total dose (all pathways) is 1.0 mrem/year and the 95th percentile value of peak dose (average of the 10 repetitions) is approximately 2.5 mrem/year. Extreme values (> 25 mrem/year) of peak total dose are associated with rare (< 1 percent) large I-129 contributions at the end of the simulation period. The extreme high end (> 25 mrem/year) of the distribution of compliance period peak dose and the factors that contribute to extreme dose peaks are considered in Appendix G, Sect. G.6.3.3.5.

Table 5.3. Compliance period peak radionuclide dose statistics

Radionuclide	Average peak dose (mrem/year)	95th percentile peak dose (mrem/year)
C-14	1.03	1.96
I-129	0.48	0.26
Tc-99	0.40	1.34
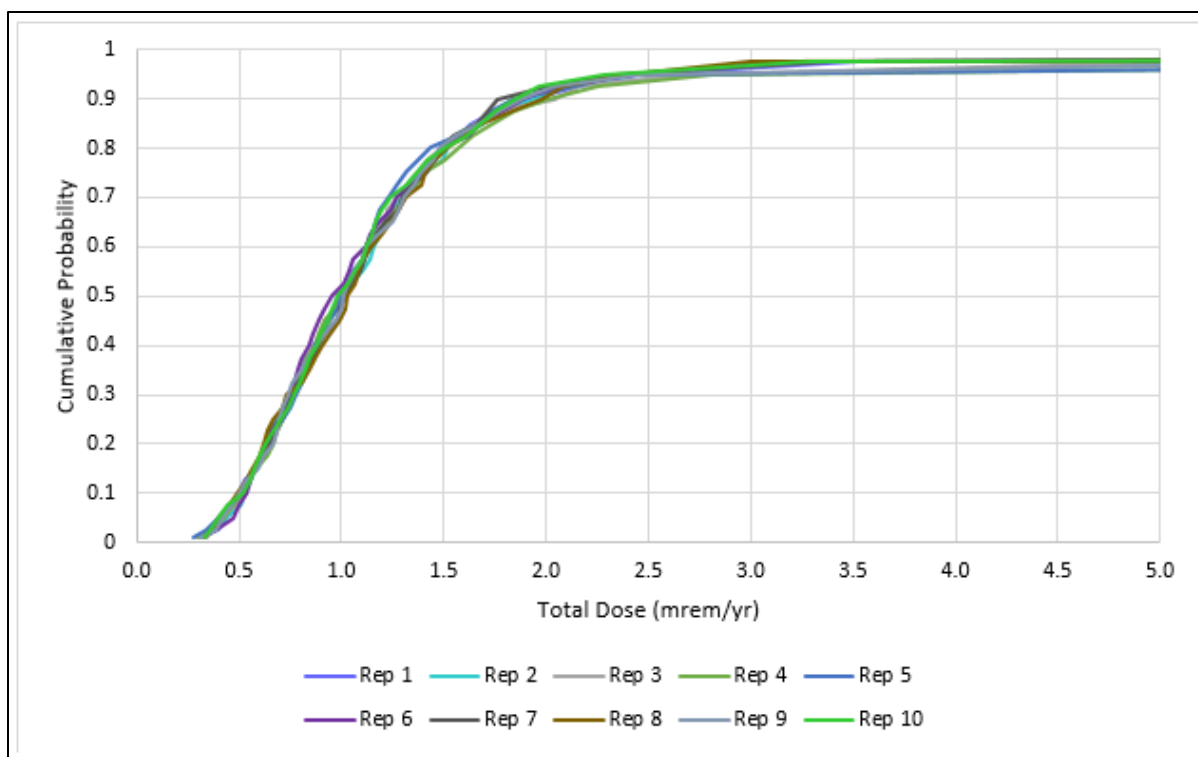
Fig. 5.13. Cumulative distribution function curves, peak all-pathways dose over 10,000 years

Regression analysis of the compliance period probabilistic peak dose output suggests that among the 33 input parameters for which probability distributions were assigned, the most influential variables fall into four categories: (1) contaminated zone parameters, (2) unsaturated zone parameters, (3) saturated zone parameters, and (4) human exposure parameters. Table G.26 of Appendix G provides a complete list of the probabilistic input parameters and the standardized rank regression coefficients calculated for each repetition of 300 simulations. For the entire range of compliance period peak doses, the five most influential parameters are:

- Runoff coefficient (cover infiltration rate)

- Release duration (affects release rate)

- Hydraulic conductivity of the saturated zone (saturated zone mixing)

- Mean residence time in the surface water body (C-14 fish ingestion dose)

- Depth of aquifer contributing to well (exposure factor, affects well water concentrations).

These results are consistent with results from the single parameter sensitivity analysis presented in Sect. 5.3, which show that total dose and timing of peaks are sensitive to changes in these parameters. Appendix G, Sect. G.6.3.3.4 provides more detailed discussion of the results of the regression analysis for the compliance period. Figure 5.14 is a summary graphic for the compliance period probabilistic results. Additional interpretation of the results of the uncertainty analysis is included in Sect. 7.4.

273

PA identifies key parameters and pathways to demonstrate dose compliance

Contaminated Zone (CZ)
- Runoff coefficient
- Release duration of I-129
- Effective porosity of CZ
- Initial releasable fraction of I-129
- Initial release time of C-14
- Longitudinal dispersivity in CZ

Unsaturated Zone (UZ)
- K_d of I-129 in UZ1
- K_d of Tc-99 in UZ1
- Thickness of UZ5

Saturated Zone (SZ)
- Hydraulic conductivity of SZ
- Mean residence time in surface water
- K_d of Tc-99 in SZ
- Effective porosity of SZ
- K_d of I-129 in SZ

Human Exposure
- Depth of aquifer contributing to well

Median and 95th Percentile Dose (mrem/yr) vs Time (yr)
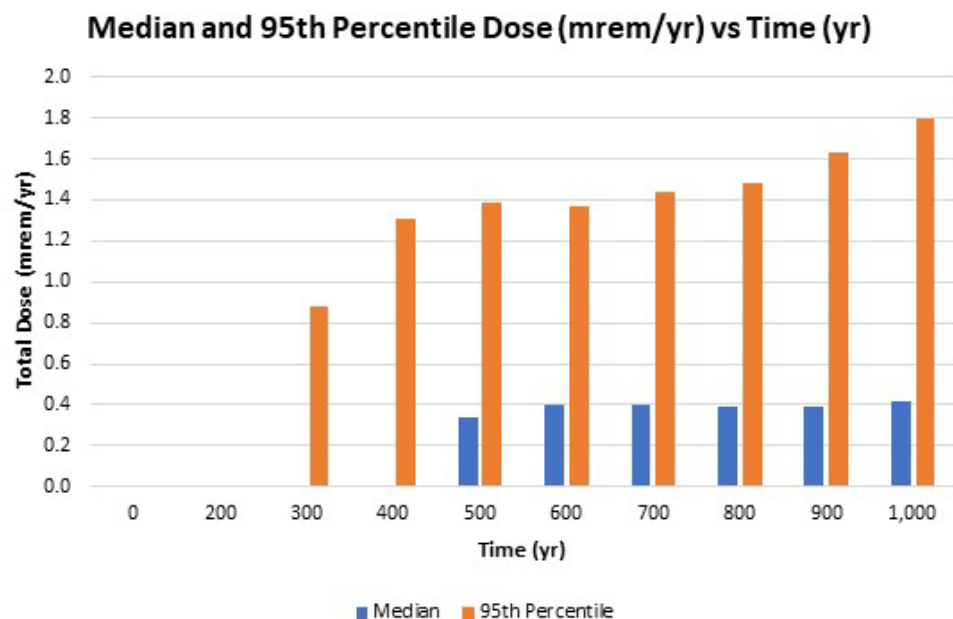
Primary Exposure Pathways
- Water ingestion
- Fish ingestion
- Meat ingestion (waterborne)

Note: Underlined parameters are the top five factors controlling peak total compliance period dose.

Fig. 5.14. Summary of influential variables, primary exposure pathways, and total dose at select reporting times for the 1000-year compliance period

274

5.4.2 Probabilistic Results – 10,000-year Simulation Period

This section presents the results of the 10,000-year simulation period probabilistic uncertainty analysis with a focus on results beyond the compliance period. The variation of median, mean, and 95th percentile dose over time for each of the 10 repetitions of 300 simulations is shown on Fig. 5.15. The deterministic base case model all-pathways dose curve is also shown on Fig. 5.15 for comparison to the probabilistic results. Results for the period prior to 1000 years were described in Sect. 5.4.1. The remainder of the simulated period can be divided into an early portion between 1000 and approximately 6000 years, and a later portion extending to 10,000 years. The early portion of the results are dominated by the fission products Tc-99 and I-129 dose contributions, whereas the later (> 6000 years) results reflect the potential impacts of the actinides included in the 10,000-year analysis (Pu-239, U-234, U-235, and U-238).
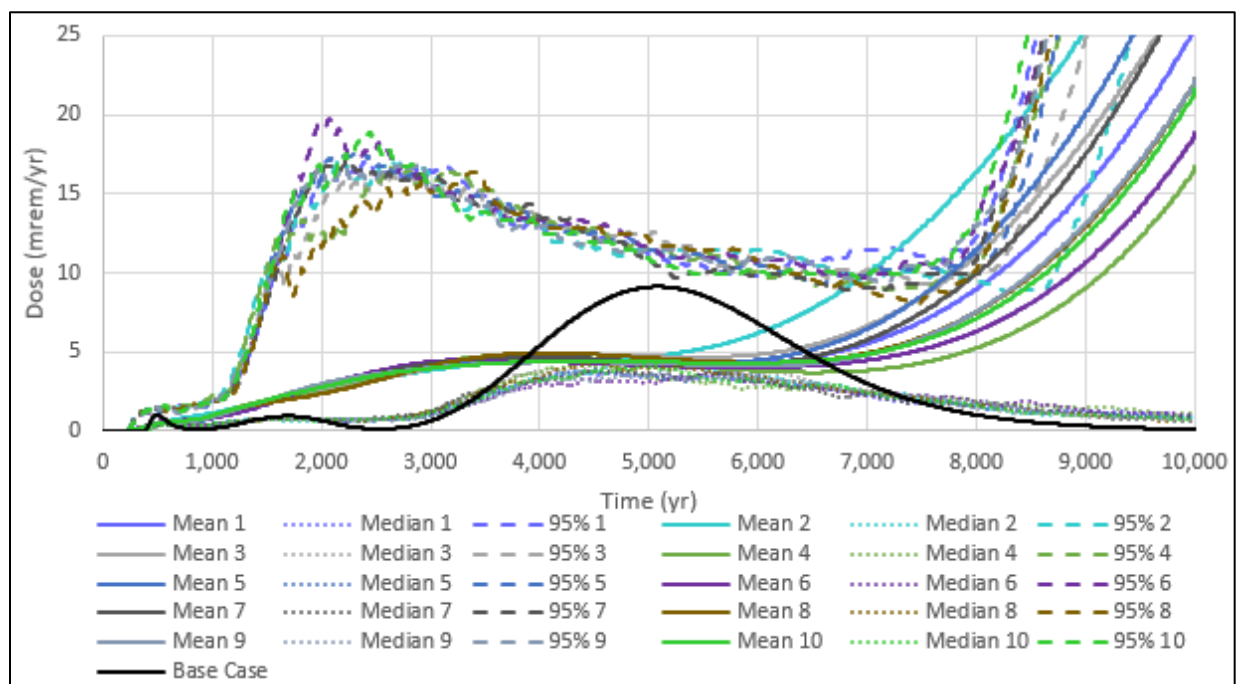
Fig. 5.15. Probabilistic total dose summary for 10 sets of 300 RESRAD-OFFSITE 10,000-year simulations, all pathways, all calculation points

The changing distribution of total dose over time reflects the varying contributions by the fission products and the actinides. The mean total dose increases gradually between 1000 years and approximately 4000 years and then remains nearly steady at just under 5 mrem/year (solid curves on Fig. 5.15). Then the mean total dose increases rapidly beginning at about 6500 years, reaching values that exceed 25 mrem/year by 10,000 years for 5 of the 10 repetitions of 300 simulations. The median simulated total dose approaches the mean total dose around 4500 years and remains below 5 mrem/year throughout the simulation period (dotted curves on Fig. 5.15). The 95th percentile of total dose increases quickly between 1000 and 2000 years to values around 15 mrem/year (fission product dose contributions) and then decreases more gradually through 8000 years. At 8000 years there is a second sharp increase in the 95th percentiles as actinide dose contributions begin to rise and simulated total doses > 25 mrem/year become more frequent. Significant dose contributions from the actinides can occur much earlier than in the deterministic base case, primarily because of lower actinide K_d values, shorter release durations, and greater cover infiltration rates. The divergence of the mean probabilistic dose from the median value (which decreases after 5000 years) reflects the strong negative skew that develops in the distribution of total dose after 5000 years, due to a large proportion of very small total doses and a small proportion of very high doses. Additional discussion

of the factors associated with the occurrence of peak total doses greater than 25 mrem/year for the 10,000-year uncertainty analysis, and the potential for these actinide peaks to be over-estimated by the RESRAD-OFFSITE model is included in Appendix G, Sect. G.6.3.4.

The largest radionuclide dose contributions for Tc-99 occur between 1000 and 2000 years post-closure, whereas for I-129 the largest doses occur between 2000 and 4000 years (refer to Appendix G, Sect. G.6.3.4.2). These fission product contributions combine to produce the period between roughly 2000 and 3000 years during which the 95th percentile of total dose exceeds 15 mrem/year (Fig. 5.15). Peak radionuclide dose statistics for I-129 and Tc-99 are provided in Table 5.4. The average values of peak dose for Tc-99 and I-129 are consistent with the deterministic base case peak values; the median peak probabilistic dose values for Tc-99 and I-129 are essentially the same as the average peak values (refer to Appendix G, Figs. G.56 and G.57). Approximately 90 percent of the peak I-129 doses occur between 2000 and 9700 years, with a mean I-129 peak time of approximately 5200 years. For Tc-99, 90 percent of the 3000 simulated peak doses occur between 900 and 2700 years, with a mean Tc-99 peak time of 1700 years. Approximately 4 percent of the simulated I-129 peak doses exceed 25 mrem/year, whereas Tc-99 peak doses are all less than 2.5 mrem/year. Peak doses greater than 25 mrem/year associated with I-129 are discussed in Appendix G, Sect. G.6.3.4.5.

Table 5.4. Peak radionuclide dose statistics

Radionuclide	Average peak dose (mrem/year)	95th percentile peak dose (mrem/year)
I-129	10.6	23.1
Tc-99	0.94	1.62

Over the 10,000-year simulation period, the median peak total dose (average of the 10 repetitions) is approximately 10 mrem/year. Seventy percent of the peak total doses were distributed evenly between about 2000 and 8000 years, and about 15 percent of the peaks occurred at the end of the simulation period. A total of 379 out of 3000 realizations (approximately 13 percent) produced a peak total dose above 25 mrem/year. Seventy-two percent of the peak total doses that exceeded 25 mrem/year occurred at the end of the simulation period (approximately 10,000 years) suggesting that these peaks were associated with combined contributions of Pu-239 and uranium nuclides. The remaining 28 percent of peak doses greater than 25 mrem/year occur prior to 3800 years. These earlier extreme peaks correspond to dose contributions from (primarily) I-129 and Tc-99. The earlier subset of peak doses (I-129 peaks greater than 25 mrem/year) are generally associated with smaller than average sampled I-129 K_d values (< 3.5 cm^3/g) and with smaller than average sampled release duration. The earlier peaks greater than 25 mrem/year also tend to be associated with larger than average modeled cover infiltration (> 0.88 in./year) and smaller than average values of the saturated zone Darcy velocity (calculated as hydraulic conductivity multiplied by hydraulic gradient, refer to Appendix G, Fig. G.60). This correlation suggests that saturated zone mixing is particularly important in determining the likelihood of peak I-129 dose exceeding 25 mrem/year. This dependence of higher I-129 dose on saturated zone mixing is consistent with the high dose conversion factor for I-129, which reflects potentially large exposures associated with small environmental concentrations. The extreme I-129 dose peaks are probably over-estimated and not likely to be realized given the combination of unrealistically large I-129 source inventory (Appendix B) and the RESRAD-OFFSITE over-estimate of peak I-129 flux to the water table relative to the more detailed STOMP model of release from the vadose zone (refer to Sect. 3.3.5).

These extreme peak total dose values should be viewed with caution given the inherent limitations and uncertainty of the RESRAD-OFFSITE release model. These limitations include the modeled cover

infiltration remaining constant rather than increasing over time, the lack of solubility limits that may lead to overestimated leachate concentrations for uranium species, and the relatively rapid release for radionuclides having $K_d > 1$ cm^3/g produced by the constant cover infiltration rate applied to the instantaneous equilibrium desorption release model. Comparison of STOMP model simulations of U-234 release to the RESRAD-OFFSITE release predictions shows that the predicted peak RESRAD-OFFSITE U-234 flux is over twice as large as the peak STOMP U-234 flux to the water table beneath the EMDF. This difference in U-234 release model predictions suggests that the RESRAD-OFFSITE peak well water concentrations are too uncertain (probably over-estimated) to draw conclusions about the very-long-term performance of the EMDF with respect to less mobile radionuclides ($K_d > 1.0$ cm^3/g) including nuclides of uranium and possibly also I-129.

This page intentionally left blank.

6.   INADVERTENT INTRUDER ANALYSIS

6.1   INADVERTENT HUMAN INTRUSION SCENARIOS

Selection of IHI scenarios was guided by consideration of EMDF site characteristics and facility design, as well as review of IHI analyses performed for other historical and proposed LLW disposal facilities on the ORR. Additional details on this IHI analysis and the other PAs that were reviewed are provided in Appendix I. The IHI analysis for the EMDF considers an acute discovery scenario that involves attempted excavation into the final cover for construction of a residence, and acute drilling and chronic post-drilling (agricultural) scenarios that involve direct contact with the waste. A summary of the three IHI scenarios analyzed for the EMDF is provided in Table 6.1.

Table 6.1. Summary of IHI scenarios analyzed for the EMDF

Scenario type/name	DOE O 435.1 performance measure	Exposure scenario description
Acute exposure –discovery (basement excavation)	500 mrem	Intruder initiates excavation into EMDF cover, but stops digging before exposing waste. Exposure to external radiation.
Acute exposure – drilling (water well)	500 mrem	Intruder drills irrigation well through waste and is exposed to waste in exhumed drill cuttings. Exposure to external radiation, inhalation and incidental ingestion of contaminated soil.
Chronic exposure – post-drilling (subsistence garden)	100 mrem/year	Intruder uses contaminated drill cuttings to amend soil in a vegetable garden. Exposure to external radiation, inhalation, and ingestion of contaminated food and soil.

DOE O = U.S. Department of Energy Order   IHI = inadvertent human intrusion
EMDF = Environmental Management Disposal Facility

The IHI analysis assumes that intrusion is an accidental occurrence resulting from a temporary loss of institutional control. The occurrence of accidental intrusion also presumes a loss of societal memory of the ORR and radioactive waste disposal facilities in the area, despite existing long-term stewardship commitments of the DOE and the likelihood of legal controls such as property record restrictions and notices. For each of the IHI scenarios, active institutional controls are assumed to preclude intrusion for the first 100 years following closure of the disposal facility.

Several important assumptions for the intruder analyses are based on the specifics of the EMDF Preliminary Design that are described in Sects. 1.3, 2.2, and Appendix C. The estimated EMDF radionuclide inventory (Appendix B) was used with the RESRAD-OFFSITE code to model doses resulting from these unlikely future intrusion scenarios. The results are used to establish compliance with DOE O 435.1 dose performance measures for IHI (DOE 2001b). The model results can also be used to evaluate the protectiveness of proposed concentration limits for radionuclides, prior to the beginning of EMDF operations.

6.2   INVENTORY SCREENING FOR IHI

The radionuclide inventory screening for the IHI analysis differs from the screening for the radionuclide release scenarios in that the sole screening criterion is a 5-year minimum half-life for radionuclides that are not radioactive progeny. Refer to Fig. 2.44 for an overview of the radionuclide screening process. Additional description of the screening and estimated source concentrations is included in Appendix I, Sect. I.2.2 and Table I.1.

6.3   ACUTE IHI SCENARIOS AND EXPOSURE PATHWAYS

Two acute exposure scenarios were evaluated. The acute discovery scenario assumes that an intruder attempts to excavate a basement for a home on the disposal site, but stops prior to excavating into the waste and moves elsewhere because of the unusual nature of the engineered material layers encountered. The acute drilling scenario assumes that an irrigation well is drilled through the waste, bringing contaminated material to the surface as drill cuttings and causing an acute exposure to the well drillers.

6.3.1   Acute Discovery Scenario (Cover Excavation)

The acute discovery analysis assumes that the intruder begins excavating but stops digging upon reaching the geotextile and HDPE geomembrane layer overlying the amended clay barrier (Fig. 6.1). The discovery and decision to cease digging occurs after excavating through 8 ft of engineered cover materials including the vegetated surface layer, filter layer, biointrusion layer, and lateral drainage layer. It is assumed that 3 ft of undisturbed barrier material remains between the bottom of the excavation and the underlying waste.

For this scenario, only the external radiation exposure pathway (for photon emissions) is considered for the hypothetical intruder. The inhalation and ingestion pathways are not considered because it is assumed that the clay barrier materials in the cover remain undisturbed and saturated and excavation does not penetrate into the waste. Shielding by the clay barrier eliminates alpha and beta-particle exposure.

6.3.2   Acute Drilling Scenario (Irrigation Well)

For the acute drilling scenario (Fig. 6.2), intruders are assumed to drill a well for irrigation on the EMDF. This scenario is highly unlikely given that drilling in more accessible areas at lower elevations would be much more cost effective due to the shallower depth to groundwater. This exposure scenario also assumes that the drilling crew is not deterred by encountering the large rocks in the biointrusion layer, structural steel, concrete, or rebar in the waste zone, or by the exhumation of any of these or other unusual materials in the drill cuttings.

The following exposure pathways were considered for the acute drilling scenario:

- External exposure to radiation from the unshielded drill cuttings that contain waste

- Inhalation of radionuclides suspended in air from the uncovered cuttings containing waste

- Incidental ingestion of soil containing radionuclides from the uncovered cuttings containing waste.

Thickness		
feet	meters	
4	1.22	Vegetated erosion control layer
1	0.30	Sand/Gravel granular filter/drainage layer
2	0.61	Large rock/rip-rap biointrusion layer
1	0.30	Gravel/sand lateral drainage layer
0.005	0.002	HDPE -Flexible Membrane Liner (not to scale)
1	0.30	Amended Compacted Clay Barrier
1	0.30	Compacted Clay Barrier
1	0.30	Contour Gravel
Zero to > 110 ft (58 ft average)		EMDF Waste Zone (contaminated soil and demolition debris)

Maximum Depth of Excavation (8 ft)

Fig. 6.1. EMDF cover system schematic and acute discovery IHI scenario
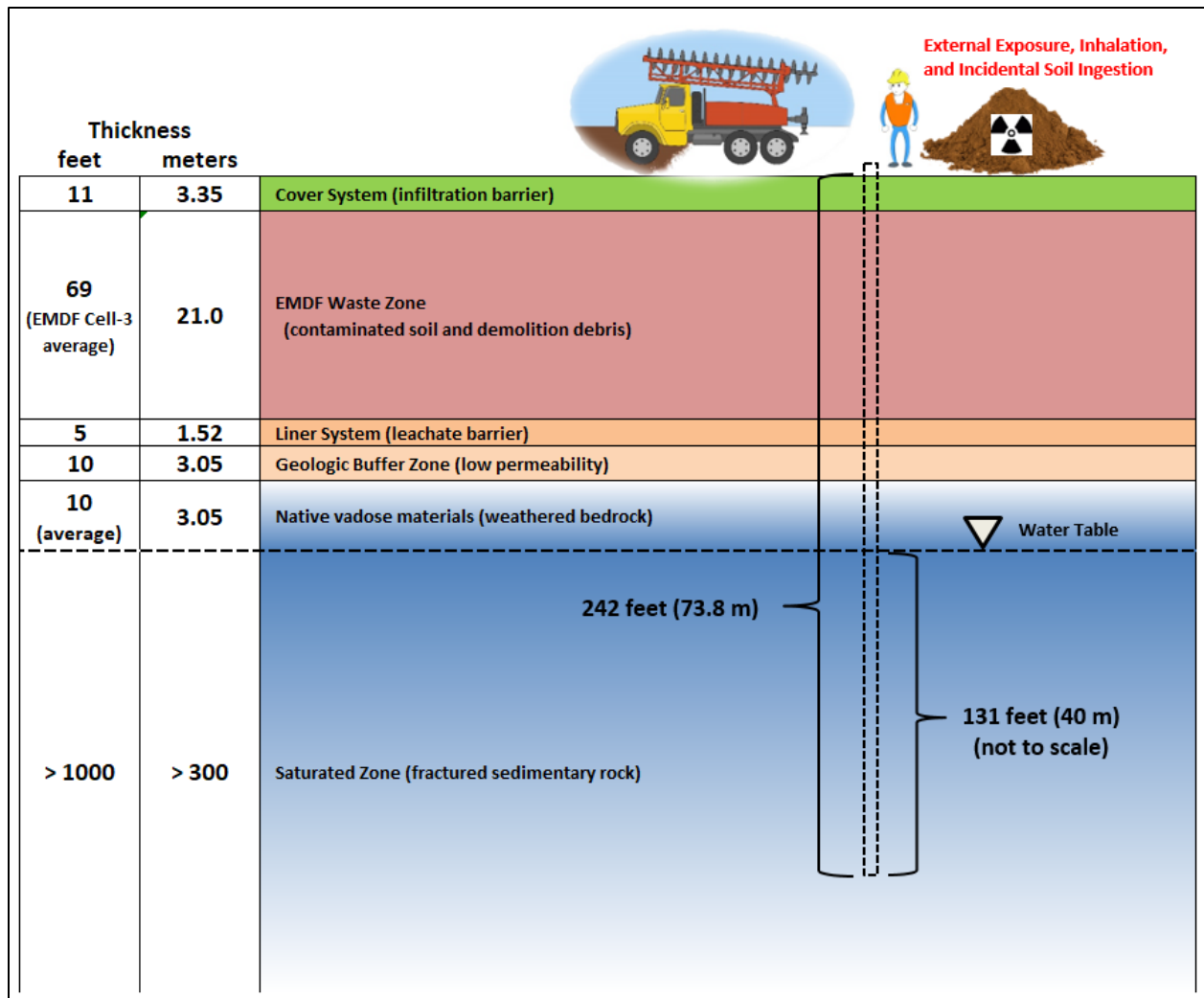
Fig. 6.2. EMDF schematic profile and acute drilling IHI scenario

6.4 CHRONIC IHI SCENARIO AND EXPOSURE PATHWAYS

The chronic IHI scenario selected for the EMDF is a post-drilling exposure to contaminated garden soil and contaminated produce grown in that soil. Intruders are assumed to drill a residential well on the EMDF and to mix the drill cuttings into the garden soil to grow food for human consumption and feed for livestock (Fig. 6.3). This scenario is highly unlikely in terms of the location selected for the well (as for the acute drilling scenario) and in the required assumption that the contaminated cuttings are indistinguishable from native soil and used to amend the garden soil. It is more likely that drill cuttings would be used to build up the area around the well to direct runoff away from the borehole.

Thickness			
feet	meters		
11	3.35	Cover System (infiltration barrier)	
69 (EMDF Cell-3 average)	21.0	EMDF Waste Zone (contaminated soil and demolition debris)	
5	1.52	Liner System (leachate barrier)	
10	3.05	Geologic Buffer Zone (low permeability)	
10 (average)	3.05	Native vadose materials (weathered bedrock)	Water Table
> 1000	> 300	Saturated Zone (fractured sedimentary rock)	

Contaminated Drill Cuttings

242 feet (73.8 m)

131 feet (40 m) (not to scale)

Agricultural Area = 2200 m² = 0.54 acre

External exposure, inhalation, and incidental soil ingestion while working in garden

Consumption of contaminated produce, milk, and meat

Fig. 6.3. EMDF schematic and chronic post-drilling IHI scenario

283

The chronic post-drilling scenario only considers exposures after drilling and construction of the residential well. The following exposure pathways were considered:

- Ingestion of vegetables grown in contaminated garden soil

- Ingestion of contaminated garden soil

- External exposure while working in the garden

- Inhalation exposure while working in the garden.

To add conservatism, other exposure pathways that are less likely to occur were also simulated, including:

- Ingestion of contaminated milk from animals eating feed from the garden

- Ingestion of contaminated meat from animals eating feed from the garden.

Groundwater transport pathways are not included in the IHI scenarios and are not modeled, consistent with *Disposal Authorization Statement and Tank Closure Documentation* (DOE 2017a) guidance. Radionuclide release associated with groundwater and surface water pathways is considered in the all pathways dose analysis of this PA (Sect. 4.5) and is evaluated relative to the 25 mrem/year performance objective for public protection. Similarly, the water resource protection analysis (Sect. 4.7) evaluates potential impacts to groundwater and surface water relative to applicable water quality standards.

6.5   IHI SCENARIO MODELING

The RESRAD-OFFSITE Version 3.2 model (Gnanapragasam and Yu 2015) was used for estimating doses to a hypothetical inadvertent intruder under each of the three exposure scenarios. For the modeling of IHI dose, it is assumed that the waste disposal in the EMDF is completed at time zero, the site is under active institutional control for the next 100 years, and that inadvertent intrusion can occur at any time after loss of active control of the site. RESRAD-OFFSITE simulations were completed to 10,000 years to provide information on long-term increases in predicted dose that occur following the 1000-year compliance period.

In general, simulation of IHI exposure using the RESRAD-OFFSITE model involves assumptions required for the calculation of average radionuclide concentrations in exhumed drill cuttings or garden soil and selection of the relevant exposure pathways for each exposure scenario. For all of the IHI scenario modeling, the RESRAD-OFFSITE release rate (leach rate for the first-order release model option) was set to zero to effectively eliminate leaching of contamination from the waste and to provide a conservative bias toward higher estimated dose. Similarly, precipitation input was set to the near-zero value of 1E-06 m/year and irrigation of the garden area was assumed to be zero for the chronic well drilling scenario. Loss of contaminated materials (cuttings or garden soil) due to erosion was not included in the analysis.

RESRAD-OFFSITE model setup and key parameter assumptions for each scenario are summarized in the following sections and described in detail in Appendix I, Sect. I.4. Additional detail on model parameterization and supporting calculations are provided in the QA documentation for the IHI analyses (UCOR 2020b).

6.5.1   Acute Discovery Scenario

The acute discovery scenario assumes that an intruder attempts to excavate a basement for a home on the disposal site. The key assumption is that the intruder stops excavation activities upon reaching the geotextile

cushion and HDPE geomembrane below the drainage layer, leaving 3 ft of earthen materials between the bottom of the excavation and the underlying waste.

For the EMDF analysis, only the dose resulting from external exposure to radiation that penetrates the residual materials (lower 3 ft of 11-ft EMDF total cover thickness) overlying the waste is modeled (Fig. 6.1). Formulation of the expression for calculating dose due to external radiation is given in the RESRAD-OFFSITE User's Manual (Yu et al. 2007, pages 6-1 to 6-2). Mathematical expressions for the conceptual model of the zone of primary contamination including a clean cover layer on top of the waste are described in detail in the user's manual for RESRAD-OFFSITE Version 2 (Yu et al. 2007, pages 2-1 to 2-3). The materials of the EMDF cover layer are assumed to remain uncontaminated because processes that could lead to contamination of the cover material such as bioturbation by burrowing animals are inhibited by the overall thickness of the cover design and robust biointrusion barrier.

Important assumptions and calculated parameter values for the EMDF acute discovery scenario modeling include the thickness of clean cover material overlying the waste (3 ft) and the assumption that excavation ceases after encountering the HDPE membrane at the interface between the lateral drainage layer and the amended clay barrier. Excavation for the acute discovery scenario is assumed to take place over 10 8-hour days for a total of 80 hours. To provide additional bias toward higher dose estimates, it is also assumed that the maximum depth of excavation is completed over the full basement area immediately, after which exposure to external radiation occurs over the assumed duration of excavation.

6.5.2   Acute Well Drilling Scenario

The acute well drilling scenario assumes that an intruder drills an irrigation well directly through a disposal unit (Fig. 6.2). The acute well drilling scenario only considers exposures during the short period of time for drilling and construction of the well, during which the hypothetical intruder could be exposed to unshielded cuttings for an extended period. Exposure to external radiation, inhalation of contaminated particulates, and (incidental) soil ingestion by a member of the drill crew is assumed to occur during the period of drilling and distribution of the drill cuttings (both clean and contaminated).

The RESRAD-OFFSITE model simulation of external exposure, inhalation, and (incidental) soil ingestion requires specifying the thickness and radionuclide concentrations of the drill cuttings to which a driller would be exposed as well as the duration of (acute) exposure. Mathematical expressions for the conceptual model of the zone of primary contamination are described in detail in the User's Manual for RESRAD-OFFSITE, Version 2 (Yu et al. 2007, pages 2-1 to 2-3). The thickness of the clean cover is assumed to be zero. Assumed values for atmospheric particulate loading and soil ingestion during drilling are also required. Formulation of the expressions for calculating dose due to external radiation and inhalation of contaminated dust are also given in the RESRAD-OFFSITE User's Manual (Yu et al. 2007, pages 6-1 to 6-3). Similarly, formulation of the expressions for calculating dose due to incidental ingestion of contaminated soil is given on pages 6-4 and 6-5 of the User's Manual.

Important assumptions and calculated parameter values for the EMDF acute well drilling scenario include the waste thickness at the well location (68.7 ft), and the average waste thickness in EMDF disposal cell #3 based on the EMDF Preliminary Design (UCOR 2020b). The average EMDF waste thickness is approximately 57.5 ft, and the maximum thickness is approximately 113 ft. The assumed thickness of waste at the well location is used to adjust the as-disposed waste concentrations to account for co-mingling of clean drill cuttings with waste as materials are brought to the surface. The borehole is assumed to be completed at a depth equivalent to 131 ft below the estimated water table elevation, or 242 ft below the surface of the disposal facility. The calculated dilution factor applied to the post-operational activity concentrations is thus equal to 68.7 ft/242 ft, or 0.284.

The borehole diameter is assumed to be 18 in., which is representative of a well designed for irrigation in East Tennessee. Use of the 18-in. diameter for the acute drilling scenario provided a degree of pessimistic bias to offset some of the uncertainty associated with simplification of the complex external exposure to drill cuttings applied in the acute scenario. The total combined volume of waste and clean drill cuttings based on the assumed borehole length and diameter is 427 ft^3. The mixed clean cuttings and exhumed waste from the borehole are assumed to be distributed over an area centered on the bore hole of 2150 sq ft, resulting in an average thickness of 0.20 ft (2.4 in.). This value is input as the thickness of the primary contamination for the RESRAD-OFFSITE dose analysis. Sensitivity of the modeled dose to assumptions that affect the calculated average thickness of cuttings is addressed in Sect. 6.6.2.

For the acute drilling scenario, the duration of exposure is assumed to be 30 hours, the equivalent of three 10-hour working days. A more realistic assumption for the time required to drill an approximately 250-ft-deep well using typical drilling equipment would be less than 30 hours. The calculated occupancy factor for the RESRAD-OFFSITE model (outdoor annual time fraction on primary contamination) is $0.0034 = (30 \text{ hours/year})/ [(365.25 \text{ days/year}) \times (24 \text{ hours/day})]$.

For both the acute drilling and chronic post-drilling scenarios, the incidental soil ingestion rate is assumed to be 100 mg/day, consistent with the RESRAD-OFFSITE default value and the EPA recommended value for outdoor workers. The average mass loading of airborne particulates for estimating inhalation exposure for both the acute drilling and chronic post-drilling scenarios was assumed to be 0.001 g/m^3, a value representative of construction activities (Maheras et al. 1997). The annual inhalation rate for both scenarios was set at the RESRAD-OFFSITE default value of 8400 m^3/year.

6.5.3   Chronic Post-drilling Scenario

The chronic post-drilling scenario assumes that a hypothetical intruder drills a residential well directly through the disposal unit and then mixes contaminated drill cuttings into the soil in a garden used to grow food for people and livestock (Fig. 6.3). The chronic IHI scenario only considers exposure that follows drilling and construction of the well. Exposure to contaminated soil (external radiation, inhalation and soil ingestion) occurs during the portion of time that the intruder works in the garden.

The RESRAD-OFFSITE model simulation of exposure to contaminated soil and ingestion of contaminated food requires specifying the thickness and radionuclide concentrations of the garden soil, as well as the duration of exposure. Mathematical expressions for the conceptual model of the zone of primary contamination are described in detail in the User's Manual for RESRAD-OFFSITE Version 2 (Yu et al. 2007, pages 2-1 to 2-3). The thickness of the clean cover is assumed to be zero. Assumed values for atmospheric particulate loading and soil ingestion during gardening are also required. Formulation of the expressions for calculating dose due to external radiation and inhalation of contaminated dust are also given in the RESRAD-OFFSITE User's Manual (Yu et al. 2007, pages 6-1 to 6-3). Similarly, formulation of the expressions for calculating dose due to of contaminated soil and food is given on pages 6-4 and 6-5 of the User's Manual.

Key assumptions and calculated parameter values for the chronic well drilling scenario include waste thickness at the well location (68.7 ft), borehole depth (242 ft), and incidental soil ingestion rate (100 mg/day), which are identical to those made for the acute drilling scenario. Inhalation parameter values are also identical to the acute drilling scenario. Values for agricultural and animal product (beef, poultry, eggs, milk) transfer factors are set to values published by PNNL (2003), which are identical to the values used in the base case model.

The borehole diameter is assumed to be 12 in., which is representative of a well designed for residential use in the region. The resulting volume of exhumed waste is 54 ft^3. The 12-in. residential water well

diameter is reasonable for the chronic IHI analysis given that the hilltop location assumed for the well construction is more appropriate for a residential supply well than an irrigation well with a larger diameter.

The total volume of contaminated drill cuttings is assumed to be completely and uniformly tilled into uncontaminated surface soil to a depth of 1 ft over an area of approximately one-half acre (2200 m^2). Average radionuclide concentrations in the amended garden soil are calculated by applying a dilution factor equal to the ratio of the volume of waste contained in drill cuttings to the total volume of uncontaminated garden soil: 54 ft^3 / (1 ft $\times$ 23,668 sq ft) = 0.00228 or approximately 0.2 percent. Calculate post-operational radionuclide concentrations (Sect. 4.2) are multiplied by the tilling dilution factor to give the input soil concentrations for the RESRAD-OFFSITE dose analysis. This approximation assumes that the volume of cuttings is negligible compared to the total soil volume, and neglects any difference in the average dry bulk densities of the waste and the garden soil. The implications of using this simplified calculation of the tilling dilution factor for the intruder dose analysis are addressed in Sect. 6.6 in the context of uncertainty and overall pessimistic bias in dose calculations.

The fraction of feed for livestock obtained from the contaminated garden is conservatively assumed to be 0.5 (50 percent). The fraction of milk consumed from the dairy cows raised on the contaminated area is assumed to be 0.5 (50 percent) and the fraction of meat (beef, poultry, eggs) from the contaminated area is assumed to be 0.25 (25 percent). The fractional duration of exposure for the external radiation, inhalation, and soil ingestion pathways is assumed to be 1/6, equivalent to 4 out of every 24 hours. This value is consistent with the (pessimistic) assumption that 50 percent of food consumed by the intruder is grown in the contaminated garden soil.

6.6   INTRUDER ANALYSIS RESULTS

6.6.1   Acute Discovery Scenario Results

Predicted dose as a function of time of intrusion for the acute discovery scenario is presented in Fig. 6.4. The total dose (i.e., dose from all simulated radionuclides summed) at 100 years post-closure is 1.3E-04 mrem. Total dose decreases to a minimum of 6.7E-05 mrem at approximately 540 years, and then gradually increases through 10,000 years as concentrations of radioactive progeny increase. Total dose at 10,000 years is 2.5E-04 mrem. The predicted dose is extremely sensitive to the assumed thickness of the uncontaminated material (clean cover) overlying the waste. Decreasing the assumed thickness from 3 ft to 1 ft increases the dose by three orders of magnitude (dashed curve in Fig. 6.4). This sensitivity case represents the assumption that a 10-ft-deep basement excavation is completed in the EMDF cover, which results in estimated dose that is three to four orders of magnitude smaller than the acute intrusion performance measure of 500 mrem.

Primary contributors to the acute discovery IHI dose prior to 1000 years post-closure include Th-232, and initially (at 100 years) Cs-137 and U-232 (Fig. 6.5). After 1000 years, other isotopes of uranium, particularly U-234 and progeny, become proportionally significant and eventually predominant dose contributors.
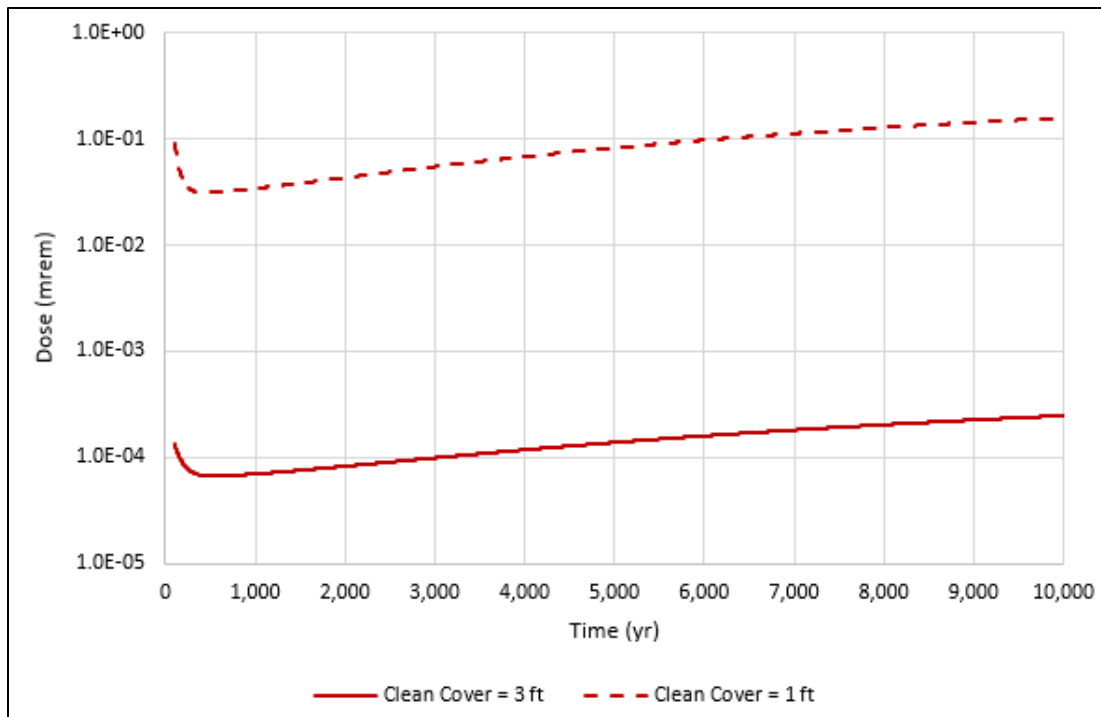
Note: Vertical axis is logarithmic for clarity.

Fig. 6.4. Acute discovery scenario total dose (all radionuclides summed)
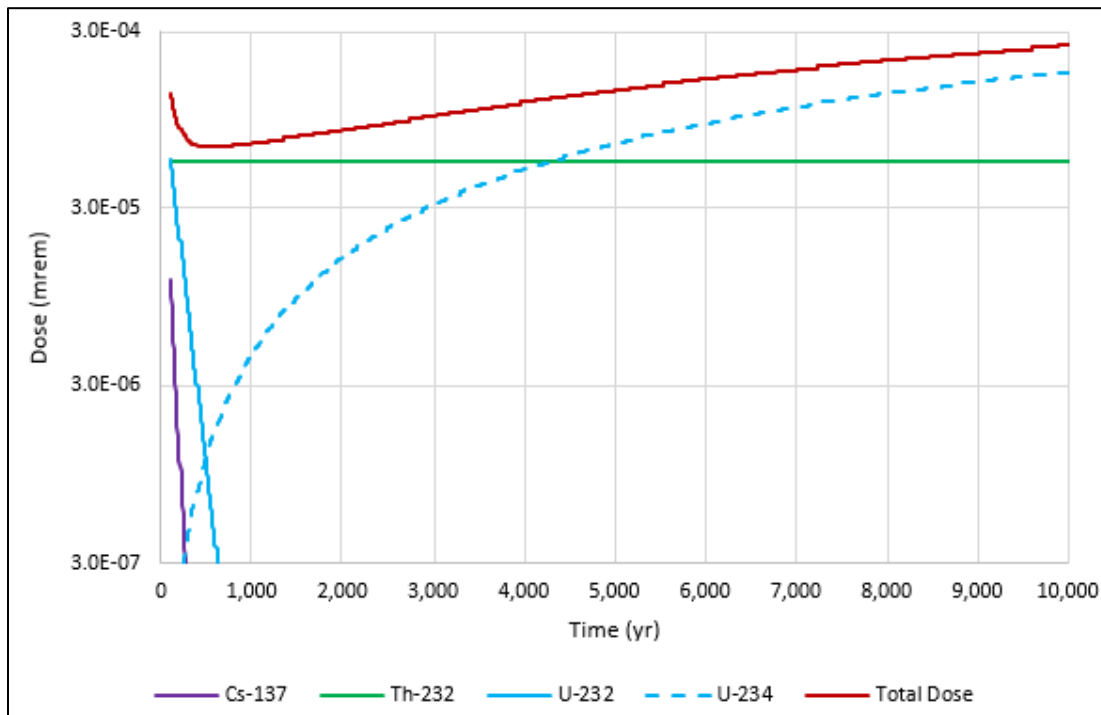
Note: Vertical axis is logarithmic for clarity.

Fig. 6.5. Acute discovery scenario dose contributions by radionuclide

288

6.6.2 Acute Well Drilling Scenario Results

Predicted dose as a function of time of intrusion for the acute drilling scenario is presented in Fig. 6.6. The total dose (all radionuclides and pathways summed) at 100 years post-closure is 0.38 mrem. Total dose decreases to a minimum of 0.17 mrem at approximately 600 years and then gradually increases through 10,000 years as concentrations of radioactive progeny increase. Total dose at 10,000 years is 0.42 mrem.
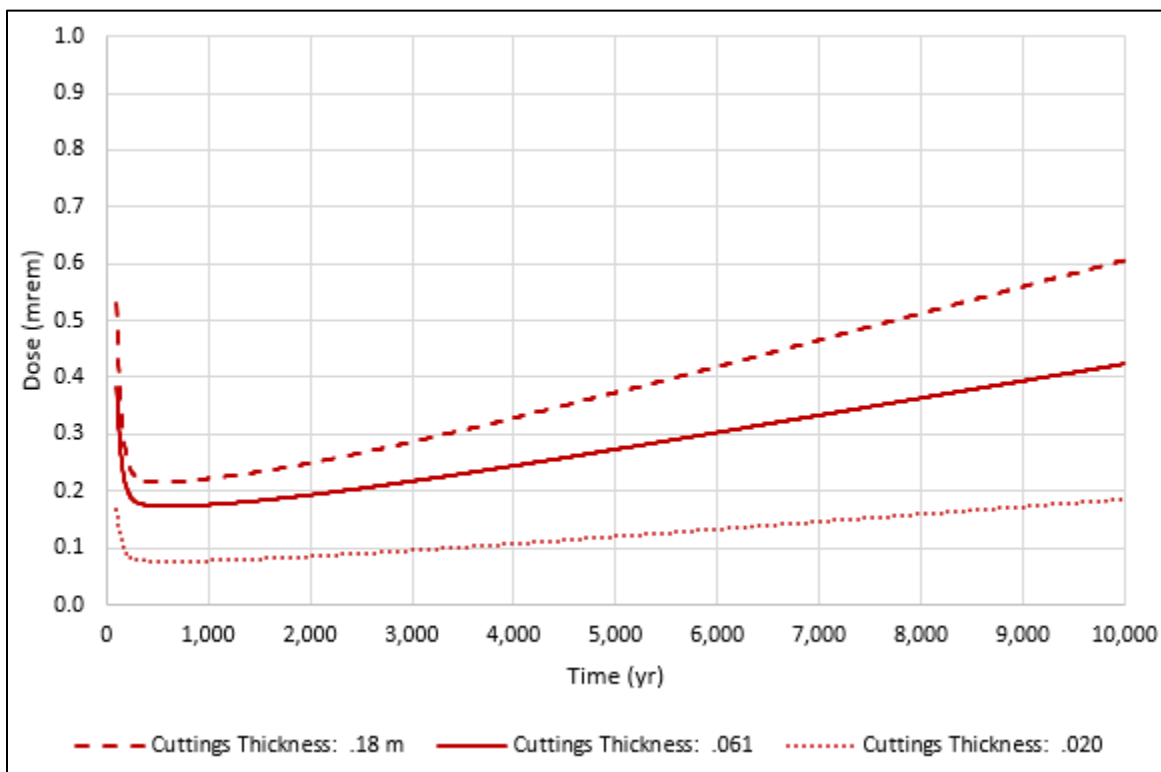
Fig. 6.6. Acute well drilling scenario total dose (all radionuclides and pathways summed)

The dotted and dashed curves shown on Fig. 6.6 represent model sensitivity to the calculated value for the thickness of mixed drill cuttings and indicate dose associated with the thickness increased by a factor of 3 (dashed) and decreased by a factor of 3 (dotted). For the increased thickness of cuttings (0.18 m), the acute dose remains less than 1 mrem between 100 and 10,000 years, a value much less than the acute intrusion performance measure of 500 mrem. Parameter values that affect the calculated average thickness of cuttings include borehole depth and diameter and the area over which cuttings are spread.

Figure 6.7 presents the dose contributions for each of the simulated exposure pathways for the acute drilling scenario: external (direct) radiation, inhalation, and incidental soil ingestion. The direct external dose (solid red curve) is the largest contributor to the total dose during the simulation period, whereas soil ingestion contributes least to the total acute drilling intruder dose.

Primary contributors to the acute drilling IHI dose prior to 1000-year post-closure include U-235, U-238, Th-232, and Cs-137 (Fig. 6.8). The increase in dose after 500 years is driven by U-234, U-235, and their progeny. Radionuclides of thorium and plutonium contribute proportionally significant, but much smaller doses through 10,000 years.
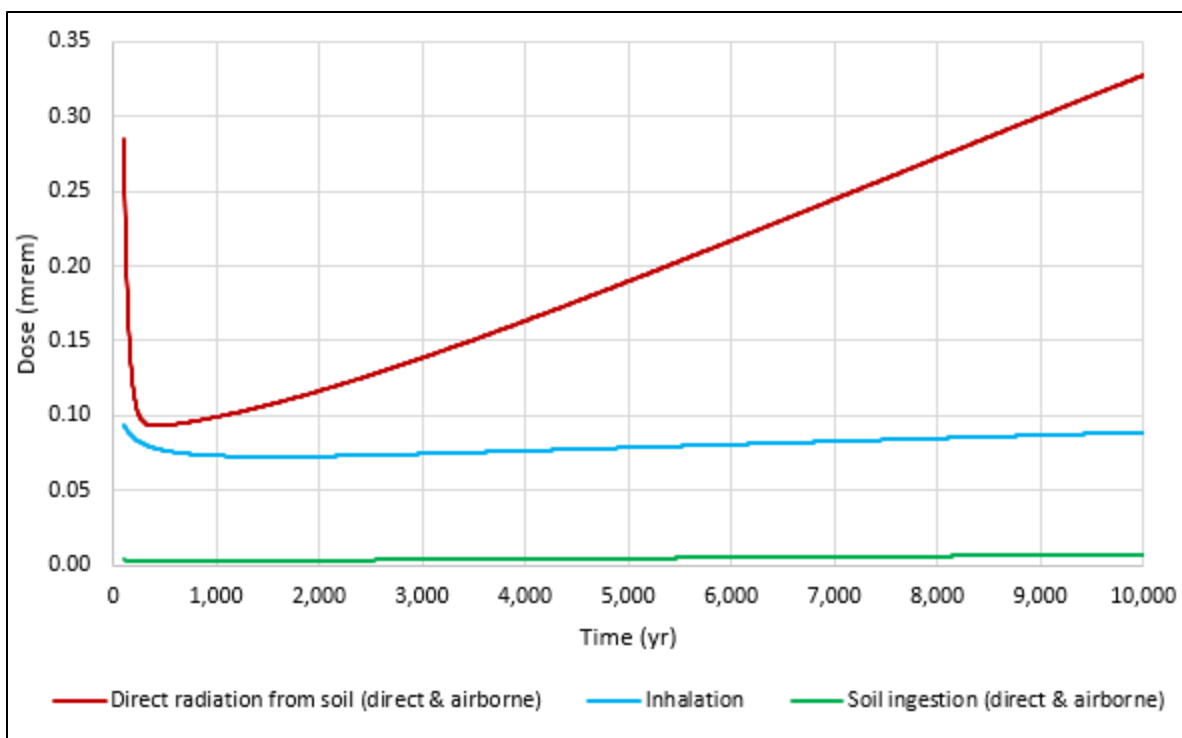
Fig. 6.7. Acute well drilling scenario radiological dose by exposure pathway for all radionuclides summed
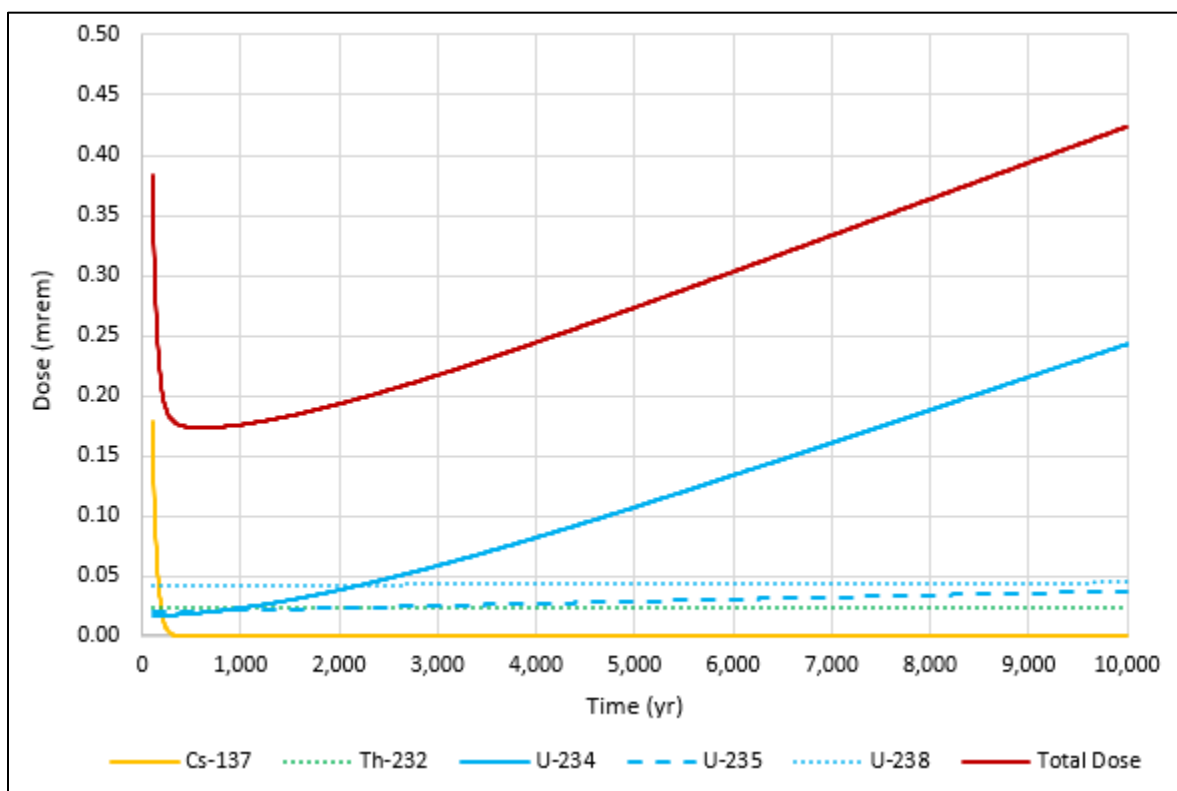
Fig. 6.8. Acute well drilling scenario dose contributions by radionuclide

290

6.6.3 Chronic Post-drilling Scenario Results

Predicted dose as a function of time of intrusion for the chronic drilling scenario is presented in Fig. 6.9. The total dose (all radionuclides and pathways summed) at 100 years post-closure is 3.56 mrem/year. Total dose decreases to a minimum of 2.95 mrem/year at approximately 340 years and gradually increases through 10,000 years as concentrations of radioactive progeny increase. Total dose at 10,000 years is 8.24 mrem/year. The maximum predicted dose is a factor of 10 lower than the chronic IHI performance measure of 100 mrem/year.

Figure 6.10 presents the dose contributions for each of the simulated exposure pathways for the chronic drilling scenario: direct radiation from garden soil, ingestion of plants, meat, and milk, inhalation, and incidental soil ingestion. The direct external and meat ingestion dose contributions comprise 90 percent or more of the total dose (dashed black curve). Plant ingestion, milk ingestion, and inhalation together comprise 2 to 7 percent. The contribution of soil ingestion (< 1 percent of the total dose) is negligible relative to the chronic IHI performance measure of 100 mrem/year.

Primary contributors to the chronic post-drilling IHI dose prior to 1000-year post-closure include U-234, U-238, Cs-137, and U-235 (Fig. 6.11). After 500 years total dose is driven by U-234, U-238, and their associated progeny.
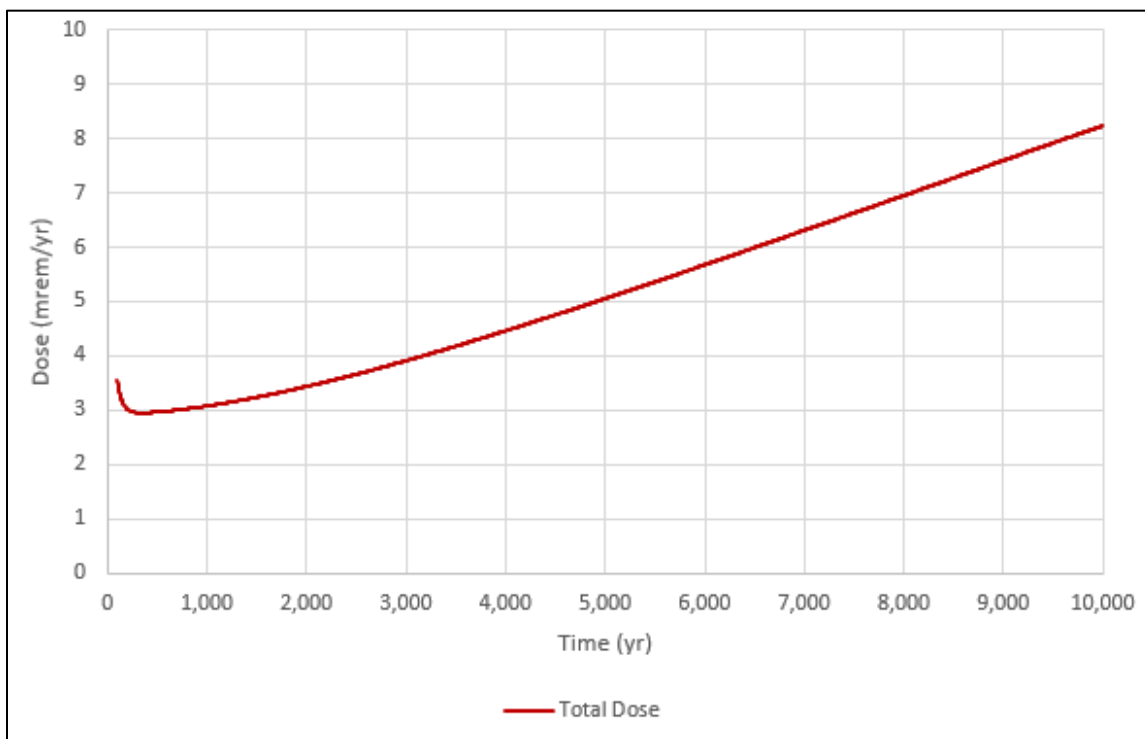
Fig. 6.9. Chronic post-drilling scenario total dose (all radionuclides and pathways summed)
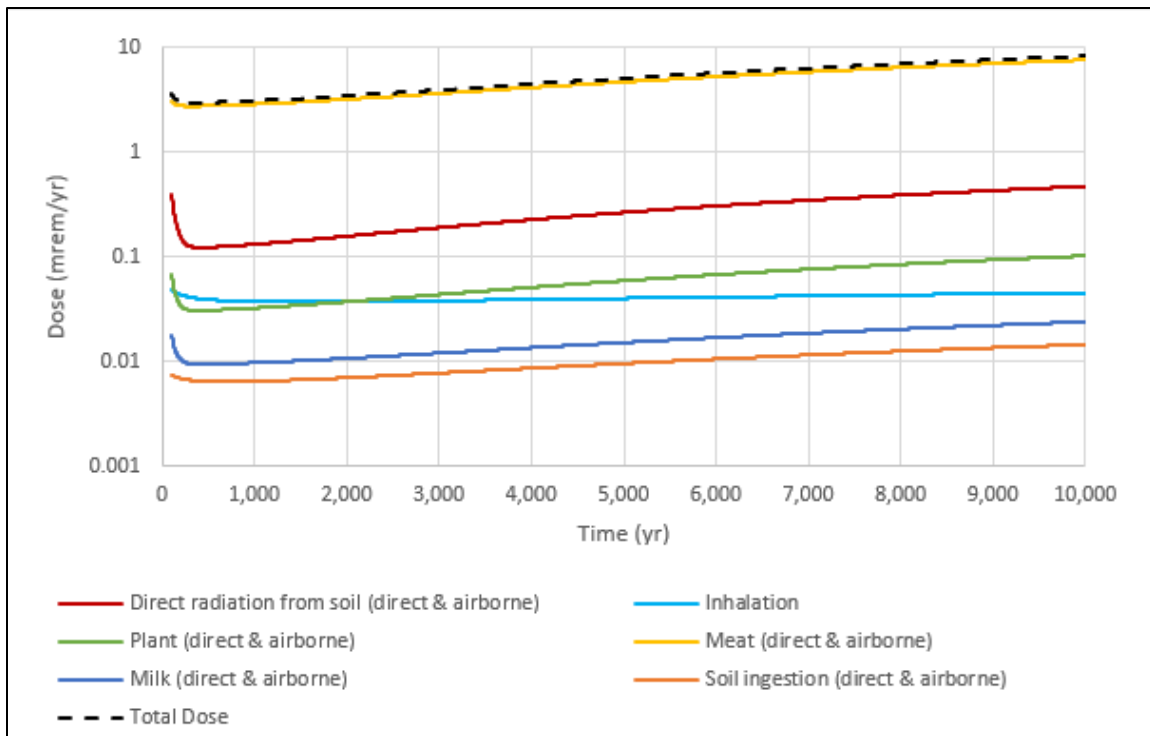
Note: Vertical axis is logarithmic for clarity.

Fig. 6.10. Chronic post-drilling scenario total dose and dose contributions by pathway
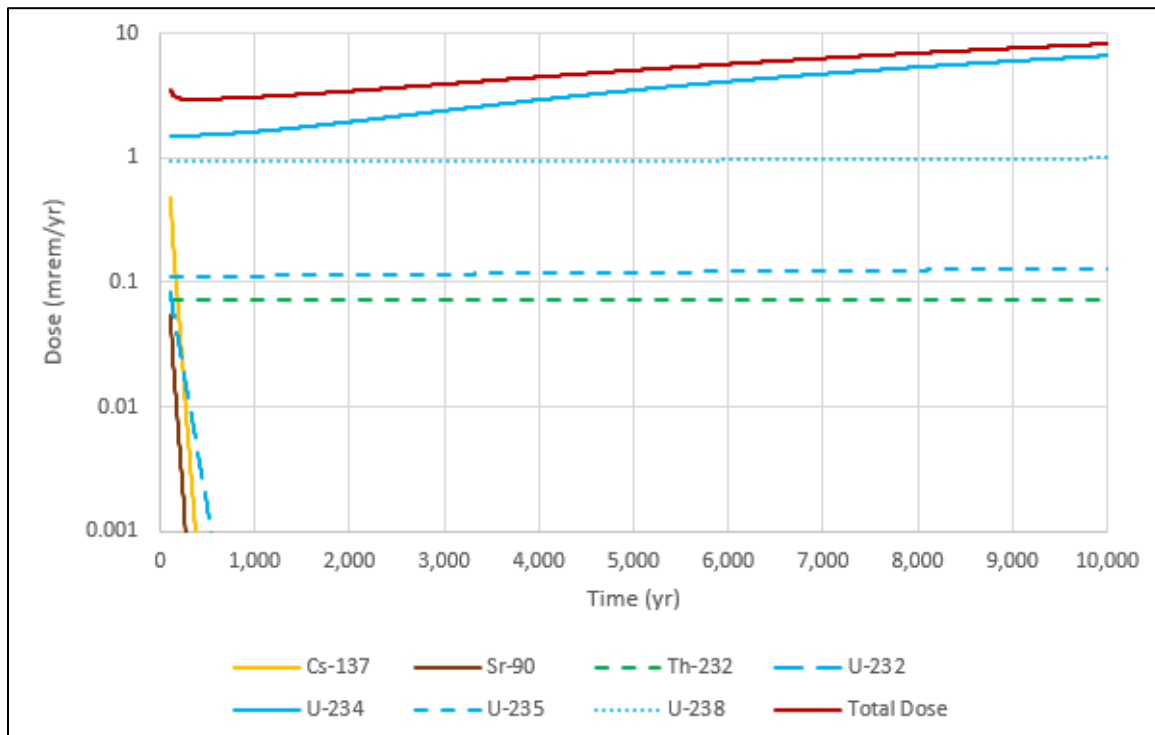
Note: Vertical axis is logarithmic for clarity.

Fig. 6.11. Chronic post-drilling scenario dose contributions by radionuclide

6.7 SUMMARY OF RESULTS AND RESRAD-OFFSITE SINGLE RADIONUCLIDE SOIL GUIDELINES

With respect to performance measures for IHI, the EMDF analysis suggests that, based on the current estimated EMDF radionuclide inventory, there is a reasonable expectation that the facility design will protect a future inadvertent human intruder for the specific IHI scenarios considered. The analysis is pessimistic in that DOE is expected to maintain control of the EMDF site indefinitely into the future.

The dose analysis suggests that, based on the estimated EMDF inventory, IHI-based radionuclide concentration limits (WAC) are not required to meet the DOE M 435.1-1 performance measures for exposure from IHI.

A summary of the results of the IHI modeling results for the period from 100 to 10,000 years post-closure is shown in Table 6.2.

Table 6.2. Summary of modeled doses for acute and chronic EMDF IHI scenarios

EMDF IHI scenario	DOE O 435.1 IHI performance measure	Modeled EMDF dose range (100-10,000 years post-closure)
Acute exposure – discovery (excavation)	500 mrem	6.7E-05 to 2.5E-04 mrem
Acute exposure – drilling (water well)	500 mrem	1.7E-01 to 4.2E-01 mrem
Chronic exposure – post-drilling (subsistence garden)	100 mrem/year	3.0E+00 to 8.2E+00 mrem/year

DOE O = U.S. Department of Energy Order   IHI = inadvertent human intrusion
EMDF = Environmental Management Disposal Facility

IHI analyses provide one basis for setting radionuclide concentration limits to ensure protection of members of the public. RESRAD-OFFSITE SRSGs are calculated activity concentrations that meet a specific dose target for a single radionuclide at a specific time, based on the modeled scenario. The SRSGs do not depend on the assumed radionuclide concentrations or the corresponding modeled doses, but only on the target dose value and the specific exposure scenario considered. Thus, the SRSGs are dose-based radionuclide concentration limits for the particular system and scenario simulated.

For the IHI scenarios presented here, the most restrictive (lowest) SRSG values are based on the 100 mrem/year dose measure associated with the chronic drilling exposure scenario. For most radionuclides, the minimum SRSG within this period occurs at either 100 or 1000 years post-closure. This approach was taken for all radionuclides except for C-14. Carbon-14 is a highly mobile radionuclide that easily transitions to the gaseous or dissolved form. In the acute and chronic drilling scenarios, the dispersed drill cuttings are exposed to the atmosphere, which causes the C-14 to volatilize from the soil completely within the first five years of the simulation. Due to the volatility of C-14, the minimum SRSG between 100 and 1000 years was calculated by adjusting the SRSG at year 0 for 100 years of radioactive decay. A detailed description of how the C-14 SRSG was calculated is provided in the QA documentation for the IHI analysis (UCOR 2020b).

The correct application of the predicted SRSG to set or evaluate waste concentration limits based on the IHI dose must account for the assumed dilution of radionuclides when mixed with the uncontaminated materials when being placed in the facility and when they are exhumed and mixed with clean drill cuttings or garden soil. The source SRSG values output by the RESRAD-OFFSITE model are divided by the dilution factor(s) applied to the waste concentrations in the IHI analysis to derive corresponding SRSG values for comparison to as-disposed (including clean fill) or as-generated activity concentrations. SRSGs calculated

for C-14, H-3, I-129, and Tc-99 are not back-adjusted to account for potential activity loss during operations as a conservative measure biased towards lower SRSGs. Table 6.3 presents the SRSG values for both the acute drilling and chronic post-drilling scenarios. The minimum SRSG values occur at 100 years post-closure unless indicated otherwise in Table 6.3. After accounting for the assumed dilution, as-disposed and as-generated SRSG values for the chronic post-drilling scenario are less than the as-disposed and as-generated SRSG values for the acute drilling scenario for all radionuclides.

Table 6.3. RESRAD-OFFSITE SRSG for acute drilling and chronic post-drilling IHI scenarios

Radionuclide	Acute drilling source SRSG (pCi/g)	Acute drilling as-disposed SRSG (pCi/g)	Acute drilling as-generated SRSG (pCi/g)	Chronic post-drilling source SRSG (pCi/g)	Chronic post-drilling as-disposed SRSG (pCi/g)	Chronic post-drilling as-generated SRSG (pCi/g)
Ac-227	2.08E+06	7.31E+06	1.38E+07	2.96E+03	1.30E+06	2.45E+06
Am-241	6.05E+05	2.13E+06	4.01E+06	1.27E+03	5.55E+05	1.05E+06
Am-243	1.78E+05	6.26E+05	1.18E+06	2.90E+02	1.27E+05	2.39E+05
Ba-133	1.00E+08	3.52E+08	6.64E+08	1.24E+05	5.45E+07	1.03E+08
Be-10	1.74E+08	6.13E+08	1.15E+09	1.36E+04	5.98E+06	1.13E+07
C-14[a]	2.79E+09[b]	9.83E+09[b]	1.85E+10[b]	7.07E+01[b]	3.10E+04[b]	5.84E+04[b]
Ca-41	1.72E+10	6.04E+10	1.14E+11	5.13E+03	2.25E+06	4.24E+06
Cf-249	1.24E+05	4.36E+05	8.22E+05	1.80E+02	7.92E+04	1.49E+05
Cf-250	7.69E+07	2.71E+08	5.10E+08	1.47E+05	6.45E+07	1.21E+08
Cf-251	2.02E+05	7.11E+05	1.34E+06	3.65E+02	1.60E+05	3.01E+05
Cm-243	2.98E+06	1.05E+07	1.98E+07	4.76E+03	2.09E+06	3.93E+06
Cm-244	3.58E+07	1.26E+08	2.37E+08	7.72E+04	3.39E+07	6.38E+07
Cm-245	2.13E+05[c]	7.48E+05[c]	1.41E+06[c]	4.00E+02[c]	1.75E+05[c]	3.30E+05[c]
Cm-246	5.55E+05	1.95E+06	3.68E+06	1.13E+03	4.97E+05	9.35E+05
Cm-247	1.12E+05[c]	3.93E+05[c]	7.40E+05[c]	1.55E+02[c]	6.81E+04[c]	1.28E+05[c]
Cm-248	3.14E+04	1.11E+05	2.08E+05	3.58E+01	1.57E+04	2.96E+04
Co-60	1.05E+10	3.69E+10	6.94E+10	1.06E+07	4.65E+09	8.76E+09
Cs-137	8.82E+05	3.10E+06	5.84E+06	5.30E+02	2.32E+05	4.38E+05
Eu-152	7.42E+06	2.61E+07	4.92E+07	8.21E+03	3.60E+06	6.78E+06
Eu-154	1.31E+08	4.62E+08	8.71E+08	1.44E+05	6.33E+07	1.19E+08
H-3[a]	3.35E+13	1.18E+14	2.22E+14	1.30E+06	5.72E+08	1.08E+09
I-129[a]	1.23E+07	4.31E+07	8.12E+07	1.38E+01	6.06E+03	1.14E+04
K-40	3.22E+05	1.13E+06	2.13E+06	4.10E+01	1.80E+04	3.39E+04
Mo-93	2.67E+08	9.39E+08	1.77E+09	1.26E+02	5.52E+04	1.04E+05
Nb-93m	1.34E+11	4.70E+11	8.85E+11	3.57E+07	1.57E+10	2.95E+10
Nb-94	3.19E+04	1.12E+05	2.11E+05	3.61E+01	1.59E+04	2.99E+04
Ni-59	2.57E+09	9.04E+09	1.70E+10	1.72E+05	7.56E+07	1.42E+08
Ni-63	2.69E+10	9.45E+10	1.78E+11	1.46E+05	6.39E+07	1.20E+08
Np-237	1.82E+05[d]	6.42E+05[d]	1.21E+06[d]	2.35E+02[c]	1.03E+05[c]	1.94E+05[c]
Pa-231	6.06E+04[d]	2.13E+05[d]	4.01E+05[d]	9.40E+01[d]	4.12E+04[d]	7.77E+04[d]
Pb-210	3.12E+07	1.10E+08	2.07E+08	4.72E+01	2.07E+04	3.90E+04

Table 6.3. RESRAD-OFFSITE SRSG for acute drilling and chronic post-drilling IHI scenarios (cont.)

Radionuclide	Acute drilling source SRSG (pCi/g)	Acute drilling as-disposed SRSG (pCi/g)	Acute drilling as-generated SRSG (pCi/g)	Chronic post-drilling source SRSG (pCi/g)	Chronic post-drilling as-disposed SRSG (pCi/g)	Chronic post-drilling as-generated SRSG (pCi/g)
Pm-146	1.86E+10	6.53E+10	1.23E+11	2.19E+07	9.61E+09	1.81E+10
Pu-238	1.14E+06	4.02E+06	7.58E+06	2.87E+03	1.26E+06	2.37E+06
Pu-239	4.71E+05	1.66E+06	3.12E+06	1.19E+03	5.22E+05	9.83E+05
Pu-240	4.75E+05	1.67E+06	3.15E+06	1.20E+03	5.27E+05	9.92E+05
Pu-241	1.77E+07	6.22E+07	1.17E+08	3.70E+04	1.62E+07	3.06E+07
Pu-242	4.94E+05	1.74E+06	3.27E+06	1.25E+03	5.47E+05	1.03E+06
Pu-244	1.09E+05[c]	3.84E+05[c]	7.24E+05[c]	1.44E+02[c]	6.31E+04[c]	1.19E+05[c]
Ra-226	2.97E+04	1.05E+05	1.97E+05	2.00E+00[d]	8.77E+02[d]	1.65E+03[d]
Ra-228	2.82E+09	9.93E+09	1.87E+10	1.64E+06	7.21E+08	1.36E+09
Re-187	SA[e]	SA[e]	SA[e]	SA[e]	SA[e]	SA[e]
Sr-90	5.75E+07	2.02E+08	3.81E+08	7.44E+02	3.26E+05	6.15E+05
Tc-99[a]	1.02E+09	3.58E+09	6.73E+09	1.09E+02	4.80E+04	9.03E+04
Th-228	SA[e]	SA[e]	SA[e]	SA[e]	SA[e]	SA[e]
Th-229	9.58E+04	3.37E+05	6.35E+05	1.44E+02	6.32E+04	1.19E+05
Th-230	7.08E+04[c]	2.49E+05[c]	4.69E+05[c]	5.48E+00[c]	2.40E+03[c]	4.53E+03[c]
Th-232	2.05E+04[d]	7.21E+04[d]	1.36E+05[d]	1.09E+01[d]	4.79E+03[d]	9.02E+03[d]
U-232	8.99E+04	3.16E+05	5.96E+05	2.69E+01	1.18E+04	2.22E+04
U-233	8.78E+05[c]	3.09E+06[c]	5.82E+06[c]	8.79E+01[c]	3.86E+04[c]	7.26E+04[c]
U-234	3.80E+06[c]	1.34E+07[c]	2.52E+07[c]	8.87E+01[c]	3.89E+04[c]	7.33E+04[c]
U-235	2.62E+05[c]	9.22E+05[c]	1.74E+06[c]	8.03E+01[c]	3.52E+04[c]	6.64E+04
U-236	5.82E+06	2.05E+07	3.86E+07	1.02E+02	4.47E+04	8.42E+04
U-238	SA[e]	SA[e]	SA[e]	9.29E+01[c]	4.08E+04[c]	7.68E+04[c]

[a]SRSG was not back-adjusted to account for activity loss during operations.
[b]SRSG equal to SRSG at 0 year adjusted for 100 years of radioactive decay.
[c]Minimum SRSG occurs at 1000 years.
[d]Minimum SRSG occurs after 100 years and before 1000 years.
[e]The SRSG is equal to or greater than the SA for the radionuclide.

IHI = inadvertent human intrusion   SA = specific activity
RESRAD = RESidual RADioactivity   SRSG = Single Radionuclide Soil Guideline

This page intentionally left blank.

7.   INTEGRATION AND INTERPRETATION OF RESULTS

This section provides a summary of key elements of the analyses that support compliance decisions for the EMDF system with respect to DOE M 435.1-1 performance objectives and measures.

7.1   RADIONUCLIDE INVENTORY

The PA analyses of the EMDF system are based on an estimated radionuclide inventory and Preliminary Design parameters. Both the facility design and the estimated inventory will be refined as the EMDF design development process proceeds and additional waste stream characterization data become available.

Base case all-pathway peak doses for each radionuclide that was not screened from further analysis (Sect. 2.3.3) indicate that for the period from EMDF closure to 10,000 years post-closure, the primary contributors to total dose are C-14, Tc-99, and I-129 (Figs. 4.8 through 4.10). The inventory component that has the greatest impact on maximum dose during the compliance period is C-14; contributions from Tc-99 and I-129 occur after 1000 years. Uncertainty in EMDF inventory of the three dose-significant radionuclides is important for understanding the likely impacts of potential future releases. There is uncertainty in the estimated waste average activity concentrations used to derive the modeled source concentrations, and uncertainty in the magnitude of operational period losses credited for reducing the post-closure inventory of C-14, Tc-99, and I-129 (Fig. 5.8).

7.2   COVER SYSTEM PERFORMANCE

7.2.1   Cover Infiltration

The EMDF cover design and assumed long-term cover performance are key elements of the performance analysis. The assumed post-closure cover infiltration rate is a primary driver of predicted dose, affecting the rate of radionuclide release from the disposal unit and peak concentrations in groundwater and surface water. Based on the RESRAD-OFFSITE sensitivity analysis, the maximum all-pathways dose during the compliance period (i.e., at 1000 years post-closure) is very sensitive to parameters that determine the rate of cover infiltration (Fig. 5.8).

Uncertainty in future annual average precipitation and the degree of cover system degradation (two fundamental controls on cover infiltration) are two of the key parameter uncertainties identified in the RESRAD-OFFSITE probabilistic uncertainty analysis (refer to Appendix G, Sect. G.6.3.3.3). The upper limit of cover infiltration evaluated for the probabilistic analysis (approximately 3.7 in./year) is much larger than is reasonably expected during the 1000-year compliance period, given the likely service life of the HDPE membrane in the cover. The assumptions applied to the HELP modeling of cover infiltration (Appendix C, Sect. C.2) regarding degradation of the lateral drainage function of the cover system are very pessimistic, particularly because the coarse materials of the biointrusion layer above the lateral drainage layer in the cover (Fig. 2.41) will provide drainage even in the event of clogging of the underlying engineered drainage layer.

Degradation of the clay infiltration barrier of the EMDF cover (increased hydraulic conductivity) should be significantly delayed relative to the base case assumptions applied to the timing of cover failure (progressive failure from 200 to 1000 years post-closure), because of the likelihood that overlying HDPE membrane will function effectively for much more than 200 years. Extended HDPE membrane longevity is expected based on existing research (Appendix C, Sect. C.1.2.2.2) and the protection from the surface

environment provided by 11 ft of overlying material (the lateral drainage layer, biointrusion barrier, and cover surface layers).

Erosion of the cover system over very long periods of time is inevitable, and long-term degradation of waste containers and stabilized waste forms may contribute to differential settlement that can impair the efficiency of the engineered lateral drainage system. However, water-driven cover erosion should facilitate effective lateral drainage even in the case of relatively severe dissection (gullying) of the cover surface, and the biointrusion layer should limit the depth of gully formation so that direct exposure of the underlying infiltration barriers is unlikely even over very long periods of time. Natural vegetation dynamics in the warm humid climate of the southeast United States should also promote cover longevity and limit the potential for severe erosion, although a forested EMDF cover would be subject to natural processes of tree-throw and weather-related forest disturbance that could also cause localized erosion. In general, the earthen cover components overlying the HDPE and clay infiltration barriers should be relatively stable under the natural range of environmental conditions, even considering natural climate fluctuations or the potential for progressive climate change.

The distributions selected for the timing and duration of cover degradation, and for the cover infiltration rate (runoff coefficient) in the RESRAD-OFFSITE probabilistic uncertainty analysis (Appendix G, Sect. G.6.3.2.1 and Table G.23) provide a robust assessment of the base case assumptions for cover performance. For the probabilistic dose analysis, the mean (average mean value for ten repetitions of 300 system realizations) of the all-pathways dose at 1000 years is approximately 1 mrem/year (Fig. 5.12), and the average 95th percentile at 1000 years is less than 2 mrem/year (20 percent of the 25 mrem/year performance objective). Higher peak doses associated with fission products (Tc-99 and I-129) and actinides occur after 1000 years. However, comparison of release predictions from the STOMP and RESRAD-OFFSITE models suggest that the post-1000 year peaks may be over-estimated by the relatively simple release and vadose zone conceptualizations implemented in RESRAD-OFFSITE.

7.2.2   Atmospheric (Vapor Phase) and Biological Release

EMDF cover performance is also a key assumption in the screening of atmospheric (vapor-phase) release from detailed analysis. The estimated inventories of H-3, C-14, and I-129 have the greatest potential for vapor-phase release, but vapor-phase release and aqueous-phase leaching of these relatively mobile radionuclides from the waste during disposal and prior to EMDF closure will reduce the amounts available for post-closure release to the atmosphere or to porewater. Post-closure release of volatile hydrocarbons incorporating H-3 or C-14 (above background levels) and release of vapor-phase radioiodine will be limited by the synthetic and clay barriers of the EMDF cover system, which are expected to remain fully functional for several centuries, and at least partially functional for the duration of the compliance period.

Following the end of post-closure care and active institutional control, development of natural vegetation and inhabitation of the cover system by various animals is likely. Biological intrusion by root systems, insects, and larger animals will contribute to the natural evolution of the cover system components. Based on the expectation of a relatively stable cover surface, and the prevention of deep burrowing by large animals or severe gully erosion by the coarse materials of the biointrusion barrier, the potential for significant biologically-driven release of radionuclides is limited, and biological release was eliminated from consideration in the PA analysis.

7.2.3   Inadvertent Human Intrusion

The analysis of IHI for the EMDF includes acute and chronic exposure scenarios that are based on the EMDF Preliminary Design for the CBCV site. The continuing presence of the HDPE liner and general stability of the cover system over the 1000-year compliance period is significant for the IHI analysis acute

discovery scenario, which is based on a hypothetical excavation of the cover that does not expose the waste. The discovery scenario credits the engineered barriers of the EMDF cover with deterring completion of an excavation into the waste that could lead to direct exposure to radionuclides in EMDF waste. Erosion of the cover system that could reduce the thickness of the cover components would not significantly impact the deterrent to excavation provided by the engineered biointrusion barrier and underlying cover system components.

7.3 RADIONUCLIDE RELEASE AND TRANSPORT MODELS

7.3.1 Release Conceptualization

Similar approaches to representation of radionuclide release from the EMDF were implemented in the more detailed models of the vadose and saturated zone and in the total system transport model. The PA models incorporate no assumptions related to the use of waste containers or stabilized waste forms that can limit or delay release of radionuclides. The relatively simple equilibrium sorption model for radionuclide release applied in the STOMP model (Appendix E) and in developing the source release boundary condition (leachate flux to the water table) for the MT3D model (Appendix F) is pessimistic given the likelihood of non-uniform cover infiltration that limits water intrusion to particular locations and flow pathways through the waste. Waste heterogeneity will also focus infiltrating water along preferred transport paths. The simplified source release representation in these two models assumes that the entire radionuclide inventory is available for aqueous release and transport as soon as cover infiltration becomes non-zero, whereas it is likely that heterogeneity in water intrusion and radionuclide transfer to the aqueous phase will limit release rates. Figures 3.31, 3.32 and 3.33 show a comparison of vadose zone flux predicted by STOMP and RESRAD-OFFSITE and the release model applied to the MT3D saturated zone transport model for Tc-99. The consistency among the model outputs and MT3D model input is good.

The potential impact of non-uniform release to the saturated zone that is possible due to sloping liner surfaces and variability in waste thickness was evaluated by applying a simple non-uniform leachate flux boundary condition to the MT3D model (Sect. 3.3.3.2). The non-uniform release was found to decrease the predicted peak Tc-99 concentration at the groundwater well (Fig. 5.5). Source release to the saturated zone in the total system model is assumed to occur uniformly over a simplified rectangular footprint area based on the EMDF preliminary design. However, sensitivity evaluation with the MT3D model suggests that the uniform source release assumption for the total system model simulations is not critical to the assessment of EMDF compliance with the 25 mrem/year performance objective. The model intercomparison for the saturated zone activity concentration results also suggests that uncertainties related to conceptual models of radionuclide release and materials in the shallow aquifer are not significant in terms of the range of predicted peak saturated zone concentrations, at least for highly mobile radionuclides like C-14 and Tc-99.

7.3.2 Assumed K_d Values for Dose-Significant Radionuclides

The PA model results are sensitive to the assumed values for partition coefficients for Tc-99 and, particularly, I-129. To account for uncertainty in waste geochemistry and release kinetics, the waste K_d values for all radionuclides are reduced by a factor of two from the assumed base case values; this is a fairly pessimistic approach because it is likely that sorption by the clean fill emplaced with the waste will be substantial. Uncertainty in assigning K_d values is significant, but the base case values for Tc-99 and I-129 are reasonably pessimistic (lower than is likely) given the available information regarding the sorptive capacity of Conasauga Group materials, and the likely range of geochemical conditions. Similarly, the assumed K_d value for uranium is probably on the lower end of the range of likely values for the materials of the EMDF system, based on the available information. Uranium sorption experiments on local clay rich soils were performed during the design phase for the EMWMF (WMFS 2000) and the results indicated that

the sorptive capacity of those materials was very high, implying $K_d > 1000$ cm^3/g. Lower than expected K_d values may result for particular chemical species and geochemical environments, but the uncertainty analysis (Sect. 5.4) evaluated K_d values as low as zero for both Tc-99 and I-129, the two radionuclides for which the uncertainty in assigning an appropriate long-term value is most significant for the results of the PA. New laboratory studies of the sorptive capacity of Conasauga Group materials for Tc-99 and I-129 are planned to reduce the uncertainty in these important model input parameters.

7.3.3 Transport Model Uncertainty

The PA applied 2-D and 3-D radionuclide transport models to the vadose and saturated zone, respectively. These models capture much of the complexity in the configuration of waste, engineered barriers, and natural geologic materials for the EMDF system. The results obtained from the more complex transport model codes (STOMP and MT3D) were compared to radionuclide release and transport output from the total system model (RESRAD-OFFSITE). This model integration step was performed to ensure that the simplified representations of the vadose and saturated zones in the RESRAD-OFFSITE model were producing results consistent with the more detailed models, and to address uncertainty associated with applying a simplified conceptualization of radionuclide release and transport to a fairly complex LLW disposal system like the EMDF.

In general, the RESRAD-OFFSITE model base case predictions of peak concentrations at the groundwater POA are larger and earlier than corresponding predictions from the more detailed MT3D transport model. Final base case values for critical RESRAD-OFFSITE input parameters that impact the simulated saturated zone concentrations, including the well depth and hydraulic gradient to the well, were adopted on this basis. This approach to managing transport model uncertainty imparts a pessimistic bias to the transport modeling because the RESRAD-OFFSITE concentration estimates are biased high relative to predictions from the more detailed models, and provide a measure of conservatism to the PA dose analysis.

7.4 ALL-PATHWAYS DOSE UNCERTAINTY

The RESRAD-OFFSITE compliance period probabilistic uncertainty analysis includes only estimated inventories of C-14, Tc-99, and I-129. These three radionuclides are the primary dose contributors for the base case EMDF performance scenario. Sensitivity of the predicted total dose to uncertainties in selected model parameters representing climate (precipitation), long-term cover performance, radionuclide mobility (K_d values), subsurface material properties, and groundwater conditions was evaluated by probabilistic sampling of input parameter values and multiple regression analysis of predicted peak total dose (Sect. 5.4).

For the probabilistic analysis, K_d values for Tc-99 and I-129 were permitted to vary independently between maximum (twice the base case values) and zero minimum values, with the result that earlier, higher additive doses can occur in the probabilistic than for the deterministic base case scenario. For the compliance period analysis, the mean probabilistic dose at 1000 years was similar to the deterministic base case peak dose, approximately 1 mrem/year (Fig. 5.12), and the 95th percentile of the probabilistic peak total dose was less than 3 mrem/year.

Although approximately 5 percent of post compliance period probabilistic peak doses between 2000 and 3000 years exceed 15 mrem/year, the mean of the probabilistic dose remains less than 5 mrem/year for simulations times before about 6000 years. Higher probabilistic uranium and plutonium dose predictions beyond about 6000 years appear to be over-estimated by the RESRAD-OFFSITE code using the instantaneous equilibrium desorption model, which appears to predict much higher peak activity flux to the saturated zone than do the STOMP model simulations for radionuclide with assigned $K_d > 1$ cm^3/g, such as I-129 and U-234 (Sect. 3.3.5). In addition, uranium solubility limits and the effect of waste containers,

waste stabilization (grouting), or treatment to reduce the mobility of some of the estimated actinide inventory are not considered in the model predictions.

These results suggest that the uncertainty in key input parameter values does not affect the conclusion that the all-pathways dose performance objective will be met during the 1000-year compliance period, and that the 25 mrem/year limit is unlikely to be exceeded within timeframes of several thousand years post-closure.

This page intentionally left blank.

8. PERFORMANCE EVALUATION

8.1 COMPARISON OF RESULTS TO PERFORMANCE OBJECTIVES

The base case analysis and sensitivity-uncertainty analysis performed for the EMDF PA demonstrate that there is a reasonable expectation that the facility will meet the established all-pathways dose performance objective during the 1000-year compliance period and within the first several thousand years post-closure. Analytical results of the EMDF performance modeling are summarized in Table 8.1.

Table 8.1. Exposure scenarios, performance objectives and measures, and base case results for the EMDF PA

Exposure scenario	Performance objective or measure	EMDF PA results
All pathways	25 mrem/year	Base case maximum dose during compliance period: 1.03 mrem/year Base case peak dose through 10,000 years: 9.13 mrem/year (at 5100 years)
Air pathway[a]	10 mrem/year[b]	Pathway screened from analysis (Sect. 3.2.2)
Radon flux	20 pCi/m^2/sec	EMDF cover surface: 5.0E-08 pCi/m^2/sec EMDF waste surface (no cover): 0.80 pCi/m^2/sec
Water resources (groundwater) • Ra-226 + Ra-228 • Gross alpha activity[c] • Beta/photon activity • H-3 • Sr-90 • Uranium (total)	5 pCi/L 15 pCi/L 4 mrem/year 20,000 pCi/L 8 pCi/L 30 µg/L	Groundwater during compliance period: • Ra-226 + Ra-228: 0.0 pCi/L (negligible) • Gross alpha activity: 0.0 pCi/L (negligible) • Beta/photon activity: 1.03 mrem/year • H-3: 0.0 pCi/L (negligible) • Sr-90: 0.0 pCi/L (negligible) • Uranium (total): 0.0 µg/L (negligible).
Water resources (surface water)	DOE DCS[d]	Bear Creek peak concentration less than DCS standard for all radionuclides in EMDF inventory (Sect. 4.7.2)
Inadvertent human intrusion • Chronic exposure • Acute exposure	100 mrem/year 500 mrem	IHI dose at 100 years (compliance period maximum): Chronic post-drilling: 3.56 mrem/year Acute discovery: 1.30E-04 mrem Acute drilling: 0.38 mrem

[a]Air pathway is screened from the EMDF PA.
[b]Excluding radon in air.
[c]Including Ra-226, but excluding radon and uranium.
[d]DOE 2011b.

DCS = Derived Concentration Standard
DOE = U.S. Department of Energy
EMDF = Environmental Management Disposal Facility

IHI = inadvertent human intrusion
PA = Performance Assessment

Results of the radon flux analysis, which are provided in Sect. 4.4 and presented in detail in Appendix H, are included in Table 8.1. The results suggest that the EMDF can meet the 20 pCi/m^2/sec radon flux performance objective even if the cover is severely eroded. Also included in Table 8.1 is a summary of the results of RESRAD-OFFSITE modeling to demonstrate protection of water resources during the 1000-year compliance period. Modeled well water and surface water concentrations are compared to maximum contaminant levels for drinking water systems and to DCSs (DOE 2011b), respectively. The results suggest

that there is a reasonable expectation that the EMDF disposal system will be protective of water resources during the compliance period.

With respect to performance measures for IHI, the EMDF analysis suggests that, based on the current estimated EMDF radionuclide inventory, there is a reasonable expectation that the facility design will protect a future inadvertent human intruder for the specific IHI scenarios considered.

8.2 USE OF PERFORMANCE ASSESSMENT RESULTS

The primary uses of this EMDF PA are to support issuance of a DAS by demonstrating the likelihood of meeting performance objectives based on the expected EMDF waste forms, estimated radionuclide inventory, preliminary facility design, and site characteristics and to identify key site, waste, and facility uncertainties that can be prioritized for further work prior to start of operations.

8.3 FURTHER WORK

Near-term priorities for research and development activities to support PA maintenance include the following:

- Perform laboratory evaluations of EMDF materials to reduce uncertainty in the assumed K_d values for Tc-99 and I-129

- Monitor EMDF design evolution through final design and assess changes through the EMDF change control process.

In parallel with these near-term PA maintenance activities, the FFA parties will approve operating limits, including WAC, and will issue a WAC compliance document prior to EMDF operations. Review of proposed activities, new regulatory requirements, or other new information that could challenge key assumptions for the EMDF performance analysis will be evaluated in accordance with the EMDF change control process to assess the potential for such changes to require a Special Analysis or revisions to the PA.

9. QUALITY ASSURANCE

The QA Report (UCOR 2020b) was prepared to comprehensively document the QA record for this Revision 2 PA (and the companion Revision 2 CA [UCOR 2020a]). This QA Report accompanies this PA and details the QA protocol applied during the preparation of this PA. It identifies the electronic files created during the modeling and their location; it identifies the modeling input parameters and documents their technical assessment; and it documents the technical review of the draft PA before it was finalized. An assessment of the QA associated with the development of this PA must include a review of the QA Report.

UCOR, in accordance with DOE O 414.1C, 10 *CFR* 830, Subpart A, federal regulations, and contractual requirements, maintains an NQA-1-compliant QA program. Drummond Carpenter, PLLC (Drummond Carpenter) and Jacobs provided groundwater and contaminant fate and transport modeling support to this PA under a UCOR Professional Services Agreement and a Request for Offsite Services, respectively. UCOR flows its QA requirements to companies providing support via the Professional Services Agreements and Requests for Offsite Services.

The salient components of the QA program that were implemented during the preparation of this PA include the following:

- Software QA procedures for code verification and documentation for each model code per *Software Quality Assurance Program* (PPD-IT-6007)

- Formal independent checking and review of calculation and data packages that document input parameter values and other model assumptions, model implementation, model output data, and post-processing activities for each PA model

- Documentation of PA model development, implementation, sensitivity-uncertainty analyses, and PA model integration contained in the EMDF PA report and report appendices

- Configuration management for PA documents and calculation packages per UCOR procedures for document control

- Maintenance of the digital modeling information archive of PA documents, model codes, model input and output files, formal QA documentation, and reference materials in compliance with requirements of the UCOR QA Program (UCOR 2019), DOE QA Program (DOE 2012, Attachments G and H), and DOE O 414.1D (DOE 2013b).

9.1 SOFTWARE QUALITY ASSURANCE

Documentation of software QA, including code validation on computers used for PA modeling follows the requirements of UCOR Software QA procedure (PPD-IT-6007). All PA model codes have been categorized as UCOR category C (Business Impacting Software). Documentation of code validation, including model input and output files for validation runs are available for each PA model code in the UCOR Software QA database system. In addition, all software QA documentation is included in the EMDF PA Library.

A management assessment of the compliance of the EMDF Project Software with the requirements in the current revision of UCOR procedure PROC-IT-6008 was conducted in March 2019. There were no observations of findings identified during this assessment. A copy of this assessment is in the QA Report.

9.2 INPUT DATA QUALITY ASSURANCE

Development and independent checking of one or more calculation packages for each EMDF PA model code is the basis for ensuring the accuracy and consistency of model input data. Data and calculation packages for each model code document input parameter values and other model assumptions, information sources, model implementation, model outputs, and post-processing activities. The calculation package for the EMDF estimated radionuclide inventory that documents the data structure and data sources used to estimate the estimated inventory is a supporting QA document for all of the radionuclide transport models.

A list of all EMDF PA calculation packages and the model(s) supported by each is shown on Table 9.1. All calculation packages, including model input and output files, data for supporting calculations, and copies of all supporting references will be maintained in electronic format (pdf) and available on digital media or in controlled hard copy form as required.

Table 9.1. Data and calculation packages for the EMDF PA

Calculation Package Title	Author	UCOR Calculation Number	Document Reference(s)
Data and Calculation Package-EMDF Radiological Inventory	UCOR	CAW-90EMDF-F898	Sect. 2.3, Appendix B
Calculation and Data Package for the HELP Model	Jacobs	CAW-90EMDF-G118	Sect. 3.3.1, Appendix C
Calculation and Data Package for the Parameter Development based on EMDF Design	Jacobs	CAW-90EMDF-G119	Sect. 2.2, Appendix C
Calculation and Data Package for the STOMP Model	Jacobs	CAW-90EMDF-G120	Sect. 3.3.2, Appendix E
Calculation and Data Package for the MODFLOW Model	Jacobs	CAW-90EMDF-G121	Sect. 3.3.3, Appendix D
Calculation and Date Package for the MT3D Model	Jacobs	CAW-90EMDF-G122	Sect. 3.3.3, Appendix F
EMDF RESRAD-OFFSITE Operational Period Inventory Depletion Calculation Package	Drummond Carpenter	CAW-90EMDF-G182	Sect. 3.2.2.5, Appendix G
EMDF RESRAD-OFFSITE Performance Assessment and Composite Analysis Calculations Package	Drummond Carpenter	CAW-90EMDF-G183	Sects. 3.3.4, 3.4, Appendix G
EMDF IHI RESRAD-OFFSITE Modeling Calculations Package	Drummond Carpenter	CAW-90EMDF-G184	Sect. 6, Appendix I
EMDF Cover Erosion Calculation (RUSLE2)	UCOR	CAW-90EMDF-G123	Sect. 3.2.1, Appendix C
EMDF Radon Flux Calculation	UCOR	CAW-90EMDF-G124	Sect. 3.2.2.2, Appendix H
EMDF Bathtub Scenario Analysis	UCOR	CAW-90EMDF-G048	Sect. 3.2.1, Appendix C
Data and Calculation Package – Average Properties of EMDF Waste	UCOR	CAW-90EMDF-G496	Sect. 3.3, Appendices C, D, E, F, G (all models except HELP)
Data and Calculation Package – EMDF Engineered Material Properties	UCOR	CAW-90EMDF-G497	Sect. 3.3, Appendices C, D, E, F, G (all models except HELP)

EMDF = Environmental Management Disposal Facility   PA = Performance Assessment
HELP = Hydrologic Evaluation of Landfill Performance   RESRAD = RESidual RADioactivity
IHI = inadvertent human intrusion

9.3　　　　　DOCUMENTATION OF MODEL DEVELOPMENT AND OUTPUT DATA

Model development and output data for each of the EMDF PA model codes is documented in the appendices to the PA report document, and additional detail is provided in model-specific calculation packages (Table 9.1). Model output files and separate electronic tabulations of model output used for plotting or post-processing are included for archival purposes as digital attachments to calculation packages.

9.4　　　　　INDEPENDENT TECHNICAL REVIEW OF THE REVISED PERFORMANCE ASSESSMENT

UCOR performed an independent technical review of the final draft of the Revision 2 EMDF PA prior to its transmittal to DOE for distribution. This review was conducted using the UCOR Form-141, "Document Review Request." These forms document the names of those reviewing the document, the scope (purpose) of the reviews, how comments on the documents were transmitted from the reviewers to the preparer, and that comments were resolved.

The scope of this review process included the following (at a minimum):

- An OREM (DOE) review (two reviewers, a technical review by a subcontractor)

- A review by the UCOR EMDF Project Manager

- A technical consistency review by the primary author of the Revision 2 PA (UCOR)

- Technical reviews by various subject matter experts (primarily geologists)

- Verification that values in the document that originated in calculation packages, modeling, etc. have been correctly transcribed to the document from those sources.

More details, as well as the competed Forms-141, are included in the QA Report.

9.5　　　　　CONFIGURATION MANAGEMENT AND MAINTENANCE OF PA MODELING INFORMATION ARCHIVE

Calculation packages have been developed according to the calculation procedures and quality management protocols of the specific company responsible for model development (UCOR, Jacobs, or Drummond Carpenter). All calculation packages have been reviewed and approved under either the existing UCOR procedure PROC-DE-0704, *Project Calculations*, or PROC-WM-2031, *Waste Management Calculations*. Configuration control of calculation packages will be governed by contractor-specific protocols for change control of calculations as well as UCOR protocol. Both of these procedures require submittal of approved calculation packages to the Document Management Center (DMC) in accordance with UCOR procedure PROC-OS-1001, *Records Management, Including Document Control*. Both of the calculation procedures also require a hardcopy submittal and an electronic copy in native format (such as Word or Excel) to the DMC when possible. This requirement is being interpreted as including digital files (such as input and output files) created during the performance modeling simulations.

Configuration control and archival of digital files for the PA, supporting data, and calculation packages have been performed in accordance with UCOR procedure PROC-OS-1001, *Records Management, Including Document Control*. This procedure allows for the submittal and defines the requirements for submitting records on media other than paper (such as input and output files from performance modeling

simulations). This PA, as well as the QA Report, were entered into the DMC upon transmittal to DOE for distribution. At that time, all associated "records" were submitted to the DMC.

10. PREPARERS

Chad Drummond, PE, D.WRE, BCEE

Chad Drummond is a Principal Engineer/Modeler with Drummond Carpenter and has over 20 years of experience conceptualizing, developing, and applying environmental numerical models for sites across the United States and in Australia. His role on the EMDF PA included RESRAD-OFFSITE model conceptualization, model parameterization, and model simulation. Documentation of the RESRAD-OFFSITE modeling is included in Appendix G, the main PA report text, and associated calculations packages.

Over his career, his technical focus has been on unsaturated flow, groundwater hydrogeology, environmental assessment and remediation/restoration, and the fate and transport of various contaminants, including emerging contaminants and radionuclides. He has nearly 12 years of project experience performing environmental modeling at several DOE sites, including the Paducah Gaseous Diffusion Plant; ORR; and the Shiprock, Rocky Flats, and Tuba City DOE Legacy Management sites.

Modeling performed at Paducah Gaseous Diffusion Plant was primarily performed as part of the RI/FS and included sitewide groundwater flow and contaminant transport simulations, volatile organic compound and radionuclide leaching simulations, radon emanation modeling, and WAC modeling. WAC modeling was performed to assess disposal criteria for nearly 100 potential contaminants of interest. His experience at ORR includes the PA documented herein, modeling to specify contaminant Authorized Limits, and reviewing the ORR sitewide model to facilitate development of the site-specific RESRAD-OFFSITE model. His tasks at the various DOE Legacy Management sites include source and plume remediation, site modeling, and configuring and assessing pump tests to provide parameters for the site groundwater models.

In addition to DOE projects, he has worked on projects for other federal entities including National Air and Space Agency, Air National Guard, U.S. Army Corps of Engineers, and the U.S. Air Force. He also has experience in private sector projects and has been accepted as an expert witness and has deposition and court testimony experience.

Mr. Drummond is a licensed Professional Engineer and his credentials include BCEE (Board Certified Environmental Engineer) by the American Academy of Environmental Engineers and Scientists (AAEES) and D.WRE (Diplomate, Water Resources Engineer) by the American Academy of Water Resources Engineers. He has taught environmental modeling and environmental engineering courses to undergraduate and graduate students.

Ryan Hupfer, MS

Ryan Hupfer is a Senior Staff Geologist with Drummond Carpenter and has 4 years of experience performing environmental assessment and remediation and aquifer characterization activities. He has developed, calibrated, and applied environmental numerical models at sites in the eastern United States. Mr. Hupfer provided RESRAD-OFFSITE modeling support to the development of the EMDF source term dose at the CA POA. Prior to that, he provided modeling support on this PA. His role on the EMDF PA included parameterizing the RESRAD-OFFSITE model, conducting inadvertent human intruder and base case model simulations, and performing the sensitivity analysis and probabilistic model simulations. Mr. Hupfer provided documentation support of the completed RESRAD-OFFSITE modeling included in Appendix G, the main PA text, and associated calculations packages.

His technical focus is on hydrogeology, geochemistry, and the predictive migration and attenuation of various contaminants, including chlorinated solvents, inorganics, and radionuclides. Mr. Hupfer's project experience includes working in a variety of geologic settings, including unconsolidated sediment, fractured bedrock, and karst environments. He has applied geographic information system platforms, computer-aided design, and Python scripting to facilitate pre- and post-processing model data. In addition to his RESRAD-OFFSITE modeling experience, he has developed and used MATLAB, Surfer, AQTESOLV, and MODFLOW to assess environmental condition. He holds a bachelor's degree and a master's degree (Rutgers) in geology and is credentialed as a Professional Geologist in Tennessee and a Geologist-in-Training in Florida.

Stephen Kenworthy, Ph.D.

Steve Kenworthy is a hydrologist and environmental scientist with StrataG in Oak Ridge, TN. Dr. Kenworthy has 7 years of experience as a postdoctoral research associate and university professor focused on field and laboratory studies of fluvial hydrology and hydraulics and earth surface processes. His research experience includes field measurements and analysis of stream flow dynamics and sediment transport in agricultural settings in Illinois, field studies of slope stability in southeast Alaska, laboratory analysis and modeling of fluvial sediment transport mechanics, field studies of topographic controls on soil moisture, field monitoring and analysis of the hydrology and suspended sediment dynamics of the Green River system in Kentucky, and field monitoring of flow, sediment transport and contaminant dynamics in karst conduits of the Mammoth Cave system.

Dr. Kenworthy has over 8 years of experience providing technical support to the OREM program, including contributions to the Mercury Technology Development project, development of the EMDF RI/FS, and was the document lead for this EMDF PA. He recently participated in an international expert review of the performance analysis prepared for licensing a LLW disposal facility near Ottawa, Ontario, Canada.

Dr. Kenworthy's contributions to preparing the EMDF PA included primary responsibility for coordination and integration of the modeling team and development of the main text of the report. He also was responsible for developing the radionuclide inventory (Appendix B) and contributed to the analysis of EMDF cover performance (HELP model and Appendix C) and the analysis of IHI (Appendix I).

Changsheng Lu, Ph.D., PG

Changsheng Lu is a Professional Geologist and senior hydrogeologist with Jacobs Engineering in Oak Ridge, Tennessee. He has over 30 years of environmental modeling application experience, including 25 years of groundwater and contaminant fate and transport modeling in BCV, including support for EMWMF and the proposed EMDF. Dr. Lu has provided technical and modeling support for the EMWMF RI/FS and CA, and for the RI/FS and PA for the onsite disposal facility at the Portsmouth Gaseous Diffusion Plant as well as many other DOE, Department of Defense, EPA, and industrial clients.

Dr. Lu's contributions to development of the EMDF PA included vadose zone flow and transport analysis (STOMP model implementation, Appendix E), 3-D saturated zone flow and radionuclide transport analysis (MODFLOW and MT3D model implementation, Appendices D and F), cover and liner performance modeling (RUSLE2 model implementation and EMDF bathtub analysis in Appendix C) and the analysis of radon flux (Appendix H).

11. REFERENCES

Albrecht and Bensen 2001. "Effect of Desiccation on Compacted Natural Clays," *Journal of Geotechnical Engineering*, Vol. 127, No. 1, Paper No. 16291, B. A. Albrecht and C. H. Benson, January.

Baes et al. 1984. *A Review and Analysis of Parameters for Assessing Transport of Environmentally Released Radionuclides through Agriculture*, ORNL-5786, Oak Ridge National Laboratory, Oak Ridge, TN, September.

Bailey and Lee 1991. *Hydrogeology and Geochemistry in Bear Creek and Union Valleys, Near Oak Ridge, Tennessee*, USGS Water Resources Investigation 90-4008, Z. C. Bailey and R. W. Lee, U.S. Geological Survey, Reston, VA.

Baranski 2009. *Natural Areas Analysis and Evaluation: Oak Ridge Reservation*, ORNL/TM-2009/201, Oak Ridge National Laboratory, Oak Ridge, TN, November.

Baranski 2011. *Aquatic Natural Areas Analysis and Evaluation: Oak Ridge Reservation*, ORNL/TM-2011/13, Oak Ridge National Laboratory, Oak Ridge, TN, April.

BJC 1999. *Predesign Site Characterization Summary Report for the Environmental Management Waste Management Facility, Oak Ridge, Tennessee*, BJC/OR-255, Bechtel Jacobs Company LLC, Oak Ridge, TN, May.

BJC 2000. *Final Site Investigation Report,* SSRS Item No. 3.5, Rev. 1*,* Bechtel Jacobs Company LLC, Oak Ridge, TN, August.

BJC 2003. *Engineering Feasibility Plan for Groundwater Suppression of the Environmental Management Waste Facility, Oak Ridge, Tennessee*, BJC/OR-1478, Bechtel Jacobs Company LLC, Oak Ridge, TN.

BJC 2010a. *Summary Report on the 2010 on the Environmental Management Waste Management Facility Groundwater Model and Fate-Transport Analyses, Oak Ridge, Tennessee*, BJC/OR-3434, Bechtel Jacobs Company LLC, Oak Ridge, TN, May.

BJC 2010b. *Calculation Package for the Analysis of Performance of Cells 1-6, with Underdrain, of the Environmental Management Waste Management Facility Oak Ridge, Tennessee*, I-60442-0001, Bechtel Jacobs Company LLC, Oak Ridge, TN, March.

Bouwer 1989. The Bouwer and Rice Slug Test – An Update, *Groundwater,* Vol. 27, Issue 3, pages 304−309.

Bouwer 1991. "Simple Derivation of the Retardation Equation and Application to Preferential Flow and Macrodispersion," *Ground Water*, Vol 29, No. 1, H. Bouwer, January-February.

Bouwer and Rice 1976. *A Slug Test for Determining Hydraulic Conductivity of Unconfined Aquifers with Completely or Partially Penetrating Wells*, Water Resources Research, Vol. 12, No. 3, pages 423−428.

Boynton and Daniel 1985. "Hydraulic Conductivity Tests on Compacted Clays", *Journal of Geotechnical Engineering*, ASCE, 111(4), 465–478. Boynton, S. S., and Daniel, D. E.

Canadell et al. 1996. *Maximum rooting depth of vegetation types at the global scale*, J. Canadell, R.B. Jackson, J.R. Ehleringer, H.A. Mooney, O.E. Sala- E.-D. Schulze. Oecologia 108:583-595.

CH2M-Hill 2000. *Phase IV Final Site Investigation Report, SSRS Item No.3.3, Rev. 1,* CH2MHill Constructors, Inc., under contract to Waste Management Federal Services, Inc., for Bechtel Jacobs Company LLC, Oak Ridge, TN, March.

City Data 2020. "Races in Oak Ridge, Tennessee (TN) Detailed Stats", https://www.city-data.com/races/races-Oak-Ridge-Tennessee.html., accessed March 12.

Clapp 1998. *Environmental Sciences Division Groundwater Program Office Report of Fiscal Years 1995- 1997*, "Water Balance Modeling," Sect. 5.1, D. Huff (ed.), Environmental Sciences Division Publication No. 4751, ORNL/GWPO-027 (ESD Publ. No, 4751), pages 13-14, R. B. Clapp, Oak Ridge National Laboratory, Oak Ridge, TN.

Connell and Bailey 1989. *Statistical and Simulation Analysis of Hydraulic Conductivity Data for Bear Creek and Melton Valleys, Oak Ridge Reservation, Tennessee*, USGS Water-Resources Investigations Report 89-4062, U.S. Geological Survey, Reston, VA.

Davis et al. 1984. *Site Characterization Techniques Used at a Low-Level Waste Shallow Land Burial Field Demonstration Facility*, ORNL-9146, E. C. Davis, W. J. Boegly, Jr., E. R. Rothschild, B. P. Spalding, N. D. Yaughan C. S. Haase, D. D. Huff, S. Y. Lee, E. C. Walls, J. D. Newbold: and E. D. Smith, Oak Ridge National Laboratory, Oak Ridge, TN, July.

DOE 1992a. *Federal Facility Agreement for the Oak Ridge Reservation*, DOE/OR-1014, U.S. Environmental Protection Agency Region 4, Atlanta, GA; U.S. Department of Energy, Oak Ridge, TN; and Tennessee Department of Environment and Conservation, Nashville, TN, January.

DOE 1992b. *Site Characterization Summary Report for Waste Area Grouping 1 at Oak Ridge National Laboratory, Oak Ridge, Tennessee Vol. 3*, DOE/OR/01-1043/V3&D1, U.S. Department of Energy, Oak Ridge, TN, September.

DOE 1997a. *Hazard Categorization and Accident Analysis Techniques for Compliance with DOE Order 5480.23, Nuclear Safety Analysis Reports*, DOE-STD-1027-92, U.S. Department of Energy, Washington, D.C., December.

DOE 1997b. *Report on the Remedial Investigation of Bear Creek Valley at the Oak Ridge Y-12 Plant, Oak Ridge, Tennessee*, DOE/OR/01-1455/V1-V6&D2, U.S. Department of Energy, Oak Ridge, TN, May.

DOE 1997c. *Feasibility Study for Bear Creek at the Oak Ridge Y-12 Plant, Oak Ridge, Tennessee*, DOE/OR/02-1525/V2&D2, U.S. Department of Energy, Oak Ridge, TN, November.

DOE 1998a. *Remedial Investigation/Feasibility Study for the Disposal of Oak Ridge Reservation Comprehensive Environmental Response, Compensation, and Liability Act of 1980 Waste*, DOE/OR/02-1637&D2, U.S. Department of Energy, Oak Ridge, TN, January.

DOE 1998b. *Addendum to Remedial Investigation/Feasibility Study for the Disposal of Oak Ridge Reservation Comprehensive Environmental Response, Compensation, and Liability Act of 1980 Waste*, DOE/OR/02-1637&D2/A1, U.S. Department of Energy, Oak Ridge, TN, September.

DOE 1999a. *Record of Decision for the Disposal of Oak Ridge Reservation Comprehensive Environmental Response, Compensation, and Liability Act of 1980 Waste*, DOE/OR/01-1791&D3, U.S. Department of Energy, Oak Ridge, TN, November.

DOE 1999b. *Proposed Plan for the Disposal of Oak Ridge Reservation Comprehensive Environmental Response, Compensation, and Liability Act of 1980 Waste*, DOE/OR/01-1761&D3, U.S. Department of Energy, Oak Ridge, TN, January.

DOE 2000. *Record of Decision for the Phase I Activities in Bear Creek Valley at the Oak Ridge Y-12 Plant, Oak Ridge, Tennessee*, DOE/OR/01-1750&D4, U.S. Department of Energy, Oak Ridge, TN, May.

DOE 2001a. *Attainment Plan for Risk/Toxicity-Based Waste Acceptance Criteria at the Oak Ridge Reservation, Oak Ridge, Tennessee*, DOE/OR/01-1909&D3, U.S. Department of Energy, Oak Ridge, TN, October.

DOE 2001b. *Radioactive Waste Management*, DOE Order 435.1 Chg 1 (PgChg), U.S. Department of Energy, Washington, D.C., August.

DOE 2004. *Environmental Management Waste Management Facility Capacity Assurance Remedial Action Report*, DOE/OR/01-2145&D2, U.S. Department of Energy, Oak Ridge, TN, September.

DOE 2008. *Oak Ridge Reservation Planning: Integrating Multiple Land Use Needs*, DOE/ORO/01-2264, U.S. Department of Energy, Oak Ridge, TN, May.

DOE 2010a. *Explanation of Significant Differences for the Record of Decision for the Disposal of Oak Ridge Reservation Comprehensive Environmental Response, Compensation, and Liability Act of 1980 Waste, Oak Ridge, Tennessee*, DOE/OR/01-2426&D2, U.S. Department of Energy, Oak Ridge, TN, May.

DOE 2010b. *Program and Project Management for the Acquisition of Capital Assets*, DOE Order 413.3B Chg5 (MinChg), U.S. Department of Energy, Washington, D.C., April.

DOE 2011a. *Radioactive Waste Management Manual*, DOE Manual 435.1-1 Chg 2, U.S. Department of Energy, Washington, D.C., June.

DOE 2011b. *Derived Concentration Technical Standard*, DOE-STD-1196-2011, U.S. Department of Energy, Washington, D.C., April.

DOE 2011c. *Final Site-Wide Environmental Impact Statement for the Y-12 National Security Complex*, DOE/EIS-0387, U.S. Department of Energy, Oak Ridge, TN, February.

DOE 2012. *EM Quality Assurance Program*, EM-QA-001 Rev. 1, U.S. Department of Energy, Washington, D.C., June 11.

DOE 2013a. *Radiation Protection of the Public and the Environment*, DOE Order 458.1, U.S. Department of Energy, Office of Health, Safety, and Security, Washington, D.C.

DOE 2013b. *Quality Assurance*, DOE Order 414.1D, Admin Chg 1, U.S. Department of Energy, Washington, D.C., May 8.

DOE 2013c. *Groundwater Strategy for the U.S. Department of Energy, Oak Ridge Reservation, Oak Ridge, Tennessee*, DOE/OR/01-2628/V2&D1, U.S. Department of Energy, Oak Ridge, TN, September.

DOE 2014. *Optimizing Radiation Protection of the Public and the Environment for use with DOE O 458.1, ALARA Requirements*, DOE-HDBK-1215-2014, U.S. Department of Energy, Washington, D.C., October.

DOE 2015a. *Oak Ridge Reservation Annual Site Environmental Report for 2014*, DOE/ORO/2502, U.S. Department of Energy, Oak Ridge, TN, September.

DOE 2015b. *2015 Remediation Effectiveness Report for the U.S. Department of Energy Oak Ridge Reservation Oak Ridge, Tennessee*, DOE/OR/01-2675&D1, U.S. Department of Energy, Oak Ridge, TN, March.

DOE 2015c. *Performance Assessment Report for the Proposed Disposal Facility at the Portsmouth Gaseous Diffusion Plant, Piketon, Ohio*, DOE/PPPO/03-0607&D2, U.S. Department of Energy, Lexington, KY.

DOE 2016a. *Oak Ridge Reservation Regional Groundwater Flow Model Development – Fiscal Year 2016 Progress Report, 2016*, DOE/OR/01-2743&D1, U.S. Department of Energy, Oak Ridge, TN.

DOE 2016b. *Sampling and Analysis Plan/Quality Assurance Project Plan for Environmental Monitoring at the Environmental Management Waste Management Facility, Oak Ridge, Tennessee*, DOE/OR/01-2734&D1, U.S. Department of Energy, Oak Ridge, TN, November.

DOE 2017a. *2017 Disposal Authorization Statement and Tank Closure Documentation*, DOE-STD-5002-2017, U.S. Department of Energy, Washington, D.C, July.

DOE 2017b. *Remedial Investigation/Feasibility Study for Comprehensive Environmental Response, Compensation, and Liability Act Oak Ridge Reservation Waste Disposal, Oak Ridge, Tennessee*, DOE/OR/01-2535&D5, U.S. Department of Energy, Oak Ridge, TN, February.

DOE 2017c. *Remediation Effectiveness Report for the U.S. Department of Energy Oak Ridge Reservation, Oak Ridge, Tennessee*, DOE/OR/01-2731&D2, U.S. Department of Energy, Oak Ridge, TN.

DOE 2018a. *Proposed Plan for the Disposal of Oak Ridge Reservation Comprehensive Environmental Response, Compensation, and Liability Act (CERCLA) Waste*, DOE/OR/01-2695&D2/R1 U.S. Department of Energy, Oak Ridge, TN, September.

DOE 2018b. *Technical Memorandum #1, Environmental Management Disposal Facility Phase 1 Field Sampling Results Oak Ridge, Tennessee*, DOE/OR/01-2785&D1, U.S. Department of Energy, Oak Ridge, TN, July.

DOE 2018c. *2018 Remediation Effectiveness Report for the U.S. Department of Energy Oak Ridge Site, Oak Ridge, Tennessee*, DOE/OR/01-2757&D2, U.S. Department of Energy, Oak Ridge, TN, September.

DOE 2019. *Technical Memorandum #2, Environmental Management Disposal Facility, Phase 1 Monitoring*, DOE/OR/01-2819&D1, U.S. Department of Energy, Oak Ridge, TN, May.

Dorsch and Katsube 1996. *Effective Porosity and Pore-Throat Sizes of Mudrock Saprolite from the Nolichucky Shale within Bear Creek Valley on the Oak Ridge Reservation: Implications for Contaminant Transport and Retardation Through Matrix Diffusion*, ORNL/GWPO-025, J. Dorsch and T. J. Katsube, Oak Ridge National Laboratory, Oak Ridge, TN, May.

Dorsch et al. 1996. *Effective Porosity and Pore-Throat Sizes of Conasauga Group Mudrock: Application, Test and Evaluation of Petrophysical Techniques*, ORNL/GWPO-021, J. Dorsch, T. J. Katsube, W. E. Sanford, B. E. Dugan, and L. M. Tourkow, Oak Ridge National Laboratory, Oak Ridge, TN.

Dreier et al. 1987. "Vol. 42, Flow and Transport Through Unsaturated Fractured Rock," *American Geophysical Union Monograph*, R. B. Dreier, D. K. Solomon, and C. M. Beaudoin, pages 51-59.

Dreier et al. 1993. *Results and Interpretation of Groundwater Data Obtained from Multiport-Instrumented Coreholes (GW-131 through GW-135), Fiscal Years 1990 and 1991*, Y/TS-803, R.B. Dreier, T.O. Early, and H.L. King, Oak Ridge National Laboratory, Oak Ridge, TN, January.

Dreier and Davidson 1994. "Fracture Spacing and Connectivity Observed in Multiport Instrumented Wells," *Geological Society of America Abstracts with Programs*, v. 25, no. 7, p. A412, R. B. Dreier and G.L. Davidson.

Driese et al. 2001. "Lithologic and pedogenic influences on porosity distribution and groundwater flow in fractured sedimentary saprolite: a new application of environmental sedimentology", S. G. Dreise, L. D. McKay, and C. P. Penfield, *Journal of Sedimentary Research*, Vol.71, No. 5, September, p.843-857.

EPA 1990. *Exposure Factors Handbook*, EPA/600/8-89/043, U.S. Environmental Protection Agency, Office of Health and Environmental Assessment, Washington, D.C.

EPA 1999. *Understanding Variation In Partition Coefficient, K_d, Values. Volume II: Review of Geochemistry and Available K_d Values for Cadmium, Cesium, Chromium, Lead, Plutonium, Radon, Strontium, Thorium, Tritium (^3H), and Uranium*, EPA 402-R-99-004B, U.S. Environmental Protection Agency, Office of Air and Radiation, Washington, D.C., August.

EPA 2000. Final Radionuclides Rule, 66 Federal Register 76708, Vol. 65, No. 236, U.S. Environmental Protection Agency, December 7.

EPA 2002a. *Radionuclides in Drinking water: A Small Entity Compliance Guide,* U.S. Environmental Protection Agency, Office of Ground Water and Drinking Water, Washington, D.C., February.

EPA 2002b. *U.S. Implementation Guidance for Radionuclides,* EPA 816-F-00-002, U.S. Environmental Protection Agency, Office of Ground Water and Drinking Water, Washington, D.C., March.

EPA 2004. *Understanding Variation in Partition Coefficient, K_d, Values*, EPA 402-R-04-002C, U.S. Environmental Protection Agency, Office of Air and Radiation, Washington, D.C., July.

EPA 2011. *Exposure Factors Handbook: 2011 Edition*, EPA/600/R-090/052F, U.S. Environmental Protection Agency, Washington, D.C., September.

Evans et al. 1996. "Application of particle tracking and inverse modeling to reduce flow model calibration uncertainty in an anisotropic aquifer system," *Proceedings of the ModelCARE 96 Conference: Calibration and Reliability in Groundwater Modelling*, E. K. Evans, C. Lu, S. Ahmed, and J. Archer, Golden, CO.

Friedman et al. 1990. *Laboratory Measurement of Radionuclides Sorption in Solid Waste Storage Area 6 Soil/Groundwater Systems*, ORNL/TM-10561, Oak Ridge National Laboratory, Oak Ridge, TN, June.

Gelhar et al. 1992. "A Critical Review of Data on Field-Scale Dispersion in Aquifer," L. W. Gelhar, C. Welty, and K. R. Rehfeldt, *Water Resources Research*, v. 28, no. 7, pages 1955-1974.

Geraghty and Miller 1986. *Aquifer Test Data and Design of Recovery Wells, S-3 Ponds*, Y/SUB/86-O0206C/3, Geraghty and Miller, Oak Ridge, TN.

Geraghty and Miller 1990. *Development of Ground-Water Flow Models for the S-3 Waste Management Area, Y-12 Facility, Oak Ridge, Tennessee*, Y/SUB/89-00206C/3, Geraghty and Miller, Oak Ridge, TN.

Gil-Garcia et al. 2008. "New best estimates for radionuclide solid–liquid distribution coefficients in soils. Part 3: miscellany of radionuclides (Cd, Co, Ni, Zn, I, Se, Sb, Pu, Am, and others)", *Journal of Environmental Radioactivity*, 100, 704–715.

Gnanapragasam and Yu 2015. *User's Guide for RESRAD-OFFSITE*, NUREG/CR-7189, ANL/EVS/TM-14/2, E. K. Gnanapragasam and C. Yu, Argonne National Laboratory, Argonne, IL, U.S. Nuclear Regulatory Commission, Rockville, MD, April.

Golder 1988a. *Task 2 – Well Logging and Geohydrologic Testing, Site Characterization, and Groundwater Flow Computer Model Application*, Vol. 1, Martin Marietta Energy Systems, Inc. (MMES) Contract No. 30X-SA706C; Golder Associates, Inc., May (copy unavailable).

Golder 1988b. *Task 5 – Contaminant Transport Model Validation, Geohydrologic Site Characterization, and Groundwater Flow Computer Model Application*, Vol. 1, MMES Contract No. 30X-SA706C; ORNL/Sub/88-SA706/5/V1, Golder Associates, Inc., September.

Golder 1989. *Task 7 – Groundwater Flow Computer Model*, MMES Contract No. 30X-SA706C, Golder Associates, Inc., September.

Gu et al. 2011. "Dissolution of technetium (IV) oxide by natural and synthetic organic ligands under both reducing and oxidizing conditions", B. Gu, Wenming Dong, Liyuan Liang, and N. A. Wall, *Environmental Science & Technology* 45, 4771-4777.

Haase 1991. *Geochemical Identification of Groundwater Flow Systems in Fractured Bedrock Near Oak Ridge, Tennessee*, C. S. Haase, Oak Ridge National Laboratory, Oak Ridge, TN. Source: info.ngwa.org/gwol/pdf/910155202.pdf.

Haase et al. 1985. *Geology of the Host Formation for the New Hydrofracture Facility at the Oak Ridge National Laboratory*, C. S. Haase, S. H. Stow, and C. L. Zucker, Waste Man agement Symposium 1985, v. 2, pages 473-480.

Haase et al. 1987. *Geochemistry of Formation Waters in the Lower Conasauga Group at the New Hydrofracture Facility: Preliminary Data from the Deep Monitoring (DM) wells*, ORNL/RAP-6, C. S. Haase, J. Switek, and S. H. Stow, Oak Ridge National Laboratory, Oak Ridge, TN.

Hatcher et al. 2012. *Large earthquake paleoseismology in the East Tennessee seismic zone: Results of an 18-month pilot study*, Special Paper 493, R. D. Hatcher, Jr., J. D. Vaughn, and S. F. Obermeier, The Geological Society of America, Boulder, CO.

IAEA 2010. *Handbook of Parameter Values for the Prediction of Radionuclide Transfer in Terrestrial and Freshwater Environments*, Technical Reports Series No. 472, International Atomic Energy Agency, Vienna, Austria.

ICRP (International Commission on Radiological Protection) 2008. *Nuclear Decay Data for Dosimetric Calculations*, Publication 107, International Commission on Radiological Protection, Ottawa, Ontario K1P 5S9, Canada.

Jackson et al. 1996. *A global analysis of root distributions for terrestrial biomes.* R.B. Jackson, J. Canadell, J.R. Ehleringer, H.A. Mooney, O.E. Sala- E.-D. Schulze. Oecologia 108:389-411.

Kaplan et al. 2000. "Iodide Sorption to Subsurface Sediments and Illitic Minerals", D. I. Kaplan, R.J. Serne, K.E. Parker, and I.V Kutnyakov, *Environmental Science and Technology*, 34 (3) pages 399-405, December.

Kaplan et al. 2013. *Radioiodine Geochemistry in the SRS Subsurface Environment*, SRNL-STI-2012-00518, D. I. Kaplan, H. P. Emerson, B. A.Powell, K. A. Roberts, S. Zhang, C. Xu, K. A. Schwehr, H. P. Li, Y. F. Ho, M. E. Denham, C. Yeager, and P. H. Santschi, Savannah River National Laboratory, Aiken, SC, May.

Kaplan et al. 2014. "Radioiodine biogeochemistry and prevalence in groundwater", D. I. Kaplan, M. E. Denham, S. Zhang, C. Yeager, C. Xu, K. A. Schwehr, H. P. Li, Y. F. Ho, D. Wellman, and P. H. Santschi, *Critical Reviews of Environmental Science and Technology*, 44, 2287-2337.

Kim et al. 2009. "Mineralogical characterization of saprolite ast the FRC background site in Oak Ridge, Tennessee", Y-J.Kim, J-W. Moon, Y. Roh, and S.C. Brooks, *Environmental Geology* 58: 1301-1307.

King and Haase 1987. *Subsurface-Controlled Geological Maps for the Y-12 Plant and Adjacent Areas of Bear Creek Valley*, ORNL/TM-10112, H. L. King and C. S. Haase, Oak Ridge National Laboratory, Oak Ridge, TN.

Kitchings and Mann 1976. *A Description of the Terrestrial Ecology of the Oak Ridge Environmental Research Park*, ORNL/TM-5073, T. Kitchings and L. K. Mann, Oak Ridge National Laboratory, Oak Ridge, TN.

Law Engineering 1983. *Results of Ground-Water Monitoring Studies at Y-12 Plant*, Y/SUB/83-47936/1, Law Engineering, Oak Ridge, TN.

Lee and Ketelle 1989. *Geology of the West Bear Creek Site*, ORNL/TM-10887 R. R. Lee and R. H. Ketelle, Oak Ridge National Laboratory, Oak Ridge, TN.

Lee et al. 1992. "Aquifer Analysis and Modeling in a Fractured Heterogeneous Medium," R. R. Lee, R. H. Ketelle, J. M. Bownds, and T. A. Rizk, *Groundwater*, vol. 30, no. 4, pages 589-597.

Lemiszki, P. J. 2000. *Geologic Map of the Bethel Valley Quadrangle, Tennessee*, Geologic Quadrangle Map 130-NE, Tennessee Division of Geology, Nashville, TN.

Lietzke et al. 1988. *Soils, Surficial Geology, and Geomorphology of the Bear Creek Valley Low-Level Waste Disposal Development and Demonstration Program Site*, ORNL/TM-10573, D. A. Lietzke, S. Y. Lee, and R. E. Lambert, Oak Ridge National Laboratory, Oak Ridge, TN.

Lozier et al. 1987. Aquifer Pump Test with Tracers, ORNL/SUB/86-32136, Golder and Associates, Inc., October.

Maheras et al. 1997. *Addendum to Radioactive Waste Management Complex Low-Level Waste Radiological Performance Assessment*, INEEL/EXT-97-00462 (formerly EGG-WM-8773), S. J. Maheras, A. S. Rood, S. O. Magnuson, M. E. Sussman, and R. N. Bhatt, Idaho National Engineering and Environmental Laboratory, Idaho Falls, ID, April.

McCracken et al. 2015. *Bat Species Distribution on the Oak Ridge Reservation*, ORNL/TM-2015/248, M. K. McCracken, N. R. Giffen, A. M. Haines, B. J. Guge, and J. W. Evans, Oak Ridge National Laboratory, Oak Ridge, TN, October.

McKay et al. 1997. "EPM Modeling of a Field-Scale Tritium Tracer Experiment in Fractured, Weathered Shale," *Groundwater*, vol. 35, no.6, pages 997–1007, L. D. McKay, P. L. Stafford, and L. E. Toran.

McKay et al. 2000. "Field-Scale Migration of Colloidal Tracers in a Fractured Shale Saprolite," *Groundwater*, vol. 38, no.1, pages 139–147, L. D. McKay, W. E. Sanford, and J. M. Strong.

Moline and Schreiber 1996. *FY94 Site Characterization and Multilevel Well Installation at a West Bear Creek Valley Research Site on the Oak Ridge Reservation*, ORNL/TM-13029, G.R. Moline and M. E. Schreiber, Oak Ridge National Laboratory, Oak Ridge, TN, March.

Moline et al. 1998. "Discussion of Nativ, et al. 1997," *Groundwater,* Vol. 36, No. 5, pages 711-712, G. R. Moline, C. T. Rightmire, R. H. Ketelle, and D. D. Huff.

Moore and Toran 1992. *Supplement to a Hydrogeologic Framework for the Oak Ridge Reservation*, ORNL/TM-12191, G. K. Moore and L. E. Toran, Oak Ridge National Laboratory, Oak Ridge, TN, November.

Nativ et al. 1997a. *The Deep Hydrologic Flow System Underlying the Oak Ridge Reservation – Assessing the Potential for Active Groundwater Flow and Origin of the Brine*, ORNL/GWPO-018, R. Nativ, A. Halleran, and A. Hunley, Oak Ridge National Laboratory, Oak Ridge, TN.

Nativ et al. 1997b. "Evidence for Groundwater Circulation in the Brine-Filled Aquitard," R. Nativ, A. Halleran, and A. Hunley, Oak Ridge, Tennessee, *Groundwater*, Vol. 35, No. 4, July-August.

Nichols et al. 1997. *STOMP – Subsurface Transport Over Multiple Phases Application Guide*, PNNL-11216 (UC-2010), W. E. Nichols, N. J. Aimo, M. Oostrom, M. D. White, Pacific Northwest National Laboratory, Richland, WA.

NRC 1984. *Radon Attenuation Handbook for Uranium Mill Tailings Cover Design*, NUREG/CR-3533, U.S. Nuclear Regulatory Commission, Washington, D.C., April.

Ogden 1993a. *Geotechnical Study, ORR Storage Facility, Site "B", Y-12 Plant, Oak Ridge, Tennessee,* Contract No. 88B-99977V, Release C-53, Ogden Environmental and Energy Services, Knoxville, TN, May.

Ogden 1993b. *Geotechnical Study, ORR Storage Facility, Site "C", Y-12 Plant, Oak Ridge, Tennessee,* Contract No. 88B-99977V, Release C-53, Ogden Environmental and Energy Services, Knoxville, TN, May.

ORNL 1984. *Site Characterization Techniques Used at a Low-Level Waste Shallow Land Burial Field Demonstration Facility*, ORNL-9146, Oak Ridge National Laboratory, Oak Ridge, TN, July.

ORNL 1987. *Geochemical Behavior of Cs, Sr, Tc, Np, and U in Saline Groundwaters: Sorption Experiments on Shales and Their Clay Mineral Components*, ORNL/TM-10364, Oak Ridge National Laboratory, Oak Ridge, TN, November.

ORNL 1992a. *Status Report on the Geology of the Oak Ridge Reservation*, ORNL/TM 12074, Environmental Sciences Division Publication No. 3860, Oak Ridge National Laboratory, Oak Ridge, TN, October.

ORNL 1992b. *Status Report: A Hydrologic Framework for the Oak Ridge Reservation,* ORNL/TM-12026, Oak Ridge National Laboratory, Oak Ridge, TN, May.

ORNL 1996. *Report on the Biological Monitoring Program for Bear Creek at the Oak Ridge Y-12 Plant, Oak Ridge, Tennessee (1989-1994)*, ORNL/TM-12884, ESD Publication No. 4357, R. L. Hinzman (ed.), Oak Ridge National Laboratory, Oak Ridge, TN, April.

ORNL 1997a. *Performance Assessment for Continuing and Future Operations at Solid Waste Disposal Area 6*, ORNL-6783/R1, Volume 1, Oak Ridge National Laboratory, Oak Ridge, TN, September.

ORNL 1997b. *Performance Assessment for the Class L-II Disposal Facility,* ORNL/TM-13401, Oak Ridge National Laboratory, Oak Ridge, TN, March.

ORNL 2002. *Oak Ridge National Laboratory Land and Facilities Plan*, ORNL/TM-2002/1, Oak Ridge National Laboratory, Oak Ridge, TN.

ORNL 2014. *Climate Normals (1981-2010) and Extremes (1948-2015) for Oak Ridge, Tennessee (Town Site) with 2015 Comparisons*, Oak Ridge National Laboratory, Oak Ridge, TN. https://web.ornl.gov/~birdwellkr/web/Normals/30YEARNorm.pdf, last accessed March 12, 2018.

ORNL 2018. *Natural Resource Assessment for the Proposed Environmental Management Disposal Facility (EMDF), Oak Ridge, Tennessee*, ORNL/TM-2018/515, Oak Ridge National Laboratory, Oak Ridge, TN, June.

Parr and Hughes 2006. *Oak Ridge Reservation Physical Characteristics and Natural Resources*, ORNL/TM-2006/110, P. D. Parr and J.F. Hughes, Oak Ridge National Laboratory, Oak Ridge, TN.

Peterson et al. 2005. *Environmental Survey Report for the ETTP: Environmental Management Waste Management Facility (EMWMF) Haul Road Corridor, Oak Ridge, Tennessee*, ORNL/TM-2005/215, M. J. Peterson, N. R. Giffen, M. G. Ryon, L. R. Pounds, and E. L. Fyan, Jr., Oak Ridge National Laboratory, Oak Ridge, TN, September.

Peterson et al. 2009. *Performance Monitoring Report for the Restored North Tributary 3 (NT-3), Bear Creek Valley, Oak Ridge, Tennessee*, ORNL/TM-2009/53, M. J. Peterson, J. G. Smith, M. G. Ryon, W. K. Roy, and J. A. Darby, Oak Ridge National Laboratory, Oak Ridge, TN.

PNNL 2003. *A Compendium of Transfer Factors for Agricultural and Animal Products,* PNNL-13421, L. H. Staven, B. A. Napier, K. Rhoads, and D. L. Strenge, Pacific Northwest National Laboratory, Richland, WA, June.

Powell et al. 1994. *A Seismotectonic Model for the 300-Kilometer-Long Eastern Tennessee Seismic Zone*, *Science*, v. 264, 29, C. A. Powell, G. A. Bollinger, M. C. Chapman, M. S. Sibol, A. C. Johnston, and R. L. Wheeler, April, pages 686–688.

Putnam et al. 1999. *Food Consumption, Prices, and Expenditure, 1970–1997,* J. J. Putnam, J. E. Allshouse, U.S. Department of Agriculture, Statistical Bulletin No. 965, Washington, D.C., April.

Robinson and Johnson 1995. *Results of a Seepage Investigation at Bear Creek Valley, Oak Ridge, Tennessee January – September 1994*, USGS Open-File Report 95-459, J. A. Robinson and G. C. Johnson, U.S. Geological Survey, Reston, VA.

Robinson and Mitchell 1996. *Gaining, Losing, and Dry Stream Reaches at Bear Creek Valley, Oak Ridge, Tennessee March and September 1994*, USGS Open-File Report 96-557, J. A. Robinson and R. L. Mitchell III, U.S. Geological Survey, Reston, VA.

Rosensteel and Trettin 1993. *Identification and Characterization of Wetlands in the Bear Creek Watershed*, Y/TS-1016, B. A. Rosensteel and C. C. Trettin, Environmental Sciences Division, Oak Ridge National Laboratory, Oak Ridge, TN, October.

Rothschild et al. 1984. *Characterization of Soils at Proposed Solid Waste Storage Area (SWSA) 7*, ORNL/TM-9326, E. R. Rothschild, D. D. Huff, B. P. Spalding, S. Y. Lee, R.B. Clapp, D. A. Lietzke, R. G. Stansfield, N. D. Farrow, C. D. Farmer, I. L. Munro, Oak Ridge National Laboratory, Oak Ridge, TN, December.

Ryon 1998. *Evaluation of Protected, Threatened, and Endangered Fish Species in Upper Bear Creek Watershed*, ORNL/M-6567, M. G. Ryon, Oak Ridge National Laboratory, Oak Ridge, TN.

Sanford and Solomon 1998. "Site characterization and containment assessment with dissolved gases", *J. Environmental Engineering*, vol. 124, no. 6, pages 572-574, W. E. Sanford and D. K. Solomon.

Sanford et al. 1996. "Dissolved gas tracers in groundwater: Simplified injection, sampling, and analysis," *Water Resources Research*, vol. 32, no. 6, pages 1635-642, W. E. Sanford, R. G. Shropshire, and D. K. Solomon.

Schreiber 1995. *Spatial Variation in Groundwater Chemistry in Fractured Rock: Nolichucky Shale, Oak Ridge, TN*, M. E. Schrieber, Master Thesis: University of Wisconsin-Madison, Madison, WI.

Schreiber et al. 1999. "Using Hydrochemical Facies to Delineate Groundwater Flowpaths in Fractured Shale," *Groundwater Monitoring Review – Winter 1999*, p. 95-109, M. E. Schreiber, G. R. Moline, and J. M. Bahr.

Schroeder et al. 1994. *The Hydrologic Evaluation of Landfill Performance (HELP) Model: Engineering Documentation for Version 3*, EPA/600/R-94/168b, P. R. Schroeder, T. S. Dozier, P. A. Zappi, B. M. McEnroe, J. W. Sjostrom, and R. L. Peyton, U.S. Environmental Protection Agency, Office of Research and Development, Washington, D.C., September.

Serne R., 2007. *Kd Values for Agricultural and Surface Soils for Use in Hanford Site Farm, Residential, and River Shoreline Scenarios,* PNNL-16531, Pacific Northwest National Laboratory, Richland, WA, August.

Sheppard and Thibault 1990. "Default Soil Solid/Liquid Partition Coefficients, K_ds, for Four Major Soil Types: A Compendium," *Health Physics*, M. Sheppard and D. H. Thibault, Vol. 59, No. 4, pages 471-481, October.

Sledz and Huff 1981. *Computer Model for Determining Fracture Porosity and Permeability in the Conasauga Group, Oak Ridge National Laboratory, Tennessee*, ORNL/TM-7695, J. J. Sledz and D. D. Huff, Oak Ridge National Laboratory, Oak Ridge, TN.

Smith and Vaughn 1985. "Aquifer test analysis in nonradial flow regimes: A case study," *Ground Water*, Vol. 23, no. 2, pages 167-175, E. D. Smith and N. D. Vaughn.

Southworth et al. 1992. *Ecological Effects of Contaminants and Remedial Actions in Bear Creek,* ORNL/TM-11977, G. R. Southworth, J. M. Loar, M. G. Ryon, J. S. Smith, A. J. Stewart, and J. A. Burris, Oak Ridge National Laboratory, Oak Ridge, TN.

Stafford et al. 1998. "Influence of fracture truncation on dispersion: A dual permeability model," *Journal of Contaminant Hydrology*, 30, p. 79-100, P. Stafford, L. Toran, and L. McKay.

Stover and Coffman 1993. *Seismicity of the United States 1568 – 1989 (Revised)*, USGS Prof. Paper 1527, C. W. Stover and J. L. Coffman, U.S. Geological Survey, Reston, VA.

Stumm, W, and J Morgan 1996. "Aquatic Chemistry, Chemical Equilibria and Rates in Natural Waters," John Wiley & Sons, Inc., New York.

Tang et al. 2010. "Long-Term Nitrate Migration and Attenuation in a Saprolite/Shale Pathway from a Former Waste Disposal Site," abstract published in *Geochinica et Cosmochimica Acta*, vol. 27, no. 12, Supplement 1 A1118 for Goldschmidt 2010 Conference, G. Tang, D. B. Watson, J. C. Parker, P. M. Jardine, and S. C. Brooks, S.C.

Tian et al. 2017. "Antioxidant Depletion and Service Life Prediction for HDPE Geomembranes Exposed to Low-Level Radioactive Waste Leachate", *Geotechnical & Geoenvironmental Engineering*, K. Tian, C. H. Benson, J. M. Tinjum, Vol. 143 Issue 6, June.

TVA 2012. *Water Use in the Tennessee Valley for 2010 and the Projected Use in 2035*, Tennessee Valley Authority, Knoxville, TN, July.

TVA 2016. Clinch River Nuclear Site License-Application for Early Site Permit (ESP), Site Safety Analysis Report (SSAR), Revision 0, May 25.

UCOR 2013. *Engineering Feasibility Plan for the Elevated Groundwater Levels in the Vicinity of PP-01, EMWMF, Oak Ridge, Tennessee*, UCOR-4517, UCOR, Oak Ridge, TN.

UCOR 2014. *Oak Ridge Reservation Regional Groundwater Flow Model Development – Fiscal Year 2014 Progress Report*, *U.S. Department of Energy Oak Ridge Reservation Oak Ridge, Tennessee*, UCOR-4634/R0, UCOR, Oak Ridge, TN, November.

UCOR 2015. *Regional Groundwater Flow Model Development – Fiscal Year 2015 Progress Report, U.S. Department of Energy Oak Ridge Reservation Oak Ridge, Tennessee*, UCOR-4753/R0, UCOR, Oak Ridge, TN, December.

UCOR 2018a. *Safety Design Strategy for the Environmental Management Disposal Facility, Y-12 National Security Complex, Oak Ridge, Tennessee*, SDS-YT-EMDF-0001/R1, UCOR, Oak Ridge, TN, September.

UCOR 2018b. *Conceptual Safety Design Report for the Environmental Management Disposal Facility, Y-12 National Security Complex, Oak Ridge, Tennessee*, CSDR-YT-EMDF-0001, UCOR, Oak Ridge, TN, February.

UCOR 2019. *URS | CH2M Oak Ridge LLC Quality Assurance Program Plan Oak Ridge, Tennessee*, UCOR-4141/R6, UCOR, Oak Ridge, TN, June.

UCOR 2020a. *Composite Analysis for the Environmental Management Waste Management Facility and the Environmental Management Disposal Facility, Oak Ridge, Tennessee*, UCOR-5095/R2 UCOR, Oak Ridge, TN, April.

UCOR 2020b. *Quality Assurance Report for Modeling of the Bear Creek Valley Low-level Radioactive Waste Disposal Facilities, Oak Ridge, Tennessee,* UCOR-5234/R0, UCOR, Oak Ridge, TN, April.

USDA 1986. *Urban Hydrology for Small Watersheds (TR-55)*, U.S. Department of Agriculture Natural Resources Conservation Service, Conservation Engineering Division Technical Release 55, June.

USGS 1988a. *A Modular Three-Dimensional Finite Difference Groundwater Flow Model,* Book 6, Modeling Techniques, Chapter A1, M. G. McDonald and A. W. Harbaugh, U.S. Geological Survey, Reston, VA.

USGS 1988b. *Preliminary Evaluation of Groundwater Flow in Bear Creek Valley, Oak Ridge Reservation, Tennessee*, WRIR 88-4010, U.S. Geological Survey, Reston, VA.

USGS 1989. *Study and Interpretation of the Chemical Characteristics of Natural Water*, U.S. Geological Survey Water-Supply Paper 2254, J. D. Hem, U.S. Geological Survey, Reston, VA.

USGS 2013. Earthquake Probability Map for Magnitude 5 and 7 within 1000 years for Oak Ridge, Tennessee, map developed at http://geohazards.usgs.gov/eqprob/2009/index.php on October 18.

USGS 2020. Earthquake Magnitude, Energy Release, and Shaking Intensity, U.S. Geological Survey, https://www.usgs.gov/natural-hazards/earthquake-hazards/science/earthquake-magnitude-energy-release-and-shaking-intensity.

Valocchi 1985. "Validity of the Local Equilibrium Assumption for Modeling Sorbing Solute Transport Through Homogeneous Soils," *Water Resources Research*, Vol 21, No. 6, pages 808-820, A. J. Valocchi, June.

Watson et al. 2004. *The Oak Ridge Field Research Center Conceptual Model,* Environmental Sciences Division, Oak Ridge National Laboratory, August.

Webster 1996. *Results of Ground-Water Tracer Tests Using Tritiated Water at Oak Ridge National Laboratory, Tennessee*, Water-Resources Investigations Report 95-4182, D. A. Webster, U.S. Geological Survey, Reston, VA.

White and Oostrom 2000. *STOMP Subsurface Transport over Multiple Phases: Theory Guide*, PNNL-12030 (UC-2010), M. D. White and M. Oostrom, Pacific Northwest National Laboratory, Richland, WA.

White and Oostrom 2006. *STOMP Subsurface Transport over Multiple Phases, Version 4.0, User's Guide*, PNNL-15782, M. D. White and M. Oostrom, Pacific Northwest National Laboratory, Richland, WA.

WMFS 2000. *Final Site Investigation Report, SSRS Item No. 3.5, Rev. 1*, August 2000, prepared for Bechtel Jacobs Company LLC, Oak Ridge, TN, August.

Xu et al. 2015. "Radioiodine Sorption/desorption and Speciation Transformation by Subsurface Sediments from the Hanford Site", *Journal of Environmental Radioactivity*, 139, pg. 43-55.

Yu et al. 2001. *User's Manual for RESRAD Version 6*, ANL/EAD-4 C. Yu, A.J. Zielen, J.-J. Cheng, D.J. LePoire, E. Gnanapragasam, S. Kamboj, J. Arnish, A. Wallo III, W.A. Williams, and H. Peterson Environmental Assessment Division Argonne National Laboratory, Argonne, IL, July.

Yu et al. 2007. *User's Manual for RESRAD-OFFSITE Version 2* ANL/EVS/TM/07-1, C. Yu, E. K. Gnanapragasam, B. M. Biwer, S. Kamboj, J.-J. Cheng, T. Klett, D. LePoire, A. J. Zielen, S. Y. Chen and W. A. Williams, Argonne National Laboratory, Argonne, IL, June.

Yu et al. 2013. *New Source Term Model for the RESRAD-OFFSITE Code Version 3*. NUREG/CR-7127, ANL/EVS/TM/11-5, C. Yu, E. Gnanapragasam, J.-J. Cheng, S. Kamboj, and S.Y. Chen, U.S. Nuclear Regulatory Commission, Office of Nuclear Regulatory Research, Washington, D.C.

Yu et al. 2015. *Data Collection Handbook to Support Modeling Impacts of Radioactive Material in Soil and Building Structures*, ANL/EVS/TM-14/4, C. Yu, J.-J. Cheng, L. Jones, Y. Wang, Y. Chia, and E. Faillace, Argonne National Laboratory for U.S. Department of Energy, Office of Science, Oak Ridge, TN, September.

Zheng 1990. *A Modular Three-Dimensional Transport Model for Simulation of Advection, Dispersion and Chemical Reactions of Contaminants in Groundwater Systems; Documentation and Users Guide*, report to the U.S. Environmental Protection Agency, C. Zheng, S.S. Papadopulos & Associates, Inc., Bethesda, MD.

Zheng and Bennett 1995. *Applied Contaminant Transport Modeling: Theory and Practice***,** John Wiley & Sons, New York, page 440.

This page intentionally left blank.

RECORD COPY DISTRIBUTION

File—DMC—RC